GRIGORE T. POPA UNIVERSITY OF MEDICINE AND PHARMACY IASI

HABILITATION THESIS

IAȘI
2021

GRIGORE T. POPA UNIVERSITY OF MEDICINE AND PHARMACY IASI

CURRENT AND MODERN CONCEPTS IN INFERTILITY: FURTHER MOLECULAR AND CLINICAL INSIGHTS

Bogdan Doroftei, MD, PhD
Associate Professor

CONTENTS

ABBREVIATIONS

WHO - World Health Organization
HPG - Hypothalamic-Pituitary-Gonadal
PID - Pelvic Inflammatory Disease
EMS - Endometriosis
AS - Asherman Syndrome
POF - Premature Ovarian Failure
FertiQol - Fertility Quality of Life Questionnaire
QOL - Quality Of Life
IIEF-5 - International Index of Erectile Function-5
PEDT - Prenature Ejaculation Diagnostic Tool
IELT - Intravaginal Ejaculatory Latency Time
PE - Premature Ejaculation
ED - Erectile Dysfunction
ADAM - Androgen Deficiency in the Aging Male
SHIM - Sexual Health Inventory for Men
TDS - Testosterone Deficiency Syndrome
IVF - *In Vitro* Fertilization
CC - Clomiphene Citrate
PMS - Premenstrual Syndrome
hMG - human Menopausal Gonadotropin
OC - Oral Contraception
COC - Combined Oral Contraception
fMRI - functional Magnetic Resonance Imaging
HC - Hormonal Contraception
E - Oestrogen
P4 - Progesterone
CI - Confidence Interval
OR - Odds Ratio
AIs - Aromatase Inhibitors
PCOS - Polycystic Ovary Syndrome
GnRH - Gonadotropin-Releasing Hormone
FF - Follicular Fluid
GSH - Glutathione
ICSI - Intracytoplasmic Sperm Injection
PTB - Preterm Delivery
IAIs - Intra-Amniotic Infections
STL - Spontaneous Preterm Labour
PPROM - Preterm Prolonged Rupture of Membranes
IC/PBS - Interstitial Cystitis/Painful Bladder Syndrome
r-hFSHs - recombinant human Follicle-Stimulating Hormones
ART - Assisted Reproductive Technology
BMI - Body Mass Index
AMH - Anti-Müllerian Hormone
OS - Ovarian Stimulation
OHSS - Ovarian Hyperstimulation Syndrome
PGT - Preimplantation Genetic Testing
ET - Embryo Transfer
LH - Luteinizing Hormone
SCSA - Sperm Chromatin Structure Assay
AI - Artificial Insemination
IUI - Intrauterine Insemination
DFI - DNA Fragmentation Index
FCM - Flow Cytometry
IMSI - Intracytoplasmic Morphologically Selected Sperm Injection
MGC - Mammary Gland Cancer
MRI - Magnetic Resonance Imaging
ROMA - Ovarian Malignancy Risk Algorithm

IEN - Intraepithelial Neoplasia
D & C - Dilation and Curettage
CT - Computed Tomography
CRL - Crown Rump Length
MCT - Mature Cystic Teratoma
DE - Deep Endometriosis
IOTA - International Ovarian Tumor Analysis
MUSA - Morphological Uterus Sonographic Assessment
USLs - Uterosacral Ligaments
RVS - Rectovaginal Septum
TVS - Transvaginal Sonography
AWE - Abdominal Wall Endometriosis
NEA - Norethindrone Acetate
FDA - Food and Drug Administration
HSG - Hysterosalpingography
IUA - Intrauterine Adhesion
SHG - Sonohysterography
SIS - Saline Infusion Sonohysterography
PGD - Preimplantation Genetic Diagnosis
CDG - Congenital Disorder of Glycosylation
PMD - Placental Mesenchymal Dysplasia
FGR - Fetal Growth Restriction
IUDF - Intrauterine Fetal Demise
RPL - Recurrent Pregnancy Loss
PGT - Preimplantational Genetic Testing
YCM - Y Chromosome Microdeletion
NOA - Nonobstructive Azoospermia
WGA - Whole Genome Amplification
MDA - Multiple Displacement Amplification
CDG-Ia - Congenital Disorder of Glycosylation Type Ia
PGT-M - Preimplantation Genetic Testing for Monogenic Diseases
HF - Hydrops Fetalis
VSD - Ventricular Septal Defect
NL - Nuchal Translucency
NIPT - Noninvasive Prenatal Test
IUGR - Intrauterine Growth Restriction
AFI - Amniotic Fluid Index
ICH - Intracerebral Hemorrhage
DMD - Duchenne Muscular Dystrophy
BRCA1 - Breast Cancer 1
BRCA2 - Breast Cancer 2
EIM - European IVF-Monitoring
DRs - Delivery rates
ED - Egg Donation
FOR - Frozen Oocyte Replacements
FER - Frozen Embryo Replacement
PGS - Preimplantation Genetic Screening
FOR - Frozen Oocyte Replacement
NGS - Next Generation Sequencing
AOA - Assisted Oocyte Activation
IVP - *In Embryo* Production
SDF - Sperm DNA Fragmentation
IVM - *In Vitro* Maturation

REZUMAT

Această teză de abilitare intitulată **„CONCEPTE ACTUALE ȘI MODERNE ÎN INFERTILITATE: INFORMAȚII SUPLIMENTARE MOLECULARE ȘI CLINICE”** prezintă realizările mele științifice, didactice și medicale în perioada postdoctorală. Se concentrează pe expertiza clinică și experimentală, cu scopul de a oferi o imagine de ansamblu integrativă asupra intereselor mele generale privind infertilitatea dintr-un punct de vedere multidisciplinar. Am reușit să delimitez acest subiect de cercetare și să-mi împart munca în patru părți, din care două subcapitole principale, după cum urmează:

INTRODUCEREA oferă o retrospectivă succintă a carierei mele academice, profesionale și științifice, respectiv a domeniilor mele de interes și a principalelor împliniri profesionale.

SECȚIUNEA I - INFERTILITATEA: CONTEXTUL MOLECULAR este atribuit așa-numiților promotori ai infertilității, indiferent de sex. Mai precis, se referă la predispoziția ridicată spre comorbidități neuropsihiatrice și la modul în care medicamentele pentru infertilitate prescrise exercită, de asemenea, efecte antagonice prin perturbarea integrității axei hipotalamo-hipofizo-suprarenale/gonadale. Deoarece este bine cunoscută producția fulminantă a speciilor reactive de oxigen în timpul stărilor de stres prelungit, stresul oxidativ este acceptat în prezent și văzut ca o componentă integrativă. Astfel, am arătat în mod sistematic că într-adevăr ar putea fi un factor declanșator al infertilității. De asemenea, induce o schimbare în interiorul eubiozei gazdei prin perturbarea funcționalității normale a axei intestin-creier, reflectată de deficiențe pe termen lung care implică mai multe componente, cum ar fi: neurologice, metabolice și genetice. Acest concept se aplică și nou-născuților care sunt livrați fie prin cezariană, fie vaginal la termen sau prematuri. Există o multitudine de factori endo- și exogeni care le modelează microbiota și influențează dezvoltarea lor ulterioară. Având în vedere că orice entitate microscopică posedă capacitatea de a modula această cale bidirecțională, este imperativ să se restabilească homeostazia cât mai curând posibil pentru a evita orice boli severe, ireversibile și care pot pune viața în pericol.

SECȚIUNEA II - APLICAȚII CLINICE reflectă încă o dată la începutul acestei secțiuni rolul jucat de microorganisme. De data aceasta se concentrează pe prevalența infecțiilor cu agenți non- și patogeni, precum și pe rezistența lor la antibiotice. Deși medicamentele convenționale pentru infecții s-au dovedit încă fiabile, infertilitatea rămâne o provocare. Pe măsură ce domeniul tehnologiilor ADN a devenit congruent cu metodologiile FIV/ART, șansele de a obține o sarcină au fost îmbunătățite exponențial în urma utilizării diferitelor medicamente recombinante. Pe de altă parte, nu trebuie omis faptul că componenta masculină este o altă cauză a incapacității de a concepe. De-a lungul carierei mele, am avut, de asemenea, șansa de a extinde acest spectru de cunoștințe cu cazuri în care instrumentele de investigare și diagnostic molecular și-au dovedit eficiența și fiabilitatea pentru femei și bebeluși care au necesitat intervenții imediate. În ultima parte a acestei secțiuni, am încercat să explic matematic statutul fertilității. Cu toate acestea, acest subiect de interes este limitat, dar sunt necesare studii suplimentare pentru a obține o imagine de ansamblu completă cu privire la modul în care se poate explica această tranziție de la fertilitate la infertilitate.

CONCLUZIILE enunță și explică direcțiile de dezvoltare profesională și cercetare științifică pe care mi le-am propus în continuare.

Secțiunea **REFERINȚE BIBLIOGRAFICE** include articole, cărți și capitole de carte care m-au ajutat la elaborarea acestei teze.

Rezultatele științifice pe o perioadă de 15 ani sunt incluse în peste 60 de articole publicate și sesiuni de conferințe (peste 35 de articole fiind publicate în reviste indexate ISI) care au adunat peste 900 de citări (index h - 10).

THESIS SUMMARY

This habilitation thesis titled **"CURRENT AND MODERN CONCEPTS IN INFERTILITY: FURTHER MOLECULAR AND CLINICAL INSIGHTS"** presents my scientific, didactic, and medical accomplishments during the postdoctoral years. As such, it provides an integrative overview of my overall expertise and interests regarding infertility from a multidisciplinary point of view. The research topic and my work with it are divided here in four parts with two main sections as follows:

The **INTRODUCTION** consists in a succinct overview of my academic, professional, and scientific career path, interests, and achievements.

SECTION I - INFERTILITY: MOLECULAR BACKGROUND focuses on the so-called promoters of infertility, regardless of sex. More precisely, it refers to the high predisposition towards neuropsychiatric comorbidities and how prescribed infertility drugs also exert antagonistic effects by perturbing the integrity of the hypothalamic-pituitary-adrenal/gonadal axis. Since the fulminant production of reactive oxygen species during prolonged stress states is well known, oxidative stress is presently accepted and viewed as an integrative component. Thus, we systematically showed that it could indeed be a trigger of infertility. Also, oxidative stress induces a shift within the host's eubiosis by disrupting the normal functionality of the gut-brain axis, reflected in long-term deficiencies which involve multiple components such as: neurological, metabolic, and genetic. This also applies to newborns that are delivered either through C-section or vaginally at full-term or preterm. There are a multitude of endo- and exogenous factors that shape their microbiota and influence subsequentdevelopment. Considering that any microscopic entity possesses the ability to modulate this bi-directional pathway, it is imperative to re-establish the homeostasis as soon as possible to avoid any severe, irreversible, and potentially life-threatening diseases.

SECTION II - CLINICAL APPLICATIONS begins with a reiteration of the role played by microorganisms. This time, the focus is on the prevalence of infections with non- and pathogenic agents, as well as on their antibiotic resistance. While conventional drugs are still reliable in addressing infections, infertility presents a significant challenge. As the field of DNA technologies became congruent with IVF/ART methodologies, the chances of obtaining a pregnancy were exponentially improved following the use of various recombinant drugs. On the other hand, it must be said that inability to conceive can also have male-related causes. Throughout my career, I have also had the chance to explore and expand this area of knowledge by analyzing cases in which investigative and molecular diagnostic tools proved their efficiency and safety for women and babies in need of immediate interventions. Last but not least, towards the end of this section, I attempt a mathematical explanation of fertility status. However, further studies are necessary to achieve a comprehensive view explaining the transition from fertility to infertility.

The **CONCLUSIONS** revisit and explain my intended directions for future professional development and scientific research.

The **BIBLIOGRAPHIC REFERENCES** section includes numerous articles, books, and book chapters that informed the writing process and the thesis itself.

The thesis encompases the scientific results obtained over a period of 15 years, and which have been communicated in over 60 published articles and conference sessions. Of these, more than 35 articles are featured in ISI-indexed journals and their 900+ citations demonstrate substantial international readership and outreach (h-index 10).

INTRODUCTION

I began my academic career in 2001 as a Junior Teaching Assistant at the "Apollonia" University in Iași following a competition-based employment process. There, I proceeded to teach 6th-year Dentistry students and to begin exploring my field of scientific interest. In 2005, I applied for a position of Junior Teaching Assistant at the "Grigore T. Popa" University of Medicine and Pharmacy Iași and was successful after an intense competition. Since then, I have been a full-time faculty member at the Department of Mother and Child Health. The high standard of teaching I encountered here as a newcomer motivated me to elevate my conduct and work style to that of my colleagues and to learn from their substantial experience and knowledge. Alongside them, I have devoted much of my time to advancing this important and fascinating field by conducting numerous research projects.

Concurrently, in my professional career as a medical practitioner, I progressed from being a young resident in 2002 to becoming a fully qualified specialist doctor in Obstetrics and Gynecology in 2007. During this time, I also completed my doctoral medical research and was awarded the title of Medical Doctor in 2006. Then, in 2009, I advanced to the position of Teaching Assistant at the Department of Mother and Child Health, once again by undergoing a competitive employment procedure. Soon after, in 2011, I attained the highest position of senior medical specialist in Obstetrics and Gynecology according to the Romanian medical ranking system ("medic primar", equivalent to senior consultant in the UK or attending physician in the US).

My interest in the field of reproductive medicine dates back to the year 2000, when I began my clinical training at the Vienna General Hospital (AKH) in Austria, immediately after my graduation from the "Grigore T. Popa" U.M.Ph. Iași. At the AKH Department of Urology, I worked on the team charged with investigating male infertility and I was fortunate to familiarize myself with the Da Vinci robotic laparoscopy system and with sonographic approaches. I then continued to pursue other clinical internships and qualifications in infertility, especially after 2005, such as a qualification in andrology at the Karolinska Institute in Stockholm, Sweden, and the exam-based European diploma program in gynecological laparoscopy skills at Clermont-Ferrand, France, in 2008, after spending one year at Auvergne University.

The internships that followed in 2008-2010 at the Human Assisted Reproduction Clinic in Ireland (HARI), focusing on *in vitro* fertilization, make up an important chapter in my training as a specialist in reproductive medicine. At the HARI, I had the opportunity to participate in clinical briefings and surgical interventions specifically related to the management of infertile couples. Upon my return, the experience, knowledge, and skills thus acquired enabled me to establish the Origyn reproductive clinic in 2010, and to subsequently secure its current position among the top three most successful Romanian clinics in terms of obtained pregnancies.

From that point onwards, I have started to gradually create an environment that combines performance and perseverance. Not only is this reflected in the daily activity over the last decade, but it also highlights my own growing interest in the spectrum of infertility from a scientific perspective. Alongside my colleagues, I successfully applied in 2019 for a project (POR/846/2/2) aiming to bring state-of-the-art equipment to improve each patient's quality of life.

Most recently, I was able to obtain the Bachelor Certificate in Endoscopy from the

European Academy of Gynaecological Surgery in 2020. This not only confirms my surgical expertise, but it also enables me to deliver training courses recognized by EAGS, and to promote minimally invasive surgery at the "Grigore T. Popa" U.M.Ph. Iași.

My postdoctoral career has integrated scientific research, professional clinical medical practice, and academic education. My clinical and scientific activity has been significantly enhanced by my mentors from Romania and abroad. In my professional development and career, I have had the privilege and honor to be guided by exceptional mentors, among whom the Romanian Prof. Mircea Rusu, Prof. Zenovia Pricop, Prof. Gheorghe Costăchescu, and Prof. Cristina Anton, as well as Prof. Revaz Botchortshvili, Dr. Edgar Mocanu, Prof. Pavel Calda, and Prof. Samir Hammamah from abroad. To them and others, I owe a debt of gratitude for all the opportunities I have had to perfect my clinical skills in minimally invasive surgery, reproductive medicine, human assisted reproductive technology, and sonography.

Academic

The teaching career is a profession with a profound impact on society, as it plays a leading role in the shaping generations to come. It is a complex profession, whose success is based not only on subject-related expertise, but also on advanced metacognition, psychological insights, adaptability, dynamism, and openness to change. An educator should always keep an open mind and strive towards the highest levels of professional development and performance. Our complicated time demands that educators remain primordially focused on the continuous aspect of their own learning by integrating innovative methods and technologies of information and communication within the teaching activity and by personifying quality in education. Now more than ever, teachers also need to be good team workers and flexible thinkers, able to entertain both innovative and critical perspectives, including those imparted by the younger generations.

Regarding my own development as a member of the teaching profession, one common denominator throughout my career has been my continuous self-assessment of my abilities in concordance to international standards of professional competence. I have always kept up to date with the latest trends in my field, and that includes my pursuit of the required teaching skills and certifications to engage in the highest quality teaching practice. Since 2001, when I began my teaching career, and especially after 2005, when I became a Junior Teaching Assistant at the "Grigore T. Popa" University of Medicine and Pharmacy, I have been passionate about engaging young and eager minds with complex knowledge related to high-stakes topics such as the conception and birth of human life.

Retrospectively, from 2018 until last year, I held the position of Head of works within the II Obstetrics-Gynecology Clinic "Grigore T. Popa". As I mentioned before, in 2020 my academic career has evolved one step further. More precisely, I managed to get the title of Associate Professor following a following an evaluation competition within "Grigore T. Popa" which I presently occupy with honor.

Throughout my academic career, I have taught numerous undergraduate courses and workshops, and I have contributed to revising the curriculum in order to update it in an accessible and interesting manner that raises awareness and sparks interest in Obstetrics and Gynecology. Concurrently, I have also authored and co-authored numerous educational materials.

Importantly, I have always been open to the feedback and suggestions of my students, and I accepted their invitations to many events organized by student associations at our University, such as to workshops and conferences by SSCR and SSMI, including to Congressis, the annual international medical congress for medical students and young

medical graduates. My contributions to such events have always been met with genuine enthusiasm and, as such, have inspired and motivated me in turn. The topics that I have covered on such extra-curricular occasions include infertility, preimplantation genetic testing, and minimally invasive procedures in Obstetrics and Gynecology.

In addition to these core teaching activities, I have been observant of the fact that quality education requires organizational skills and commitments in support of the academic and professional community. In this respect, I have been a member of evaluation committees charged with awarding or promoting faculty members to various university titles and positions, as well as a member of committees advancing physicians in the Romanian medical ranking system.

To summarize, my academic strengths moving forward are my substantial experience and expertise in both curricular content and teaching, enhanced by my inspirational relationship with my mentors, colleagues, and students, as well as by my ambitious and competitive nature. Last but not least, my readiness to formalize my role as mentor for medical graduates interested in advanced doctoral studies is confirmed both internally, by my own sense of maturity, and by my peers who seek my guidance and trust my support.

Scientific research

My clinical and educational activities have consistently been informed and complemented by research subsequently shared as published chapters in specialized textbooks, monographs, articles, as well as presented in various scientific events. My contributions to international journals some of which rated as high impact, amount to more than 70 research articles of different types.

After the successful completion of my doctoral research, I have involved myself consistently in various national / university research projects and grants, such as:

1. **THE MOLECULAR DIAGNOSIS OF TUBAL FACTOR INFERTILITY WITH MICROBIAL ETIOLOGY**, a 36-month research project granted by U.M.Ph. Iași at the Ministry of Research through the IDEAS Program (contract no. 338/1.10.2007)
2. **BIOELECTRA – NEW BIOMEDICAL METHODS AND TECHNIQUES FOR NON-INVASIVE INVESTIGATION, DIAGNOSIS, AND MONITORING USING NON-IONOGENIC ELECTROMAGNETIC RADIATIONS**, another 36-month research project (contract PN II no. 41089/2007)
3. **BIOMAG – NEW HIGH-RESOLUTION BIOMAGNETOMETRIC METHODS AND TECHNIQUES IN BIOMEDICAL INVESTIGATION AND DIAGNOSIS**
4. **COMPLEX NON-PHARMACOLOGICAL METHODS IN THE PROPHYLAXIS AND TREATMENT OF CERVICAL AND UTERINE MEDICAL CONDITIONS**, a bilateral cooperation project with the Republic of Moldova
5. **THE MOLECULAR DIAGNOSIS AND PROTEOMIC IMPLICATIONS OF INFERTILITY WITH MICROBIAL ETIOLOGY**, another bilateral cooperation project with the Republic of Moldova (contract no. 423/04.06.2010)
6. **ASSESSING THE ANTIFUNGAL EFFECT OF THE NANOCONJUGATES OF A NEW β-CYCLODEXTRIN PROPICONAZOLE DERIVATIVE,** http://www.uaiasi.ro/PN_2/MXP4509/
7. **I3IDT – INFERTILITY, A THREE-PIECE PUZZLE: THE ASSESSMENT OF THE COUPLE, THE DIAGNOSIS OF THE CONDITION, AND THE POTENTIAL THERAPEUTIC APPROACH,** a 30-month project worth 3,499, 970 RON which I coordinated as Project Manager (contract no. 448 / 2013).

Clinical medical practice

Considering that Obstetrics and Gynecology is a compulsory clinical discipline in the medical curriculum, my medical practice has provided a solid foundation and platform for my own continuing education as well as for the applied, interactive teaching of students.

My body of clinical work speaks to the level of expertise that I have attained in this field. Below I include a succinct overview of my hospital experience, practical competences, professional memberships, and public recognition which qualify me as a seasoned practitioner able and ready to coordinate and supervise:

- competent provision of medical care for the full spectrum of pathologies since 2001 in a tertiary reference center for the region of Moldova, the "Cuza Vodă" Clinical Hospital of Obstetrics and Gynecology in Iași
- more than 17,000 hours of on-call duties in Obstetrics and Gynecology specifically since 2002, amounting to over 2,000 workdays (8h)
- over 13,000 abdominal and transvaginal sonographies up to now
- 2,438 interventions in the last 6 years: C-sections, surgical interventions, diagnostic and therapeutic laparoscopies (mainly laparoscopic salpingectomies and cystectomies), diagnostic and surgical hysteroscopies, myomectomies, and hysteroplasties.
- admission and monitoring of more than 400 female patients/year from a total of 1,400 annual admissions in the Obstetrics I and II wards, as well as consulting more than 300 female patients/year during on-call duties at the hospital's emergency room.

Professional competencies acquired in Romania in the following fields:

- obstetric and gynecologic ultrasonography
- hysteroscopy
- gynecologic laparoscopic surgery
- assisted reproduction
- sanitary management

Professional competencies acquired abroad in the following fields:

- Andrology (qualification diploma from Karolinska Institute in Stockholm, Sweden, 2007)
- gynecologic laparoscopy (Diplome Europeéne d'Endoscopie Opératoire, 2008-2009, Université d'Auvergne, Clermont Ferrand, France)
- Endoscopic surgery (Bachelor in Endoscopy Surgeon Certificate from the European Academy of Gynecological Surgery, 17.03.2020).

Noteworthy training period abroad:

- Training internship in reproductive medicine at the HARI in Dublin, Ireland, during 01.09.2009-01.03.2010, under the supervision of Dr. Edgar Mocanu

Memberships:

Concurrent with and instrumental to my scientific, clinical, and academic endeavors, I have always been interested in actively joining professional organizations from Romania and abroad in the fields of Obstetrics and Gynecology, and especially Reproductive Medicine.

Thus, I am a member of the Romanian Society of Obstetrics and Gynecology, the European Society of Human Reproduction and Embryology, the European Society of Gynecologic Endoscopy, and the American Society of Reproductive Medicine. I am also a founding member of the Romanian Society affiliated with the International Federation of Fertility Societies.

It is worth mentioning that I was elected twice as the Romanian delegate at the European Society of Human Reproduction and Embryology (ESHRE), where I contributed actively to EU legislation initiatives. Last but not least, I am a member of the committee charged with reporting medical outcomes from across Europe and, as such, I participate in annual meetings and draft reports for Romania.

Awards:

In my clinical practice, I strived to apply my innate enterprising spirit to advancing the level of care available in our geographical area. My initiatives received public recognition at the Gala Medica 2013 when I was awarded the prize and title of Young Medical Entrepreneur by the Romanian Medical Council (http://gala2013.cmr.ro).

Managing activity

My interest in management started in 2015 when I became Head of the Gynecology Department at "Cuza Vodă" Hospital in Iași a position I held until 2016. In these two years of managerial activity, my main focus was to enable a fluid and proactive work environment for my fellow surgeons, resulting in the best care for the patients. I also made considerable efforts to facilitate the transition to minimally invasive procedures such as laparoscopy, allowing patients to recover faster, with fewer complications and shorter hospitalization.

Later, in 2018, I took on a great responsibility by accepting the position of Medical Director of "Cuza Vodă" Clinical Hospital Iași, which I continue to hold. The level of expertise and engagement required to fulfill this job successfully is considerable, to say the least. As Medical Director, I have provided leadership in this sizeable healthcare organization I have devised protocols and guidelines for the clinical staff, I have supervised and evaluated performance with the view to ensuring optimal healthcare for our patients.

After more than 10 years of practice in the area of Infertility, my main subject of interest and passion, I decided to set up in Iași a medical center specialized in Infertility and Human Reproduction, and fulfill a vision I was able to conjure after visiting several such centers throughout Europe. This is how the Origyn Fertility Centre was born. Since its establishment, I have strived to offer state-of-the-art services for patients struggling with infertility. Thereby, from 2012 to 2018 I was Medical Director at Origyn, and Head coordinator since 2018 until now, supervising the clinical activity and staff, ensuring that all the medical and administrative procedures are conducted appropriately.

In 2020, in the context of the Covid-19 pandemic and the acute need for timely testing of the population, Origyn began to offer RT-PCR testing for Covid-19 in our laboratory, using the latest technology and devices. Moreover, Origyn has gradually been broadening its scope and range of medical services to include Genetics, Nutrition and Dietetics, Endocrinology, Urology, Clinical Psychology, and Cardiology.

SECTION I. INFERTILITY: MOLECULAR BACKGROUND

Chapter I

Infertility can be defined as the impossibility to procreate, carry, or deliver a baby naturally after having tried for at least one year. However, there are provisions which add different nuances to this general view, such as the WHO recommendation to consider at least two years of unprotected intercourse in order to validate these guidelines [1].

Infertility affects an estimated 10-15% of couples of reproductive age worldwide [2,3]. Female infertility is responsible for one-third of the cases, the remaining two-thirds consisting of male or mixed infertility. Assessing the causes of female infertility is essential and there are two key areas of interest: the structure of the reproductive organs and the function of the hormonal HPG axis [4,5].

There are multiple causes for female infertility, including structural factors such as pelvic adhesions after chronic infection and PID resulting in tubal obstruction, EMS, uterine fibroids, endometrial polyps or uterine congenital abnormalities or the AS [6]. Hormonal imbalances may cause anovulatory cycles and genetic factors may lead to POF [7].

Personal contribution - published papers:

Doroftei, **B**.; Ilie, O.-D.; Puiu, M.; Ciobica, A.; Ilea, C. Mini-Review Regarding the Applicability of Genome Editing Techniques Developed for Studying Infertility. *Diagnostics (Basel, Switzerland)* ***2021***, *11*, 246. **IF: 3.706**

Simionescu, G.; **Doroftei**, **B**.; Maftei, R.; Obreja, B.-E.; Anton, E.; Grab, D.; Ilea, C.; Anton, C. The complex relationship between infertility and psychological distress (Review). *Exp Ther Med* ***2021***, *21*, 306. **IF: 2.447**

Armeanu, T.; Simionescu, G.; Nicolaiciuc, D.; Plopa, N.; **Doroftei**, **B.**; Maftei, R. Infertility and borderline malignant ovarian tumors: a case of successful pregnancy after fertility-preserving management of the disease. *Eur. J. Gynaecol. Oncol.* ***2020*** *41*, 284–288. **IF: 0.196**

Personal contribution - published papers:

Simionescu, G.; Ilie, O.-D.; Ciobica, A.; **Doroftei**, **B**.; Maftei, R.; Grab, D.; McKenna, J.; Dhunna, N.; Mavroudis, I.; Anton, E. Mini-Review on the Possible Interconnections between the Gut-Brain Axis and the Infertility-Related Neuropsychiatric Comorbidities. *Brain Sci.* ***2020***, *10*, 384. **IF: 3.394**

Simionescu, G.; **Doroftei**, **B**.; Maftei, R.; Obreja, B.-E.; Anton, E.; Grab, D.; Ilea, C.; Anton, C. The complex relationship between infertility and psychological distress (Review). *Exp Ther Med* ***2021***, *21*, 306. **IF: 2.447**

I.1 Infertility-related neuropsychiatric comorbidities

I.1.1 Psychological stress

Infertility can have profound consequences on a person's psychology, often through the perception of losing control on one's own life [8]. The issue of infertility can become centric to a relationship, with anger and confusion replacing reason [9]. This is because, for an adult, the desire to conceive is often an important aspect of progression through life and identity itself [10]. Cousineau reviewed extensively the cultural and social effects of infertility, including its influence on marital status, decision making, and relevant psychological support [11]. Infertility treatment places a great deal of stress on a couple, which can culminate in an attitude of resignation; the dream of having a child of one's own is replaced by resorting to adoption or by remaining child free [12].

Many couples find it difficult to accept and adapt to such an unintended trajectory, defining a new vision for their lives beyond the temporary crisis [13]. They must often make radical lifestyle adjustments, such as re-evaluate decisions surrounding career options, with other important aspirations often postponed [14]. Aside from the individual lifestyle upheaval, one must adapt to a rigorous medication program as well [15]. Women are more prone to mixed anxiety-depressive

disorders (MAAD) than men. In Table 1, all the large-cohort studies conducted between 2010-2020 are summarized (≥1000 patients per sample).

Table 1. Associations between infertility and the predisposition for upcoming health issues

Number of Patients	Main Observations	Reference
1,000 patients (couples)	After the completion of the fertility problem inventory (FPI)-derived questionnaire prior to the beginning of the procedure, confirmatory factor analysis (CFA) was partially validated. A post hoc exploratory factor analysis (EFA) explained two associated factors and the invariance between genders regarding stress-related states.	[16]
1,146 infertile patients	Using generalized anxiety disorder-7 (GAD-7) in parallel with a simple and multiple logistic method of classification revealed that generalised anxiety is common among infertile women, which was positively correlated with four specific indices.	[17]
1,506 infertile patients	In accordance with patient health questionnaire-9 (PHQ-9) scores and through a simple and multiple logistic method of classification, the authors concluded that depression is predominant in women, a series of variables being positively correlated with its triggering.	[18]
511 infertile women and 1,017 controls	Based on a personalised version of 36-short form health survey (SF-36), family members were found to exert significant impact upon decision making, more precisely towards divorce, remarriage or adoption, independently of social status.	[19]
1,620 infertile women	Women recorded low scores in FertiQol in three specific subscales and high scores in SCREENIVF, which indicates that they are at higher risk for developing emotional problems compared to their partners, both during and after the procedure.	[20]
2,180 patients, of whom 1,049 were men and 1,131 women	After the measurement of the severity of depression-like symptoms and infertility distress using the mental health inventory-5 (MHI-5) and COMPI Fertility Problem Stress Scales, the predisposition for neuropsychiatric disorders was almost three times higher, which directly correlated with infertility-related distress in both groups.	[21]
338 infertile patients and 1,953 controls	Based on composite international diagnostic interview (CIDI), beck depression inventory (BDI), and 12-item general health questionnaire (GHQ-12), approximately 29% of the patients who had experienced infertility, especially women, had increased risks for persistent depressive disorder (PDD) and anxiety compared with controls. Those who already had a child were more prone to panic disorder, while in men there was a reduction in the quality of life (QOL).	[22]
1,468 infertile men and 942 controls	IIEF-5, PEDT and IELT, concomitant with self-rating anxiety scale (SAS) and self-rating depression scale (SDS) revealed that, compared with controls, the incidence of PE and ED was significantly higher for infertile patients, and the results were similar for anxiety and depression. Negative associations were noticed for anxiety and depression in the IELT and IIEF-5 datasets.	[23]
2,783 men	In total, 1,750 men completed the ADAM and the SHIM questionnaires. Through a multivariable logistic model, positive correlations between the prevalence for ED and the results obtained in ADAM were seen. After the serum measurements of a series of biomarkers, no associations between T values with the symptoms of ED or TDS were reported.	[24]
5,936 infertile women	1,031 women who had never sought specialised advice for their infertility problem presented higher risk of depression, ovulation and metabolic disorders. Even though 728 pursued with treatment, 303 manifested increased chances to develop depression, tumours, menstrual disorders or urinary tract infections.	[25]

6,567 women with or without a history of IVF	With a median follow up of seventeen years and by using a multivariate predictor, the authors found that 411 women from the cohort were admitted with diagnoses of mental disorders during the studied period. Of them, 93 had previously pursued IVF and 318 had not.	[26]
9,175 infertile women and 9,175 controls	Women who had previously received treatment were less likely to be hospitalised for mental disorders or substance abuse/intoxication compared to controls. This risk was statistically significant, similar for hospitalisation during a decade post-treatment follow-up, but with exceptions in two indices. Furthermore, those who had given birth were less predisposed to anxiety, depression, and substance abuse/intoxication in contrast with those who had not, the hospitalisation rates being identical between women who did not have a baby and controls.	[27]
13,027 infertile men and 23,860 controls	Infertile men were found to be predisposed to metabolic and cardiovascular disorders, as well as to substance abuse compared to those who underwent testing only or were vasectomised.	[28]
98,320 women	Whenever a pregnancy failed, women were at increased risk of psychiatric disorders and substance abuse compared with the women who managed to give birth after the infertility evaluation. No significant differences were noted regarding the prevalence of anxiety, eating disorders or obsessive-compulsive disorder (OCD).	[29]
HUNT 2006–2008 *n* = 9,200 women HUNT 1 and HUNT 2 *n* = 5,873 sub-fertile women and HUNT 2 *n* = 12,987 women	The North-Trøndelag Health Study is one of the largest series of cross-sectional population-based studies ever designed to determine the predisposition of central nervous system (CNS) disorders. Nevertheless, the results obtained are antithetical. No conclusive evidence was found in two of the studies to link the incidence of infertility with common mental health disorders, while the third confirmed the causality.	[30–32]

I.1.2 Infertility medication

It has been suggested that intestinal microflora may reduce or even inhibit the treatment for infertility [33] and, in parallel, gradually promote neuropsychiatric disorders. In Table 2, our overview of available studies focuses only on medication usually administered for infertility and which may cause side effects that include the promotion of a psychiatric disorder.

Table 2. Infertility drugs with known to potentially induce pronounced mood fluctuations as a side effect

Type of Drug	Number of Patients	Main Observations	Reference
CC	50 patients (25 couples)	CC triggered exacerbated symptoms of PMS in 9 out of 14 women only (e.g. irritability and mood swings)	[34]
CC	1 male patient	The patient in this study was diagnosed with oligoteratospermia and received CC. The treatment culminated in depressive symptoms for five consecutive days. After the treatment was discontinued, it took an additional seven days until he made a full recovery.	[35]
CC and hMG	454 (139 women who had not previously taken any drug and 315 who had previously received medication)	This cross-sectional, self-reported study concluded that both CC (*n* = 162) and hMG (*n* = 153) act as agonists and could trigger disorders such as depression according to the state-trait anxiety inventory (stai) through a disturbance of the hypothalamic-pituitary-adrenal (HPA) axis. Significant differences were noted between the groups, with those women taking either CC or hMG reporting a higher incidence	[36]

		of psychological effects.	
OC	34 women (17 COC and 17 placebo)	During the seven-day study period, the COC users displayed more depressive symptoms when compared to the placebo cohort according to the cyclicity diagnoser (CD) scale. This was highlighted by a specific reactivity at the level of the insular cortex, respectively, the first one-third and the lowest portion of the frontal lobe through fMRI both before as well as during the treatment.	[37]
OC	76 women (38 OC and 38 placebo)	A significant percentage (77%) of the total adolescent cohort had one side effect manifested. Interestingly, the number and type of side effects were identical in both the OC and placebo groups after the completion of center for epidemiologic studies depression scale (CES-D).	[38]
HC	1,061,997 Danish women	Compared with the relative low risk with aging, adolescents were found to be more predisposed to the subsequent usage of antidepressants following the administration of HC.	[39]
HC	2532 women (232 E-progestin, 58 progestin only and 948 with no treatment)	The use of combined hormone contraception was higher in Caucasians with major depression disorder (MDD), while those on P4 monotherapy displayed more hypersomnia, weight gain, and relatively worse physical functioning. Those with the COC were singnificantly less depressed than those in the other two groups according to the 16-item quick inventory of depressive symptomatology (QIDS) score.	[40]
HC	75,528 postpartum women	Of all the women in this study, 7.8% were prescribed antidepressants, while 5% were diagnosed with depression.The percentages differ depending on the type of hormonal contraception. It should be noted that the women had previously served in the US army.	[41]
HC	815,662 Swedish women	The high confident interval of 95% OR indicates a strong correlation between psychotropic drug usage among adolescents compared with the older women.	[42]
CC versus AIs for PCOS as well as gonadotropins versus CC versus AIs in patients with an unknown cause of infertility	3,258 patients (1,650 women and 1,608 men)	In women who were not previously taking any antidepressants, major depression (MD) did not negatively influence the fertility chances, but instead slightly increased the likelihood of pregnancy. However, in 90 of the women who had taken antidepressants previously, there was an increased risk of miscarriage, while in men, active major depression reduced the likelihood for conception.	[43]
GnRHa	29 women (agonist)	GnRHa correlated positively with a pronounced depression-like symptomatology, analogue with anxiety, but this was considered an overlap of the pre-existing condition in euthymic participants according to the hamilton scales for anxiety (HAM-A), hamilton scales for depression (HAM-D) and Visual Analogue Scale for Anxiety (VAS-A) and visual analogue scale for depression (VAS-D).	[44]

Based on the studies summarized above, we may conclude that infertility drugs do indeed exert antagonistic effects upon the neurohormonal axis by disrupting its normal functionality. Unfortunately, not enough is known regarding the side effect profile of infertility medication. It is difficult for patients and clinicians to figure out which responses are psychological and which are

caused by medication, but it is vital to identify the causes in order to establish optimal countermeasures.

I.1.3 Therapies

Psychotherapy

Psychotherapy is an important approach that should be recommended to couples suffering from any form of infertility. Therefore, counselling should ideally begin before patients start any medical intervention to help with infertility [45]. Research has found that addressing psychological problems such as depression, anxiety, and stress may help increase the chance of conception [45]. Also, interpersonal treatment, which focuses on enhancing relationships or resolving disputes with others, and cognitive behavioural therapy, can help infertile patients deal with depression and anxiety [46,47]. In addition, psychotherapy can be provided individually, to couples or in community settings, with excellent results [48,49].

Relaxation techniques

In addition to the psychological help that couples who cannot conceive a baby should receive, other complementary interventions should also be advocated for. Given that infertility and its therapy often cause significant stress, multiple relaxation techniques are recommended by specialists: meditation, deep breathing, guided imagery, and yoga.

Previous studies emphasised the effect of yoga on decreasing psychological stress among individuals undergoing infertility treatment [50–52]. Specifically, a study demonstrated that yoga intervention increased the quality of life and decreased negative feelings and thoughts that were associated with infertility. It revealed that participating in yoga classes also decreased symptoms of anxiety and depression in women undergoing IVF [51]. In another study, structured yoga classes lasting six weeks were found to decrease anxiety by 20% and anxiety scores by 12% [52].

Personal contribution - published papers:

Anton, C.; Ciobica, A.; **Doroftei**, **B**.; Maftei, R.; Ilea, C.; Darii Plopa, N.; Bolota, M.; Anton, E. A Review of the Complex Relationship between Irritable Bowel Syndrome and Infertility. *Med.* ***2020***, *56*, 592. **IF: 2.430**

Doroftei, **B**.; Ilie, O.-D.; Cojocariu, R.-O.; Ciobica, A.; Maftei, R.; Grab, D.; Anton, E.; McKenna, J.; Dhunna, N.; Simionescu, G. Minireview exploring the biological cycle of Vitamin B3 and its influence on oxidative stress: Further molecular and clinical aspects. *Molecules* ***2020***, *25*, 3323. **IF: 4.411**

Antioch, I.; Ilie, O.-D.; Ciobica, A.; **Doroftei**, **B**.; Fornaro, M. Preclinical considerations about affective disorders and pain: A broadly intertwined, yet often under-explored, relationship having major clinical implications. *Med.* ***2020***, *56*, 504. **IF: 2.430**

Ilie, O.-D.; Ciobica, A.; McKenna, J.; **Doroftei**, **B**.; Mavroudis, I. Minireview on the Relations between Gut Microflora and Parkinson's Disease: Further Biochemical (Oxidative Stress), Inflammatory, and Neurological Particularities. *Oxid. Med. Cell. Longev.* ***2020***, *2020*, Article ID 4518023. **IF: 6.543**

I.2 State-of-the-art: Oxidative stress as a promoter of infertility

Perhaps the most important variable that may explain this relationship is stress related. Reactive oxygen species (ROS) are created by cells in some physiological and pathological situations. The main reactive oxygen species are O_2^-, OH^-, H_2O_2, $^1O_2$ and NO. These reactive oxygen species are known to respond to all macromolecules, lipids, proteins and carbohydrates. However, they particularly react with polyunsaturated fatty acids (PUFAs) on the membrane of the cell. Cell injury and ultimately cell death occurs after the initial reaction with main reactive oxygen species and after the following chain reaction is initiated [53]. Reactive oxygen species-started oxidative stress (OS) can be controlled by the antioxidant defense system. The antioxidant defense mechanism includes enzymatic and nonenzymatic antioxidants. The main enzymes that have antioxidant properties are

superoxide dismutase (SOD), catalase (CAT) and gluthatione peroxidase (GPx). Regarding the nonenzymatic antioxidants, these are represented by vitamin E, vitamin C, and flavonoids [54].

Thus, oxidative stress results when the generation of reactive oxygen species surpasses the ranging capacity of antioxidants as a result of two possible situations: high levels of reactive oxygen species and/or deficient intake or elevated usage of antioxidants. The majority of reactive oxygen species are created as a result of the mitochondrial respiratory chain. However, reactive oxygen species can also be created by various exogenous factors. These exogenous factors include alcohol consumption, tobacco smoking, and various environmental pollutants [55].

According to researchers, niacin supplementation could have an important role in treating POF. Also, B_3 promotes follicular growth and an increase in the level of two markers, both involved in mediating apoptosis in cultured cell lines from mice [56].

Lactobacillus plantarum YW11 [57], *Lactobacillus plantarum* CCFM10 [58], and *Enterococcus durans* MTCC 3031 [59] were found to restore microbial integrity in aging murine models through normalization of the redox ratio. On the other hand, gut metabolism in mice could be disrupted following administration of antibiotics, which was characterized by a shift of the redox potential after just 24h [60].

Diet also plays a pivotal role in optimizing the function of gastrointestinal microbiota (GM). The rodent diet consists of oxidized animal proteins and results in significant impairment of the mucosal barrier. The disbalance is characterized by a reduction of several beneficial strains such as *Akkermansia*, *Lactobacillus*, and *Desulfovibrio*, to the detriment of proinflammatory strains like *Escherichia-Shigella* and *Mucispirillum* [61].

Extruded sorghum flour (ESF) was found to improve the intestinal microbiota of obese rats by enhancing the proportion of the Bacteroidetes phylum, and lowering that of the Firmicutes phylum. Extruded sorghum flour also diminished the concentration of a series of proinflammatory biomarkers, and subsequently increased the overall antioxidant capacity [62].

I.2.1 The impact on males (in)fertility

In male subjects, targeted studies demonstrated that a high level of oxidative stress leads to decreased sperm motility, sperm number, and sperm-oocyte fusion [63]. The exact mechanism behind the negative influence of oxidative stress on male infertility is connected to spermatozoa. A human spermatozoon is a cell type that has the capacity to generate ROS when incubated under aerobic conditions. The production of reactive oxygen species by sperm is considered a common physiologic process [64]. The problem occurs when an imbalance between reactive oxygen species generation and scavenging activity develops. This imbalance is associated in the literature with male infertility because it is detrimental to the sperm [65,66].

Therefore, it is vital to detect the sources from where reactive oxygen species is produced in order to understand the impact of high levels of reactive oxygen species on the spermatozoa, especially in those phases that are vital for fertilization.

Thus, human spermatozoa have the capacity to produce reactive oxygen species by starting the peroxidation of the unsaturated fatty acids that are found in the sperm plasma membrane [67]. This process plays an important role in the etiology of male infertility.

These molecules have a relatively short half-life and limited diffusion, which is accordant with their physiologic function in acrosome reaction and hyper activation. Therefore, a major cause of defective sperm function in cases of male infertility may be the intrinsic reactivity of the aforementioned metabolites in peroxidative damage. This may be induced by high levels of reactive oxygen species production, particularly H_2O_2 and the O_2^- anion [68].

In addition, the two main sources of reactive oxygen species production in the male reproductive system are the spermatozoa and infiltrating leukocytes [69]. Although both spermatozoa and leukocytes have the capacity to produce reactive oxygen species, leukocytes are known to produce much more elevated levels [70]. It is important to mention that the clinical significance of leukocyte production of reactive oxygen species in semen is controversial. Seminal plasma contains enzymes that scavenge reactive oxygen species, such as catalase and superoxide dismutase, offer protection against reactive oxygen species damage. Therefore, a number of defense mechanisms can

be used to reduce the levels of oxidative stress caused by excessive reactive oxygen species production [71].

Therefore, developing effective therapies to overcome excessive reactive oxygen species production is important in order to help reduce male infertility, given that reactive oxygen species production can have both positive and negative effects on the spermatozoa and equilibrium between the levels of reactive oxygen species produced and the levels of reactive oxygen species scavenged will decide if a given sperm function will be promoted or endangered [72].

Thus, precise measurement of reactive oxygen species production levels is vital, because it will help clinicians identify patients that may or may not respond to specific therapeutic plans and, perhaps more importantly, it will help elucidate the fertility status of an individual.

However, the possible benefits of various antioxidant supplements for fertility purposes must be cautiously investigated, until proper clinical trials validate them. From the current available data it appears that there is still no single adjuvant treatment that is able to enhance the fertilizing ability of sperm in infertile males [73]. A more feasible approach would be a combination of various medications that are not toxic in the administered dosages.

I.2.2 The impact on females (in)fertility

On the other hand, animal models, *in-vitro* data, and human studies demonstrated that high levels of oxidative stress may negatively affect female fertility [74]. However, the exact mechanism behind this observed correlation has not yet been discovered in subjects who are trying to conceive.

High levels of oxidative stress negatively influence both natural and assisted fertility [75]. Various oxidative stress biomarkers have been discovered in different locations in the female reproductive tract. These findings suggest that oxidative stress biomarkers are playing important roles in various physiological functions [76]. However, a number of studies point to reactive oxygen species production as a causative factor of infertility. This causal link may explain various types of infertility, such as peritoneal factor, tubal factor, EMS, and unexplained infertility [76]. However, the scientific cause of unexplained infertility remains unclear, hence its name, but oxidative stress may soon be proven to play an important role in its pathophysiology.

The role of oxidative stress in other types of infertility is not completely discovered either. Many studies have measured the potential role of various markers of the oxidative stress in tubal factor infertility, EMS, and peritoneal factor infertility [77]. The results reported so far show that the tubal and peritoneal microenvironments impact fertilization and early embryonic growth. If high concentrations of reactive oxygen species are found in these environments, they might produce negative effects both in the Fallopian tube and the peritoneal cavity, on the spermatozoa, oocytes, sperm-oocyte interaction and fetus [78]. Furthermore, activated macrophages have been found to play an important role in the process of pathogenesis of EMS. In the peritoneal environment affected by EMS, these macrophages are capable of producing high levels of reactive oxygen species.

On the other hand, Siristatidis et al., reported opposing findings and showed that, following measurement of reactive oxygen species in blood samples at oocyte retrieval and in FF, there was no association between reactive oxygen speices and the quality of embryos following IVF [79].

However, evaluating antioxidant status may help to predict IVF outcome. This was the case reported by Nishihara et al., in a study where they showed that patients with a low fertilization rate also had low levels of GSH following ICSI. In turn, those with a high fertilization rate had high levels of 8-oxo-2'-deoxyguanosine (8-OHdG) in the FF. The authors also suggested that oxidative stress in infertile women are associated with EMS [80]. Their observations were reinforced by the results of Borowiecka et al., who revealed that an elevated FF lipid level and the process of protein peroxidation could negatively influence IVF outcome, after analysis of thiobarbituric-acid-reactive substances (TBARS) in pregnant women [81].

Tulić et al., demonstrated that reactive oxygen species do not negatively influence IVF outcomes, but significant differences were noted between protocols. A GnRH-agonist protocol was proven to be more reliable in terms of developing mature oocytes and fertilization when compared with a GnRH antagonist. There were no differences between the number of biochemical pregnancies, miscarriage, or live birth rate. By measuring superoxide dismutase, malondialdehyde (MDA) and

sulfhydryl group (SH) in serum, the authors concluded that the superoxide dismutase was significantly lower in contrast with malondialdehyde and sulfhydryl group [82].

In addition to disturbing the body's internal parameters, heavy [83] and trace elements [84] act as exogenous stressors, as they cause an increase in the production of specific oxidative biomarkers. Possible therapies include treatment with micronutrients that may optimize the host microenvironment against reactive oxygen species [85].

I.2.3 Long-term gastrointestinal dysfunctions

The digestive tract is another important anatomical feature whose overall functionality was proven to correlate positively with bipolar disorder (BD) and major depression disorder [86]. This was due to the fact that ROME IV has offered a more conclusive perspective. More precisely, with the inclusion of affective and neurological components, any idiopathic cause indicates a functional gastrointestinal disorder (FGID) [87].

Thus, functional gastrointestinal disorders such as irritable bowel syndrome (IBS), which is the most common functional gastrointestinal disorder, is recognized as a disturbance of the gut-brain axis (GBA) and hypothalamic-pituitary-adrenal axis [87]. Despite the fact that irritable bowel syndrome' underlying mechanism of action is still obscure, it possesses a clear clinical panel: abdominal pain and/or discomfort and altered bowel function are predominant symptoms reported by patients [88].

In the literature, relatively few studies have attempted to elucidate the interplay between bipolar disorder and/or major depression disorder in the context of irritable bowel syndrome [86]. On three distinct occasions, in patients suffering from major depression disorder (onset or recurrent episode), the prevalence was found to range between 27-29% and 47,3% [89,90]. A cross-sectional study was conducted by Karling et al., [91]. On the other hand, those in remission did not differ from the control group in terms of gastrointestinal (GI) symptoms.

One possible explanation for the pain felt in irritable bowel syndrome relates to the gradual degradation of the kynurenine pathway and serotonin (5-HT) depletion. Having, as a result, a pro-inflammatory cascade, these modifications of the homeostasis could, in the future, be considered as a potential biological basis in order to certify the high comorbidity between irritable bowel syndrome and the neuropsychiatric disorders [92,93].

Unfortunately, no reliable and efficient therapy or treatment has yet been found for major depression disorder-irritable bowel syndrome patients. In several studies, the authors tried a recovery of host's eubiosis using probiotics [94,95] and dietary changes [96], or even hypothesized that, in fact, the inflammasome-gut microflora system could be responsible [97,98], but only robust or negative data have been since obtained.

Results regarding the relevance of irritable bowel syndrome in bipolar disorder are even more controversial. Crane et al., [99] and Mykletun et al., [100] have demonstrated that irritable bowel syndrome is not associated with bipolar disorder. On the contrary, they concluded that under certain circumstances, irritable bowel syndrome' severity is completely independent or slightly correlated with a reduction. The same conclusion was reached by Mykletun et al., [100] following the epidemiological study conducted on irritable bowel syndrome women diagnosed with anxiety or depression.

Liu et al., [101] contradicted these findings following the comparison of a cohort consisting of 30,796 irritable bowel syndrome patients and an identical matched control group. The authors have concluded that irritable bowel syndrome could represent a promoter of bipolar disorder. On the basis of a recent meta-analysis and nationwide studies, irritable bowel syndrome appears to be behind the development of bipolar disorder. It seems that the risk ratios primarily depend on time as the crucial variable, but the prevalence persists even after half a decade [102,103].

Analogous to major depression disorder, Järbrink-Sehgal [104] summarized all the available reports regarding the involvement of the gastrointestinal microflora in bipolar disorder following the analysis of the 16S rRNA and one shotgun metagenomics sequencing analysis. However, we did not identify any study in the literature currently where probiotics were used in order to diminish bipolar disorder-related symptomatology.

Although the relationship between fertility and irritable bowel syndrome has been examined in the literature, relatively little is known regarding the reproductive disorders faced by patients who suffer from irritable bowel syndrome. Therefore, the available studies that examine male infertility in irritable bowel syndrome patients reported results showing that infertility is more prevalent in individuals with irritable bowel syndrome compared to the general population [105]. Furthermore, one case control study [106] concluded that the number of children born to individuals with irritable bowel syndrome is significantly lower when compared to patients suffering from other gastrointestinal disorders, such as ulcerative colitis (UC), and the general population. The same study also showed no statistically significant difference in the number of children that individuals with ulcerative colitis have and the general population [107]. Moreover, the significant differences observed between patients with irritable bowel syndrome and controls could not be explained by the fecundability or the frequency of the sexual intercourse as these two measured variables did not differ significantly in the two groups [108,109].

Another interesting explanation of these results was proposed by Heetun et al., who suggested that the decision to limit family size may be explained by fear of passing irritable bowel syndrome predisposition genes rather than a physical effect of the disease itself [110]. This hypothesis is backed by another study which showed that irritable bowel syndrome suffering individuals presented a reduction in fertility up to 50% with no significant difference measured in the reproductive capacity [111].

However, even if irritable bowel syndrome itself does not seem to physically influence fertility, the medications which are commonly prescribed to treat this disorder could definitely affect one's ability to procreate. An unwanted surgical procedure or malnutrition resulting from irritable bowel syndrome may provoke various sexual dysfunctions that may finally lead to infertility [112].

Therefore, patients suffering from irritable bowel syndrome should consider changing their prescribed pharmaceutical treatment. For example, individuals who have a prescription for sulfasalazine (SASP), should substitute this drug with a different 5-aminosalicylic acid (5-ASA). It is recommended that this change in medication be made at least 4 months before any attempt to conceive [113]. Furthermore, in order to restore fertility, patients with irritable bowel syndrome who are on mesalazine are also advised to discontinue the treatment [114]. However, to avoid any potential escalation of irritable bowel syndrome symptoms, corticosteroids can be prescribed in order to control the active disorder [115]. In addition, although some authors recommend the interruption of methotrexate (MTX) treatment 4 months prior to attempting to conceive, there is simply not enough evidence to support this guidance. The risk of an acute increase in irritable bowel syndrome symptoms as a result of methotrexate discontinuation might eclipse any hypothesized benefits regarding fertility [116]. The interruption of the treatment is suggested only if erectile dysfunctions are present. Similarly, there is not enough data to endorse interruption of thiopurines and anti-tumor necrosis factor (TNF) agents such as infliximab (IFX) [117]. Moreover, to individuals who intend to undergo proctocolectomy, sperm banking prior to the procedure should be offered because postoperative anejaculation, although rare, is a possible permanent complication [118].

Besides medication, other possible explanations for the observed high levels of infertility in men with irritable bowel syndrome are active inflammation, alcohol consumption, smoking habits, use of over the counter medications, and unhealthy nutritional intake [119]. Therefore, before any infertility treatment is prescribed, it is important to try to manage all these variables that may worsen irritable bowel syndrome symptoms. For example, if the individual has unhealthy nutritional habits, optimizing their food intake should be an objective, e.g. proper macro and micronutrients partitioning [120]. Likewise, smoking cessation should strongly be advocated if the patient has a smoking habit.

In the majority of the available studies, the molecular mechanism behind the connection between irritable bowel syndrome and infertility is related to GnRH [121]. This hormone is the hypothalamic hormone in the sex hormone axis. GnRH is known to stimulate the release of E and P4 [121]. GnRH neurons are known to control fertility in all mammalian species [122]. In addition, studies show that humans who present a dysfunction connected to the GnRH neurons are also infertile [123]. Animal models also proved that mice with defective GnRH biosynthesis are also sterile [53].

Another explanation for the correlation between infertility and irritable bowel syndrome is IVF intervention. The problem occurs when IVF is prescribed repeatedly to women who are struggling to conceive, the same aforementioned population most likely to be affected by irritable bowel syndrome

[121]. Although this hypothesized correlation has not been studied extensively, available data shows that irritable bowel syndrome symptoms do occur after IVF [124].

As can be seen in Table 3, all infertility factors in patients who are suffering from irritable bowel syndrome from our review are also linked to oxidative stress. Therefore, we decided to explore the available literature to analyze both oxidative stress-infertility and oxidative stress-irritable bowel syndrome relationships.

Table 3. Possible causes of infertility in IBS patients

Factors	**Studies**
Obesity	Roberts et al., [125], Ehrmann [126], Stamets et al., [127], Moran et al., [128]
IBS Medication	Sands et al., [114], Shin et al., [115]
Smoking	Feagins et al., [113]
Alcohol consumption	Feagins et al., [113]
Poor nutritional habits	El-Tawil [129]
Psychological factors	Heetun et al., [110], Tavernier et al., [111]

For example, in the context of neurodegenerative diseases, aside from motor dysfunctionalities, patients with Parkinson's disease (PD) also manifest metabolic disturbances with half of them suffering from constipation prior to the onset of other clinical features. This suggests a possible link between early gastrointestinal problems and Parkinson's disease later on [130]. Over the last half decade, a limited number of studies were conducted with the aim of exploring the impact of the gastrointestinal microbiota in the prodromal and early stages of Parkinson's disease [131,132]. Since gastrointestinal deficiencies like constipation significantly contribute toward the morbidity in Parkinson's disease, a recent clinical study identified that regular intakes of *Lactobacillus casei Shirota* could diminish such disturbances and bowel movement in Parkinson's disease [133]. Vitamin D3 prevented deterioration in the Hoehn and Yahr stage in Parkinson's disease patients, and vitamin D exerted beneficial activity both *in vivo* and *in vitro* against 6-hydroxydopamine (6-OHDA) [134,135]. Another study identified that following a twenty-four-week administration of riboflavin, there was a significant increase in the motor capacity in Parkinson's disease patients by normalising vitamin B6 status and after all red meat was eliminated. Symptomatology did not reappear even if the treatment was interrupted for several days; this suggests that low levels of vitamin B6 may promote motor impairment [136].

Heintz-Buschart et al., [137] propose that the gastrointestinal microbiota alteration most likely precedes the development of motor symptoms in Parkinson's disease. The genus *Ralstonia* was responsible for proinflammatory reactions in the mucosa compared to the controls [138]. In some cases, it was observed that there was an alteration of several metabolic pathways (lipopolysaccharide - LPS and ubiquinone and bacterial emission and xenobiotic metabolism or tryptophan) [138–140]. in addition, low levels of faecal short-chain fatty acids (SCFAS) were reported in parkinson's disease patients by a theoretically deteriorating enteric nervous system (ENS) [141].

Barichella et al., [142] evaluated atypical parkinsonism, more specifically, the composition of the gut in multiple system atrophy (MSA) and Steele-Richardson-Olszewski syndrome, in which some bacterial taxa have undergone changes similar to Parkinson's disease, while drug-naïve persons displayed low abundance of *Lachnospiraceae*, almost 43% reduction identified in contrast to *Bifidobacterium* [143].

The gram-negative *Prevotella* population was diminished to almost 78% compared to controls with 38.9% specificity in Parkinson's disease [144]. Dysbacteriosis that occurred in Chinese patients promoted features such as disease duration, levodopa equivalent doses (LED), and cognitive impairment, while in the German cohort, alpha and beta analysis highlighted a similar pattern, with the exception of the *Barnesiella* genus and *Enterococcaceae* family which were present in abundance [145,146]. Furthermore, cellulose-degrading bacteria (CDB) concentration lessened, whereas putative pathobionts dramatically increased [147].

A similar pattern was also found in human patients with cardiovascular or kidney disease. Measurements of plasma and serum biomarkers have indicated a fluctuation between strains, low

richness, and increased levels of oxidative stress, proinflammatory cascades, and endotoxemia [148,149].

On the other hand, silver nanoparticle (AgNP) usage as a potential treatment for colorectal cancer (CRC) negatively influenced the metabolism of *Enterococcus durans*. Even in the presence of low silver nanoparticle concentrations, increased intracellular hydroxyl radical and extracellular folic acid concentrations were observed [150]. Environmental arsenic trioxide (As_2O_3) exerts a similar effect upon gene(s) expression, modifying the overall microbial diversity and the pathways of synthesis involved in a variety of functions in mice [151].

Personal contribution - published papers:

Cojocariu, R.O.; Balmus, I.M.; Lefter, R.; Ababei, D.C.; Ciobica, A.; Hritcu, L.; Kamal, F.; **Doroftei, B**. Behavioral and Oxidative Stress Changes in Mice Subjected to Combinations of Multiple Stressors Relevant to Irritable Bowel Syndrome. *Brain Sci.* ***2020***, *10*, 865. **IF: 3.394**

Aim of the study

In the current study we aimed to investigate the effect of stress exposure on behavior, intestinal transit and oxidative status in mice by using combinations of previously validated irritable bowel syndrome stress-based paradigms. Our hypothesis was that the intensity of cumulative stress comprising of early and adult life stressors would alter intestinal motility, affective and cognitive states in mice more than either of the separate stressors. We also assumed that a disturbed antioxidative balance in brain and in colon as a result of psychological stress would accompany and correlate with behavioral changes, which might help to explain the biochemical mechanisms underlying irritable bowel syndrome.

Materials and methods

Animal housing and habituation

Male Swiss mice at an initial body mass of 30-40g were habituated in constant environmental conditions (20˚C, 55-60% humidity, natural light-dark cycle, and free access to water and food) in polyacrylic cages containing woodchip bedding (5 animals/cage). The Romanian and European laws regarding animal use in biomedical research were observed during animal care and experimental procedures. This study was approved by the local committee (no. USAMV Iasi 385/04.04.2019), and efforts were made to reduce the number of animals and their suffering.

Experimental design

Forty male mouse pups were selected and four groups were created for the experiment (n = 10). Three groups were subsequently exposed to different stress combinations as described below and established as irritable bowel syndrome animal models. The remaining group served as the control group and was subjected to identical environmental conditions in the absence of any studied stress factors.

Two of the three irritable bowel syndrome groups (n = 20), were subjected to neonatal maternal separation (MS) for 3h/day between postnatal days (PD) 1 and 14. The third irritable bowel syndrome group and the Control group were left unhandled. Beginning with postnatal day 90, the third irritable bowel syndrome group and one of the previously maternal separation groups were subjected to 7 days (postnatal days 90-96) of combined multifactorial stress-exposure consisting of (a) unpredictable mild stressors (UMS) and (b) a repetitive stress factor. During the 7 days of stress-exposure the (a)-type stressors were applied in the morning, with the exception of the food/water deprivation stressors that were administered continuously over a 24h period (Table 4). In the second part of the day, the mice were subjected for 1h/day to the (b) type stressor represented by water avoidance stress (WAS) paradigm. The sequence of unpredictable mild stressors included: (1) restraint stress [152], 30 min/day, (2) exposure to predator sounds (birds of prey cries lasting 10 min

at ambient level), (3) 24h water deprivation, (4) injection simulation, (5) tilt cages backwards at 45 degrees during 1 to 4h, (6) 1 min tail pinch at 1 cm from the end of the tail, (7) 24h food deprivation. The one-hour water avoidance stress procedure consisted in placing each mouse on a small platform (2.5 cm diameter) in the middle of a small plastic basin filled with warm water (22˚C) at the height level of the platform. Control group mice were placed on the same platform but in a waterless container for 1h.

Table 4. The types of stressors applied in each experimental group of mice

Group 1 (MS)	**Group 2 (MF)**		**Group 3 (MS+MF) maternal separation multifactorial stress**		**Group Control**
maternal separation					
	multifactorial stress				
	a. unpredictable	b. repetitive	a. unpredictable	b. repetitive	
	(1) restraint stress	daily water avoidance stress	(1) restraint stress	daily water avoidance stress	
	(2) predator sound		(2) predator sound		
	(3) water deprivation		(3) water deprivation		
	(4) injection stimulation		(4) injection stimulation		
	(5) tilt cage		(5) tilt cage		
	(6) tail pinch		(6) tail pinch		
	(7) food deprivation		(7) food deprivation		

Following stress exposure, all the animals were subjected to behavioral assessment during postnatal day 101 – postnatal day 109 in the following order: Y Maze Test in postnatal day 101, Elevated plus Maze in postnatal day 103 and forced swim test (FST) in postnatal day 106 – postnatal day 109. The biological samples were collected in postnatal day 111 (Figure 1). The woodchip bedding from the cages was changed periodically. After the last stress session all the fecal pellets were collected, counted, and evaluated in terms of consistency. The evaluation of fecal output was conducted for each cage of animals, not individually. Animals were divided into four groups depending on the type of stressor applied: (1) control, (2) neonatal maternal separation+multifactorial stress, (3) multifactorial stress exposed group, (4) maternal separation group. Early-age stress maternal separation reflecting a certain genetic vulnerability that would add to the burden of the later stressful events constituted one of the stressors (maternal separation), often cited as risk factor in [153]; multiple chronic stressors associated with restraint stress and water avoidance stress in adult stage made up the second combination suggestive for a highly stressful adult environment (multifactorial stress+ water avoidance stress); the third combination was the most complex by merging all the above stressors (maternal separation+multifactorial stress), in order to replicate a diathesis-stress model based on genetic predisposition and highly stressful events.

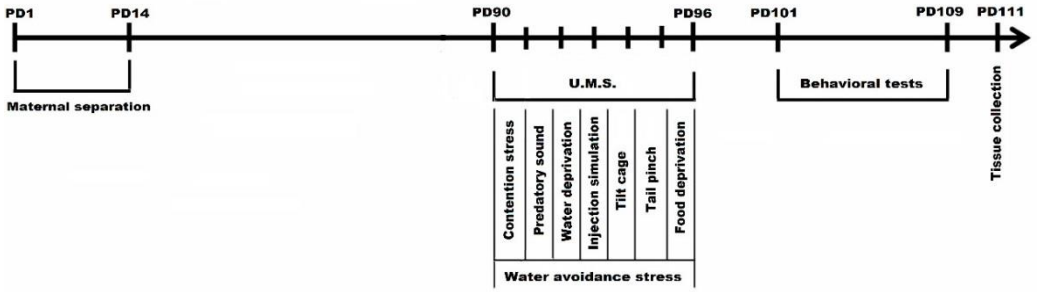

Figure 1. Experimental design of maternal separation and chronic UMS combination in a complex IBS mice model (PD1-PD111)

Behavioral testing

Following animal model development, the animals were subjected to behavioral tests in the following order: Y maze test, elevated-plus maze and forced swim test.

Y maze test

The Y maze test was used for short-term memory evaluation by assessing the exploratory behavior of the three arms of the Y-shaped apparatus, according to the protocol described by Kokkinidis group [154]. The maze consisted of three arms (40 cm length, 8 cm width, and 15 cm height, attached at 120 degrees angles) and an equilateral triangular central area. Each mouse was placed at the end of one arm and allowed to freely explore the maze for 8 min. For evaluating short-term memory we assessed the spontaneous alternation indicator, defined by the entries into all three arms on consecutive choices. For further statistical analyses the spontaneous alternation percentage (%) was calculated as the ratio of spontaneous alternation entries per total entries.

Elevated plus maze

Elevated plus maze, a cross-like four-arm apparatus elevated 50 cm off the ground, with two arms enclosed by walls 30 cm high and the other two exposed, was used to assess anxious behaviors. Each animal was placed at the juncture of the open and closed arms and was let to freely explore the maze for 5 min. During this period the entries and time spent in each arm and grooming bouts were recorded as indicators for anxiety recorded during a 5-min test according to the protocol described by Pellow group [155].

Forced swim test

Behavioral despair was assessed using an adapted variant of Porsolt's forced swim test [156] for mice. The protocol consists of maintaining the individuals in a transparent glass cylinder (30 cm in diameter, 59 cm high) filled with water (15 cm, 26°C) while the swimming patterns of the escape behavior are assessed. The animals were exposed to the experimental conditions for 6 min – the first two minutes for acclimatization and the last 4 min for measuring a series of behavioral parameters that serve as indicators of depressive state: swimming, immobility (floating), and struggling behavior.

Tissue Collection and Preparation

Biological samples were obtained in day after behavioral evaluation in total anaesthesia conditions (ketamine 100 mg/kg, xylazine 10 mg/kg). The brains and colons were collected from the animals and the colons were emptied of all contents and washed twice with physiological saline. Following this, 0.2g of tissues were used for sampling using tissue extraction buffer (0.328 g TRIS, 1.304g KCl_2 and distilled water to 200 mL volume, pH = 7.4) and then subjected to biochemical assessment.

Biochemical determinations

Superoxide dismutase enzymatic activity was determined using a spectrophotometric SOD Assay Kit (Sigma, Darmstad, Germany) according to the manufacturer's instructions. The indirect measurement of superoxide dismutase activity was obtained based on the water soluble tetrazolium (WST) salt reaction with superoxide anion producing a water-soluble formazan dye.

Gluthatione peroxidase enzyme activity was assessed using the GPx Cellular Activity Assay Kit CGP-1 (Sigma). The indirect determination method of the gluthatione peroxidase activity is based on the NAPDH concentration decrease in the reaction media during which nicotinamide adenine dinucleotide phosphate (NADPH) is oxidized to $NADP^+$.

Lipid peroxidation as reflected by malondialdehyde levels was assessed using thiobarbituric-

acid-reactive substances determination method [157]. Trichloroacetic acid (TCA) (50%, 0.25 mL), Thiobarbituric acid (TBA) (0.73%, 0.255 mL) and tissue extracts (0.05 mL) were mixed and vortexed. Afterwards, a 20 min incubation at 100°C (boiling water bath), and a 10 min centrifugation (3000 rpm) were performed. The supernatants were exposed to a 532 nm spectrometry system and the absorbance was read against malondialdehyde standard curve (the results were expressed as mmol MDA/mL tissue extract).

Statistical analysis

The numerical data obtained by behavioral and biochemical evaluation was statistically analyzed using ANOVA tests and the software Minitab 17 (Pennsylvania University, US, 2017). The results below were expressed as means ± SEM and were considered statistically significant at $p < 0.05$. Statistical correlations were expressed as Pearson's linearity coefficient while $p < 0.05$ Post-hoc analysis included Bonferroni corrected student *t*-test.

Results

Behavioral parameters evaluation

The Effect of Various Combinations of Stress Factors on Gastrointestinal Tract Habits

Regarding the animals' bowel habit changes we observed that the exposure to different stress factors combinations can induce significant increases in bowel transit time. Thus, slowed defecation observed by fecal pellet count/24 h after stress exposure appeared in all three cases of stressor combinations compared to the control group (Figure 2). However, the differences were clearer for the combination of early-life maternal separation stress and adult-life multifactorial stress for maternal separation+multifactorial stress vs. control (F (1, 18) = 24.13, $p = 0.001$).

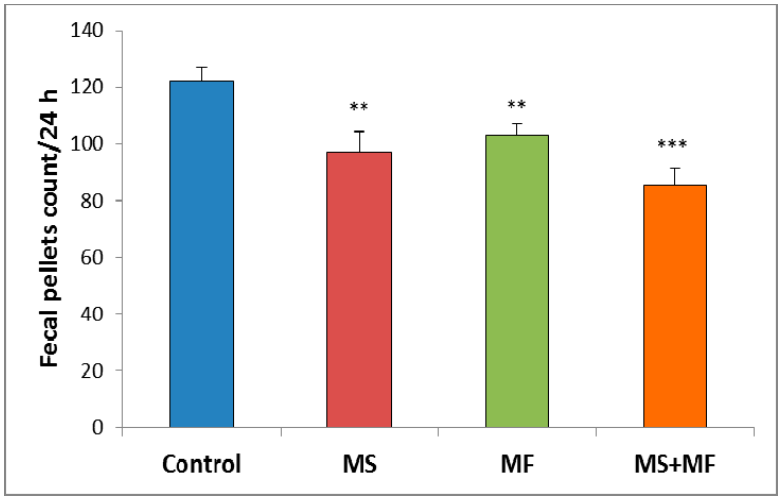

Figure 2. The effect of various combinations of stress factors on gastrointestinal tract habits, as given by fecal pellets count per 24h. The values are mean ± S.E.M ($n = 10$ per group, ** $p < 0.01$, *** $p < 0.001$)

The effects of various combinations of stress factors in the y-maze test

The behavioral analysis of the short-term memory performance showed no significant overall differences between the experimental groups (F (3, 36) = 2.28, $p = 0.09$) in terms of spontaneous alternation (%). However, post-hoc analysis showed significant decreases of spontaneous alternation in the multifactorial stress group (F (1, 18) = 4.42, $p = 0.04$; t(18) = 2.11, $p = 0.02$) and maternal separation+multifactorial stress group (F (1, 18) = 5.65, $p = 0.02$; t(18) = 2.03, $p = 0.03$), as compared to the control group (Figure 3).

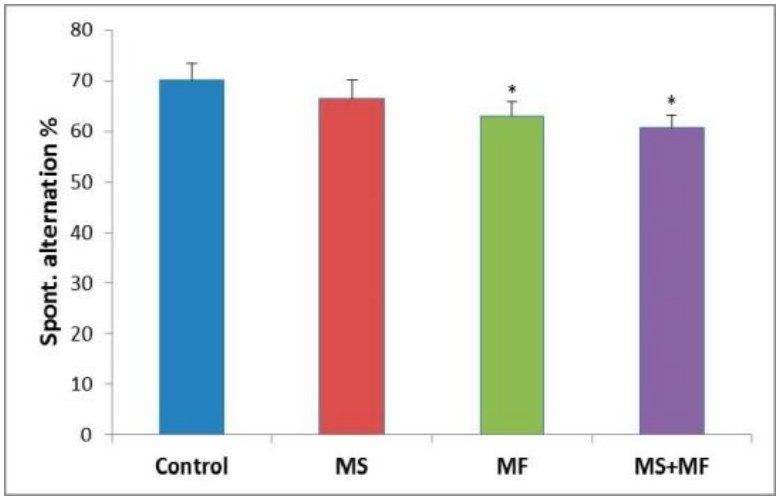

Figure 3. The effects of various combinations of stress factors in the Y-maze test, as showed by the spontaneous alternation parameter. The values are mean ± S.E.M (n = 10 per group, * $p < 0.05$ vs. control)

The effects of various combinations of stress factors on the parameters evaluated in elevated plus maze

Regarding the number of open arms entries (OEA), a parameter for which lower values are consistent with anxiogenic-like behavior since it is based on the rodents' natural aversion for open spaces, noticeable decreases were observed for all stress-exposed groups compared to the control group. These were statistically significant in the maternal separation+multifactorial stress group ($F(1, 18) = 6.18$, $p = 0.023$; $t(9) = 2.75$, $p = 0.01$) and almost significant in the maternal separation group ($F(1, 18) = 3.92$, $p = 0.063$; $t(16) = 1.97$, $p = 0.03$) (Figure 4a). The time spent in the open arms (Figure 4b), one of the most suggestive indicators for anxiolytic effects, decreased for all stress-exposed groups compared to the control group, but to a significant degree only for multifactorial stress ($F(1, 18) = 4.52$, $p = 0.047$; $t(10) = 2.12$, $p = 0.02$) and maternal separation+multifactorial stress groups ($F(1, 18) = 4.42$, $p = 0.049$; $t(18) = 2.10$, $p = 0.03$) vs. control. Interestingly, when we analyzed the number of entries in the closed arms (Figure 4c), a locomotor oriented parameter, we found a significant decrease in the exploration of the maze's closed arms in the maternal separation group ($F(1, 18) = 5.44$, $p = 0.037$; $t(16) = 2.33$, $p = 0.01$) vs. control, whereas the other two stress-exposed groups showed less significant decreases. Moreover, the grooming bouts (Figure 4d), another anxiety indicator, showed no significant variations between groups, except for a moderate increase in the same maternal separation group ($F(1, 18) = 4.64$, $p = 0.044$; $t(12) = -2.15$, $p = 0.01$) vs. control.

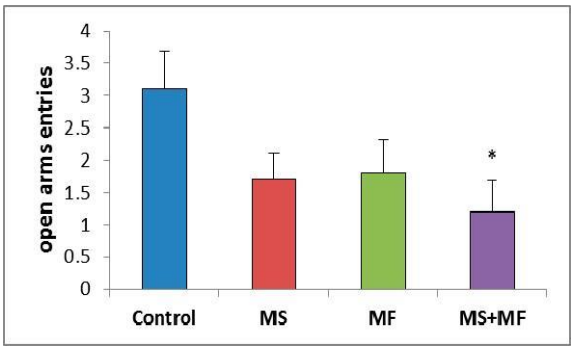

(a)

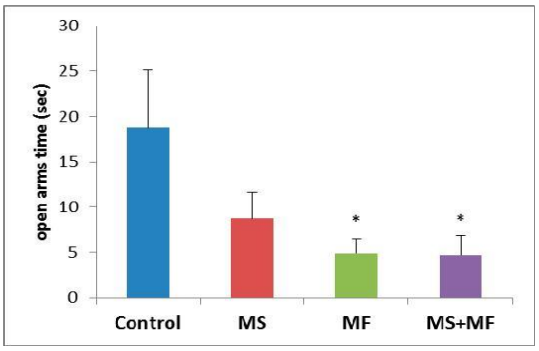

(b)

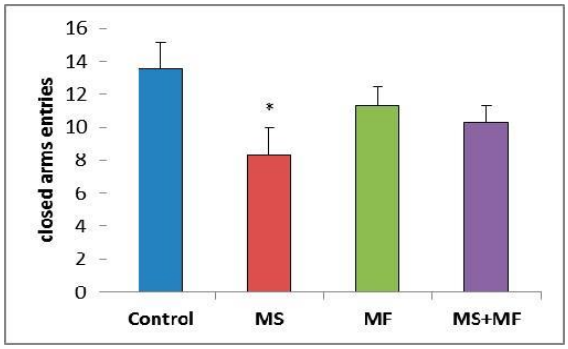

(c)

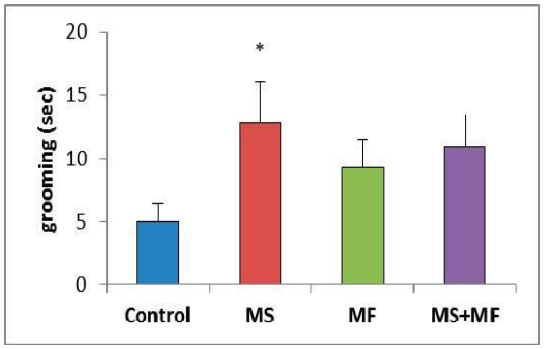

(d)

Figure 4. The effects of various combinations of stress factors on the parameters evaluated in elevated plus maze: (a) open arms entries, (b) open arms time - OAT, (c) closed arms entries and (d) grooming time. The values are mean ± S.E.M (n = 10 per group, * $p < 0.05$ vs. control)

Effects of various combinations of stress factors on the parameters evaluated in forced swim test

In the forced swim test, statistical analysis of the swimming time showed significantly low mobility for the maternal separation group ($F(1,18) = 6{,}69$, $p = 0.018$; $t(17) = 2.58$, $p = 0.009$) and close to significant low mobility for the other two stressed groups (Figure 5a). Post-hoc analysis showed significant overall differences between groups for the floating time ($F(3, 36) = 2.874$, $p = 0.04$) and, reversely, increased floating time in all three stress-exposed groups, significant in the multifactorial stress group ($F(1, 18) = 3.64$, $p = 0.048$; $t(18) = -2.10$, $p = 0.02$) and the maternal separation+multifactorial stress groups ($F(1, 18) = 6.614$, $p = 0.019$; $t(14) = -2.57$, $p = 0.01$) vs. control (Figure 5b). Moreover, we observed a significant group difference in terms of struggling duration ($F(3, 36) = 5.433$, $p = 0.03$), and a significant decrease in maternal separation+multifactorial vs. control group ($F(1, 18) = 7.154$, $p = 0.015$; $t(13) = 2.67$, $p = 0.009$) and also vs. maternal separation group ($F(1, 18) = 4.21$, $p = 0.05$; $t(10) = 3.62$, $p = 0.02$) (Figure 5c). Interestingly, we observed an almost significant increase in struggling in the maternal separation group vs. control, which may be suggestive of anxious behavior ($F(1,18) = 3.928$, $p = 0.06$; $t(13) = -1.98$, $p = 0.03$).

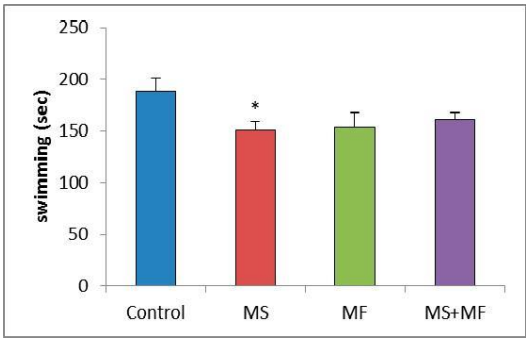

(a)

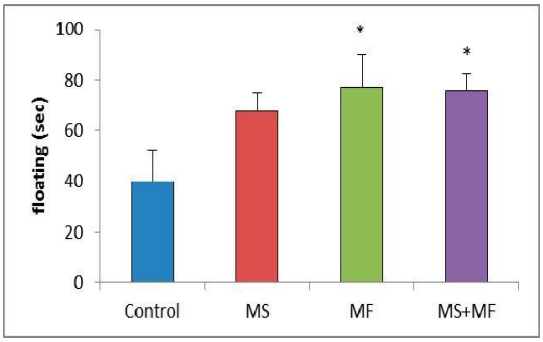

(b)

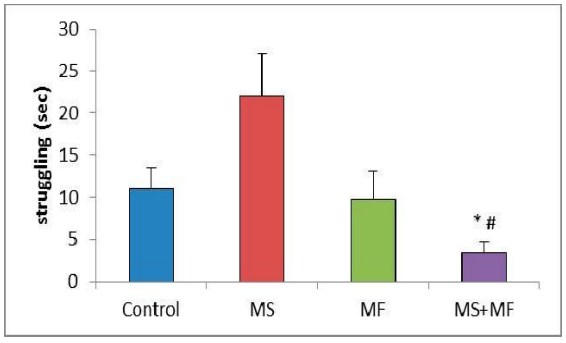

(c)

Figure 5. Effect of various combinations of stress factors on the parameters evaluated in the forced swim test: (a) swimming, (b) floating and (c) struggling time (seconds). The values are mean ± S.E.M ($n = 10$ per group, * $p < 0.05$ vs. control and # $p < 0.05$ vs. MS group

Biochemical evaluation of brain tissue

Regarding the brains' oxidative stress status, post-hoc analysis showed no significant variations between groups in the antioxidant activity of superoxide dismutase (Figure 6a), although visually slightly lower superoxide dismutase values were obtained in the maternal separation+multifactorial stress group ($F(1, 18) = 4.27$, $p = 0.53$; $t(18) = 2.06$, $p = 0.02$) vs. control and slightly higher in the multifactorial stress group. However, the glutathione peroxidase levels were generally decreased in the stress-exposed groups, and significant decreases were detected in the multifactorial stress and maternal separation+multifactorial stress groups compared to the control group ($F(1, 18) = 15.33$, $p = 0.002$; $t(12) = 3.916194657$, $p = 0.002$) and ($F(1, 18) = 8.44$, $p = 0.009$; $t(17) = 2.90$, $p = 0.04$), respectively (Figure 6b). In what concerns brain malondialdehyde levels, significant overall differences were observed ($F(3, 36) = 3.21$, $p = 0.03$) suggesting the effect of stress exposure on this oxidative stress parameter. We found significantly increased malondialdehyde levels in the multifactorial stress group ($F(1, 18) = 8.604$, $p = 0.008$; $t(15) = -2.93$, $p = 0.005$) vs. control and maternal separation+multifactorial stress ($F(1, 18) = 7.516$, $p = 0.013$; $t(14) = -2.74$, $p = 0.007$) vs. control, but not in the maternal separation group (Figure 6c).

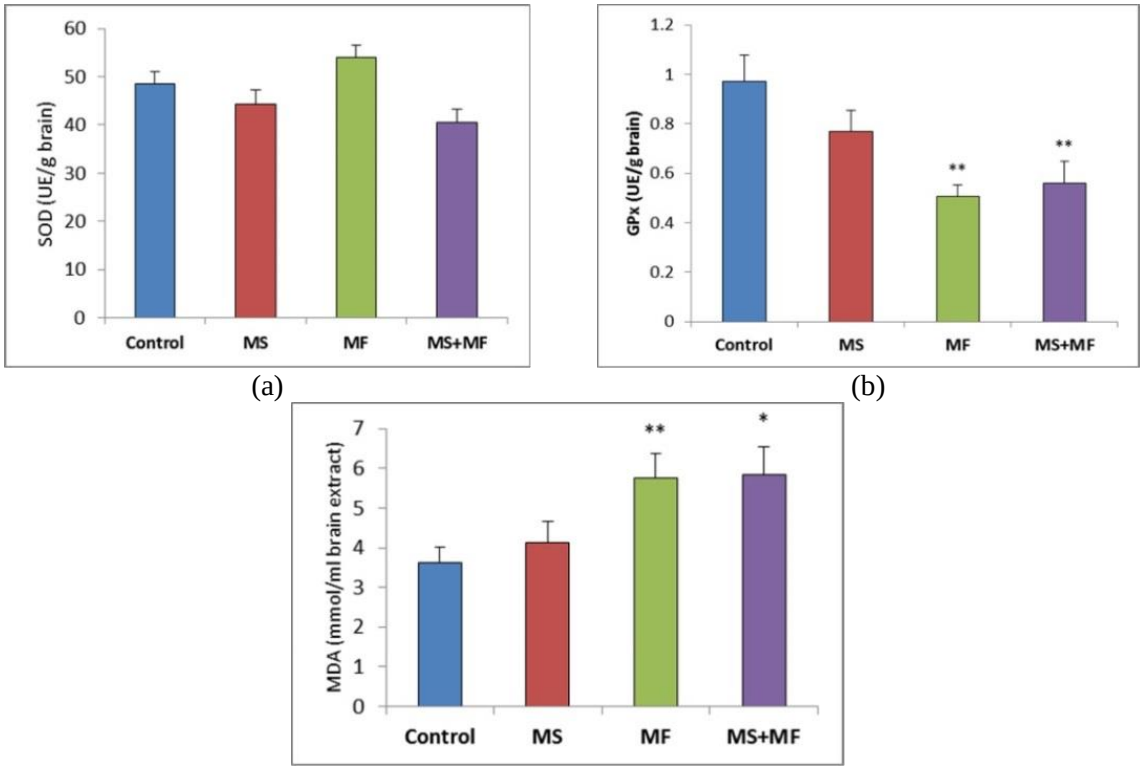

Figure 6. The effect of various combinations of stress factors on oxidative stress markers in the mice brain: (a) superoxide dismutase activity, (b) gluthatione peroxidase activity and (c) malondialdehyde levels. The values are mean ± S.E.M. ($n = 10$ per group, * $p < 0.05$, and ** $p < 0.01$)

Biochemical evaluation of bowel tissue

When evaluating the oxidative stress markers in bowel tissues, no significant differences in superoxide dismutase specific activity were detected between groups (Figure 7a). Similarly, glutathione peroxidase enzymatic activity in the stressed groups did not vary significantly relative to the control mice, except for a significant decrease in the maternal separation group ($F(1, 18) = 7.77$, $p = 0.012$; $t(18) = 2.788445607$, $p = 0.006$) (Figure 7b). Regarding the colon malondialdehyde levels, a significant elevation was observed in the maternal separation+multifactorial stress group ($F(1, 18) = 7.241$, $p = 0.0149$; $t(15) = -2.69104995$, $p = 0.008$), whereas the other two stress-exposed groups had no significant increases compared to the controls (Figure 7c).

Correlations between behavioral and biochemical parameters

Analysis of Pearson's linearity coefficient revealed several significant correlations between behavioral and biochemical parameters. We found moderate negative and positive correlations between depression and anxiety indicators, such as floating duration in forced swim test versus frequency of open arms entries in elevated maze test (r = −0.705, while $p < 0.0001$) (Figure 8b), mobility duration in forced swim test and frequency of open arms entries (r = 0.649, $p < 0.0001$) (Figure 8a), mobility duration and open arms time (r = 0.602, $p < 0.0001$) (Figure 8c). Correlations between the spontaneous alternation memory indicator and other indicators were also moderate (r = −0. 437 vs. open arms entries; r = 0.454 vs. swimming duration) or weak.

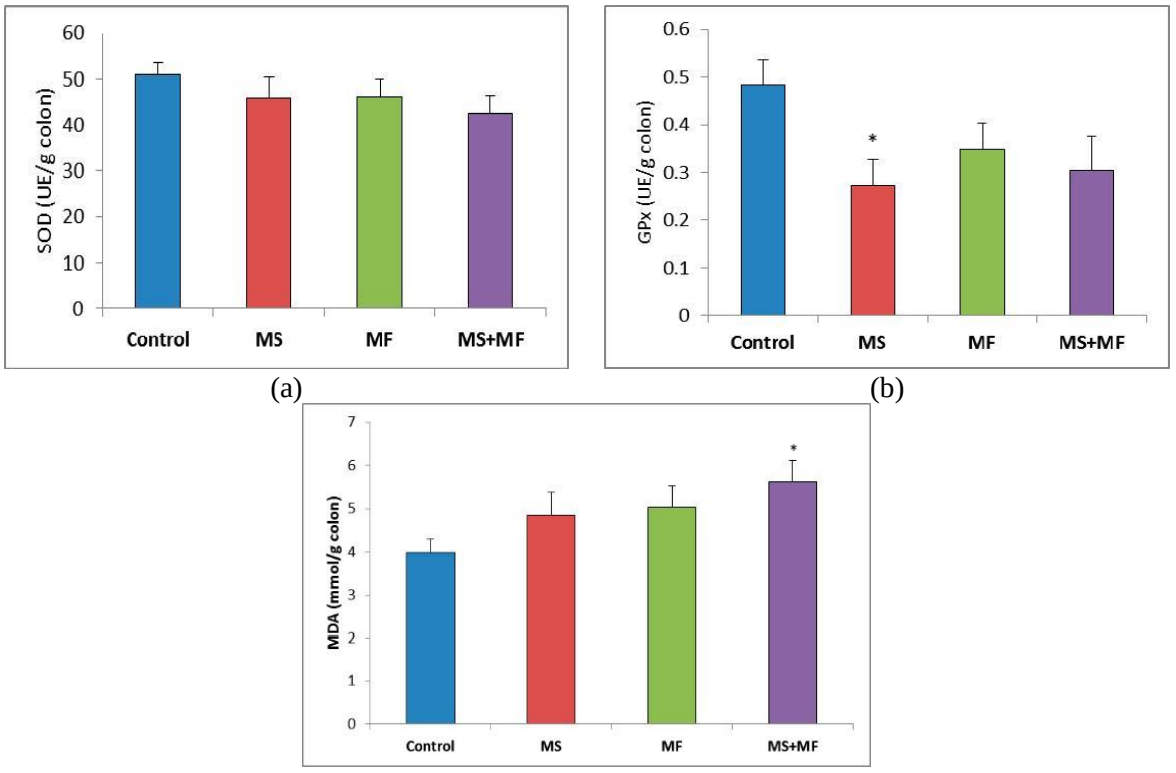

Figure 7. The effect of various combinations of stress factors on oxidative stress markers in the mice bowel tissue: (a) superoxide dismutase activity, (b) glutathione peroxidase activity and (c) malondialdehyde levels. The values are mean ± S.E.M. ($n = 3$ per group), * $p < 0.05$ vs. control

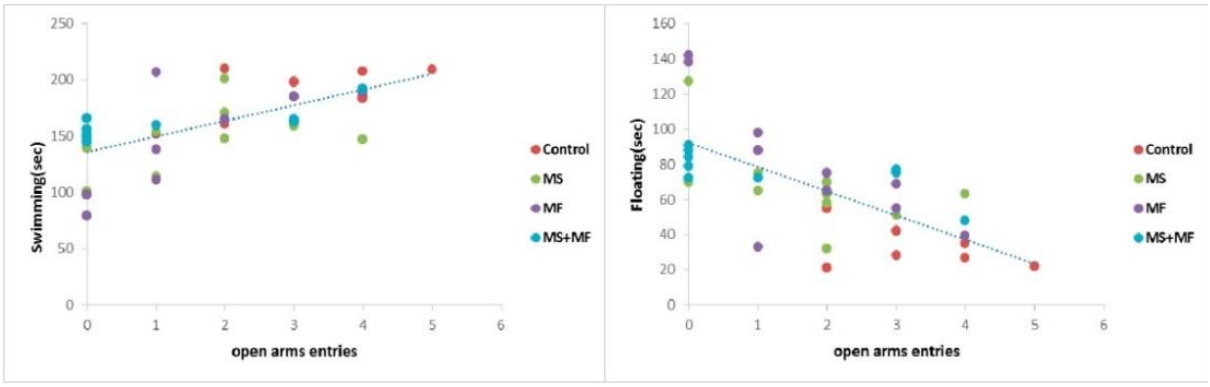

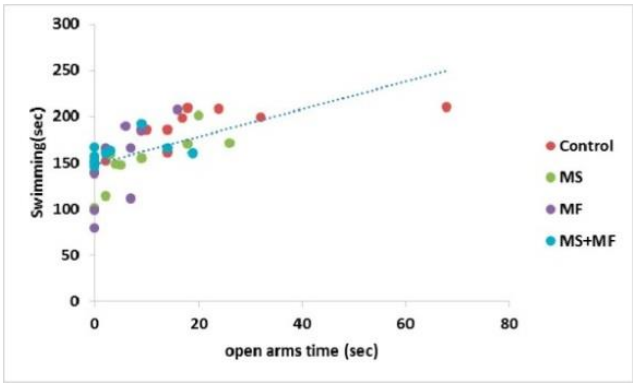

(c)

Figure 8. Statistical correlations between behavioral parameters: (a) swimming vs. frequency of open arms entries, (b) floating duration vs. frequency of open arms entries, (c) swimming vs. open arms time (n = 40)

Regarding behavioral and oxidative stress parameters (Figure 9), Pearson's coefficients presented a series of moderate correlations for anxiety and depression indicators vs. brain tissue oxidative biomarkers, such as: moderate positive correlation between floating duration and malondialdehyde brain levels (r = 0.731, p < 0.001) (Figure 9a), moderate negative correlation between swimming and malondialdehyde brain levels (r = −0.653, p < 0.001), moderate negative correlation between floating and glutathione peroxidase activity (r = −0.694, p < 0.001) (Figure 9c), moderate negative correlation between open arms time and malondialdehyde brain levels (r = −0.615, p < 0.0001) (Figure 9b), moderate positive correlation between open arms entries and glutathione peroxidase activity (r = −0.582, p < 0.001) (Figure 9e), moderate positive correlation between the spontaneous alternation and brain superoxide dismutase activity (r = 0.685, p < 0.01) (Figure 9d). For behavioral and oxidative stress parameters evaluated from the colon, we found a moderate positive correlation between floating duration and bowel malondialdehyde levels (r = 0.558, p < 0.001) (Figure 9f).

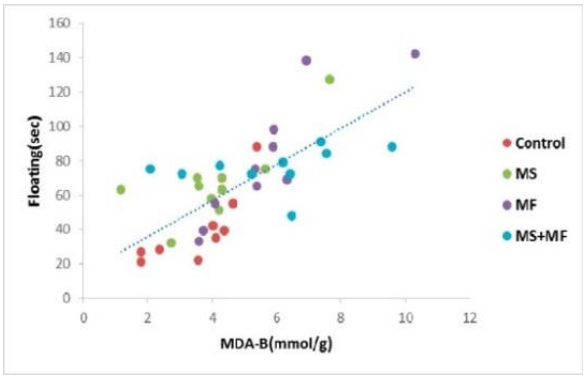

(a)

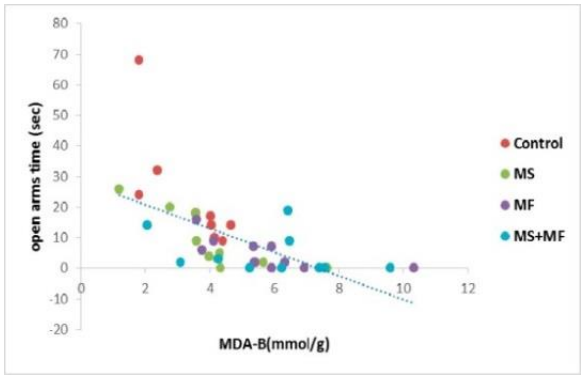

(b)

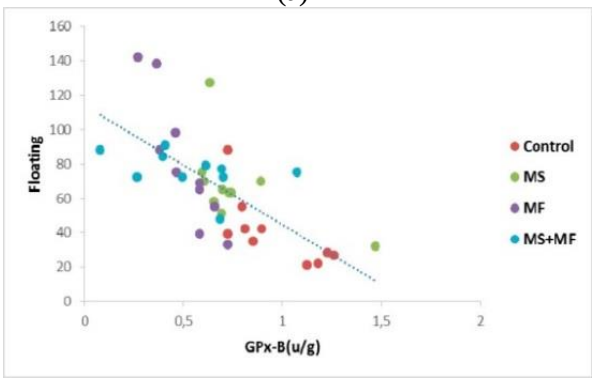

(c)

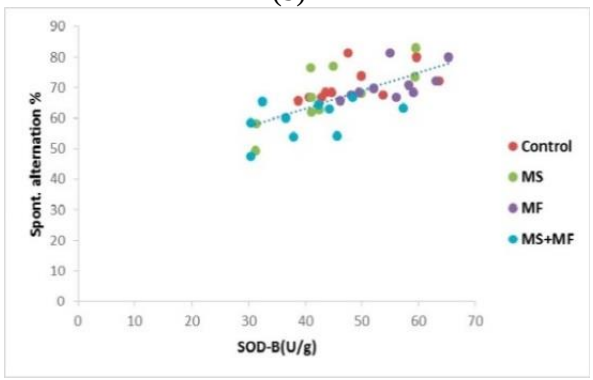

(d)

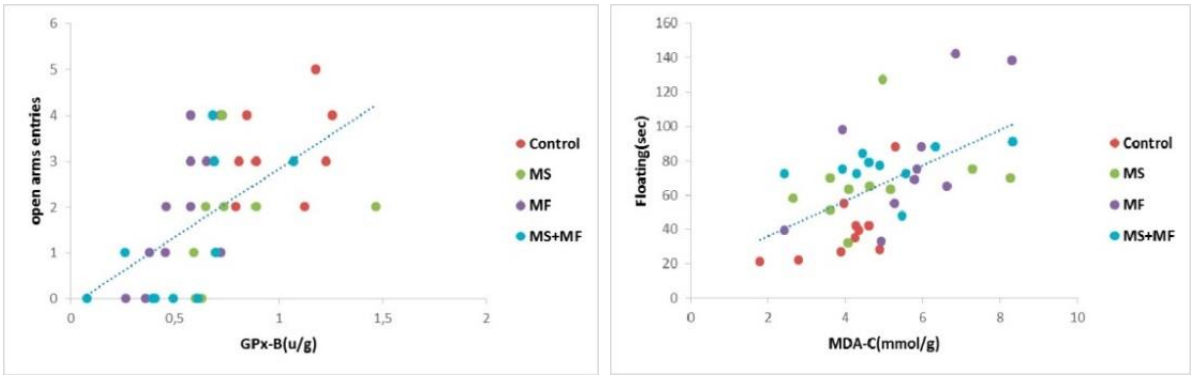

(e) (f)

Figure 9. Statistical correlations between behavioral parameters: (a) floating duration vs. malondialdehyde brain levels, (b) open arms time vs. malondialdehyde brain levels, (c) floating vs. brain glutathione peroxidase activity, (d) spontaneous alternation vs. brain superoxide dismutase activity, (e) open arms entries vs. brain glutathione peroxidase activity, (f) floating and bowel malondialdehyde levels (n = 40)

Furthermore, we analyzed Pearson's correlational significance between oxidative stress parameters evaluated from brain and bowel tissues. Thus, we found a moderate negative correlation between glutathione peroxidase activity in brain and malondialdehyde levels in brain (r = −0.725, while p = 0.001) (Figure 10a), and similarly, a mild negative correlation between glutathione peroxidase activity in bowel and malondialdehyde levels in bowel tissue (r = −0.505, p = 0.001) (Figure 10b). Also, we found moderate negative correlations between brain glutathione peroxidase activity versus malondialdehyde levels in bowel (r = −0.524, while p = 0.001) (Figure 10c), weak positive correlations between brain glutathione peroxidase and bowel glutathione peroxidase activity (r = −0.458, while p = 0.002) (Figure 10d) and weak positive correlations between brain malondialdehyde and bowel malondialdehyde levels (r = −0.479, while p = 0.001) (Figure 10e).

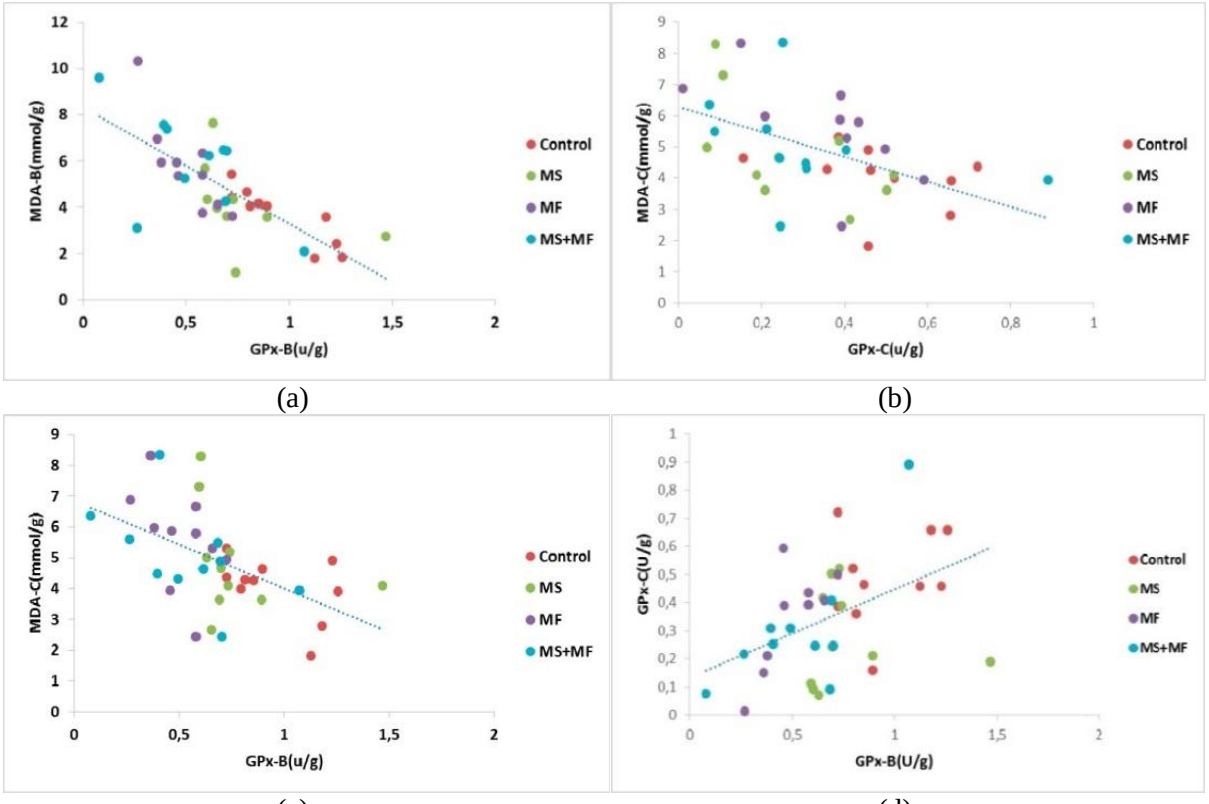

(a) (b)

(c) (d)

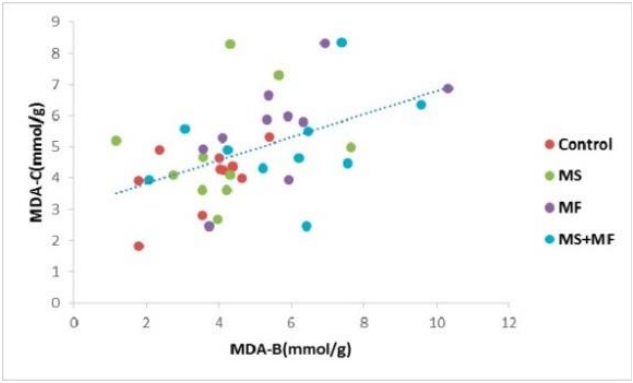

(e)

Figure 10. Statistical correlations between oxidative stress parameters in brain and colon: (a) brain GPx activity vs. brain malondialdehyde levels, (b) bowel glutathione peroxidase activity vs. bowel malondialdehyde levels, (c) brain glutathione peroxidase activity vs. bowel malondialdehyde levels, (d) brain glutathione peroxidase and bowel glutathione peroxidase activity, (e) brain malondialdehyde and bowel malondialdehyde levels (n = 40)

Discussion

This study was designed to evaluate the effectiveness of three different combinations of stress factors relevant for mimicking irritable bowel syndrome typical manifestations in rodents. Our results showed that all stress combinations chronically slowed intestinal transit and led to depressive and anxiety-like behaviors mimicking the irritable bowel syndrome comorbidities [158]. On the whole, a cumulative stress generated by early and later life stressors was the more effective in modulating gastroenterological features accompanied by depressive and anxious-like behavioral changes; however, the multifactorial stress exposure was seemingly a more influential factor in modulating behavioral symptoms and oxidative stress, as the supplementary stress load in the maternal separation+multifactorial stress combination rarely differed significantly in symptoms exhibition. Lipid peroxidation increases were observed in brain and bowel tissues, suggesting that mild oxidative stress occur in intestinal cells as a result to stress exposure, but to a greater extent in brain tissue. Furthermore, these biochemical changes, in particular at brain level, can be correlated to a certain degree with behavioral symptoms.

With regard to the gastrointestinal symptoms occurrence, our initial assumption was confirmed, namely that the higher the intensity of the stress factors combination, the more efficient its effect on gastrointestinal habits. A combination between restraint stress and maternal separation could lead to significantly slowed intestinal transit, as demonstrated by our data and comparative analysis regarding the fecal pellets count per 24h. The gastrointestinal transit modifications seen in mice following chronic stress exposure are suggestive of slow-transit constipation, but, interestingly, during and shortly after the restraint stress routine, mice presented acute diarrhea that did not persist for more than 30 min. Others reported similar results of watery diarrhea in rats after restraint stress [159]. A large body of literature showed that, in rodents, stress provokes the stimulation of large intestinal activity and increased fecal excretion [160–162]. However, exactly how different forms and combinations of stress modulate colonic motility in animals remains to be established. German et al., demonstrated the tendency towards diarrhea and constipation in shelters containing cats and suggested stress due to relocation into the shelter as a possible cause of fecal retention [163]. Also, initially accelerated colonic transit caused by restraint stress in rats is slowed down gradually under chronic exposure due to adaptation [164]. Several other studies in mice report similarly decreased fecal pellet output following early-life maternal separation stress [165] or chronic psychosocial stress [166,167] and suggest the timepoint as an important factor to be considered when measuring colonic motor function, due to fast adaptations in the colon in response to chronic stress [167].

The presented data also point to the deleterious effects of stress exposure on affective states, which correspond to the abnormalities observed in gastrointestinal functioning. Zhang group [168] recently reported the correlation between slowed intestinal transit (constipation) and depressive behaviors in a chronic stress-induced depression rat model. The idea of a correlation between the affective status and gastrointestinal response has been highlighted since 1968 when Lieblich and

Guttman showed that defecation intensity is strongly associated to specific emotional context response [169]. In our study, all three stress factors-exposed groups were significantly vulnerable to depressive-like states, as suggested by the decreased swimming in the maternal separation group and increased floating durations in the multifactorial stress and maternal separation+multifactorial stress groups. The non-uniformity exhibited by the stressed groups when considering struggling is more difficult to interpret, given also the ambiguous significance of this parameter. In the literature, swimming is considered sensitive to serotonergic compounds like selective serotonine reuptake inhibitors and serotonine receptor antagonists, while struggling is sensitive to tricyclic antidepressants and drugs with effects on catecholaminergic transmission [170,171]. If we regard struggling as an escape-directed behavior driven by anxiety state [172], we could presume that the maternal separation stress factor nature could predispose to anxious behavior, whereas an increased stressful load, as in the case of the maternal separation+multifactorial stress group, would overcome anxiety threshold and shift it to depressive behavior, when struggling significantly decreases and becomes relevant for installation of a depressive state in which individuals no longer try to escape.

Regarding the assessment of anxiety in the elevated plus maze, we observed some significant changes in the exhibition of anxiogenic behaviors. Based on the significantly lessened tendency of entering/staying in the open arms of the maze, anxiety-like responses were more intense in the multifactorial stress and maternal separation+multifactorial stress group than in the maternal separation group. This role of chronic multifactorial stress and restraint stress in producing anxiety-like behavior, has been reported previously in rodents following restraint stress [173] or chronic stress exposure [174]. On another note, maternal separation group exhibited a significant decrease in the closed arm entries during the elevated maze test task. While closed arm entries may serve as a measure of spontaneous motor activity [175], in this case they may actually be relevant for the installation of anxiety-states, if we consider the increased grooming frequency measured for this group. According to a study of Yoon et al., [176] on chronic non-social stress exposure in mice, the depression and anxiety-related circuits modified by stress can be dissociated in the mouse brain and different stress types address different brain circuits, according to their social/non-social profile. In this light, we may suggest that the stress combinations in our study modulated affective states with largely similar outcome, but, due to being based on stressors with distinct social relevance (the social maternal separation stressor vs. the non-social multifactorial stress stressors), they activated preferentially different brain circuits, hence the variation of phenotypic manifestations.

Regarding the short-term memory, our results indicated that stress exposure generally exerts an altering effect on cognitive process; however, the most significant effects were observed in the case of multifactorial stress and multifactorial stress combined with maternal separation. Short-term memory impairment was previously obtained by applying restraint stress [177] and by multifactorial unpredictable stress [178,179] in animal models, and may be the consequence of elevated activity of hypothalamic-pituitary-adrenal axis and increase in stress hormones levels [180]. We have found less significant deficits in short-term memory during the Y maze task in the case of maternal separation exposure. The disruption of the mother-infant relationship exhibits life-long influence on the behavioral and endocrine responses to stress [181], however, the effect of maternal separation on short-term memory performance is controversial, and decreased cortisol levels were reported in maternal separation juvenile squirrel monkeys [182].

Mild inflammatory response and low intensity oxidative stress were described in irritable bowel syndrome pathology, as reflected by increased colon mast cell density [183], low activity of plasma antioxidant enzymes and significantly higher malondialdehyde and nitric oxide concentrations [184,185]. We hypothesized that the psychological stressors we used would produce alterations in the brain and colon oxidative stress that would be also reflected by behavioral modifications. In the literature, the association between oxidative stress and systemic inflammation and chronic unpredictable mild stress or chronic restraint stress exposure was previously documented in rodents [186–188]. We have found significantly increased lipid peroxidation processes in the brain in the multifactorial stress and maternal separation+ multifactorial stress groups, and less accentuated lipid peroxidation in the bowel tissues, with significant increase only in the maternal separation+ multifactorial stress group. The antioxidant enzymes superoxide dismutase did not register significant variations for these groups, but glutathione peroxidase activity at the brain level was significantly decreased in both groups and also statistically correlated with the increased malondialdehyde levels.

Brain susceptibility to oxidative injury due to its structural particularities and increased oxygen consumption, previously documented [186], may explain the association between chronic stress exposure and oxidative stress more tangible in the brain. No significant variations in oxidative stress markers were observed in the maternal separation group with the sparse exception of a significant decrease of bowel glutathione peroxidase activity when compared to control group. These results should not, however, overrule the occurrence of oxidative stress in the maternal separation group; instead they may indicate a different oxidative stress mechanism. The reactive oxygen species target not only lipids but also cause protein oxidation and nitration and DNA damage [189], and in this line, recent reports on the effects of maternal separation stress in rats highlight an abnormal elevated nitrosylation profile in the hypothalamus [190], or, in accordance with our results, no differences in antioxidant enzymes activities (superoxide dismutase, glutathione peroxidase and catalase), but an increased index of DNA breaks in hippocampus [191].

The significant correlations between the behavioral indicators and oxidative stress markers, identified predominantly at the brain level, but also a number of weak to moderate correlations between brain and bowel oxidative markers may arguably offer a perspective on the oxidative stress effects: centrally more acute, where it appears directly correlated to neuropsychiatric affective and cognitive symptoms, as in prior published work by our group [192,193], and less pronounced peripherally, in gastrointestinal tissues, possibly occurring alongside a low-grade inflammatory response, as reported by other studies [194]. Thus, our results suggest that gastrointestinal tissue oxidative damage follows central nervous system damage, with a similar pattern for oxidant/antioxidant markers, and further demonstrate the connection between brain and gut, described in the literature [195].

In summary, the present data show that exposure to combined early and adult life stress including an original sequence of predictable and unpredictable stressors results in significant altered intestinal transit, anxiety and depression-like behaviors and decreased short term cognitive capacity. Its more significant effect compared to either of single stressors was accompanied by increased oxidative stress in colon and predominantly in brain, which suggests the involvement of a neurologic component in the pathogenesis of irritable bowel syndrome. Out of the two separate stressors, maternal separation and multifactorial stress, we found only for the latter a similar pattern with the combined stress group in terms of oxidative stress markers dynamics, suggesting that what is driving the effect is mostly the multifactorial stress exposure. This would not rule out the impact of the maternal separation factor on the antioxidant balance, as some oxidative aggravations were observed in its case as well, but may point to different oxidative pathways or even to some degree of inconsistency in the maternal separation protocol as some studies suggested previously [196]. Heterotypical stress exposure could arguably determine a more immediate central response than early-life stress, but, overall, the combination of the two types of stressors reflected more accurately irritable bowel syndrome visceral and affective specific symptoms, advocating for a more precise irritable bowel syndrome model in mice.

This study provides additional evidence on the effect of stress exposure on the gastrointestinal and neurological status, in a multifactorial animal model of irritable bowel syndrome. The combination of early-life and chronic unpredictable adult-life stress can lead to important depressive and anxiety-like behaviors accompanying alterations of intestinal transit. Oxidative stress may play an important role in irritable bowel syndrome development, acting on central and peripheral levels.

I.3 Bacteria - from eubiosis to homeostasis and development

I.3.1 Mechanistic aspects

It has been well established that all microorganisms populating our body are grouped into four major ecosystems. The greatest number of associations is at the level of the digestive tract, with a density of 10^{14}. This is approximately ten times more entities than the total number of cells involved in the structure of an individual. The human microbiome possesses over one hundred and fifty times more bacterial genes and a biomass production weighing equivalent to that of the human brain. The average total number of microbes populating a reference male with a normal constitution is close to forty trillion. Increased numbers of pluricellular organisms could be viewed as ideal amphitrions,

alongside our tenants (large collections of archaea, bacteria, fungi, and viruses), ensuring an invisible endo- and exoskeleton thanks to this symbiotic bond [197–200].

From what it is known, key roles fulfilled by the enteric microflora include the following: (I) antimicrobial compound synthesis in order to block pathogen overgrowth, (II) secretion of immunoglobulin A (IgA) for the fortification of the intestinal epithelium, (III) nutrient absorption, and, finally, (IV) maturation of the immune system [201].

The intestinal lumen-blood barrier is the main guardian that ensures symbiosis, and alongside commensal microorganisms, it prevents the adherence of pathogens to the intestinal wall by protecting intestinal epithelial cells (IECs) [202], while Paneth cells may allow possible disruption of intestinal epithelium [203]. Intestinal epithelial cells are protected on the plasma surface by a series of glycoproteins, enterocytes, and gut-associated lymphoid tissue (GALT) which perform similar functions [204].

The goblet cells (GCs) of the small intestine secrete mucin and mucin 2 (MUC2) [205,206], alongside antimicrobial peptides (AMPs), which strengthen the barrier against any pathogenic entity [207]. Some goblet-derived products such as trefoil factor 3 (TFF3) and resistin-like molecule-β (RELMβ) form a physical barrier in response to inflammatory reactions, and resistin-like molecule-β assists mucin 2 in the regulation of adaptive lymphocytes and macrophages [208].

As mentioned above, there are enterocytes that are directly involved in host-defense that possess some pattern-recognition receptors (PRRs) for the detection of harmful species. These sensors contain toll-like receptors (TLRs) and nucleotide oligomerization domain-like receptors (NODs). In return, nucleotide oligomerization domain-like receptors perform an action similar to those of enterocytes, by targeting some microbial templates known as microbe-associated molecular patterns (MAMPs). This, in turn, activates nuclear factor kappa-light-chain-enhancer of activated B cells (NF-Kb), nucleotide oligomerization domain-like receptor, and, subsequently, damage-associated molecular patterns (DAMPs) [209].

However, a dysbacteriosis will inevitably occur, and this is the case when all pathogens are engulfed and as antigen-presenting cells (APCs) are directed to dendritic cells (DCs) [209]. Microfolding cells present the antigen to naïve cluster of differentiation 4 (CD4) and allow differentiation into T helper cells (Th cells) and production of immunoglobulin A [210].

In addition, we can also find conserved motifs known as pathogen-associated molecular pattern-recognition receptors amongst the gut flora which present on the surface of pathogens, and a "leaky gut" has the potential to exacerbate reactive oxygen species production. Bacterial lipopolysaccharide and other toxins are recognized by these pattern-recognition receptors and initiate downstream signals by activating nuclear factor kappa-light-chain-enhancer of activated B cells [211], protecting the blood-brain barrier (BBB) against harmful products of metabolism [212].

The latest evidence suggests that many colonies of bacteria in our intestines have defined roles in food processing [213] and metabolic potency [214]. The fluctuations of gut colonies are the most conclusive and under normal circumstances have a pivotal role in host eubiosis [215]. This is highlighted by a wide range of metabolites [216,217], especially short-chain fatty acids. These metabolites result from fermentation of fiber and carbohydrates, but more specifically, acetate, butyrate, and propionate, which contribute to energy production for enterocytes [218]. They contribute to the optimal functionality of the neurohormonal axes [219] and act against age-induced disorders [220,221].

I.3.2 Disruptive Factors in Enteric Eubiosis and the Influence on Colonisation in Neonates

One of the earliest interactions of the foetus with the maternal urogenital microbiota take place once the foeus passes into the birth channel [222]. The colonisation process could actually be initiated *in utero*; Collado et al., [223] identified that *Proteobacteria* is the most prevalent phylum in both the placenta as well as the amniotic fluid. Data obtained following the analysis of the meconium suggest a mother-foetal transfer, with infants' microbiota being similar to that found in the colostrum after almost one week. The neonatal microbial communities are influenced by several processes such as preterm deliveries along with the method of delivery.

Aagaard et al., [224] highlighted the existence of a temporary niche formed during pregnancy, which unites four phyla: *Firmicutes*, *Tenericutes*, *Proteobacteria*, *Bacteroidetes* and

the *Fusobacteria* genus. While *Bifidobacterium*, *Lactobacillus*, *Bacteroides* and *Clostridium* are passed via the placenta [225,226], Lauder et al., [227] concluded that there are no significant differences between the number of copies following a quantitative polymerase chain reaction (q-PCR) analysis between the placental strains and the negative controls.

However, whether or not the placenta possesses beneficial microorganisms is still under question, mainly because some recent evidences supports the notion of favourable conditions for certain pathogen proliferation - in particular, Group B streptococcus [228].

Stout et al., [229] established that 27% of the basal plates of placentas possess intracellular bacteria which is, therefore, a possible route for intra-uterine colonisation. The finding of placental intracellular bacteria was found in 54% of the studied cohort who had a spontaneous PTB, and in only 26% of term-spontaneous deliveries. There were no major differences in the predisposition for IAIs or Group B Streptococcus in preterm births.

Intrauterine infections are known to be a cause of both STL and/or PPROM [230,231]. As the bacterial DNA has been detected in 70% from all the placental tissues, the authors concluded that the placental membranes possess bacteria, but it is not a cause of preterm labour or PPROM [232] following a C-section. On the other hand, no signatures of bacterial DNA have been detected compared with term vaginal deliveries, the positivity being around 50% [233].

PRM is a significant cause of premature birth and can cause complications of a term task. Considerable research on RPM has led to a better understanding of the mechanism of spontaneous breakage of membranes, risk factors, and good results for newborns resulting from such obstetrical events. Spontaneous rupture of the membranes increases the risk of intrauterine infection and umbilical cord compression as well as the risk of premature detachment of placenta. Newborn babies resulting from RPM have an increased risk of morbidity compared to GA, and the risk of infection is increased compared with other premature babies due to ancillary causes. If RPM occurs in the second trimester, there is an additional risk of PH and hip dysplasia. Pre-term conservative treatment prolongs latency to birth. Antibiotics reduce the risk of infection while corticosteroid treatment (dexamethasone) reduces respiratory complications and interventricular haemorrhage without increasing the risk of infection. Birth is necessary or unavoidable in many cases by RPMs and because conservative treatment is often ineffective. That is why more studies are needed to identify all risk factors and the need to treat pregnant women at risk of RPM.

The GA of an infant can correlate with the diversity seen in the commensal bacteria that are acquired by the infant, which is suggestive of prenatal influences [234,235]. Interestingly, Hu et al., [236] concluded that the meconium unites microbial strains, arguing that the mode of birth does not influence the microbial diversity. However, the microbial composition of the meconium was significantly influenced by the maternal diabetes status. Diabetes is characterized by a complex disorder of the body's energy metabolism that affects both the use of lipids, carbohydrates and proteins, as well as the other metabolisms. The most frequent complication caused by diabetes at the level of the eye is diabetic retinopathy (DR).

In one study we aimed to evaluate the changes related to diabetic retinopathy (no changes, small or moderate changes) in patients with glaucoma and diabetes using artificial intelligence (AI) instruments: support vector machines (SVM) in combination with a powerful optimization algorithm - diabetes mellitus - DE. In order to classify the diabetes mellitus changes and to make predictions in various situations, an approach including support vector machines optimized with diabetes mellitus was applied. The role of the optimizer was to automatically determine the support vector machines parameters that lead to the lowest classification error.

The study was conducted on a sample of 52 patients: particularly, 101 eyes with glaucoma and diabetes mellitus who presented at the Ophthalmology Clinic I of the "St. Spiridon" Clinical Hospital in Iaşi. The criteria considered in the modelling action were: normal or hypertensive open-angle glaucoma (OAG), intraocular hypertension, and associated diabetes. The patients with other types of glaucoma pseudoexfoliation (PXF), pigment, cortisone, neovascular and primitive angle-closure, and those without associated diabetes were excluded. The assessment of diabetic retinopathy changes was carried out with Volk lens and Fundus Camera Zeiss retinal photography on the dilated pupil, inspecting all quadrants. The criteria for classifying the diabetic retinopathy (early treatment diabetic retinopathy study - ETDRS) changes were: no changes (absence of diabetic retinopathy), mild forma nonproliferative diabetic retinopathy (the presence of a single micro aneurysm), moderate form (micro

aneurysms, hemorrhages in 2-3 quadrants, venous dilatations and soft exudates in a quadrant), severe form (micro aneurysms, hemorrhages in all quadrants, venous dilatation in 2-3 quadrants) and proliferative diabetic retinopathy (disk and retinal neovascularization in different quadrants). Any new clinical element that occurred in subsequent checks, which led to their inclusion in severe nonproliferative or proliferative forms of diabetic retinopathy, was considered to be the result of the progression of diabetic retinopathy. The results obtained were very good; the accuracy in the testing phase was 95.23% and only one sample was wrongly classified. The research demonstrated the effectiveness of the classification algorithm (support vector machines) developed in optimal form with diabetes mellitus and used in predictions of retinal changes related to diabetes.

It is intriguing that one of the microbes involved in the metabolism of levodopa in patients with Parkinson's disease has been identified in meconium samples. With a rate of 1 to 5 samples, *Enterococcus faecalis* has been identified in almost 80% of all the samples after the meconium has passed within the first two hours [237]. Hansen et al., evaluated the microbiota contained within the meconium, and they found that bacteria was detectable in two-thirds of the meconium samples through the use of fluorescence in situ hybridization (FISH) and 7% by standard polymerase chain reaction (PCR), while a significant percentage of sterile samples have been defined by a minimum inhibitory concentration (MIC) [238]. *Enterococcus*, *Streptococcus*, *Staphylococcus*, or *Propionibacterium* were the predominant strains in the umbilical blood cord [237], while in the amniotic fluid the bacterial composition was dominated by species such as *Sneathia sanguinegens*, *Leptotrichia amnionii* and an uncharacterised bacteria [239]. Shao et al., identified that the bacterial composition can be influenced by delivery method, as they demonstrated a disruption to the transmission of the maternal *Bacteroides* in C-section, with C-sections proving to detriment the *Enterococcus*, *Enterobacter* and *Klebsiella* species [240]. In addition, preterm infants often receive treatment with antibiotics in order to prevent possible infections, but a recent research article showed the subsequent existence of resistome as a result of prolonged exposure to various drugs [241], suggesting that an infant's commensal microbiome will be impacted by these antibiotics.

A series of factors should be taken into consideration by the obstetrician before considering inducing labor. There are studies that compare the use of oxytocin (OXT) with prostaglandins (PGs) for labor induction and the results are in favor of prostaglandins for the lower rate of pregnancies completed by segmental transversal cesarean. However, administration of oxytocin may increase the risk of pregnancy termination through segmental transversal cesareans. In contrast to oxytocin and prostaglandins, the mechanical methods of inducing labor may increase the risk of both maternal and neonatal infectious. The decision to trigger labor requires the obstetrician to carefully analyze the timing of induction of birth and the risks and benefits, considering, for each patient, the most effective method of triggering. Thus, we emphasize the necessity of developing protocols to guide obstetricians, since there is no consensus on the doses that should be administered. The cost-effectiveness of the treatment should also be considered.

I.3.3 Enteric Microbial Variations in Childhood: The Heritable and Social Components

Turnbaugh et al., revealed that even monozygotic (MZ) pairs have distinct signatures of commensal microbiota. The stool samples collected were compared to 1,095 bacterial communities that are commonly found in the gut and other body habitats, from related and unrelated individuals. In over one million bacterial reads, the α-diversity indicated approximately 800 following the analysis of the hypervariable V2 region [242].

Goodrich et al., managed to replicate an association between the lactic bacteria belonging to the *Bifidobacterium*, which is usually heritable between the UK twins, and the LCT gene locus, being responsible for the hydrolysation of lactose in the upper gastrointestinal tract [243].

The faecal samples collected from monozygotic and dizygotic (DZ) twin individuals from the United States and South Korea revealed the existence of a unique microbiome. Based on the sequences obtained following the analysis of the bacterial V2 region, Lee et al., concluded that this variation seems to be the result of a combination between certain temporal and spatial variables [244].

This hypothesis also applies to a much smaller degree in brothers. In a study conducted by Schloss et al., a metagenomic shotgun analysis of 16S rRNA's V3-V5 region was conducted with the aim of distinguishing the microbial communities of each family member, using as reference

individuals which live in the same geographic area. *Bifidobacterium* and *Escherichia* were the most dominant strains encountered in all siblings, with the mention that the microbiota of the two-year-old was more similar to her weaned siblings. Twelve operational taxonomic units (OTUs) were identified within the family, from which four were location specific, belonging to the genus *Bacteroides* and *Subdoligranulum* and family *Lachnospiraceae* [245].

Recently, Kato et al., revealed the presence of the CC genotype in 1068 Japense adults at rs4988235 and the GG at rs182549, in addition to those previously reported (rs145946881, rs41380347, rs41525747 and rs869051967) [246]. They found that there was positive correlation between the CC genotype and a low abundance of *Bifidobacterium* [247,248]. C/T(-13910) has been mainly reported as the predominant lactase locus in Europeans, while G/A(-22018) in Japanese-Brazilian and Chinese populations [249]. In addition, bathtub water was proven to be a potential vehicle for the bacterial transfer and it is not strictly a mother-to-infant axis.

Odamaki et al., enrolled 21 Japanese individuals from five families and, after the isolation of the faecal and bathtub samples, *Bifidobacterium longum* was shown to be the most abundant microorganism exchanged between the members, compared with those which do not adopt this tradition [250]. A comparative study conducted by the same author demonstrated that *Bifidobacterium longum* subsp. *longum* is present throughout life, regardless of age. Their results suggest that some bacteria are distributed across family members [251].

Laursen et al., evaluated how early infections, having older brothers or pets could disrupt the normal colonisation of the gut [252]. David Strachan's hygiene hypothesis was confirmed by the positive correlation between the presence of older siblings and bacterial diversity and abundance of *Firmicutes* and *Bacteroidetes* or *Faecalibacterium prausnitzii* [253]. On the other hand, pets or early infections had less contribution towards the gut flora, without any significant data correlation.

Dill-McFarland et al., have emphasised in his study an attribute acquired as social human beings [254]. The analysis of the faecal samples collected from 177 individuals, from which 94 were spouses and 83 were siblings, revealed that their taxa was more similar and diverse when compared to those of related or unrelated individuals, with the cause-effect relating to dietary habits.

The faecal samples collected over during two years showed no major fluctuations within these communities throughout the entire study period. The only minor difference was in the case of one person after an intervention that required medication, and no foreign or major change regarding species density was reported [255].

Obesity, allergies, anaphylactic reactions to asthma, and autoimmune diseases are a few examples of conditions which may be influenced by the commensal bacteria and thus the delivery method. It is evident that C-section indirectly promotes various diseases through the effect of the neonatal microbiota [256,257].

In a recent study, researchers discovered that the resistome (gigantic tank of antibiotic resistance determinants - ARDs) of infants born prematurely is already preformed because of the antibiotics used in order to prevent different infections, with gene-drug-type studies becoming possible through mobile-clustered regularly interspaced short palindromic repeats interference (CRISPRi). By using dedicated techniques, they revealed distinctive patterns and an emerging multidrug resistance of *Enterobacteriaceae* during and after hospitalization [241,258]. Ciprofloxacin, an antibiotic usually administered to treat bacterial infections, has a long-term effect upon bacterial diversity even after half a year since after the end of the treatment [259].

I.3.4 How Is the Hypothalamic-Pituitary-Adrenal Axis Influenced?

A reduction in the host's innate eubiosis triggers a pro-inflammatory cascade [260]. If this state is prolonged, it may lead to gastrointestinal disorders [211,261], as well as neurodegenerative [262] or neuropsychiatric disorders [263]. In such cases, the hypothalamic-pituitary-adrenal axis exerts an antagonistic effect upon the organism. It has been shown that the patients with a major depression disorder have high serum levels of cortisol [264] and reduced levels of oxytocin [265]. The results obtained in another study, conducted with a similar design to the previous one, provides additional evidence and further consolidates this strong correlation between the brain and the digestive tract [266].

There is a lot of controversy regarding the interconnections between the neurological and gastrointestinal disorders [211,263] and even if these disturbances of the central nervous system are irremediable, at least the symptoms can be reduced by enhancing the gastrointestinal microbiota. A number of conventional alternatives have been developed in recent years [267,268], presently being considered the most powerful vehicles for the acquisition of the beneficial microorganisms intended for the reconstruction of the gastrointestinal microbiota

I.3.5 Gut microbiota and the novel coronavirus?

A recent review discussed the crosstalk between lung and gut microbiota in the elderly. According to the authors, age could be responsible for the high predisposition of elder people to severe acute respiratory syndrome coronavirus 2 (SARS-CoV-2) infections. It seems that age is directly correlated with an increased gut permeability and the associated gastrointestinal deficiencies, which suggests a potential for fecal-oral transmission [269].

Even though no study has yet been published on this topic, early studies on COVID-19 highlighted a low [270–273] to medium [274–277] incidence of gastrointestinal deficiencies (Table 5). The most common symptom was diarrhea [278–281], which suggests a potential route of action of COVID-19 at the level of digestive tract.

Based on these initial considerations, it should be also mentioned that gastrointestinal dysfunctions (e.g., diarrhea) are part of a cluster of specific symptoms displayed by patients suffering from irritable bowel syndrome [282]. In Table 5, we have summarized the data related to these abnormalities which may result from disturbances along the gut-brain axis [283].

Table 5. Frequency of the most uncommon gastrointestinal symptoms displayed by severe acute respiratory syndrome coronavirus 2-infected patients

Number of Patients Included	Occurrence	Reference
99	2 (2%)	[272]
41	1/38 (3%)	[271]
1,099	42 (3.8%)	[270]
62	3 (8%)	[273]
651	74 (8.14%)	[274]
191	9 (5%)	[275]
138	14 (10.1%)	[276]
95	58 (24.2%)	[277]
274	77 (28%)	[284]

Over the years, analytical biochemical analysis has been introduced as an integrated component alongside molecular biology. Thus, the optimization of techniques (e.g., enzyme-linked immunosorbent assay - ELISA) has allowed fecal calprotectin - FC to evolve as a reliable biomarker that allows the identification of intestinal inflammation [285].

Using a cohort consisting of 40 patients, Effenberger et al., aimed to measure the level of fecal calprotectin. According to their data, 45% of patients did not report gastrointestinal symptoms, in 55% of cases diarrhea has ceased after two days, and in nine patients, diarrhea persisted beyond the two days. They demonstrated that patients with or without diarrhea had fecal calprotectin levels significantly correlated with interleukin-6 (IL-6) concentration, but not with that of c-reactive protein (CRP) or ferritin [286].

Contrary to the hypothesis that people with additional diseases are more prone to infection, those with inflammatory bowel disease (IBD) were not at increased risk of COVID-19 and the associated mortality in one observational, case-series study [287]. What is certain is that there is controversy around this topic, because we also identified antithetical studies.

For example, we encountered a report of a patient diagnosed with an acute, severe ulcerative colitis flare who died. As part of the management of the inflammatory bowel disease, the patient

received high intravenous dose of corticosteroids. He subsequently developed pneumonia and was found to have COVID-19 based on a nasopharyngeal swab [288].

To date, only two large clinical trials have been conducted with the aim of assessing gastrointestinal symptoms and detecting the virus following the analysis of fecal samples [274,277]. Among all patients (n = 651), Jin et al., concluded that on the basis of gastrointestinal dysfunctions, only 11.4% (74 cases) had digestive problems, of which 28% did not manifest any respiratory difficulties [274]. Lin et al., offered a more conclusive perspective, showing that 61.1% (58/95) of patients had gastrointestinal dysfunctions, the most frequent being diarrhea, nausea, vomiting, and liver impairment. Thus, it was possible to identify the niches in which severe acute respiratory syndrome coronavirus 2 was detected [277], with it being observed even in the stool samples on day 7, up to twelve days [273,289–291].

It has been hypothesized that severe acute respiratory syndrome coronavirus 2 could even be transmitted postmortem [292], persisting in the body after clearance of the respiratory tract [293], with viral signatures being found 1 month later after admission [291].

There is an increasing trend in the literature regarding the underlying mechanism or possible interconnections between COVID-19 and the myriad microscopic entities that are gathered at the level of every human gastrointestinal tract [294].

In this context, an immunopathological mechanism and novel therapeutic targets have been revealed. Using a machine-learning (ML) model dedicated to exploring core microflora in order to predict the outcome, it was possible to identify an increased expression and exacerbated levels in fourteen proinflammatory cytokines [295,296].

Mechanically, the main gateway of the virus could be represented by the angiotensin system, or, more precisely, the angiotensin-converting enzyme 2 (ACE2) as a viable receptor [297]. Angiotensin-converting enzyme 2 can mediate intestinal inflammation [298], which explains its high expression on the epithelial cells [299] and lymphocytes' exhaustion status [300,301]. By analyzing single-cell RNA sequencing data, it was discovered that angiotensin-converting enzyme 2 is highly expressed in the small intestine [281].

The latest reports have revealed the importance of enteric microflora in regulating the neuroimmune network [302–304]. Severe acute respiratory syndrome coronavirus 2 is not only dependent on the presence of the angiotensin-converting enzyme 2 receptor. The structural composition and proportions by which angiotensin-converting enzyme 2 is expressed are distinct in the digestive tract (e.g., esophagus, gastric, ileum, and colon). Therefore, this could explain how the spike (S) protein is cleaved on the cell membrane and the interplay between transmembrane protease, serine 2 and 4 (TMPRSS2/4) [305] and how the gut enterocytes are gradually infected [306].

Even though polymerase chain reaction-based methods have proven efficient and are used at a global scale, a recent report demonstrated that eight out of ten "infected" children could be false positives. Even when initial nasopharyngeal testing was negative, rectal swabs were not [307]. Through electron microscopy, it was possible to detect patients who did not have diarrhea but were positive, which strongly suggests once again an oral-fecal transmission [308].

In one study, at approximately three weeks after onset, a seroconversion of immunoglobulin G (IgG) and immunoglobulin M (IgM) took place in all 285 patients [309].

Because there is no active treatment against this infection, mouth rinses containing β-cyclodextrin combined with citrox were said to potentially exert a beneficial effect, but this remains a theoretical proposition [310], as does the usage of hydroxychloroquine (HCQ) [311]. On the other hand, mouthwash containing chlorhexidine (CHG) was associated with a richness of several strains of *Firmicutes* and *Proteobacteria*, but negatively correlated with *Bacteroidetes*, *Saccharibacteria*, Candidate division TM 7, Candidate division SR1, and *Fusobacteria*, inducing massive shifts among the microorganisms found inside the oral cavity by leading to a more acidic pH [312].

Modeling daily cases are pivotal for management and future directions. Estimating COVID-19 possible evolution or regression through mathematical and statistical models is groundbreaking to determine short and long-term case estimates. Such approaches are viable not only to predict the COVID-19 spreading course, but also to allocate the resources necessary to restrict the virus spreading [313].

Distinct approaches have been applied with relatively high accuracy for different prediction purposes. Some examples are represented by statistical methods aiming to predict epidemic cases.

These include time series [314], or simulation models [315,316], multivariate linear regression [317], backpropagation neural network [318–320], and gray forecasting [321,322].

Personal contribution - published papers:

Ilie, O.-D.; Cojocariu, R.-O.; Ciobica, A.; Timofte, S.-I.; Mavroudis, I.; **Doroftei**, **B**. Forecasting the spreading of COVID-19 across nine countries from Europe, Asia, and the American continents using the arima models. *Microorganisms **2020**, 8,* 1158. **IF: 4.128**

Aim of the study

The present study aims to estimate the prevalence trend in Ukraine, Romania, the Republic of Moldova, Serbia, Bulgaria, and Hungary as Central European countries. Moreover, we will also consider the most affected countries presently, such as USA, Brazil, and India.

Materials and methods

Data

The daily prevalence data of COVID-19 was taken from The Ministry of Internal Affairs of Romania, the WHO, and the EUROPEAN CENTRE FOR DISEASE PREVENTION AND CONTROL (ECDC)[1]. MS Excel was used to build a time-series database. Descriptive statistics of the COVID-19 data for the established intervals (March 10 and July 10) are given in Table 6. In order to create an optimum autoregressive integrated moving average (ARIMA) model, at least 30 observations are needed [323].

Table 6. Descriptive statistics on the prevalence and incidence of coronavirus (COVID-19) in the established countries

(a) Prevalence

Continents	Country	Mean	SE Mean	St. Dev	Minimum	Maximum	Skewness	Kurtosis
Central and Eastern Europe	Ukraine	17,545.34	1424.02	15793.16	1	52,043	0.5836	-0.8257
	Romania	13,958.65	837.07	9283.60	25	31,381	-0.0447	-1.1718
	Republic of Moldova	6341.02	516.67	5730.20	3	18,666	0.6936	-0.7263
	Serbia	8159.77	468.22	5192.87	5	17,342	-0.3619	-1.1779
	Bulgaria	2063.34	151.29	1677.90	4	6672	0.7943	-0.0721
	Hungary	2618.48	138.75	1538.90	12	4.220	-0.5892	-1.2725
South and North America, and South Asia	USA	1,242,336.35	80,297.41	890,541.35	696	3,038,325	0.1309	-1.1182
	Brazil	405,199.86	45,415.32	503,680.30	25	1,713,160	1.1576	0.0707
	India	168,929.42	19,430.70	215,496.91	50	793,802	1.3365	0.7176

(b) Incidence

Continents	Country	Mean	SEMean	St. Dev	Minimum	Maximum	Skewness	Kurtosis
Central and Eastern Europe	Ukraine	423.10	25.90	287.33	0	1366	0.3931	-0.0052
	Romania	255.00	11.65	129.25	6	614	0.2298	-0.0560
	Republic of Moldova	151.74	10.03	111.27	0	478	0.7573	0.1075
	Serbia	140.98	10.22	113.38	0	445	0.8188	-0.4346
	Bulgaria	54.21	5.08	56.44	0	330	1.9756	4.8870
	Hungary	34.23	3.09	34.36	0	210	1.6979	4.7398
South and North America, and South Asia	USA	24,697.99	1152.30	12,779.70	0	64,630	0.1378	0.8261
	Brazil	13,927.92	1307.41	14,499.97	0	54,771	0.8961	-0.3030
	India	6453.31	644.93	7152.72	0	26,506	1.1402	0.2809

[1] https://www.mai.gov.ro/informare-covid-19-grupul-de-comunicare-strategica, https://covid19.who.int/?gclid=CjwKCAjwi_b3BRAGEiwAemPNUYzgrAMkQXN5Z848tjCmGZLJecod03yWxqW_bN248wjgdezXeYg0RoCeFcQAvD_BwE, and https://www.ecdc.europa.eu/en

The analyzed data corresponds to the period between March 10 and July 10. The data set was used to perform and analyze a case estimation model by applying autoregressive integrated moving average that could help us to predict the severe acute respiratory syndrome coronavirus 2 evolution in the future.

For this study, a time series containing at least 45 data points was used to predict COVID-19 prevalence in six Central and Eastern European countries (Romania, Bulgaria, Serbia, Ukraine, Republic of Moldova, and Hungary). The same concept was applied for one country from South America (Brazil), one from North America (United States of America), and one from South Asia (India) over the subsequent fourteen days, with 95% relative CI.

As seen in Figure 11, the COVID-19 outbreak hit Ukraine harder than the other five countries between the established period. The first case in Ukraine was reported on the 3rd of March, 2020. In contrast with the related regions, the COVID-19 pandemic had started earlier in Romania (26 February) and later in the other four (March 4 in Hungary, March 6 in Serbia, March 7 in the Republic of Moldova, and March 8 in Bulgaria). In Ukraine, the total number of confirmed cases of COVID-19 reported during the period is 52,043, the highest number of new cases reported being 1,366 registered on July 6.

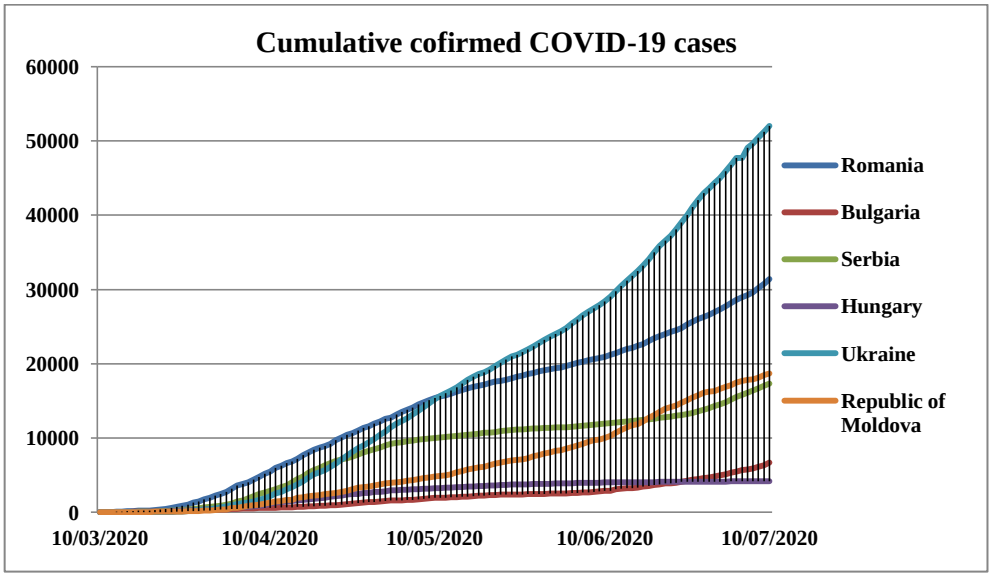

(a)

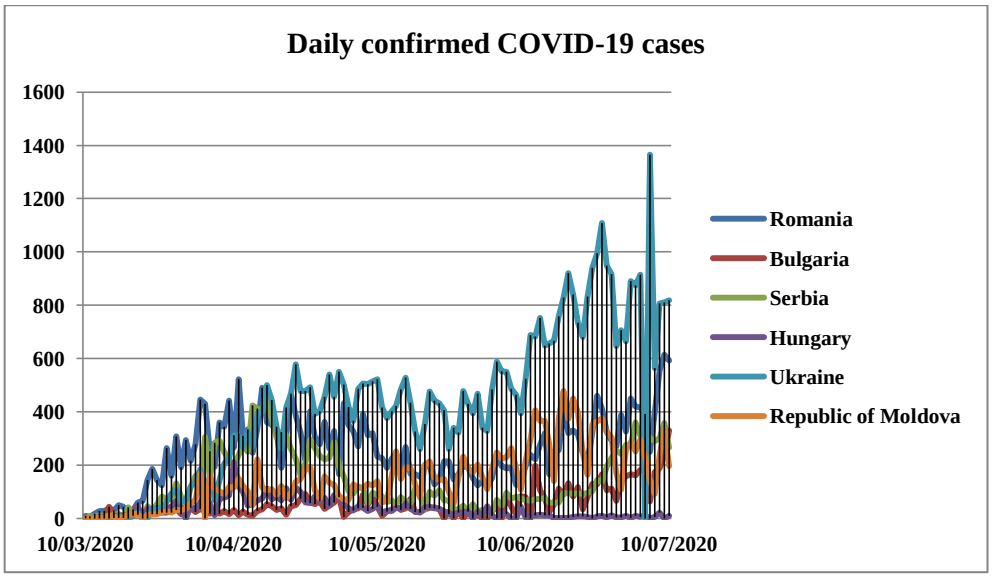

(a')

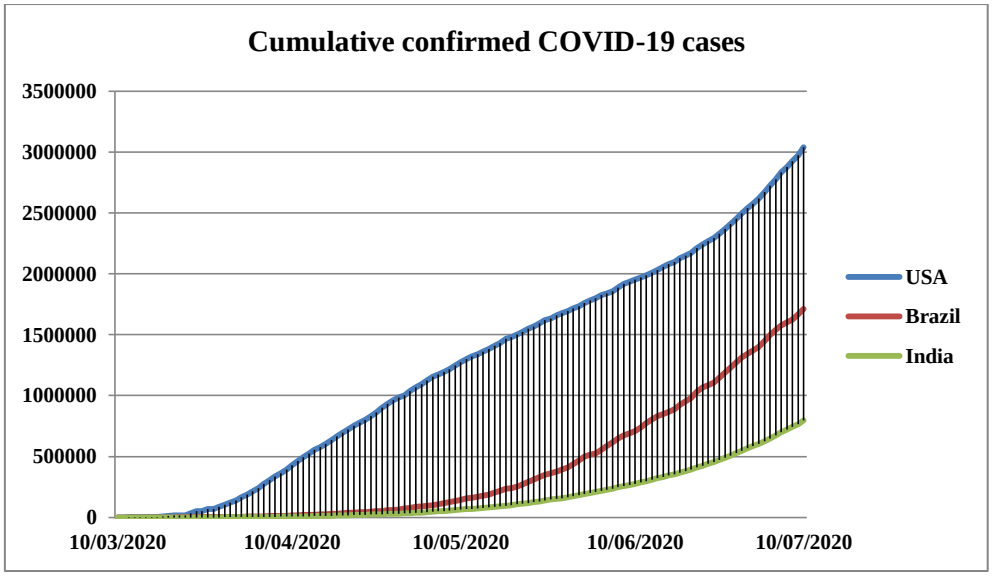

(b)

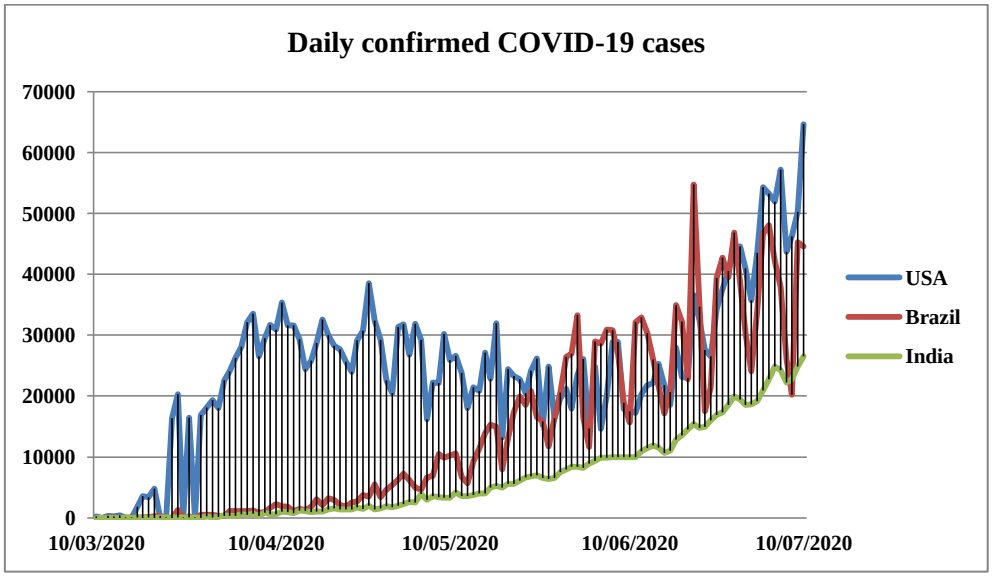

(b')

Figure 11. The (a,b) prevalence and (a',b') incidence of the COVID-19 within the established countries

The overall prevalence for Romania was 31,381, making it the second hardest-hit region, followed by the Republic of Moldova with 18,666, then Serbia with 17,342, Bulgaria with 6,672, and Hungary with 4,220 cases. Also, the second highest incidence between the remaining five regions was in Romania with 614 new cases on July 9, followed by the Republic of Moldova with 478 on June 18, 445 in Serbia on April 17, 330 in Bulgaria on July 10, and 210 in Hungary on April 10.

Elsewhere, the first case in the USA was reported on January 20, almost one week later compared with Romania. The second hardest-hit region was Brazil, where the first case was reported on February 26, while in India on January 30. The overall prevalence for these three countries at the time of conducting our study was as follows: USA with 3,038,325, Brazil with 1,713,160, and India with 793,802 cases. Concerning the incidence, the highest was as expected in the USA with 64,630 on July 10, followed by Brazil with 54,771 on June 21, and last, India with 26,506 on July 10.

Autoregressive integrated moving average models

A time series is simply a series of time-dependent data points [324] used for analyses dedicated to revealing reliable and meaningful statistical data for the subsequent prediction of values of a series

[325]. Since it was introduced by Box and Jenkins approximately half a century ago, autoregressive integrated moving average has been used at much larger scales [323]. In most cases, autoregressive integrated moving average is chosen because it takes into account all trends and periodic changes, even random disturbances. Thus, autoregressive integrated moving average is suitable for a large spectrum of data, from seasonality to cyclicity. In this context can be modeled a temporal dependency in a flexible manner. Non-seasonal autoregressive integrated moving average models are defined by three parameters (*p*, *d*, *q*) where *p* is the order of autoregression, *d* is the degree of differencing, and *q* the order of moving average [326]. autoregressive integrated moving average offers the possibility to be modified so that can be conducted different and simple AR, I, or MA models.

AR (p) usually explains the present value $Y_{t,}$ unidirectionally it terms of its previous values Y_{t-1}, Y_{t-2}, ..., Y_{t-p}, and the current residuals ε_t. MA (q) refers to the current value of the time series Y_t in terms of its current and previous residuals ε_{t-1}, ε_{t-2},…, ε_{t-q}. The general formula of AR (p) and MA (q) can be expressed in Equations (1) and (2).

$$Y_t = \Phi_1 Y_{t-1} + \Phi_2 Y_{t-2} + \ldots + \Phi_p Y_{t-p} + \varepsilon_t \quad (1)$$

$$Y_t = \theta_1 \varepsilon_{t-1} - \theta_2 \varepsilon_{t-2} - \ldots \theta_p \varepsilon_{t-p} + \varepsilon_t \quad (2)$$

where:
p - past value;
Φ and θ - parameters that indicate the autoregression, and moving average, respectively;
t - time;
Y_t - observed value at a time t;
ε_t - value of the random shock dependent by t;
p - past value.

In other words, ARMA (p,q) model express the current values, as well as its previous ones and residuals linearly. The corresponding formula is given in the below equation:

$$Y_t = \alpha + \Phi_1 Y_{t-1} + \Phi_2 Y_{t-2} + \ldots + \Phi_p Y_{t-p} + \varepsilon_t - \theta_1 \varepsilon_{t-1} - \theta_2 \varepsilon_{t-2} - \ldots \theta_p \varepsilon_t - q \quad (3)$$

where:
α - constant;
ε_{t-1} - value of the previous random shock;

Model selection

In our study, three performance criteria entitled root mean square error (RMSE), mean absolute error (MAE) and mean absolute percentage error (MAPE) were applied to test the predictive accuracy of the current autoregressive integrated moving average model. Mathematically, the equations for these three criteria are presented above:

$$RMSE = \sqrt{\frac{1}{n}\sum_{t=1}^{n} e_t^2}$$

$$MAE = \frac{1}{n}\sum_{t=1}^{n} |e_t|$$

$$MAPE = \frac{100\%}{n}\sum_{i=1}^{n} \left|\frac{e_t}{y_t}\right|$$

where:
y_t - value observed at a time t;
e_t - difference between values;
n - number of time points;

For a better fit of the data, root mean square error, mean absolute error, and mean absolute percentage error must have low values. All analyses were performed using STATGRAPHICS Centurion (v.18.1.13) software with a statistically significant level of $p < 0.005$.

Results and discussions

Forecasting the prevalence of COVID-19 pandemic using the autoregressive integrated moving average model

The autoregressive integrated moving average modeling is composed of four repetitive steps: assessment of the model, estimation of parameters, diagnostic checking, and prediction. The first step is to control whether the time series' mean, variance, and autocorrelation constancy over time are stationary and seasonal for a better accuracy [327]. In this context, Time Series plot, autocorrelation function (ACF), and partial autocorrelation function (PACF) (Figure 12) graphs were constructed to verify the seasonality and stationarity. On one hand, , autocorrelation function can determine whether the previous values from the series are related to the following one, while partial autocorrelation function highlights the degree of correlation between a variable and a lag of the said variable [328]. Estimated autocorrelations for the time series of the established countries are shown in Figure 13. Straight lines represent two standard deviations limits, while bars that extend beyond the lines indicate statistically significant autocorrelations.

ACF for Ukraine (a)

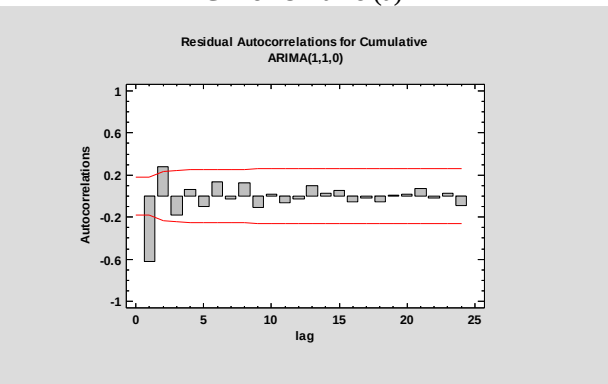

PACF for Ukraine (b)

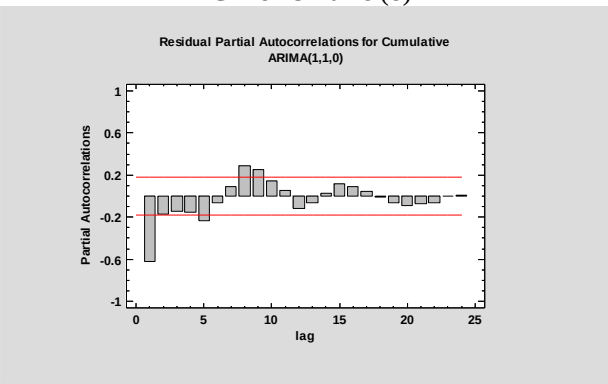

ACF for Romania (a)

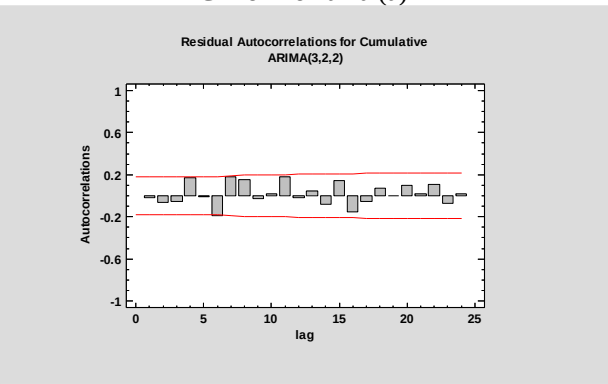

PACF for Romania (b)

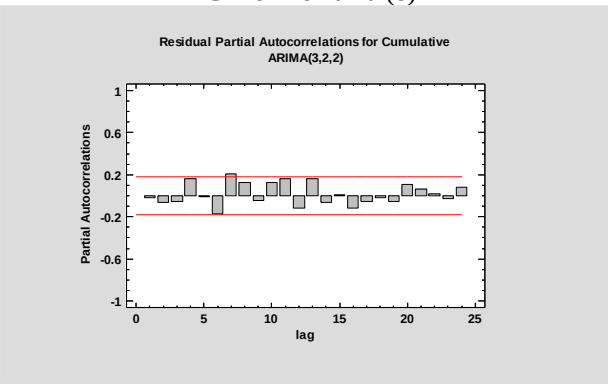

ACF for the Republic of Moldova (a)

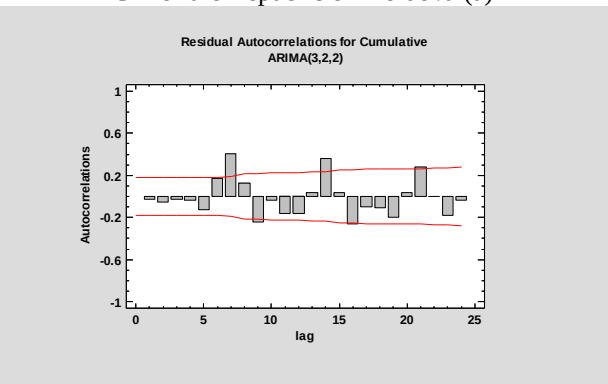

PACF for the Republic of Moldova (b)

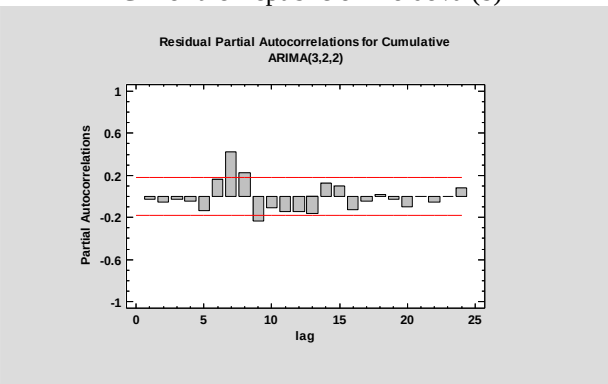

ACF for Serbia (a)

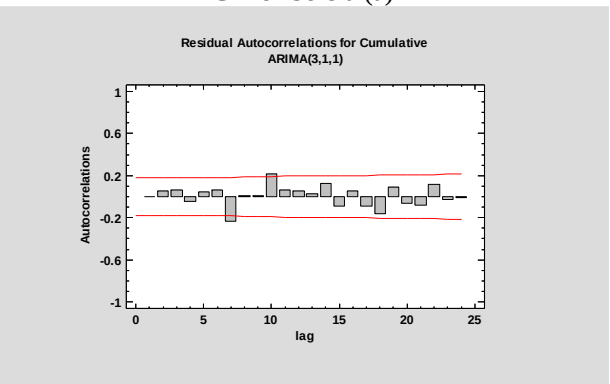

PACF for Serbia (b)

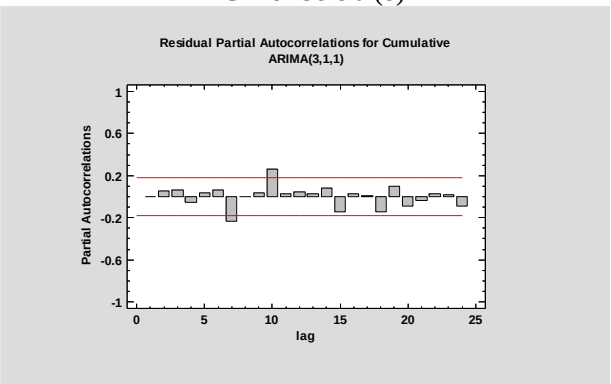

ACF for Bulgaria (a)

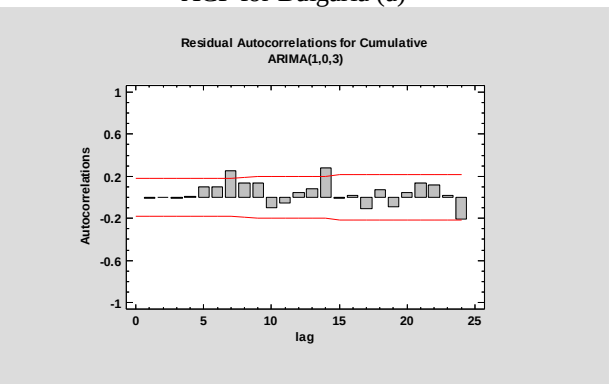

PACF for Bulgaria (b)

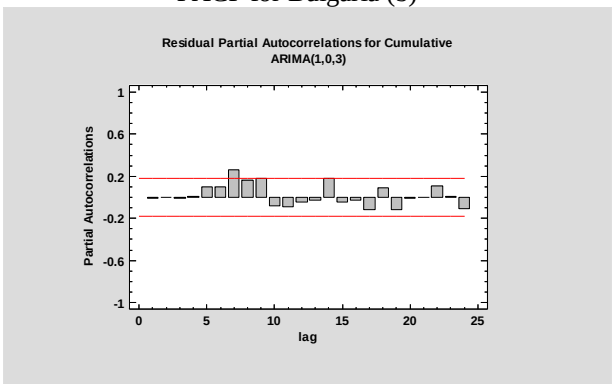

ACF for Hungary (a)

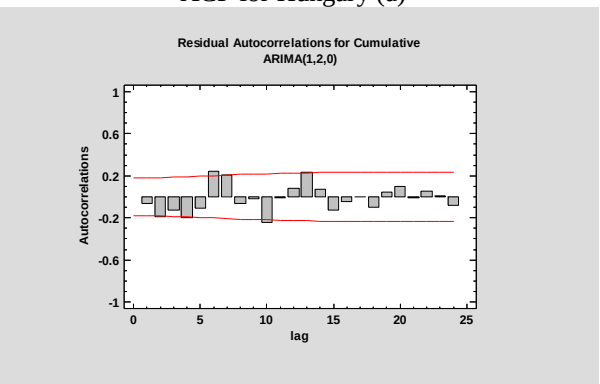

PACF for Hungary (b)

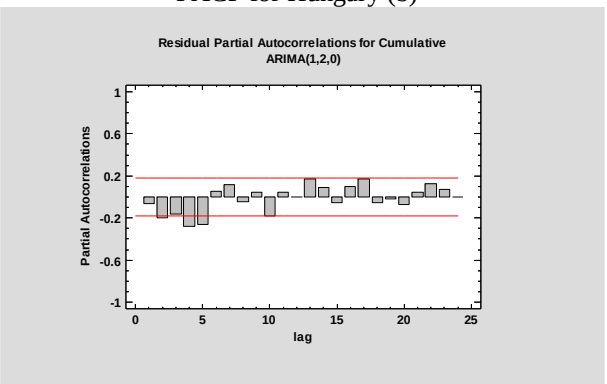

ACF for USA (a)

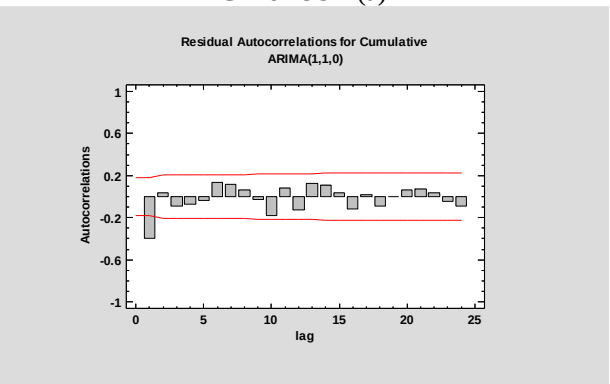

PACF for USA (b)

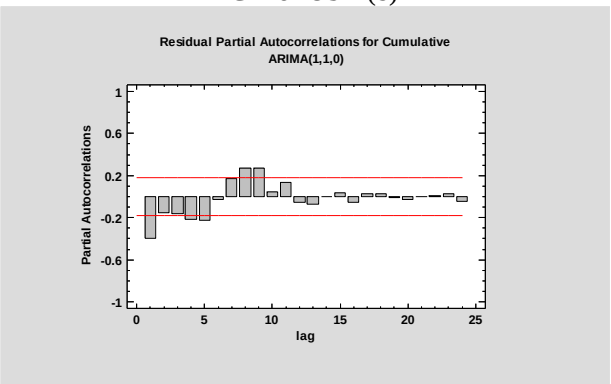

ACF for Brazil (a)

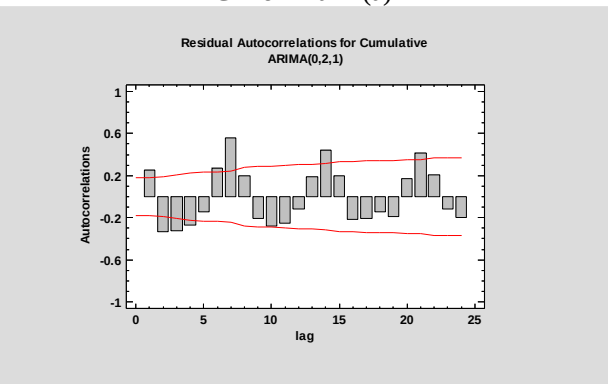

PACF for Brazil (b)

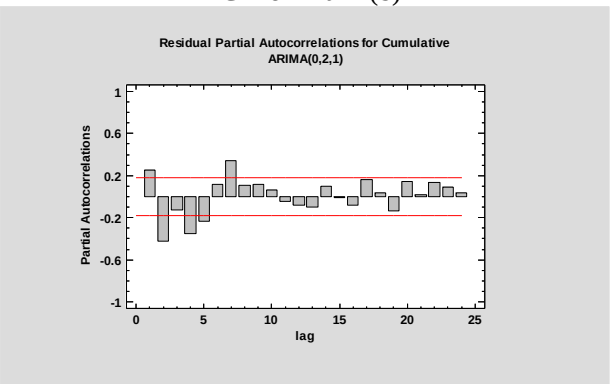

ACF for India (a)

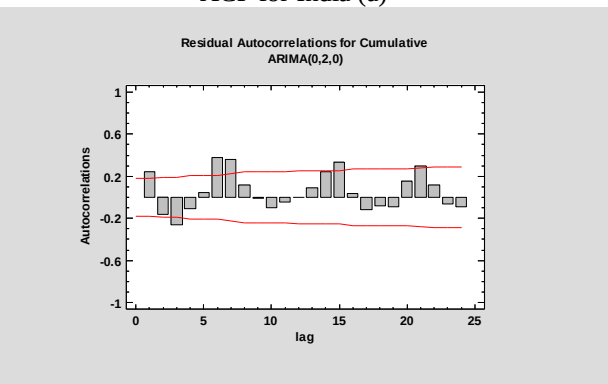

PACF for India (b)

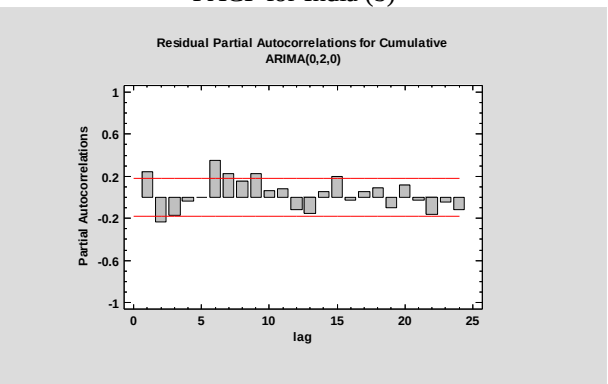

Figure 12. The estimated ACF (a) and PACF (b) graphs to predict the epidemiological trend of COVID-19 prevalence for Ukraine, Romania, the Republic of Moldova, Serbia, Bulgaria, Hungary, USA, Brazil and India

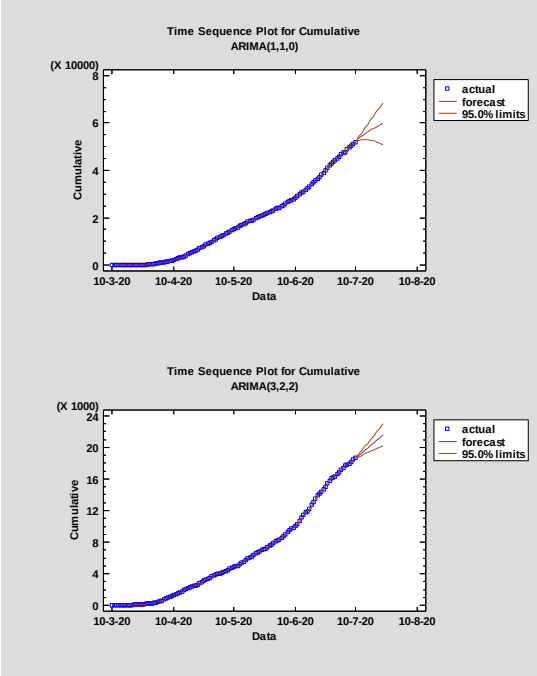

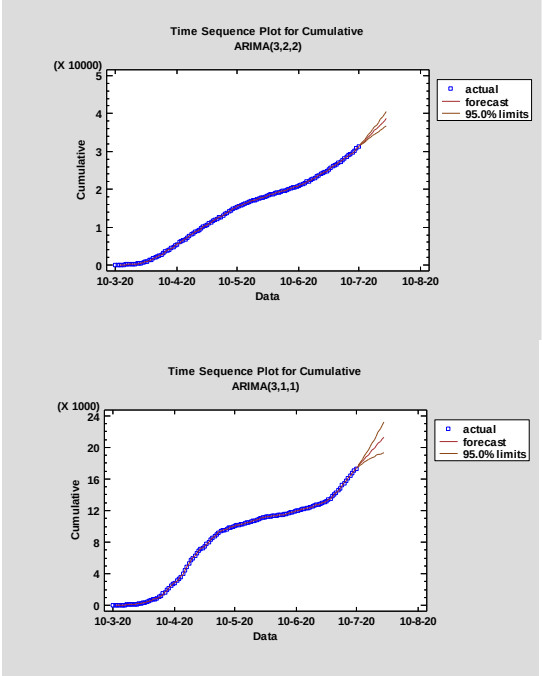

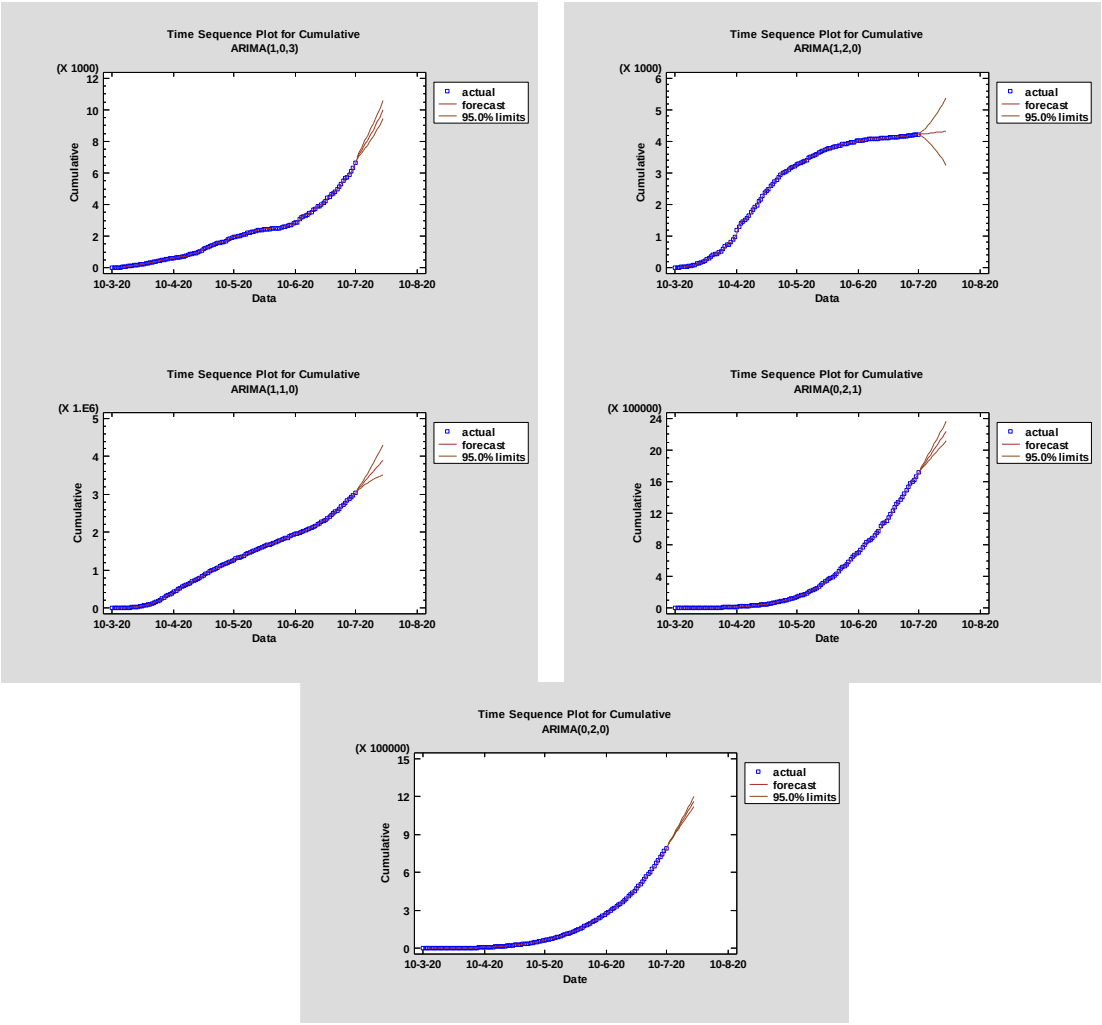

Figure 13. Time-series plots for the best autoregressive integrated moving average models

Additionally, a series of autoregressive integrated moving average models was also created, and their performance was compared using various statistical tools. All statistical procedures were performed on the transformed COVID-19 data. Autoregressive integrated moving average models with the minimum mean absolute percentage error values were selected as the best model. Among the tested models, the ARIMA (1, 1, 0), ARIMA (3, 2, 2), ARIMA (3, 2, 2), ARIMA (3, 1, 1), ARIMA (1, 0, 3), ARIMA (1, 2, 0), ARIMA (1, 1, 0), ARIMA (0, 2, 1), and ARIMA (0, 2, 0) models were chosen as the best models for Ukraine, Romania, the Republic of Moldova, Serbia, Bulgaria, Hungary, USA, Brazil, and India. The models fitted the COVID-19 data are presented in Figure 12 and Table 7 and Table 8 with a minimum $MAPE_{Ukraine}$ = 4.70244, $MAPE_{Romania}$ = 1.40016, $MAPE_{Republic\ of\ Moldova}$ = 2.76751, $MAPE_{Serbia}$ = 2.16733, $MAPE_{Bulgaria}$ = 2.98154, $MAPE_{Hungary}$ = 2.11239, $MAPE_{USA}$ = 3.21569, $MAPE_{Brazil}$ = 4.10596, $MAPE_{India}$ = 2.78051.

Table 7. Comparison of tested autoregressive integrated moving average models

Country	Model	RMSE	MAE	MAPE
Ukraine	(1,1,0)	182.403	86.857	4.70244
	(0,2,0)	184.534	84.6694	4.75145
	(3,2,0)	140.184	87.0874	4.86564
	(3,0,0)	140.834	83.9104	5.02043
	(2,2,0)	141.809	86.6818	5.08194
Romania	(3,2,2)	72.2811	54.8283	1.40016
	(1,2,3)	77.4246	57.1017	1.45906
	(2,2,3)	74.5154	55.2809	1.48125
	(3,2,3)	76.4564	56.4977	1.52647
	(2,2,2)	78.7986	58.4657	1.53212
Republic of Moldova	(3,2,2)	61.1658	43.5817	2.76751

	(3,2,1)	60.7849	43.5131	2.77257
	(2,2,1)	60.6597	43.5749	2.77809
	(3,2,3)	61.6063	43.8593	2.84718
	(2,2,3)	61.341	43.8542	2.85937
Serbia	(3,1,1)	43.0079	28.8086	2.16733
	(2,1,3)	43.0409	29.127	2.17147
	(1,1,3)	42.8633	29.1174	2.17271
	(3,1,0)	42.8659	28.847	2.17729
	(2,1,2)	42.8686	29.1841	2.17814
Bulgaria	(1,0,3)	33.4732	23.1431	2.98154
	(2,0,2)	33.7635	23.0537	3.04647
	(3,0,0)	33.5995	22.8279	3.08918
	(3,2,0)	35.4064	23.7486	3.08997
	(2,2,2)	78.7986	58.4657	1.53212
Hungary	(1,2,0)	23.0452	15.101	2.11239
	(0,2,3)	21.7985	13.6316	2.15973
	(3,2,0)	22.6729	14.2714	2.16096
	(3,0,0)	22.6563	14.488	2.16571
	(2,2,3)	21.9873	13.6272	2.16876
USA	(1,1,0)	6539.46	4673.82	3.21569
	(0,2,0)	6541.2	4710.64	3.2431
	(3,2,1)	5818.42	4379.88	3.29508
	(1,2,3)	5868.51	4434.36	3.29553
	(2,2,3)	5888.31	4430.09	3.29999
Brazil	(0,2,1)	6134.91	3838.17	4.10596
	(2,1,0)	6493.37	3521.69	4.14127
	(2,2,1)	5454.19	3118.73	4.15452
	(1,2,0)	6515.51	3598.89	4.16568
	(3,2,1)	5457.52	3082.2	4.1698
India	(0,2,0)	642.607	416.132	2.78051
	(1,1,0)	574.812	376.235	2.7951
	(2,1,0)	570.378	373.247	3.06874
	(1,1,2)	524.071	358.294	3.19978
	(3,0,1)	543.562	358.125	3.29689

Table 8. Parameters of autoregressive integrated moving average models

Country and best model	**Parameters**	**Estimate**	**Standard Error**	**t-statistic**	**p-value**
Ukraine (1,1,0)	AR(1)	0.943844	0.0325404	29.0053	0.000000
Romania (3,2,2)	AR(3) MA(2)	-0.410628 -0.758911	0.103264 0.0916899	-3.97648 -8.27702	0.000122 0.000000
Republic of Moldova (3,2,2)	AR(3)	-0.162489	10.6563	-0.0152482	0.987860
	MA(2)	0.341459	26.5106	0.0128801	0.989746
Serbia (3,1,1)	AR(3)	0.241924	1.06252	0.227689	0.820282
	MA(1)	-0.572339	2.98064	-0.192018	0.848058
Bulgaria (1,0,3)	AR(1)	1.02769	0.00227845	451.048	0.000000
	MA(3)	-0.267346	0.0937488	-2.85172	0.005128
Hungary	AR(1)	-0.401032	0.0836831	-4.79227	0.000005
USA (1,1,0)	AR(1)	0.99441	0.0217047	45.8154	0.000000
Brazil (0,2,1)	MA(1)	0.758422	0.0565645	13.4081	0.000000
India (0,2,0)	no parameter(s)				

Table 8 shows the parameter estimates for the best models. The *p*-values of the associated with the parameters are less than 0.005, so the terms are considerably different from zero at the 95.0% CI. The fitted and predicted values are presented in Figure 13. As seen in Table 9, the next 14-day estimate of confirmed cases may be between 52,816-59,679 in Ukraine, 31,838-38,650 in Romania, and 18,836-21,601 in the Republic of Moldova, 17,639-21,313 in Serbia, 6931-10,000 in Bulgaria, 4225-4319 in Hungary, 3.10259×10^6-3.90611×10^6 in USA, 1.75087×10^6 - 2.24113×10^6 in Brazil, and 8.20308×10^5 - $116{,}489 \times 10^6$ in India, respectively.

Table 9. Prediction of total confirmed cases of COVID-19 for the next fourteen days according to autoregressive integrated moving average models with 95% confidence interval

Ukraine ARIMA (1,1,0)

		Lower 95%	**Upper 95%**
Period	Forecast	Limit	Limit
11-7-20	52,816.0	52,454.9	53,177.1
12-7-20	53,545.6	52,756.2	54,335.0
13-7-20	54,234.2	52,941.6	55,526.9
14-7-20	54,884.2	53,031.4	56,736.9
15-7-20	55,497.6	53,040.6	57,954.7
16-7-20	56,076.7	52,980.2	59,173.1
17-7-20	56,623.2	52,859.4	60,386.9
18-7-20	57,139.0	52,685.5	61,592.4
19-7-20	57,625.8	52,464.9	62,786.7
20-7-20	58,085.3	52,202.9	63,967.7
21-7-20	58,519.0	51,904.2	65,133.8
22-7-20	58,928.3	51,573.0	66,283.7
23-7-20	59,314.7	51,212.8	67,416.6
24-7-20	59,679.3	50,826.8	68,531.9

Romania ARIMA (3,2,2)

		Lower 95%	**Upper 95%**
Period	Forecast	Limit	Limit
11-7-20	31,838.2	31,694.9	31,981.5
12-7-20	32,261.6	32,023.7	32,499.5
13-7-20	32,719.8	32,386.2	33,053.5
14-7-20	33,267.3	32,849.6	33,685.1
15-7-20	33,872.9	33,362.9	34,383.0
16-7-20	34,469.6	33,845.7	35,093.5
17-7-20	35,003.7	34,237.5	35,769.8
18-7-20	35,477.4	34,549.7	36,405.1
19-7-20	35,938.6	34,844.5	37,032.8
20-7-20	36,438.8	35,182.0	37,695.7
21-7-20	36,992.8	35,575.4	38,410.2
22-7-20	37,572.2	35,988.4	39,156.0
23-7-20	38,132.9	36,369.6	39,896.1
24-7-20	38,650.7	36,693.2	40,608.1

Republic of Moldova ARIMA (3,2,2)

		Lower 95%	**Upper 95%**
Period	Forecast	Limit	Limit
11-7-20	18,836.6	18,715.5	18,957.8
12-7-20	19,037.2	18,806.5	19,268.0
13-7-20	19,259.3	18,940.0	19,578.5
14-7-20	19,478.9	19,081.4	19,876.5
15-7-20	19,691.4	19,211.9	20,170.8
16-7-20	19,901.5	19,332.3	20,470.6
17-7-20	20,113.1	19,448.2	20,778.0
18-7-20	20,326.1	19,561.3	21,090.8
19-7-20	20,539.0	19,670.8	21,407.3
20-7-20	20,751.6	19,775.9	21,727.3
21-7-20	20,964.0	19,876.7	22,051.2
22-7-20	21,176.4	19,973.7	22,379.1
23-7-20	21,389.0	20,067.1	22,710.8
24-7-20	21,601.5	20,156.8	23,046.2

Serbia ARIMA (3,1,1)

		Lower 95%	**Upper 95%**
Period	Forecast	Limit	Limit
11-7-20	17,639.6	17,554.5	17,724.8
12-7-20	17,927.0	17,765.1	18,088.8
13-7-20	18,214.2	17,956.8	18,471.6
14-7-20	18,501.8	18,135.5	18,868.0
15-7-20	18,786.8	18,300.4	19,273.2
16-7-20	19,072.0	18,454.5	19,689.5
17-7-20	19,355.4	18,597.4	20,113.5
18-7-20	19,638.3	18,730.5	20,546.1
19-7-20	19,919.9	18,854.1	20,985.8
20-7-20	20,200.7	18,968.8	21,432.6
21-7-20	20,480.4	19,075.0	21,885.8
22-7-20	20,759.2	19,173.2	22,345.2
23-7-20	21,036.9	19,263.5	22,810.3
24-7-20	21,313.7	19,346.4	23,281.0

Bulgaria ARIMA (1,0,3)

		Lower 95%	**Upper 95%**
Period	Forecast	Limit	Limit
11-7-20	6931.5	6865.22	6997.79
12-7-20	7179.18	7065.11	7293.25
13-7-20	7405.16	7239.7	7570.63
14-7-20	7610.22	7392.89	7827.55
15-7-20	7820.95	7559.81	8082.1
16-7-20	8037.53	7736.95	8338.1

Hungary ARIMA (1,2,0)

		Lower 95%	**Upper 95%**
Period	Forecast	Limit	Limit
11-7-20	4225.99	4180.36	4271.62
12-7-20	4233.59	4147.54	4319.64
13-7-20	4240.54	4102.74	4378.34
14-7-20	4247.75	4051.78	4443.73
15-7-20	4254.86	3993.94	4515.78
16-7-20	4262.01	3930.38	4593.64

17-7-20	8260.09	7922.85	8597.34
18-7-20	8488.83	8116.76	8860.89
19-7-20	8723.89	8318.28	9129.5
20-7-20	8965.47	8527.2	9403.73
21-7-20	9213.73	8743.44	9684.02
22-7-20	9468.87	8966.96	9970.78
23-7-20	9731.07	9197.81	10,264.3
24-7-20	10,000.5	9436.04	10,565.0

17-7-20	4269.14	3861.35	4676.93
18-7-20	4276.28	3787.29	4765.27
19-7-20	4283.42	3708.46	4858.38
20-7-20	4290.56	3625.12	4955.99
21-7-20	4297.69	3537.49	5057.89
22-7-20	4304.83	3445.76	5163.91
23-7-20	4311.97	3350.08	5273.86
24-7-20	4319.11	3250.6	5387.62

USA ARIMA (1,1,0)

		Lower 95%	**Upper 95%**
Period	Forecast	Limit	Limit
11-7-20	3.10259E6	3.08965E6	3.11554E6
12-7-20	3.1665E6	3.13762E6	3.19539E6
13-7-20	3.23006E6	3.18183E6	3.27828E6
14-7-20	3.29325E6	3.2228E6	3.3637E6
15-7-20	3.3561E6	3.26091E6	3.45129E6
16-7-20	3.41859E6	3.2964E6	3.54077E6
17-7-20	3.48073E6	3.3295E6	3.63196E6
18-7-20	3.54253E6	3.36035E6	3.7247E6
19-7-20	3.60398E6	3.3891E6	3.81885E6
20-7-20	3.66508E6	3.41586E6	3.91431E6
21-7-20	3.72585E6	3.44073E6	4.01097E6
22-7-20	3.78627E6	3.46379E6	4.10876E6
23-7-20	3.84636E6	3.48513E6	4.2076E6
24-7-20	3.90611E6	3.5048E6	4.30743E6

Brazil ARIMA (0,2,1)

		Lower 95%	**Upper 95%**
Period	Forecast	Limit	Limit
11-7-20	1.75087E6	1.73873E6	1.76302E6
12-7-20	1.78858E6	1.76922E6	1.80795E6
13-7-20	1.8263E6	1.79985E6	1.85275E6
14-7-20	1.86401E6	1.83027E6	1.89775E6
15-7-20	1.90172E6	1.86038E6	1.94306E6
16-7-20	1.93943E6	1.89016E6	1.98871E6
17-7-20	1.97714E6	1.91958E6	2.03471E6
18-7-20	2.01486E6	1.94866E6	2.08105E6
19-7-20	2.05257E6	1.9774E6	2.12774E6
20-7-20	2.09028E6	2.0058E6	2.17476E6
21-7-20	2.12799E6	2.03387E6	2.22211E6
22-7-20	2.16571E6	2.06163E6	2.26978E6
23-7-20	2.20342E6	2.08907E6	2.31776E6
24-7-20	2.24113E6	2.11621E6	2.36605E6

India ARIMA (0,2,0)

		Lower 95%	**Upper 95%**
Period	Forecast	Limit	Limit
11-7-20	820,308	819,036	821,580
12-7-20	846,814	843,969	849,659
13-7-20	873,320	868,560	878,080
14-7-20	899,826	892,858	906,794
15-7-20	926,332	916,897	935,767
16-7-20	952,838.	940,702	964,974
17-7-20	979,344	964,291	994,397
18-7-20	1.00585E6	987,679	1.02402E6
19-7-20	1.03236E6	1.01088E6	1.05383E6
20-7-20	1.05886E6	1.0339E6	1.08382E6
21-7-20	1.08537E6	1.05675E6	1.11399E6
22-7-20	1.11187E6	1.07944E6	1.14431E6
23-7-20	1.13838E6	1.10197E6	1.17479E6
24-7-20	1.16489E6	1.12435E6	1.20542E6

In the present study using autoregressive integrated moving average, the best model forecast for future data is given by a parametric model relating the most recent data value to previous data values and previous noise, or residuals in this context. The output summarizes the statistical significance of the terms in the forecasting model. Terms with *p*-values less than 0.05 are statistically significantly different from zero at the 95.0% CI. The *p*-value for the AR(x) or term is less than 0.05, so it is significantly different from 0. The *p*-value for the MA(x) term is less than 0.05, so it is significantly different from 0. When the trend is increasing, in order to obtain a linearity or central trend, the model also chooses q. The estimated standard deviation (SD) of the input white noise depends on the best model that was selected during the simulations performed.

According to our knowledge, this would be the first study in the literature to date. The idea of a cluster of nations and the rate of the spread between them is novel. This is also the first study to

address the situation of the most affected nations globally. The COVID-19 pandemic in Ukraine, Romania, the Republic of Moldova, Serbia, Bulgaria, Hungary, USA, Brazil, and India is reviewed, and the ongoing trend and extent of the outbreak estimated by the autoregressive integrated moving average model.

Most of the relevant studies in the literature evaluate the situation from western and southern Asia. Reports regarding the status of Europe are elusive for unknown reasons, and, as a consequence, Europe gradually became the second mainland (Table 10).

Table 10. Studies using distinct statistical approaches to predict COVID-19 spread

Disease	Method(s)	Reference
COVID-19	Hybrid ARIMA-WBF	[329]$
	SutteARIMA	[330]*
	Seasonal ARIMA	[331]*
	ARIMA NARNN LSTM	[332]*
	ARIMA	[333]*
	ARIMA	[334]$
	ARIMA	[335]$
	ARIMA	[336]$
	ARIMA HWAAS TBAT Facebook's Prophet DeepAR N-Beats	[337]$

Effective strategies are now all more imperative to control the spreading of COVID-19. Thus, estimating epidemiological trends is crucial for the allocations of medical resources and production activities.

Among the most effective measures turns out to be quarantine. Chintalapudi et al., discussed the beneficial impact lockdown had within the Italian population in terms of transmissibility. A data-driven model analysis demonstrated a decrement up to 35% of total registered cases, concomitantly with an increase up to 66% of recovered cases after lockdown and self-isolation. The accuracy of these two parameters was 93.75 and 84.4%, respectively [331].

This tendency of regression proved to be true according to the results obtained by another group of authors. The accuracy of six performance metric models has been tested. Long short-term memory (LSTM) was found to be the most accurate during the study, perspective predictions within the next two weeks being made. Thus, a slight decrease in the number of the total cumulative cases was expected [332].

These observations are strengthened by the results of Papastefanopoulos et al., [337]. Six different time series approaches were utilized to test the accuracy concerning the COVID-19 outbreak for the top ten most affected countries. Machine learning time series methods were efficiently used to estimate the percentage of the population that would be affected.

By using a stochastic modified susceptible-exposed-infectious-recovered (SEIR) model and due to lack of effective pharmaceutical interventions against severe acute respiratory syndrome coronavirus 2, López et al., concluded that social confinement should remain in place for the next two months. Behavior, awareness, and immunity decay was attributed to 99% of the current wave. The gradual incorporation of up to 50% of daily working proportion should be also considered [338].

It has been shown recently that Black and South Asian people are more prone to infection and subsequently death than the rest. Age, being male, deprivation, diabetes, asthma, and numerous other medical conditions were found to be risk factors following the analysis of a cohort consisting of 17,278,392 UK individuals [339].

According to the latest reports by the WHO, if all social restrictions are not respected, humanity will face a second wave of infections much more severe than the previous one [334]. Most certainly,

governments' internal politics and capability in managing the current situation would be definitory during this temporary crisis [330,333–335].

Assuming that 20% of the population of each country in the US will be infected, age-specific mortality patterns show that certain counties will probably be heavily affected. These findings suggest the adequate allocation of the medical care resources per capita needed to outside communities to restrain the spread [340].

Chakraborty et al., revealed that to people over the age of 65 should be paid more attention, which is why intensive care and social isolation are recommended in their case [329]. In addition, the authors suggest that the lockdown period must be extended, concurrent with increasing the number of beds in medical centers.

Furthermore, Demongeot et al., presented a new perspective regarding the important role temperature has on COVID-19 spread, reflected by the total number of active cases. It seems that high temperature directly reduces contagion rates, but this does not mean seasonal temperature could not support the later reappearance following the usage of time series methods [336].

Forecasting the prevalence of a disease is crucial for health departments to create an optimum environment and conditions for patients. As has been presented throughout this manuscript, time series models play an important role in disease prediction. In this study, ARIMA time series models were successfully applied to estimate the overall prevalence of COVID-19 in nine countries, six of them being neighbors, while the other three are the most affected today

Personal contribution - published papers:

Ilie, O.-D.; Ciobica, A.; **Doroftei**, **B**. Testing the Accuracy of the ARIMA Models in Forecasting the Spreading of COVID-19 and the Associated Mortality Rate. *Med.* ***2020***, *56*, 566. **IF: 2.430**

Aim of the study

Unlike the other studies conducted, the present study aims to estimate COVID-19 cases through autoregressive integrated moving average using two distinct statistical software (IBM SPSS and STATGRAPHICS) in order to test their reliability and accuracy. It also aims to present the evolution of the mortality rate in Romania considering the high, almost double reports between the number of positive cases/deaths in the last thirty days compared to the same intervals of the previous months.

Material and methods

Data

The daily prevalence data of COVID-19 was taken from The Ministry of Internal Affairs of Romania (https://www.mai.gov.ro), and compared to the figures reported by the WHO (https://covid19.who.int/). MS Excel was used to build a time-series database.

Even though the first case in Romania was reported back on February 27, we decided the following: (1) in order to test the accuracy of the autoregressive integrated moving average models, the established interval was divided into small (1 month) subdivisions with fourteen days forecast of the next month and comparing the numbers reported daily by the Romanian Government and WHO; (2) to perform a forecast from the so-called point zero (February 27) until August 31, with an additional fourteen-day forecast.

Descriptive statistics of the COVID-19 data for the established intervals (March 1 – March 31, April 1 – April 30; May 1 – May 31; June 1 – June 30; July 1 – July 31, August 1 – August 31, and February 27 – August 31) are summarized in Table 11. The situation in Romania at the end of AugustI was as follows: 85,833 confirmed cases and 3,539 deaths. At least thirty observations are recommended for an optimum autoregressive integrated moving average model [323].

Table 11. Descriptive statistics on the prevalence (a) and incidence (b) of COVID-19 in Romania

(a) Prevalence							
Interval	Mean	SE Mean	St. Dev	Minimum	Maximum	Skewness	Kurtosis
March	482.866	118.415	648.588	3	2245	1.49	1.21
April	7603.551	540.324	2909.737	2738	12,240	−0.03	−1.23

May	16,502.933	346.883	1899.957	12,732	19,257	−0.37	−0.90
June	22,776.689	427.610	2302.754	19,517	26,970	0.31	−1.16
July	36,874.3	1287.582	7052.379	27,746	50,886	0.61	−0.94
August	70,602.366	1930.889	10,575.917	53,186	87,540	−0.03	−1.19
March 1 – August 31	25,840.071	1751.969	23,700.201	3	87,540	1.04	0.17

(b) Incidence							
Interval	Mean	SE Mean	St. Dev	Minimum	Maximum	Skewness	Kurtosis
March	74.733	17.058	93.434	0	308	1.33	0.69
April	337.241	16.016	86.250	190	523	0.31	−0.38
May	223	14.369	78.704	124	431	1.08	0.59
June	261.103	16.507	88.896	119	460	0.40	−0.39
July	786.333	59.450	325.623	250	1356	0.19	−1.28
August	1180.966	42.478	232.664	733	1504	−0.63	−0.85
March 1 – August 31	478.344	31.352	424.128	0	1504	1.03	−0.24

The data set was used to conduct and analyze a case estimation model with the potential benefit of being able to predict the further evolution of COVID-19 in Romania. A time-series containing at least 45 data points was used to predict severe acute respiratory syndrome coronavirus 2 prevalence in Romania over the following two weeks with a 95% CI.

Initially, the outbreak did not affect Romania significantly, but starting from July 23, the number of new positive cases exceeded 1,000. Since then, days with <1,000 new cases per day were only August 4, 11, 18, 24, 25, and the highest number was reported on August 28, when 1,504 new cases and 38 deaths were confirmed.

The autoregressive integrated moving average model

A time-series, as the name suggests, is just a succession of data points indexed in a time order [324] dedicated to generating statistical data. More precisely, are used to perform predictions of values of a series [325], autoregressive integrated moving average becoming a simple-to-use algorithm since it was introduced in the 1970s [323]. Autoregressive integrated moving average is preferred to the detriment of other models due to the fact it takes into account all (in)dependent variances. Nevertheless, beyond fitting for a large sphere of data, through seasonality to cyclicity a temporal dependency can be modeled.

In summary, autoregressive integrated moving average technique is used for tracking linear tendencies, the entire concept constituting a mixture or being denoted by three orderly parameters. Non-seasonal autoregressive integrated moving average's parameters AR(p) (auto regression) represents the order of autoregression, MA(q) (moving average) the order of moving average, whereas I(d) is the degree of difference.

Viewed or described as a time-series, Yt represents a succession of independent arguments on the basis of a time t [341]. A deterministic/stochastic time-series could be explained by the following function, Yt = $f/X(t)$, where X is just a random variable. Thus, AR(p) (Equations (1a) and (1b)) predict the future value based on previous p-time observations as inputs, θ or Φ is the multiplying coefficient, ε_t or ω is the random error or white noise at a time t and μ, the mean of a series. In cases of a stationary time-series, the average of the ε_t or ω_t is 0, the variance being noted as σ^2:

$$Y_t = \alpha + \Phi_1 Y_{t-1} + \Phi_2 Y_{t-2} + \cdots + \Phi_p Y_{t-p} + \varepsilon_t \quad (1a)$$

or

$$Y_t = \mu + \sum_{i=1}^{p} (\Phi_i Y_{t-i}) + \omega_t \quad (1b)$$

Here, δ or α have the same value = constant. The polynomial's MA(q) (Equation 2a and 2b) time-series as a q^{th} degree can be found such as follows:

$$Y_t = \mu + \varepsilon_t + \theta_1 \varepsilon_{t-1} + \theta_2 \varepsilon_{t-2} + \cdots + \theta_q \varepsilon_{t-q} \quad (2a)$$

or

$$Y_t = \mu + \sum_{j=1}^{q} (\theta_j \omega_{t-1}) + \omega_t \quad (2b)$$

Therefore, AR(*p*)MA(*q*)'s expression is obtained by combining *p* and *q*, mathematically being represented in Equation 3a and 3b [342].

$$Y_t = \delta + \Phi_1 Y_{t-1} + \cdots + \Phi_p Y_{t-p} + \varepsilon_t + \theta_1 \varepsilon_{t-1} + \cdots + \theta_q \varepsilon_{t-q} \quad (3a)$$

or

$$Y_t = \mu + \sum_{i=1}^{p} (\Phi_i Y_{t-i}) + \sum_{j=1}^{q} (\theta_j \omega_{t-j}) + \omega_t \quad (3b)$$

On the other hand, there are also circumstances when the time-series is not stationary. In such cases, it should be verified if this condition is satisfied or not; if not, it can be made stationary by adding another variable *d*. Once ΔY "take over" Yt's non-stationary differences, ΔY can be explained as follows: (Equation 4), with *L* representing the likelihood of the data.

$$\Delta Y_t = Y_t - Y_{t-1} = Y_t - LY_t = Y_t' \quad (4)$$

For testing the accuracy of our model, we analyzed the performance of three factors known under the name of root mean square error, mean absolute error and mean absolute percentage error (Equations 5,6,7).

$$MAE = \frac{1}{n} \sum_{i=1}^{n} \left| Y_i - \widehat{Y_i} \right| \quad (5)$$

$$MAPE = \frac{100}{n} \, x \sum_{i=1}^{n} \left| \frac{Y_i - \widehat{Y_i}}{Y_i} \right| \quad (6)$$

$$RMSE = \sqrt{\sum_{i=1}^{n} \frac{(\widehat{Y_i} - Y_i)\text{^}2}{n}} \quad (7).$$

For congruity, mean absolute error, mean absolute percentage error, and mean absolute percentage error's values must be low, all analyses being performed using STATGRAPHICS Centurion (v.18.1.13) and IBM SPSS (v.20.0.0) software with a statistically significant levels of $p<0.05$.

Mortality rate

We collected data aiming to determine the mortality rate depending on the sex of each individual, the median age ranging between <10 as the minimum and >80 as the maximum limit of people who have died, who had associated comorbidities, and were hospitalized in intensive care units (ICUs) between the established intervals, using Excel software. We were able to collect data for a period of several months up to June 11 for sex, median age, and associated comorbidities, and up to March 17 for intensive care unit patients. We encountered certain limitations: the figures related to the sex of patients, the median age, the associated comorbidities, and at intensive care unit were incomplete as a consequence of lack of data management from the Romanian government during this pandemic.

Results

Building an autoregressive integrated moving average model for any given time-series involves the checking of four steps: assessment of the model, estimation of parameters, diagnostic checking, and prediction. The first, which is otherwise imperative, is to verify if the mean, variance, and autocorrelation of the time-series are consistent throughout the established interval [327]. Therefore, two-time-series plots, autocorrelation function, and partial autocorrelation function (Figure 14) graphs

were generated to test the seasonality and stationarity. Autocorrelation function is a statistical metric that determines whether the prior values are related to the latest values of not, while partial autocorrelation function the value of the correlation coefficient between its time lag and the variable [328]. Both are imperative in detecting misspecification, the model performance being measured by Akaike information criteria expression, and the bayesian information criterion of schwarz (BIC) [343]. Estimated autocorrelations for Romania are presented in Figure 14; the straight lines indicate the limit of two standard deviations and the bars that extend beyond the lines suggest statistically meaningful autocorrelations.

(a) STATGRAPHICS Centurion (v.18.1.13)

ACF (March)

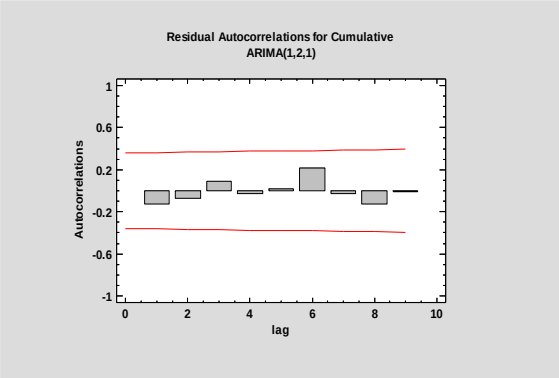

PACF (March)

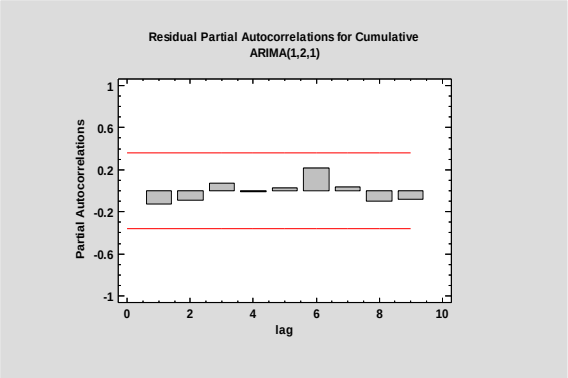

ACF (April)

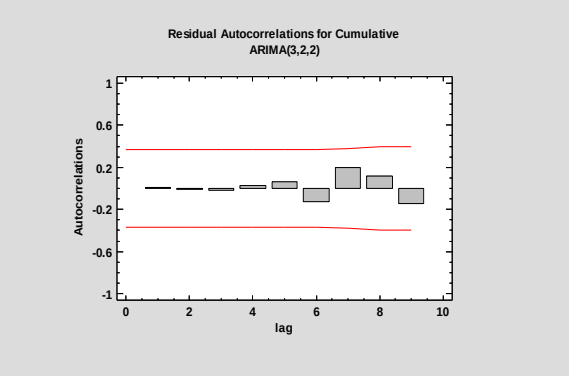

PACF (April)

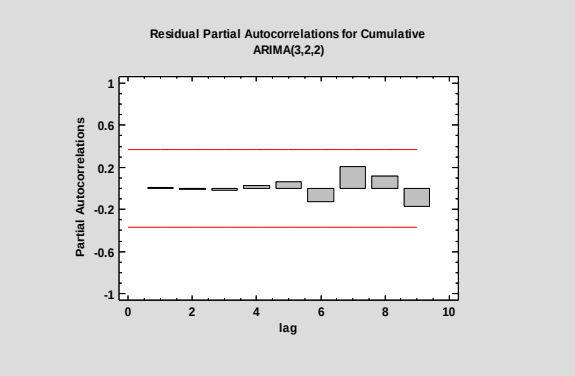

ACF (May)

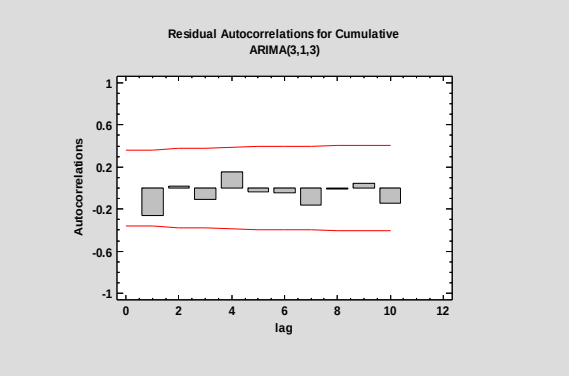

PACF (May)

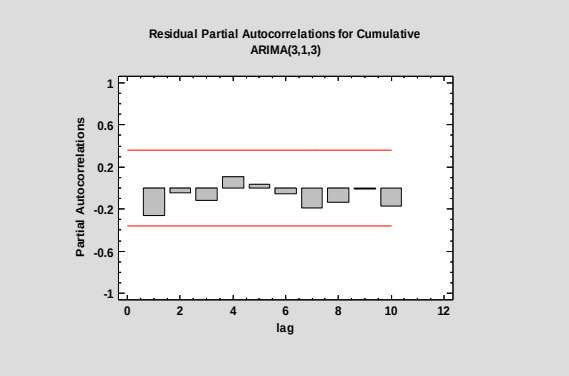

ACF (June)

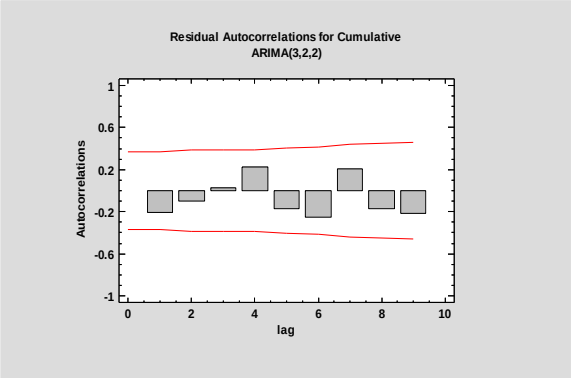

PACF (June)

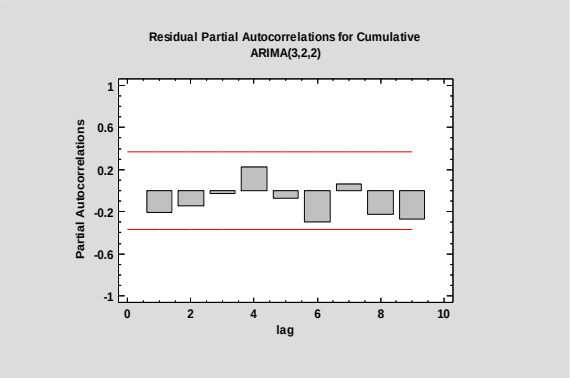

ACF (July)

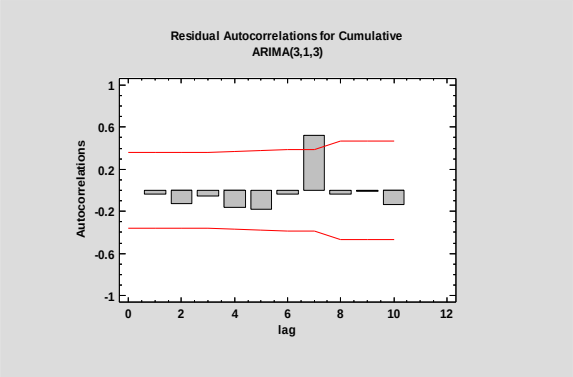

PACF (July)

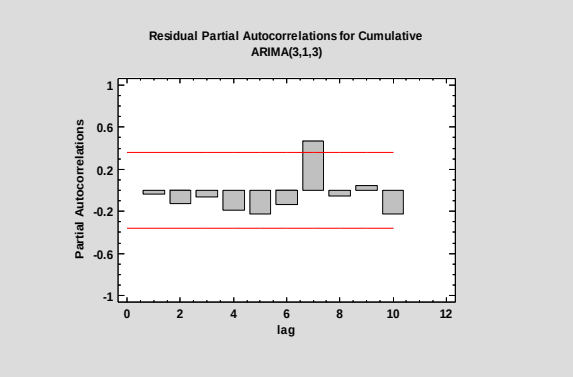

ACF (August)

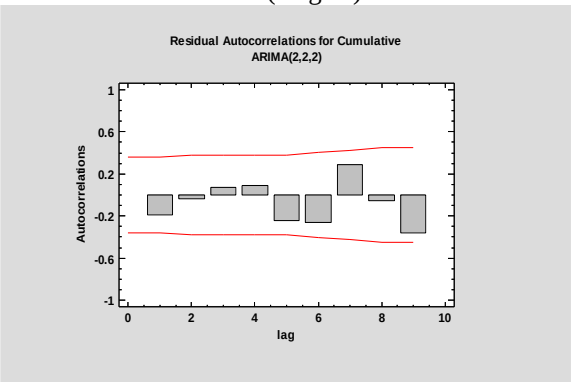

PACF (August)

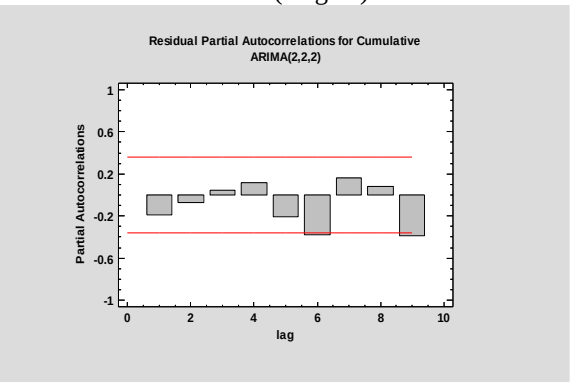

ACF (March–August)

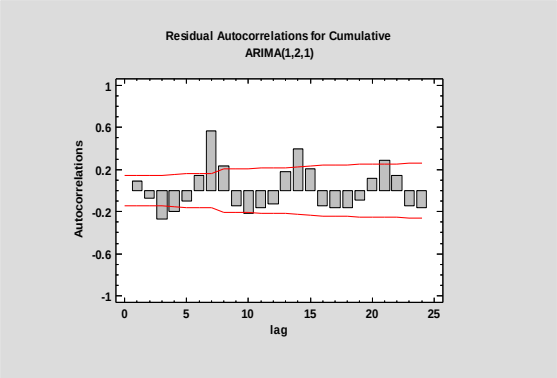

PACF (March–August)

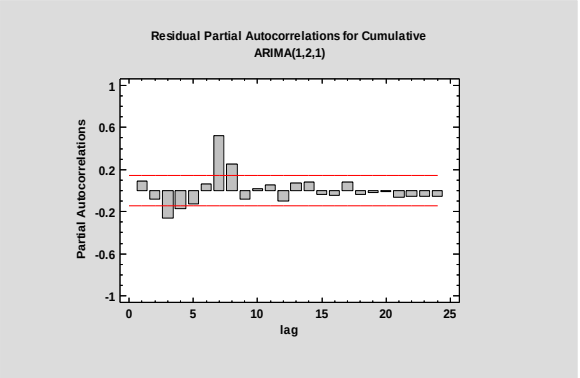

(b) IBM SPSS (v.20.0.0)

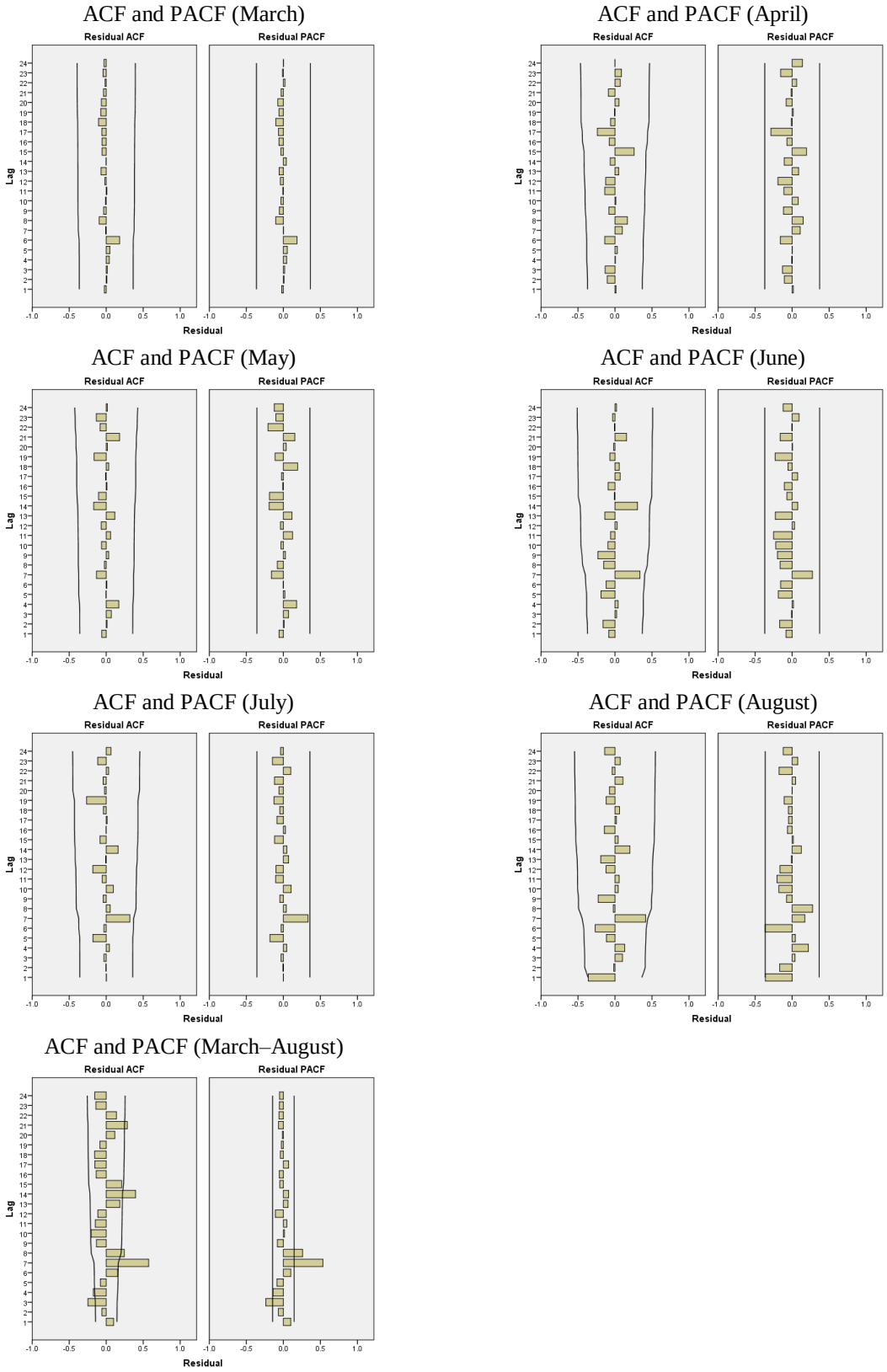

Figure 14. The estimated ACF and PACF graphs to predict the epidemiological trend of COVID-19 in Romania performed by using (a) STATGRAPHICS Centurion (v.18.1.13) and (b) IBM SPSS (v.20.0.0)

Additionally, a series of autoregressive integrated moving average models were created, and their performances were compared using various statistical tools. All statistical procedures were performed on the transformed COVID-19 data. Autoregressive integrated moving average models

with the lowest MAPE values were considered the most optimum model. Among the tested models, ARIMA (1,2,1), ARIMA (3,2,2), ARIMA (3,1,3), ARIMA (3,2,2), ARIMA (3,1,3), ARIMA (2,2,2), ARIMA (1,2,1) were chosen as the best models for Romania. The models where COVID-19 data fitted are presented in Figure 14 and Table 12 and Table 13 with a minimum $MAPE_{March}$ = 9.3225, $MAPE_{April}$ = 0.975287, $MAPE_{May}$ = 0.227675, $MAPE_{June}$ = 0.161412, $MAPE_{July}$ = 0.243285, $MAPE_{August}$ = 0.163873, $MAPE_{March-August}$ = 2.29175, $MAPE_{March}$ = 57.505, $MAPE_{April}$ = 1.152, $MAPE_{May}$ = 0.259, $MAPE_{June}$ = 0.185, $MAPE_{July}$ = 0.307, $MAPE_{August}$ = 0.194, and $MAPE_{March-August}$ = 6.013, respectively.

Table 12. Comparison of tested ARIMA models

(a) STATGRAPHICS Centurion (v.18.1.13)				
Romania	**Model**	**RMSE**	**MAE**	**MAPE**
March	(1,2,1)	40.2064	21.7726	9.3225
	(2,2,0)	40.1344	21.8332	9.33149
	(2,1,0)	37.1349	22.3392	9.42158
	(3,2,0)	40.7137	22.252	9.50679
	(3,0,0)	36.317	21.4381	9.58606
April	(3,2,2)	84.4845	62.4813	0.975287
	(3,2,3)	91.4283	64.3356	0.978607
	(3,2,1)	86.0235	63.5418	0.988232
	(1,2,3)	86.1254	66.3094	1.03015
	(0,2,3)	84.8321	66.818	1.03804
May	(3,1,3)	55.1218	35.4972	0.227675
	(3,2,3)	51.5543	37.7316	0.233695
	(3,2,2)	52.2601	37.5565	0.235246
	(3,2,1)	52.0651	37.7596	0.235816
	(3,2,0)	51.9334	38.9065	0.243301
June	(3,2,2)	53.3883	36.8425	0.161412
	(3,2,3)	55.042	36.8814	0.161561
	(3,1,3)	66.319	45.2191	0.195068
	(2,1,3)	66.8927	47.8626	0.207124
July	(3,1,3)	117.982	87.1512	0.243285
	(2,1,1)	113.198	88.1797	0.24369
	(2,1,2)	115.679	88.7863	0.245774
	(1,1,2)	115.307	92.5001	0.256055
August	(2,2,2)	153.804	113.314	0.163873
	(3,2,2)	155.701	114.742	0.164574
	(3,2,3)	159.39	115.195	0.165348
March–August	(1,2,1)	121.674	85.2619	2.29175
	(3,2,3)	118.411	82.2194	2.37771
	(1,2,3)	118.36	82.5649	2.37918
	(3,2,1)	113.778	80.2205	2.40063
	(3,2,0)	121.301	84.6413	2.41403

(b) IBM SPSS (v.20.0.0)				
Romania	**Model**	**RMSE**	**MAE**	**MAPE**
March	(1,2,1)	38.127	24.651	57.505
April	(3,2,2)	96.089	68.365	1.152
May	(3,1,3)	68.403	39.996	0.259
June	(3,2,2)	58.588	41.854	0.185
July	(3,1,3)	156.476	106.572	0.307
August	(2,2,2)	179.309	129.350	0.194
March–August	(1,2,1)	121.054	85.524	6.013

Table 13. Parameters of ARIMA models

(a) STATGRAPHICS Centurion (v.18.1.13)					
Romania	**Parameters**	**Estimate**	**Standard Error**	***t*-Statistic**	***p*-Value**
March (1,2,1)	AR(1)	−0.865514	0.194131	−4.45841	0.000131
	MA(1)	−0.209212	0.291261	−0.718298	0.478744
April (3,2,2)	AR(3)	−0.329312	0.225307	−1.46161	0.157377
	MA(2)	−0.528086	0.247375	−2.13475	0.043660
May (3,1,3)	AR(3)	0.625887	0.145922	4.28918	0.000253
	MA(3)	0.570657	0.0544548	10.4795	0.000000
June (3,2,2)	AR(3)	−0.312216	0.209998	−1.48676	0.150660
	MA(2)	−0.964198	0.0269271	−35.8077	0.000000
July (3,1,3)	AR(3)	−0.560219	0.258752	−2.16508	0.040545
	MA(3)	−0.0478648	0.274587	−0.174315	0.863080
August (2,2,2)	AR(2)	−0.826566	0.112664	−7.33655	0.000000
	MA(2)	−0.782937	0.171731	−4.5591	0.000117
March–August (1,2,1)	AR(1)	0.479999	0.122096	3.93133	0.000120
	MA(1)	0.781228	0.0765947	10.1995	0.000000

(b) IBM SPSS (v.20.0.0)						
ARIMA Model Parameters						
					Estimate	Standard Error
Cumulative-Model (March)	Cumulative	No Transformation	Constant		8.881	3.986
			AR	Lag 1	−0.740	0.206
			Difference		2	
			MA	Lag 1	0.037	0.287
					t-statistic	*p*-value
Cumulative-Model (March)	Cumulative	No Transformation	Constant		2.228	0.035
			AR	Lag 1	−3.595	−0.001
			Difference			
			MA	Lag 1	0.130	0.898
					Estimate	Standard Error
Cumulative-Model (April)	Cumulative	No Transformation	Constant		−0.902	1.468
			AR	Lag 1	0.210	0.486
				Lag 2	−0.216	0.203
				Lag 3	−0.268	0.257
			Difference		2	
			MA	Lag 1	1.527	22.293
				Lag 2	−0.528	11.600
					t-statistic	*p*-value
Cumulative-Model (April)	Cumulative	No Transformation	Constant		−0.615	0.545
			AR	Lag 1	0.432	0.670
				Lag 2	−1.065	0.298
				Lag 3	−1.042	0.309
			Difference			
			MA	Lag 1	0.069	0.946
				Lag 2	−0.046	0.964
					Estimate	Standard Error
Cumulative-Model (May)	Cumulative	No Transformation	Constant		216.917	46.423
			AR	Lag 1	−0.013	0.498
				Lag 2	0.252	0.348
				Lag 3	0.480	0.348
			Difference		1	
			MA	Lag 1	−0.641	3.924
				Lag 2	−0.258	4.043
				Lag 3	0.591	3.576

					t-statistic	*p*-value
Cumulative-Model (May)	Cumulative	No Transformation	Constant		4.673	0.000
			AR	Lag 1	−0.026	0.980
				Lag 2	0.725	0.476
				Lag 3	1.381	0.181
			Difference			
			MA	Lag 1	−0.163	0.872
				Lag 2	−0.064	0.950
				Lag 3	0.165	0.870
					Estimate	Standard Error
Cumulative-Model (June)	Cumulative	No Transformation	Constant		8.194	1.482
			AR	Lag 1	0.161	0.487
				Lag 2	−0.159	0.291
				Lag 3	−0.451	0.234
			Difference		2	
			MA	Lag 1	0.914	4.922
				Lag 2	0.080	0.849
					t-statistic	*p*-value
Cumulative-Model (June)	Cumulative	No Transformation	Constant		5.529	0.000
			AR	Lag 1	0.332	0.743
				Lag 2	−0.549	0.589
				Lag 3	−1.928	0.067
			Difference			
			MA	Lag 1	0.186	0.854
				Lag 2	0.094	0.926
					Estimate	Standard Error
Cumulative-Model (July)	Cumulative	No Transformation	Constant		837.899	505.059
			AR	Lag 1	0.274	20.176
				Lag 2	0.753	3.824
				Lag 3	−0.087	15.011
			Difference		1	
			MA	Lag 1	−0.629	20.192
				Lag 2	0.259	14.442
				Lag 3	−0.003	3.383
					t-statistic	*p*-value
Cumulative-Model (July)	Cumulative	No Transformation	Constant		1.659	0.111
			AR	Lag 1	0.014	0.989
				Lag 2	0.197	0.846
				Lag 3	−0.006	0.995
			Difference			
			MA	Lag 1	−0.031	0.975
				Lag 2	0.018	0.986
				Lag 3	−0.001	0.999
					Estimate	Standard Error
Cumulative-Model (August)	Cumulative	No Transformation	Constant		−4.351	1.253
			AR	Lag 1	1.120	0.139
				Lag 2	−0.832	0.107
			Difference		2	
			MA	Lag 1	1.978	6.107
				Lag 2	−0.995	6.084
					t-statistic	*p*-value
Cumulative-Model (August)	Cumulative	No Transformation	Constant		−3.474	0.002
			AR	Lag 1	8.077	0.000
				Lag 2	−7.804	0.000
			Difference			

			MA	Lag 1	0.324	0.749
				Lag 2	−0.164	0.871
					Estimate	Standard Error
Cumulative-Model (March–August)	Cumulative	No Transformation	Constant		5.885	3.318
			AR	Lag 1	0.501	0.126
			Difference		2	
			MA	Lag 1	0.820	0.084
					t-statistic	*p*-value
Cumulative-Model (March–August)	Cumulative	No Transformation	Constant		1.773	0.078
			AR	Lag 1	3.985	0.000
			Difference			
			MA	Lag 1	9.712	0.000

In Table 13, the parameter estimates for the best models are presented. The fitted and predicted values are presented in Figure 15. As seen in Table 14 for both software, the next two weeks estimate of confirmed cases may be between 2450.74-5673.29, 12,616.5-16,896.3, 19,400.9-21,280.5, 27,404.9-32,340.9, 52,247.6-75,717.2, 88,483.4-103,777, 88,427.4-101,440, respectively through STATGRAPHICS Centurion (v.18.1.13). For IBM SPSS (v.20.0.0), the forecast for the next two weeks is as follows: 2478.78-6715.00, 12,599.76-16,756.08, 19,412.18-21,910.55, 27,405.69-33,181.42, 52,168.29-67,467.42, 88,444.38-103,059.41, and 88,451.83-102,656.81 for March, April, May, June, July, August, and March–August.

(a) STATGRAPHICS Centurion (v.18.1.13)

March (1,2,1)

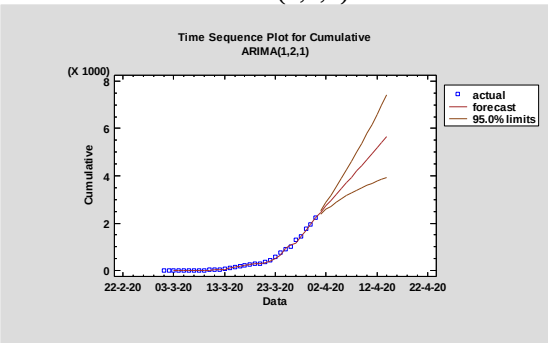

April (3,2,2)

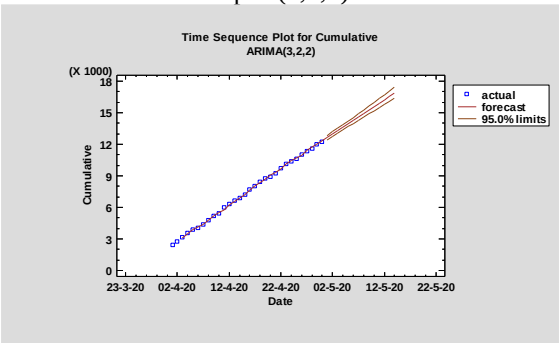

May (3,1,3)

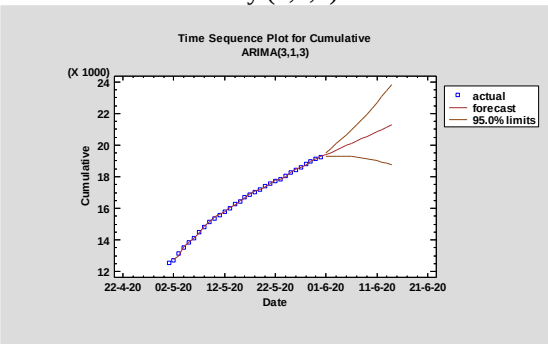

June (3,2,2)

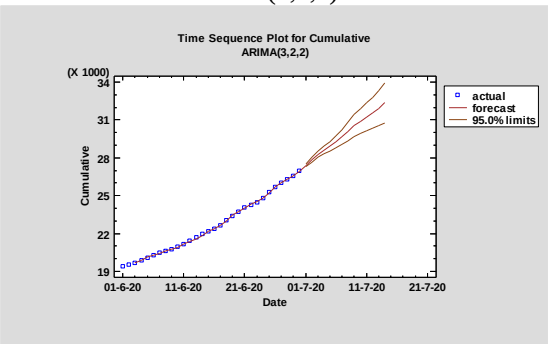

July (3,1,3)

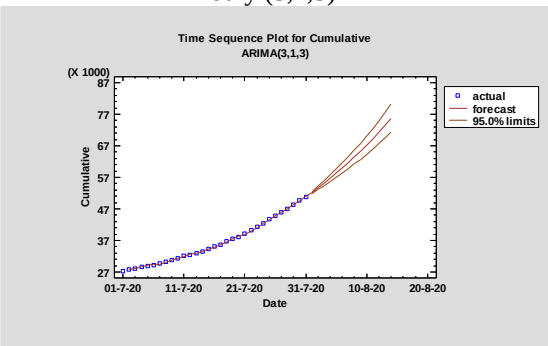

August (2,2,2)

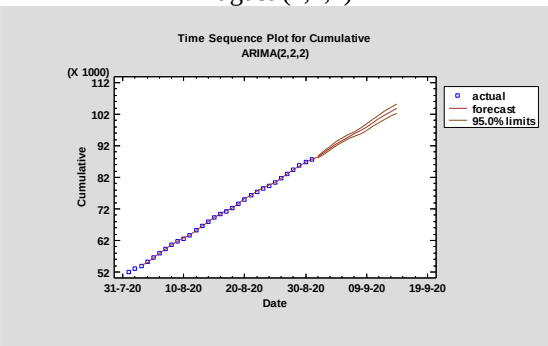

March–August (1,2,1)

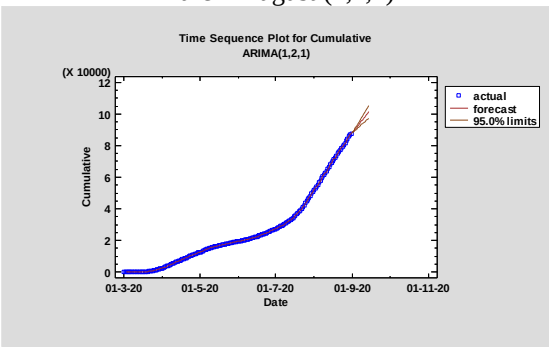

(b) IBM SPSS (v.20.0.0)

March (1,2,1)

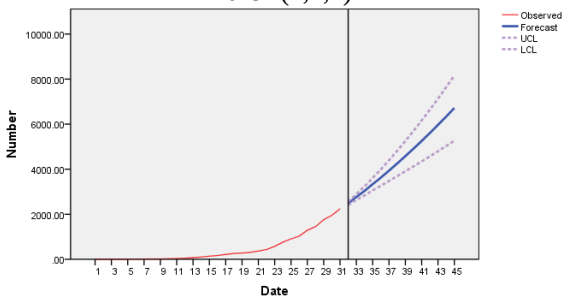

April (3,2,2)

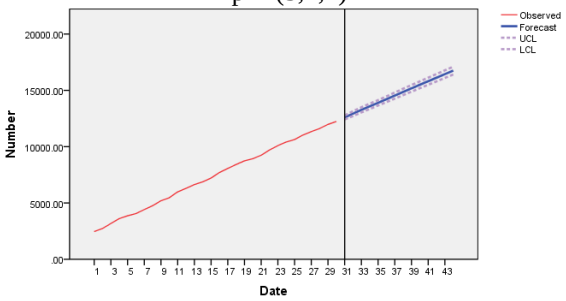

May (3,1,3)

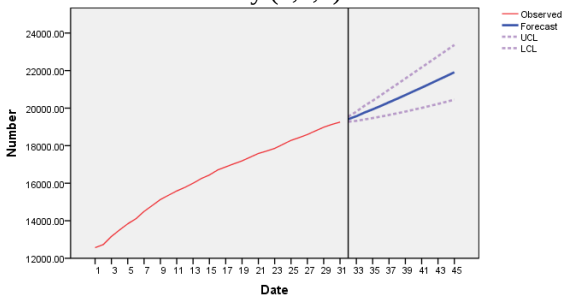

June (3,2,2)

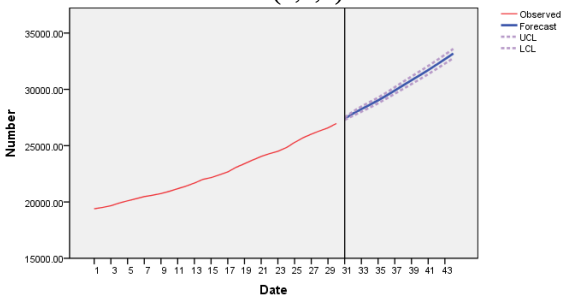

July (3,1,3)

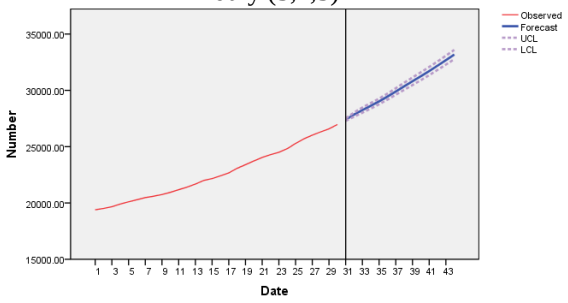

August (2,2,2)

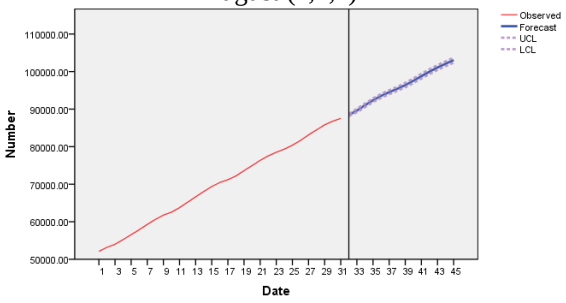

March – August (1,2,1)

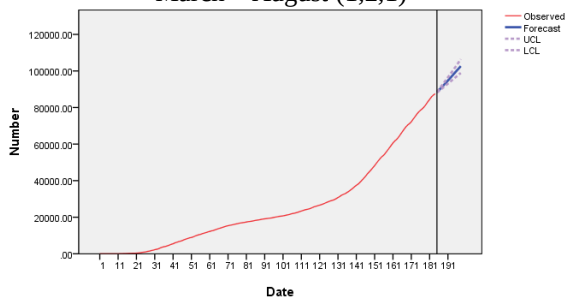

Figure 15. Time-series plots for the best ARIMA models through (a) STATGRAPHICS Centurion (v.18.1.13) and (b) IBM SPSS (v.20.0.0)

Table 14. Prediction of total confirmed cases of COVID−19 for the next two weeks through (a) STATGRAPHICS Centurion (v.18.1.13) and (b) IBM SPSS (v.20.0.0)

(a) STATGRAPHICS Centurion (v.18.1.13)

March (1,2,1)

		Lower 95%	*Upper 95%*
Period	*Forecast*	*Limit*	*Limit*
01-4-20	2450.74	2368.24	2533.23
02-4-20	2732.0	2593.82	2870.18
03-4-20	2947.89	2716.13	3179.66
04-4-20	3220.37	2900.32	3540.42
05-4-20	3443.87	3011.65	3876.09
06-4-20	3709.76	3166.05	4253.47
07-4-20	3938.96	3266.6	4611.32
08-4-20	4199.91	3397.23	5002.6
09-4-20	4433.39	3487.15	5379.63
10-4-20	4690.65	3597.86	5783.43
11-4-20	4927.32	3677.29	6177.34
12-4-20	5181.81	3770.81	6592.81
13-4-20	5420.88	3839.91	7001.84
14-4-20	5673.29	3918.22	7428.36

April (3,2,2)

		Lower 95%	*Upper 95%*
Period	*Forecast*	*Limit*	*Limit*
01-5-20	12,616.5	12,440.4	12,792.5
02-5-20	12,959.9	12,738.5	13,181.4
03-5-20	13,302.9	13,061.4	13,544.4
04-5-20	13,615.5	13,368.8	13,862.3
05-5-20	13,932.3	13,674.7	14,189.9
06-5-20	14,257.0	13,975.5	14,538.5
07-5-20	14,592.6	14,276.6	1,4908.7
08-5-20	14,927.5	14,579.7	15,275.3
09-5-20	15,257.2	14,883.3	15,631.0
10-5-20	15,582.2	15,184.3	15,980.1
11-5-20	15,907.6	15,482.8	16,332.4
12-5-20	16,235.9	15,779.8	16,692.0
13-5-20	16,566.2	16,076.4	17,056.0
14-5-20	16,896.3	16,372.8	17,419.8

May (3,1,3)

		Lower 95%	*Upper 95%*
Period	*Forecast*	*Limit*	*Limit*
01-6-20	19,400.9	19,280.2	19,521.5
02-6-20	19,533.0	19,286.3	19,779.8
03-6-20	19,689.2	19,296.5	20,081.9
04-6-20	19,831.8	19,307.7	20,355.9
05-6-20	19,971.4	19,290.8	20,651.9
06-6-20	20,122.2	19,270.7	20,973.7
07-6-20	20,265.2	19,240.9	21,289.5
08-6-20	20,408.1	19,194.8	21,621.5
09-6-20	20,556.2	19,143.4	21,968.9
10-6-20	20,699.9	19,081.8	22,318.0
11-6-20	20,844.3	19,009.0	22,679.7
12-6-20	20,991.0	18,929.9	23,052.1
13-6-20	21,135.4	18,841.3	23,429.4
14-6-20	21280.5	18744.1	23816.9

June (3,2,2)

		Lower 95%	*Upper 95%*
Period	*Forecast*	*Limit*	*Limit*
01-7-20	27,404.9	27,291.5	27,518.3
02-7-20	2,7860.4	27,673.0	28,047.7
03-7-20	28,267.6	28,019.4	28,515.8
04-7-20	28,608.4	28,307.9	28,908.9
05-7-20	28,916.8	28,551.9	29,281.8
06-7-20	29,253.3	28,792.0	29,714.6
07-7-20	29,652.8	29,060.9	30,244.7
08-7-20	30,097.5	29,360.4	30,834.6
09-7-20	30,533.1	29,658.3	31,407.9
10-7-20	30,914.6	29,916.3	31,912.9
11-7-20	31,243.0	30,126.4	32,359.6
12-7-20	31,562.8	30,317.0	32,808.5
13-7-20	31,924.0	30,526.8	33,321.1
14-7-20	32,340.9	30,772.3	33,909.5

July (3,1,3)

August (2,2,2)

		Lower 95%	*Upper 95%*
Period	*Forecast*	*Limit*	*Limit*
01-8-20	52,247.6	51,999.2	52,496.1
02-8-20	53,668.7	53,169.6	54,167.9
03-8-20	55,147.3	54,390.9	55,903.6
04-8-20	56,685.2	55,656.5	57,714.0
05-8-20	58,282.6	56,976.8	59,588.5
06-8-20	59,942.3	58,346.7	61,537.9
07-8-20	61,665.3	59,772.1	63,558.4
08-8-20	63,454.6	61,250.0	65,659.3
09-8-20	65,311.9	62,784.7	67,839.2
10-8-20	67,240.4	64,374.9	70,106.0
11-8-20	69,242.1	66,024.5	72,459.8
12-8-20	71,320.4	67,733.2	74,907.6
13-8-20	73,477.6	69,504.9	77,450.3
14-8-20	75,717.2	71,340.0	80,094.4

		Lower 95%	*Upper 95%*
Period	*Forecast*	*Limit*	*Limit*
01-9-20	88,483.4	88,163.3	88,803.4
02-9-20	89,735.8	89,186.2	90,285.4
03-9-20	91,171.6	90,521.1	91,822.0
04-9-20	92,553.1	91,883.1	93,223.0
05-9-20	93,723.4	93,050.4	94,396.4
06-9-20	94,707.0	94,020.1	95,393.9
07-9-20	95,660.3	94,899.8	96,420.7
08-9-20	96,734.6	95,825.9	97,643.3
09-9-20	97,966.8	96,901.4	99,032.2
10-9-20	99,272.2	98,093.1	100,451.
11-9-20	100,527.	99,273.2	101,781.
12-9-20	101,667.	100,347.	102,986.
13-9-20	102,721.	101,316.	104,126.
14-9-20	103,777.	102,249.	105,305.

March – August (1,2,1)

		Lower 95%	*Upper 95%*
Period	*Forecast*	*Limit*	*Limit*
01-9-20	88,427.4	88,187.3	88,667.5
02-9-20	89,378.4	88,905.1	89,851.7
03-9-20	90,359.9	89,641.2	91,078.7
04-9-20	91,356.1	90,382.1	92,330.1
05-9-20	92,359.3	91,120.4	93,598.2
06-9-20	93,365.8	91,851.8	94,879.9
07-9-20	94,374.0	92,574.3	96,173.7
08-9-20	95,383.0	93,286.8	97,479.2
09-9-20	96,392.3	93,988.7	98,796.0
10-9-20	97,401.8	94,679.8	100,124.
11-9-20	98,411.4	95,360.3	101,463.
12-9-20	99,421.1	96,030.1	102,812.
13-9-20	100,431.	96,689.5	104,172.
14-9-20	101,440.	97,338.6	105,542.

(b) IBM SPSS (v.20.0.0)							
Forecast							
Model		**Day 1**	**Day 2**	**Day 3**	**Day 4**	**Day 5**	**Day 6**
Cumulative-Model (March)	Forecast	2478.78	2771.81	3036.46	3337.56	3627.14	3940.69
	UCL	2557.11	2895.56	3237.39	3612.37	3992.87	4399.42
	LCL	2400.44	2648.06	2835.53	3062.74	3261.42	3481.96
Model		**Day 7**	**Day 8**	**Day 9**	**Day 10**	**Day 11**	**Day 12**
Cumulative-Model (March)	Forecast	4251.96	4580.37	4911.55	5256.13	5606.25	5967.72
	UCL	4814.73	5251.20	5698.58	6164.03	6641.61	7135.33
	LCL	3689.20	3909.55	4124.53	4348.24	4570.89	4800.11

Model		**Day 13**	**Day 14**
Cumulative-Model (March)	Forecast	6336.24	6715.00
	UCL	7641.78	8163.17
	LCL	5030.71	5266.84

Forecast							
Model		**Day 1**	**Day 2**	**Day 3**	**Day 4**	**Day 5**	**Day 6**
Cumulative-Model	Forecast	12,599.76	12,935.87	13,271.55	13,584.87	13,898.80	14,216.66

(April)	UCL	12,774.44	13,150.93	13,500.98	13,816.96	14,136.69	14,467.65
	LCL	12,425.08	12,720.81	13,042.12	13,352.78	13,660.91	13,965.67
Model		**Day 7**	**Day 8**	**Day 9**	**Day 10**	**Day 11**	**Day 12**
Cumulative-Model (April)	Forecast	14,540.05	14,862.45	15,181.23	15,496.84	15,811.68	16,126.86
	UCL	14,808.71	15,145.84	15,475.55	15,800.64	16,125.74	16,452.34
	LCL	14,271.39	14,579.05	14,886.92	15,193.03	15,497.61	15,801.38

Model		**Day 13**	**Day 14**
Cumulative-Model (April)	Forecast	16,441.99	16,756.08
	UCL	16,779.10	17,104.18
	LCL	16,104.88	16,407.98

Forecast

Model		**Day 1**	**Day 2**	**Day 3**	**Day 4**	**Day 5**	**Day 6**
Cumulative-Model (May)	Forecast	19,412.18	19,569.68	19,763.17	19,935.78	20,118.83	20,313.78
	UCL	19,543.30	19,816.82	20,130.38	20,397.32	20,688.05	20,989.84
	LCL	19,281.05	19,322.54	19,395.96	19,474.23	19,549.62	19,637.71
Model		**Day 7**	**Day 8**	**Day 9**	**Day 10**	**Day 11**	**Day 12**
Cumulative-Model (May)	Forecast	20,501.17	20,696.67	20,895.88	21,093.45	21,295.88	21,499.60
	UCL	21,277.17	21,576.47	21,877.30	22,173.28	22,473.47	22,773.08
	LCL	19,725.17	19,816.88	19,914.45	20,013.63	20,118.28	20,226.12

Model		**Day 13**	**Day 14**
Cumulative-Model (May)	Forecast	21,703.75	21,910.55
	UCL	23,071.27	23,369.65
	LCL	20,336.23	20,451.44

Forecast

Model		**Day 1**	**Day 2**	**Day 3**	**Day 4**	**Day 5**	**Day 6**
Cumulative-Model (June)	Forecast	27,405.69	27,851.25	28,248.97	28,627.75	29,018.52	29,447.71
	UCL	27,520.95	28,038.23	28,481.50	28,874.60	29,273.56	29,714.32
	LCL	27,290.42	27,664.28	28,016.44	28,380.90	28,763.48	29,181.10
Model		**Day 7**	**Day 8**	**Day 9**	**Day 10**	**Day 11**	**Day 12**
Cumulative-Model (June)	Forecast	29,901.63	30,359.87	30,809.40	31,257.55	31,716.79	32,193.86
	UCL	30,190.48	30,674.74	31,145.84	31,609.14	32,081.24	32,572.50
	LCL	29,612.78	30,045.00	30,472.95	30,905.96	31,352.35	31,815.21

Model		**Day 13**	**Day 14**
Cumulative-Model (June)	Forecast	32,684.53	33,181.42
	UCL	33,079.98	33,594.43
	LCL	32,289.08	32,768.41

Forecast

Model		**Day 1**	**Day 2**	**Day 3**	**Day 4**	**Day 5**	**Day 6**
Cumulative-Model (July)	Forecast	52,168.29	53,426.67	54,674.30	55,902.11	57,118.49	58,317.76
	UCL	52,449.73	54,031.51	55,633.07	57,264.85	58,911.15	60,573.52
	LCL	51,886.84	52,821.82	53,715.54	54,539.37	55,325.84	56,061.99
Model		**Day 7**	**Day 8**	**Day 9**	**Day 10**	**Day 11**	**Day 12**
Cumulative-Model (July)	Forecast	59,505.46	60,678.11	61,839.43	62,987.33	64,124.34	65,249.25
	UCL	62,244.36	63,923.34	65,606.40	67,292.68	68,979.84	70,666.96
	LCL	56,766.56	57,432.88	58,072.46	58,681.98	59,268.84	59,831.54

Model		**Day 13**	**Day 14**
Cumulative-Model (July)	Forecast	66,363.83	67,467.42
	UCL	72,352.60	74,035.96
	LCL	60,375.05	60,898.88

Forecast

Model		**Day 1**	**Day 2**	**Day 3**	**Day 4**	**Day 5**	**Day 6**
Cumulative-Model (August)	Forecast	88,444.38	89,634.01	91,015.67	92,372.04	93,537.29	94,506.51
	UCL	88,730.43	90,079.75	91,493.00	92,852.85	94,048.38	95,027.52
	LCL	88,158.32	89,188.27	90,538.35	91,891.23	93,026.19	93,985.50
Model		**Day 7**	**Day 8**	**Day 9**	**Day 10**	**Day 11**	**Day 12**
Cumulative-Model (August)	Forecast	95,412.10	96,406.37	97,549.71	98,783.13	99,990.33	101,090.16
	UCL	95,938.80	96,978.64	98,171.45	99,421.94	100,629.11	101,728.19
	LCL	94,885.41	95,834.09	96,927.97	98,144.32	99,351.54	100,452.13

Model		Day 13	Day 14
Cumulative-Model (August)	Forecast	102,088.51	103,059.41
	UCL	102,726.16	103,708.74
	LCL	101,450.85	102,410.08

Forecast							
Model		Day 1	Day 2	Day 3	Day 4	Day 5	Day 6
Cumulative-Model (March-August)	Forecast	88,451.83	89,445.12	90,482.12	91,543.96	92,621.15	93,708.98
	UCL	88,690.71	89,912.30	91,185.57	92,489.10	93,813.54	95,154.94
	LCL	88,212.96	88,977.94	89,778.67	90,598.81	91,428.77	92,263.03
Model		Day 7	Day 8	Day 9	Day 10	Day 11	Day 12
Cumulative-Model (March-August)	Forecast	94,805.08	95,908.24	97,017.89	98,133.72	99,255.59	100,383.41
	UCL	96,511.68	97,883.14	99,269.09	100,669.45	102,084.15	103,513.14
	LCL	93,098.47	93,933.34	94,766.69	95,598.00	96,427.02	97,253.68

Model		Day 13	Day 14
Cumulative-Model (March-August)	Forecast	101,517.16	102,656.81
	UCL	104,956.35	106,413.66
	LCL	98,077.97	98,899.95

Regarding the mortality rate, since June 11 until August 31 a total of 2,261 new patients were identified, of whom 1,356 (59.97%) were male and 905 (40.02%) were female. The most affected age group were people aged between 70 and 79 years, where severe acute respiratory syndrome coronavirus 2 caused the death of 709 people, followed by people between 60 and 69 years with 621 deaths and >80 with 526 deaths (Figure 16). On the other hand, a total of 405 people died, from which 260 had between 50 and 59 years, 104 between 40 and 49 years, 30 between 30 and 39 years, 10 between 20 and 29 years, 1 between 10 and 19 years, and 0 with less than 10 years old. From the total number of 2,261 people, 2,184 had comorbidities (96.6823%), and 77 did not. Also, since March 17, when the first 4 people were confirmed, the total number reported until August 31 was 506 (Figure 17).

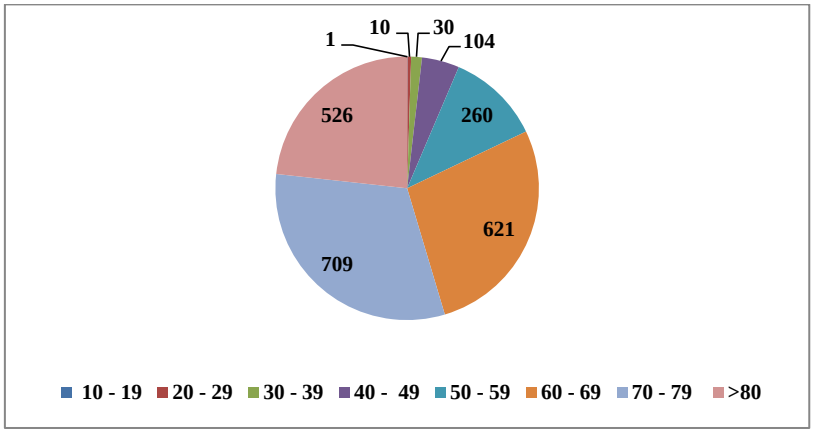

Figure 16. The number of deaths depending on the age group

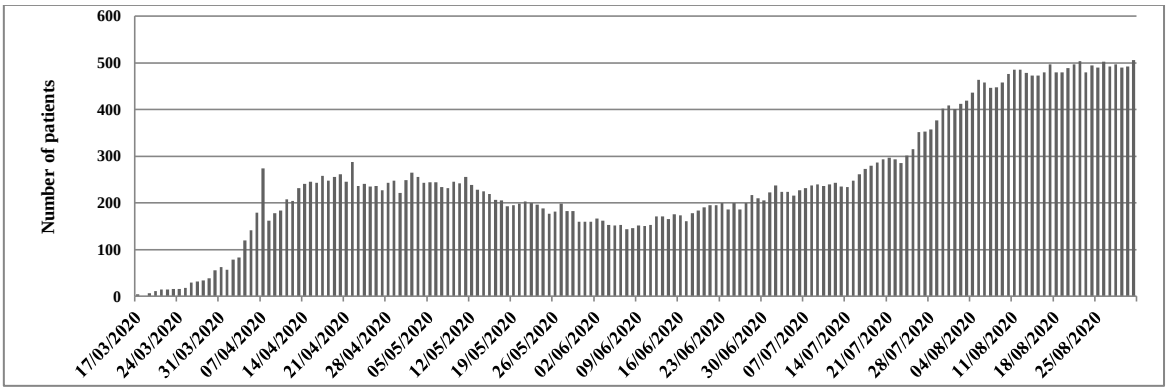

Figure 17. The total number of patients hospitalized in intensive care unit

Discussion

Based on these results, we can predict that Romania will face an even higher number of infections, possibly even more than one hundred thousand. In terms of deaths, Romania does not compare to other countries such as Italy, Spain, or France. The probability of exceeding 1,000 is very small, especially due to the superior longevity rates in these countries vs. Romania.

According to the latest available literature, this is the first study of its kind. The idea of testing the accuracy of the autoregressive integrated moving average model using two distinct statistical software processings is novel. Also, middle-class countries do not have the resources necessary or a reliable strategy in restraining the rate of contagion or transmissibility in such conditions, and most studies have focused on Westernized or China's neighboring countries.

Recently, a team of authors proposed three new methods for studying the epidemiological course of COVID-19. The first one is a universal physics-based model designed to assess the COVID-19 dynamics in Europe. The model folds within the existing curve due to the fact that the results obtained following simulation indicate an evolution curve related to that describing the current status. This "overlap" can be explained by the fact that this approach is based on a universal mechanism, having as a structural concept, the "diffusion over a lattice". In this context, it has been successfully applied for seven European countries, and further offers the chance to study the memory effects through autocorrelation within the epidemiological dynamical systems [344]. Furthermore, Demertzis et al., applied an exploratory time-series analysis built on a recent conceptualization. More specific, is dedicated in detecting connective communities by developing a novel spline regression in which the knot vector is represented by the community detection in a complex network. Through this approach, the authors demonstrated the reliability of this exploratory time-series analysis in decision-making in Greece, mainly because diagnostic testing, services, and resources strategies vary between countries [345]. Finally, Tsiotas et al., used the modularity optimization algorithm in which the visibility graphs generated describe a sequence of different typologies that this disease has. According to their results, the current pandemic in Greece is about to reach the second half in a decreasing manner, whereas the chances for a "maximum infection" are low due to the saturation point reached [346].

Quarantine is the first option – in Italy, Chintalapudi et al., demonstrated that this approach promoted a reduction up to 35% of the total registered cases, in parallel with a significant percentage (66%) of recovered cases [331].

Considering the emphatic nature of humankind, self-isolation or quarantine could have far reaching repercussions on humans' psychological profile. The psycho-social impact is exponential, with post-traumatic stress disorder (PTSD) and depression representing just two examples [347]. The gut-brain axis component should not be neglected, since it is already known that a long-term loss of host eubiosis can promote psychiatric or neurodegenerative disorders [348].

Based on the above, from our point of view, social confinement is a double edged sword. López et al., considered that social confinement should remain valid for at least 8 weeks because 99% of the current wave was attributed to humans intervention and recommended a resumption of daily activities up to 50% [338]. Chakraborty et al., concurred with López taking into consideration that people >65 years are more prone, and highlighted the necessity of an adequate medical center arrangement [329].

A study conducted by Williamson et al., on over 17 million people from the UK demonstrated an increased risk among Black and South Asian people, predisposition attributed to age, sex, and related medical conditions [339]. Miller et al., worked on the scenario in which around 20% of the US population would be infected, especially certain counties compared to the rest of the country. The authors generated a pattern based on a series of assumptions such as transmission, contact patterns, basic reproductive rate, and how efficient quarantine really is [340].

There were authors who signaled that, without taking social restrictions and other measures seriously, we could face a second wave that would be much more severe [349], and this was indeed reflected in the number of deaths reported each day. A similar pattern was recorded as a consequence of disregarding prevention measures in Romania.

An investigation of 12,343 severe acute respiratory syndrome coronavirus 2 genome sequences collected from 6 distinct geographical regions revealed that ORF1ab 4715L and S protein 614G variants were in direct correlation with fatality rates. The authors of this particular study also showed

that the bacillus calmette-guérin (BCG) vaccine and the frequency of several HLA alleles were associated with fatality rates and the number of infected cases [350].

In conclusion, Eastern European countries such as Romania are at particular risk because of the vulnerabilities in the health system, corruption, and emigration of doctors. Delays and poor organization are lingering consequences of the communist regime even after more than three decades. It should be noted that Romania has also faced several economic crises, including as recently as February 2020 [351].

Identical to Western models, and consistent with WHO guidelines (distance between people of about 1.5 m, wearing a mask, isolation, and massive testing), restrictive measures have also been implemented in Romania. Despite all the efforts made, the sums allocated for carrying out tests are insignificant, the equipment is missing, the staff is not qualified, and the hospitals are at full capacity.

Cumulatively, all these negative aspects are certified by an increasing number of infected people in contrast to the rest of Europe where the situation has reached the upper limit and is now stabilizing. What is certain is that Romania does not yet have an effective strategy to reduce the number of patients.

Forecasting the prevalence of severe acute respiratory syndrome coronavirus 2 is imperative to date, especially for health departments. As has been described and demonstrated throughout this study, time-series models play a crucial role in disease prediction. In this study, autoregressive integrated moving average time-series models were applied with success with the aim of estimating the overall prevalence of COVID-19 in Romania. However, based on our expertise and although both software have proven effective, Statgraphics has a much wider spectrum of possibilities in terms of speed, analysis, and utility. To these arguments is added the current pandemic, where providing a clear perspective in a short interval is vital for every individual.

Personal contribution - published papers:

Ilie, O.-D.; Ciobica, A.; McKenna, J.; **Doroftei**, **B**.; Mavroudis, I. Minireview on the Relations between Gut Microflora and Parkinson's Disease: Further Biochemical (Oxidative Stress), Inflammatory, and Neurological Particularities. *Oxid. Med. Cell. Longev.* ***2020***, *2020*, Article ID 4518023. **IF: 6.543**

Ilie, O.-D.; Ciobica, A.; Riga, S.; Dhunna, N.; McKenna, J.; Mavroudis, I.; **Doroftei**, **B**.; Ciobanu, A.-M.; Riga, D. Mini-Review on Lipofuscin and Aging: Focusing on The Molecular Interface, The Biological Recycling Mechanism, Oxidative Stress, and The Gut-Brain Axis Functionality. *Med.* ***2020***, *56*, 626. **IF: 2.430**

Simionescu, G.; Ilie, O.-D.; Ciobica, A.; **Doroftei**, **B**.; Maftei, R.; Grab, D.; McKenna, J.; Dhunna, N.; Mavroudis, I.; Anton, E. Mini-Review on the Possible Interconnections between the Gut-Brain Axis and the Infertility-Related Neuropsychiatric Comorbidities. *Brain Sci.* ***2020***, *10*, 384. **IF: 3.394**

Doroftei, **B**.; Ilie, O.-D.; Cojocariu, R.-O.; Ciobica, A.; Maftei, R.; Grab, D.; Anton, E.; McKenna, J.; Dhunna, N.; Simionescu, G. Minireview exploring the biological cycle of Vitamin B3 and its influence on oxidative stress: Further molecular and clinical aspects. *Molecules* ***2020***, *25*, 3323. **IF: 4.411**

Doroftei, **B**.; Ciobica, A.; Ilie, O.-D.; Maftei, R.; Ilea, C. Mini-Review Discussing the Reliability and Efficiency of COVID-19 Vaccines. *Diagnostics* ***2021***, *11*, 579. **IF: 3.706**

Anton, N.; Dragoi, E.N.; Tarcoveanu, F.; Ciuntu, R.E.; Lisa, C.; Curteanu, S.; **Doroftei**, **B**.; Ciuntu, B.M.; Chiseliţă, D.; Bogdănici, C.M. Assessing Changes in Diabetic Retinopathy Caused by Diabetes Mellitus and Glaucoma Using Support Vector Machines in Combination with Differential Evolution Algorithm. *Appl. Sci.* ***2021***, *11*, 3944. **IF: 2.679**

Nicolaiciuc D, Simionescu G, Darii N, Bolota M, Anton SC, **Doroftei**, **B**. SYSTEMATIC REVIEW REGARDING PSYCHOLOGICAL AND PHYSIOLOGICAL PROCESS ASPECTS ABOUT THE METHODS OF INDUCING LABOR. *Rev. Med. Chir. Soc. Med. Nat., Iaşi* ***2018***, *122*, 507–514.

Bolota, M.; Simionescu, G.; Nicolaiciuc, D.; **Doroftei**, **B**.; Diaconu, I.; Anton, C.R.; Anton, E.; Filipeanu, D. RESEARCHES RELATED TO THE REDUCTION OF PREMATURITY THROUGH PREMATURE RUPTURE OF MEMBRANES IN 2017. *Manag. Intercult.* ***2017***, 55–60.

SECTION II. INFERTILITY: FROM BENCH TO BEDSIDE

Chapter II

II. 1 Infections

The implications of *Helicobacter pylori* in dyspepsia and gastritis are well documented. In Parkinson's disease, it appears to be associated with an increased severity of motor functions [352], by inhibiting and controlling dopamine levels in the brain [353]. Antimicrobial treatments against *H. pylori* improved absorption of levodopa [354]. However, due to the lack of clinical trials, no clear conclusions can so far be drawn regarding the implications of *H. pylori* in Parkinson's disease beyond the proven fact that the presence of *H. pylori* in the gastrointestinal tract can interfere with different Parkinson's disease treatment regimens by initiating autoimmune or inflammatory reactions [355–357].

There are increased populations of intestinal bacteria in patients with Parkinson's disease with estimates alluding to an overpopulation of greater than 50% when compared to the intestinal microbiota populations of patients without Parkinson's disease [358,359]. Parkinson's disease treatments often fail, with a recent randomised trial suggesting that possible eradication of surplus will not affect the pharmacokinetics of L-dopa [360]. Another study analysed the role of infection as a cause for Parkinson's disease by analysing the serum antibody titre through enzyme-linked immunosorbent assay. The authors analysed the antibody titres to common pathogens including cytomegalovirus (CMV), herpes simplex virus type 1 (HSV-1), *Helicobacter pylori*, epstein-barr virus (EBV), *Borrelia burgdorferi*, and *Chlamydophila pneumonia*, concluding that the bacterial and viral burden was independently associated with Parkinson's disease [361].

Matheoud et al., provided a pathophysiological model following an infection with *Citrobacter rodentium* [362]. PINK1 is a repressor of the immune system and, as a result, it is engaged in mitochondrial antigen presentation and autoimmune mechanisms that elicit the establishment of cytotoxic T cells in the brain. Any alteration of PINK1 can induce tumorigenesis, while parkin, encoded by the PARK2 gene, is usually involved in the early-onset of parkinsonism.

In a 16S rRNA next generation sequencing (NGS) and quantitative polymerase chain reaction analysis, the viral infection with *Influenza A* induced insignificant changes at the level of the tracheobronchial tree and minor reactivity of the immune system, but in the intestines there was a depletion of the bacterial composition with an increase in the host defence peptides (HDPs) in Paneth cells and a tear of the mucous membrane [363].

In 2005, Nerius et al., initiated the largest prospective German study (individuals with an average age of 50 or older), with the main objective of determining the prevalence of Parkinson's disease in patients who have previously suffered from common gastrointestinal infections [364]. The study identified that 77.9% did not suffer from any gastrointestinal infections, while 22.1% reported previous infections. The results suggested that the predisposition to of Parkinson's disease is significantly higher ($p < 0.001$) in people who have suffered from common gastrointestinal infections when compared to the control group.

The gradual dysfunction of the enteric nervous system amplifies the probability of small intestinal bacterial overgrowth (SIBO). There are extensive cross-sectional studies which highlight an increased prevalence of small intestinal bacterial overgrowth in Parkinson's disease patients compared with the control groups [365]. This is supported by a study revealing that small intestinal bacterial overgrowth is a condition that could be treated with an appropriate treatment regime, such as rifaximin 200 mg 3 times per day for 1 week, which improves not only gastrointestinal symptoms but also motor fluctuations [366].

In addition, the clinical features of irritable bowel syndrome, which include bloating and flatulence, are also common symptoms in Parkinson's disease patients, while constipation or rectal tenesmus, present in patients with Parkinson's disease, does not define the clinical panel of irritable bowel syndrome [365]. However, an unusual case of early Parkinson's disease treated with antibiotics and colchicine was reported recently. These drugs improved constipation and diminished the

Parkinson's disease-like symptoms [366].

Sexually transmitted diseases (STDs) have become more common in recent decade(s). Left untreated, the consequences are characterized by a series of potentially life-threatening pathologies [367–369]. We refer to Mycoplasma hominis (MH) and Ureaplasma urealyticum (UU), whose high tropism has been positively associated with various disorders [370,371], some irreversible, even in asymptomatic patients [372,373]. In 2004, Stellrecht et al., revealed that 40% of infants born from carrier mothers of Mycoplasma hominis and Ureaplasma urealyticum were diagnosed with neonatal conjunctivitis and meningitis. The authors maintained that an ascending route crossing the placenta via the birth canal could exist [374].

Even though there are numerous reports on the incidence of genital mycoplasmas infections worldwide, studies that aim to establish the prevalence, antibiotic resistance patterns, types, and transmission of Mycoplasma hominis and Ureaplasma urealyticum in Romania are limited or non-existant [375].

The evaluation of an infertile individual comprises a broad panel of investigations – a detailed history, a complex physical examination, and comprehensive laboratory analyses in order to identify the main cause of the patient's impossibility to contribute to the conception of a child [376]. Genital infections are a common cause of infertility and they often go undiagnosed because of the non-specificity of clinical manifestations. Among the microorganisms involved in women's infertility, the literature mentions the following bacterial species: Chlamydia Trachomatis (CT), Ureaplasma parvum (UU/UV), Mycoplasma hominis, and Neisseria Gonorrhoeae (NG) [376]. Both Ureaplasma urealyticum and Mycoplasma hominis are sexually transmitted bacterial pathogens undoubtedly implied in impairment of reproductive status, although numerous and often contradictory papers concerning their real pathogenic potential have been published in recent years. Spreading to other body areas is also possible; Mycoplasma hominis and Ureaplasma urealyticum have detected in synovial fluid in high amounts - up to 10^7 colony forming units (CFU)/ml [377].

Unlike conventional bacteria, Mycoplasma hominis does not have a rigid cell wall. Hence, they are not susceptible to Penicillins and other antibiotics that act on this structure. They are, however, susceptible to a variety of other broad-spectrum antibiotics, most of which only inhibit their multiplication and do not actually kill them. The Tetracyclines have always been in the forefront of antibiotic usage, particularly for genital tract infections, but the newer Macrolides, Ketolides, and Quinolones have equal or sometimes greater activity. Mycoplasmas may be difficult to eradicate from human or animal hosts by antibiotic treatment because of resistance to the antibiotic, or because it lacks cidal activity, or because the invasion of eukaryotic cells by some mycoplasmas. The Quinolones have the additional advantage of exhibiting some cidal activity [378]. Fluoroquinolones are also attractive choices for treating genito-urinary tract *Ureaplasma* infections.

Data on antimicrobial resistance in ureaplasmas are very limited, because *Ureaplasma spp*. cultures are rarely obtained for clinical purposes and *in vitro* susceptibilities are almost never performed. Different studies are showing that the level of resistance to Doxycycline, Josamycin, Tetracycline, Azithromycin, Clarythromycin and Pristinamycin is generally low, but the rate of resistance to Fluoroquinolones (Ofloxacin, Ciprofloxacin) is showing an increasing rate in different studies. For example, Xie and Zhang reported <50% resistance in a large number of strains isolated during 1999 and 2004 [379]. Clinical isolates of Fluoroquinolone-resistant *Ureaplasma spp*. have been also described thus far from France [380,381] and USA [382]. Duffy et al., reported the first case of naturally occurring Fluoroquinolone resistance in *Ureaplasma spp*. from the United States, probably developed as a result of mutations in the *gyrA* and *parC* genes of the DNA gyrase/topoisomerase IV complex that occurred in the presence of antimicrobial selective pressure [382].

Fungemia due to different Candida species is the 4th most common occurrence, after systemic nosocomial infections caused by coagulase-negative staphylococci, enterococci, and *Staphylococcus aureus*. The species that are implied in the etiology of fungemia present a particular pattern of susceptibility toward main antifungal agents - the percentage of Fluconazole-resistant strains is significantly increased especially in *Candida glabrata* and *Candida krusei* [383–387]. In this context, there is growing interest in developing new antifungal drugs and improving the bioavailability of the existing agents [388].

Cyclodextrins (CDs) act as host molecules to form inclusion complexes at nano-level with a

wide range of guest molecules, the largest field of their practical utilization being based on their solubilizing capacity [389]. A large variety of drugs encapsulated through noncovalent interactions into the Cyclodextrin cavity were described [389–391]. Such a complexation of the drug offers the possibility to improve the aqueous solubility without any modification of the original structure and allows a homogeneous delivery, thus increasing its bioavailability. The new compound MXP-4509 is a nanoparticle-formulated Propiconazole derivative (beta-cyclodextrin being the carrier molecule) whose antifungal activity was previously demonstrated [392]. Its mechanism of action is the disruption of ergosterol biosynthesis by inhibiting the 14-α-demethylase, this being a common feature for all Triazoles [393,394]. Unpublished data regarding acute toxicity studies performed on Wistar SD1 NRM1 White/C57Bi6 outbred mice have shown that the LD50 is 280 mg/kg body weight, classifying the drug as a class 2 substance (moderately hazardous), accordingly to WHO [395]. This toxicity value is quite similar to that of Voriconazole - an approved antifungal drug for human usage [396].

Unlike fungaemia, superficial yeast infections are not life-threatening, but they are a public health problem with increasing incidence, especially mucocutaneous ones, and they often have a significant negative impact on the quality of life [397]. Individuals with diabetes mellitus, broad-spectrum antibiotic therapy, malignancies or an impaired immune system are particularly susceptible to this type of infections, which can also lead to subsequent invasive mycosis [397,398]. Genetic predisposition may also be a risk factor, especially in the case of recurrent vulvovaginal candidiasis (VVC) [399].

A tendency to focus on candidaemia and *Candida* isolates from sterile sites can be noticed in the literature lately, due to their severity and the difficulty in discriminating infection from colonisation in case of isolates from non-sterile sites. Nevertheless, an important number of investigations have analysed clinical yeast isolates from all body sites. Some cover yeasts in general [400–402], while others are limited to *Candida* species [383,403]. Some are global surveys, but most are limited to certain geographic areas of variable extension.

The data regarding the geographic distribution of pathogenic yeast species that these studies offer is important for epidemiology. Accurate susceptibility pattern comparisons are, however, challenging and difficult to accomplish, due to different testing protocols [404,405] and because of different and changing breakpoints (BPs) used to define the categories of susceptibility [406]. In the current literature, various reference testing protocols can be encountered: the clinical and laboratory standards institute (CLSI) M27-A3 broth micro-dilution method [407,408], the clinical and laboratory standards institute M44-A disk diffusion method [383,409], a modified deutsches institut für normung (DIN) 58940-84 method [401,409] with a mix of changing breakpoints from various sources and the european committee for antimicrobial susceptibility testing (EUCAST) EDef 7.1 method [402,410], with various changing breakpoints versions, as well as commercial methods [411].

Regarding the species distribution and the susceptibility pattern of fungal clinical isolates, there are no extensive data reported from Romania, except some preliminary data from our team [412].

Personal contribution - published papers:

Ilie, O.-D.; Ciobica, A.; McKenna, J.; **Doroftei**, **B**.; Mavroudis, I. Minireview on the Relations between Gut Microflora and Parkinson's Disease: Further Biochemical (Oxidative Stress), Inflammatory, and Neurological Particularities. *Oxid. Med. Cell. Longev.* ***2020***, *2020*, Article ID 4518023. **IF: 6.543**

Doroftei, **B**.; Ilie, O.-D.; Armeanu, T.; Anton, E.; Scripcariu, I.; Maftei, R. The Prevalence of Ureaplasma Urealyticum and Mycoplasma Hominis Infections in Infertile Patients in the Northeast Region of Romania. *Med.* ***2021***, *57*, 211. **IF: 2.430**

Mihai, M.; Valentin, N.; **Doroftei**, **B**.; Carmen, C.M.; Coralia, B.; Demetra, S. Antibiotic susceptibility profiles of Mycoplasma hominis and ureaplasma urealyticum isolated during a population-based study concerning women infertility in northeast romania. *Braz. J. Microbiol.* ***2011***, *42*, 256–260. **IF: 1.091**

Mareș, M.; Năstasă, V.; Moraru Ramona, F.; **Doroftei**, **B**.; Ștefanache, A. Comparative In Vitro Activities of Fluconazole, Voriconazole, and MXP-4509 Against Romanian Blood Yeast Isolates. *Mycopathologia* ***2011***, *172*, 487–492. **IF: 2.574**

Minea, B.; Nastasa, V.; Moraru, R.F.; Kolecka, A.; Flonta, M.M.; Marincu, I.; Man, A.; Toma, F.; Lupse, M.; **Doroftei**, **B**.; et al. Species distribution and susceptibility profile to fluconazole, voriconazole and MXP-4509 of 551 clinical yeast isolates from a Romanian multi-centre study. *Eur. J. Clin. Microbiol. Infect. Dis.* ***2015***, *34*, 367–383. **IF: 3.267**

Personal contribution - published papers:

Doroftei, **B**.; Ilie, O.-D.; Armeanu, T.; Anton, E.; Scripcariu, I.; Maftei, R. The Prevalence of Ureaplasma Urealyticum and Mycoplasma Hominis Infections in Infertile Patients in the Northeast Region of Romania. *Med.* ***2021***, *57*, 211. **IF: 2.430**

Aim of the study

Even though in the current literature, a substantial number of reports regarding the worldwide incidence of genital mycoplasmas infections can be found, studies that aim to establish the prevalence, antibiotic resistance patterns, types, and transmission of Mycoplasma Hominis and Ureaplasma urealyticum in Romania are limited or do not exist.

Materials and methods

Study participants

Our study was conducted between 2017 and 2019 at the Origyn Fertility Center in Iasi, Romania. Four hundred and eleven women were included (mean 31.85, range 18-51 years old) based on the following criteria: (I) a confirmed diagnosis of infertility, and (II) absence of Chlamydia trachomatis infection. There was no maximum age limit for participation in this study.

Sample collection and processing

All endocervical samples were collected from patients using an Aptima Unisex Swab Specimen Collection Kit for Endocervical and Male Urethral Swab Specimens (San Diego, CA 92121, USA). As we continued with the investigation, samples were transferred to Synevo (n = 130) and Regina Maria (n = 281) laboratories for further analysis. The Synevo laboratory used Mycoplasma IES (Autobio Diagnostics, Zhengzhou, China) to identify and test the antimicrobial susceptibility of Ureaplasma urealyticum and Mycoplasma hominis to 11 antibiotics, namely, Macrolide class (Clarithromycin, Erythromycin, Joysamicin, Roxithromycin), Fluoroquinolones (Ciprofloxacin, Ofloxacin, Levofloxacin), Tetracycline (Minocycline, Tetracycline), Streptogramins (Pristinamycin), and Lincosamides (Clindamycin). The Regina Maria laboratory used Mycoplasma IST2 (bioMérieux, Marcy-l'Etoile, France) to detect and assess the sensitivity of Mycoplasma hominis and Ureaplasma urealyticum to 8 antibiotics, members of 4 distinct classes, namely, Macrolide class (Josamycin, Erythromycin, Azithromycin), Tetracycline (Doxycycline, Tetracycline), Fluoroquinolones (Ofloxacin, Ciprofloxacin), and Streptogramins (Pristinamycin).

Ethical approval

The present study was approved by the ethics committee of the Origyn Fertility Center, Iasi, Romania (no 115/565; 25 January 2021) and was conducted in accordance with the Helsinki Declaration of human rights, as well as the national and European regulations on biomedical research. Participants signed written informed consent forms for their voluntary contribution to this study. They did not receive any remuneration for their participation.

Statistical analysis

Data analysis was carried out using Microsoft Excel 2010 and Minitab 19 software (Minitab Inc., State College, Pennsylvania, USA, 2019). Microsoft Excel was used for editing, sorting, and coding. Statistical analysis was performed with Minitab 19.

Results

The prevalence of Mycoplasma hominis and Ureaplasma urealyticum was (n = 2) 0.48% and 28.46% (n = 117). We also noted that 2.91% (n = 12) of all participants had coinfections. The overall

detection rate was up to 31.87% (*n* = 131). There is a fluctuating tendency of Ureaplasma urealyticum infections among early adulthood and middle-aged women. We identified only two cases characterized strictly by a Mycoplasma hominis infection within the group between 30 and 35 years old. Even though coinfections were reported in a small percentage if we refer to associated figures for Ureaplasma urealyticum, the pattern in terms of predisposition is identical to that of Ureaplasma urealyticum affecting the same age groups (Figure 18).

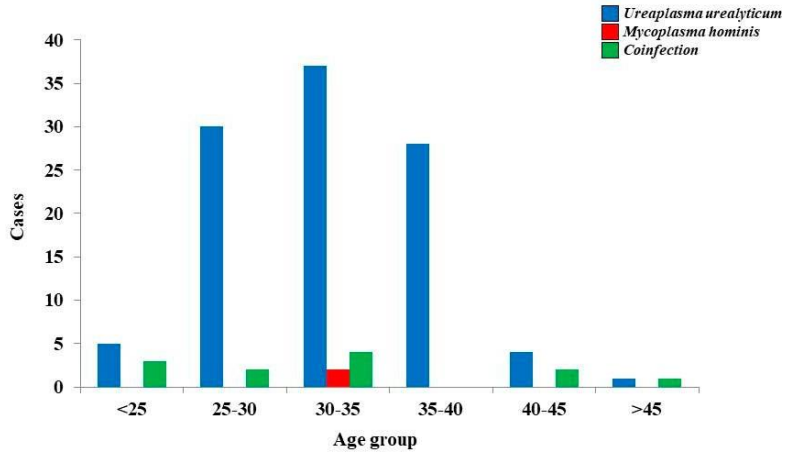

Figure 18. Prevalence of UU and MH infection by age

Samples were unequally sent to 2 laboratories for additional analyses. From the total number of samples collected, 68.46% (*n* = 281) were processed by Regina Maria laboratory. The overall detection rate was 20.28% (*n* = 57), as shown in Table 15. Pristinamycin and Josamycin were fully efficient (100%) against Ureaplasma urealyticum and Mycoplasma hominis. Furthermore, Doxycycline (98.23%) and Tetracycline (96.48%) were highly effective and we knew they could be used as agents to eradicate Ureaplasma urealyticum and Mycoplasma hominis pathogens. Azithromycin and Erythromycin also demonstrated a potent reactivity rate that reached 78.94% and 70.17%. By contrast, Ciprofloxacin and Ofloxacin were considered unsuitable, since their potency was variable, reflected by an intermediate response (61.40%) towards the gained resistance status (50.87%) of Ureaplasma urealyticum (Figure 19). The most susceptible groups were women aged 20-40, suggesting a direct correlation between the presence of Ureaplasma urealyticum and Mycoplasma hominis and age (Table 15).

Table 15. The susceptibility of Ureaplasma urealyticum and Mycoplasma hominis depending on s = sensitivity, i = intermediate, and r = resistant status (Regina Maria)

Antibiotics	**Ureaplasma urealyticum (positive, n = 55) and Mycoplasma hominis (positive, n = 2)**					
	Cumulative results		**Results based on the age**			
			20-30 (n=19)	**30-40 (n=33)**	**40-50 (n=4)**	**>51 (n=1)**
Doxycycline	S = 54; 94.73% I = 1; 1.75% R = 0; 0.00%	S = 2; 3.50% I = 0; 0.00% R = 0; 0.00%	S = 18 I = 1 R = 0	S = 33 I = 0 R = 0	S = 4 I = 0 R = 0	S = 1 I = 0 R = 0
Josamycin	S =55; 96.49% I = 0; 0.00% R = 0; 0.00%	S = 2; 3.50% I = 0; 0.00% R = 0; 0.00%	S= 19 I = 0 R = 0	S = 33 I = 0 R = 0	S = 4 I = 0 R = 0	S = 1 I = 0 R = 0
Ofloxacin	S = 11; 19.29% I = 35; 61.40% R = 9; 15.78%S	S = 2; 3.50% I = 0; 0.00% R= 0; 0.00%	S = 4 I = 12 R = 3	S = 9 I = 19 R = 5	S = 0 I = 3 R = 1	S = 0 I = 1 R = 0
Erythromycin	S = 40; 70.17% I = 14; 24.56% R = 1; 1.75%	S = 0; 0.00% I = 0; 0.00% R = 2; 3.50%	S = 13 I = 6 R = 0	S = 24 I = 6 R = 3	S = 2 I = 2 R = 0	S = 1 I = 0 R = 0
Tetracycline	S = 53; 92.98%	S = 2; 3.50%	S = 17	S = 33	S = 4	S = 1

	I = 1; 1.75% R = 1; 1.75%	I = 0; 0.00% R = 0; 0.00%	I = 1 R = 1	I = 0 R = 0	R = 0 I = 0	I = 0 R = 0
Ciprofloxacin	S = 5; 8.77% I = 21; 31.84% R = 29; 50.87%	S = 2; 3.50% I = 0; 0.00% R = 0; 0.00%	S = 1 I = 7 R = 11	S = 6 I = 13 R = 14	S = 0 I = 0 R = 4	S = 0 I = 1 R = 0
Azithromycin	S = 45; 78.94% I = 10; 17.54% R = 0; 0.00%	S = 0; 0.00% I = 0; 0.00% R = 2; 3.50%	S = 17 I = 2 R = 0	S = 25 I = 6 R =2	S = 2 I = 2 R = 0	S = 1 I = 0 R = 0
Pristinamycin	S = 55; 96.49% I = 0; 0.00% R = 0; 0.00%	S = 2; 3.50% I = 0; 0.00% R = 0; 0.00%	S = 19 I = 0 R = 0	S = 33 I = 0 R = 0	S = 4 I = 0 R = 0	S = 1 I = 0 R = 0

Coinfection (n = 12)			
20-30 (n=5)	**30-40 (n=4)**	**40-50 (n=3)**	**>51 (n=0)**
S = 5 I = 0 R = 0	S = 4 I = 0 R = 0	S = 3 I = 0 R = 0	S = 0 I = 0 R = 0
S = 4 I = 1 R = 0	S = 3 I = 1 R = 0	S = 2 I = 0 R = 1	S = 0 I = 0 R = 0
S = 2 I = 3 R = 0	S = 2 I = 1 R = 1	S = 1 I = 2 R = 0	S = 0 I = 0 R = 0
S = 0 I = 0 R = 5	S = 0 I = 1 R = 3	S = 0 I = 1 R = 2	S = 0 I = 0 R = 0
S = 5 I = 0 R = 0	S = 4 I = 0 R = 0	S = 3 I = 0 R = 0	S = 0 I = 0 R = 0
S = 0 I = 3 R = 2	S = 1 I = 1 R = 2	S = 1 I = 0 R = 2	S = 0 I = 0 R = 0
S = 0 I = 2 R = 3	S = 0 I = 1 R = 3	S = 0 I = 1 R = 2	S = 0 I = 0 R = 0
S = 5 I = 0 R = 0	S = 4 I = 0 R = 0	S = 3 I = 0 R = 0	S = 0 I = 0 R = 0

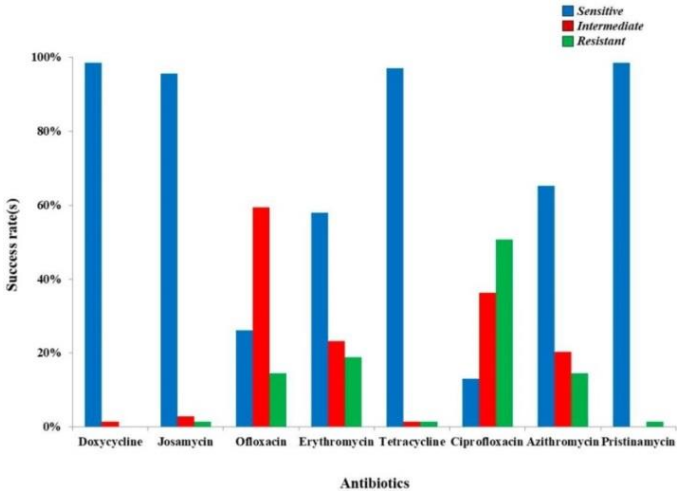

Figure 19. Drug susceptibility of Ureaplasma urealyticum and Mycoplasma hominis based on antibiograms from Regina Maria

The other laboratory, Synevo, was responsible for processing 31.54% of the samples (*n* = 130), the number of cases in which we had cogent data being only fifty. Despite the wide spectrum of antibiotics used, Pristinamycin was the sole antibiotic with complete efficiency. Except for Erythromycin and Josamycin, with viability over 90%, Minocycline had a 96% success rate against Ureaplasma urealyticum. Clarithromycin and Roxithromycin exerted beneficial activity (88.00%) in countering the persistence of Ureaplasma urealyticum, further highlighting a high sensitivity of this microorganism to Levofloxacin (82.00%). As indicated in Table 16, the susceptibility of Ureaplasma urealyticum to Tetracycline was 68.00%, significantly lower if we refer to the results reported previously. The data are contradictory for Ofloxacin (60.00%), since above it had only 19.29% sensitivity. Unfortunately, Clindamycin and Ciprofloxacin were ineffective in 66.00% and 82.00% of cases for infections with Ureaplasma urealyticum (Figure 20). Analogous to our previous results, the most susceptible groups were also women that were 20 to 40 years old, a downward trend being positively correlated with age (Table 16).

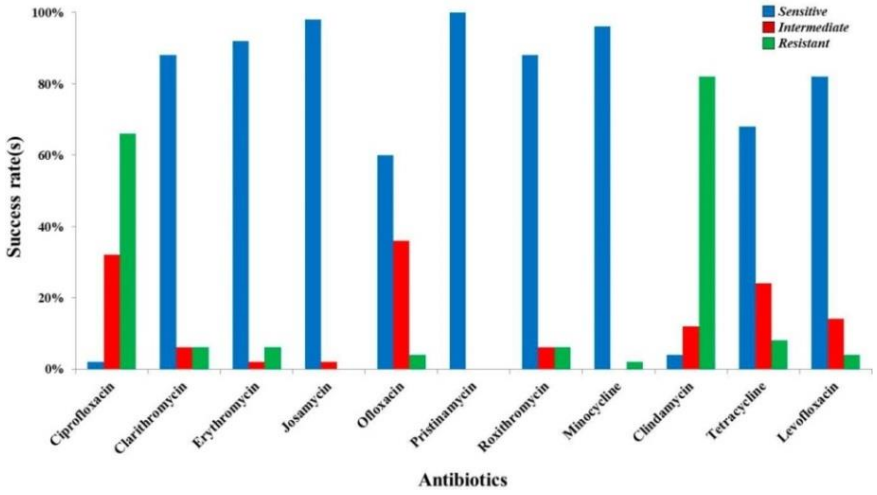

Figure 20. Drug susceptibility of Ureaplasma urealyticum and Mycoplasma hominis based on antibiograms from Synevo

Table 16. Data revealing the susceptibility of Ureaplasma urealyticum depending on s = sensitivity, i = intermediate, and r = resistant status (Synevo)

Antibiotics	**Ureaplasma urealyticum (positive, n = 50) and Mycoplasma hominis (positive, n = 0)**					
	Cumulative results		**Results based on the age**			
			20-30 (n=16)	**30-40 (n=33)**	**40-50 (n=1)**	**>51 (n=0)**
Ciprofloxacin	S = 1; 2.00% I = 16; 32.00% R = 33; 66.00%	S = 0; 0.00% I = 0; 0.00% R = 0; 0.00%	S = 0 I = 6 R = 10	S = 1 I = 10 R = 22	S = 0 I = 0 R = 1	S = 0 I = 0 R = 0
Clarithromycin	S = 44; 88.00% I = 3; 6.00% R = 3; 6.00%	S = 0; 0.00% I = 0; 0.00% R = 0; 0.00%	S =14 I = 1 R = 1	S = 29 I = 2 R = 2	S = 1 I = 0 R = 0	S = 0 I = 0 R = 0
Erythromycin	S = 46; 92.00% I = 1; 2.00% R = 3; 6.00%	S = 0; 0.00% I = 0; 0.00% R = 0; 0.00%	S = 15 I = 0 R = 1	S = 30 I = 2 R = 2	S = 1 I = 0 R = 0	S = 0 I = 0 R = 0
Josamycin	S = 49; 98.00% I = 1; 2.00% R = 0; 0.00%	S = 0; 0.00% I = 0; 0.00% R = 0; 0.00%	S = 16 I = 0 R = 0	S = 32 I = 1 R = 0	S = 1 I = 0 R = 0	S = 0 I = 0 R = 0
Ofloxacin	S = 30; 60.00% I = 18; 36.00% R = 2; 4.00%	S = 0; 0.00% I = 0; 0.00% R = 0; 0.00%	S = 10 I = 6 R = 0	S = 19 I = 12 R = 2	S = 1 I = 0 R = 0	S = 0 I = 0 R = 0
Pristinamycin	S = 50; 100% I = 0; 0.00%	S = 0; 0.00% I = 0; 0.00%	S = 16 I = 0	S = 33 I = 0	S = 1 I = 0	S = 0 I = 0

	R = 0; 0.00%	R = 0; 0.00%	R = 0	R = 0	R = 0	R = 0
Roxithromycin	S= 44; 88.00% I = 3; 6.00% R = 3; 6.00%	S = 0; 0.00% I = 0; 0.00% R = 0; 0.00%	S = 14 I = 1 R = 1	S = 29 I = 2 R = 2	S = 1 I = 0 R = 0	S = 0 I = 0 R = 0
Minocycline	S = 48; 96.00% I = 0; 0.00% R = 1; 2.00%	S = 0; 0.00% I = 0; 0.00% R = 0; 0.00%	S = 15 I = 0 R = 0	S = 32 I = 0 R = 1	S = 1 I = 0 R = 0	S = 0 I = 0 R = 0
Clindamycin	S = 2; 4.00% I = 6; 12.00% R = 41; 82.00%	S = 0; 0.00% I = 0; 0.00% R = 0; 0.00%	S = 1 I = 0 R = 15	S = 1 R = 6 R = 25	S = 0 I = 0 R = 1	S = 0 I = 0 R = 0
Tetracycline	S = 34; 68.00% I = 12; 24.00% R = 4; 8.00%	S = 0; 0.00% I = 0; 0.00% R = 0; 0.00%	S = 11 I = 4 R = 1	S = 23 I = 7 R = 3	S = 0 I = 1 R = 0	S = 0 I = 0 R = 0
Levofloxacin	S = 41; 82.00% I = 7; 14.00% R = 2; 4.00%	S = 0; 0.00% I = 0; 0.00% R = 0; 0.00%	S = 14 I = 2 R = 0	S = 26 I = 5 R = 2	S = 1 I = 0 R = 0	S = 0 I = 0 R = 0

Discussion

Ureaplasma urealyticum was prevalent among all samples analyzed. The single Ureaplasma urealyticum, Mycoplasma hominis, and dual infections accounted for 28.46% (n = 117), (n = 2) 0.48%, and 2.91% (n = 12), respectively. Even though Ureaplasma urealyticum and Mycoplasma hominis are non-pathogenic commensal bacteria, part of the normal genital flora, some factors could perturb the host's eubiosis [413].

These arguments were strengthened on two distinct occasions. Ureaplasma urealyticum was identified in ≥1 site in 52.9% of the cases, while Mycoplasma hominis in 3.3%, but always in association with Ureaplasma urealyticum. Figures reached 23% in cord blood cultures, being more common in infants of nonwhite women under twenty years of age (27.9% vs. 16.8%; p = 0.016). Even though the cultures were initially positive in cases of spontaneous, preterm, or early gestational age (34.7% vs. 3.2%; p = 0.001), the therapeutic regimen led to a depletion of these strains [414]. This topic should be of interest because elevated levels of interleukin-6 and placental histology were noted, showing that the risk of systemic inflammation (41.3% vs. 25.7%; p = 0.007), funisitis [415], and bronchopulmonary dysplasia (26.8% vs. 10.1%; p = 0.0001) is significantly higher in neonates [416].

In order to offer a conclusive overview regarding all studies performed to date with a similar objective to our study, we searched bibliographic databases available online and found five studies in which the authors included a total number of 34,698 Chinese participants. Cumulatively, the scholars demonstrated that Ureaplasma urealyticum had a prevalence of 22.01% (n = 7639), 2.37% Mycoplasma hominis (n = 824), and 3.74% coinfection (n = 1300). One common observation was that women are more predisposed than men (p < 0.001), regardless of age and health status, also inflicting changes in semen parameters. Josamycin, Clarithromycin, Roxithromycin, Doxycycline, Minocycline, and Tetracycline could be recommended in both symptomatic and asymptomatic individuals for clinically treating Ureaplasma urealyticum and Mycoplasma hominis infections since the success rate of these three antibiotics was 94.6%, 100%, and 84.3%, respectively [417–421].

Concerning sperm integrity, Lee et al., were the first to prove the existence of a positive correlation with Ureaplasma urealyticum [422]. In their research, Ureaplasma urealyticum was prevalent among infertile individuals of both sexes (p = 0.022), 48% from infertile men and 40% in infertile women, whereas the results were 25% and 22.9% in fertile men and women, respectively. Salmeri et al., reached a similar conclusion, since 41% infertile men presenting to their clinic had urogenital symptoms (Ureaplasma urealyticum - n = 39; MH - n = 9; mixed - n = 1), oligo-astheno-teratozoospermia (Chi-square = 127.3; p < 0.05), and asthenozoospermia (Chi-square = 5.74; p < 0.05), in contrast to non-infected infertile patients [423].

In 2019, Moridi et al., conducted a systematic review and meta-analysis regarding the prevalence of Ureaplasma urealyticum and Mycoplasma hominis in Iran in the previous 19 years [424]. Based on a total of forty-four articles selected for data extraction, the authors concluded that Ureaplasma urealyticum and Mycoplasma hominis prevalence was 17.53% and 9.68%, respectively, especially in central provinces compared to other parts of Iran.

Even though antibiotics proved their efficiency, the beneficial activity of lactic bacteria remained under-explored, yet crucial, having major clinical implications. Daniele et al., found that bacteriocins L23 and L60 produced by *Lactobacillus fermentum* and *Lactobacillus rhamnosus* are two novel inhibitors of bacterial infection [425]. The minimum inhibitory concentration of L23 ranged between 320 and 160/80 UA mL^{-1} for 78%/95% of the Mycoplasma hominis and Ureaplasma urealyticum, respectively, whereas L60 was still active at 160/80 UA mL^{-1} for 56%/53% of the Mycoplasma hominis and Ureaplasma urealyticum infection, respectively.

Fortunately, we now have the knowledge and equipment to detect both Ureaplasma urealyticum and Mycoplasma hominis from a molecular point of view, and polymerase chain reaction remains the method of choice due to its high specificity and sensitivity as opposed to direct fluorescence antibody (DFA) [426–428].

It is worth mentioning that IC/PBS is associated with EMS and infertility. According to a recent review by Garzon et al., there is no reliable strategy for IC/PBS due to scarce evidence and limited approaches [429]. Unfortunately, current methodologies are not applied in a personalized manner and depend on pathophysiological causes. The only applied technique involves the use of conservative options that are more invasive, targeting the bladder.

Patnaik et al., conducted another review referring to the underlying mechanisms of IC/PBS [430]. Congruent with the conclusions reached by Garzon et al., the etiology is not clearly understood. They estimated the prevalence to be in the range of 45/8 per 100,000 in women and men. The joint prevalence in both sexes was up to 10.6 cases per 100,000. A series of etiological theories were issued to find novel diagnostic strategies and biomarkers. Patnaik et al., claimed that there are no "gold standards" of IC/PBS, the only alternative being to classify the patients based on symptoms and with emphasis on the phenotype.

It can be concluded that the persistence of Mycoplasma hominis and Ureaplasma urealyticum exerts a detrimental activity in certain circumstances, such as dysbacteriosis or other pathologies, by negatively affecting the human fertility status. We can successfully reduce infections and infertility risks by educating and screening the population, and adequately treating individuals who test positive. Avoiding unreliable treatment of these infections contributes to reducing multidrug resistance and conserving drug susceptibility.

Personal contribution - published papers:

Mihai, M.; Valentin, N.; **Doroftei**, **B**.; Carmen, C.M.; Coralia, B.; Demetra, S. Antibiotic susceptibility profiles of Mycoplasma hominis and ureaplasma urealyticum isolated during a population-based study concerning women infertility in northeast romania. *Braz. J. Microbiol.* ***2011***, *42*, 256–260. **IF: 1.091**

Aim of the study

The purpose of this paper was to determine the antibiotic susceptibility profile of Mycoplasma hominis and Ureaplasma urealyticum isolated during a population-based study concerning women infertility in northeast Romania and to identify the most prevalent resistance markers in the respective strains.

Patients

Our study consisted in a screening of 1,068 infertile women who presented for initial evaluation in our outpatient clinic from May 2008 to September 2009. The median age of the patients enrolled in the study was 31 years (range 26-42). Approval for the study was granted by the Research Ethics Committee from the "Gr. T. Popa" University of Medicine and Pharmacy, Iasi (Romania). The study was conducted accordingly to the Declaration of Helsinki 2000.

Sample collection

Endocervical samples were collected in duplicate from all patients using Chlamydia

Swab/Brush Collection Kit (Bio-Rad Laboratories, France).

Sample processing

Soon after sampling, the swab was processed using Mycoplasma IST2 kits (bioMérieux, France) in order to identify Mycoplasma hominis and Ureaplasma urealyticum, and to evaluate the susceptibility of the strains to 9 antibiotics, i.e. Doxycycline, Josamycin, Ofloxacin, Erythromycin, Tetracycline, Ciprofloxacin, Azithromycin, Clarythromycin, and Pristinamycin.

Bacteria detection

The brush was subjected to DNA extraction using the DNA-Sorb-A kit (Sacace Biotechnologies, Italy). All extracted DNA samples were processed in an Applied Biosystems 7300 Real Time PCR system (Applera, USA) using the Mycoplasma hominis Real-TM and Ureaplasma urealyticum/Ureaplasma parvum Real-TM kits (Sacace Biotechnologies, Italy). The parameters of amplification were as follows: 95°C for 15 min, followed by 10 cycles of 95°C for 20 s, 65°C for 20 s and 72°C for 20 s, with a last stage of 35 cycles of 95°C for 25 s, 60°C for 30 s and 72°C for 15s. After incubation of Mycoplasma IST2 strips, the positive samples have been registered and compared with the results obtained after RT-PCR assay in order to choose only the positive samples for Mycoplasma hominis and/or Ureaplasma urealyticum in the two tests. After the samples processing, we have selected 80 positive samples for Mycoplasma hominis and 372 for Ureaplasma urealyticum, respectively. For these samples, the susceptibility profiles to the mentioned above antibiotics were analyzed using the manufacturer recommendations.

There were considerable differences in levels of resistance to the antibacterial agents for the two bacterial species. However, the Mycoplasma hominis strains showed generally higher resistance rates than Ureaplasma urealyticum ones. For Mycoplasma hominis, the highest resistance rates were registered for Ciprofloxacin (77.27%), followed by Macrolides (Azithromycin 38.88%, Clarythromycin and Erythromycin - 33.33% each) and Ofloxacin (27.77%). Lower resistance rates (p=0.028) were registered for Tetracycline, Josamycin, Pristinamycin, and Doxycycline, i.e. 16.66%, 11.11%, 11.11%, and 11.11% respectively (Figure 21). For Ureaplasma urealyticum isolates, the Ciprofloxacin resistance was also very high (51.72%), while the resistance rates to the other tested antibiotics were significantly lower (p=0.022), i.e. Ofloxacin (16.09%), Erythromycin (16.09%), Clarythromycin (9.19%), Azithromycin (8.05%), Tetracycline (5.75%), Pristinamycin (3.45%), Josamycin (2.30%) and Doxycycline (2.30%) (Figure 21).

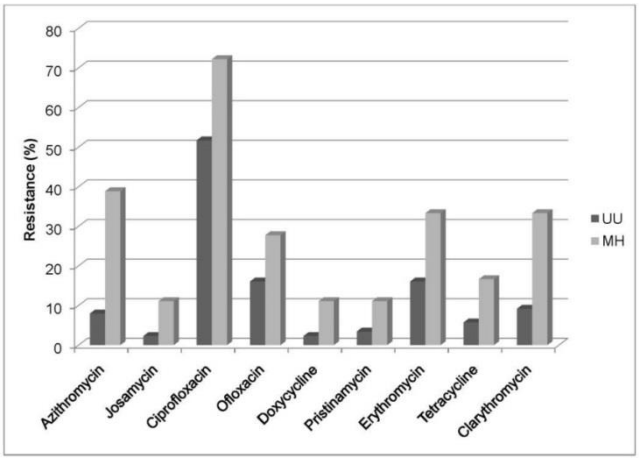

Figure 21. Resistance of *Mycoplasma hominis* and *Ureaplasma urealyticum* strains to antibacterial agents

For this study, we also reviewed the resistance rates of Mycoplasma hominis and Ureaplasma urealyticum isolated from genital swabs taken from women with infertility problems over the period from May 2008 to September 2009.

These bacteria are members of the class Mollicutes, commonly referred to as mycoplasmas. The Mollicutes are the smallest known free-living microorganisms. Mycoplasma hominis is involved

in the etiology of salpingitis and PID, but its occurrence in sexually active population is lower than Ureaplasma urealyticum, with an average of 10% [376,431,432]. Thus, Ureaplasma urealyticum is the most common bacteria of the human urogenital tract (with a detection rate of 67% in sexually active women and 50% in men, respectively) that can cause lower pregnancy rates (PRs) after IVF, higher abortion rate of spontaneous pregnancies, increasing of the risk of premature contractions and PTB, puerperal endometritis, orchitis, epididymitis, spermatocystitis, prostatitis, urethritis, increased apoptosis in human spermatogens, impairment of semen parameters, less stable chromatin and DNA denaturation spermatozoa [433–439]. Although mycoplasmas evolved from Gram-positive ancestors, the mycoplasmas lack a cell wall and are usually treated with Quinolones, Tetracyclines, or Erythromycin. However, the number of resistant Mycoplasma hominis and Ureaplasma urealyticum strains is increasing every year following the widespread use of these agents.

The susceptibility rates showed that there was a considerable difference in levels of resistance to various antibacterial agents, and that the rate of change was related to the degree of antibacterial use. Doxycycline is still highly effective against Mycoplasma hominis and Ureaplasma urealyticum. Erythromycin, which is one of the most widely used antibiotics elsewhere, demonstrated high resistance rates in Mycoplasma hominis. Ciprofloxacin, which was commonly used in treating patients with diarrhoea and other infections has demonstrated a high resistance rate in both tested microorganisms. The high resistance rates to Ciprofloxacin observed in our strains could be indeed correlated with the antibiotic treatment history in the analyzed patients. Because the history of the patients reported a treatment with Fluoroquinolones in the last 12 months (Ciprofloxacin in 68 cases, Ofloxacin in 56 cases, both in 28 cases and Norfloxacin in 4 cases), it is likely that Mycoplasma hominis and Ureaplasma urealyticum isolates could become resistant to these antibiotics used for the treatment of other bacterial infections.

For Romania, the explanation of this high resistance percentage to Fluoroquinolones occurred in Mycoplasma hominis and Ureaplasma urealyticum strains isolated from human patients is the frequent prescription of these drugs by the general practitioners for the treatment of urinary and respiratory tract infections, pneumonia or otitis, due to their reduced price and lack of side reactions. The mechanism of resistance is probably the occurrence post exposure to Fluoroquinolones, of a target alteration located in the DNA gyrase and topoisomerase IV subunits [380,440].

We further analyzed the presence of Chlamydia trachomatis antigen, Ureaplasma urealyticum, Mycoplasma hominis and Neisseria gonorrhoeae in the endocervical secretions and Chlamydia trachomatis antibodies immunoglobulin A, immunoglobulin G, immunoglobulin M in the serum of 125 infertile women as well as in 30 pregnant women in the 3rd trimester of pregnancy, as a control group. In infertile women, the prevalence rate of the four bacterial markers was: Chlamydia trachomatis antigen 1/125 (0.80%), Chlamydia trachomatis immunoglobulin G antibodies 19/125 (15.20%), Mycoplasma hominis 6/125 (4.80%), Ureaplasma urealyticum 51/125 (40.80%) and Neisseria gonorrhoeae 1/125 (0.8%). From the control group, none was positive for Chlamydia trachomatis antigen, but 1/30 (3.33% of patients) was positive for Chlamydia trachomatis immunoglobulin A while the prevalence rate for Mycoplasma hominis and Ureaplasma urealyticum were 16.66% and 43.33% respectively.

Concluding, fluoroquinolones resistance was very high among Mycoplasma hominis and Ureaplasma urealyticum isolates, while macrolides resistance was low in Ureaplasma urealyticum and high in Mycoplasma hominis. Doxycycline was active against both organisms, exhibiting a low percentage of resistance.

These results highlighted the emergence of antibiotic resistance in genital mycoplasmas from northeast Romania. Thus, the treatment of such infections should be guided by antibiotic susceptibility testing and local antibiotic resistance pattern.

Personal contribution - published papers:

Mareș, M.; Năstasă, V.; Moraru Ramona, F.; **Doroftei**, **B**.; Ștefanache, A. Comparative In Vitro Activities of Fluconazole, Voriconazole, and MXP-4509 Against Romanian Blood Yeast Isolates. *Mycopathologia* ***2011***, *172*, 487–492. **IF: 2.574**

Aim of the study

The aim of this study was to evaluate the *in vitro* activity of a new triazole formulation (MXP-4509) in comparison with Fluconazole and Voriconazole against clinical yeast strains isolated in Romania. This article presents the preliminary data concerning the susceptibility to Fluconazole and Voriconazole for clinical isolates of yeasts recovered from blood cultures in the first Romanian Fungemia Surveillance Study.

Materials and methods

Clinical isolates

A total number of 182 clinical isolates of yeasts collected between 2007 and 2009 from bloodstream infections (BSI) in three tertiary hospitals from Romania were assessed. The clinical isolates were recovered from blood cultures using BacT/ALERT bottles (bioMe´rieux, Marcy l'Etoile, France) and subsequently plated onto Sabouraud Dextrose Agar (Merck, Darmstadt, Germany) in order to prepare a stock suspension in 10% glycerol. After that, they were stored at -80°C until the identification and susceptibility testing have been performed. All the clinical isolates were identified using standard laboratory procedures including morphological and biochemical methods using ID32C strips (bioMe´rieux, Marcy l'Etoile, France).

Of a total 182 yeast isolates, 56 (30.76%) were *Candida albicans*, 112 (61.54%) were other Candida species, and the rest - 14 (7.70%) belonged to different genera (i.e., Cryptococcus, Geotrichum, Rhodotorula, Saccharomyces, and Trichosporon). The non-albicans Candida species were represented by 60 isolates of *C. parapsilosis* (32.96%), 18 isolates of *C. glabrata* (9.88%), 8 isolates of *C. pelliculosa* (4.40%), 8 isolates of *C. krusei* (4.40%), 6 isolates of *C. guilliermondii* (3.30%), 4 isolates of *C. lusitaniae* (2.20%), 4 isolates of *C. tropicalis* (2.20%), 2 isolates of *C. dubliniensis*, and 2 isolates of *C. intermedia* (1.10% each).

Antifungals

Pure powders of Fluconazole, Voriconazole, and MXP-4509 were used. Fluconazole was purchased from Sigma (St. Louis, USA) and Voriconazole from Pfizer Ltd. (Sandwich, UK), respectively. MXP-4509 was synthesized at the ''Petru Poni'' Institute of Macromolecular Chemistry (Iași, Romania). The final concentrations of antifungal ranged between 0.125 and 64 mg/l for Fluconazole and 0.0156-8 mg/l for Voriconazole and MXP-4509. Microplates were prepared and stored frozen at -20°C until their use (no more than 1 month).

Susceptibility testing

In vitro susceptibility was assessed by following the guidelines of AFST-EUCAST E. Def. 7.1 [410]. The tests were performed in RPMI-1640 medium buffered with MOPS and supplemented with 2% glucose. The final size of inoculum was adjusted to 105 CFU/ml. Minimum inhibitory concentrations were determined spectrophotometrically after 24 or 48 h of incubation at 36°C (depending on the species), using the MR-96A microplate reader (Mindray, China). The minimum inhibitory concentration endpoint was defined as 50% or more reduction in growth compared to that in the drug-free well. Two reference strains, *Candida krusei* ATCC 6258 and *C. parapsilosis* ATCC 22019, were included in each set of determinations to assure the quality of results. After acquirement of the minimum inhibitory concentration values, the following parameters were calculated using specific statistical software: minimum inhibitory concentration $_{50}$, minimum inhibitory concentration $_{90}$, and geometric mean (GM). The minimum inhibitory concentrations$_{50}$ and minimum inhibitory concentrations$_{90}$ of the tested isolates were determined only for which at least 5 or 10 isolates were available, respectively [441]. The interpretation of the minimum inhibitory concentration values and subsequently determination of the susceptibility of a given isolate were made according to EUCAST recommendations as shown in Table 17 [442–444]. All *C. krusei* strains were considered intrinsically resistant to Fluconazole.

Table 17. EUCAST clinical changing breakpoints and ECOFF for Fluconazole and Voriconazole

Antifungal agent	Method	Species	MIC by category (mg/l)			ECOFF
			S[a]	SDD[b]	R[c]	
Fluconazole	EUCAST	*C. albicans*	≤2	-	>4	1
		C. glabrata	-	-	-	32
		C. krusei	-	-	-	128
		C. parapsilosis	≤2	-	>4	2
		C. tropicalis	≤2	-	>4	2
Voriconazole	EUCAST	*C. albicans*	≤0.125	-	>0.125	0.125
		C. glabrata	-	-	-	1
		C. krusei	-	-	-	1
		C. parapsilosis	≤0.125	-	>0.125	0.125
		C. tropicalis	≤0.125	-	>0.125	0.125

ECOFF Epidemiological cutoff
[a] Susceptible
[b] Susceptible dose dependent
[c] Resistant

Results and discussions

A detailed description of the antifungal activity of Fluconazole, Voriconazole, and the new triazole formulation MXP-4509 against tested clinical isolates is shown in Table 18.

Table 18. *In vitro* activity of Fluconazole, Voriconazole, and MXP-4509 against 182 yeast isolates collected from three tertiary hospitals in Romania

Species (no. of isolates)	Antifungal agent	MIC (mg/l)			
		Range	MIC_{50}	MIC_{90}	GM
C. albicans (n = 56)	FCA[a]	0.125-0.5	0.25	0.5	0.205
	VOR[b]	0.0156-0.0312	0.0156	0.0156	0.0159
	MXP[c]	0.0156-0.0625	0.0156	0.0312	0.0194
C. parapsilosis (n = 60)	FCA	0.125-2	0.5	1	0.535
	VOR	0.0156	0.0156	0.0156	0.0156
	MXP	0.0156-0.25	0.0625	0.0625	0.0484
C. glabrata (n = 18)	FCA	0.25-64	32	64	17.281
	VOR	0.0156-8	0.125	8	0.340
	MXP	0.0156-8	0.125	4	0.231
C. pelliculosa (n = 8)	FCA	2-8	4	ND	4
	VOR	0.0312-0.125	0.0625	ND	0.074
	MXP	0.0625-0.5	0.0625	ND	0.105
C. krusei (n = 8)	FCA	16-64	32	ND	38.054
	VOR	0.25-0.5	0.25	ND	0.353
	MXP	0.25-1	0.5	ND	0.500
C.	FCA	0.5–4	0.5	ND	1

guilliermondii (n = 6)	VOR	0.0156–0.0312	0.0156	ND	0.0196
	MXP	0.0625–0.25	0.25	ND	0.157
C. lusitaniae (n = 4)	FCA	0.125–1	ND	ND	0.353
	VOR	0.0156	ND	ND	0.0156
	MXP	0.0156	ND	ND	0.0156
C. tropicalis (n = 4)	FCA	0.5–64	ND	ND	5.656
	VOR	0.0156–2	ND	ND	0.176
	MXP	0.0625–8	ND	ND	0.707
S. cerevisiae (n = 4)	FCA	4-16	ND	ND	8
	VOR	0.0156-0.0625	ND	ND	0.0312
	MXP	0.0312-0.0625	ND	ND	0.0441
T. asahii (n = 4)	FCA	4-32	ND	ND	11.313
	VOR	0.0156-0.25	ND	ND	0.0624
	MXP	0.0312	ND	ND	0.0312
C. dubliniensis (n = 2)	FCA	0.0625-0.25	ND	ND	0.125
	VOR	0.0156	ND	ND	0.0156
	MXP	0.0156	ND	ND	0.0156
C. intermedia (n = 2)	FCA	0.125-0.5	ND	ND	0.25
	VOR	0.0156	ND	ND	0.0156
	MXP	0.0156-0.0625	ND	ND	0.0312
C. neoformans (n = 2)	FCA	2-8	ND	ND	4
	VOR	0.0156	ND	ND	0.0156
	MXP	0.0625-0.25	ND	ND	0.125
G. capitatum (n = 2)	FCA	4	ND	ND	4
	VOR	0.0156-0.0625	ND	ND	0.0312
	MXP	0.0156	ND	ND	0.0156
R. mucilaginosa (n = 2)	FCA	16-64	ND	ND	32
	VOR	0.5-2	ND	ND	1
	MXP	8	ND	ND	8

ND not determined
[a] Fluconazole
[b] Voriconazole
[c] MXP-4509

After analysis of minimum inhibitory concentration values, the overall susceptibility to Fluconazole in our study was 84.62%, while the rate of resistance was 15.38%, and this fact may be correlated with an important rate of clinical resistance and treatment failure especially in yeast species other than *C. albicans* and *C. parapsilosis*. The explanation for a high *C. parapsilosis* incidence in our study despite the susceptibility of this organism to Fluconazole may be the fact that *C. parapsilosis* adheres to the surface of indwelling central venous catheters and forms biofilm, therefore becoming resistant to usual antifungal agents, particularly Fluconazole [445].

The higher resistance rate was registered for *C. glabrata* (33.33%), significantly higher than in other studies [385,387]. We think this is due to the rather empirical use of Fluconazole in our country,

both for prophylactic and for therapeutic purposes in majority of patients at risk. Despite these findings, at least in Romania, Fluconazole remains an active, safe, and cheaper antifungal drug that is indicated as pre-emptive therapy in patients colonized or infected with *C. albicans* and *C. parapsilosis*.

Voriconazole performed better, only 2.19% of the tested strains presenting minimum inhibitory concentrations outside the susceptibility interval. This value is significantly different from that obtained by Pfaller et al., [446] (11.9%) and quite similar to that reported by others - 1% [447]. Voriconazole was highly potent *in vitro* against the majority of Fluconazole-resistant isolates although one isolate of *C. tropicalis* and three of *C. glabrata* were resistant. For these species, Fluconazole resistance may predict resistance to Voriconazole as suggested by Lyon et al., [385].

Overall, the activity of MXP-4509 was comparable to that of Voriconazole (MIC_{50}: 0.0312 mg/l vs. 0.0156 mg/l; MIC_{90}: 0.25 mg/l vs. 0.25 mg/l) and obviously higher to that of Fluconazole (MIC_{50}: 0.0312 mg/l vs. 0.5 mg/l; MIC_{90}: 0.25 mg/l vs. 32 mg/l). MXP-4509 exhibited significant lower geometric mean values than Voriconazole for *C. glabrata*, *T. asahii*, and *G. capitatum* strains ($P<0.05$). It had good activity (minimum inhibitory concentrations≤1 mg/l) against 78.57% of Fluconazole resistant isolates belonging to different species. The results suggest that MXP-4509 may be a useful antifungal drug, and more pharmacological and microbiological investigations are needed in order to prove its activity on animal models of invasive fungal infections, to establish changing breakpoints for *in vitro* susceptibility testing, and to evaluate the pharmacokinetic and pharmacodynamic aspects.

Personal contribution - published papers:

Minea, B.; Nastasa, V.; Moraru, R.F.; Kolecka, A.; Flonta, M.M.; Marincu, I.; Man, A.; Toma, F.; Lupse, M.; **Doroftei**, **B**.; et al. Species distribution and susceptibility profile to fluconazole, voriconazole and MXP-4509 of 551 clinical yeast isolates from a Romanian multi-centre study. *Eur. J. Clin. Microbiol. Infect. Dis.* ***2015***, *34*, 367–383. **IF: 3.267**

Aim of the study

The aim was to determine the aetiological spectrum and susceptibility pattern to Fluconazole, Voriconazole and the novel compound MXP-4509.

Materials and methods

Clinical isolates processing

During a two-year period (2010-2011), 551 clinical yeast isolates were collected in four tertiary hospitals from different regions of Romania (i.e. Iasi, Cluj-Napoca, Timisoara and Târgu Mureș). Of these, 174 were recovered from blood culture-confirmed bloodstream infections, 93 from deep-seated mycoses (DEEP) (lower respiratory tract in patients without oropharyngeal mycosis, upper urinary tract in non-catheterised patients, peritoneal cavity, cerebrospinal fluid (CSF) and 284 from superficial mycoses (SUP) (oropharyngeal, female genital tract, gastro-intestinal tract, other sites). The isolates were collected from patients who presented at least two of the following risk factors simultaneously: low birth weight (65 years), insulin-dependent diabetes mellitus, recent major surgery, broad-spectrum antibiotic therapy, central venous catheter, organ transplantation, prolonged intensive care unit stay (>48 h), immunosuppression- human immunodeficiency virus (HIV) infection or other predisposing conditions, total parenteral nutrition or mechanical ventilation.

We included the gastrointestinal isolates in the category of superficial infections, since they all came from antibiotics induced dysbiosis and generated high microbial loads, which, we considered, advocated against mere colonisation. Moreover, the dysbioses did not involve the penetration of the intestinal mucosal barrier.

The isolates were presumptively identified by local hospital laboratories using routine microbiological methods - germ tube test, API® Candida strips (bioMérieux, France) or the Vitek® 2 system (bioMérieux, France), and chromogenic culture media (bioMérieux, France) and then

submitted to our centre (Laboratory of Antimicrobial Chemotherapy, "Ion Ionescu de la Brad" University, Iasi, Romania). All isolates were checked for purity and stored in 10% glycerol at −70°C until the final processing and antifungal susceptibility testing. The final identification was performed using ID32C strips (bioMérieux, France). Isolates identified as *Candida albicans* or *C. dubliniensis* were additionally tested using duplex polymerase chain reaction, a molecular method previously described [448]. Yeasts without conclusive identification based on the ID32C strips (e.g. Saccharomyces spp., arthroconidial yeasts, the *C. parapsilosis* complex) were further processed for matrix-assisted laser desorption ionisation time-of-flight mass spectrometry (MALDI-TOF MS) testing at the CBSKNAW Fungal Biodiversity Centre. For isolates where the MALDI-TOF MS result was not reliable, sequence analyses of the internal transcribed spacer (ITS) and D1/D2 domains of the large subunit (LSU) of the ribosomal DNA were used for final identification.

Identification by MALDI-TOF MS Biotyper 3.0 (Bruker Daltonics, Bremen, Germany) was carried out using the Bruker Daltonics GmbH protocol of ethanol/formic acid extraction, as reported by Kolecka et al., [27]. As a positive control, 1 µl of Bacterial Test Standard solution (Bruker, Bremen, Germany) was used in duplicate. For each tested isolate, 1 µl of the crude protein extract was spotted twice on a 96-spot polished steel target plate (Bruker, Bremen, Germany). After air drying, all spots were overlaid with 1 µl of the alpha-cyano-4-hydroxycinnamic acid (HCCA) matrix solution (Bruker, Bremen, Germany), prepared according to the protocol of the manufacturer and, after air drying, measured in automatic runs.

Identification runs were operated by FlexControl v.3.3.108.0, simultaneously with a commercially available Bruker database BDAL (4,110 MSP) and an in-house CBS-KNAW library of 510 MSP of clinically relevant yeasts, generated by Bruker Daltonics. The identification results generated by MALDI-TOF MS were scored as the log values according to: correct genus and species identification (>2.0), secure genus identification (1.7-2.0) and no reliable identification (<1.7).

DNA extraction and sequencing was performed as described by Kolecka et al., [449]. Briefly, genomic DNA was extracted from yeasts grown on GYPA plates incubated at 30°C for 48 h. DNA extractions were performed following the phenol-chloroform-isoamyl alcohol method, as reported by Cendejas-Bueno et al., [450]. The primers reported by White et al., [451] were used for internal transcribed spacer, while the D1/D2 large subunit region was amplified using the primers suggested by Vilgalys and Hester [452]. The polymerase chain reaction and sequencing conditions were as reported by Cendejas-Bueno et al., [450]. Sequence alignments were assembled and edited using SeqMan version 8.0.2 software (DNASTAR, Inc., Madison, WI, USA) and aligned with MEGA version 5. The sequences were manually corrected. Consensus sequences were compared by the basic local alignment search tool (BLAST) with sequences available from the in-house CBS sequences and the GenBank™ database for correct identification.

Antifungal agents and susceptibility testing

In vitro susceptibility testing was performed following the EUCAST EDef 7.1 guidelines [410], with the updates in EUCAST EDef 7.2 regarding Cryptococcus [453], for three antifungal agents: Fluconazole (Sigma, St. Louis, MO, USA), Voriconazole (Pfizer Ltd., Sandwich, UK) and the MXP-4509 compound ("Petru Poni" Institute of Macromolecular Chemistry, Iasi, Romania). The stock solutions were prepared using dimethyl sulfoxide (DMSO) as a solvent for Fluconazole and Voriconazole, and deionised water for MXP. The concentration ranges of the tested antifungals were 0.125-64 mg/L for Fluconazole and 0.0156-8 mg/L for Voriconazole and MXP. The minimum inhibitory concentrations were determined spectrophotometrically at 405 nm, after 24 h or 48 h of incubation at 35°C (30°C for Cryptococcus isolates), using an iMark Microplate Absorbance Reader (Bio-Rad Laboratories, Hercules, CA, USA). A 50% reduction in growth (compared with the drug-free well) was used as the minimum inhibitory concentration endpoint for all the tested drugs. Three reference strains (*C. albicans* ATCC 90028, *C. krusei* ATCC 6258 and *C. parapsilosis* ATCC 22019) were used for quality control purposes.

The interpretation of Fluconazole and Voriconazole minimum inhibitory concentrations was done according to the recent EUCAST document "Antifungal agents. Breakpoint tables for interpretation of minimum inhibitory concentrations", version 6.1 [454]. For species without an established specific changing breakpoint, the epidemiological cut-off value (ECOFF), if available,

was preferred to a non-specific changing breakpoint. For Voriconazole, a value suggested in the EUCAST document "EUCAST Technical Note on voriconazole" [443] was used as a non-specific BP. All C. *krusei* isolates were considered intrinsically resistant to Fluconazole. By applying these criteria, the following changing breakpoints resulted (expressed in mg/L): S≤2 and R>4 for Fluconazole against *C. albicans*, *C. parapsilosis* and *C. tropicalis*; S≤0.002 and R>32 for Fluconazole against *C. glabrata*; S≤2 and R>4 as nonspecific changing breakpoints for Fluconazole; S≤0.125<R for Voriconazole against *C. albicans*, *C. parapsilosis* and *C. tropicalis*; S≤1<R for Voriconazole against *C. glabrata* and *C. krusei*; and S≤0.25<R as a non-specific changing breakpoint for Voriconazole. When reporting reduced susceptibility to any of the two azoles, we used the criteria suggested by Pfaller et al., [400], namely, less than 75 % susceptible isolates for a certain species or group.

Statistical analysis

A range of parameters [mode, MIC_{50} for n≥5, MIC_{90} for n≥10 and geometric mean for n≥2 overall (i.e. regardless of infection type) and n≥5/infection type, where n is the number of isolates] were calculated for the minimum inhibitory concentrations of each tested drug using Microsoft® Excel® 2010 [401,455]. The geometric means of the minimum inhibitory concentrations were calculated as the antilogarithm of the arithmetic mean of the natural logarithms of the minimum inhibitory concentrations using as a base the following array formula: EXP(AVERAGE(LN(x))), where "x" is a range of minimum inhibitory concentration values. This formula was extended with various logical arguments using the IF function. To calculate the 95 % CIs of proportions and to perform statistical tests, a fully functional trial version of GraphPad Prism version 6.04 for Windows (GraphPad Software, La Jolla, CA, USA; http://www.graphpad.com) was used. The 95 % CIs of proportion were calculated using the method of Clopper and Pearson. The Kruskal-Wallis test followed by Dunn's multiple comparison test were used to compare the distribution of the minimum inhibitory concentration between infection types. The Wilcoxon matched-pairs signed-rank test, using the method of Pratt for ties, was run to compare the activities of Voriconazole and MXP-4509. Two-tailed *p*-values were calculated and $p<0.05$ was considered significant. For large samples, the software calculated approximate *p*-values (indicated by the "≈" sign).

To calculate the geometric means and run the statistical tests, right-censored values (minimum inhibitory concentration>the maximum tested concentration) were considered as the next theoretical value [455]. In other words, >64 and >8 were considered as 128 and 16, respectively (all expressed in mg/L).

Results

Species distribution

The overall species distribution and the calculated statistical parameters of the minimum inhibitory concentrations, for species and various defined groups of species, are shown in Table 19. The table also provides the teleomorphic names where available [456], but we based our analysis on the names most widely used by clinicians and the various routine identification systems which are most often those of the anamorphs. Thirty species that belong to nine genera were identified. Both overall and within each category of infections, the artificial genus Candida was dominant, with isolates that belong to 20 species.

Table 19. Overall species (n>1) distribution and *in vitro* susceptibility

Species/group (no. of isolates, % of all isolates	95% CI of proportion	Compound	MIC (µg/ml)				
			Range	Mode	MIC_{50}	MIC_{90}	GM[a]
Candida spp. (521, 94.56%)	92.32-96.30 %	FLC	≤0.125->64.0	0.25	0.5	16.0	0.7482
		VOR	≤0.0156->8.0	0.0156	0.0156	0.25	0.0304
		MXP	≤0.0156-8.0	0.0156	0.0156	0.125	0.0352

C. albicans (278, 50.45%)	46.20-54.71 %	FLC	≤0.125-32.0	0.25	0.25	0.5	0.2762
		VOR	≤0.0156-1.0	0.0156	0.0156	0.0156	0.0163
		MXP	≤0.0156-0.25	0.0156	0.0156	0.0312	0.0193
C. parapsilosis (70, 12.70%)	10.04-15.78 %	FLC	≤0.125-4.0	0.5	0.5	1.0	0.6156
		VOR	≤0.0156-0.0625	0.0156	0.0156	0.0312	0.0196
		MXP	≤0.0156-0.25	0.0625	0.0625	0.125	0.0544
C. glabrata (60, 10.89%)	8.41-13.79 %	FLC	≤0.125->64.0	32.0	16.0	32.0	12.9960
		VOR	≤0.0156->8.0	0.5	0.25	1.0	0.2806
		MXP	≤0.0156-8.0	0.125	0.0625	0.25	0.0894
C. krusei (TM[b]: *Pichia kudriavzevii*) (27, 4.90%)	3.25-7.05 %	FLC	16.0->64.0	32.0	32.0	64.0	36.3828
		VOR	0.125-0.5	0.25	0.25	0.5	0.2916
		MXP	0.125-4.0	0.25	0.25	1.0	0.3581
C. tropicalis (25, 4.54%)	2.96-6.63 %	FLC	≤0.125->64.0	0.5; 1.0	0.5	8.0	0.9202
		VOR	≤0.0156->8.0	0.0156	0.0312	0.5	0.0559
		MXP	≤0.0156-8.0	0.0625	0.0625	0.25	0.0824
C. kefyr (TM: Kluyveromyces marxianus) (21, 3.81%)	2.37-5.77 %	FLC	0.25–2.0	0.5	0.5	0.5	0.4102
		VOR	≤0.0156-0.0625	0.0156	0.0156	0.0156	0.0172
		MXP	≤0.0156-0.0312	0.0156	0.0156	0.0156	0.0167
C. lusitaniae (TM: Clavispora lusitaniae) (10, 1.81%)	0.87-3.31 %	FLC	≤0.125-1.0	0.125; 0.5	0.25	1.0	0.3299
		VOR	NA[c]	0.0156	0.0156	0.0156	0.0156
		MXP	≤0.0156-0.0312	0.0156	0.0156	0.0156	0.0167
C. dubliniensis (6, 1.09%)	0.40-2.35 %	FLC	0.25–0.5	0.25	0.25	NA	0.2806
		VOR	NA	0.0156	0.0156	NA	0.0156
		MXP	NA	0.0156	0.0156	NA	0.0156
C. guilliermondii (TM: *Meyerozyma guilliermondii)* (6, 1.09%)	0.40-2.35 %	FLC	0.25-4.0	0.5; 4.0	0.5	NA	1.0000
		VOR	≤0.0156-0.125	0.0312	0.0312	NA	0.0312
		MXP	0.0625-0.5	0.25	0.25	NA	0.2227
C. pelliculosa (TM: *Wickerhamomyces anomalus*) (4, 0.73%)	0.20-1.85 %	FLC	2.0-8.0	4.0	NA	NA	4.0000
		VOR	0.0312-0.125	0.125	NA	NA	0.0743
		MXP	0.0625-0.5	0.0625	NA	NA	0.1051
C. rugose (3, 0.54%)	0.11-1.58 %	FLC	4.0-8.0	8.0	NA	NA	6.3496
		VOR	0.125-0.5	0.125	NA	NA	0.1984
		MXP	0.125-0.5	0.125	NA	NA	0.1984
C. inconspicua (2, 0.36%)	0.04-1.30 %	FLC	NA	32.0	NA	NA	32.0000
		VOR	NA	0.25	NA	NA	0.2500
		MXP	0.0312-0.125	NA	NA	NA	0.0624
C. lipolytica (TM: Yarrowia lipolytica) (2, 0.36%)	0.04–1.30 %	FLC	0.5–1.0	NA	NA	NA	0.7071
		VOR	NA	0.0156	NA	NA	0.0156
		MXP	NA	0.0156	NA	NA	0.0156
Unique *Candida* spp.[d] (7, 1.27%)	0.51-2.60 %	FLC	0.25-64.0	0.25; 16.0	16.0	NA	5.3836
		VOR	≤0.0156-0.5	0.0156	0.0312	NA	0.0624
		MXP	≤0.0156-0.5	0.0312	0.0312	NA	0.0624
Non-*albicans Candida* spp. (243, 44.10%)	39.91-48.36 %	FLC	≤0.125->64.0	0.5	1.0	32.0	2.3397
		VOR	≤0.0156->8.0	0.0156	0.0312	0.5	0.0621
		MXP	≤0.0156-8.0	0.0625	0.0625	0.25	0.0698
Non-*Candida* spp. (30, 5.44%)	3.70-7.68	FLC	≤0.125-32.0	2.0; 4.0	2.0	8.0	2.5198

	%	VOR	≤0.0156-1.0	0.0156	0.0312	0.25	0.0519
		MXP	≤0.0156-8.0	0.0312	0.0312	0.125	0.0484
Saccharomyces cerevisiae (11, 2.00%)	1.00-3.54 %	FLC	0.5-8.0	MM[e]	4.0	8.0	2.9190
		VOR	≤0.0156-0.25	MM	0.0625	0.125	0.0551
		MXP	≤0.0156-0.125	0.0625	0.0625	0.0625	0.0428
Geotrichum candidum (5, 0.91%)	0.30-2.10 %	FLC	≤0.125-8.0	NA	2.0	NA	1.1487
		VOR	0.0312-0.125	0.0312	0.0312	NA	0.0473
		MXP	0.0312-0.0625	0.0312	0.0312	NA	0.0412
Trichosporon asahii (4, 0.73%)	0.20-1.85 %	FLC	2.0-32.0	2.0	NA	NA	4.0000
		VOR	≤0.0156-0.25	NA	NA	NA	0.0624
		MXP	0.0312-0.0625	0.0312; 0.0625	NA	NA	0.0442
Cryptococcus neoformans (3, 0.54%)	0.11-1.58 %	FLC	1.0-4.0	NA	NA	NA	2.0000
		VOR	≤0.0156-0.0312	0.0156	NA	NA	0.0197
		MXP	0.0312-0.125	0.0312	NA	NA	0.0496
Magnusiomyces capitatus (2, 0.36%)	0.04-1.30 %	FLC	NA	4.0	NA	NA	4.0000
		VOR	0.0312-1.0	NA	NA	NA	0.1766
		MXP	≤0.0156-0.125	NA	NA	NA	0.0442
Unique non-*Candida* spp.[f] (5, 0.91%)	0.30-2.10 %	FLC	≤0.125-32.0	NA	4.0	NA	2.9720
		VOR	≤0.0156-1.0	0.0156	0.0156	NA	0.0512
		MXP	≤0.0156-8.0	0.0312	0.0312	NA	0.0565
Yeast total		FLC	≤0.125->64.0	0.25	0.5	16.0	0.7994
		VOR	≤0.0156->8.0	0.0156	0.0156	0.25	0.0313
		MXP	≤0.0156-8.0	0.0156	0.0312	0.125	0.0358

[a] GM = geometric mean
[b] TM = teleomorph
[c] NA = not applicable
[d] Species with n=1 (MICs in parentheses): *C. famata*/*Debaryomyces hansenii* (FLC 32.0, VOR 0.5, MXP 0.5), *C. haemulonii* (FLC 64.0, VOR 0.5, MXP 0.25), *C. intermedia* (FLC 0.25, VOR 0.0156, MXP 0.0312), *C. lambica*/*Pichia fermentans* (FLC 16.0, VOR 0.0156, MXP 0.0312), *C. norvegensis*/*Pichia norvegensis* (FLC 16.0, VOR 0.0312, MXP 0.0312), *C. pulcherrima*/*Metschnikowia pulcherrima* (FLC 0.25, VOR 0.0156, MXP 0.0156), *C. utilis*/*Lindnera jadinii* (FLC 4.0, VOR 0.125, MXP 0.0625)
[e] MM = multi-modal (more than two modes)
[f] Species with n=1 (MICs in parentheses): *Lodderomyces elongisporus* (FLC 0.125, VOR 0.0156, MXP 0.0156), *Pichia burtonii* (FLC 1.0, VOR 0.0156, MXP 0.0312), *Rhodotorula mucilaginosa* (FLC 32.0, VOR 1.0, MXP 8.0), *Trichosporon coremiiforme* (FLC 4.0, VOR 0.0156, MXP 0.0312), *Trichosporon moniliiforme* (FLC 8.0, VOR 0.0625, MXP 0.0312)

For each category of infections analysed separately, the same type of information is presented in Table 20. The most abundant category was superficial mycoses, followed by bloodstream infections and deep-seated mycoses. With 22 species, superficial mycoses had the highest species diversity, followed by bloodstream infections, with 17 species, and deep-seated mycoses, with ten species.

Five *Candida* spp. (*C. albicans*, *C. glabrata*, *C. krusei*, *C. parapsilosis* and *C. tropicalis*) and one non-*Candida* spp. (*Trichosporon asahii*) were present in all three types of infection. Seven *Candida* spp. (*C. dubliniensis*, *C. inconspicua*, *C. lambica*, *C. norvegensis*, *C. pulcherrima*, *C. rugosa* and *C. utilis*) and three non-*Candida* spp. (*Geotrichum candidum*, *Pichia burtonii* and *Trichosporon moniliiforme*) were only found in superficial mycoses. Three *Candida* spp. (*C. haemulonii*, *C. intermedia* and *C. pelliculosa*) and three non-*Candida* spp. (*Lodderomyces elongisporus*, *Rhodotorula mucilaginosa* and *Trichosporon coremiiforme*) were isolated exclusively from bloodstream infections. Only one species, *C. famata*, was unique to deep-seated mycoses.

C. albicans was the most prevalent species overall, in superficial mycoses and in deep-seated mycoses. In bloodstream infections, however, there were two leading species, namely, *C. parapsilosis*, followed by *C. albicans*. Other frequently isolated species were *C. glabrata*, overall and in every infection type, *C. lusitaniae* overall, and *C. parapsilosis*, *C. krusei*, *C. tropicalis* and *C. kefyr*, overall and in superficial mycoses. The most frequently occurring non-*Candida* spp. isolates were of

Saccharomyces cerevisiae, followed by *Geotrichum candidum*.

Table 20. Species (n≥5) distribution and *in vitro* susceptibility according to infection type

Infection site and species (no. of isolates, % of infection type	95% CI of proportion	Compound	MIC (µg/ml)				
			Range	Mode	MIC_{50}	MIC_{90}	GM[a]
Bloodstream infections (174)							
Candida spp. (167, 95.98%)	91.89-98.37 %	FLC	≤0.125-≥64.0	0.25	0.5	32.0	0.8435
		VOR	≤0.0156->8.0	0.0156	0.0156	0.5	0.0324
		MXP	≤0.0156-8.0	0.0156	0.0312	0.25	0.0456
C. parapsilosis (59, 33.91%)	26.92-41.46 %	FLC	≤0.125–2.0	0.5; 1.0	0.5	1.0	0.5964
		VOR	≤0.0156–0.0312	0.0156	0.0156	0.0312	0.0190
		MXP	≤0.0156–0.25	0.0625	0.0625	0.125	0.0494
C. albicans (57, 32.76%)	25.85-40.27 %	FLC	≤0.125–32.0	0.25	0.25	0.5	0.2324
		VOR	≤0.0156–1.0	0.0156	0.0156	0.0156	0.0168
		MXP	≤0.0156–0.25	0.0156	0.0156	0.0312	0.0187
C. glabrata (25, 14.37%)	9.52-20.48 %	FLC	≤0.125-≥64.0	16.0	16.0	64.0	13.1775
		VOR	≤0.0156->8.0	1.0	0.25	2.0	0.2716
		MXP	≤0.0156-8.0	0.125	0.125	0.25	0.1058
C. guilliermondii (TM[c]: *Meyerozyma guilliermondii*) (5, 2.87%)	0.94-6.58 %	FLC	0.25-4.0	0.5; 4.0	0.5	NA[b]	1.0000
		VOR	≤0.0156-0.125	0.0156; 0.0312	0.0312	NA	0.0312
		MXP	0.0625-0.5	0.25	0.25	NA	0.2176
C. krusei (TM: Pichia kudriavzevii) (5, 2.87%)	0.94-6.58 %	FLC	16.0-64.0	32.0; 64.0	32.0	NA	36.7583
		VOR	0.25-0.5	0.25	0.25	NA	0.3299
		MXP	0.25-1.0	0.5	0.5	NA	0.5000
C. tropicalis (5, 2.87%)	0.94-6.58 %	FLC	≤0.125-64.0	0.5	0.5	NA	0.8706
		VOR	≤0.0156-2.0	0.0156; 0.0312	0.0312	NA	0.0543
		MXP	0.0312-8.0	0.0625	0.0625	NA	0.1435
Rare *Candida* spp.[d] (11,	3.20-11.03 %	FLC	≤0.125-64.0	MM[e]	1.0	8.0	1.3704

6.32%)		VOR	≤0.0156-0.5	0.0156	0.0156	0.125	0.0377
		MXP	≤0.0156-0.5	0.0156	0.0312	0.25	0.0428
Non-*albicans Candida* spp. (110, 63.22%)	55.59-70.39 %	FLC	≤0.125->64.0	0.5	1.0	32.0	1.6451
		VOR	≤0.0156->8.0	0.0156	0.0156	0.5	0.0456
		MXP	≤0.0156-8.0	0.0625	0.0625	0.25	0.072
Non-*Candida* spp.[f] (7, 4.02%)	1.63-8.11 %	FLC	≤0.125-32.0	MM	8.0	NA	5.3836
		VOR	≤0.0156-1.0	0.0156	0.0312	NA	0.0566
		MXP	≤0.0156-8.0	0.0312	0.0312	NA	0.0624
Yeast BSI total		FLC	≤0.125-≥64.0	0.25	0.5	32.0	0.9088
		VOR	≤0.0156->8.0	0.0156	0.0156	0.5	0.0331
		MXP	≤0.0156-8.0	0.0156	0.0312	0.25	0.0461
Deep-seated infections (93)							
Candida spp. (89, 95.70%)	89.35-98.82 %	FLC	≤0.125-≥64.0	0.25	0.25	32.0	0.7438
		VOR	≤0.0156->8.0	0.0156	0.0156	0.5	0.0340
		MXP	≤0.0156-8.0	0.0156	0.0156	0.25	0.0315
C. albicans (61, 65,59%)	55.02-75.14 %	FLC	≤0.125-1.0	0.25	0.25	0.5	0.2707
		VOR	≤0.0156-0.0312	0.0156	0.0156	0.0156	0.0158
		MXP	≤0.0156-0.0625	0.0156	0.0156	0.0312	0.0183
C. glabrata (11, 11.83%)	6.05-20.18 %	FLC	4.0->64.0	32.0	32.0	64.0	19.3294
		VOR	0.125->8.0	0.5	0.5	1.0	0.4408
		MXP	≤0.0156-8.0	0.0312; 0.25	0.125	0.25	0.1173
C. kefyr (TM: *Kluyveromyces marxianus*) (5, 5.38%)	1.77-12.10 %	FLC	0.25-1.0	0.5	0.5	NA	0.5000
		VOR	NA	0.0156	0.0156	NA	0.0156
		MXP	NA	0.0156	0.0156	NA	0.0156
C. krusei (TM: *Pichia kudriavzevii*) (5, 5.38%)	1.77-12.10 %	FLC	16.0->64.0	16.0	32.0	NA	36.7583
		VOR	0.25-0.5	0.25	0.25	NA	0.3299
		MXP	0.125-4.0	0.5	0.5	NA	0.5000
Rare *Candida* spp.[g] (7,	3.08-14.89 %	FLC	0.25->64.0	1.0	1.0	NA	2.4380

7.53%)		VOR	0.0312->8	0.0312; 0.0625	0.0625	NA	0.1682
		MXP	≤0.0156-0.5	0.25	0.125	NA	0.1025
Non-*albicans Candida* spp. (28, 30.11%)	21.03-40.50 %	FLC	0.25->64.0	32.0	8.0	>64.0	6.7272
		VOR	≤0.0156->8.0	0.5	0.25	1.0	0.1811
		MXP	≤0.0156-8.0	0.0156	0.125	0.5	0.1025
Non-*Candida* spp.[h] (4, 4.30%)	1.18-10.65 %	FLC	1.0-4.0	2.0	NA	NA	2.0000
		VOR	≤0.0156-0.0312	0.0156	NA	NA	0.0186
		MXP	0.0312-0.125	0.0312	NA	NA	0.0525
Yeast DEEP total		FLC	≤0.125-≥64.0	0.25	0.25	32.0	0.7762
		VOR	≤0.0156->8.0	0.0156	0.0156	0.5	0.0331
		MXP	≤0.0156-8.0	0.0156	0.0156	0.25	0.0322
Superficial infections (284)							
Candida spp. (265, 93.31%)	89.75-95.92 %	FLC	≤0.125-≥64.0	0.25	0.25	16.0	0.6952
		VOR	≤0.0156-1.0	0.0156	0.0156	0.25	0.0282
		MXP	≤0.0156-1.0	0.0156	0.0156	0.125	0.0311
C. albicans (160, 56.34%)	50.35-62.19 %	FLC	≤0.125-16.0	0.25	0.25	0.5	0.2960
		VOR	≤0.0156-0.5	0.0156	0.0156	0.0156	0.0164
		MXP	≤0.0156-0.125	0.0156	0.0156	0.0312	0.0200
C. glabrata (24, 8.45%)	5.49-12.31 %	FLC	0.25-32.0	16.0; 32.0	16.0	32.0	10.6787
		VOR	≤0.0156-1.0	0.25	0.25	1.0	0.2360
		MXP	≤0.0156-0.25	0.0625; 0.125	0.0625	0.25	0.0662
C. krusei (TM: *Pichia kudriavzevii*) (17, 5.99%)	3.53-9.41 %	FLC	16.0–>64.0	32.0	32.0	64.0	36.1637
		VOR	0.125–0.5	0.25	0.25	0.5	0.2712
		MXP	0.125–4.0	0.25	0.25	0.5	0.2943
C. kefyr (TM: Kluyveromyces marxianus) (16, 5.63%)	3.25-8.99 %	FLC	0.25-2.0	0.25	0.25	0.5	0.3856
		VOR	≤0.0156-0.0625	0.0156	0.0156	0.0312	0.0178
		MXP	≤0.0156-0.0312	0.0156	0.0156	0.0312	0.0170
C. tropicalis (16, 5.63%)	3.25-8.99 %	FLC	≤0.125-8.0	0.25; 1.0	0.5	2.0	0.7071

		VOR	≤0.0156-0.5	0.0156	0.0312	0.125	0.0371
		MXP	≤0.0156-1.	0.125	0.0625	0.25	0.0681
C. parapsilosis (10, 3.52%)	1.70-6.38 %	FLC	≤0.125-4.0	0.5	0.5	4.0	0.8123
		VOR	≤0.0156-0.0625	0.0156	0.0156	0.0312	0.0221
		MXP	≤0.0156-0.25	0.125	0.125	0.25	0.1088
C. dubliniensis (6, 2.11%)	0.78-4.54 %	FLC	0.25-0.5	0.25	0.25	NA	0.2806
		VOR	NA	0.0156	0.0156	NA	0.0156
		MXP	NA	0.0156	0.0156	NA	0.0156
C. lusitaniae (TM: *Clavispora lusitaniae*) (6, 2.11%)	0.78-4.54 %	FLC	≤0.125-1.0	0.125; 0.5	0.25	NA	0.3150
		VOR	NA	0.0156	0.0156	NA	0.0156
		MXP	≤0.0156-0.0312	0.0156	0.0156	NA	0.0175
Rare *Candida* spp.[i] (10, 3.52%)	1.70-6.38 %	FLC	0.25–32.0	MM	8.0	32.0	6.0629
		VOR	≤0.0156-0.5	0.0156; 0.125	0.125	0.25	0.0769
		MXP	≤0.0156-0.5	0.0312; 0.125	0.0312	0.125	0.0583
Non-*albicans Candida* spp. (105, 36.97%)	31.34-42.87 %	FLC	≤0.125->64.0	0.25	2.0	32.0	2.5533
		VOR	≤0.0156-1.0	0.0156	0.0625	0.5	0.0645
		MXP	≤0.0156-4.0	0.0156	0.0625	0.25	0.0608
Non-*Candida* spp. (19, 6.69%)	4.08-10.25 %	FLC	≤0.125-8.0	2.00	2.00	8.00	2.0000
		VOR	≤0.0156-1.0	2.00	0.0625	0.25	0.0625
		MXP	≤0.0156-0.125	0.0312	0.0312	0.125	0.0434
Saccharomyces cerevisiae (9, 3.17%)	1.46-5.93 %	FLC	0.5-8.0	2.0; 4.0	2.0	NA	2.3331
		VOR	≤0.0156-0.25	0.125	0.0625	NA	0.0625
		MXP	≤0.0156-0.125	0.0625	0.0625	NA	0.0425
Geotrichum candidum (5, 1.76%)	0.57-4.06 %	FLC	≤0.125-8.0	NA	2.0	NA	1.1487
		VOR	0.0312-0.125	0.0312	0.0312	NA	0.0473
		MXP	0.0312-0.0625	0.0312	0.0312	NA	0.0412
Rare non-*Candida* spp.[j]	0.57-4.06 %	FLC	1.0-8.0	2.0	2.0	NA	1.7411
		VOR	≤0.0156-1.0	NA	0.0625	NA	1.7411

		MXP	0.0312-0.125	0.0312	0.0312	NA	0.0442
Yeast SUP total		FLC	≤0.125-≥64.0	0.25	0.5	16.0	0.7461
		VOR	≤0.0156-1.0	0.0156	0.0156	0.25	0.0297
		MXP	≤0.0156-4.0	0.0156	0.0156	0.125	0.0318

[a] GM = geometric mean
[b] NA = not applicable
[c] TM = teleomorph
[d] Species with n<5 (number of isolates in parentheses): *C. lusitaniae*/*Clavispora lusitaniae* (4), *C. pelliculosa*/*Wickerhamomyces anomalus* (4), *C. haemulonii* (1), *C. intermedia* (1), *C. lipolytica*/*Yarrowia lipolytica* (1)
[e] MM = multi-modal, i.e. more than two modes
[f] Species with n<5 (number of isolates in parentheses): *Lodderomyces elongisporus* (1), *Magnusiomyces capitatus* (1), *Rhodotorula mucilaginosa* (1), *Saccharomyces cerevisiae* (2), *Trichosporon asahii* (1), *Trichosporon coremiiforme* (1)
[g] Species with n<5 (number of isolates in parentheses): *C. tropicalis* (4), *C. famata*/*Debaryomyces hansenii* (1), *C. guilliermondii*/*Meyerozyma guilliermondii* (1), *C. parapsilosis* (1)
[h] Species with n<5 (number of isolates in parentheses): *Cryptococcus neoformans* (2),*Trichosporon asahii* (2)
[i] Species with n<5 (number of isolates in parentheses): *C. rugosa* (3), *C. inconspicua* (2), *C. lambica*/*Pichia fermentans* (1), *C. lipolytica*/*Yarrowia lipolytica* (1), *C. norvegensis*/*Pichia norvegensis* (1), *C. pulcherrima*/*Metschnikowia pulcherrima* (1), *C. utilis*/*Lindnera jadinii* (1)
[j] Species with n<5 (number of isolates in parentheses): *Cryptococcus neoformans* (1), *Magnusiomyces capitatus* (1), *Pichia burtonii* (1), *Trichosporon asahii* (1), *Trichosporon moniliiforme* (1)

Minimum inhibitory concentration distribution

Overall, most MIC_{50} values were within a ± 2 $\log_2$ dilutions range: 0.25-2 mg/L for Fluconazole and 0.0156-0.125 mg/L for Voriconazole and MXP. For Fluconazole, *C. krusei*, *C. glabrata* and *S. cerevisiae*, as well as the "Unique *Candida*" and "Unique non-*Candida*" groups were exceptions to this rule, with MIC_{50} values that were one to four dilutions above the mentioned range. For Voriconazole, *C. krusei* and *C. glabrata* were the exceptions, both with one dilution higher MIC_{50} values. For MXP, *C. krusei* and *C. guilliermondii* were the exceptions, both one dilution higher (Table 20).

There were six right-censored isolates for Fluconazole: three of *C. glabrata* (2 bloodstream infections+1 deep-seated mycoses), two of *C. krusei* (1 deep-seated mycoses+1 superficial mycoses) and one of *C. tropicalis* (deep-seated mycoses). For Voriconazole, there were three right-censored isolates: two of *C. glabrata* (1 bloodstream infections+1 deep-seated mycoses) and one of *C. tropicalis* (deep-seated mycoses); all were also right-censored for Fluconazole.

The distribution of MXP minimum inhibitory concentration for the "Candida spp." group differed between infection types (p<superficial mycoses (p≈0.0091). All the other comparisons showed no significant differences between infection types, with p-values ranging from 0.25 to 0.67.

Resistance

Data regarding susceptibility and resistance for species with a minimum of ten isolates and various groups of species are summarised in Table 21. When applying a combination of the above-mentioned specific and non-specific changing breakpoints, 56 isolates were found to be Fluconazole-resistant (Fluconazole-R), with 27 of them identified as *C. krusei*. This species was followed, in terms of the number of resistant isolates, by *C. glabrata*, *C. albicans*, *S. cerevisiae* and *C. tropicalis*. Of the species with at least ten isolates, *S. cerevisiae* had the highest resistance rate, followed by *C. tropicalis*, *C. glabrata* and *C. albicans*. Compared to the entire *Candida* genus, the "Non-*albicans Candida* spp." group had an almost doubled resistance rate, while the "Non-*Candida*" group had an even higher one, but with only a few isolates.

Regarding infection types, superficial mycoses had the highest Fluconazole resistance rate,

followed by bloodstream infections and deep-seated mycoses. *C. krusei* was the leading resistant pathogen in all three categories, followed by *C. albicans* in superficial mycoses and *C. glabrata* in bloodstream infections and deep-seated mycoses.

Resistance to Voriconazole was detected in only 14 out of 551 isolates. Bloodstream infections had the highest resistance rate, followed by deep-seated mycoses and superficial mycoses. The "Non-*albicans Candida* spp." group accounted for most of the Voriconazole-resistant (VOR-R) isolates and, consequently, had a much higher resistance rate than the whole *Candida* genus or the overall value, while the "Non-*Candida*" group had an even higher rate, but with few isolates. *C. glabrata* was the species with the most resistant isolates, followed by *C. tropicalis*. None of the groups or species with a minimum of ten isolates showed Voriconazole decreased susceptibility, yet the possibility was not always ruled out by the 95 % CIs.

There were 44 exclusively Fluconazole-R isolates, 12 isolates that were both Fluconazole-R and Voriconazole-R and, a little unusual, two isolates that were resistant to Voriconazole but intermediately susceptible to Fluconazole (one *C. glabrata* and one *Magnusiomyces capitatus*).

Table 21. Resistance data for species (n≥10) and groups of species

Species/group	FLC				VOR	
	Resistant *n*, %	95% CI	Susceptible *n*, %	95% CI	Resistant *n*, %	95% CI
Overall						
Candida spp.	49, 9.40 %	7.04-12.24 %	448, 85.99 %	82.71-88.85 %	12, 2.30 %	1.20-3.99 %
C. albicans	4, 1.44 %	0.39-3.64 %	273, 98.20 %	95.85-99.41 %	2, 0.72 %	0.09-2.57 %
C. glabrata	6, 10.00 %	3.76-20.51 %	37, 61.67 %	48.21-73.93 %	4, 6.67 %	1.85-16.20 %
*C. kefyr (*TM: *Kluyveromyces marxianus*)	0, 0.00 %	0.00-16.11 %	21, 100.00 %	83.89-100.00 %	0, 0.00 %	0.00-16.11 %
C. krusei (TM: *Pichia kudriavzevii*)	27, 100.00 %	87.23-100.00 %	-	-	0, 0.00 %	0.00-12.77 %
C. lusitaniae (TM: *Clavispora lusitaniae*)	0, 0.00 %	0.00-30.85 %	10, 100.00 %	69.15-100.00 %	0, 0.00 %	0.00-30.85 %
C. parapsilos	0, 0.00 %	0.00-5.13 %	68, 97.14 %	90.06-99.65 %	0, 0.00 %	0.00-5.13 %
C. tropicalis	3, 12.00 %	2.55-31.22 %	22, 88.00 %	68.78-97.45 %	3, 12.00 %	2.55-31.22 %
Other *Candida* spp.[a]	9, 30.00 %	14.73-49.40 %	17, 56.67 %	37.43-74.54 %	3, 10.00 %	2.11-26.53 %
Non-*albicans Candida* spp.	45, 18.52 %	13.84-23.98 %	175, 72.02 %	65.92-77.57 %	10, 4.12 %	1.99-7.44 %
Non-*Candida* spp.	7, 23.33 %	9.93-42.28 %	15, 50.00 %	31.30-68.70 %	2, 6.67 %	0.82-22.07 %
Saccharomyces cerevisiae	3, 27.27 %	6.02-60.97 %	5, 45.45 %	16.75-76.62 %	0, 0.00 %	0.00-28.49 %
Other non-*Candida* spp.[b]	4, 21.05 %	6.05-45.57 %	10, 52.63 %	28.86-75.55 %	2, 10.53 %	1.30-33.14 %
Overall total	56, 10.16 %	7.77-12.99 %	463, 84.03 %	80.70-86.99 %	14, 2.54 %	1.40-4.23 %
BSI						
Candida spp.	13, 7.78 %	4.21-12.94 %	146, 87.43 %	81.42-92.04 %	6, 3.59 %	1.33-7.66 %
C. albicans	1, 1.75 %	0.04-9.39 %	56, 98.25 %	90.61-99.96 %	1, 1.75 %	0.04-9.39 %
C. glabrata	4, 16.00 %	4.54-36.08	15, 60.00 %	38.67-78.87	3, 12.00 %	2.55-31.22

		%		%		%
C. parapsilosis	0, 0.00 %	0.00-6.06 %	59, 100.00 %	93.94-100.00 %	0, 0.00 %	0.00-6.06 %
Other *Candida* spp.*c*	8, 30.77 %	14.33-51.79 %	16, 61.54 %	40.57-79.77 %	2, 7.69 %	0.95-25.13 %
Non-*albicans Candida* spp.	12, 10.91 %	5.77-18.28 %	90, 81.82 %	73.33-88.53 %	5, 4.55 %	1.49-10.29 %
Non-*Candida* spp.[d]	4, 57.14 %	18.41-90.10 %	1, 14.29 %	0.36-57.87 %	1, 14.29 %	0.36-57.87 %
BSI total	17, 9.77 %	5.80-15.18 %	147, 84.48 %	78.23-89.52 %	7, 4.02 %	1.63-8.11 %
DEEP						
Candida spp.	9, 10.11 %	4.73-18.33 %	76, 85.39 %	76.32-91.99 %	3, 3.37 %	0.70-9.54 %
C. albicans	0, 0.00 %	0.00-5.87 %	61, 100.00 %	94.13-100.00 %	0, 0.00 %	0.00-5.87 %
C. glabrata	2, 18.18 %	2.28-51.78 %	5, 45.45 %	16.75-76.62 %	1, 9.09 %	0.23-41.28 %
Other *Candida* spp.[e]	7, 41.18 %	18.44-67.08 %	10, 58.82 %	32.92-81.56 %	2, 11.76 %	1.46-36.44 %
Non-*albicans Candida* spp.	9, 32.14 %	15.88-52.35 %	15, 53.57 %	33.87-72.49 %	3, 10.71 %	2.27-28.23 %
Non-*Candida* spp.	0, 0.00 %	0.00-60.24 %	3, 75.00 %	19.41-99.37 %	0, 0.00 %	0.00-60.24 %
DEEP total	9, 9.68 %	4.52-17.58 %	79, 84.95 %	76.03-91.52 %	3, 3.23 %	0.67-9.14 %
SUP						
Candida spp.	27, 10.19 %	6.82-14.48 %	226, 85.28 %	80.43-89.32 %	3, 1.13 %	0.23-3.27 %
C. albicans	3, 1.88 %	0.39-5.38 %	156, 97.50 %	93.72-99.31 %	1, 0.63 %	0.02-3.43 %
C. glabrata	0, 0.00 %	0.00-14.25 %	17, 70.83 %	48.91-87.38 %	0, 0.00 %	0.00-14.25 %
C. kefyr (TM: *Kluyveromyces marxianus*)	0, 0.00 %	0.00-20.59 %	16, 100.00 %	79.41-100.00 %	0, 0.00 %	0.00-20.59 %
C. krusei (TM: *Pichia kudriavzevii*)	17, 100.00 %	80.49-100.00 %	-	-	0, 0.00 %	0.00-19.51 %
C. parapsilosis	0, 0.00 %	0.00-30.85 %	8, 80.00 %	44.39-97.48 %	0, 0.00 %	0.00-30.85 %
C. tropicalis	1, 6.25 %	0.16-30.23 %	15, 93.75 %	69.77-99.84 %	1, 6.25 %	0.16-30.23 %
Other *Candida* spp.[f]	6, 27.27 %	10.73–50.22 %	14, 63.64 %	40.66–82.80 %	1, 4.55 %	0.12–22.84 %
Non-*albicans Candida* spp.	26, 24.76 %	16.86-34.14 %	70, 66.67 %	56.80-75.57 %	2, 1.90 %	0.23-6.71 %
Non-*Candida* spp.[g]	3, 15.79 %	3.38-39.58 %	11, 57.89 %	33.50-79.75 %	1, 5.26 %	0.13-26.03 %
SUP total	30, 10.56 %	7.24-14.74 %	237, 83.45 %	78.61-87.58 %	4, 1.41 %	0.39-3.57 %

[a] Species with n<10. Resistant isolates: *C. famata*/*Debaryomyces hansenii* 1 FLC/VOR, *C. haemulonii* 1 FLC/VOR, *C. inconspicua* 2 FLC, *C. lambica*/*Pichia fermentans* 1 FLC, *C. norvegensis*/*Pichia norvegensis* 1 FLC, *C. pelliculosa*/*Wickerhamomyces anomalus* 1 FLC, *C. rugosa* 1 FLC/VOR+1 FLC

[b] Species with n<10. Resistant isolates: *Geotrichum candidum* 1 FLC, *Magnusiomyces capitatus* 1 VOR, *Rhodotorula mucilaginosa* 1 FLC/VOR, *Trichosporon asahii* 1 FLC, *Trichosporon moniliiforme* 1 FLC

[c] Species with n<10. Resistant isolates: *C. haemulonii* 1 FLC/VOR, *C. krusei*/*Pichia kudriavzevii* 5 FLC, *C. pelliculosa*/*Wickerhamomyces anomalus* 1 FLC, *C. tropicalis* 1 FLC/VOR

[d] Species with n<10. Resistant isolates: *Rhodotorula mucilaginosa* 1 FLC/VOR, *Saccharomyces cerevisiae* 2

FLC, *Trichosporon asahii* 1 FLC

[e] Species with n<10. Resistant isolates: *C. famata*/*Debaryomyces hansenii* 1 FLC/VOR, *C. krusei*/*Pichia kudriavzevii* 5 FLC, *C. tropicalis* 1 FLC/VOR

[f] Species with n<10. Resistant isolates: *C. inconspicua* 2 FLC, *C. lambica*/*Pichia fermentans* 1 FLC, *C. norvegensis*/*Pichia norvegensis* 1 FLC, *C. rugosa* 1 FLC/VOR+1 FLC

[g] Species with n<10. Resistant isolates: *Geotrichum candidum* 1 FLC, *Magnusiomyces capitatus* 1 VOR, *Saccharomyces cerevisiae* 1 FLC, *Trichosporon moniliiforme* 1 FLC

Susceptibility to fluconazole

Because EUCAST changing breakpoints also defines an intermediate category of susceptibility for Fluconazole, unlike for Voriconazole, information regarding susceptibility cannot be simply deduced from the resistance data or *vice versa*. In our study, most of the isolates were Fluconazole-susceptible (FLC-S). Within infection types, the Fluconazole susceptibility rates were similar, with deep-seated mycoses having the highest rate, followed by bloodstream infections and superficial mycoses.

"*Candida* spp.", as a group, was Fluconazole-S overall and in each infection type, with similar rates. The "Non-*albicans Candida* spp." and "Other *Candida* spp." groups showed decreased susceptibility in deep-seated mycoses, superficial mycoses and overall. The "Other *Candida* spp." group had decreased susceptibility in bloodstream infections too. "Non-*Candida* spp." exhibited decreased Fluconazole susceptibility in bloodstream infections and superficial mycoses.

Considering the species with at least ten isolates (to avoid excessively wide CIs) and excluding the intrinsically resistant *C. krusei*, overall decreased Fluconazole susceptibility was only present in *C. glabrata* and *S. cerevisiae*. Also, the 95 % CIs do not rule out decreased susceptibility for *C. lusitaniae* and *C. tropicalis*.

Using the same criteria for infection types, only *C. glabrata* showed decreased susceptibility in all three categories, but the 95 % CIs did not exclude normal susceptibility (>75 %). Conversely, because of their CIs, decreased susceptibility cannot be ruled out for either *C. parapsilosis* or *C. tropicalis* in superficial mycoses.

MXP vs. Voriconazole

The Wilcoxon matched-pairs test showed a higher average sum of ranks for MXP against *Candida* spp. (Figure 22a). The average sum of ranks was higher for Voriconazole when the activity against non-*krusei Candida* spp. Fluconazole-R isolates (Figure 22b), *Candida* spp. Voriconazole-R isolates (Figure 22c) and *C. glabrata* isolates (Figure 22d) was compared.

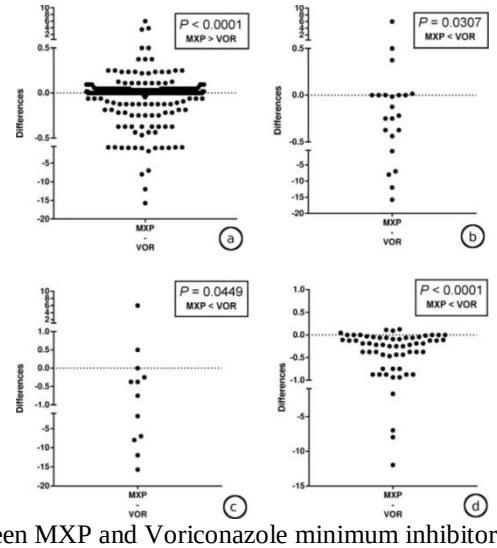

Figure 22. Differences between MXP and Voriconazole minimum inhibitory concentrations against: a all *Candida* spp. isolates; b all *Candida* spp. Fluconazole-R isolates except *C. krusei*; c all *Candida* spp. Voriconazole-R isolates; d all *C. glabrata* isolates

Discussion

Candida albicans continues to be reported as the most frequently isolated yeast pathogen, but in varying degrees [383,403]. In our study, the proportion of this species was inferior to worldwide (65.3%) and European (67.9 %) values reported by Pfaller et al., [383] in their global study, and closer to the results of a German-Austrian study (54%) [401]. The high diversity and proportion of the non-*albicans Candida* species adds further confirmation to the trend of increasing frequency that is reported for this category of yeasts [383].

Despite the geographic differences, the top five yeasts, which account for the vast majority of the isolates, are the same - *C. albicans*, *C. parapsilosis*, *C. glabrata*, *C. tropicalis* and *C. krusei* - with the order changing according to the area investigated [383]. This also applied to our study, where 88.3% of all *Candida* spp. isolates belong to these top five yeasts, a value that is, nonetheless, low compared with the previously mentioned studies. This, correlated with the high number of identified species, indicates an important contribution of yeasts normally considered as rare or emerging to the replacement of *C. albicans*. The present study confirmed a notable isolation frequency in Eastern Europe for *C. krusei*, as reported by Pfaller et al., [383]. We were not able, however, to confirm similar reports of the same study regarding *C. inconspicua* and *C. norvegensis*.

Compared to other studies [400–402], both the diversity and the proportion of non-*Candida* yeasts were relatively high, which shows that this group also contributes to the replacement of *C. albicans*. To the best of our knowledge, invasive fungal infection with *Lodderomyces elongisporus* is reported here for the first time in Europe, adding to the very few cases reported worldwide [457].

The overall Fluconazole resistance in our study was high. Along with the acquired resistance of the normally susceptible species, another main reason for this is the high percentage of *C. krusei* - more than double compared with a global survey [383]. On the other hand, the same species is an important reason for the low overall Voriconazole resistance, which is comparable to the worldwide level (3%). All its isolates exhibited Fluconazole-R/Voriconazole-S phenotypes, confirming the tendency reported in the same global survey. Fluconazole susceptibility was lower than the 90.2% global level.

C. albicans and *C. parapsilosis* were susceptible to both commercial azoles, which is in agreement with the previously reported global and European values [383]. *C. glabrata* had lower values of azole resistance than those reported for Europe [383], although the 95 % CIs were wide. Compared with the Spanish study [402], we observed equal MIC_{90} values but higher MIC_{50} values. Ranking second in Fluconazole resistance and first in Voriconazole resistance, *C. glabrata* isolates from Romania confirm the potential of this species to acquire resistance to both azoles [383].

C. tropicalis had high resistance rates to both commercial antifungals and low susceptibility to Fluconazole. Compared with the Spanish study [402], the MIC_{50} was higher for Fluconazole, while the MIC_{90} was higher for both azoles. Our data confirm a trend towards decreased susceptibility to Voriconazole reported for *C. tropicalis* [383]. Several investigations report high MIC_{50} and MIC_{90} values as well as frequent resistance to azoles for *C. guilliermondii* [383,402], on the potential to acquire Fluconazole resistance for *C. dubliniensis* [458,459] and on the occurrence of azole resistance for *C. kefyr* [383]; in our study, these species did not exhibit high minimum inhibitory concentrations.

In accordance with the documented tendency of many isolates to be less susceptible to Voriconazole after having acquired Fluconazole resistance [383], five out of seven isolates with acquired Fluconazole resistance (*C. albicans*, *C. parapsilosis* and *C. tropicalis*) were also Voriconazole-R.

The percentages of Fluconazole-S isolates in the "Other *Candida*" and "Non-*Candida*" groups, as well as their 95 % CIs, support the observed trend of reduced Fluconazole susceptibility in rare species [383].

In the "Non-*Candida*" group, *S. cerevisiae* had reduced Fluconazole susceptibility. Fluconazole resistance was present in the *Saccharomyces*, *Trichosporon*, *Rhodotorula* and *Geotrichum* genera, which is consistent with other reports [400,460–462]. The group remained susceptible to Voriconazole, although resistance was detected in the *Rhodotorula* and *Magnusiomyces* genera.

Unlike for Fluconazole, the EUCAST has not officially recommended a non-specific changing breakpoint for Voriconazole. We have, therefore, used R>0.25 mg/L, a value that was only suggested by the EUCAST [443]. The same document, however, states that "voriconazole trough blood levels

above 5.5 mg/L have been associated with an increase in toxicity". Therefore, minimum inhibitory concentration>1 could also be considered as an alarming threshold. In our tests, only six isolates (1.1 %, 95 % CI=0.4–2.4 %) exceeded this value, namely, four of *C. glabrata* (3 bloodstream infections+1 deep-seated mycoses) and two of *C. tropicalis* (1 bloodstream infections +1 deep-seated mycoses).

Considering the bloodstream infections, the fact that *C. albicans* was second in prevalence, with a relatively low proportion, confirms its noted worldwide decline as a cause of fungaemia in favour of non-*albicans Candida* species [463–466], especially *C. glabrata*, *C. parapsilosis* and *C. tropicalis* [408,466].

The dominant non-*albicans* species in bloodstream infections vary geographically. *C. glabrata* has been reported for North America, the northern and central parts of Europe, and the North Hemisphere in general [465–467]. *C. tropicalis* has been reported for the Southern Hemisphere and the Asia-Pacific region [383,403,465,468,469], while *C. parapsilosis* (sensu lato) was reported for the Southern Hemisphere, the Southern Europe and the Middle East [465,468,470–472]. With the latter species surpassing *C. albicans* and taking the first place, but also with a significant presence of *C. glabrata*, which took the third place, our survey indicates an intermediary situation for Romania, with Southern European tendencies. This could pose serious problems to Romanian clinicians in treating fungal infections prior to species identification, since *C. glabrata* has reduced susceptibility to Fluconazole [473] and increasing resistance to echinocandins [474], and *C. parapsilosis* (sensu lato) has been reported to exhibit reduced susceptibility to echinocandins [467,475].

With a small number of isolates, *C. tropicalis* has a situation similar to that reported for Central [465] and Northern Europe [467]. *C. krusei* was also relatively infrequent in bloodstream infections, in accordance with reports from both the south [476] and the north of Europe [467].

The susceptibility of bloodstream infections isolates to both azoles was high (>80 % for Fluconazole and >90 % for Voriconazole) and accompanied by low levels of resistance. Similar to other reports [408], the susceptibility rate is even higher if *C. glabrata* and *C. krusei* are analysed separately. The two species were responsible for 60 % of the Fluconazole resistance in *Candida* spp., while 13.3 % came from isolates with acquired resistance. The latter value, though, is still higher than that reported from Denmark [467]. In bloodstream infections, 64.7 % of the Fluconazole-R isolates remained Voriconazole-S. In accordance with the Danish study [467], reduced Fluconazole susceptibility occurred with *C. glabrata* and the less common *Candida* species, as well as with non-Candida spp. Consistent with reports of azole resistance for *Rhodotorula* spp. [460,477,478], the isolate from Romania was resistant to both triazoles.

Regarding superficial infections, all reviews notice a dominance of *C. albicans*, which is even more pronounced in vulvovaginal infections, where it can be responsible for up to 95% of the cases [397,399,479,480]. The non-*albicans Candida* species, though, especially *C. glabrata* and *C. tropicalis*, are reported to be emerging [398,481–483]. As a particularity of the oropharyngeal infections, a significant isolation rate of *C. dubliniensis* can be noticed [482,484,485]. It is worth mentioning that all our *C. dubliniensis* isolates were of oral origin. Although slightly reduced in some studies [486,487], the reported proportion of *C. albicans* in superficial infections remained elevated in other parts of Europe [488–490]. Our research revealed a lower proportion of this species, though it remained dominant. In the "Non-albicans *Candida* spp." group, *C. glabrata* and *C. tropicalis* were frequent, but so were *C. krusei* and *C. kefyr*.

Reported Fluconazole resistance values for yeasts in superficial mycoses are variable, ranging from 0 % to over 30 % [481,491–494]. We measured 10.2 % Fluconazole resistance for *Candida* spp. When subtracting *C. krusei*, however, the remaining isolates had a lower rate of Fluconazole resistance in superficial mycoses (4.9 %) compared with bloodstream infections (7.1 %). Therefore, the resistance was partially acquired and partially due to the distribution of the species (the high percentage of *C. krusei*).

Deep-seated infections are an artificial group composed of a heterogeneous assembly of yeasts, with organisms originating most likely from pre-existent superficial mycoses or bloodstream infections, or from the commensal microbiome. The majority of our isolates in this category were collected from the lower respiratory tract. The presence of *Candida* spp. in this part of the human body is mostly attributed to contamination [495]. Furthermore, the lung, until recently regarded as a sterile environment, appears to have its own microbiome [496]. Nevertheless, we included these isolates on the basis of the observed high microbial loads and, as previously stated, the presence of at

least two risk factors. Furthermore, the patients were negative for oropharyngeal mycosis. In general, this category showed a species distribution more similar to superficial mycoses, especially due to the high proportion of *C. albicans*. The observed higher minimum inhibitory concentration parameters were, however, closer to those of isolates from bloodstream infections, which suggests a possible transitional state from superficial mycoses towards bloodstream infections.

The new compound MXP-4509 exhibited a good antifungal activity, comparable to that of Voriconazole (Figure 22a) or better, especially against azole-resistant isolates (Figure 22b, c). Furthermore, it was particularly active against *C. glabrata* (Figure 22d), a species that frequently exhibits high azole minimum inhibitory concentrations and stands out with elevated and increasing isolation rates worldwide, and an apparent predilection for bloodstream infections [446,497]. These important and desirable properties make MXP-4509 worthy of further investigation and development.

In summary, our study provides much needed data regarding yeast infections in Romania, one of the larger countries in Eastern Europe, which, until now, has insufficiently investigated these matters. We performed both an overall analysis (i.e. regardless of the infection type) and one based on distributing the isolates in three categories of infections. The percentage of nonalbicans *Candida* isolates was large, in line with the worldwide reports of *C. albicans* replacement by other yeasts. A large part of the high Fluconazole resistance was not acquired but resulted from the high frequency of *C. krusei*. The present study offers valuable susceptibility data of isolates that belong to some rare yeast species that are characterised by intrinsic susceptibility patterns which are not specifically addressed in general treatment guidelines [460].

The results provide a starting point for future comparisons and for detecting trends in fungal species distribution and azole susceptibility patterns. They also complement existing data concerning yeast infections in other parts of Europe and the rest of the world.

Personal contribution - published papers:

Moraru, R.; Minea, B.; Năstasă, V.; **Doroftei**, **B**.; Mares, M. Comparative evaluation of the antifungal activity of voriconazole and a new propiconazole derivative (MXP-4509) against 278 Candida albicans clinical isolates. *Lucr. Ştiinţifice - Med. Vet. Univ. Ştiinţe Agric. şi Med. Vet. "Ion Ionescu la Brad" Iaşi* ***2013****, 56,* 468-473.

Aim of the study

The purpose of this study was to determine the spectrum and susceptibility pattern to fluconazole, voriconazole and the novel compound MXP-4509.

Materials and methods

Antifungal agents

Pure powders of Fluconazole and MXP-4509 were used. Voriconazole was used as VFEND. Fluconazole was purchased from Sigma (St. Louis, USA) while VFEND was purchased from Pfizer Ltd. (Sandwich, UK). MXP-4509 was synthesized at the "Petru Poni" Institute of Macromolecular Chemistry (Iaşi, Romania). The new compound is a bionanoconjugate based on a Propiconazole derivative and a Ciclodextrin. Its synthesis and characterisation have been previously published [498]. Prior to use the antifungal agents were dissolved in distilled water.

Isolates

A number of 278 *C. albicans* clinical isolates were tested. The isolates were collected in the 2010-2011 time frame, from 4 tertiary hospitals located in various regions of Romania (Cluj, Iaşi, Tg. Mureş and Timişoara). The *C. albicans* strain used for quality control belongs to Romanian Type Culture Collection (RTCC) from the Laboratory of Antimicrobial Chemotherapy of Iaşi, Romania.

Yeast identification

The microorganisms were presumptively isolated using various techniques - germtube test, manual and automatic Vitek 2®, Api Candida®. The isolates were centralized by our laboratory where they were rechecked for purity and they were kept in a 20% glycerol aqueous solution, at -80°C, until analysis. The identification was redone using ID 32 C® (BioMerieux). The isolates identified as *C. albicans* or *C. dubliniensis* were further analysed by polymerase chain reaction duplex [499]. Prior to susceptibility testing, each *Candida* isolate was cultivated on YPD agar and incubated at 36±1°C for 24-48 h.

Antifungal susceptibility testing

Minimum inhibitory concentrations for the three compounds were assessed using the EUCAST (ESCMID) broth microdilution method described in the EUCAST Definitive Document EDef 7.1 [410]. Briefly, 100 µL of two-fold dilution series of the antifungal agents, at double the final strength, in a modified RPMI-1640 medium (containing 2% glucose), also at double the final strength and at a 7.0 pH, were 1:1 mixed with 100 µL of inocula at double the final density, in 96 well microplates. This way, the final concentrations for each dilution and for the medium as well as the final density for each inoculum were obtained. The ranges of final antifungal concentrations tested were 0.125 µg/mL - 64 µg/mL, for Fluconazole, and 0.0156 µg/mL - 8 µg/mL, for Voriconazole and MXP-4509. For the preparation of the inoculum, a yeast suspension in sterile 0.9% saline solution, adjusted to a turbidity equivalent to the 0.5 McFarland standard, was made for each isolate. These initial suspensions were 1:10 diluted with distilled water and used for the inoculation of the microplates that contained the antifungal agents dissolved in medium. The final density of the inocula was 0.5-2.5 × 10^5 CFU/mL [410]. Minimum inhibitory concentrations for *Candida* spp. isolates were determined after a 24 h incubation period, at 36±1°C. Minimum inhibitory concentrations were established, according to EUCAST E. Def. 7.1, as the smallest concentrations that induced an obvious reduction of turbidity (spectrophotometrically measured 50% growth reduction) compared to the positive control.

Microbiological resistance

The isolates were classified as resistant according to the EUCAST BPs, version 6.1, valid from 11/03/2013 [454].

Data analysis

The D'Agostino-Pearson omnibus normality test was used to check the normality of the log(MIC) values of each compound or of the differences between the paired log(MIC) values of the two compounds. Since none of the data passed the normality test and sample size was not small, non-parametric tests were used [500]. To analyse whether the minimum inhibitory concentrations of each compound were different between infection types, the Kruskal-Wallis test was used followed by Dunn‘s multiple comparison test. To compare the minimum inhibitory concentrations of the two compounds the Wilcoxon matched-pairs signed-rank test was run. In case of ties, the method of Pratt for ties was used [500]. The tests were run using a fully functional trial version of GraphPad Prism version 6.02 for Windows, GraphPad Software, San Diego California USA, www.graphpad.com. Two-tailed P values were calculated. P values smaller than 0.05 were considered as indicative of statistical significance.

The geometric mean of the minimum inhibitory concentrations was calculated as the antilogarithm of the arithmetic mean of the natural logarithms of the minimum inhibitory concentrations using as a base the following array formula in Microsoft® Excell® 2010: EXP(AVERAGE(LN(x))), where x is a minimum inhibitory concentrations value or a range of values. This formula was extended with various logical arguments using the IF function. Right-censored values (greater than the maximum tested concentration) were considered as the next theoretical value (double of the maximum tested concentration).

Results and discussions

The 278 yeasts tested were isolated from various sources: blood, bronchial aspirate, cerebrospinal fluid, draining tube, peritoneal fluid, sputum, urine, balanitis, bile, bronchial catheter, faeces, onychomycosis, oral infection and vaginal infection. These sources were grouped into three infection types: blood stream infections (blood), deep seated infections (bronchial aspirate, cerebrospinal fluid, draining tube, peritoneal fluid, sputum and urine) and superficial infections – superficial mycoses (balanitis, bile, bronchial catheter, faeces, onychomycosis, oral infection and vaginal infection). The largest number of isolates came from superficial infections (160 - 57.56%) seconded by deep seated infections with 61 isolates (21.94%) while blood stream infections came last with 57 isolates (20.50%) (Figure 23).

Two of the *C. albicans* isolates (one bloodstream infection and one superficial mycosis) showed Voriconazole resistance.

The distribution of minimum inhibitory concentrations for both Voriconazole ($P\approx0.6051$) and MXP-4509 ($P\approx0.2536$) was not different between the three infection types.

On *C. albicans* isolates Voriconazole had a statistically significant superior activity to that of MXP-4509, both overall ($P<0.0001$) and within infection types (bloodstream infection-$P=0.001$, deep-seated mycosis-$P=0.002$, superficial mycoses-$P<0.0001$). Statistical significance, however, doesn‘t necessary imply a very big difference, as it can be seen from Table 22 and Figures 23 to 26. Table 22 shows identical values for the minimum inhibitory concentration Mode and the MIC_{50} across all groups. The MIC_{90} of MXP-4509 is always one order of magnitude higher and, consequently, its geometric mean is slightly higher in all cases. The minimum inhibitory concentration Range, however, is, with one exception, always narrower or, to be more precise, it extends less to the right in the case of MXP-4509.

Figures 23 to 26 show a large number of zero differences (the median of differences was also zero) and that the positive differences between MXP-4509 and Voriconazole minimum inhibitory concentrations never went past 0.5 mg/L and rarely past 0.0156 mg/L.

Although slightly inferior, the activity of MXP-4509 against *C. albicans* clinical isolates is very much comparable to that of Voriconazole. The minimum inhibitory concentration Range and the MIC_{50} and MIC_{90} suggest a minimum inhibitory concentration distribution curve slightly shifted to the right but more peaked, with more kurtosis and less skewness, for MXP-4509 in comparison with that of Voriconazole, but more data is necessary to confirm such a supposition.

Given the comparable antifungal activity and the fact that Propiconazole, the raw material for MXP-4509, is cheaper than Voriconazole, MXP-4509 presents itself as an interesting compound that deserves further research regarding its in vivo antifungal activity as well as its pharmacokinetics and pharmacodinamics.

Table 22. Minimum inhibitory concentration characteristics for the C. albicans clinical isolates tested

Infection type	Compound	MIC (mg/L)				
		Range	Mode	MIC_{50}	MIC_{90}	GM
Overall	VOR	≤0.0156 - 1.0	0.0156	0.0156	0.0156	0.0163
	MXP-4509	≤0.0156 - 0.25	0.0156	0.0156	0.0312	0.0193
BSI	VOR	≤0.0156 - 1.0	0.0156	0.0156	0.0156	0.0168
	MXP-4509	≤0.0156 - 0.25	0.0156	0.0156	0.0156	0.0187
DEEP	VOR	≤0.0156 - 0.0312	0.0156	0.0156	0.0156	0.0158
	MXP-4509	≤0.0156 - 0.0625	0.0156	0.0156	0.0156	0.0183
SUP	VOR	≤0.0156 - 0.5	0.0156	0.0156	0.0156	0.0164
	MXP-4509	≤0.0156 - 0.125	0.0156	0.0156	0.0156	0.0200

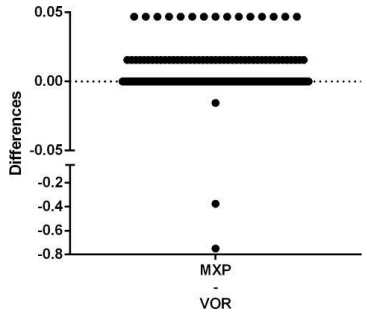

Figure 23. Differences between MXP and VOR MICs for all isolates

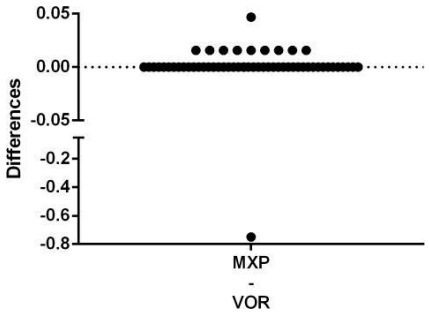

Figure 24. Differences between MXP and VOR MICs for BSI isolates

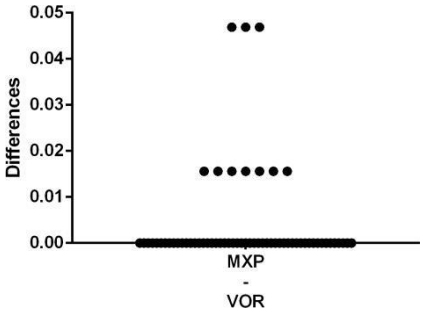

Figure 25. Differences between MXP and VOR MICs for DEEP isolates

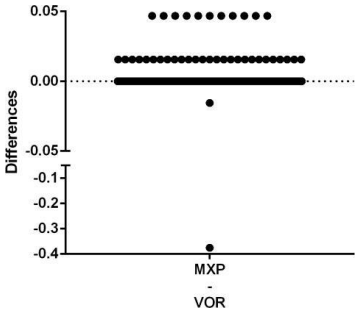

Figure 26. Differences between MXP and VOR MICs for SUP isolates

Personal contribution - published papers:

Minea, B.; Moraru, R.; Năstasă, V.; **Doroftei**, **B**.; Marincu, I.; Mares, M. Comparative evaluation of the antifungal activity of voriconazole and a new propiconazole derivative (MXP-4509) against fluconazole-resistant yeast isolates. *Lucr. Ştiinţifice - Med. Vet. Univ. Ştiinţe Agric. şi Med. Vet. "Ion Ionescu la Brad" Iaşi* ***2013***, *56*, 474-480.

Aim of the study

The scope of the present study was to assess the spectrum and susceptibility pattern to fluconazole, voriconazole and the novel compound MXP-4509.

Antifungal agents

Pure powders of Fluconazole and MXP-4509 were used. Voriconazole was used as VFEND. Fluconazole was purchased from Sigma (St. Louis, USA) while VFEND was purchased from Pfizer Ltd. (Sandwich, UK). MXP-4509 was synthesized at the "Petru Poni" Institute of Macromolecular Chemistry (Iaşi, Romania). The new compound is a bionanoconjugate based on a Propiconazole derivative and a Ciclodextrin. Its synthesis and characterisation have been previously published [498]. Prior to use the antifungal agents were dissolved in distilled water.

Isolates

A number of 57 clinical yeast isolates were tested. The isolates were collected in the 2010-2011 time frame, from 4 tertiary hospitals located in various regions of Romania (Cluj, Iaşi, Tg. Mureş and Timişoara). The strains used for quality control belong to the Romanian Type Culture Collection (RTCC) from the Laboratory of Antimicrobial Chemotherapy of Iaşi, Romania: *C. albicans, C. krusei*, and *C. parapsilosis.*

Yeast identification

The microorganisms were presumptively isolated using various techniques - germtube test, manual and automatic Vitek 2®, Api Candida®. The isolates were centralized by our laboratory where

they were rechecked for purity and they were kept in a 20% glycerol aqueous solution, at -80°C, until analysis.

The identification was redone using ID 32 C® (BioMerieux). The isolates identified as *C. albicans* or *C. dubliniensis* were further analysed by polymerase chain reaction duplex [499]. In cases where the identity of the yeast remained unclear, MaldiTof was used for identification [449]. The rare species, for which even this method yielded doubtful profiles, were identified by DNA sequencing.

Prior to susceptibility testing, each *Candida* isolate was cultivated on YPD agar while the non-*Candida* isolates were cultivated on Sabouraud agar (Bio-Rad, France). All were incubated at 36±1°C for 24-48 h.

Antifungal susceptibility testing

Minimum inhibitory concentrations for the three compounds were assessed using the EUCAST (ESCMID) broth microdilution method described in the EUCAST Definitive Document EDef 7.1 [410]. Briefly, for each isolate, 100 µL of two-fold dilution series of the antifungal agents, at double the final strength, in a modified RPMI-1640 medium (containing 2% glucose), also at double the final strength and at a 7.0 pH, were 1:1 mixed with 100 µL of inoculum at double the final density, in 96 well microplates. This way, the final concentrations for each dilution and for the medium as well as the final density for each inoculum were obtained.

The ranges of final antifungal concentrations tested were 0.125 µg/mL - 64 µg/mL, for Fluconazole, and 0.0156 µg/mL - 8 µg/mL, for Voriconazole and MXP-4509. For the preparation of the inocula, a yeast suspension in sterile 0.9% saline solution, adjusted to a turbidity equivalent to the 0.5 McFarland standard, was made for each isolate. These initial suspensions were 1:10 diluted with distilled water and used for the inoculation of the microplates that contained the antifungal agents dissolved in culture medium. The final inoculum density was 0.5-2.5 × 105 CFU/mL (EUCAST E. Def. 7.1).

Minimum inhibitory concentrations for *Candida* spp. isolates were determined after a 24 h incubation period, at 36±1°C. The incubation for *Cryptococcus neoformans* isolates was longer, of 70-74 h [453,501]. Minimum inhibitory concentrations were established, according to EUCAST E. Def. 7.1, as the smallest concentrations that induced an obvious reduction of turbidity (spectrophotometrically measured 50% growth reduction) compared to the positive control.

Microbiological resistance

The isolates were classified as resistant according to the EUCAST BPs, version 6.1, valid from 11/03/2013 [502]. In the case of species for which changing breackpoints have not yet been determined, the ECOFFs were applied, when available, otherwise two non-specific changing breakpoints were used. For Fluconazole, the 4 µg/mL EUCAST non-specific changing breakpoint was used. For Voriconazole, a 0.25 µg/mL value, mentioned in the EUCAST Technical Note on voriconazole [443] as a possible non-specific BP, was used.

Data analysis

The comparison of minimum inhibitory concentrations was done with the Wilcoxon matched-pairs signed-rank test [500] using a fully functional trial version of GraphPad Prism version 6.02 for Windows, GraphPad Software, San Diego California USA, www.graphpad.com. In case of ties, the Pratt method was used. Two-tailed P values were calculated. P values smaller than 0.05 were indicative of statistical significance. Right-censored values (greater than the maximum tested concentration) were considered as the next theoretical value (double of the maximum tested concentration).

Results and discussions

The 57 resistant yeasts were isolated from various sources: blood, bronchial aspirate, peritoneal fluid, sputum, urine, faeces, oral infection and vaginal infection. These sources were grouped into

three infection types: blood stream infections (blood), deep seated infections (bronchial aspirate, peritoneal fluid, sputum, urine) and superficial infections (faeces, oral infection and vaginal infection). The largest number of resistant isolates came from superficial infections (30 - 52.63%) seconded by blood stream infections with 18 isolates (31.58%) while deep seated infections came last with 9 isolates (15.79%) (Figure 27).

The distribution of isolates according to species and infection type is presented in Table 23. *Candida* spp. was the dominant group with 53 resistant isolates while the non-*Candida* group only had 4 resistant isolates. *C. krusei* accounted for almost half of all the resistant isolates, followed at a distance by *C. glabrata* and *C. albicans*. Only C. krusei and *C. tropicalis* had isolates in all three infections types. 12 of the 57 Fluconazole-resistant isolates also showed Voriconazole resistance. As Figure 28 shows, in this case bloodstream infection was the most abundant infection class with 7 isolates (50%) followed by superficial mycoses with 4 isolates (29%) and deep-seated mycoses with 3 isolates (21%).

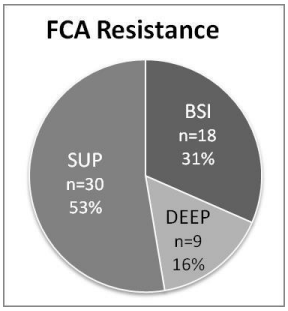

Figure 27. Distribution of Fluconazole-resistant isolates according to infection type

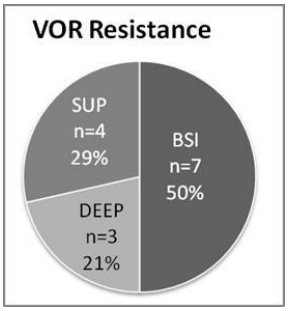

Figure 28. Distribution of Voriconazole-resistant isolates according to infection type

Table 23. Fluconazole-resistant isolates distribution according to species and infection type

Group	Species	Bloodstream infection	Deep-seated mycosis	Superficial mycosis	Total
Candida spp.	*C. albicans*	1	-	3	4
	C. famata	-	1	-	1
	C. glabrata	4	2	-	6
	C. haemulonii	1	-	-	1
	C. inconspicua	-	-	2	2
	C. krusei	5	5	17	27
	C. lambica	-	-	1	1
	C. norvegiensis	-	-	1	1
	C. parapsilosis	1	-	-	1
	C. pelliculosa	1	-	-	1
	C. robusta	2	-	1	3
	C. rugosa	-	-	2	2
	C. tropicalis	1	1	1	3
Non-*Candida* spp.	*Geotrichum candidum*	-	-	1	1
	Rhodotorula mucilaginosa	1	-	-	1
	Trichosporon asahii	1	-	-	1
	Trichosporon moniliiforme	-	-	1	1

The *Candida* sp. group was again dominant with 11 isolates (6 bloodstream infections, 3 deep-seated mycoses and 2 superficial mycoses) while the non-*Candida* group had only one isolate (superficial mycosis). The distribution of Voriconazole resistant isolates according to species and infection type is presented in Table 24. In general, MXP-4509 had a better activity than Voriconazole

against *Candida* spp. Fluconazole-resistant isolates (P=0.0058) (Figure 29) as well as against all Fluconazole-resistant isolates (P=0.0047).

Table 24. Voriconazole-resistant isolates distribution according to species and infection type

Group	Species	Bloodstream infection	Deep-seated mycosis	Superficial mycosis	Total
Candida spp.	C. albicans	1	-	1	2
	C. famata	-	1	-	1
	C. glabrata	2	1	-	4
	C. haemulonii	1	-	-	1
	C. rugosa	-	-	1	1
	C. tropicalis	1	1	1	3
Non-*Candida* spp.	Rhodotorula mucilaginosa	1	-	-	1

Since *C. krusei* isolates account for almost half of all the resistant isolates, it made sense to separate them and then analyze the two resulting groups, i.e. *C. krusei* and *C.* non-*krusei*. The superiority of MXP-4509 became even more obvious in the *C.* non-*krusei* group (P=0.0039) (Figure 30). In the *C. krusei* group, however, MXP-4509 had a slightly inferior but still comparable activity to that of VOR (P=0.041).

MXP-4509 showed a very good antifungal activity against Voriconazole-resistant isolates (Figure 31) and it seems to be especially efficient against *C. glabrata* isolates, but the results were not statistically significant (P=0.1133 for Voriconazole-resistant isolates and P=0.0625 for *C. glabrata* isolates).

The P values, show the need for further research in both cases. The same can be said about *C. krusei* where the P value, although it shows statistical significance, is very close to the 0.05 threshold.

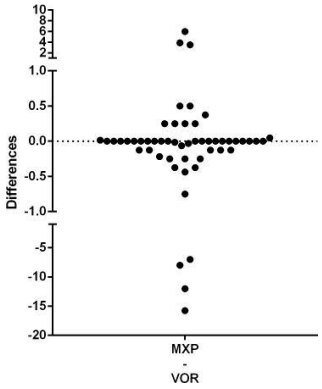

Figure 29. Differences between MXP and Voriconazole minimum inhibitory concentrations for Candida spp. Fluconazole-resistant isolates

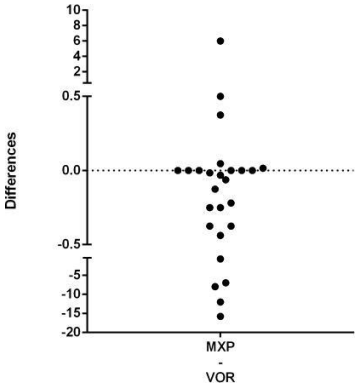

Figure 30. Differences between MXP and Voriconazole minimum inhibitory concentrations for C. non-krusei Fluconazole-resistant isolates

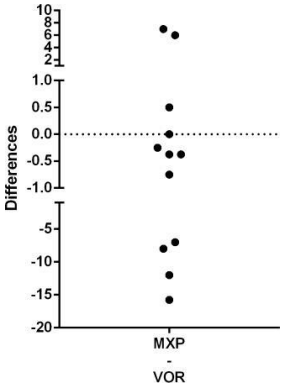

Figure 31. Differences between MXP and Voriconazole minimum inhibitory concentrations for all Voriconazole-resistant isolates

Personal contribution - published papers:

Mares, M.; Socolov, D.; **Doroftei**, **B**.; Botezatu, A.; Goia, C. The prevalence of some bacterial markers in female patients undergoing an initial infertility evaluation in North-East Romania. *Roum. Arch. Microbiol. Immunol.* ***2009***, *68*, 171–174.

Personal contribution - published papers:

Doroftei, **B**.; Ilie, O.-D.; Dabuleanu, A.-M.; Diaconu, R.; Maftei, R.; Simionescu, G.; Ilea, C. Follitropin Delta as a State-of-the-Art Incorporated Companion for Assisted Reproductive Procedures: A Two Year Observational Study. *Med.* ***2021***, *57*, 379. **IF: 2.430**

II.2 Recombinant drugs

Fortunately, the fulminant ascension of recombinant DNA technologies promoted the current success of IVF procedures. Scientists have been able to optimize these protocols and to create recombinant gonadotropins, currently making r-hFSHs the method of choice [503]. Three r-hFSHs are administered within the current clinical practice as part of the ART protocols [504]. The fourth is still under development. Follitropin delta is the only human-derived r-hFSH that possesses a defined dosing algorithm [505]. Considering the half-life of endogenous FSH, a long-acting formula was necessary.

Compared with follitropin alfa and/or beta [506,507] and corifollitropin alfa [508], whose pharmacokinetics is calculated based on a 150 UI dose, follitropin delta emphasize the actual tendency. More precisely it ensures the transition between standardized and personalized doses [509]. Specifically, corifollitropin alfa is a molecular hybrid, with it an effect that ranges between 59 and 82 h. Its terminal rate varies from 68.2 to 73.1 h at 100 to 150 µg at 0.225 L/h. However, it is dependent on the BMI [508].

The AMH level is the main predictor to set out ovarian reserve and the response to exogenous gonadotropins. The BMI, is used, on the other hand, as a determinant after exposure to follitropin delta [510–513].

Personal contribution - published papers:

Doroftei, **B**.; Ilie, O.-D.; Dabuleanu, A.-M.; Diaconu, R.; Maftei, R.; Simionescu, G.; Ilea, C. Follitropin Delta as a State-of-the-Art Incorporated Companion for Assisted Reproductive Procedures: A Two Year Observational Study. *Med.* ***2021***, *57*, 379. **IF: 2.430**

Aim of the study

The present study aims to assess a series of parameters (follicles, oocytes, and embryos) and further by the outcomes in women following the administration of follitropin delta.

Materials and methods

Study participants

This study was conducted between January 1, 2018, and December 31, 2020, at the Origyn Fertility Center in Iasi, Romania. A total of two hundred and five women consented and participated (mean-33.45, range 21-43 years). The AMH level varied from 0.11 to 16.00 ng/dL (mean-2.89).

Inclusion criteria and limitations

The main inclusion criteria were: (I) tubal infertility; (II) EMS; (III) male-component infertility; and (IV) both regular and irregular menstrual cycles.

Even though the fertility status is typically dependent on the age of the recipient, there were situations when treatment is ineffective. Also, due to heterogeneity between groups, we were unable to perform standard statistical analyses.

Study design

The OS protocol with follitropin delta began on day two of the menstrual cycle. According to the established methodology, we harvested the hormonal profile (FSH, LF, P4, and E2), and endovaginal ultrasound was performed on the same day. If the hormonal profile was favorable (FSH < 10 and the ovaries do not present an ovarian cyst), the short antagonist (hCG) stimulation protocol was initiated. All doses were administered according to the algorithm provided by the manufacturer. Each patient received the recommended dose of follitropin delta daily, in the afternoon (between 18:30 and 20:00).

On day 6 of stimulation (day 7 of the menstrual cycle) the administration of the antagonist (Orgalutran® 0.25 (ganirelix)/day) started in the morning (between 8:00 and 11:00) after harvesting the hormonal profile. Endovaginal ultrasound was performed to monitor the growth of follicles. On day eight and ten of stimulation, the hormonal profile (E and P4) was harvested again, together with the endovaginal ultrasound to follow the adequate development of the follicles.

Whenever more than 3 follicles over 18 mm were detected via ultrasound, ovulation was triggered by administrating hCG Pregnyl 5000 IU. At 36 h, the ultrasound-guided ovarian puncture took place under deep anal sedation.

Ethical approval

Prior to participation, each woman signed an informed consent form explaing the procedures. We also obtained the approval of the Ethics Committee at the Origyn Fertility Center (118/565/January/10/2021), and the agreement was signed off by the Medical Director of the center as well. The study was conducted in accordance with the Helsinki Declaration of human rights, and the national and European regulations on Biomedical Research. Women did not receive any remuneration for their participation since it was voluntary.

Statistical analysis

Data analysis, editing, sorting, and coding was carried out using Microsoft Excel 2010.

Results

As presented in Table 25, a total of 2,532 follicles over 18 mm were obtained following the administration of follitropin delta to 205 women. From these, 1,719 (67.89%) belonged to women under the age of 35, and 814 (32.14%) to women older than 35. There were 1,891 oocytes in both groups – 1,279 (67.63%) from women under the age of 35 and 612 (32.36%) from women older than 35. Last but not least, 978 embryos resulted from 205 women, of which 677 (69.22%) from the younger group and 301 (30.77%) from the other, respectively.

The protocol was canceled in several cases in which either the recipient manifested no response or due to moderate (OHSS; one 36-year-old woman, one 37 years, and one 43). Additionally, we performed a series of interventions such as PGT (n = 4 - 1.95%), ET on day 3 (n = 4 - 1.95%), and freezing all embryos on day 4 (n = 1 - 0.48%) throughout the entire established interval.

Table 25. Ovarian response in women following the administration of follitropin delta

Parameters	**Under 35 Years**	**Above 35 Years**
	(n = 122)	**(n = 83)**
AMH level	Mean - 3.46	Mean - 2.04

Parameters	Under 35 Years	Above 35 Years
	(*n* = 122)	(*n* = 83)
	SE - 0.22	SE - 0.17
	SD - 2.53	SD - 1.58
	CI 95% - 0.45	CI 95% - 0.34
	STDev - 2.54	STDev - 1.59
	SE Mean - 0.23	SE Mean - 0.17
Duration of stimulation (days)	Mean - 10.11	Mean - 9.62
	SE - 0.17	SE - 0.14
	SD - 1.91	SD - 1.35
	CI 95% - 0.34	CI 95% - 0.29
	STDev - 1.91	STDev - 1.36
	SE Mean - 0.17	SE Mean - 0.15
Daily dose (ng/mL)	Mean - 9.18	Mean - 10.63
	SE - 0.20	SE - 0.20
	SD - 2.31	SE - 1.89
	CI 95% - 0.41	CI 95% - 0.41
	STDev - 2.32	STDev - 1.89
	SE Mean - 0.21	SE Mean - 0.21
Follicles >18 mm	*n* = 1719	*n* = 814
	Mean-14.09	Mean-9.92
	SE - 0.73	SE - 0.77
	SD - 8.15	SD - 7.00
	CI 95% - 1.46	CI 95% - 1.54
	STDev - 8.15	STDev - 7.01
	SE Mean - 0.74	SE Mean - 0.77
Oocytes retrieved	*n* = 1279	*n* = 612
	Mean - 10.48	Mean - 7.65
	SE - 0.59	SE - 0.61
	SD - 6.57	SD - 5.50
	CI 95% - 1.17	CI 95% - 1.22
	STDev - 6.58	STDev - 5.51
	SE Mean - 0.60	SE Mean - 0.62
Embryo day 3	*n* = 677	*n* = 301
	Mean-5.73	Mean-4.01

Parameters	Under 35 Years	Above 35 Years
	(*n* = 122)	(*n* = 83)
	SE - 0.46	SE - 0.41
	SD - 5.08	SD - 3.62
	CI 95% - 0.92	CI 95% - 0.83
	STDev - 5.09	STDev - 3.63
	SE Mean - 0.47	SE Mean - 0.42

A total of 58 pregnancies were subsequently confirmed, more precisely 45 (36.88%) in women under 35 years and 13 (15.66%) in women above 35 years. Unfortunately, in the younger group, nine pregnancies (7.37%) ceased to evolve, and twelve pregnancies (*n* = 8 - 6.55%) could not be carried to term (which also happened in the older group, *n* = 4 - 4.81%). There were also three situations in which mothers suffered an abortion (one women under 35 and two older than 35). Multiple pregnancies were, however, noted in one case of a 39-year-old woman with twins (1.20%). Six pregnancies were ongoing at the time of drafting the results for publication purposes, all in the group under 35 (4.91%). In both groups there was a case where the result was expected, without any information regarding the status of the current pregnancy (*n* = 1 - 0.81%, and 1.20% - *n* = 1), respectively (Figure 32).

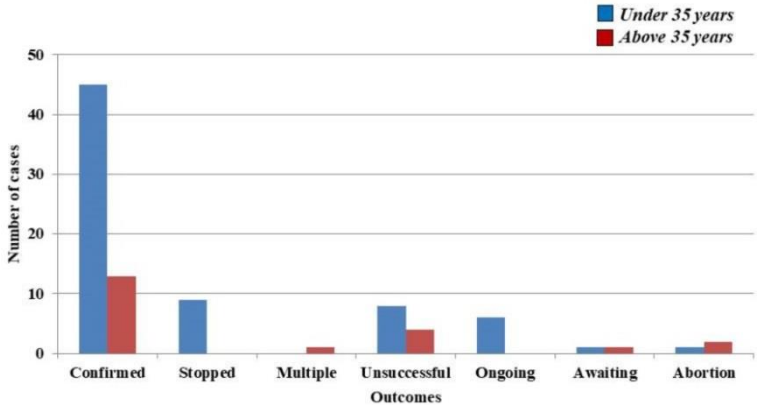

Figure 32. Main outcomes over a period of two years in women who received follitropin delta

Discussion

Follitropin delta can be successfully used in OS to achieve a pregnancy. We achieved that in both groups and obtained 45 pregnancies (36.88%) in women that were under 35 years of age and 13 (15.66%) in females above 35 years of age. We encountered only three cases when the procedure needed to be stopped (*n* = 2 were non-responders and *n* = 1 exhibited moderate adverse reactions). Even though the number of volunteers is not comparable with that of Martin and co-authors [514], the number of follicles, oocytes, and embryos was higher in women under 35 years compared with those over 35 years even though the groups were unequal; *n* = 1719 - 95% CI 1.46, *n* = 1279 - 95% CI 1.17, and *n* = 677 - 95% CI 0.92 and *n* = 814 - 95% CI 1.54, *n* = 612 - 95% CI 1.22, and *n* = 301 - 95% CI 0.83.

Regarding the effectiveness of follitropin alfa and delta, from 824 ongoing pregnancies, approximately 5.6% (*n* = 25) ended electively because of major congenital malformations.

The fact that fifteen women (8.15%) did not respond to treatment at different stages suggests that the treatment's kinetics are modulated by age and weight: eight did not achieve a pregnancy (4.81%) and three had abortions (1.80%) [515–517]. Based on the existing literature, we identified only two other studies in which women with similar conditions were enrolled.

In our study, nine pregnancies were stopped (4.39%), twelve pregnancies could not be continued (5.85%), and three were electively terminated (1.46%). Thankfully, at the time of writing up the results for publication, a twin pregnancy had been confirmed (0.48%). We also noted six ongoing pregnancies (2.92%), and in two cases we are unfamiliar with the outcome (0.97%).

To date, the Evidence-based Stimulation Trial with Human recombinant Follicle Stimulating Hormone (rFSH) in Europe and Rest of World (ESTHER-1) remains the largest research project dedicated to deepening the understanding of follitropin delta's reliability. The aim was to compare both conventional and standardized methodologies based on AMH level and BMI index using follitropin delta of 150 IU/day. Ongoing pregnancies and live birth rates were similar in both groups with fewer poor responders, respectively, and hyper-responders following the administration follitropin delta via an individualized manner [518].

By using a subset from ESTHER-1, patients had the possibility to undergo new stimulation cycles in ESTHER-2. It has been demonstrated that the treatment-induced incidence rate of anti-FSH antibodies was between 0.8% and 1.1% in cycle 2 and 3. Similar figures were noted after the first cycle as well. This further support the high efficacy of follitropin delta [519].

Using as reference the serum clearance, its agonistic potential was influenced in part by the hepatic asialoglycoprotein receptor (ASGPR). On the other hand, follitropin alfa was unaffected by asialoglycoprotein receptor in experimental models [520,521].

Arce et al., conducted a recent study aiming to establish the daily follitropin delta dose by further providing a similar ovarian response to 150 IU/day follitropin alfa [521]. For this, the authors analyzed the ovarian response in 1,591 IVF/ICSI cases that underwent OS. Daily doses of follitropin delta (10.0 µg (95% CI 7.9 - 12.8) and 10.3 µg (95% CI 9.7 - 10.8)) were shown to promote the formation of an identical number of oocytes as 150 IU/day follitropin alfa in both phases. When they analyzed patients with either normal or high ovarian reserve and no dose changes, the number of oocytes obtained was the same in all three situations: 150 IU/day follitropin alfa and daily doses of follitropin delta of 9.7 µg (95% CI 7.5 - 12.4) and 9.3 µg (95% CI 8.6–10.1). Between 9.5 and 10.4 µg was considered the optimal dose that corresponds to 150 IU/day follitropin alfa for serum E2 concentration and the number of follicles ≥ 12 mm.

A multinational clinical trial entitled "Follitropin Delta in Long GnRH Agonist and GnRH Antagonist Protocols" (BEYOND) (ClinicalTrials.gov Identifier: NCT03809429) was in the recruitment phase when we first learned about it. Seventeen institutions from seven states are involved in this project and it is scheduled for completion this year at the end of September. In this interventional study, 415 consenting participants were randomized, the main objective being to compare the efficacy and safety of follitropin delta and its personalized dosing algorithm in controlled OS for IVF/ICSI by using a long GnRH agonist protocol compared with a short GnRH antagonist protocol.

In conclusion, follitropin delta proved to be a safety biomolecule that can be used in OS protocols, which is why we encourage the usage on an even larger scale. To the best of our knowledge, this is the first observational study conducted in Romania, but also in the northeastern region of Europe that addresses such a perspective and brings conclusive evidences in this context.

Personal contribution - published papers:

Simionescu, G.; **Doroftei**, **B**. Efficacy and safety of corifollitropin alfa administration in poor ovarian responders undergoing IVF treatment cycle. *Fertil. Steril.* ***2013****, 100,* S521. **IF: 7.329**

Aim of the study

The current survey aims to investigate the effect of corifollitropin alfa administration in women undergoing an IVF treatment cycle, stated as poor ovarian responders according to the Bologna criteria.

Materials and methods

Stimulation parameters and treatment outcomes were documented for 33 female infertile patients undergoing an IVF long protocol with agonist GnRH. The patients were given a 150 mg single dose of corifollitropin alfa on cycle day 2 or 3 to sustain the first 6 days of OS. Daily hMG administration was initiated on stimulation day 7, for 3 to 8 days. The following parameters were assessed: the number of follicles greater than or equal to 11 mm and the oestradiol value on day 8 and on the trigger day, the number of stimulation days, the number of retrieved oocytes, the fertilization rate, the number of good-quality embryos obtained and transferred and, also, the pregnancy rate.

Results

The mean age of the studied population was 37 years, with a mean value of the AMH of 1.01 ng/mL. Stimulation lasted a median of 11 days. Significant correlations were noted between the age of the female participants and the following variables: the number of follicles bigger than or equal to 11 mm on the trigger day ($p<0.05$), the number of retrieved oocytes ($p<0.05$) and the number of stimulation days ($p<0.02$). The desired ovarian development was achieved in 98.5% of cycles and ET took place in 85.7% of cycles, with an average of 2 embryos transferred. The clinical pregnancy rate was 18.18% and no OHSS was observed.

OHSS is a rare but serious and potentially life-threatening iatrogenic complication of IVF cycles, which occurs in approximately 1-14% of ART cycles [522,523]. The OHSS is typically associated with exogenous gonadotrophin stimulation and is only rarely observed with use of other agents (CC and GnRH) [524].

Pathophysiology of this syndrome is still a subject of debate, the main mechanism is the release of vasoactive peptides from the granulosa cells causing an increase of vascular permeability. The ultimate OHSS trigger is hCG which induces the overexpression of vascular endothelial growth factor (VEGF) in granulosa cells and a rise in serum vascular endothelial growth factor concentrations [525,526].

Because of its homology with LH, in IVF treatments, hCG is the most used trigger for final oocyte maturation, and due to its long half-life, in some patients hCG trigger can cause OHSS. Recent good clinical practice recommends that in patients at high risk of OHSS a short GnRH antagonist protocol with GnRH agonist trigger for final oocytes maturation and "freeze-all strategy" proves the safest.

Personal contribution - published papers:

Simionescu, G.; **Doroftei**, **B**. Efficacy and safety of corifollitropin alfa administration in poor ovarian responders undergoing IVF treatment cycle. *Fertil. Steril.* ***2013***, *100*, S521. **IF: 7.329**

Maftei, R.; Simionescu, G.; Neculai-Valeanu, A.S.; Mocanu, E.; **Doroftei**, **B**. Ovarian hyperstimulation syndrome after GnRH agonist trigger and rhCG luteal rescue protocol. *Arch. Clin. Cases* ***2016***, *03*, 149–152.

Darii, N.; Pavlovic, M.; **Doroftei**, **B**.; Anton, E. Unsuspected adverse effect of albumin in severe ovarian hyperstimulation syndrome: a case report. *JBRA Assist. Reprod.* ***2019***, *23*, 430-433

Personal contribution - published papers:

Maftei, R.; Simionescu, G.; Neculai-Valeanu, A.S.; Mocanu, E.; **Doroftei**, **B**. Ovarian hyperstimulation syndrome after GnRH agonist trigger and rhCG luteal rescue protocol. *Arch. Clin. Cases* ***2016***, *03*, 149–152.

Case presentation 1

We revisit the case of a 24 year-old woman with a history of primary infertility related to male factor (severe asthenozoospermia), and who underwent a procedure of IVF in a center from Romania. She then presented at our hospital with symptoms of early severe OHSS. The patient's BMI was 20.2, the menstrual periods were regular, at 28 days, and the AMH was 3.51 ng/mL. The treatment was

carried out with GnRH antagonist downregulated protocol using Cetrorelix (Cetrotide; Merck Serono, UK).

OS was started on the second day of menstruation with a daily dose of 125 IU of rFSH (Puregon; MSD, Oss) until the 7th day of stimulation, afterwards, the stimulation continued with a combination of 50 IU of rFSH (Puregon; MSD, Organon) and 75 IU of hMG (Menopur; Ferring, UK).

On the 6th day of stimulation, when the leading follicle diameter was 14mm, the GnRH antagonist was started. The oestradiol concentration on the day of trigger (day 10) was 10267.7 pmol/L. Final oocyte maturation was triggered by administration of 0.3 mg Triptorelin (Diphereline, Ipsen).

After 36 hours a total of 18 oocytes were retrieved. IVF was carried out for all the oocytes and 14 embryos were obtained (fertilization rate: 77.7%). On day 5, two embryos were transferred and 6 embryos were frozen. During oocyte pick up, 125 mcg of recombinant hCG (Choriogonadotrophin alfa; Ovitrelle, Serono) was administered and another 125 mcg in the day of ET. From the day of ET, 2 mg/day of oestradiol valerate (CycloProgynova, Bayer) and 600 mg/day of progesterone (Utrogestan, Laboratories Besins International) were started. The day following ET, the patient was admitted to the emergency department of our hospital with moderate abdominal pain, abdominal distention (abdominal circumference 80 cm), nausea, vomiting and oliguria. Ultrasound evaluation revealed enlarged ovaries (left ovary: 8.7 cm and right ovary: 7.9 cm) and free fluid in the pouch of Douglas. Laboratory results indicated hemoconcetration: hemoglobin: 17.7 g/dl; hematocrit: 52%, white blood cells count 31800 µL and K: 5.31 mmol/L.

The treatment was initiated immediately with albumin (25%) in doses of 50 g infused over 4 h and repeated at every 12 h in the first 2 days, lactated ringers solution (1000 mL/day) in the first 2 days and low molecular weight heparin (Clexane; 6000 IU daily) during hospitalization. The patient was discharged after 10 days of hospitalization, and the pregnancy was confirmed biochemically (βhCG on day 10 after ET was 37 mIU/mL). After two weeks, an ultrasound revealed it as a twin pregnancy. At 34 weeks of gestation, due to uterine contraction and fetal distress, she underwent a C-section to delivere one girl (weight 1900 g, APGAR score 9) and a boy (weight 1700 g, APGAR score 9).

Personal contribution - published papers:

Darii, N.; Pavlovic, M.; **Doroftei**, **B**.; Anton, E. Unsuspected adverse effect of albumin in severe ovarian hyperstimulation syndrome: a case report. *JBRA Assist. Reprod.* ***2019***, *23*, 430-433

Case presentation 2

A 29-year-old woman (G0P0) underwent controlled OS using an antagonist protocol (Cetrotide™ 0.25mg, Merck Serono, London UK) after being informed that IVF was indicated due to male factor infertility (severe oligoasthenoteratozoospermia). Her ovarian reserve showed an AFC of 17 and a FSH level of 4.5mIU/mL. Recombinant FSH (Gonal-F™, Merck Serono, London, UK) was administered for a period of 13 days, with a total dose of 3,487.5IU. On day 6, ultrasound examination showed 10 ovarian follicles measuring more than 7mm in diameter and 14 ovarian follicles measuring less than 5mm in diameter for both ovaries, with an estradiol level of 198pg/ml.The patient did not report any abdominal discomfort or dyspnea.

The FSH antagonist cetrorelix (Cetrotide™ 0.25mg,Merck Serono, London, UK) was added on day 9 when at least one follicle measured 13mm in diameter. Ovulation was induced by the administration of 10,000IU hCG (Pregnyl™, Merck & Co., Brussels, Belgium) on day 13 when the estradiol level was 898pg/dl and 16 follicles measured more than 15mm in diameter. According to Kovács et al., [527], when the estradiol level is within a comfortable level (between 1,500 and 2,500pg/ml), human chorionic gonadotropin can be administered and the cycle will continue.

Two days later, 24 oocytes were retrieved because small follicles were also aspirated. After fertilization, nine embryos were obtained. On the day of ET, no clinical or ultrasound signs of OHSS were detected. Despite the high number of oocytes retrieved, we decided to transfer only one 10-cell-stage embryo after counselling the patient.

Seven days after oocyte pick-up, the patient was admitted to the emergency department for

abdominal pain, bloating, nausea and dyspnea, indicative of OHSS. Clinical examination revealed blood pressure of 90/60mmHg, a heart rate of 94/min, oxygen saturation of 96%, and a temperature of 36.6°C. Ultrasound examination showedcomparable ovarian size (75x48x51mm for the right ovary and 71x57x63mm for the left ovary), but significant ascites in the Douglas pouch (81x27x12mm), in the Retzius space (72x73x57mm) and around the liver (95x43mm). According to the SOGC-CFAS clinical practice guidelines [528], the OHSS was classified as severe, based on hemoconcentration, hyponatremia, elevated liver enzymes, presence of significant ascites, pleural effusion and clinical symptoms.

The patient was admitted for intensive follow-up. We administered NaCl 0.9% perfusion in order to correct the electrolytic balance, as well as low-molecular-weight heparin nadroparin 0.3ml/day (Fraxiparine®, GSK, Inc) and compressive stockings for thromboembolic prevention. Due to severe dyspnea, thoracocentesis was carried out onday one (admission) and intravenous albumin was given.

Pleural and abdominal ascites were drained. Pregnancy was confirmed by positive hCG (92.5mIU/ml). hCG evolution was correct (Figure 33) and vaginal ultrasound performed a few days later revealed a single intrauterine gestational sac.

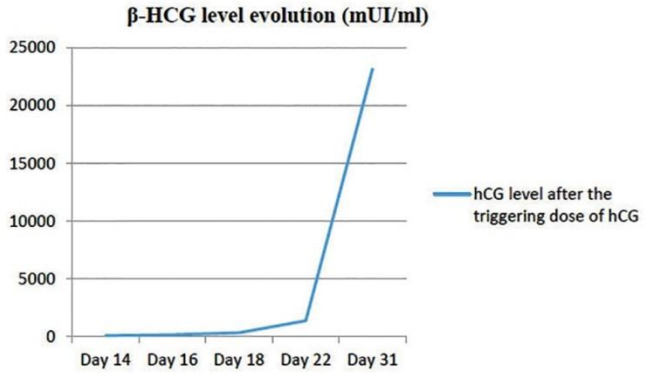

Figure 33. hCG evolution

Seven paracenteses (between 1,000 and 2,100 ml of exudate) and 5 thoracocenteses (between 1,100 and 1,600 ml of exudate) under ultrasound guidance were required to decrease patient dyspnea and improve her comfort. A total of 19,900 ml of exudate was extracted by the two procedures. Crystalloids (normal saline 1,000 ml a day) and colloids (human albumin 20% 100 ml twice a day then 100 ml three times a day) were administered to counterbalance the loss of osmotic pressure related to albumin loss in the third space, but effusions persisted despite this strategy (Table 26). We finally suspected that the pleural and abdominal effusions werebeing sustained by our initial treatment. It was decidedto stop albumin perfusion after 24 days of the admission. Surprisingly, the patient's clinical and paraclinical status improved within 4 days of stopping albumin, with reduction of ascites and pleural fluid synthesis. She was subsequently discharged on day 29 (day 35 after HCG injection) without dyspnea and gave birth to a 2.800 g girl at term and by the vaginal route.

Table 26. Patient evaluation

Date	Hb	Hct	L	Alb level	HCG	P + or T	Perf	Albumina DM	T (°C)	Ovarian size(cm)	Patient weight
Day 7	16.1	45.5	8.06	3033		0			36.6	74x48x51(L); 71x57x63(R)	
Day 8	13.5	38.1	7.74	2010		3000	3500	2	36.8		55.5
Day 9	12.1	34.6	7.74	2495		2000	3500	2	36.5		54.4
Day 10						0	1000	2	36.2		55.0
Day 11	12.3	35.8	7.74	2997		1900	1000	2	37.3		55.0

Day 12						0	1000	2	37.3		55.7
Day 13						0	1000	2	36.9		55.4
Day 14	13.8	40.9	7.74	2954	92.5	1400	1000	2	36.9		56.0
Day 15						0	1000	2	36.0		55.5
Day 16					158.3	1900	1000	2	36.9		55.6
Day 17						0	1000	2	37.2		57.1
Day 18	12.3	35.9	9.13	2949	333.3	1000	1000	2	37.1		57.1
Day 19						0	1000	2	37.0		56.9
Day 20						0	1000	2	37.0		55.9
Day 21						0	1000	3	36.8		55.4
Day 22	10.5	30.8	6.62		1381.2	1900	1000	3	37.2		55.5
Day 23	10.9	32.1	6.55	3607		1500	1000	3	37.2		56.1
Day 24						0	1000	3	37.3		56.9
Day 25	10.2	30.1	6.08	3774		1100	1000	3	36.7		56.0
Day 26						1100	1000	3	36.6		56.4
Day 27						0	1000	3	37.3		57.9
Day 28	10.1	29.6	6.61	4300		1400	1000	2	37.0	64x69x76(L); 120x76x74 (R)	57.6
Day 29						0	1000	2	36.8		56.9
Day 30						0	1000	2	37.0		57.1
Day 31	10.5	30.7	6.83	4301	2315 4.4	1700	1000	0	37.1		55.4
Day 32						0	1000	0	37.1		53.8
Day 33	10.8	31.0	7.45	3734		0	1000	0	37.2		53.9
Day 34						0	1000	0	36.7		53.6
Day 35	10.4	30.6	7.72	3774		0	1000	0	37.2	74x40x50(L); 115x72(R)	52.9

Date, day after triggering dose of hCG; Hb, hemoglobin (g/dL); Hct, haematocrit; L, leucocytes x100/µL; albumin level, mg/ dL; alb level, albumin level (mg/dL); HCG, human chorionic gonadotropin (mUI/mL); P, paracenteses (ml); T, thoracocenteses(ml); perf, perfusions (ml); albumin adm, albumin administration (albumin humaine C.R. 20%100ml); T, temperature (Celsius); patient weight (kg)

Discussion

OHSS is one of the most serious iatrogenic IVF complications to occur after OS. The pathogenesis of OHSS is not entirely understood but the most accepted mechanism is an overexpression of of vascular endothelial growth factor [529]. This mediator of angiogenesis acts as a potent stimulator of vascular permeability and inflammation, which hypovolemia, hydroelectrolytic disorders, multi-organ failure and sometimes, death as potential consequences. High

molecular weight plasma proteins could also accumulate in extravascular fluid under mediation of vascular endothelial growth factor [530,531]

For severe cases of OHSS, multidisciplinary counsel and close clinical and biological monitoring are recommended [532]. The goal of treatment is to preserve intravascular blood volume. Guidelines and most studies [528,530,532,533] recommend use of macromolecules like albumin to maintain this intravascular fluid. Albumin is a blood-derived plasma expander, and it has been suggested that the binding and transport properties of human albumin result in binding and inactivation of the vasoactive intermediates responsible for the pathogenesis of OHSS. The osmotic function is the most well-known property of albumin, whose role is to maintain intravascular volume in the event of capillary leakage, thus preventing the sequelae of hypovolemia, ascites and hemoconcentration. However, because vascular permeability is compromised, albumin could accumulate in the interstitium, drawing fluid into the extracellular space and leading to impaired re-expansionof the intravascular space [528,534]. Vandoorne et al., showed that large serum proteins, like albumin extravasate through large fenestration and vesiculo-vacuolar organelles and can accumulate selectively in the extravascular spacein regions with elevated vascular permeability [530]. In a pilot study on rabbits, Orvieto et al., showed that, in animals treated with bovine serum albumin (BSA), body weight and ascites formation were higher than in animals not treated with bovine serum albumin treatment [535]. It appears that plasma albumin concentrations in patients with severe OHSS are significantly lower than in controls and ascitic fluid obtained from patients with OHSS contains large amounts of this protein [531]. Thus, the potential protective action of albumin perfusion could be less than commonly believed, and it may even promote edema formation by further increase of extra-vascular colloid oncotic pressure [534]. Repeated ascitic fluid aspiration is usually necessary in case of severe OHSS in order to improve clinical parameters and to reduce hospitalization time [536] and it is usually recommended to give human albumin in order to limit the rapid reconstitution of the third space. The quantity of aspirated fluid may varyup to significant value and consequently the quantity of albumin extracted. For this reason, albumin administration is recommended. The more albumin is administered the more will cross the capillary wall in this context of vascular hyperpermeability.

In our opinion, this theory could explain the vast quantities of liquid extracted by numerous paracenteses and thoracocenteses. Moreover, in the case of our patient, after stopping the albumin perfusion, the ascitis formation was ceased despite the woman being in the 7^{th} week of pregnancy so with rise in hCG (hCG peaked between 56 and 68 day) [537]. Albumin perfusion for OHSS also has other disadvantages, such as risks of exacerbation of ascites, nausea, vomiting, febrile reactions, allergic reactions, anaphylactic shock and possible virus and prion transmission [538].

Synthetic colloids such as gelatins, dextrans and hydroxyethyl starches (HES) may also be utilized as plasma expanders. Conversely, in patients with increased vascular permeability, like human albumin, these colloid molecules may themselves leak into the interstitium and exert a reverse osmotic effect. Hydroxyethyl starches are macromolecules that have been extensively used in the treatment of severe OHSS, but very few studies have compared its efficacy with that of intravenous albumin. Many studies show the beneficial role of hydroxyethyl starches in maintaining plasma volume. However, Kissler et al., [539] reported a case of detrimental role of hydroxyethyl starches in OHSS due to increase in capillary permeability with loss of this colloidal substance into the third space and prolong clinical OHSS symptoms. Moreover, hydroxyethyl starches run a greater risk of adverse renal and coagulation effects than albumin and there is still uncertainly regarding their use in pregnancy.

Other treatment options for OHSS include oral antidiabetics (glibenclamide), dopamine and dopamine agonists in addition to crystalloids and colloids or anti-vascular endothelial growth factor agents [532,533], but more studies are needed to assess the safety of these treatments if OHSS is associated with pregnancy.

Based on the aforementioned report, this case of OHSS resulting from luteal phase use of hCG highlights the danger of pursuing such protocols with patients at high risk of OHSS. The IVF therapy was developed as a way to help infertile couples who are otherwise unable to conceive a child but, unfortunately, IVF is not free of side effects and complications.

The most serious complication of controlled ovarian hyperstimulation cycles is the development of OHSS. The trigger of OHSS is represented by hCG, which determine the

overexpression vascular endothelial growth factor in granulosa cells and raises in serum vascular endothelial growth factor concentrations and can have different grades of severity. The incidence of severe OHSS, which can be life-threatening, is 2-3% [540].

The risk factors for OHSS can be divided in two groups: primary (factors that can be identified before the initiation of stimulation) and secondary (factors that becomes obviously during stimulation). In general, patients at risk to develop OHSS are patients with AMH levels above 3.3 ng/dL [541,542], age below 30 years, low BMI, PCOS, previous OHSS, E2 levels more than 3000 pg/mL in the day of trigger, rapidly rising of oestradiol levels during stimulation and number of oocyte collected >15. Depending on the onset, OHSS can be late (after more than 10 days after trigger) which is primarily related to the ongoing pregnancy and early OHSS, which is an iatrogenic complication of IVF (in the first 10 days after trigger) caused by luteotrophic effect of hCG.

The patient described here had both types of risk factors for OHSS: primary (AMH>3.3 ng/dL, age <30 years, low BMI) and secondary (rapidly rising of oestradiol levels during stimulation: 2856/6086/10267 pmol/L in day 5/8/11, number of oocyte collected more than 15 [543]) therefore, the GnRH agonist triggering was mandatory.

Should an ET take place in such cases? When a patient is identified as high risk, the use of an antagonist protocol with GnRH analogue trigger has been proven to prevent early OHSS [544]. The only protocol to prevent late OHSS is adopting a “freeze all” procedure with cryopreservation of all embryos obtained.

The proponents of ET in these high risk cases use the so called “luteal rescue” protocol with hCG to correct the luteal defect. The most used protocol is administration of 1500 IU of hCG at 35 h after trigger [545–547]. In this case, a higher dose, 125 mcg of rhCG which is equivalent of 3250 IU of hCG, were used, on two occasions. Furthermore, two embryos were transferred, resulting in a twin pregnancy and a more severe form of OHSS as well as premature delivery.

II.3 Semen integrity

Spermatozoa are produced in the testicles during a process of differentiation known as spermatogenesis. The sperm cell is composed of a head, neck, mid-piece and flagellum (tail and end-piece) [548], the genetic material being located in the head, along with the acrosome. The flagellum contains axoneme and a set of mitochondria that supply energy required for sperm cell motility. The acrosome is located in the apical region of the spermatozoon covering the anterior extremity of the nucleus and has been described by Moreno and Alvarado [549] as a secretory vesicle that produces acrosin, acrogranin, hyaluronidase as well as other enzymes present in classic organelles, such as peroxisome, lysosome [550]. Unlike the somatic cells in which the chromatin has a loose structure, in sperm cells the chromatin is characterized by a tightly compact structure due to the unique associations between the DNA and sperm nuclear proteins also known as protamines [551].

During spermatogenesis, the spermatid nucleus is remodeled and condensed, and the histones are replaced [552]. The DNA compaction is the result of disulfide bonds generated by protamines. These bonds have the purpose to protect the genetic material from stressing agents such as reactive oxygen species and high temperatures during the transit through the male and female reproductive tract [553–555].

There are also other factors that might affect chromatin integrity such as cryopreservation, although the precise underlying mechanism it is not completely understood. A study conducted by Thomson et al., reported that the sperm DNA-damage induced by cryopreservation is generated mainly by oxidative stress and less by apoptosis [556]. According to Mukhopadhyay et al., the percentage of sperms with DNA fragmentation is consecutive cryopreservation is relatively higher in bulls with poor semen quality [557].

The semen quality evaluation includes routinely assessed parameters such as motility, viability, morphology but recent studies suggest that markers of sperm DNA integrity may offer a better perspective of male fertility potential as compared to conventional parameters [558]. The study of

sperm DNA integrity is particularly relevant in an era where advanced forms of assisted reproductive biotechnologies are frequently used in both human and animal reproductive programs. According to Cho et al., there appears to be a solid relationship among sperm DNA damage (i.e., DNA fragmentation, abnormal chromatin condensation) and embryo development [559]. In bulls, the level of sperm with damaged chromatin has been negatively correlated with motility and viability [560,561]. Sperm chromatin integrity has been shown to affect the reproductive potential in several studies [562,563].

Over the past decade, *in vitro* assays have become very common as a means to determine sperm intactness and measure sperm function. These assays have improved the andrological diagnosis and have contributed to the optimization of semen processing methods, as summarized in multiple reviews [564,565].

Sperm DNA damage can be assessed either directly (fragmentation, oxidation) or indirectly (sperm chromatin compaction). Direct assessment of DNA damage can be made by single-cell gel electrophoresis assay, by Comet assay, or TUNEL assay [566]. Indirectly, the DNA damage may be measured by means of sperm chromatin integrity assays and by evaluation of nuclear protein levels [567].

Toluidine blue (TB) is a classic nuclear dye that has been used to evaluate the sperm chromatin integrity. The principle of the method is based on the detection of rupture or absent disulfide bonds. It has been used to determine sperm chromatin integrity in several species, such as bulls, horses, rabbits, buffaloes and humans [568–572] but it is not introduced as a routine analysis in semen quality evaluation. Toluidine blue stain was high correlated with SCSA, TUNEL and AO [570,573] in human sperm; while in rabbits, a study conducted by Beletti and Mello, [569] showed a high correlation with Feulgen reaction.

Personal contribution - published papers:

Doroftei, **B**.; Neculai-Valeanu, A.S.; Simionescu, G. HORMONAL MODULATION OF THE SPERM ACROSOME REACTION. *Lucr. Ştiinţifice USAMV Iaşi – Ser. Med. Vet. ISSN 1454-7406* ***2014***, *57*, 20–28.

Simionescu, G.; Maftei, R.; Anton, E.; Valeanu, S.; **Doroftei**, **B**. TIME-LAPSE MICROSCOPY ROLE IN IMPROVING THE OUTCOME OF IVF/ICSI CYCLES BY MONITORING AND SELECTION OF EARLY EMBRYO. *Manag. Intercult.* ***2016***, 345–349.

Personal contribution - published papers:

Doroftei, **B**.; Neculai-Valeanu, A.S.; Simionescu, G. THE UTILITY OF TOLUIDINE BLUE STAIN IN ASSESSING CHROMATIN INTEGRITY OF HUMAN AND BULL SPERM. *Lucr. Ştiinţifice USAMV Iaşi – Ser. Med. Vet. ISSN 1454-7406* ***2014***, *57*, 13–19.

Aim of the study

The purpose of this preliminary study was to observe the possible relationship between sperm chromatin integrity as assessed by toluidine blue stain and other semen parameters such as motility and morphology, in order to establish the utility of this analysis in routine semen evaluation.

Material and methods

The study summarized next was conducted as two separate experiments (Experiment 1 and Experiment 2) using human and bull semen.

Experiment 1

Semen samples

Ejaculates were collected from bulls used for artificial intelligence with the help of an artificial vagina. After routine evaluation, only ejaculates that reached the minimum quality standards established by the Bull Center were processed and loaded into commercial straws of 0.25 mL, which were then frozen in liquid nitrogen.

Motility and morphology in thawed bull semen

The straws were thawed in a water bath at 37°C for 30 seconds, motility being immediately estimated subjectively under a light microscope at x 400 magnification. For the sperm morphology evaluation, eosin-nigrosin stain was used as described by Tamuli and Watson [574]. Briefly, 15 μL of semen were mixed with 10 μL of eosin-nigrosin stain for 30 seconds. Wet smears were prepared onto a pre-warmed glass slide and the percentage of sperm cell with normal morphology was determined under light microscope at x 1000 magnification by counting at least 200 spermatozoa. The mean motility and mean morphology was determined.

Chromatin integrity in thawed bull semen

Sperm chromatin integrity was assessed using the toluidine blue stain according to the protocol described by Agarwal and Said [575]. Semen smears were air dried and fixed in an freshly prepared mixture of ethanol: acetone (1:1 v/v) solution for 30 minutes and then hydrolyzed for 5 minutes in 0.1 N HCl. Consecutively, the smears were washed in distilled water two times, each time for 2 minutes. The air-dried smears were stained for 10 minutes with a 0.05% toluidine blue (pH 4) prepared using McIlvain buffer. The final step consisted in evaluation under a light microscope at x 1000 magnification. Sperm cells with normal chromatin were stained light blue or green, whereas sperms with damaged chromatin were stained dark blue or violet. The percentage of sperm with abnormal chromatin was established after counting 300 spermatozoa. Additionally, the mean percentage of sperms with abnormal chromatin was determined.

Experiment 2

Semen samples

The subjects of the present study were 5 male partners younger than 35 from couples attending a fertility clinic. Semen samples were collected at the clinic site, by masturbation, into sterile containers, after a period of sexual abstinence of 2-7 days. After liquefaction for 30 minutes at room temperature, each sample was routinely assessed using light microscopy.

Motility and strict morphology in human semen

Complete semen analysis was carried out after sample liquefaction at 37°C. The following parameters were taken into account: semen volume, total motility, morphology and sperm chromatin integrity. All parameters, except motility, were determined according to WHO.

Chromatin integrity in human semen

Sperm chromatin integrity of human sperm was assessed according to the same protocol as described previously for frozen thaw bull semen.

Results

In experiment 1, the mean motility was 64.54 (± 3.72%), while the percentage of sperms with normal morphology was 81.8 (± 4.65). The percentage of sperm cells with damaged chromatin was 5.28 (± 0.85%). Normal morphology was positively correlated with motility (r=0.950, p=0.013), and negatively correlated with damaged chromatin sperms (r= - 0.892, p=0.021). Furthermore, motility percentage was also negatively correlated with the percentage of sperms with damaged chromatin (r= -0.772, p=0.049) (Table 27).

In experiment 2, semen was analyzed according to the WHO criteria, the mean motility being 38,33 (± 5.34). The tested samples had a mean strict morphology of 5.9% ± 3.6%, and a mean abnormal chromatin structure of 24.1% ± 14.5%. The percentage of sperms with abnormal chromatin structure was negatively correlated with the strict morphology (r= - 0.738, p= 0.047) and motility (r= - 0.483, p= 0.329. A positive relationship was observed between strict morphology and motility (r=0.412, p=0.035) (Table 28).

Table 27. Percentage of motility, normal morphology and abnormal sperm chromatin in frozen thaw bull sperm

Bulls	Motility	Normal Morphology	Abnormal sperm chromatin
1	59.66a	75a	6.7a
2	64.5b	82b	5.44b
3	65.25c	85b	4.9c
4	63.33a	80ab	4.6b
5	70d	87d	3.77d

Values with superscript in the same column differ significantly ($p<0.05$)

Table 28. Percentage of motility, normal morphology and abnormal sperm chromatin in human sperm

Patient	Motility	Normal Morphology	Abnormal sperm chromatin
1	23a	4.78	34.2
2	59	5.31	20.1
3	16	5.52	23.7
4	20	4.58	28.5
5	67	5.87	22.3

Discussion

Sperm quality has been routinely assessed upon certain parameters such us concentration, motility or morphology, however these classical parameters may not reveal subtle defects such as sperm DNA damage or offer a clear view over the male's fertility potential. Evenson et al., [576], revealed, that at least in humans, the chromatin damage may be responsible for embryo death in the early stages of embryonic development.

The results in our study showed that the overall level of sperm chromatin damage in the examined bulls was relatively low (5.28 ± 0.85%), whereas in men, the degree of sperm cell with damaged chromatin was significantly higher (24.1% ± 14.5%). One possible explanation for these results might lie with the sperm chromatin protamination. Studies conducted by Gatewood et al., [577], Bench et al., [578] showed that bull, stallion, hamster and mouse sperm nuclei contain

significantly higher amounts of protamines (about 95%) compared to human sperm nuclei (about 85%). As a consequence, in animals, the degree of sperm chromatin condensation is higher, thus chromatin resistance to fragmentation would be higher [579].

In contrast to human sperm, which contains protamines P1 and P2, bull, boar, ram and cat spermatozoa contain only P1 protamines which are more abundant in cysteine residues, contributing to the formation of disulfide bridges and the stabilization of sperm chromatin [580]. These differences between human and animal sperm may suggest that bull sperm chromatin is more resistant to damage than human sperm chromatin.

There are studies that either confirm the relationship between sperm chromatin integrity and other sperm characteristics [555,581] or contradict this [582]. However, studies conducted by Bochenek et al., [582] on animal semen, as well as those conducted on human semen [555,576,583] revealed a close relationship between the extent of sperm chromatin damage and fertility potential.

In our study, the sample size was not statistically significant and neither of the experiments included data regarding the clinical outcomes such as IUI or pregnancy rate. Although the results are preliminary, we may conclude that toluidine blue stain proved to be a rapid, useful and nonetheless cheap method for assessing sperm chromatin integrity.

In conclusion, the toluidine blue stain could be introduced as additionally assay in the routine semen analysis for the couples with infertility history. In the case of bulls, where the sperm chromatin damaged is lower than in humans, the sperm chromatin integrity assay could detect subfertility, condition which usually passes beneath the radar in the routine semen analysis.

Personal contribution - published papers:

Neculai-Valeanu, A.S.; Simionescu, G.; **Doroftei**, **B**.; Cumpata, S. Sperm Chromatin Structure and the Sperm Parameters characteristics after Processing by the Density Gradient. *Curr. Opin. Biotechnol.* ***2013***; 24S: S48-S143. **IF: 9.740**

Aim of the study

This study was designed to study the efficiency of the density gradient media in recovering the spermatozoa with a high degree of motility, normal morphology and a low level of damaged chromatin.

Material and methods

A total of 20 samples were included in the study mentioned next. The semen samples were collected by masturbation. After 30 min homogenization, an aliquot of semen was spread on a slide and the remaining part of the sample was prepared by the density gradient technique, using PureCeption 40% and PureCeption 80% (SAGE Cooper Surgical USA). The recovered spermatozoa were evaluated for total motility, normal morphology and sperm chromatin structure. Sperm chromatin structure was assessed using the TB stain.

Results

There were significant differences in the sperm parameters characteristics before and after processing by density gradient technique. The spermatozoa recovered after processing presented a significant lower level of damaged chromatin, improved total motility and normal morphology. Density gradient sperm preparation has proven to be efficient in separating motile spermatozoa with a

higher level of normal morphology and healthy chromatin structure. This method will improve pregnancy rate and increase selection of high quality sperm.

Personal contribution - published papers:

Doroftei, **B**.; Emerson, G.; Cumpata, S.; Simionescu, G.; Maftei, R.; Zlei, M. Time-lapse monitoring of early embryo development may aid in the validation of the effect of sperm DNA fragmentation assay on reproductive outcomes - preliminary findings. 31st Annual Meeting of the European-Society-of-Human-Reproduction-and-Embryology (ESHRE); ***2015***; O-270.

Study question:

Can time-lapse study of early embryonic development aid in the validation of the effect of DNA fragmentation assay (DFI) on ART?

Summary answer:

Sperm DFI assessed by SCSA by flow cytometry (FCM) impacts on the embryo-development and reproductive outcome of IVF/ICSI/IMSI in a group of couples with male infertility. Morphokinetics of early embryo development may aid in validation of new cut-off values for DFI.

What is known:

Available literature suggests that, when the sperm DFI value is above 25%, couples with infertility may have greater success with IVF/ICSI/IMSI procedures instead of IUI. However, when sperms with high DFI are involved, there are still uncertainties regarding the repair capacity of the egg and its further embryo-development.

Study design, size, duration:

A retrospective comparative analysis of 23 sperm samples from men undertaking ART in a private IVF center (May-December, 2014) focused on the reproductive outcome and morphokinetic parameters (EmbryoViewer-Vitrolife) between patients groups divided by the DFI cut-off value of 25. Mean ± SD and p values with a significance threshold of 0.5 were calculated.

Participants/materials, setting, methods:

Semen samples from patients (aged 35.6 ± 4.9 years) were analysed by SCSA (FACSAriaIII-BDBiosciences). Group A had a DFI <25 (n = 17) and Group B had DFI 25 (n = 6). Twenty six treatment cycles were performed (23% IVF, 50% ICSI, 27% IMSI) and the development of 218 fertilised eggs was monitored by time-lapse imaging (EmbryoScope-Vitrolife).

Main results and the role of chance:

All female partners were under 36 years of age and had >4 eggs collected. The following morphokinetic parameters were found to be significantly different in Group A vs. Group B: lower t3-tPNF (time to 3 cells minus time to pro-nucleai fading, in hours) (4.73 ± 4.57 versus 9.31 ± 4.57, respectively, p = 0.0259, lower t3-t2 (5.64 ± 7.65, 12.68 ± 9.73, p = 0.0466, lower t5-t3 (9.23 ± 12.60, 23.46 ± 13.82, p = 0.0173, lower t7-tPNF (12.66 ± 13.13 vs. 29.31 ± 6.16, p = 0.0044, lower t8-tPNF (17.08 ± 15.53 vs. 34.51 ± 10.28, p = 0.0111) respectively and a reduced value of fragmentation time recording (57.86 ± 7.39 vs. 68.71 ± 6.53, p = 0.0089). A significant difference was found between the group of couples with positive (pregnancy rate of 61%) versus negative biochemical pregnancy (DFI of 13.5 ± 5.6 vs. 31.7 ± 23, p = 0.042).

Limitations, reason for caution:

When the relationship of DFI with the reproductive outcome is assessed, the female bias cannot be completely excluded, although age and ovarian competence have been considered. However, with larger cohorts of patients, a more cautious selection should be possible.

Wider implications of the findings:

When strictly controlled female factors and stable incubation conditions are available, the sperm DFI impact on embryo development can be properly assessed and, with larger study cohorts, new cut-off DFI values may be validated and used in conjunction with quantitative morphokinetic parameters for selecting viable embryos.

We systematically reviewed the available evidence regarding the assessment of embryo quality through both conventional monitoring and time-lapse microscopy for couples undergoing IVF or ICSI. Some of the retrospective studies conducted after 2010 have highlighted a correlation between time-lapse parameters and embryo viability as defined by the developmental competence and subsequently by the confirmation of clinical pregnancy. Other authors have undertaken a more critical appraisal of the potential benefit that time-lapse monitoring may bring to ART. Even if time-lapse monitoring is likely to revolutionize the field of embryology by enabling an objective, automatize monitoring and selection of embryos, further randomized studies reporting clinical outcomes after IVF and ICSI are needed before adopting this technology for routine use in the laboratory.

II.4 Tumor-related and other potentially life-threatening cases

Breast cancer is the most common oncology disease in women and one of the major public health issues worldwide. It is also the second leading cause of cancer-related deaths in women and a cancer research priority in laboratories across the world with a view to uncover the causes of the malignant process, understand the mechanisms of development, and, most of all, to discover early diagnostic methods and effective treatment [584].

Ignorance, fear of diagnosis, lack of health education and of efficient programmes for prevention and screening often delays the diagnosis of the disease until it reaches advanced stages when treatment options are mainly palliative and very expensive, with immense personal costs and suffering for the patients.

This is also very important since MGC is one of the most common malignant tumors in women. In 2008, MGC morbidity was extremely high especially in Eastern Europe, e.g. 38% in Ukraine, 25.4% in the Republic of Moldova, 38.2% in Russia, and around 39.8% in Romania. Also, in the economically developed countries it represents up to 15-20% of all cases of death by cancer in women and 3-5% of all deaths [585].

It is generally believed that conservative surgical treatment for the mammary gland represents a surgical operation by which the tumor with the adjacent mammary glandular tissue is removed with the evidation of the axillary and subclavicular lymph nodes, but keeping the organ (the so-called organ saving surgery).

The contemporary stage in surgery is characterized by an increasing share of organ saving operations in MGC stage I. Also, the most published sources indicate that the best results after organ saving operations were obtained in stage I of MGC [586,587]. The frequency of organ saving operations during treatment of MGC depends, in the first place, on the proportion of registered patients with the early stages of the MGC.

Moreover, due to various causes (e.g. suspicious multicentre tumor growth, affecting central quadrant, and suspicious metastatic involvement of axillary lymph nodes) the share of mastectomies in the surgical treatment of MGC remains high. Also, taking into account the fact that theaverage age of patients with MGC has decreased in the recent years, the organ saving surgical interventions and keeping of the mammary gland have become more and more significant, especially in reducing the mental trauma of the patients with MGC [588]. So far, there is no firm decision regarding the selection of the optimal order in the stages of treatment. In this way, these could represent very

important aspects which could contribute to an increase in the survival of MGC patients.

Apart from breast cancer, cervical cancer is the second most common malignancy in women, over 12,000 cases of invasive cervical cancer being annually diagnosed. Although the average patient age at diagnosis is around 50 years old, younger women are also at risk of developing it, around 20% of the patients diagnosed being younger than 40.

In the past decade, several screening programs have been developed for the most frequent types of cancers in women, aiming at systematically applying a routine test in the asymptomatic population to identify people with pre-cancerous, incipient lesions, perfectly curable by appropriate treatment. The European Union Public Health provided financial support for the development of screening programmes for cancer. Thereby, in many EU countries, screening programs for reproductive age women are becoming a trend, facilitating early detection (FIGO IA1-IB1), an essential condition if fertility preservation is desired. In contrast to the global rate, in the EU, the incidence of cervical cancer is low due to the effective implementation of cervical cancer screening programs.

The incidence of cervical cancer is comparatively low in the EU due to the effective implementation of cervical cancer screening. Unfortunately, the incidence of cervical cancer in our country, as well as mortality from this cause, places Romania at the top of the Eastern Europe region and EU ranking despite the screening programs that have been implemented through the national health system in our country.

The treatment for cervical cancer has evolved considerably in the recent years and is now focused on preserving fertility of the oncological patients of reproductive age. Dissimilar to standard cancer treatment which may include surgery, chemotherapy, radiotherapy or a combination thereof, and aims solely at treating the condition, the radical trachelectomy represents a new surgical approach that emphasis on treating the malignant disease and retain fertility in patients wanting to conceive [589].

Although not cited as one of the most frequent causes of female infertility, ovarian tumors are certainly worth looking into, as they may affect the reproductive outcome in more than one way: by decreasing the follicle count from the tissue surrounding the tumoral ovarian mass and the destructive potential of abnormally proliferative tissue [590].

The challenge when managing young patients with tumoral ovarian masses is to strike the fine balance between correct diagnosis and adequate treatment in order to lower the chances of recurrence and, at the same time, preserve conceiving potential. With an incidence of approcimately 1.8 - 4.8 per 100,000 women per year, low malignant potential ovarian tumors are masses exhibiting an atypical epithelial proliferation greater than in the benign counterpart, but without stromal invasion[591].

This histological entity was first described in 1929 as less aggressive than invasive epithelial ovarian tumors. Since 1971, the term borderline tumor was agreed upon and is now widely-used. To avoid confusion, it is worth mentioning that three terms are used to define this entity: borderline tumors, tumors of low malignant potential, and atypical proliferative tumors. They account for 10% to 20% of all ovarian epithelial tumors and one-third of the cases are diagnosed in women of less than 40 years of age, making this an area of interest and a great challenge when it comes to infertility, fertility-sparing surgery, and medical management of the disease in women of childbearing age [592].

In order to offer an in-depth overview, primitive neuroectodermal tumor (PNT) and Ewing's sarcoma should be also extensively discussed. These round-cell tumors are characterized by the presence of the t(11; 22)(q24; q12) chromosomal translocation. A review of the literature revealed only 38 previously reported cases of vulvar primitive neuroectodermal tumor and Ewing's sarcoma and 15 vaginal primitive neuroectodermal tumor and Ewing's sarcoma. Although rare, these types of tumors should be taken into consideration when making a differential diagnosis for vulvar or vaginal tumors. The currently available data is limited, and therefore, case reports are essential for improving knowledge and management of these types of extremely rare tumors. However, further molecular and histopathological studies are essential for an improved understanding of these conditions and for an early, correct diagnosis. The literature demonstrates that the outcome of these types of cancer are more favorable compared with outcomes observed for carcinomas in more typical locations.

Personal contribution - published papers:

Anton, E.; Botnariuc, N.; Ancuta, E.; **Doroftei**, **B**.; Ciobica, A.; Anton, C. THE IMPORTANCE OF CLINICAL AND INSTRUMENTAL DIAGNOSTIC IN THE MAMMARY GLAND CANCER. *Rev. Med. Chir. Soc. Med. Nat., Iasi* ***2015****, 119,* 410–418.

Anton, E.; Ancuta, E.; **Doroftei**, **B**.; Ioanid, N.; Anton C. THE RELEVANCE OF CYTOLOGICAL DIAGNOSTIC IN THE MAMMARY GLAND CANCER. *Rev. Med. Chir. Soc. Med. Nat., Iași* ***2016****, 120,* 363-370.

Armeanu, T.; Simionescu, G.; Nicolaiciuc, D.; Plopa, N.; **Doroftei**, **B.**; Maftei, R. Infertility and borderline malignant ovarian tumors: a case of successful pregnancy after fertility-preserving management of the disease. *Eur. J. Gynaecol. Oncol.* ***2020*** *41*, 284–288. **IF: 0.196**

Nicolaiciuc, D.; Simionescu, G.; **Doroftei**, **B.;** Anton, S,C.; Bolota, M.; Ioanid, N.; Anton, E. ABDOMINAL RADICAL TRACHELECTOMY AS A METHOD OF PRESERVING FERTILITY IN PATIENTS WITH CERVICAL CANCER. *Rev. Med. Chir. Soc. Med. Nat., Iasi. **2018**, 122,* 96–101.

Tintila, A.; **Doroftei**, **B**.; Grab, D.; Simionescu, G.; Anton, E.; Maftei, R.; Ilea, C.; Anton, C. Importance of studying primitive neuroectodermal tumors and extraosseous Ewing's sarcoma of the vagina and vulva (Review). *Oncol Lett* ***2021****, 21,* 171. **IF: 2.967**

Personal contribution - published papers:

Anton, E.; Botnariuc, N.; Ancuta, E.; **Doroftei**, **B**.; Ciobica, A.; Anton, C. THE IMPORTANCE OF CLINICAL AND INSTRUMENTAL DIAGNOSTIC IN THE MAMMARY GLAND CANCER. *Rev. Med. Chir. Soc. Med. Nat., Iasi* ***2015****, 119,* 410–418.

Anton, E.; Ancuta, E.; **Doroftei**, **B**.; Ioanid, N.; Anton C. THE RELEVANCE OF CYTOLOGICAL DIAGNOSTIC IN THE MAMMARY GLAND CANCER. *Rev. Med. Chir. Soc. Med. Nat., Iași* ***2016****, 120,* 363-370.

Aim of the study

The present study aims at highlighting the crucial role clinical, instrumental and cytological diagnostic have in the mammary gland cancer.

Material and methods

Clinical and laboratory data on the diagnosis and treatment of 680 patients selected between 1996 and 2004 were collected and analyzed. The patients in this study were divided into 3 groups: the retrospective group, the prospective group, and the control group. The retrospective group included 496 stages I MGC patients diagnosed and treated during the mentioned period. The retrospective group was divided into 2 groups according to the type of clinical development of tumoral process after treatment: the 1st group had 419 patients without progress for 5 years after the treatment, and the 2nd group was made of 77 patients with progressing tumoral process after treatment. The prospective group included 66 stages I MGC patients diagnosed and treated between 2007-2008. For the patients in the prospective group, the molecular expressions of the HER2/neumolecular markers, CEA tumoral markers, CA-15.3, hormonal receptors (E and P4) E receptor (RE) and P4 receptor (RP), hormonal homeostasis and immunological indices were all assessed. Finally, the control group was comprised of 118 patients, of whom 56 patients with Ha, Ilb, or lila stage MGC, and 62 patients with benign diseases. In the control group, the immunological and homeostasis hormonal parameters were studied for comparison with the stage I MGC.

A special data collection tool was developed for this study, covering 150 parameters of body or tumor features, methods of investigation, and the results of the different treatment variants applied.

Data analysis

The decisive prognostic factors were determined by means of discriminate analysis, including the decisive prognostic factors of the clinical evolution variance in the stage I MGC patients from the

retrospective groups.

Results

Regarding the clinical diagnosis of stage I MGC, for the 496 stage I MGC patients, stage I MGC was established during the primary clinical investigation only in 165 (33.3%) patients, while in 232 (46,8%) patients the diagnosis of suspected MGC was reached first. In other cases, the pathological process in the mammary gland was found as benign disease - fibroadenoma (6.0%), fibrocystic disease nodules in 8.7% or other variations - in 5.2% cases (Table 29).

Table 29. The variance of the clinical diagnosis variants in stage I MGC and age

No	Clinical diagnosis	The age of the patients						Total	
		<35 years old		35-49 years old		>50 years old			
		31 patients		224 patients		241 patients		496 patients	
		No. abs.	%	No. abs.	%	No. abs.	%	No. abs.	%
1	Cancer	6	19.4	61	27.2	98	40.7	165	33,3
2	Cancer susp.	10	32.3	107	47.8	115	47.7	232	46.8
3	MFC	3	9.7	33	14.7	7	2,9	43	8.7
4	FA	11	35.5	14	6.3	5	2.1	30	6.0
5	Other*	1	3.2	9	4.0	12	5.0	26	5.2

According to literature data, in terms of instrumental diagnosis - mammography, ultrasonography in MGC stage I - it seems that the assessment of pathological process features in the mammary gland is problematic in young patients, especially due to the proliferating changes in the mammary glandular tissue adjacent to the tumor, which contribute to the lessening of the clinical picture, including the palpable one. This decreases the possibility of accurate clinical assessment regarding the character of the pathological process in the mammary gland.

By analyzing the frequency of correct clinical diagnosis of stage I MGC during the clinical primary investigation by age, we found the following: for the patients up to 35 years old, the correct diagnosis of MGC was established in only 19.4% cases, while for the patients aged between 35-49 years old, 27.2% cases were accurately detected. Moreover, in the patients over 50 years, when the adjacent background featured adipose metaplasia of mammary glandular tissue, allowing correct assessment of the size, density, surface and character of the tumor, the frequency of accurate diagnosis was the highest - 40,7% cases. In other words, for menopausal women with glandular tissue metaplasia, the correct diagnosis of stage I MGC was established in less than half of cases based on clinical data only.

Also, our analysis of the frequency of correct diagnosis at the first clinical investigation in relation to the tumor dimensions showed that, in tumors with a diameter <0.5 cm, the clinical diagnosis was correct in a mere 11.6% of cases, while for tumors 0.6 – 1.0 cm in diameter the frequency of correct MGC diagnosis essentially increased up to 41.6% of cases. In larger tumors 1.1 – 2.0 cm in diameter, 38.4% cases were diagnosed correctly from the start (Table 30)

Table 30. Clinical diagnosis variants in stage I MGC and tumor dimensions

No	Clinical diagnosis	The dimensions of the tumors						Total	
		< 0.5 cm		0.6-l.0 cm		l.l-2.0 cm			
		43 patients		166 patients		219 patients		428 patients	
		No. abs.	%	No. abs.	%	No. abs.	%	No. abs.	%
1	Cancer	5	11.6	69	41.6	84	38.4	158	36.9
2	Cancer susp.	17	39.5	72	43.4	112	51.1	201	47.0
3	MFC	10	23.3	14	8.4	10	4.6	34	7.9
4	FA	6	14.0	4	2.4	6	2.7	16	3.7
5	Other*	5	11.6	7	4.2	7	3.2	19	4.5

In addition, the instrumental investigation, the mammography in particular, is considered a superior diagnostic method than clinical approaches and it is recommended for preclinical detection in patients with suspected MGC, including for prophylactic investigations in women after age 35,

when the adipose metaplasia of breast glandulartissue occurs. In our study, complex investigations mammography was performed in 287 cases (57.9%) and the correct diagnosis of mammary gland cancer was established in 70 of them. Analyzing the frequency of mammographies leading to the correct diagnosis of stage I MGC from the perspective of the patients' age (Table 31), correct diagnosis of stage I MGC for patients under 35 years of age was reached in 50% of cases; for the age group 35-44, the rate was 66.9% cases, and for patients older than 50 was 74.1% cases of accurately identified using this method.

Table 31. Mammographic findings in stage I MGC and age

No	Mammographic conclusions	The age of the patients						Total	
		< 35 years old		35 - 49 years old		> 50 years old			
		8 investigated patients		136 investigated patients		143 investigated patients		287 patients	
		No. abs.	%	No. abs.	%	No. abs.	%	No. abs.	%
1	Cancer	4	50,0	91	66,9	106	74,1	201	70,0
2	FAM	1	12,5	36	26,5	29	20,3	66	23,0
3	FA	3	37,5	9	6,6	8	5,6	20	7,0

$\mathbf{X^2} = 2.96$ $\mathbf{p} > 0.05$

Additionally, in out analysis of mammographic findings and tumor size, the following results were obtained: for tumors with size TIa: < 0.5 cm, the correct mammographic conclusion of cancer of the mammary gland was established 4 times more frequently compared to via clinical examination (52.2% versus 11.6%).

Also, for tumor size TIb: 0.6 - 1.0 cm, the correct mammographic diagnosis was established in 70.7% cases, and it was even more effective for tumor sizes Tic: 1.1 - 2.0 cm, as 76.2% of which were found in this way (Table 32).

Table 32. Mammographic findings in stage I MGC patients and tumor diameter

Mammographic conclusions	The dimensions of the tumor						Total	
	< 0.5 cm.		0.6-l.0 cm.		l.l-2.0 cm.			
	No. abs.	%	No. abs.	%	No. abs.	%	No. abs.	%
Cancer	12	52,2	70	70,7	96	76,2	178	71,8
MFC	9	39,1	19	19,2	24	19,0	52	21,0
FA	0	0	9	9,1	5	4,0	14	5,6
Solitary chistum	2	8,7	1	1,0	1	0,8	4	1,6
Total investigations	23	100	99	100	126	100	248	100

In patients younger than 35 years, and younger than 30 in particular, the mammographic investigation may not be effective because glandular breast tissue can lack signs of pronounced metaplasia. In 85 cases, the method of instrumental diagnosis was the mammary glands UGS. The correct conclusion of MGC presence was established in only 40 of the cases, which does not essentially improve the frequencyof correct diagnosis when compared to clinical diagnosis.

Moreover, for patients under the age of 35, the correct MGC conclusion was reached in 27.3% cases, while for those between 35-49 MGC was found in 39.5 cases. For women over the age of 50 the rate was 44.4%. Also, MGC was suspected in 9.4% of the USG investigated patients, while 38.8% of the cases were concluded by the MFC and 7.1% by FA, 4.7% cases through solitary cyst presence.

Therefore, independently of age, the correct diagnosis of MGC by MG investigation was more informative than by ultrasound investigation (Table 33).

Table 33. Ultrasound findings in patients with stage I MGC and age

USG Conclusions	The age of the patients			Total
	< 35 years old	35 - 49 years old	> 50 years old	

	11 patients investigated		38 patients investigated		36 patients investigated		85 patients investigated	
	No. abs.	%	No. abs.	%	No. abs.	%	No. abs.	%
Cancer	3	27.3	15	39.5	16	44.4	34	40.0
Cancer suspicion	2	18.2	1	2.6	5	13.9	8	9.4
MFC	4	36.4	17	44,7	12	33.3	33	38.8
FA	2	18.2	2	5.3	2	5.6	6	7.1
Solitary chistum	0	0	3	7.9	1	2.8	4	4.7

In addition, with regard to tumor size, the MGC ultrasonographic diagnosis for tumors < 0.5 cm proved to be correct in 25% cases, with an informative value 2 times lower than that provided by mammographic investigation for tumors with the same dimensions, but 2 times more frequent by than clinical examination for tumors sized 0.5 - l.0 cm, for which the diagnosis was correct in 37.8% cases and for tumor diameter between 1.1 - 2.0 cm - 46.7% cases (Table 34).

Table 34. Ultrasonographic assessment for stage I MGC patients and the size of the tumor

USG Conclusions	Tumoral dimensions						Total	
	< 0.5 cm		0.6-1.0 cm		1.1-2.0 cm			
	8 patients investigated		37 patients investigated		30 patients investigated		75 patients investigated	
	No. abs.	%	No. abs.	%	No. abs.	%	No. abs.	%
Cancer	2	25.0	14	37.8	14	46.7	30	40.0
Cancer suspicion	1	12.5	4	10.8	2	6.7	7	9.3
MFC	3	37.5	15	40.5	11	36.7	29	38.7
FA	0	0	3	8.1	2	6.7	5	6.7
Solitary chistum	2	25.0	1	2.7	1	3.3	4	5.3

Cytology results

The cytological investigation conducted on 475 patients confirmed the diagnosis of cancer of the mammary gland only in 146 patients, which represented 30.7% cases. The cytological confirmation correlates with the age of the stage I MGC patients (Table 35).

Table 25. The accuracy of cytological confirmation of the malignant process in stage I breast cancer patients by age

No	Patients age	No. of recorder patients	Cytological confirmed diagnosis	
			No. abs	%
1	<35 years	27	6	22.2
2	35-49 years	216	52	24.1
3	>50 years	232	88	37.9
4	Total:	475	146	30.7

$\chi 2 = 11.06$, $p < 0.05$

As a matter a fact, as shown in Table 35, the diagnosis of MGC was confirmed cytologically in 22.2% cases for patients younger than 35, 24.1% cases for those aged 35-49, and in 37.9% cases for the patients 50-year-old and older (Table 35). Also, the cytological conclusions were: cancer (30.7%), suspicion of cancer (18.9%), and atypical proliferative process (19.4%).

For the other cases, other variants of cytological diagnosis, without suspicion of cancer, have been established. The cytological conclusion for 1 in each 3 patients (17.5%) - consisted in normal glandular epithelial cells without proliferation or atypical signs (Table 36).

Table 36. Cytological conclusion variants in stage I MGC versions by the number of conducted aspiration biopsies

No	Cytological analyses	Quantity of conducted aspiration biopsies			
		1	2	3-4	Total

	conclusion	283 patients		138 patients		54 patients		475 patients	
		No.	%	No.	%	No.	%	No.	%
1	Cancer	117	41.3	24	17.4	5	9.3	146	30.7
2	Suspicion of cancer	34	12.0	35	25.4	21	38.9	90	18.9
3	Proliferation with	22	7.8	509	36.2	20	37.0	92	19.4
4	Glandular epithelial cells	46	16.3	29	21.0	8	14.8	83	17.5
5	Lipids, erythrocytes	64	22.6	0	0	0	0	64	13.5

$\chi 2 = 38.37$, $p < 0.01$

In addition, as shown in Table 36, the results for the cytological confirmations by number of conducted aspiration biopsies were: the first biopsy provided cytological confirmation in 41.3% of cases. For the second biopsy, the cytological investigation of the smear from the samples allowed for the diagnosis by cytological confirmation in 17.4% cases, while the aspiration biopsies repeated 3-4 times resulted in cytological confirmation of the diagnosis in only 9.3% of cases.

Also, we have to mention that the prevalence analysis of correct cytological conclusions from the perspective of tumor diameter revealed that, for tumors < 0.5 cm, the correct conclusion of MGC was attained in a mere 10.3% of cases. For tumors 0.6 - l.0 cm in diameter, the accuracy was 40%, and those sized l.l - 2.0 cm were correctly identified in 34.3% of cases (Table 37).

Table 37. The frequency of the cytological confirmation for the malignant process in patients with stage I MGC and the size of the tumor

No.	Size of tumor	No. of marked patients	Cytological confirmed diagnosis	
			No. abs.	%
1	<0.5 cm	39	4	10.3
2	0.6-1.0 cm	160	64	40.0
3	1.1-2.0 cm	213	73	34.3
4	Total:	412	141	34.2

$\chi 2 = 35.0$, $p > 0.05$

Moreover, the frequence of cytological confirmation of the diagnosis depends on the histopathological form and type of tumor growth: 31.6% cases of ductal form, 24.4% lobular, 12.5% mixed (ductal and lobular), and 41.7% rare forms of highly differentiated MGC (tubular, papillary, medullar, mucinous and other) (Table 38).

Table 38. Frequency of cytological confirmation in patients with stage I MGC and tumor morphology

No.	Morphopathological variants	No. of patients	Cytological confirmation	
			No. abs.	%
1	Ductal	345	109	31.6
2	Lobular	86	21	24.4
3	Ductal and lobular	8	1	12.5
4	Rare forms	36	15	41.7
5	Total:	475	146	30.7

$\chi 2 = 65.0$, $p > 0.05$

In addition, the prevalence of cytological confirmation differed depending on the morphological type of tumor: 66.1% of the solid growth and 37.5% of the schiros growth MGCs were confirmed, while the lowest rate of cytological confirmation was for the mixed forms – only 7.7% of cases (Table 39).

Table 39. Frequency of cytological confirmation in patients with stage I MGC by tumor morphology

No.	Morphological type	No. of patients	Cytological confirmation	
			No. abs.	%

1	Solid	59	39109	66.1
2	Schiros	56	21	37.5
3	Rare forms	260	20	7.7
4	Unknown	100	-	-
5	Total:	475	146	30.7

$\chi 2 = 5.0$ $p > 0.05$

It must also be mentioned that, although the cytological diagnosis was confirmed in 146 patients who represented only 30.7% of cases overall, for the other 329 patients (69.3%) the morphopathological diagnosis was determined by intraoperative extemporaneous histological investigations.

Discussion

The results as seen through the 5-year survival, within each stage of the MGC are determined, firstly, by the type of applied treatment. This is very important, since the type of treatment and the potential administration of a neoadjuvant treatment depend on the informational value of the diagnostic methods used.

In the extended forms of MGC, ultrasound and mammography semiotics does not present any difficulties and the correct conclusions could be reached in up to 92-98% cases. By contrast, these two instrumental methods performed rather poorly in detecting early MGC forms (only 20.75%) [593]. At the same time, correct conclusions in USG and MG investigations together with the clinical picture enables clinicians identify the exact site for aspiration biopsy in order to obtain cytological confirmation of the tumoral process.

Additionally, another very important aspect of the present study referred to the selection for the prognostic decisive factors in the biological development variance of the tumoral process for the elaboration of optimal treatment schemes in stage I MGC. It is generally accepted that current methods of MGC treatment (which include surgery, radiotherapy, chemotherapy and hormone therapy) could ensure a 90-95% rate of survival beyond the 5-year mark for patients diagnosed with stage I MGC [594]. At the same time, the selection of the surgical intervention volume for the radiotherapy and role of chemotherapy in the treatment of stage I MGC cannot be considered definitively established.

In recent studies, authors demonstrate that patients diagnosed in the early stages of MGC can be successfully cured by means of surgical intervention only [595]. Other researchers regard the inclusion of radiotherapy and chemotherapy mandatory in the treatment schemes of early MGC [596]. There are also scientists who consider using radiotherapy only in patients subjected to organ saving surgery [597], as well as some who found that, for patients older than 55 years and with tumors of up to 2.0 cm in size, mammary gland sectoral resection can be effective without radiotherapy [598].

For these reasons, chemotherapy in combination with radiotherapy is only generally recommended against preclinical metastases, especially in the context of still insufficient randomized studies for a comprehensive meta-analysis to provide a clear answer on optimal treatment schemes. This is a matter of ongoing interest and discussion, as illustrated by the proceedings of international conferences such as in San-Gallen in 2005, 2007, 2009 [599].

In addition, establishing immunological hormonal homeostasis peculiarities depending on the degree of expression of molecular markers can be used to clarify the mechanisms of unfavorable clinical course in tumors with different degrees of expression of the E receptor and P4 receptor hormonal receptors and the HER2/neumolecular marker.

As the criteria for defining the best treatment tactics of stage I MGC patients are being considered, the factors that characterize these tumors (the molecular marker indices, molecular receptors indices, tumor size etc.) must be individually assessed. For instance, in patients with tumors <1.0 cm in diameter and negative lymph nodes, only the surgical treatment is recommended.

Concurrenltly, although the literature points to increased frequency of hormonal disorders in MGC patients, hormone therapy is still limited to the indication of anti-estrogens or progestins. It would be necessary for hormonal therapy to also include hormonal homeostasis regulation, since MGC

patients may present hypothyroidism, hyperprolactinemia, and other hormonal imbalances with various causes.

Likewise, the patients' immunological status should be taken into account, because it is known to influence treatment outcomes.

In addition, convincing data has been published about the fact, that in MGC (including stage I), the degree of expression of molecular markers affects clinical development. Compared with stages II to IV, in stage I MGC, the expression of E receptor and P4 receptor is more pronounced [600]. This can be explained by the fact that, alongside tumoral progression, the degree of tumor differentiation decreases. This could reflect an inverse relationship, as the low degree of differentiation contributes to high rates of tumor growth, explaining the more substantial local or local-to-regional spread at the addressing point [601].

MGC represents a polymorphic and pathogenic disease and it cannot be admitted that all subgroups of patients will obtain identical results from one tactic of treatment determined for all the patients with MGC. Thus, the concept of MGC both clinical and patho morphological, combines different cell clones depending on its microstructure and biology. As a result, the evolution of the disease, the prognosis and the effectiveness of the treatment may vary in different patients at the same stage, depending on the degree of malignancy of the tumor, its histopathological structure, the degree of expression of molecular markers identification and also immunoresistance. Also, some numbers-related conclusions could be represented by the fact that: collecting samples through fine-needle aspiration biopsy allows the cytological confirmation of the diagnosis of stage I MGC in 30.7% cases. In stage I MGC young patients, under 35 years, the cytological confirmation rate is 22.2% and is lower as compared to the cytological confirmation rate in patients older than 35 years which is 37.9%. For a tumor diameter < 0.5 cm, the prevalence of cytological confirmation was only 10.3%, while for the diameter of 0.6 – 1.0 cm the cytological confirmation was around 40.0%. Therefore, in order to improve the cytological diagnosis confirmation, rate the tumor biopsy through the USG of the mammary glands is required. The cytological investigation of the smear obtained by the first and second puncture was instrumental in confirming the diagnosis in 41.3% and 17.4% cases; the subsequent repetition of the punctures was not useful as it helped to confirmation of the diagnosis only in 9.3% cases. Moreover, the frequency of diagnosis cytological confirmation depends of the tumor, histopathological form and type of growth. Thus, the lowest prevalence was in the mixed forms – 12.5% cases, lobular cancer – 24.4% cases, while regarding the type of growth, for the rare forms the cytological confirmation rate was 7.7% and 31.5% cases for the schiros growth type.

It is generally accepted that the treatment methods for MGC, which include surgery, radiotherapy, chemotherapy, and hormone therapy, could ensure a 90 - 95% 5-year survival rate in stage I MGC [594]. Still, the cytological confirmation of the diagnosis allows us to perform the preoperative radiotherapy treatment or poly-chemotherapy, which is why we analyzed the informative value of these diagnostic methods in stage I MGC.

Even if the mammographic or ultrasonographic clinical assessment of the malignant character of the pathological process in the mammary gland is available, the neoadjuvant treatment becomes feasible only when the diagnosis is confirmed by one of the morphopathological methods, such as the cytological or the histopathological method. According to the international literature, the cytological confirmation in the tumors smaller than 2.0 cm is problematic and does not exceed a rate of 20-25% [602].

Another way to assess the progression of mammary neoplasia is by means of serum tumoral markers: the carcinoembryonic antigen and the CA 15.3 (cancer antigen 15.3) [603]. The CA 15.3 concentration occurs in women with the diagnosis of breast cancer, and its usefulness lies in evaluating the evolution of the illness, treatment response, and relapse. The CA 15.3 tumor marker is a mucin-like antigen with high molecular weight, issued primarily by cells of mammary glandular carcinoma. CA 15.3 is defined by its reactions with two monoclonal antibodies: one of them (115D8) binds to an antigen from human milk; the other (DF3) bounds to a membrane fraction of the carcinomatous cells.

The CA 15.3 blood titer increases in patients with advanced illness, drops after chemotherapy treatment and rises again in the case of relapses or metastasis (in particular bone metastasis). Although the sensitivity of this marker in detecting early stages is reduced, lately there has been a tendency to introduce it as a method of screening in the female population in the 45-54 age group

(pre-and postmenopausal), which is considered to be the age group most prone to breast cancer. Also, determining molecularmarkers is an important tool for the diagnosis, treatment, assessment of therapy response. A slight physiological increase of the CA 15.3 antigen is registered in 4-7% of the nursing women and in about 8% of the pregnant women [603].

Concurrently, the carcinoembryonic antigen is a specific marker for digestive tract cancers (colorectal, stomach, pancreas, liver, biliary vesicle), but clinical studies have shown an increase in other malignant diseases (lung, mammary gland, ovary, cervix, prostate). Historically speaking, the carcinoembryonic antigen was first described in 1965 by Gold and Freedman in a patient with colorectal carcinoma. The carcinoembryonic antigen is a glycoprotein with the molecular weight of 220 kDa, containing approximately 40% proteins and 60% carbohydrates. It is one of the onco-fetal products during embryonic life and fetal development. Its production is suppressed after birth, reaching very low levels into adulthood (less than 3 ng/ml in non-smokers and less than 5 ng/ml in smokers). Immunohistological, the carcinoembryonicantigen can be found in elevated concentrations in the fetal gastrointestinal tract and pancreas, as well as in colorectal adenocarcinoma, and in lower concentrations in the normal intestinal tissue, intestinal mucosa, exocrine pancreas, as well as in the liver. It function is not fully known; it is assumed that the carcinoembryonic antigen bound to the cellular membrane serves as mechanism for intracellular recognition functioning as a receptor. In addition, carcinoembryonic antigen is also assigned an immuno-suppressive effect through the induction of macrophages and suppressor T lymphocytes [604].

Also historically speaking, we could also mention the unique research carried out in 1962 by H. Bloom, W. Richardson, and E. Harries. They were able to retrace the fate of 250 untreated patients mainly in stage III - IV MGC between the years 1805 and 1933: the median survival was 2.7 years, and the last patient died in the 19th year of monitoring without any treatment [605].

Of particular relevance in this context is also the fact that the prediction factors mirror the relations of reciprocity between tumor biology and treatment (for example, E receptor, P4 receptor and hormonotherapy; HER2/neuand herceptin therapy) [606]. In fact, the prediction factors may also have prognosis significance. In this way, MGC is considered to be a heterogeneous pathology with clinical evolution ranging in various patients from severe aggressiveness to the relatively benign.

Personal contribution - published papers:

Armeanu, T.; Simionescu, G.; Nicolaiciuc, D.; Plopa, N.; **Doroftei**, **B.**; Maftei, R. Infertility and borderline malignant ovarian tumors: a case of successful pregnancy after fertility-preserving management of the disease. *Eur. J. Gynaecol. Oncol.* ***2020*** *41*, 284–288. **IF: 0.196**

Case presentation 1

The authors present the case of a 26-year-old female with no medical history of gynecological surgical pathology and/or clinical symptoms other than primary infertility for three years and heavy menstrual flow.

Informed and written informed consent was obtained from the patient to present the information related with their medical records. The study protocol and the publication of the manuscript were approved by the Ethical Committee at the Origyn Fertility Center, where the investigations took place.

During the first fertility checkup, the patient was submitted to a medical interview, a clinical exam, and a transvaginal ultrasound. According to the anamnesis, the patient was a non-smoker, with no significant comorbidities or relevant family-associated diseases, regular periods, no history of past pelvic infections and normal results at the annual Pap smears. The patient did not complain of abdominal or pelvic pain and the bimanual palpation exam showed no tenderness at the moment of the exam. The transvaginal ultrasound revealed three intrauterine hyperechoic endometrial findings suggestive of polyps, the larger being 12 mm in size. The uterus was normal in size and the structure of myometrium was homogenous. In the rectouterine pouch of Douglas, no signs of PID or free fluid were observed. Furthermore, the cervix was examined, and both the length and structure were normal. Upon examination of the adnexae and the ovaries, the right adnexa showed no abnormalities. The

right ovary, which was 37×21×17 mm in size presented four antral follicles, without any signs of cystic masses or adhesions.

In contrast, the left ovary was significantly larger in size, 80×55×21 mm with a cystic appearance (Figure 34), intracystic vegetation, and increased color flow Doppler signal (Figure 35). The patient was advised to undergo a series of blood analysis and a magnetic resonance imaging MRI scan. At the follow-up exam, the blood tests revealed elevated serum levels of CA 19-9 (79.76 U/ml reference value less than 27), ROMA score 33.36% chance of malignancy (reference value less than 11% for the age group), and an AMH level of 1.24 ng/ml. The first MRI scan describes the cystic lesion on the left ovary with mixed content both fluid and solid sized 55×58 mm to be suggestive for endometriod or haemorrhagic cyst, and no other pathological findings other than a small quantity of fluid in the Douglas pouch (normal uterus and cervix, normal right adnexa) and no sign of secondary lesions in the thorax, abdomen or ischiorectal fossae.

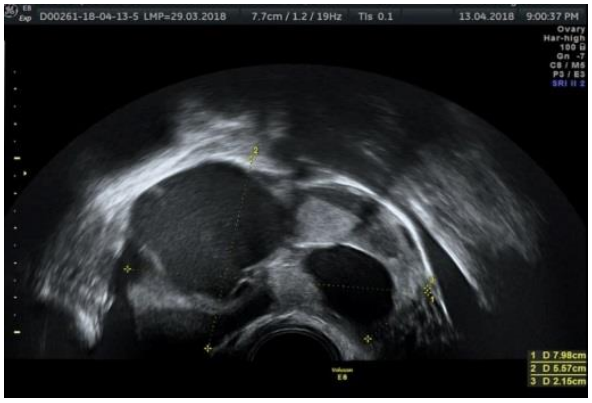

Figure 34. Transvaginal pelvic ultrasound revealing an enlarged left ovary with an abnormal multiloculated mass with mixed cystic-solid content

Figure 35. Actual Doppler signal flow

Taking into consideration all the aforementioned clinical and paraclinical data, the patient underwent a surgical procedure, the medical team opting for a less invasive laparoscopic approach. At the intraoperative inspection of the peritoneal cavity, the left ovary was visibly enlarged, with a large cystic mass having superficial cortex vessels visible on its surface, adherent to the left Fallopian tube, while the left side of the uterus presented velamentous adhesions. No macroscopic lesions were found on the peritoneum or liver. The mass was incised and a small tissue sample was sent to extemporaneous exam during surgery.

The preliminary pathology exam showed endometrioid borderline tumor with focal IEN. Left adnexectomy was performed with the extraction of the ovary and tube in an endobag, to prevent intraperitoneal malignant cell dissemination. Furthermore, peritoneal tissue biopsy and peritoneal washing cytology was performed to further exclude malignant cell contamination. Additionally, uterine D & C was also performed and the tissue samples were sent for cell atipy screening, to exclude endometrial malignancy. There were no intraoperative complications or haemorrhage and the vital signs remained stable throughout entire intervention, with normal postoperative standard biochemical analysis.

The postoperative evolution of the patient was favorable under antithrombotic, antibiotic prophylaxis and antalgic treatment, subsequently being discharged from the hospital two days later. The final pathology report showed no abnormal cells with signs of atypical mitotic activity in the peritoneal washing sample, in the peritoneal tissue samples, and the endometrial tissue harvested during the uterine curettage.

The final histologic tissue pathology report of the excised surgical specimen was conclusive and in accordance with the extemporaneous report. The examined sections captured the following aspects: papillary proliferation composed of epithelial elements arranged in simple or branching tubular glands, with mild to moderate cytonuclear atypia, low mitotic rate, and squamous morules, embedded in a sparse fibromatous stroma. Microscopic foci of intraepithelial carcinoma are present (atypical hyperplasia with rare atypical mitotic figures), composed of irregular crowded glands

disposed in a cribriform pattern, embedded in dense fibrous stroma, with dystrophic calcifications, but no inflammatory response. No vascular invasion nor any tumoral necrosis were identified in the examined area. The fragmented biopsy did not enable the assessment of the integrity of the capsule (Figures 36-39). The patient was further referred to an oncological committee who established that the tumor was a pT1aNxMxG1 and did not require any other medical or surgical interventions other than close follow up at six-month intervals after normal postoperative CT scan showed no remaining or secondary lesions and the ROMA score had dropped to 4.75% risk of malignancy.

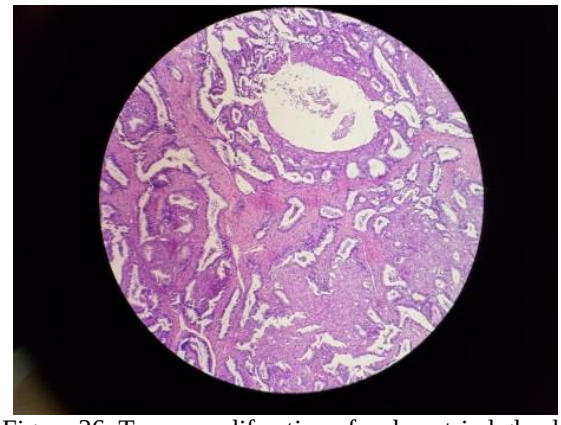

Figure 36. Tumor proliferation of endometriod glands with mildcytonuclear atypia, squamous metaplasia, and fibrous stroma

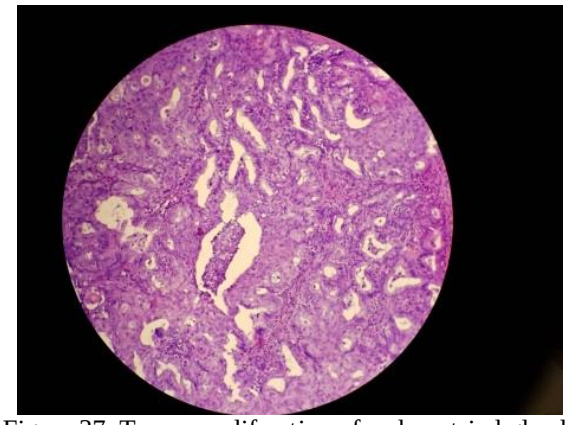

Figure 37. Tumor proliferation of endometriod glands with squamous metaplasia and fibrous stroma (HE, ×10)

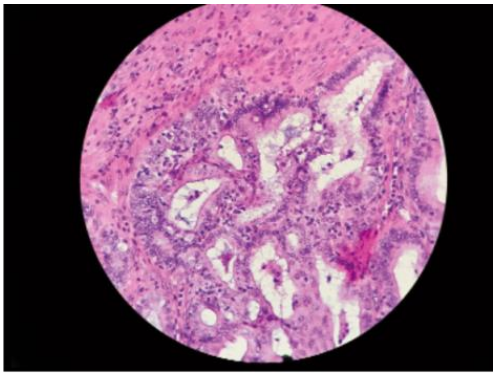

Figure 38. Endometroid intraepithelial neoplasia (HE, x 20)

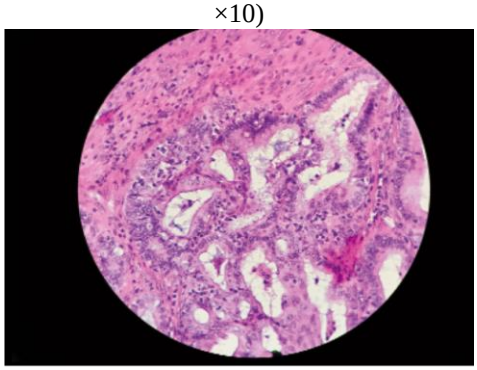

Figure 39. Endometroid intraepithelial neoplasia (HE, x 40)

Taking into consideration that the ovarian mass was an incidental finding during an infertility check-up and that the surgical management of the case preserved the remaining right ovary and Fallopian tube, the patient requested to undergo further tests to assess her chances of conceiving. Due to the removal of the left ovary, the serum level of the AMH decreased from 1.24 ng/ml prior to surgery to 0.74 ng/ml afterwards. During fertility investigations, a routine sperm analysis was also performed and the exam results were normozoospermia. In the light of the decreased ovarian reserve, the patient decided to undergo an IVF procedure. At the beginning of the following cycle, controlled OS was commenced, using a short antagonist protocol by administrating 200 units of follitropinum beta per day, for a period of nine days.

Oocyte maturation was triggered by the subcutaneously administration of chorionic gonadotropin alpha in a dosage of 250 micrograms, 36 hours prior oocyte retrieval. Nine follicles were punctured through ovum pick up method and a total number of nine mature oocytes were retrieved. Subsequently, ICSI was performed, resulting in four fertilized oocytes (fertilization rate 44.4%). The embryos were culture in time lapse system (embryoscope), until blastocyte stage (ExB1/1, HB1/2, ExB1/1, ExB2/1) and then vitrified with the purpose of performing a frozen-thawed single ET afterwards. Next month, the patient complained of a menstrual delay, therefore a hCG

analysis was recommended. The result of the first determination was 2,081 mUI/ml and the result of the second determination, performed 36 hours later, was 3,968 mUI/ml, thereby a spontaneous pregnancy was confirmed. Transvaginal ultrasound at seven weeks showed a regularly shaped intrauterine gestational sac with a CRL of 9 mm, normal yolk sack size, and shape and positive embryo cardiac activity of 144 beats per minute. At the moment the patient was ten weeks pregnant with no obstetrical complications (Figures 40 and 41).

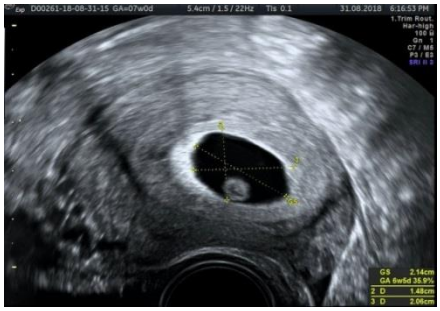

Figure 40. Transvaginal ultrasound at seven weeks of amenorrhea showing an ongoing early intrauterine pregnancy

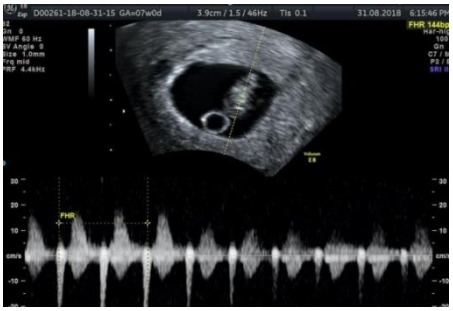

Figure 41. Actual cardiac activity of the embryo

Discussion

The aim of the article summarized here was to present the case of a 26-year-old woman diagnosed incidentally with a borderline ovarian tumor during an infertility check-up, and who obtained a spontaneous pregnancy two months after laparoscopic unilateral adnexaectomy. The prognosis for patients with borderline ovarian tumors seems to be quite favourable, with survival rates at five years for early-stage disease of approximately 98% [607].

Regarding the causes and the risk factors associated with borderline ovarian tumors, although there is no certain and evident single cause established, they do seem to originate from the surface epithelium of the ovary [608] and nulliparous women are at greater risk of developing them compared to parous ones [609]. Based on histological findings, borderline ovarian tumors are classified as serous (50%), mutinous (45%), endometrioid, clear cell or Brenner tumors [610].

There has been great controversy regarding the safety of conservative versus radical surgery in these types of tumors diagnosed at an early stage. Recurrence rates seem to be slightly higher in patients undergoing fertility-sparing surgery than in those undergoing radical surgery [611,612], however the survival rate seems unaltered since recurrent lesions seem to be also of borderline nature and completely curable through surgical resection. For first stage disease, conservative surgery consists of unilateral salpingo-oophorectomy or even cystectomy for young women willing to preserve their fertility, while bilateral salpingo-oophorectomy or even total hysterectomy with bilateral adnexaectomy may be considered for women of menopausal age, who already conceive or do not intend to preserve their fertility.

The laparoscopic approach is safe, feasible, well-tolerated, and cost effective for both radical and conservative management. Notwithstanding the benefits of this type of interventions, studies [613,614] that highlighted the negative impact on the ovarian reserved, as measured by serum AMH levels. A study carried out by Doroftei et al., [615] on 5,069 Romanian women showed a mathematical relation between age and ovarian reserve, emphasizing once more on the usefulness of this biomarker in making clinical decisions in ART. In the present case, the patient's AMH decreased significantly from 1.24 ng/ml prior to surgery to 0.74 ng/ml postoperative, thereby the authors considered that a longer waiting period between surgery and the start of an IVF cycle may have a negative impact on fertility due to deterioration of the ovarian reserve. Furthermore, studies conducted by Somegliana et al., [616] and Ho et al., [617] showed that a significantly lower number oocytes were retrieved from the operated ovaries compared to the contralateral ovary during IVF treatment.

Since infertility is frequently observed in patients with borderline ovarian tumors [616,617] and conservative treatment is applied, the question that arises is if ovarian stimulation or IVF should be proposed to these patients? Some studies have linked ovarian hyper stimulation to a higher risk of

onset of borderline ovarian tumors or even ovarian cancer, however the link remains unclear. Results so far suggest that infertility drugs and assisted reproduction techniques may be safely used in patients who experience infertility after conservative treatment of an early-stage gynaecological cancer [618,619], however particular monitoring and a joint cooperation bewteen oncologists and specialists in assisted reproduction is essential [620].

The authors may conclude that the advancements from the field of human assisted reproduction molecular biology and oncologic surgery brought new opportunities to women of childbearing age and fertility-preserving management should be highly considered for this category of patients.

Laparoscopy is widely recognized as a procedure of choice for gynaecological surgery. Myomectomy and hysterectomy are the most frequently performed surgical procedures in gynaecology. A morcellator is often used in myomectomies or subtotal hysterectomies, but morcellation may cause rare complications, such as parasitic iatrogenic myoma or adenomyoma. To improve patient counselling, proper risk estimation as well as risk factor identification should be acknowledged. Despite both conditions having an iatrogenic origin, iatrogenic parasitic myoma and adenomyoma are two different entities in terms of clinical manifestations as well as intraoperative particularities, with a common point: iatrogenic complication. A possible solution to avoid these iatrogenic complications is by using in-bag morcellation or switching to another surgical procedure (e.g., a vaginal or abdominal approach). It is concluded that parasitic myoma and iatrogenic adenomyoma are two different iatrogenic morcellator-related complications. In patients with a history of uterus or myoma morcellation who report pelvic symptoms, iatrogenic parasitic myoma or adenomyoma should be considered in the differential diagnosis.

Personal contribution - published papers:

Simionescu, G.; Neculai-Valeanu, A.S.; Maftei, R.; Anton, E.; **Doroftei**, **B**. Spontaneous pregnancy after laparoscopic cystectomy. *Arch. Clin. Cases **2016**, 03*, 59–63.

Case presentation 2

A 28 year-old Romanian woman with no history of pregnancy or gynecological pathology presented to our clinic with pelvic pain irradiated in the left inferior member, accentuated during sexual intercourse and physical activity. The patient also experienced pollakiuria, lumbar pain, low abdominal distension, bloating and perturbation of the intestinal transit and defecation, which debuted 6-8 months before, but became acute in the last weeks. A primary infertility left uninvestigated for 2 years was also declared by the patient.

According to the anamnesis, menarche commenced at the age of 15 years, with subsequent irregular cycles and moderate dysmenorrhea. The patient`s weight was 65 kg and her height 175 cm. Deep abdominal palpation revealed sensitivity in the left flank, irradiating towards the hypogastric region and sigmoid colon. The bimanual vaginal examination showed a mobile retroverted uterus, with normal dimensions. On the left adnexal topography, a voluminous mass, with imprecise limits was observed. The tumor mass, whose appurtenance was established at the ovary, presented tenderness. The endovaginal echography showed a highly deviated uterus towards the right side, although the dimensions and aspect were normal. The left ovary was enlarged in volume, presenting a well-defined mass, 11.3/11/10 mm, with thick membrane, clear content, without any proliferations or intracystic septa (Figures 42 and 43).

Figure 42. Ultrasound image of anechoic cyst. No septa were observed; thin walls and a nodule without flow onDoppler was present on the posterior wall

Figure 43. Normal ultrasound of right ovary. A part of left ovarian mass, compressing the right adnexa and the uterus

The Doppler signal was low, and the resistance index was normal. The torsion of the annexes was excluded and no intracystic bleeding was observed. According to the biochemical exam, the markers of ovarian tumors risk were within normal limits: CA 125: 15.59 U/ml (normal value <35), CA 19-9: 4.8 U/ml (normal value <27) ACE: 0.497 ng/ml (normal value<4.3), results that are consisted with studies conducted by Outwater et al., [621].

The MRI evaluation confirmed the endovaginal ultrasonography results. Thus, an extremely voluminous cystic formation (134/116/110 mm) (cranio-caudal/transversal/AP), located in the pelvis and in the hypogastrium area was revealed. The well-defined formation presented hyper-intensity in T2 and T2 iso-signal with moderate restriction,inhomogeneous diffusion and a discreet outlet contrast at the level of the thin wall (2mm). The lesion, which originated in the left ovary, showed significant mass effect on the urinary bladder, uterus, right ovary, sigmoid colon and intestinal loops, as well as strong compressionsyndrome on the common and external iliac veins. At the upper pole of ovarian cyst formation, a wide oval area of 30/10 mm, hyper-signaling in T1, T2, with diffusion restriction and nonspecific appearance was observed plated on the right anterolateral wall. The uterus, which was shifted posteriorly, presented normal size and structure. Thedimensions of the right ovary were normal, although few small follicular cysts were present. Based on the ultrasound report, MRI evaluation, and biochemical markers, we decided to evacuate the cystic fluid throughout a minimal invasive procedure.

The surgical protocol consisted in the transvaginal aspiration of the cyst (intracystic fluid), followed by laparoscopic aboard using 3trocars which were placed in the left and right iliac fossa, as well as, the umbilical area. Around 1.3 liters of fluid were evacuated by transvaginal puncture and aspiration, using echo-guidance. The shirt of the cyst was removed (cystectomy) and the normal, functional ovary was preserved (Figures 44 and 45). After the intervention, the patient was hospitalized for 3 days. It was established that the tumor mass was a MCT, which presented epidermal cells and thyroid tissue.

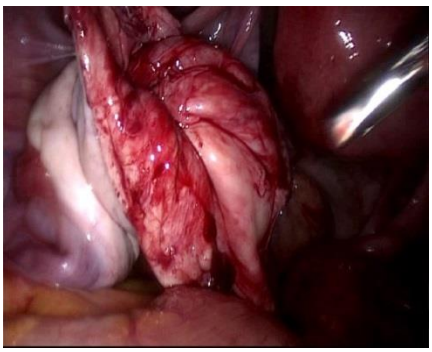

Figure 44 and 45. Intraoperatory images of the tumor

The histological exam revealed smooth cystic walls, serous fluid and no vegetationinside. One

month after intervention, the patient presented with a positive pregnancy test, the single intrauterine gestational sac being confirmed by ultrasound scan (Figure 46).

Figure 46. Pregnancy confirmed by ultrasound

The luteal corpus was observed on the left ovary, which was previously affected by the tumor. The pregnancy was carried out smoothly and was completed by the natural birth, at term, of healthy fetus, weighting 3.600 grams.

Discussion

MCT, also called dermoid cyst, is the most common ovarian benign germ cell tumor in women of reproductive age (from teens to forties) [622]. Future fertility is one of the major concerns among these women. Therefore, the management of the tumor must focus on preserving ovarian tissue and minimizing adhesion formation. The particular nature of this case resides in the fact that the left ovary whose ovulatory and gametogenic function was inhibited by presence of the tumor mass, and then regained its activity in the first month after the laparoscopic removal of the cyst. This mechanism is similar to the one observed in PCOS patients [623] who undergo cuneiform resection of the ovary [624,625].

Future fertility is one of the major concerns among these women and therefore the management of the tumor must focus on preserving ovarian tissue and minimizing adhesion formation. The particularity of this case resides in the fact that the left ovary, whose ovulatory and gametogenesis function has been inhibited by presence of the tumoral mass, regained its activity in the first month after the laparoscopic removal of the cyst. According to the available literature regarding the surgical treatment of Stein-Leventhal syndrome, this mechanism is similar to the one observed in PCOS patients, which were submitted to cuneiform resection of the ovary. Laparoscopic management offers many advantages for the patient: accurate diagnosis, minimal bleeding, reduced need for analgesia, less adhesion formation, fast recovery, better cosmetic results, shorter hospital stays (one-day surgery in selected cases), and reduced costs for the patient and hospital [623–626].

Retrospectively, the first paper that signaled the use of ultrasound in the diagnosis of EMS was published in 1978 [627]. Since then, numerous studies have focused on ultrasound findings in DE and a consensus was reached in 2016 regarding the nomenclature, definitions and measurements of endometriotic lesions depending on their localization [628]. Ultrasound for these specific lesions is a topic that has been the promoter of many other articles published. Furthermore, the objective was to test through the prism of specificity and sensibility with other protocols involving MRI and laparoscopy. From our point of view, ultrasound should become routine for DE diagnosis. Unfortunately, it is still limited to diagnosis of ovarian endometrioma [629–631].

Laparoscopic cystectomy after transvaginal punction and drainage of the fluid requires minimal recovery time, medical case period, low costs, and not the least, is an efficient method of preserving fertility in a certain number of patients.

Personal contribution - published papers:

Doroftei, **B**.; Armeanu, T.; Maftei, R.; Ilie, O.-D.; Dabuleanu, A.-M.; Condac, C. Abdominal Wall Endometriosis: Two Case Reports and Literature Review. *Med.* ***2020***, *56*, 727. **IF: 2.430**

Case presentation 3 and 4

Case 3

A 38-year-old Caucasian woman with a history of two C-sections (G2P2), the last of which was in November 2015, presented to our outpatient department with complaints of a painful, palpable, small, firm mass of approximately 2 to 3 cm, located in the lower abdomen wall, at the site of the C-section scar, with no mobility to the deeper anatomical planes. The patient described her pain as relatively cyclic and timed the onset of the symptoms at 3 months after her last C-section. The patient was known to suffer from a mild form of hereditary thrombophilia, which required prophylaxis during her two pregnancies and had no other known EMS lesions elsewhere. The rest of the patient's history was unremarkable: no natural births and no complications at the time of the two C-sections, no other relevant family history, no smoking or alcohol consumption, and no medications at the time of presenting**.**

The ultrasound revealed an irregular, heterogeneous, hypoechoic, oblong solid mass with ill-defined margins, located within the subcutaneous fat, with some infiltration in the abdominal muscle but no mobility to the deeper anatomical planes (Figure 47).

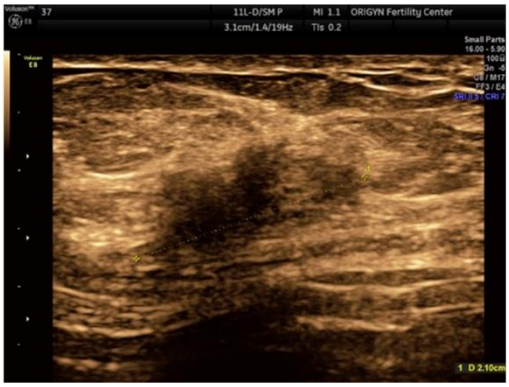

Figure 47. Ultrasound image hypoechoic solid mass with a polylobulated aspect and ill-defined margins

The excised specimen in both cases was microscopically described as a fragment of connective-muscle-fat tissue with glandular components and endometrial-like stroma, with intra- and extracellular hemosiderin deposits, lymphoplasmacytic infiltrate, and fibrosis. Therefore, the presumed diagnosis of parietal EMS was histologically confirmed (Figure 48).

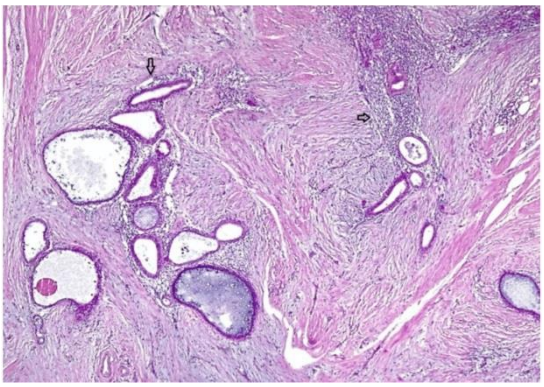

Figure 48. A histological aspect of the mass showing endometrial glands and stroma (arrows) included within conjunctive tissue

Case 4

A 36-year-old Caucasian woman, G1P1 (one birth by C-section two years prior, in 2016), presented complaining of cyclic pain on the C-section scar, as well as of moderate to severe dysmenorrhoea and dyspareunia, two symptoms well known to be associated with EMS. She also pointed to a painful, palpable, small firm mass of ~3 cm in the lower abdomen wall, at the site of the caesarean section scar (Figure 49).

Figure 49. At the level of Pfannenstiel scar (yellow arrow) a prominent painful mass around 3 cm (red circle) without mobility to the deep anatomical planes

This patient had a history of ovarian endometrioma of ~6 cm removed by laparoscopy in 2014. Similar to the previous case, she was thrombophilic and had been administered Enoxaparin during pregnancy. Otherwise, her family history and her C-section were unremarkable, and there had been no natural births. She, too, was a non-smoker and a non-drinker and was not on any medication.

Upon the endovaginal ultrasound examination of the posterior wall of the uterus, we found a nodular, 25/26 mm mass with imprecise margins, diffuse Doppler signal, intramyometrial varicose veins, sliding sign absent posteriorly and present anteriorly. The right ovary, sized 35 mm/24 mm/13 mm, was adherent to the posterolateral wall of the uterus and sensitive upon mobilization with the probe. The left ovary, sized 32 mm/16 mm/10 mm, was also adherent to the posterior wall of the uterus and the left uterosacral ligament, and there was a cystic mass measuring 13/14 mm, suggestive of ovarian endometrioma. There was no sign of free fluid in the Douglas pouch. Transabdominal ultrasound revealed a heterogeneous, hypoechoic solid mass with a polylobulated aspect and ill-defined margins, located in the subcutaneous fat near the C-section scar. The mass had some scattered internal echoes and absent Doppler signal. Surgical excision was difficult due to invasion and lack of cleavage plans. The nodule section revealed a typical aspect (Figure 50), and the histologic exam confirmed the diagnosis (Figure 51).

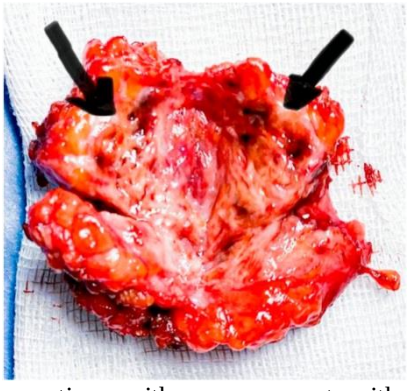

Figure 50. Sectioning revealed a fibrous tissue with numerous cysts with chocolate-like liquid (black arrows)

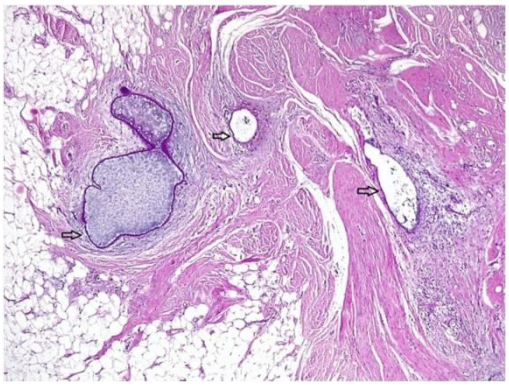

Figure 51. A histological aspect of the mass showing scarce endometrial glands and stroma (arrows) embedded within conjunctive and adipose tissue

Personal contribution - published papers:

Doroftei, **B**.; Maftei, R.; Ilie, O.-D.; Simionescu, G.; Anton, E.; Armeanu, T.; Dabuleanu, A.-M.; Mihalceanu, E.; Condac, C.; Ilea, C. Transvaginal Ultrasound as a First-Line Approach in Deep Endometriosis: A Pictorial Essay. *Diagnostics* ***2021***, *11*, 444. **IF: 3.706**

Materials and methods

The transvaginal ultrasound technique used for detecting DE was performed according to IDEA guidelines [628].

Study participants

Our study enrolled twenty-one women (mean age 33.6 ranging between 25–43) reporting painful symptoms associated with EMS for at least 12 months (dysmenorrhea, dyspareunia or dysuria).

Protocol

Prior to the actual procedure, each woman underwent an MRI investigation. Endometriotic lesions were subsequently confirmed following a histologic examination and surgery.

All the patients suspected of DE were kindly advised to follow a low residue diet for 2-3 days and to take oral laxatives a few hours before the intervention. We further recommended that the patients partially empty their bladder for better visualization of endometriotic lesions.

The images with EMS-like symptoms were obtained with a Voluson E8 expert ultrasound machine (GE Healthcare, Chicago, IL, USA) at the Origyn Fertility Center, Iasi, Romania.

Procedure

At the beginning of the ultrasound examination, the uterus and adnexa were evaluated to identify and describe separately every endometriotic lesion. The presence of “soft markers” was assessed by bimanual examination: a transvaginal probe was gently pushed towards the ovary and transabdominal pressure was applied with the other to notice if the ovary would glide freely along the pelvic sidewall and uterus. The status of the Douglas pouch was appraised using the “sliding-sign” technique. If the rectum glided freely against the uterus and the posterior vaginal fornix, this would be considered as a positive “sliding sign”. The examination concluded with a survey of DE in the anterior and posterior compartments.

Follow-up

Patients were under continuous postoperative follow-up for at least 1 year to evaluate the

evolution of symptoms. It should be also mentioned that were placed under standard treatment for at least 3 months on postoperative hormones (dienogest or COC) in continuous administration between 90-120 days, respectively).

Ethical approval

The study was approved by the Ethical Committee of the Origyn Fertility Center (no 117/565/January/25/2021). Additionally, all patients gave their signed consent for ultrasound images presented here to be used for research and publication purposes.

Results and discussions

Adnexa

The assessment of the adnexa involves the evaluation of ovaries, Fallopian tubes and the detection of "soft markers". A clear mapping of the left and right side should be performed especially in the cases of patients with ovaries kissing and important anatomic distortion; also, the examiner must try to establish the origin of the lesion, weather ovary, uterus, fallopian tube or other organs. For the description of ovarian lesions, we used the terminology proposed by the IOTA group [632].

Endometrioma or ovarian EMS is one of the most common forms of EMS with characteristic aspects of a cystic lesion with "ground-glass" echogenicity (Figure 52) and low Doppler signal.

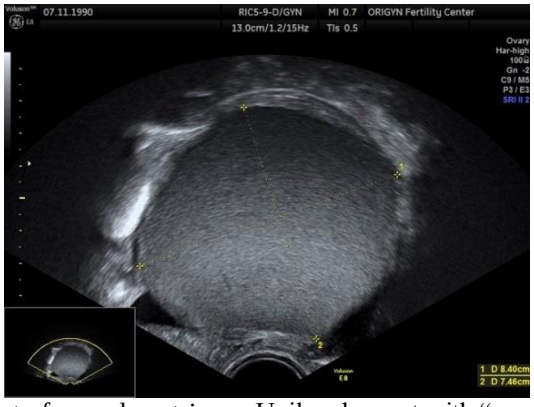

Figure 52. Typical aspect of an endometrioma. Unilocular cyst with "ground-glass" echogenicity

According to a recent study, the ultrasound appearance of endometrioma changes with the patient's age [633]. While in premenopausal women 75% of lesions have a "ground-glass" echogenicity, only 62% of lesions in peri- and post-menopausal women have this aspect. In addition to the typical appearance of unilocular cysts with "ground-glass" echogenicity, atypical forms of endometrioma can also be found, such as multilocular cysts (Figure 53), papillary projections or solid areas (Figures 54 and 55).

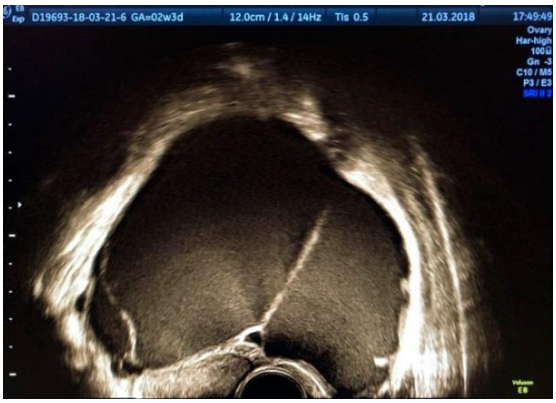

Figure 53. Multilocular endometrioma with "ground-glass" appearance

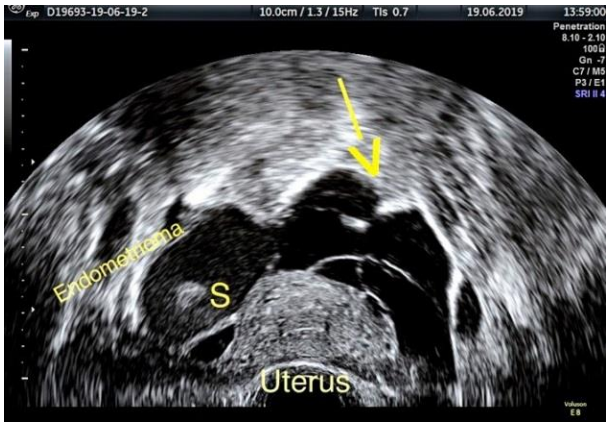

Figure 54. Ovarian endometrioma containing a hyperechoic area (S). Paraovarian multiple adhesions and free fluid (yellow arrow)

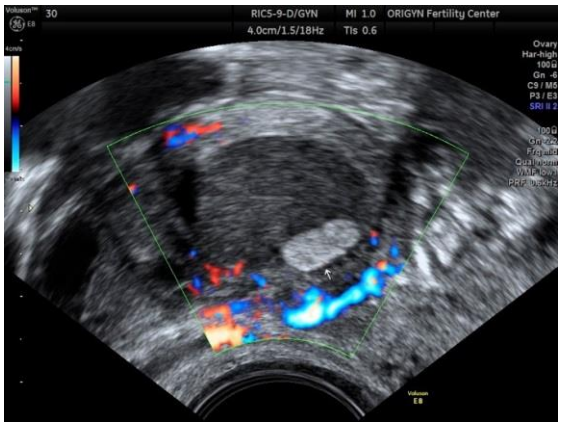

Figure 55. Ovarian endometrioma containing a hyperechoic area (white arrow) without Doppler signal

In the presence of endometrioma, due to adhesions, the Fallopian tubes can be affected, resulting in hydrosalpinx or hematosalpinx. In one study, ovarian endometrioma was linked to the severity of DE, thus having the potential to serve as a marker and a warning sign of gynecologists [634]. In addition, the surrounding ovarian bowel should be carefully checked for the presence of endometriotic lesions (Figure 56).

The evaluation of soft markers for EMS detected by transvaginal ultrasound includes ovarian mobility and site-specific tenderness (SST). The assessment of ovarian mobility is made by applying light pressure with the vaginal transducer in the direction of the ovary. In some cases, the operator can use his/her left hand to apply pressure on the iliac fossa region for a better evaluation of ovarian mobility. Normally, the ovary should glide freely along the pelvic sidewall and uterus. The assessment of the site-specific tenderness consists of applying pressure with the probe and asking the patient about the onset and site of pain. We recommend that the assessment of site-specific tenderness be done at the end of the examination to reduce the patient's physical and psychological discomfort.

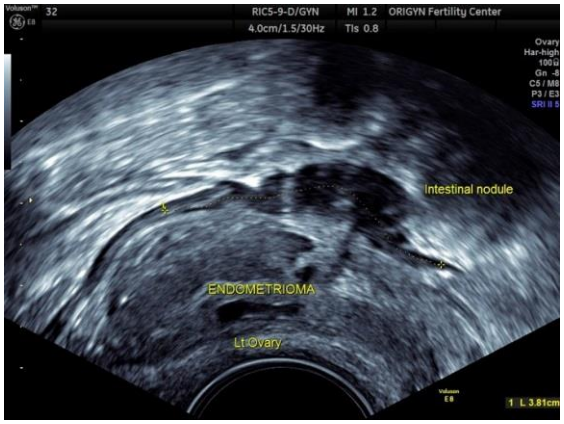

Figure 56. Left ovary with an endometrioma having a typical appearance. Right behind the ovary, a loop of the small intestine with an endometriotic nodule is very adherent to the ovary

Adenomyosis

The uterine evaluation should be done according to the MUSA consensus for a better characterization of lesions, especially when in the case of associated pathology like myoma [635]. Adenomyosis is a benign condition defined by the presence of endometrial glands and stroma at the level of the uterine muscle wall. The existence of endometrial-like tissue in the uterine wall induces hypertrophy and hyperplasia of the surrounding myometrium, creating a globose aspect of the uterus and an increased uterine volume.

Based on the histologic and ultrasonographic aspects, we can distinguish three types of adenomyosis: diffuse adenomyosis (Figures 57 and 58), focal adenomyosis (Figures 59 and 60) and adenomyoma.

Figure 57. Ultrasound image of diffuse adenomyosis showing an enlarged uterus with fan-shaped shadowing: enlarged uterus with loss of the normal aspect of the myometrium: multiple myometrial cysts, fan-shaped shadowing, echogenic islands and an interrupted junctional zone

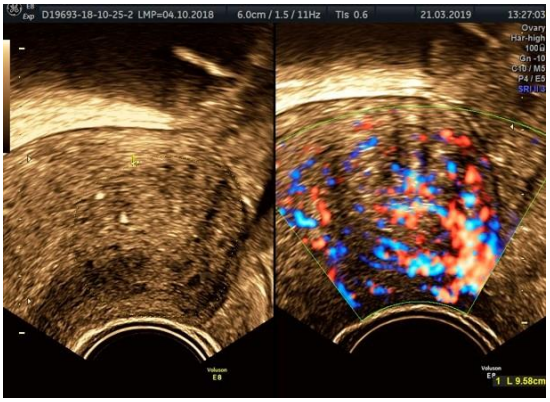

Figure 58. Ultrasound image of diffuse adenomyosis showing translesional blood flow in Doppler mode

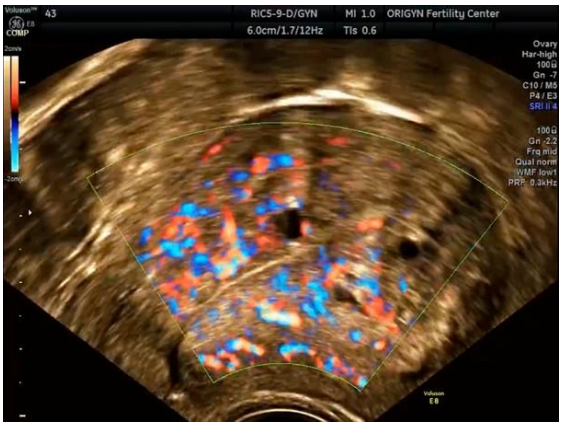

Figure 59. Ultrasound aspects of focal adenomyosis: myometrial cysts surrounded by echogenic rim and blood flow in Doppler mode

Figure 60. Focal adenomyosis in 3D coronal view showing cystic lesions

Posterior compartment

The last step of the IDEA approach consists of assessing the posterior compartment, which includes: the uterosacral ligaments (USLs), the posterior vaginal fornix, the recto-vaginal septum and the bowel. We recommend starting this evaluation with the bowel because 9-22% of all women with proven EMS will have this type of lesions [636]. With the probe oriented in the direction of the sacrum bone, the pressure is applied gently on the entrance into the vagina. Once the bowel wall is identified, slow progression is made following the bowel curves. Most commonly, the lesions are located in the anterior wall of the bowel, but sometimes it may be possible to find an endometriotic nodule in the lateral wall or even in the posterior wall of the bowel. This is the reason why we suggest assessing the bowel in the longitudinal and transversal planes.

The normal thickness of the rectosigmoid wall measured in our case was 1-2 mm (Figure 61).

Figure 61. Ultrasound appearance of a normal bowel loop

Any focal thickening of the bowel wall that suggests an endometriotic nodule should be followed by gentle pressure with the probe to elongate the intestinal loop and to exclude an artifact or superposition of images. Another helpful tip is to observe the peristalsis of the surrounding bowel because the nodule will remain immobile. Any lesions detected during the ultrasound examination should be described under the IDEA consensus statement (Figures 62-66).

Figure 62. Ultrasound image showing the bowel with an endometriotic nodule (white arrow, “pulling sleeve sign”) adherent to the uterine torus, in extrinsic retraction. In this case the sliding sign was absent

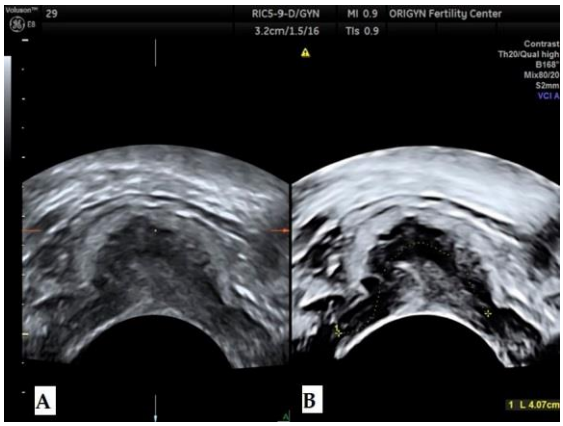

Figure 63. (A) Ultrasound image showing a deep infiltrating endometriosis (DIE) nodule with a regular outline (absence of “spikes”). (B) the same nodule is viewed in 3D with TUI (tomographic ultrasound imaging)

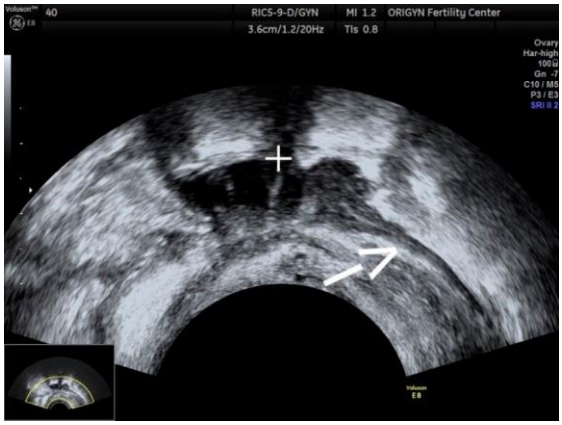

Figure 64. Ultrasound image showing a DIE nodule (+) with progressive narrowing, like a “tail” (white arrow), also known as a “comet” sign

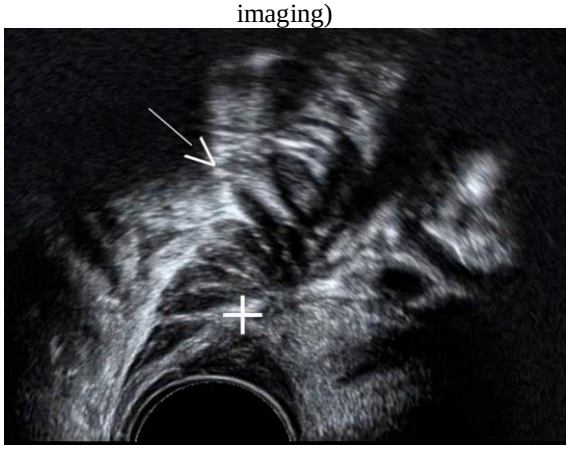
Figure 65. Ultrasound image showing a DIE nodule (+) with prominent spikes towards the bowel lumen (white arrow, “Indian headdress sign”)

Figure 66. Ultrasound image showing a big DIE nodule with some spikes towards the bowel lumen, in extrinsic retraction. In this case, the sliding sign was absent

When evaluating intestinal endometriotic nodules, the 3D ultrasound has demonstrated its usefulness, because such imagery allows for better visualization of lesion borders (Figure 67).

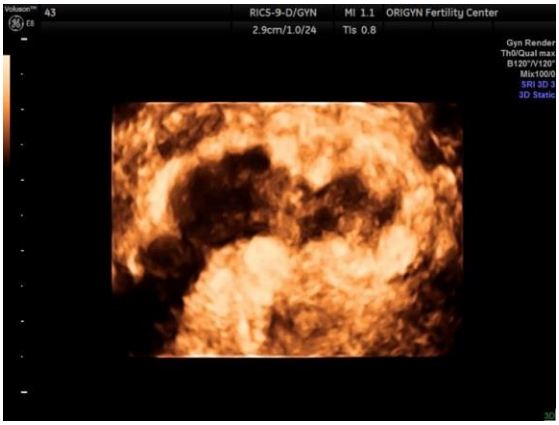

Figure 67. Three-dimensional findings of a rectosigmoid nodule in the coronal plane

Another important region that needs to be checked for DE is the RVS. This is located in the retroperitoneum, between the posterior wall of the vagina and the anterior wall of the rectum. This structure establishes a strong connection between the vagina and the rectum, containing collagen, elastic fibers, small vessels, smooth muscle cells and nerves from the inferior hypogastric plexus. The ultrasound examination of the RVS is made with the probe oriented in the same manner as for bowel evaluation. According to the IDEA group definition, the nodule should be visualized below the line passing along the lower border of the posterior lip of the cervix (Figure 68) [628].

Figure 68. Ultrasound image depicting an endometriotic nodule of the RVS. (+) the vaginal wall as a hypoechogenic line and an endometriotic nodule (*) with discreet vaginal wall infiltration

It is very important to use this landmark for better differentiation between RVS EMS and retrocervical EMS. In the former case, the anterior wall of the rectum is usually infiltrated, which implies bowel resection during surgery, while in the case of retrocervical EMS, the bowel wall is not affected, so a local excision or ablation of the lesion is sufficient.

The ultrasound evaluation of the posterior fornix should be a tenderness-guided examination. The ultrasound beam is gently placed into the posterior fornix and the patient is asked to inform the examiner about the onset and the site of any pain experienced during the examination. In addition to the size of the lesion, the operator should pay attention to the relationship with other endometriotic lesions and evaluate the mobility and the status of the sliding sign (Figure 69).

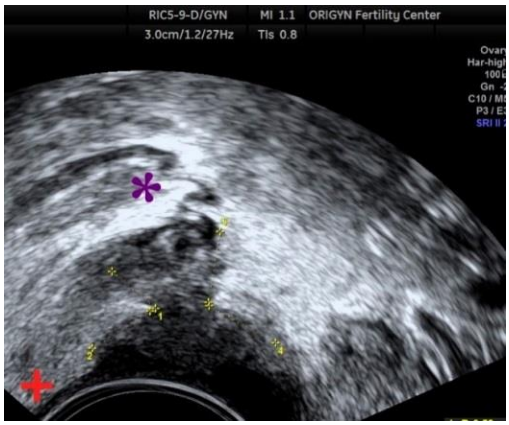

Figure 69. Ultrasound image showing a big nodule infiltrating the posterior vaginal fornix and the anterior wall of the rectum. (+) the vaginal wall, (*) the bowel. Diablo-like nodule

Normally, USLs are two anatomic structures invisible to ultrasound examination and, according to one meta-analysis [637], the overall pooled sensitivity of TVS for detection of USL EMS was only 53% (95% CI, 35-70%). During the examination, the ultrasound beam is gently placed into the posterior fornix, at the midline, in a sagittal plane and then the probe is swept inferolateral to the cervix. Endometriotic lesions of the USL appear as a hypoechoic thickening and may be isolated or may be included in a big DE nodule (Figures 70 and 71). The nodule should be measured in three orthogonal planes.

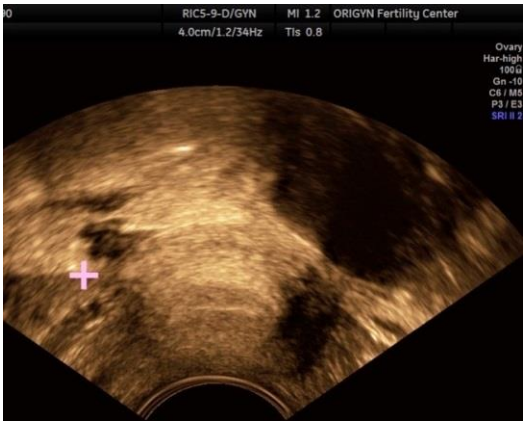

Figure 70. Transverse image of the cervix with a uterosacral ligaments (USL) DE hypoechoic nod- ule (+), with irregular outline

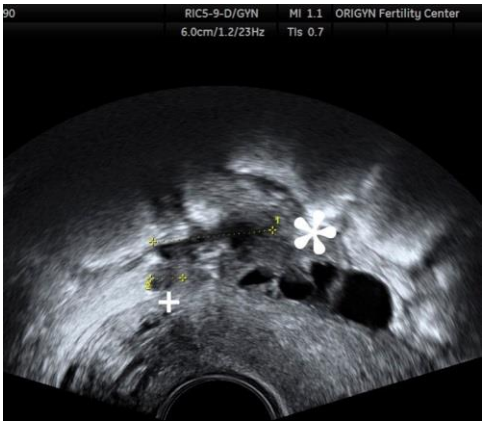

Figure 71. Sagittal image of the cervix showing a hypoechoic USL DE nodule (+) along with a bowel nodule adherent to a DE nodule of the uterine torus and a USL nodule

Another important step is the evaluation of the ureter. Ureteral EMS may be intrinsic or extrinsic, affecting one or both ureters. Intrinsic ureteral EMS is due to direct infiltration of the ureteral wall by the endometrial glands and stroma. Extrinsic EMS is more common and is a consequence of an intensive fibrotic process due to DE. The pelvic portion of the ureters can easily be

evaluated by transvaginal ultrasound. The first step is to identify the urethra in a longitudinal section and then the probe should be moved slowly to each part of the lateral pelvic wall. Ureters appear as hypoechoic tubular structures surrounded by a hyperechoic layer, measuring around 1.7 mm at rest and 2.9 mm during peristalsis (Figure 72).

Figure 72. Transvaginal ultrasound of a normal ureter during peristalsis. Notice the flow of urine into the bladder

As in the case of bowel lesions, if a ureteral nodule is visualized when the probe is fixed, the nodule will remain immobile during peristalsis. Usually, the ureters are narrowed by DE at the level of the crossing with the uterine artery. This is the reason why we recommend the inspection of the ureter until this level with the ultrasound device in Doppler mode (Figure 73). In the case of a urethral JJ stent, TVS is very helpful in evaluating the position and peristalsis (Figure 74).

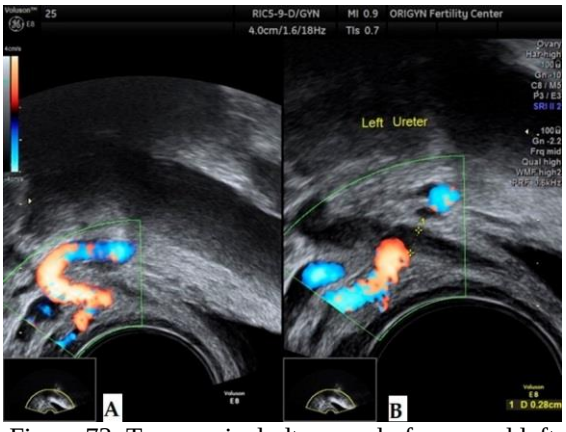

Figure 73. Transvaginal ultrasound of a normal left ureter (A) and of the crossing of the uterine artery when viewed in Doppler mode (B)

Figure 74. Transvaginal ultrasound of the bladder showing the ureter and the JJ stent in a normal position. (+ sign in the figure plays the role of a pointer to highlight a specific feature)

Scar EMS is an entirely iatrogenic disease with an incidence of 0.03-1% in women with a history of Caesarean births [638]. It can also occur following gynecological surgeries (invasive or laparoscopic) if the uterine cavity is involved. It is very difficult to predict the time between the surgery and the onset of the disease. Data from case reports show that the time frame can range from 6 months up to 10 years [639].

The diagnosis is usually delayed because the signs and symptoms are not specific, and cyclic abdominal pain is not a pathognomonic sign for scar EMS. The differential diagnosis should be made with granuloma, desmoid tumor, lipoma, abscesses, sebaceous cysts, ventral hernias, or metastasis [640]. In our cases, the diagnosis was delayed around 2-3 years even if in the first case the pain has appeared 3 months after C-section. In our case, the patient considered that the pain was due to the surgery itself, and this led to a delayed diagnosis. The variable time between surgery and symptoms, the fact that this disease is rare, and similarities with other diseases determine a delayed diagnosis. It

is still unknown what makes some forms aggressive with deep invasion into the abdominal wall, while most cases are limited up to abdominal aponeurosis because a direct link between surgery and diagnosis is not seen.

In addition to the anamnesis and clinical examination, the ultrasound should be the first-line imagistic method for diagnosis. High-frequency linear transducers are best for such assessment [641]. Upon ultrasound, a round or oval lesion with imprecise borders can be found at the site of the scar. The lesion typically appears as a hypoechoic area surrounded by a hyperechoic ring, with low or even absent blood flow when viewed in Doppler mode.

The treatment of scar EMS consists of wide lesion excision with a minimum 1 cm safe margin in order to avoid recurrence. In cases of incomplete excision of the lesion, the risk of recurrence varies between 12.5-28.6% [642]. In our cases, ultrasound evaluation 3 months after surgery shows no signs of residual or recidivant lesions. The interval dedicated to monitoring the patient after surgery to investigate whether there are outstanding or recurrent reminiscences is not yet clearly defined. The best way to prevent scar EMS is to avoid contamination with endometrial cells.

Scar EMS is, unfortunately, a disease with increasing incidence due to the rising rate of births by C-section and delays in diagnosis leading to abdominal wall invasion and serious health risks for the patient. It is very important to consider such a diagnosis in all patients of reproductive age who present with painful masses at the level of their scars. Among the various complications, delayed diagnosis can cause the patient to have to undergo complex and invasive surgical procedures, which may significantly impact their quality of life. The ultrasound is an accessible imagistic method and should be used routinely to evaluate any scar-related masses. Once a first nodule is detected, the entire scar must be assessed, and an ultrasound evaluation for ovarian EMS and DE should be performed [643].

Management strategies are controversial. Because of the relatively low incidence of AWE, there is a relatively small body of evidence in the current literature. There are situations when surgery can be avoided, especially in cases of endometriomas or recurrent endometriomas that can be medically managed. Surgical intervention becomes imperative for patients that report perpetual pain, structures that are possibly malignant, infertility, or gradual increases in size.

Discrepancies regarding the usage of oral medication have been noted. They improve the overall health condition, but the success rate is low, and the recurrence chances once the treatment is ceased are high [15]. In contrast to oral contraceptives, danazol, P4, and GnRH, leuprolide is efficient during the first year, particularly for patients close to menopause. Unfortunately, it is associated with long-term repercussions and further correlated with adverse effects and does not reduce the size of lesions [644]. Therapy with oral contraceptives, progestins, medroxyprogesterone acetate, and GnRH agonists has been tried with minimal success. In some patients, the effects can be relatively long-lasting, but complete and long term regression of EMS is rare with hormonal therapy.

GnRH is also widely used for alleviating pain and slowing the progression of EMS, but its pharmacokinetics is controversial matter. While some authors argue that GnRH has no beneficial effect [645,646], we identified one study in which the size of lesions decreased after 6 months of use [647]. AIs, GnRH agonists, and danazol are also dedicated agents, but the usefulness of these alternatives in endometrioma therapy has not been sufficiently researched [648,649].

Recently, the role of danazol has been explored from various perspectives. Considering that it is well absorbed, this synthetic steroid causes gastrointestinal deficiencies in patients and a clinical panel identical to that observed in severe acute respiratory syndrome coronavirus 2-infected patients. Specific phenotypes that reflect metabolic and psychiatric disturbances have also been documented quite frequently [650].

Given the available data, dienogest is a novel adjuvant to surgery and it possesses an effective and tolerable compound that has enjoyed rather sudden interest in recent years. Retrospectively, Bedaiwy et al., summarized in their narrative review all existing information regarding the role of dienogest. From eighteen studies, the authors concluded individually that dienogest is useful not only for preventing post-surgical recurrence, but also to reduce the associated symptomatology [651].

To add to this discussion, it seems that oral contraceptives were successfully used to lower the prevalence of endometrioma at the initial laparoscopy [652]. Based on these initial observations, it was hypothesized that the formation of endometrioma can be bypassed by suppression [653,654]. Intriguingly, recurrence could be viewed as an integrated phenomenon in approximately 30% of the

cases [655]. In support of this argument, we identified three other studies that point to the beneficial role of suppression [656–658]. Moreover, the risk is up to four times diminished following cystectomy, and women are prescribed twenty-four to seventy-two weeks of COCs versus no treatment [30]. In a recent systematic review and meta-analysis, the potent results obtained after the use of GnRH were further discussed [27], whereas those regarding levonorgestrel-releasing intrauterine device placement were considered inferior compared to ovarian suppression [31,32,33]. Overall, COCs are the most eligible alternative for reducing large endometriomas [34], not even NEA being totally risk-free despite its low costs and approval from FDA. Nevertheless, the regression of cysts in the first twelve weeks of treatment has been recently shown [659].

We identified only one study in which EMS was treated with ultrasound-guided ethanol injection. Bozkurt et al., employed this technique on a 25-year-old woman with two previous C-sections diagnosed with a 3-cm abdominal wall endometrioma in the rectus muscle [660]. The authors performed an MRI and an ultrasound-guided needle aspiration which helped identify endometrial glands and stroma. The protocol they followed was as follows: (I) an injection of 1 mL of 95% ethanol; (II) administration for twelve weeks of oral contraceptives; (III) twelve weeks follow-up.

On the other hand, surgery remains the method of choice for clinicians since it offers two viable options; treatment and definitive diagnosis. It is crucial to first remove the nodule(s) and the adjacent fascia thoroughly. Unfortunately, the risk of novel lesions or reoccurrence of AWE is relative [661]. Some recommended strategies use separate needles for the uterine and the abdominal closure, thorough washing and cleaning of the peritoneal cavity, and closing the uterine incision with care and without suturing the endometrium.

Sclerotherapy by ethanol injection before surgical resection represents another option, but intralesional ethanol injection may result in difficult-to-repair necrosis on the anterior muscles of the abdominal wall in large lesions. In EMS foci extending into the intraperitoneal region, it may also cause complications including chemical peritonitis and severe pain as a result of alcohol penetration into the peritoneum. In such patients, therefore, injections may be given in several sessions instead of a single session. Compared with the complications of surgical excision, the complications of sclerotherapy by ethanol are at a more acceptable level. Along with ethanol sclerotherapy, plasma energy is also attributed to such interventions, being less invasive, and optimal for women desiring to conceive [662].

Distinct surgical approaches may include polypropylene-mesh-closing, reserved for the cases with massive wall defect due to the invasion of the aponeurosis, a technique meant to lessen tissue tension. In wide surgical resections, complications including foreign substance reactions, mesh migration, and eventual incidence of hernia may appear due to the propylene mesh used. In the literature, abdominoplasty with polypropylene mesh is recommended for abdominal wall reconstruction in large lesions to reduce hernia development [662].

Although ultrasound is the most cost-efficient method of imaging evaluation, it is highly recommended and preferable that, in the case of AWE, further more detailed imaging investigations be conducted, such as CT/MRI. Such exams can offer important aspects regarding those lesions such as the extent of the tissue involvement and the state of all of the structures that come in close contact with the lesion.

There has been recent discussion about the usefulness of CT in the diagnosis of EMS. CT does not visualize pelvic organs but rather can be used to detect ureteral involvement and/or renal insufficiency [663].

However, the experience of the radiologist is essential considering that the average acquisition time for both high- and low-resolution MRI was twenty-four minutes. The values of specificity, sensitivity, and positive and negative predictive values (NPV/PPV) did not differ significantly, which is why both are considered valuable tools for detecting DE extension [664]. Bermot et al., investigated the detection performance of MRI of anterior pelvic endometriotic lesions, and while the two radiologists obtained identical sensitivity (89.5%), the specificity value reached by one was 100% and 89.5% by the other [665].

One relevant study is by Burkett et al., [666], who aimed to quantify the value of pre-operative MRI in the management of women suffering from EMS. Out of one hundred and thirty-six patients, the associated methodology needed to be changed in 18.4% of the cases (n = 25). Whereas major changes were made in 8.1% (n = 11), minor changes were necessary in 13.2% (n = 18) of patients.

Yap et al., analyzed 98 MRIs, of which 76 identified deep infiltrating EMS and 22 were normal. According to their results, 65 patients did not undergo any record, whereas the remaining subgroup underwent laparoscopy, operative and/or pathology investigations (n = 37). With a 195-day average time interval, middle compartment sensitivity (79.4% / specificity of 95.1%), posterior compartment sensitivity (76.5% / specificity of 99.4%) and the overall sensitivity and specificity of detecting bowel EMS of 94.4%, and 94.7% respectively, system benchmark diagnostic performance can be achieved through 3 T MRI [667].

In another retrospective study conducted by Bazot et al., in which 666 patients were enrolled between 2005 and 2009, the overall prevalence of deep infiltrating EMS was 91.6% (n = 76 out of 83). The sensitivity, specificity, positive and negative predictive values were 83.3%, 98.6%, 90.9% and 97.2%, respectively [668]. Despite such data, it was recently demonstrated that laparoscopy is superior to MRI ($p < 0.0001$) especially in the diagnosis of chronic pelvic pain, but the MRI agreement with histopathology or laparoscopy was poor ($p < 0.0455$). The second diagnostic criterion was significantly improved in 96.9% of the cases ($p < 0.0000$) [669].

To date, no evidence seems to lean towards or against the suture of the peritoneum concerning the incidence of AWE, nor is the change of gloves during the surgery recommended when completing the hysterorrhaphy. For AWE, total surgical excision is considered to be the gold standard for both diagnosis and treatment [670].

The gold standard treatment in such cases is surgical, consisting of the excision of the mass within safe margins. This also allows for the specimen to be histopathologically analyzed to confirm the diagnosis. Moreover, an interesting approach would be finding an explanation regarding why some women are more susceptible to developing this condition while others are not and thereby determining if there are other factors involved such as genetics and environmental ones.

A detailed ultrasound examination using the steps of the IDEA consensus statement could detect endometriotic lesions that would otherwise be omitted during laparoscopy (i.e., bowel lesions, ureteral nodules) and contribute to a correct referral of patients suffering from advanced endometriosis to centers of excellence in endometriosis, where they can undergo minimally invasive surgery.

Although there is ample evidence that the technique for uterine closure can be crucial for uterine scar healing, the same cannot be said about which are the optimal techniques, and there are no national or international guidelines that obstetricians and gynecologists can rely on. Most randomized trials that have evaluated the uterine closure technique during caesarean have focused on the short-term operative complications without evaluating the impact on future pregnancies or the risk of developing caesarean scar EMS. Since there is no consensus on the matter, it is up to the surgeon and his clinical experience to adapt the techniques given the intraoperative findings [671].

Along with the classic technique of assessing tubal permeability - HSG, which has its limits, and the invasive technique (celioscopy with chromotubation), sonohysterosalpingography with saline as a contrast agent (hysteroscopy contrast - HYCOSY) is an outpatient method, which complements the standard endovaginal ultrasound in assessing uterine pathology and tubal permeability.

Personal contribution - published papers:

Socolov, D.; Lupaşcu, I.A.; Danciu, E.; **Doroftei**, **B.**; Boian, I.; Boiculese, L.; Pintilie, P.; Miron, N. [Sonohysterosalpingography versus hysterosalpingography in the evaluation of uterine and tubal infertility]. *Rev. Med. Chir. Soc. Med. Nat., Iasi* ***2009***, *113*, 803–808.

Material and methods

In a prospective study of 95 infertility patients 25-40 years old (median age 31), HYCOSY was compared with HSG with regard to the diagnostic acuracy for uterine cavity pathology and tubal patency, and compared to laparoscopy with dye test combined with hysteroscopy as gold standard.

Results

The sensibility, specificity, positive and negative predictive values for the diagnostic of uterine

cavity pathology were: HYCOSY versus hysteroscopy of 72.1%, 96.15%, 93.93% and 80.64% respectively; HSG versus hysteroscopy was 83.3%, 60.7%, 63.6% and 81.6%; both methods combined versus hysteroscopy 95.34%, 61.53%, 67.21% and 94.11%. The same parameters for the tubal patency were: HYCOSY versus dye test laparoscopy 81.39%, 87.69%, 67.30% and 97.79%; HSG versus dye test laparoscopy 61.9%, 85.3%, 56.5% and 87.9%; both methods combined versus dye test 86%, 76%, 52.9% and 94.6%.

Retrospectively, HSG was the first-line tool able to confirm the presence of IUAs. It is still considered valid by many gynecologists for detecting filling abnormalities. It is cost effective, and it features a sensitivity between 0% and ~100%, and a specificity between >30% and 100%. In terms of imaging, both HSG and SHG were equally sensitive [672]. HSG was found to be as accurate as hysteroscopy despite the fact that the nature of the filling defects was detected by hysteroscopy, as was demonstrated in a retrospective study of 400 patients [673]. It was also shown that approximately 38.3% of HSG examinations were false-positive [674]. In a cohort of 65 women, of whom five had hysteroscopic evaluation, HSG yielded a sensitivity of 75% of IUA detections and 50% predictive value when compared to hysteroscopy, according to the results of Soares et al., [675].

A recent systematic review and meta-analysis appraised SIS accuracy in detecting intrauterine abnormalities, and concluding that SIS has a pooled sensitivity and specificity of 82% up to 99% [676]. Another retrospective study of 149 cases revealed a significant difference between the HSG group and SHG group (50.3% and 81.8%) [677]. Due to its design, SHG is superior to transvaginal ultrasonography at detecting IUAs [678]. Among 65 infertile women, SHG had a sensitivity of up to 75% and a specificity of around 42.9% to HSG [675]. A non-invasive procedure usually applied when HSG is not possible is ultrasonography. It was used in two previous occasions by Conforti et al., [679] and by Schlaff and Hurst [680], but both sensitivity and specificity levels were quite low. Other researchers obtained sensitivity values of up to 52% [681], and 11% specificity [678].

Despite the fact that transvaginal ultrasound revealed a substantially thinner endometrium between the AS group (n = 16) and control group (n = 50) [682], its accuracy is still low [678,681]. However, it is cheaper compared to laparoscopy, with no significant differences concerning IUA incidence [683]. Both unenhanced transvaginal ultrasonography and contrast SIS have a finite diagnostic capacity [681], near 0% specificity and sensitivity [675], and moderate to high positive and negative predictive values (98% and 43%) [675,681].

Few scientists have used three-dimensional ultrasonography aiming to detect IUAs [678,684]. It even succeeds with a specificity of around 45% [678]. It was found that 3D-SHG has a sensitivity and specificity around 91.1% and 98.8%, respectively [685], which was then confirmed by Abou-Salen et al., [686]. Three-dimensional ultrasound was compared with hysteroscopy, confirming a variation that ranges between 16% and 100% based on a series of criteria, as shown in a recent Taiwanese study involving 110 women [687]. There are rare situations when MRI is indeed valuable as a supplementary diagnostic tool [688][689].

Despite all the research and developments, hysteroscopy is rightly called the gold standard due to the fact that it allows direct real view visualization of the endometrial cavity. Moreover, it can be performed "in office" with minimal discomfort compared to a blind HSG [688]. Virtual hysteroscopy could play the key role in the future in the diagnosis of IUAs [690].

Personal contribution - published papers:

Doroftei, **B**.; Mambet, C.; Zlei, M. It's Never over until It's over: How Can Age and Ovarian Reserve Be Mathematically Bound through the Measurement of Serum AMH-A Study of 5069 Romanian Women. *PLoS One* ***2015***, *10*, e0125216. **IF: 3.240**

Darii, N.; Anton, E.; **Doroftei**, **B**.; Ciobica, A.; Maftei, R.; Anton, S.C.; Mostafa, T. Iatrogenic parasitic myoma and iatrogenic adenomyoma after laparoscopic morcellation: A mini-review. *J. Adv. Res.* ***2019***, *20*, 1–8. **IF: 10.479**

Doroftei, **B**.; Dabuleanu, A.-M.; Ilie, O.-D.; Maftei, R.; Anton, E.; Simionescu, G.; Matei, T.; Armeanu, T. Mini-Review of the New Therapeutic Possibilities in Asherman Syndrome—Where Are We after One Hundred and Twenty-Six Years? *Diagnostics* ***2020***, *10*, 706. **IF: 3.706**

II.5 Operative interventions with and without a genetic substrate

It has long been hypothesized that infertility has an idiopathic cause, but recent studies have demonstrated the existence of a genetic substrate. Over forty-four genes in total are dispensable for fertility in both sexes without affecting host homeostasis. However, there are genes whose loss-of-function induces moderate to severe phenotypic changes in both sexes. There were situations in which authors reported infertility, exhibited by the experimental model, or other pathologies such as cryptorchidism, cataracts, or reduced motor activity. Overall, zinc-finger nucleases, transcription activator-like effector nucleases, and CRISPR/Cas9 are techniques that offer a wide range of possibilities for studying infertility, even to create mutant variants.

PGD is a technique performed in conjunction with IVF, dedicated at identifying possible genetic defects in embryos obtained through human ART [691]. Usually, PGD is performed for couples in which one or both partners suffer from a genetic disorder. Therefore, embryos may be tested to reveal whether they are affected by the same abnormalities. Over 350 different medical conditions may be diagnosed with an accuracy of about 99.5% [692].

Unlike other well-known methods of prenatal diagnosis (e.g. amniocentesis, which is only available when the pregnancy is established), PGD is performed before implantation. It can aid both the medical team and the patients in choosing the most genetically suitable embryo(s). In contrast to amniocentesis, where the parents may risk being faced with the dramatic decision to terminate an ongoing pregnancy, PGD may improve the likelihood of obtaining a normal pregnancy [693].

The successful implementation of PGD technique in an IVF clinic involves collaboration between several specialties such as IVF, genetics and single cell diagnosis laboratories. Notwithstanding, the ability of the PGD test to enable parents affected by a genetic disease to have a healthy child, there are some legal, ethical and medical implications in Romania which were highlighted before [694], but unfortunately still remain unanswered.

CDG represents a multisystemic group of mild to severe neuro(metabolic) disorders, inherited in an autosomal recessive manner [695]. Forty-six relevant genes being so far identified [696]. Since the first case reported by the paediatrician Jaak Jaeken [697], remarkable discoveries have been made during these three and a half decades regarding CDG's underlying mechanism [698].

Mechanically speaking, CDG is defined by a series of defects occurring in the synthesis of the glycan moiety of the glycoconjugates and the coupling of these polysaccharides to proteins and lipids [699]. The latest studies have revealed that CDGs are divided into O-linked disorders, as a result of an attachment of the O-glycans to the hydroxyl group of threonine or the serine of proteins, a process that takes place within only one cellular compartment. It is tissue-specific and possesses a distinct clinical panel, less severe than that of the N-linked group [700].

However, it took fifteen years to unveil the gene responsible for PMM2-CDG [701] (OMIN # 212065), and it has been established that PMM2, which is located on chromosome 16 [702], is the result of an attachment of N-glycans to an amino group of asparagine of proteins. Compared with O-linked, which takes place only in the Golgi apparatus, the N-linked occurs within the cytosol, endoplasmic reticulum (ER), and Golgi apparatus. More precisely, PMM2 encodes phosphomannomtase (PMM) during the second step of the mannose pathway [703] by converting man-6-P into the Man-1-P necessary to produce guanosine diphosphate (GDP)-Man for the mannosylation of glycans [702].

Among all twenty-five pure N-linked disorders that have been highlighted [699], the PMM2 phenotype is the most frequently encountered [700], with almost 100 mutations known to date [704]. More than 800 cases have been reported worldwide [705], with a frequency rate of 1:12,000, and up to 1:20,000 births [706].

As previously mentioned, several cohort studies have already been conducted in different countries in which both related and unrelated individuals were used [707–717]. Given that most of the reports have focused on the paediatric population [718–720], the long-term course during adolescence, respectively, adulthood has also provided additional conclusive data [707,714,717,719,721–724].

PMD is a rare benign disorder of the placenta characterized by placentomegaly and grapelike vesicles that can resemble at ultrasound examination with a molar pregnancy [725]. PMD was

described initially by Moscoso et al., [726] as stem villous hyperplasia with elevated maternal serum alpha-feto-protein (AFP) and enlarged placentas with ultrasound features that are suggestive of partial mole. This condition may resemble a partial hydatidiform mole (HM), however in contrast to partial mole throphoblastic proliferation is absent, the disorder being characterized by aneurysmal dilatation of vessels on the fetal surface of the placenta with dilated stem villi. Although some papers reported an incidence of around 0.02% of pregnancies, [727] the true incidence of PMD is unknown because previously it used to be reported under a variety of names such as "placentomegaly with massive hydrops of placental stem villi" and "pseudopartial moles." [728,729]. Moreover, PMD is associated with FGR in the majority of the cases and in approximately one quarter of the reported cases with Beckwith-Wiedemann syndrome (BWS) [728,730] or IUFD, but can also be associated with normal appearing fetuses.

RPL may be defined by two or more failed clinical pregnancies confirmed by ultrasound or histopathologic examination. This entity affects 2-5% of the couples trying to conceive. Genetic abnormalities are among the most common causes of first trimester pregnancy loss, identified in more than 50% of the cases [731,732]. In almost 4% of the cases of recurrent pregnancy loss, the chromosomal abnormalities are determined by unbalanced Robertsonian translocation, a chromosomal anomaly involving 2 acrocentric chromosomes [733]. One of the most frequent subtype present in clinical practice, strongly associated with male infertility, severe oligoasthenozoospermia and RPL is Robertsonian translocation (45,XY,der(13;14)(q10;q10)), and for those couples trying to conceive and have such a genetic disorder, an IVF cycle associated with PGT may be the solution [734].

Personal contribution - published papers:

Doroftei, **B**.; Ilie, O.-D.; Puiu, M.; Ciobica, A.; Ilea, C. Mini-Review Regarding the Applicability of Genome Editing Techniques Developed for Studying Infertility. *Diagnostics (Basel, Switzerland)* ***2021***, *11*, 246. **IF: 3.706**

Doroftei, **B**.; Cumpata, S.; Nemtanu, L.; Ilie, O.; Ivanov, I.; Avasiloaiei, A.; Anton, E.; Mocanu, E.; Maftei, R. First Romanian live birth after Preimplantation Genetic Testing in a couple with Severe Oligospermia determined by Y Chromosome Microdeletions Copy Right@ Ovidiu-Dumitru Ilie. *Am. J. Biomed. Sci. Res.* ***2020***, *9*, 64-70.

Doroftei, **B**.; Nemtanu, L.; Ilie, O.-D.; Simionescu, G.; Ivanov, I.; Anton, E.; Puiu, M.; Maftei, R. In vitro fertilisation (Ivf) associated with preimplantation genetic testing for monogenic diseases (pgt-m) in a romanian carrier couple for congenital disorder of glycosylation type ia (cdg-ia): A case report. *Genes (Basel).* ***2020***, *11*, 697. **IF: 4.096**

Doroftei, **B**.; Neculai-Valeanu, S.; Simionescu, G.; Grab, D.; Plopa, N.; Anton, E.; Maftei, R. A case report of placental mesenchymal dysplasia: A rare case of a genetically normal fetus with severe intrauterine growth restriction. *Medicine (Baltimore).* ***2019***, *98*, e14554–e14554. **IF: 1.889**

Personal contribution - published papers:

Doroftei, **B**.; Cumpata, S.; Nemtanu, L.; Ilie, O.; Ivanov, I.; Avasiloaiei, A.; Anton, E.; Mocanu, E.; Maftei, R. First Romanian live birth after Preimplantation Genetic Testing in a couple with Severe Oligospermia determined by Y Chromosome Microdeletions Copy Right@ Ovidiu-Dumitru Ilie. *Am. J. Biomed. Sci. Res.* ***2020***, *9*, 64-70.

Case presentation 1

A 28 year-old female patient and her 30-year-old male partner presented for fertility advice after unsuccessfully trying to conceive for almost 2 years. The initial consultation aimed to assess the medical history of the patients, the potential risk factors, as well as the results of previous investigations. Both patients were submitted to a viral screening for hepatitis and HIV (Ag HBs, Ac HBc, Ac HCV, Anti HIV1+ 2, VDRL), and both tested negative.

For the female patient, a series of clinical and paraclinical investigations were carried out. The physical examination revealed pain in the right flank. Consecutive the evaluation of the genital tract

through ultrasound with 3D/4D reconstruction, the presumptive diagnosis of bilateral hydrosalpinx was established. In order to confirm the diagnosis, the patient underwent laparoscopy.

Further on, the paraclinical investigations involved the determination of endocrine markers (TSH, P4, estradiol, FSH, LH, prolactin), the values ranging between the normal values. The ovarian reserve was assessed and AMH was 9.09 ng/ml.

The TORCH screening (Rubeola IgG, Varicella IgG, Toxoplasma IgM and IgG, Citomegalovirus IgG, Herpes IgG) revealed that the patient tested positive for Citomegalovirus (IgG 245.1 UA/ml), Rubella (IgG anti Rubella 162 UI/ml), Herpes (IgG Herpes I+II 5.46 U/ml).

Additionally, immunological investigations for infectious diseases (Chlamydia IgG + IgA in blood), microbiological investigations (Ureaplasma and Mycoplasma in col) and hematological investigations (hemoleucogram, APTT, fibrinogenemia, 25-OH-vitamin D, coagulogram composed of INR, Quick time) were performed and the results were within normal limits given the sex and age of the patient.

For the partner, semen quality was assessed by performing a spermogram and semen culture. The patient was diagnosed with severe oligospermia (0.2x 106/ml) and asthenozoospermia. Additionally, the sperm fragmentation index was determined through SCSA, the integrity of the sperm DNA being considered moderate according to the result (22.3%).

In light of the information obtained from the anamnesis and the clinical and paraclinical investigations, the medical team decided to recommend a genetic screening for both patients. It consisted in determining the karyotype for the female patient and detecting the microdeletions in the Y chromosome structure for the male patient.

The study was conducted by an interdisciplinary team between 2015 and 2017. The infertility consultation and the medical investigations, as well as the IVF procedure, embryo culture and subsequent embryo biopsy were carried out at the Origyn Fertility Center, Iasi, Romania. The genetic investigations and PGD procedure were performed at the Regional Oncology Institute, the Department of Molecular Biology, in Iasi, Romania. The antenatal routine monitoring of the patient was performed at the Origyn Fertility Center, while the neonatal evaluation was carried out at Clinical Hospital of Obstetrics and Gynecology “Cuza Voda” Iasi, Romania, where the birth took place.

Blood samples from the couple were obtained and the cytogenetic analysis was carried out on *in vitro* cultured peripheral lymphocytes. In the case of the female patient, a total number of 33 metaphases were examined and 4 of them were karyotyped. No chromosomal numerical or structural abnormalities were detected.

DNA extraction and molecular analysis was performed on blood samples from the male patient. Multiplex-PCR method was used with the purpose of identifying the presence of 24 microdeletions in AZFa, AZFb or AZFc loci. The analysis revealed the absence of the following markers: SY153, SY155, SY254, SY255, SPGY, SY277, SY158, SY243, and SY269.

The couple signed a consent form according to the internal ethical protocol of our fertility center regarding the procedures of IMSI and PGD, after being previously counseled by the medical team with respect to the IVF procedure, the risks associated with the OHSS, the probability of obtaining pregnancy, the risks of complications during pregnancy, the necessity of performing the prenatal screening and possible risks associated with the embryo biopsies, the measures to be taken in case of obtaining embryos with genetic disorders, as well as the possibility of cryopreserving the supernumerary embryos obtained following IVF treatment.

The treatment was carried out with GnRH antagonist down-regulated protocol using ganirelix (Orgalutran; Organon, Oss). OS was started on the second day of menstruation with a daily dose of 125 IU of rFSH (Puregon; MSD, Oss) until the 8th day of stimulation. Afterwards, the stimulation was continued with 100IU of rFSH (Puregon; MSD, Oss). Final oocyte maturation was triggered by administration of 0.2mg triptorelin (Diphereline; Ipsen).

The oocyte retrieval was carried out 36 hours afterwards. Subsequently, the oocytes were inseminated using IMSI and the resulting embryos were cultured and monitored until day 3 using a time-lapse system (EmbryoScope, Vitrolife, Denmark). On day 3, the blastomere biopsy was carried out by an embryologist and 7 embryos were biopsied.

Briefly, the embryo biopsy was performed in drops of 20 ml of flushing media containing HEPES-buffered solution (FertiPro, Belgium) under a layer of Mineral Oil (Irvine Scientific). A laser beam (company, details) was used to puncture the zona pellucida, and 1-2 cells were obtained using

embryo biopsy micropipettes. Immediately after the biopsy was carried out, the cells were washed carefully using the same flushing media, placed in Eppendorf PCR microtubes in drops containing 3ml of flushing media. The embryos were subsequently cryopreserved according to published vitrification protocols (Kitazato, Japan) and stored in liquid nitrogen.

The entire genome of the embryos was scanned using the Microarray-CGH technique using the Agilent GenetiSure Pre-Screen test (Agilent Genomics, USA). We have used the Agilent Single Cell Recommended Analysis Method. The embryos were compared with both male and female controls and reports considered only the abnormalities identified in comparison with both controls (larger than 5 Mbases). Smaller variants were considered technical artifacts.

Results and discussions

The analysis of the 7 embryos revealed an affected genotype in 4 of biopsies and a non-affected genotype in 3 of the biopsies. Two of the unaffected embryos were female and one was male (Figures 75,76, 77).

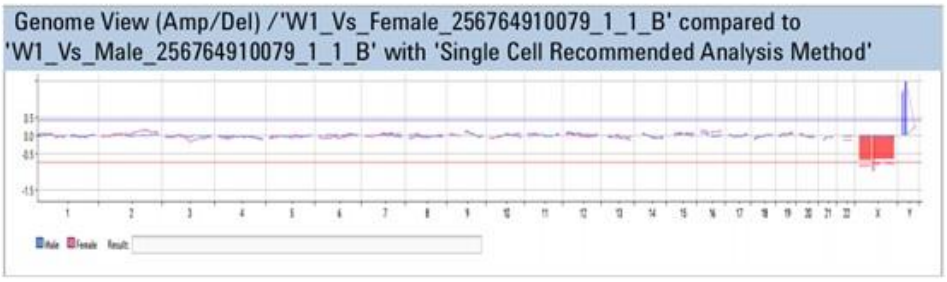

Figure 75. Male embryo, normal genetic analysis

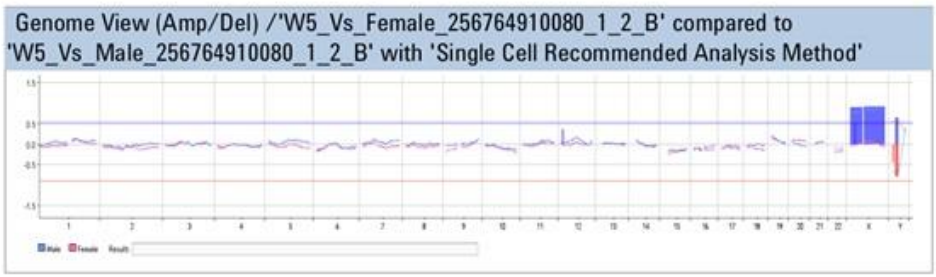

Figure 76. Female embryo, normal genetic analysis

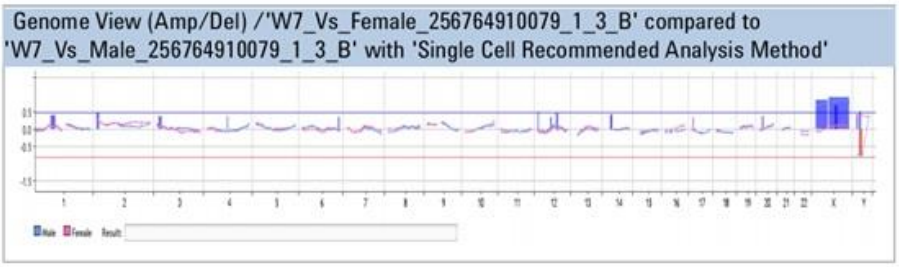

Figure 77. Female embryo, normal genetic analysis (with very small regions of additions but only in comparison with one of the controls female or male)

At the couple's request and considering the reproductive impact of a deleted Y chromosome in a male offspring, it was decided to carry out the transfer of the most suitable female embryo. Embryos W1 and W5 (Figure 75 and 76) were considered good quality, whereas embryo W7 (Figure 77) was only satisfactory due to the presence of very small regions of additions (artefacts). Since from the 3

embryos suitable for transfer, only W5 and W7 were female, we chose number W5 for transfer (Figure 78).

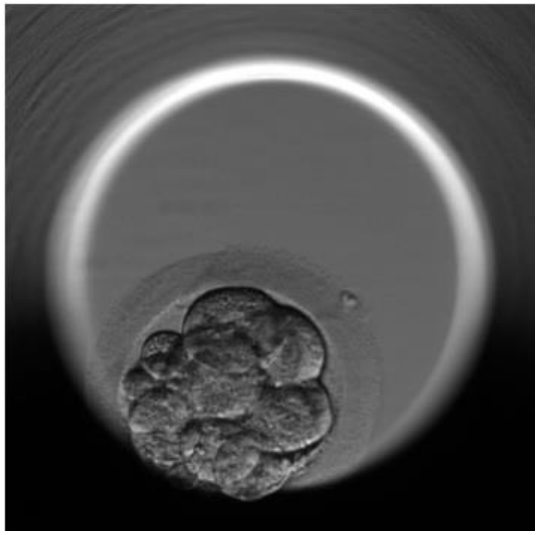

Figure 78. Embryo 4, day 3, Embryoscope image

Embryo W3 (Figure 79), which presented a small addition on chromosome 8 was considered as an alternative for transfer in case the transfer of the aforementioned embryos would fail.

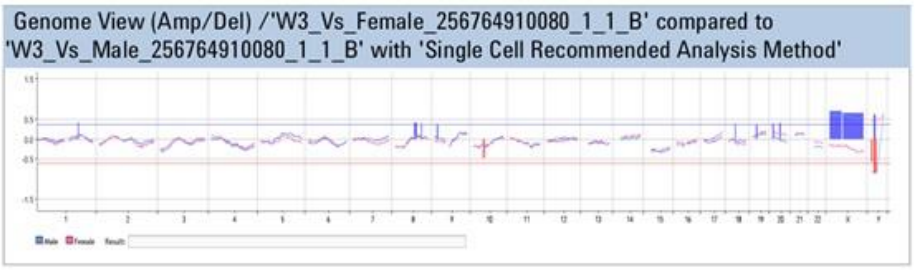

Figure 79. Female embryo with genetic anomalies: add-chr8 q21.2-q22.1 (8.4M)

The other embryos presented multiple abnormalities such as trisomies of chromosomes 2, 10 and 16, and other four chromosomes with large deletion, and/or additions (chromosomes 3, 5, 9 and 11) (Figure 80, 81 and 82).

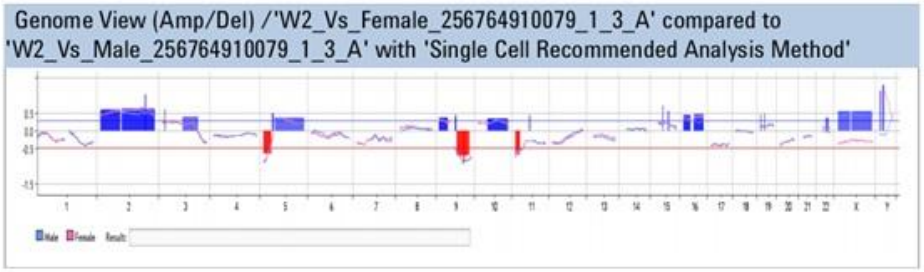

Figure 80. Male embryo with multiple genetic anomalies: add-chr2 p25.3-p11.2; add-chr2 q11.1-q37.3; del-chr5 p15.33-p13.2; add-chr5 p13.1-p11; add-chr9 p24.3-p13.1; add-chr9 q21.11-q21.13; del-chr9 q21.2-q33.3; add-chr10 q11.21-q26.2; del-chr11 p15.5-p14.3; add-chr11 q12.3-q13.2; add-chr16 p13.3-p11.2; add-chr16 q12.1-q24.3

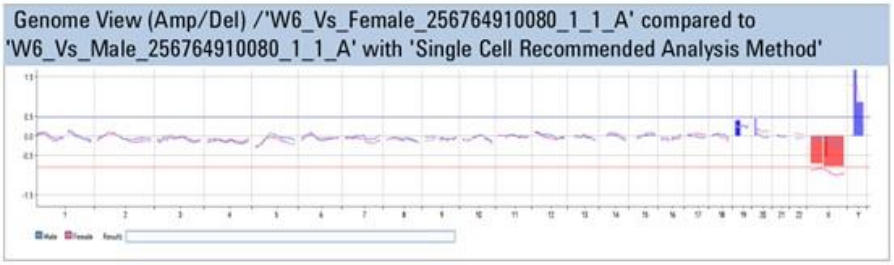

Figure 81. Male embryo with genetic anomalies: add-chr19 p13.3-p12 (23M)

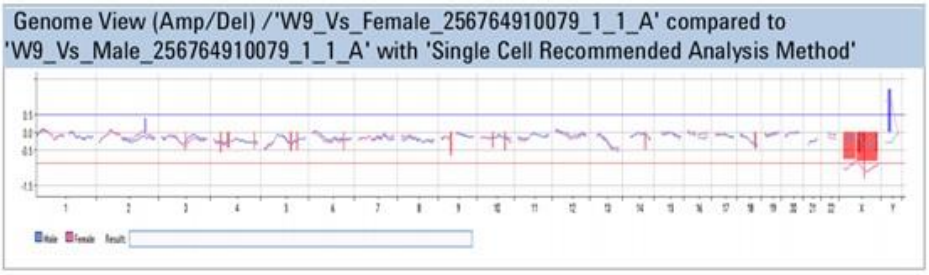

Figure 82. Male embryo with genetic anomalies: del-chr5 q23.1-q23.2 (5.7M) , del-chr9 p13.1-p11.2 (8.2M), del-chr14 q31.1-q31.3 (5.4M)

A hormone replacement therapy was used for ET. Endometrial preparation was initiated in the first day of menstruation with oral estradiol valerate (Cyclo-Progynova; Bayer, Germany) 2mg/t.i.d and a first transvaginal ultrasound was performed in day 10 of the treatment when endometrial thickness was 10mm and from day 11 natural micronized P4 (Utrogestan; Lab. Besins Int., France) was started at a dose of 600mg/day. ET was performed in day 5 of P4 administration. The chosen embryo was thawed, evaluated and transferred, the biochemical pregnancy being confirmed by beta-hCG determination 15 days after the ET. A clinical intrauterine singleton pregnancy was confirmed by ultrasound 21 days post-transfer. Following uncomplicated antenatal care the patient delivered through C-section, at 39 weeks, a female baby, with an APGAR score of 10, weighting 3300 grams. The baby was evaluated by the neonatologist and successfully adapted to extrauterine life.

YCM is a genetic disorder characterised by the absence of certain gene(s) in the Y chromosome. The Y chromosome is composed of a short arm and a long one, which in turn is divided into 3 regions, AZFa, AZFb and AZFc, each of them with a specific role. It has been shown that Y chromosome-related infertility is characterised by azoospermia (absence of spermatozoa) or different forms of oligozoospermia (reduced number of spermatozoa) [735]. According to a study conducted in Romania, the incidence of genetic defects is higher in infertile patients diagnosed with severe oligospermia [736]. Over 60% of microdeletions observed in the structure of the Y chromosome are located in the AZFc region. Since this region is not close to the center of the Y chromosome as the AZFa or AZFb regions, the microdeletions at this level have a less profound impact on sperm production and thereby, some patients diagnosed with AZFc deletions present with a reduced total number of spermatozoa (oligospermia) [737]. The deletions in the AZFc region of the Y chromosome are the most frequent cause of spermatogenic failure that can be defined molecularly [738]. In a couple of studies, it has been revealed that the AZFc deletions are responsible for almost 20% of cases with NOA or severe oligozoospermia [739,740]. Moreover, a recent study revealed that the development of embryos obtained through ICSI from partners diagnosed with AZFc microdeletions and from those without microdeletions was comparable, suggesting that AZFc microdeletions would not affect the outcome of ICSI procedure [741]. Since female offspring inherit only the X chromosome from the father, they are not at risk. It has been suggested that in IVF therapy for couples where the male has a Y deletion, PGD is recommended in order to establish the gender of the embryos and to clarify the presence of the Y chromosome microdeletions. Surprisingly, two recent studies highlighted the probability of obtaining female embryos is higher when using IMSI compared to ICSI.

Therefore IMSI was considered to be the method of choice in the case of this couple [742,743]. Preimplantation screening array comparative genomic hybridization technique is a valuable technique. Since the biopsy is performed using a single cell (third day biopsy) or from a small group of trophoectoderm cells (fifth day biopsy), test results may offer an altered image of the entire embryo.

However, the identification of major chromosomal abnormalities such as trisomy or monosomes (aneuploidy) in embryos with good or very good morphology and with satisfactory evolution confirms that PGT has a defining role in the right and informed choice of the appropriate embryo. We also have to keep in mind that interpreting the results of array comparative genomic hybridization tests should not be rigid, small anomalies that cannot be linked in a clinical context may actually be technical artifacts as they work on an artificially amplified DNA by WGA using MDA technique. It is worth mentioning that for this couple, starting from the cause of infertility (Y microdeletion), it would have been enough to achieve a simpler technique that would highlight the presence of the Y chromosome (fluorescence in situ hybridization or polymerase chain reaction). The array technique brought very valuable information about of the entire genome which resulted in a pregnancy and the birth of a normal girl and the avoidance of embryonic transplants by attempting.

Personal contribution - published papers:

Doroftei, **B**.; Nemtanu, L.; Ilie, O.-D.; Simionescu, G.; Ivanov, I.; Anton, E.; Puiu, M.; Maftei, R. In vitro fertilisation (Ivf) associated with preimplantation genetic testing for monogenic diseases (pgt-m) in a romanian carrier couple for congenital disorder of glycosylation type ia (cdg-ia): A case report. *Genes (Basel).* ***2020****, 11*, 697. **IF: 4.096**

Case presentation 2

A 28-year-old female and her 30-year-old partner were presented within Origyn Fertility Center with a recommendation for genetic counselling - IVF combined with PGT for monogenic diseases (PGT-M) and, respectively, the identification of the c.470T>C and c.385G>A in embryos. The initial consultation aimed to assess the couple's medical history, possible risk factors, as well as the results of the previous investigations.

According to their medical history, the couple previously achieved two spontaneous pregnancies, but, unfortunately, both foetuses died at two and six months after birth. The echographic examination during the first semester was normal, with no visible abnormalities in terms of the length of the long bones and cranial biometry. However, during the second trimester, analogous for both pregnancies, discrepancies were observed regarding the length of the long bones and cranial biometry. Even though the first pregnancy did not require hospitalisation, an admission was necessary at 17 weeks during the second one.

Moreover, with the suspicion of chromosomal abnormalities, an amniocentesis and prenatal screening were recommended. No molecular aneuploidies of chromosomes 13, 18, and 21 were detected.

The third-trimester examination revealed a pronounced discrepancy between the length of the long bones, cranial and abdominal biometrics, and non-immune HF diagnosis. In the case of the second foetus, a massive polyhydramnios was observed.

Considering the medical history and death of the first foetus, a series of extensive genetic investigations were carried out for the second one because of the suspicion of metabolic disease. Although there were suspicions of Gaucher disease (GD), the genetic tests conducted ultimately confirmed that the foetus suffered from the CDG-type 1 syndrome.

The necropsy exam revealed cerebral edema, venous stasis in the kidneys, lungs, and liver. The histopathological examination confirmed the presence of hyperemia in the cerebellum, brain, liver, and lung. The second foetus also displayed foetal abnormalities, such as the persistence of the arterial canal and VSD.

The genetic investigations carried out for the couple have revealed that both of them are carriers for the congenital disorder of glycosylation, with different mutations of the PMM2 gene, more precisely on exon 5 (father) and exon 6 (mother).

In light of the information obtained from the anamnesis, the couple was counselled by an interdisciplinary team in order to undergo an IVF cycle, followed by an embryo biopsy and PGT-M.

The partners were admitted to a viral screening for hepatitis and HIV (HBs Ag, Anti-HBc, Anti HCV, Anti HIV1 + 2, VDRL), both testing negative. Further on, the paraclinical investigations involved the determination of endocrine markers (TSH, progesterone, estradiol, FSH, LH, prolactin), the values ranging between normal limits. The ovarian reserve had been previously assessed by determining the AMH, the result being 0.66 ng/mL. The TORCH screening (Rubeola IgG, Varicella IgG, Toxoplasma IgM and IgG, Cytomegalovirus IgG, Herpes IgG) revealed that the male partner was positive for Cytomegalovirus (IgG 10.2 UA/mL) and Rubella (IgG anti-Rubella 97.1 UI/mL), and negative for Herpes, Toxoplasma, and Listeria.

Additionally, the haematological investigation (hemoleucogram, APTT, fibrinogenemia, 25-OH-vitamin D, coagulogram composed of International Normalized Ratio, Quick time) were performed and the results were in normal limits, according to sex and age. The semen quality was previously evaluated, the results indicating normozoospermia.

According to the internal ethic protocol, the medical team offered comprehensive information regarding the ICSI technique, the possible risks related to OS, the chances of obtaining a pregnancy, as well as the possible risks associated with the embryo biopsy and of PGT. The couples signed an informed consent, according to which a single embryo would be transferred if no genetic abnormalities were detected by PGT-M. In the case of a positive result after PGT-M, the procedure would be ceased.

The treatment was carried out by using a GnRH antagonist protocol. The OS was started on the second day of menstruation, with a daily dose of 200 UI rFSH (Puregon, Merck Sharp & Dohme, NJ, USA) and 150 UI rFSH (Menopur, Merck Sharp & Dohme, NJ, USA) until day 10. The final oocyte maturation was triggered following the administration of 10.000 hCG (Pregnyl, Merck Sharp & Dohme, NJ, USA).

Ultrasound monitoring of the ovarian stimulation revealed a total of 17 follicles, with 14 oocytes being retrieved 36 h after the trigger had been administered. Subsequently, the oocytes were inseminated using ICSI and the resulting embryos were cultured and monitored by a time-lapse system (EmbryoScope, Vitrolife, FertiliTech, Arhus, Denmark) until day 5. A total of 11 oocytes had normal fertilisation, and by day 5, four embryos degenerated. Therefore, seven embryos have been biopsied, three of them on day 5 and the other four on day 6 at blastocysts stage.

Agilent oligonucleotide arrays were used according to the instruction of Agilent GenetiSure Pre-Implantation Array-Based CGH for Aneuploidy Screening (Agilent Technologies, Santa Clara, CA. USA). The DNA amplification step uses a PCR-based method optimised for samples containing 3-10 human cells collected from a day 5 trophectoderm. Two experimental samples were hybridised on the same array and compared to a male and female reference sample co-hybridised to another array on the slide, for a total of 14 experimental samples on one 8 × 60 K slide. The PicoPLEX WGA kit (PicoPLEX WGA Kit; Rubicon Genomics, Ann Arbor, MI, USA), which increases the amount of DNA, was used for the whole genome amplification, as well as for the DNA samples of the female and male reference. The amplified DNA was labelled by random priming using either Cy5-dUTP or Cy3-dUTP. After columns-purification, probes were denatured and pre-annealed with human Cot-1 DNA. Hybridisation was performed using an 8 × 60 K slide at 67°C for 16 h. The array was washed and scanned using the Agilent DNA micro-array scanner and analysed with Feature Extraction Software (Agilent Feature Extraction Software (v10.7), Santa Clara, CA, USA). Subsequently, the results were interpreted with DNA analytics Software.

Of the seven embryos analysed by PGT-M, only three embryos were euploids (Figure 83, 84, and 85), one of which presented compound heterozygosity (PMM2 exon 5 and PMM2 exon 6) (Figure 86), while the other three were simple heterozygotes, one PMM2 exon 5, and the other PMM2 exon 6 (Figure 87, Figure 88, Figure 89). After an interdisciplinary consultation, it was decided to transfer the embryo - the carrier of the mutation on exon 5, c.385G>A.

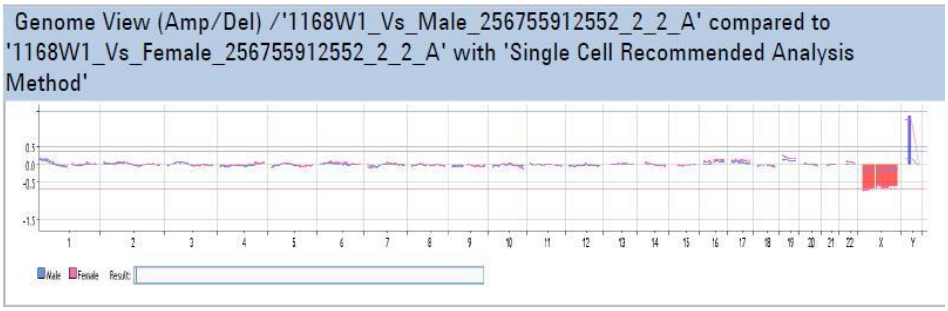

Figure 83. Male embryo, euploid, exon 6, c.470T>C

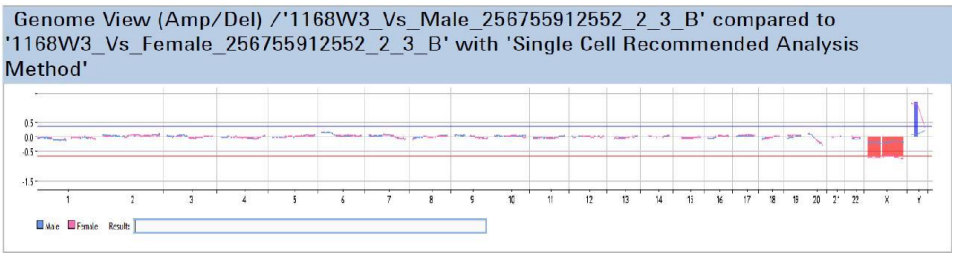

Figure 84. Male embryo, euploid: father mutation on PMM2, exon 5, c.385G>A, and mother mutation on PMM2, exon 6, c.470T>C

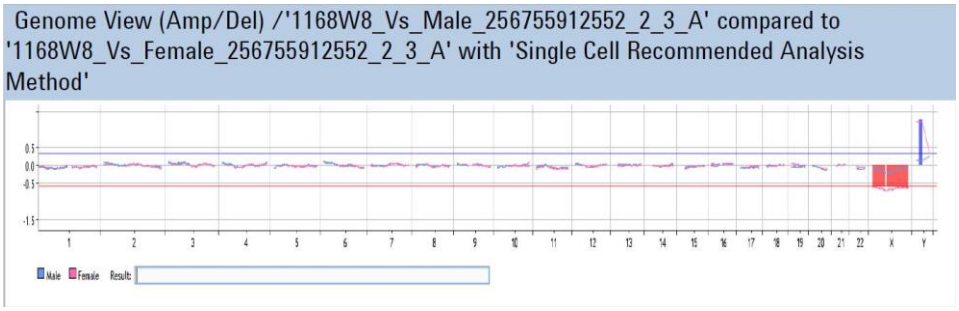

Figure 85. Male embryo, euploid, exon 5, c.385G>A

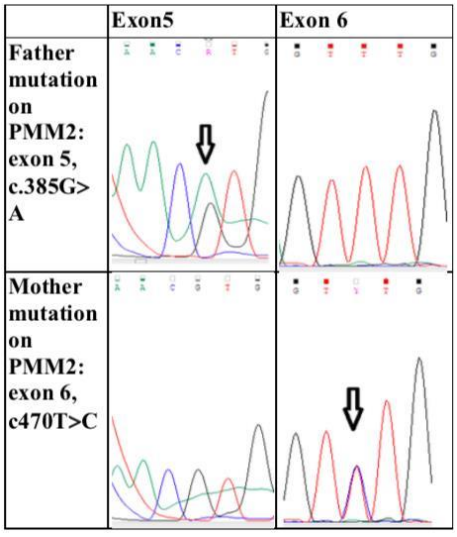

Figure 86. Male embryo with father mutation on PMM2, exon 5, c.385G>A, and mother mutation on PMM2, exon 6, c.470T>C

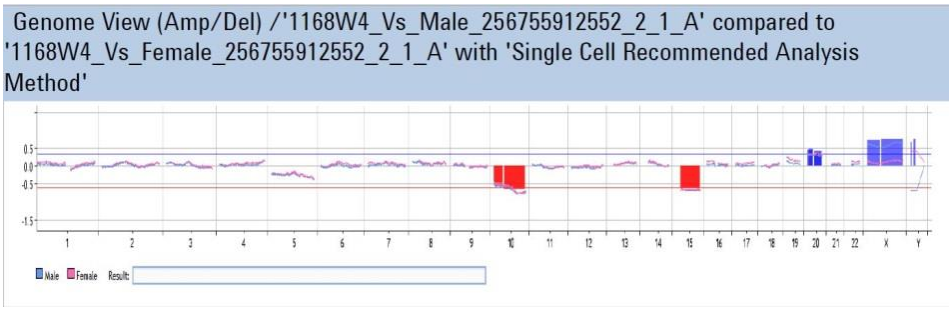

Figure 87. Male embryo, aneuploid, monosomy 10, monosomy 15, trisomy 20

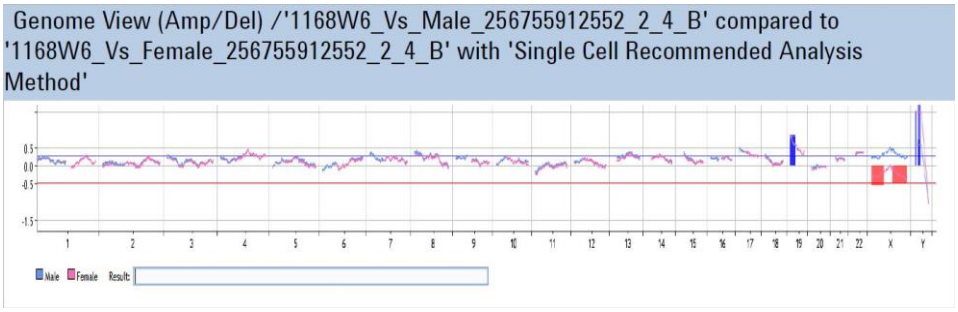

Figure 88. Male embryo, aneuploid, arr. 19p13.3p12(606,030-23,686,458)x3

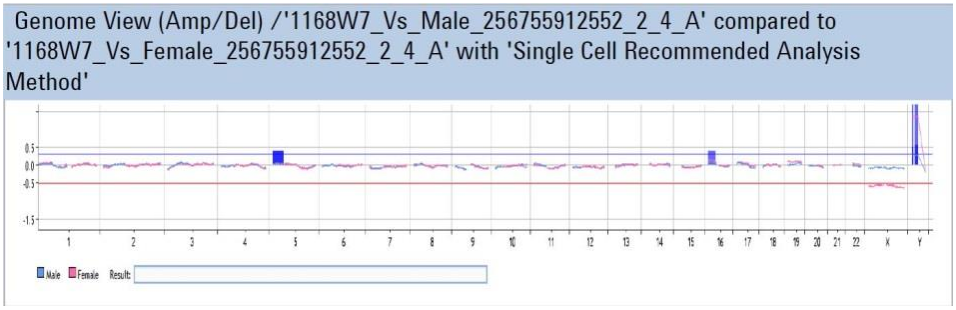

Figure 89. Male embryo, aneuploid, arr. 5p15.33p12(981,535-44,667,248)x3, 16p13.3p11.2(261,626-32,165,798)x3

Prior to the transfer of the chosen embryo, hormone replacement therapy was used. On the first day of the menstrual cycle, the endometrial preparation was initiated by using oral estradiol valerate (Cyclo-Progynova; Bayer Pharma AG, Berlin, Germany) 2 mg/t.i.d and, on day 7, the endometrial thickness was evaluated through a transvaginal ultrasound. Accordingly, 2 mg/q.i.d was prescribed until day 15, and beginning with day 16, natural micronized P4 (Utrogestan; Laboratories Besins International, Paris, France) was started at a dose of 600 mg/day. The chosen embryo (W8) was thawed, evaluated, and transferred on the fifth day of P4 administration. Fifteen days after the ET, a biochemical pregnancy was confirmed by determining the β-hCG, 55.60 mUI/mL. Subsequently, a second β-hCG was carried out 48 h later, the results being 36.75, which indicated that the pregnancy was not developing properly. Eventually, the pregnancy was clinically unconfirmed by ultrasound echography. The patients have discussed the outcome of the procedure with the medical team and it was determined that, in the future, the transfer of the remaining euploid embryos may be attempted.

We obtained ethical approval for this study from the Ethical Committee and the Medical Director of the Origyn Fertility Center. Confidentiality was guaranteed during and after the study. Written informed consent was obtained from the couple for the publication of this case report and any accompanying images.

Discussion

In this case, both partners in were carriers for the CDG-Ia. The first foetus died two months after birth. Imperative for CDG-Ia, the second baby died at six months, the necropsy exam revealing a hyperaccumulation of fluid in the cerebellum, as well as a slow blood flow in the kidneys, lungs, and liver, respectively, and an increased amount of blood in the cerebellum, brain, liver, and lung. Additional abnormalities, such as the persistence of the arterial canal and VSD were also noted.

CDG-Ia is an inborn condition which usually affects every system of organs, its type and magnitude ranging between individuals, even within the same family [744]. Depending on the mutation, there have been identified distinct phenotypes, varying from physical dysmorphism and intellectual disability, to polycystic kidney syndrome and thrombosis [745].

Vega et al., aimed to reveal the molecular pathogenesis using a prokaryotic expression system [704]. With a small group consisting of 22 Spanish PMM2 patients, and the analysis of fourteen nucleotide change, they discovered six loss-of-function proteins, seven having residual activities up to more than 50%, and one normal variant change.

In 9 out of 54 patients, Grünewald et al., [746] observed similar residual activities of proteins in fibroblasts up to 70%. An abnormal transferrin pattern and a high reduced phosphomannomtase activity defined this subgroup. However, a subset of six patients were characterised by reduced phosphomannomtase activity, which proved to be the result of the mutation that occurred in C241S.

Based on study design and methodology, the results obtained by Citro et al., are somewhat antithetical to the previous two studies [747]. They demonstrated that PMM2 was very tolerable to mutations and that the CDG-related phenotype could be the result of mutations occurring in other associated genes(s). One potential inhibitor for missense mutations is CID2876053 (1-(3-chlorophenyl)-3,3-bis(pyridine-2-yl)urea). It has a strong binding affinity for D65Y mutant but also displayed a strong interaction with the I132N, I132T, and 183S [748].

The biochemical parameters tested were in normal limits, according to the results obtained by Casado et al., [749]. However, the cranial MRI revealed distinct particularities in both patients. Both babies were heterozygous, but they had different features regarding the transferrin pattern following the tests performed. The suspicion of PMM2-CDG had been confirmed based on two atypical features such as tremor and the global cerebellar atrophy with vermis hypoplasia.

Considering that CDG-Ia affects several systems of organs, around 20% of infants usually do not survive the first months [750]. Unfortunately, the parents that are carriers for certain mutation(s) often find out when they conceive a child. In our case, the couple found out after the death of their second child.

In our case, we started from the assumption that each unexplained HF could represent a relevant pointer when talking about PMM2-deficiency. Thus, we found it appropriate to summarize the existing literature regarding the accumulation of fluid within the body compartments, as shown in Table 40. Moreover, mutations of ALG1 [751,752], ALG8 [753], Ih [753], and Ix [720], have been also associated with HF, but also with ascites or edema.

Table 40. The outcomes and consequences related to PMM2 gene mutation(s)

PMM2-CDG phenotype	Pregnancy status	Molecular analysis	Reference
Postnatal	Full-term (death at four weeks) and ultrasound echography at twenty gestational weeks	c.691G>A p.Val231Met c.710C>G p.Thr237Arg	[754]
At fifty days	Full-term (death at eight weeks) and ultrasound echography at birth	c.357CNA p.Phe119Leu c.470 TNC p.Phe157Ser	[755]
Both in day two	Birth at thirty-two, respectively thirty-six gestational weeks through Caesarean section. Death at day 7 and an ultrasound echography was carried out at twenty-nine gestational weeks. Death in week eight and an ultrasound echography was carried out at thirty-five	c.160_161insG c.357CNA p.Phe119Leu c.357CNA p.Phe119Leu c.470 TNC p.Phe157Ser	[756]

	gestational weeks		
After birth, before week eight	Siblings - Both birth at thirty-six gestational weeks through Caesarean section and died at three, respectively 8 weeks. Only one ultrasound echography was carried out at thirty-one gestational weeks. Not specified for the other one	c.161_162insG c.385GNT p.Val129L	[757]
Not specified	Full-term from which one died at six years and the third at four months. Not specified for the second infant. An ultrasound echography was carried out at birth for all three	c.357CNA p.Phe119Leu c.422GNA p.Arg141His c.691GNA p.Val231Met c.640-15479CNT c.563ANG p.Asp188Gly c.104 T>A p.Leu35	[758]

As shown in Table 40, HF has been reported in three studies [754,756,757], but it should also be mentioned that skin edema is usually considered the first clinical sign specific to CDG [755,758]. Apart from the previously mentioned clinical signs, pericardial effusion, large heart, thrombocytopenia, and ascites have also been encountered in cases of cardiomegaly [754–758].

Schollen et al., found that, from 92 independent pregnancies, in which both partners were at risk for CDG-Ia, the percentage of affected foetuses was around 34% [759]. This could be explained by the high frequency of the R141H mutation in the PMM2 gene, concluding that the recurrence risk is close to one-in-three in CDG-Ia families.

Unlike the western countries in which such genetic investigations are reimbursed through the public health system [760], for a mid-income country such as Romania, the costs are quite prohibitive. On the other hand, the field of assisted human reproduction has expanded significantly in Romania in recent years, such as by the development of a national IVF program [761].

Based on the established methodology and following the transfer of the frozen embryo(s), only a biochemical pregnancy was obtained, despite our best efforts. Of the six embryos tested, three were euploids, one of which had compound heterozygosity (PMM2 at exon 5 and 6) and the other two were simple heterozygotes (PMM2 at exon 5 and 6). Even if PGT is commonly used in current clinical practice, this is the first case of IVF associated with PGT-M, according to our best of knowledge.

Personal contribution - published papers:

Doroftei, **B**.; Neculai-Valeanu, S.; Simionescu, G.; Grab, D.; Plopa, N.; Anton, E.; Maftei, R. A case report of placental mesenchymal dysplasia: A rare case of a genetically normal fetus with severe intrauterine growth restriction. *Medicine (Baltimore)*. ***2019***, *98*, e14554–e14554. **IF: 1.889**

Case presentation 3

Next, we revisit the case of a 42-year-old woman, Gravida 1, Para 1, who presented to the hospital due to diminished fetal activity in July 2017. Before obtaining this spontaneous pregnancy, the patient was previously diagnosed with a history of almost 10 years of infertility, uterine poly-fibromatosis, hypertension, and obesity grade II. The first ultrasound was performed at 11 weeks and 6 days and revealed a single intrauterine pregnancy. The following parameters were determined during the ultrasound exam: CRL (51.8mm), NL (1.3mm), nasal bone present, and ductus venosus flow (Figure 90).

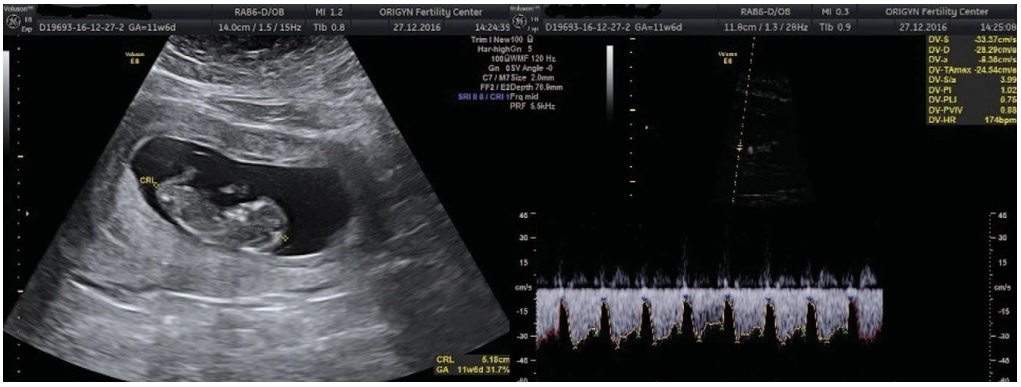

Figure 90. Ultrasound examination at 11 weeks showing a normal appearance of the placenta, normal ductus venosus flow, and CRL corresponding to gestational age

The patient underwent a NIPT and the results were: “low risk”, sex male fetus, and a 4.1% fetal fraction. Further on, the physical examination of the patient revealed that the patient measured 170 cm in height and 113 kg in weight, having a BMI of 39.1. The blood pressure was 140/90mm Hg thereby the patient was advised to undergo a cardiologic examination in order to change the treatment for the pre-existing hypertension. Unlike the second trimester morphology, which was performed at 21 weeks and had normal results, the ultrasound examination performed at 30 weeks showed severe IUGR (780 g) <2.9 percentile, oligoamnios AFI: 7, ductus venosus with a negative wave, umbilical artery with reversed diastolic flow and placentomegaly with multicystic appearance without vascular flow (Figure 91).

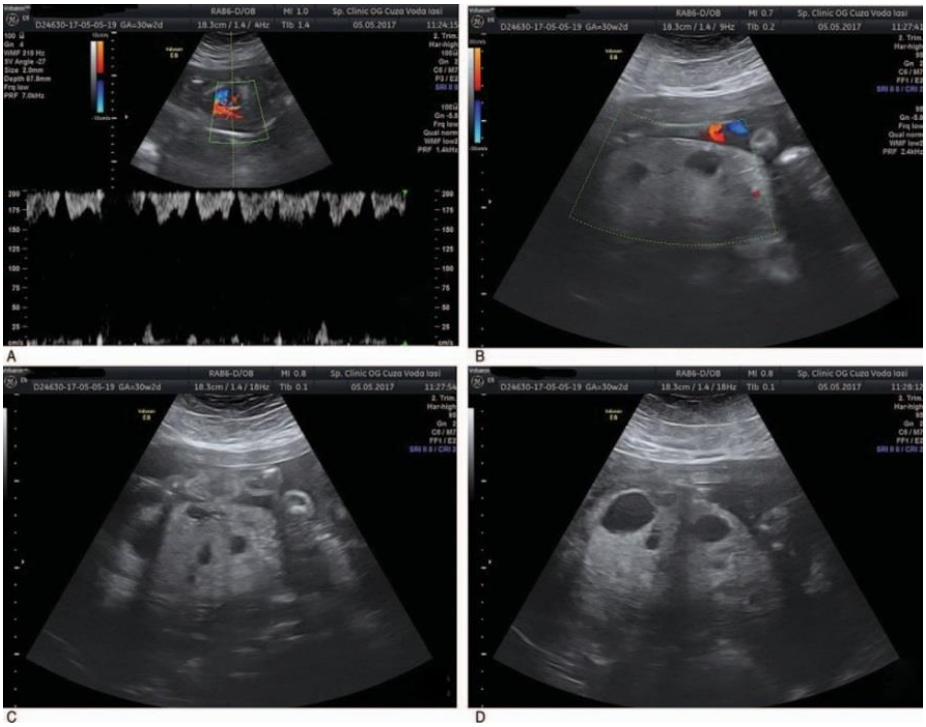

Figure 91. A: ductus venosus with negative a wave; B–D: placentomegaly with multicystic appereance without vascular flow

Due to these findings, the patient was referred as an emergency to the department of obstetrics and gynecology of “Cuza Voda” Clinical Hospital. Upon hospital admission, her blood pressure was 160/110mmHg and the medical team initiated treatment with Dopegyt 1tb/6 h and Nifedipine 1tb/12 h. A non-stress test was performed and revealed low reactivity, thereby an amniocentesis was performed and treatment with dexamethasone 6mg/12 h was initiated. Subsequently, after 48 hours a C-section was performed resulting a male fetus with normal appearance, weighting 700 g,

Appearance, Pulse, Grimace, Activity, Respiration score 3. The result from amniocentesis confirmed the absence of genetic anomalies, but the fetus died 4 days later after a massive ICH. The milestones related to diagnosis and interventions are outlined in Table 41.

Table 41. Important milestones related to diagnosis and interventions

	Time interval	**Diagnosis**	**Intervention/recommendations**
Infertility evaluation	Beginning of 2016	Primary infertility	Nutritional consult for weight loss Hormonal profile Cardiologic evaluation
Pregnancy confirmation	Autumn 2016	Spontaneous pregnancy confirmed at another medical center	Normal pregnancy in evolution
11 weeks of pregnancy	December 2016	Single intrauterine pregnancy, normal development; Noninvasive prenatal test	Cardiologic consult to change the treatment for the pre-existing hypertension (blood pressure was 140/90mmHg). Visit with a nutritionist to monitor the patient's BMI (39.1) The prenatal test results were low risk; male fetus
17 weeks of pregnancy	January 2017	Normal results	Routine checkout; blood pressure under control
Second trimester morphology (performed at 21 weeks)	February 2017	Normal results	
30 weeks checkout	May 2017	Severe IUGR (780 g)	Referred in emergency to the department of obstetrics and gynecology of Cuza Voda Clinical Hospital; blood pressure was 160/110mmHg initiated treatment with Dopegyt 1tb/6 h and Nifedipine 1tb/12 h non-stress test with low reactivity; amniocentesis; initiated treatment with dexamethasone 6mg/12 h was initiated
	48 h after hospital admission	Performed C-section and delivered a male fetus with normal appearance, weighting 700 gs, APGAR score 3	The result from amniocentes is confirmed and genetic anomalies are absent. The fetus died 4 days later after a massive intra-cerebral hemorrhage.

Additionally, the macroscopic evaluation showed that the placenta was markedly enlarged, weighting 680 g and measuring 14X15X4 cm. The umbilical cord was 58 cm long and 1 cm in diameter with 3 vessels. The surfaces of the placenta showed an admixture of normal-looking areas and numerous clusters of grape-like fluid-filled vesicles measuring up to 2.0 cm in diameter (Figure 92).

Figure 92. Gross image of enlarged placenta with multiple grape-like vesicles at maternal surface, especially around the cord insertion

The umbilical cord presented an eccentric insertion. Next, 2 types of villi populations were observed microscopically, a mostly normal for the GA population and the second type of villi was represented by enlarged stem villi with hydropic changes and central cistern formation, with thick-walled vessels at the periphery and myxoid stroma (Figure 93).

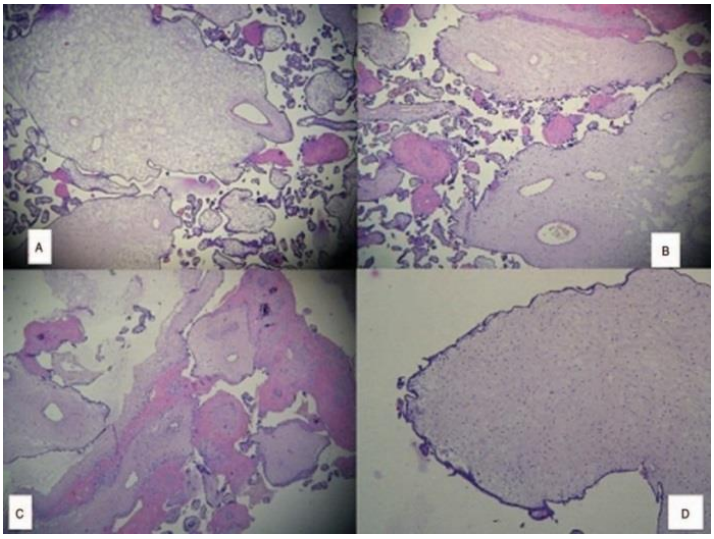

Figure 93. A large, edematous stem villi with central cistern formation and peripheral thick-walled vessels (40x). B, C Stem villus with myxomatous stroma and peripheral distribution of thick-walled vessels, in a mixed background of small normal and dysmature villi (40x). D, A stem villus with increased stromal mesenchymal cells (100x)

Discussion

PMD is a rare benign condition with unknown underlying causes. One hypothesis is that PMD is a congenital malformation of the mesoderm due to mesenchymal hyperplasia in stem villi. The enlarged stem villi contain acid mucopolysaccharide, which is found in the connective tissue layers of the normal chorionic mesoderm [762]. Moreover, the most common karyotype associated with PMD, according to Pham et al., [763] is 46,XX in 82% of cases and 20% of cases also have BWS, but Kaiser-Rogers et al., proposed an androgenetic/biparental mosaicism as the etiological factor [764]. Other types of genetic alterations found in PMD are: 11p15.5, which may affect the expression of IGF-2 [729] and Xp22.31, which is expressed as Vascular Endothelial Growth Factor D (VEGF-D) [763].

The reported incidence of this pathology is of around 0.02% of pregnancies [727] with a preponderance of 3.6-4/1 female/male [765,766]. The sex of the fetus is another particularity of the case. In our case the fetus was normal (46, XY) but Cohen et al., described 3 cases of PMD associated with fetal aneuploidy: trisomy 13 (47,XX, t(1:3) (q32;q32)+ 13), Klinefelter syndrome (47, XXY), and triploidy (69, XXX) [767].

It is highly important to distinguish PMD from a partial mole with an abnormal triploid fetus, because this diagnosis may result in pregnancy termination, while a fetus from a pregnancy with PMD may still develop normally without severe maternal complications. The sonographic features of PMD are very similar to those of partial moles [726] and usually evidenced between 17 and 20 weeks of gestation or sometimes in the third trimester of pregnancy if the progressive development of vascular malformations secondary to circulatory disorders of the dysplastic villi is slow. Sonographic findings of PMD revealed a thickened placenta with multicystic appearance without vascular flow [768]. The umbilical cord anomaly may be found like single umbilical artery, excessively long cord, marked twisted cord, and abnormal insertion like eccentrically insertion which was observed in our case.

The etiology of IUGR includes infections, placental insufficiency and other types of pathology (chorioangioma, PMD), hypertension, genetic anomalies, uterine pathology, and age. In this case, it is very difficult to say the exact etiology of the IUGR because the patient had 4 factors for IUGR: age,

polyfibromatosis, hypertension, and PMD. Late apparition of the growth restriction as well as PMD ultrasound images makes us suspect that PMD was the cause of growth restriction. The exact incidence of IUGR in pregnancies with PMD is unknown. For a small cohort of 11 patients, Pham et al., reported an incidence of IUGR of around 50% and approximately 43% intrauterine fetal demise [763]. According to Faye-Petersen, fetuses and newborns with PMD are at risk for fetomaternal hemorrhage [766], which is also one reason why we suspected that in our case the ICH could be due to PMD rather than prematurity.

Natal and neonatal teeth, also known as dentitia praecox, dens connatalis, congenital teeth, fetal teeth or precocious dentition, have been the subject of research since 59 BC, when Titus Livius first reported such a case [769].

Personal contribution - published papers:

Simionescu, G.; **Doroftei**, **B**.; Cumpata, S.; Nemtanu, L.; Ivanov, I.; Maftei, R.; Grab, D.; Neculai-Valeanu, S.; Anton, E. EMBRYO SELECTION ON MORPHOKINETIC CRITERIA THROUGH TIME-LAPSE TECHNOLOGY ALONG WITH PREIMPLANTATION GENETIC TESTING (PGT) IN A COUPLE WITH RECURRENT PREGNANCY LOSS. CASE REPORT. *Rev. Med. Chir. Soc. Med. Nat., Iaşi* ***2018****, 122*, 807–812.

Case presentation 4

Next, we discuss the case of a couple, a 35-year-old female and a37-year-old male with a history of infertility of almost 15 years. The anamnesis revealed that patients had RPLs in the first trimester, thereby a series of specific investigations, including genetic karyotyping were recommended. A balanced Robertsonian translocation (Tr crs 13,22) 45, XY, der (13,22) (q10; q10) was identified in the male karyotype. In light of this information, patients were referred to genetic counseling and were guided to follow an IVF procedure associated with PGT.

OS was started on 2nd day of the menstrual cycle, using GnRH antagonist ganirelix (Orgalutran, Organon, Oss), after a previous ultrasound assessment and hormonal blood work. Subsequently, hMG 375 IU per day (Menotropine Menopur, Ferring Pharmaceuticals) was administered for the following 9 days. Final oocyte maturation was triggered by administration of 0.2 mg triptorelin (Diphereline; Ipsen). Accordingly, the oocyte retrieval was carried out 37 hours after the administration of the trigger and resulted in 20 eggs (17 M II).

The oocytes were evaluated and inseminated using IMSI and the resulting embryos were cultured and monitored until day 5 using a time-lapse system (EmbryoScope, Vitrolife, Denmark). After that, daily information regarding the embryos was provided by the Embryoscope software by monitoring the morphokinetic parameters and the images of the embryo's development, without removing the cell from controlled environment. Based on the information from by the time-lapse system, the following parameters were assessed for the embryos that reached blastocyst stage and expressed as hours: tPnf; t2; t3; t4; t5; t8; tEB (Table 42).

Table 42. Morphokinetic parameters of embryos cultured in time-lapse system

Embryo	t Pnf	t2	t3	t4	t5	t8	tEB
W2	26.80	30.30	41.80	42.56	50.7	63.75	135.75
W4	25.31	29.20	43.22	46.11	57.21	72.74	120.74
W5	27.06	28.81	43.57	47.43	56.94	72.49	121.50
W7	27.32	30.32	43.07	44.32	59.19	63.77	128.51
W10	28.33	30.33	43.59	45.33	60.96	63.61	110.85

*t 2 = time to 2 cells; t 3 = time to 3 cells; t 4 = time to 4 cells;
t 5 = time to 5 cells; t 8= time to 8 cells; t EB= time to expanded blastocyst

Additionally, the length of the third cell cycle (CC3=t5-t3) and the interval t5-t2, were also calculated, based on a model proposed previously by Basile et al., [770], according to which these two

variables, t5- t2<20.5 hours, respectively 11 hours<CC3<18 hours may be used to predict the probability of selecting chromosomally normal embryos using morphokinetic parameters.

A number of 16 embryos achieved 2 PN stage, however, only 5 blastocysts had the proper quality to be biopsied and frozen. The embryo biopsy was performed by removing cell from the inner cell mass.

The genetic material was amplified with the PicoPLEX® WGA Kit (Rubicon Genomics Rubicon Genomics) as instructed by the manufacturer. Array comparative genomic hybridization was performed on a blade with 8x60,000 (60K) samples covering the whole human genome with a spatial resolution of ~ 5 Mb DNA (G5963A, design ID: 067559, UCSC hg19, GRCh37, February 2009, Agilent). The files obtained from the scan were interpreted with Cyto Genomics software v3.0 from Agilent, using standard cell parameters. The analysis revealed that four of the embryos were abnormal, their transfer being contraindicated. One of the embryos pre- sented a duplication on the region 9p11.2p21.2, as compared to the female reference (Table 43). Since the duplication was small, it was considered to be non-pathogenic.

Table 43. Parameters with defined optimal ranges for ploidy predictionand results from the genetic screening for the biopsied embryos

	Morphokinetic parameters with defined optimal ranges			Aneuploidy Screening
Embryos	t5 (47.2-58.2)	CC3 (11.7-18.2)	t5-t2 (<20.5)	
W2	50.7	12.2	20.39	Arr9p11.2p21.2 (31,127,576-44, 059, 743) x 3
W4	57.21	13.99	28.01	Trisomy 13, Trisomy 16, Trisomy 21
W5	56.94	13.37	28.12	Trisomy 19, Trisomy 22
W7	59.19	16.12	28.87	Trisomy 16
W10	60.96	17.37	30.63	Multiple aneuploidy

A hormone replacement therapy was used for frozen ET, consisting in the administration of oral estradiol valerate (Cyclo-Progynova; Bayer, Germany) 6 mg/t.i.d, from the first day of menstrual cycle. The first transvaginal ultrasound was performed on day 10 of the treatment, when endometrial thickness was 10 mm and from day 11 natural micronized progesterone was started at a dose of 600 mg/day (Utrogestan; Lab. Besins Int., France). ET was performed on day 5 of progesterone administration.

The euploid blastocyst wasted, evaluated and transferred with a soft catheter, under ultrasound guidance. The biochemical pregnancy was confirmed by beta-hCG determination 12 days after the transfer and clinically, by ultrasound, 21 days post-transfer. The pregnancy evolved without obstetrical complications and the baby was delivered at 38 weeks through C-section, with a 9 APGAR score and weighting 3,050 grams. The following neonatal assessments did not reveal any development problems.

Discussion

RPL is a multifactorial disorder that causes significant physical and psychological distress to patients and challenges medical providers engaged in the management of this reproductive health issue [771,772].

According to the guideline developed by ESHRE [773], patients with abnormal karyotype should receive genetic counseling. A study conducted by Ikuma et al., showed that miscarriage rates may be lower when PGT is used along with IVF [774]. The introduction of a new method of embryo selection, called time-lapse monitoring, has been long awaited. Unlike the conventional routine embryo evaluation, the time lapse monitoring of embryos provides a stable micro-climate for embryo culture, certain potentially stressful factors such as variation in temperature or pH being avoided because the embryos are cultured continuously, without being removed from the incubator for daily

routine evaluation [775,776].

A study conducted by Rubio et al., showed that embryos cultured in the Embryo Scope® system have a higher implantation potential and are associated with lower rates of early pregnancy loss, one of the possible explanations being the more stable culture environment, which ensures a better protection against OS [777]. Furthermore, studiesconducted by Campbell et al., [777], Basile et al., [770], Chawla et al., [778], concluded that the kinetic pattern differs among chromosomally normal and abnormal embryos, euploid embryos having a more defined pattern. Additionally, a study conducted by Del Carmen Nogales et al., showed that the subtypes of chromosomal abnormalities such as complex aneuploidy exhibit modified morpho kinetics parameters (t3 and t5) [779].

In our case study, only the morphokinetic parameters registered for the embryo selected for transfer (W2), were in the optimum interval proposed by Basile [770]. However, due to the limited number of analyzed embryos, no statistical analysis was performed to reveal any significant statistical differences as compared to the other embryos which were identified as aneuploid with PGT. Nevertheless, there is evidence showing that morphokinetic parameters may reflect the implantation potential of embryos, significant increased pregnancy and live birth rate, as well as reduced early pregnancy loss being observed when embryos classified as low risk were transferred [780–783].

Embryo-selection by morphokinetics criteria-time lapse imaging, may be considered as a complementary method and an option for those couples with multiple implantation failure, especially in those clinics where PGT is not available, the procedure is forbidden by law or to reduce costs associated with this procedure.

To conclude, in the era of human assisted reproduction, state of the art biotechnologies such as time-lapse embryo monitoring and PGT should be use in synergy in order to complement the overall picture and enhance the process of decision making in the quest of obtaining a healthy offspring.

Personal contribution - published papers:

Anton, E.; **Doroftei, B**.; Grab, D.; Forna, N.; Tomida, M.; Nicolaiciuc, O.S.; Simionescu, G.; Ancuta, E.; Plopa, N.; Maftei, R.; et al. Natal and Neonatal Teeth: A Case Report and Mecanistical Perspective. *Healthc.* ***2020***, *8*, 539. **IF: 2.645**

Case presentation 5

A female newborn baby was thoroughly examined by a neonatologist at the "Cuza Vodă" Maternity Hospital in Iași six hours after birth due to difficulty of breastfeeding and presence of two tooth-like structures on the lower jaw. According to the medical records, the patient was delivered at full term, vaginally, without any perinatal complication, weighing 3,700 g at birth. The pregnancy was monitored from the beginning, without any complications. Except obesity (BMI: 35.4 kg/m2) and PCOS, the mother of the infant had no other personal pathological history. Also, the mother did not take any edication during pregnancy except for vitamins. No other relatives had had natal/neonatal teeth. All ethical aspects regarding this case were strictly respected: written consent was obtained from both parents regarding participation in the present case report.

The examination of the baby's oral cavity revealed two tooth-like structures covered by gingival tissue, in the anterior mandibular region, at the lower central incisor position (Figure 94).

Figure 94. Two-day-old female infant with natal teeth

The remaining gum pads, tongue and intraoral mucosa appeared normal. According to Miller's classification of mobility, the clinical condition was natal teeth with grade II mobility, while the appearance was categorized according to Hebling's classification into category number 4. Two days later, the newborn was referred to the Department of Oral and Maxillofacial Surgery at "Sf. Spiridon" University Hospital and "Grigore T. Popa" University of Medicine and Pharmacy in Iasi, Romania. After a complete examination, the care plan proposed by the medical team included a radiographic exam of the gingival area and teeth extraction, taking into consideration Miller's classification and the high risk of aspiration. Subsequently, the plan of treatment was comprehensively explained to the parents, but written consent was obtained only for the extraction and not for the radiographic exam. The two natal teeth were extracted with extraction forceps under topical anesthesia which was well tolerated by the patient.

The shape, size and color of the two teeth were similar to normal teeth (Figure 95).

Figure 95. Extracted natal teeth

Curettage of the socket was performed to prevent ongoing development of cells of the dental papilla (Figure 96). Postoperatively, there were no complications such as bleeding or infection. Instructions of oral hygiene for the newborn baby were given to the mother and, upon re-evaluation two days later, the wound was found to be healed. Therefore, the mother was allowed to resume breastfeeding.

Figure 96. Postoperative site

The child developed normally, however, the two-year post-extraction examination revealed the presence of all age-specific teeth with the exception of the mandibular central incisors, suggesting that the extirpated natal teeth were actually part of temporary dentition. Additionally, instead of the lower left temporary central incisor, a residual tooth-like structure with solid and immobile aspect was observed, most likely due to the ongoing development of dental papilla cells. Furthermore, it could be seen that a tooth-like structure instead of the lower left temporary central incisor, and no considerable space loss occurred following the extraction (Figure 97).

Figure 97. Clinical follow-up done after two years

Discussion

The presence of teeth on newborn babies is uncommon and, as such, this phenomenon is linked tovarious myths in many cultures. For example, in British culture, it is believed that infants born with natal teeth would become popular warriors, whereas those infants are considered to be bearers of misfortune in China, India and Poland. They are predicted to be the world's potential conquerors in France and Italy, because, apparently, historical figures such as Napoleon Bonaparte and Julius Caesar were born with this condition [784].

This specific condition is usually diagnosed at birth during the general inspection performed by the neonatologist. With regard to the causes and risk factors associated with natal teeth, there is no evident or established single cause. Researchers have incriminated various hypothetical causes such as infection (congenital syphilis), osteoblastic activity in the germ region, congenital syndromes, maternal exposure to environmental toxins (polychlorinated biphenyls and dibenzofurans), febrile episodes during pregnancy and nutritional deficiency (hypovitaminosis) [785]. Another cause of this condition is thought to be endocrine disturbances in the mother's body due to excessive secretions of the pituitary, thyroid or gonad. Yet, the most acceptable theory is the one postulated by Hal in 1957, according to which presence of natal/neonatal teeth is due to superficial position of the tooth germ [786]. This implies that the tooth is not located in an alveolus, but below the surface of the alveolar bone, above the germ of the permanent successor. Furthermore, this theory was demonstrated by Boyd and Miles on the mandibular anatomical sections of a stillborn fetus [787]. Therefore, this unusual location predisposes the tooth to erupt earlier and is related to a hereditary factor [788]. Another paper that confirmed this hypothesis was a study led by Kates et al., in 1984 [789]. These researchers found that 7 out of 38 infants with natal/neonatal teeth had a family history of natal or neonatal teeth: two siblings, one mother, three paternal grandfathers and one paternal grandmother.

On the other hand, Štamfelj et al., examined the size, ultrastructure and microhardness of two natal teeth without permanent successor germs, extracted from a female patient when she was 7 years old. This group of researchers compared the characteristics of both natal teeth and normal primary teeth, and concluded that the natal teeth were prematurely erupted regular primary mandibular incisors. They related the occurrence of natal teeth, associated with agenesis of their primary successors, to an accelerated or premature pattern of dental development, rather than to superficial positioning of the teeth germs [790].

Regarding the shape of natal/neonatal teeth, they are frequently smaller and more conical compared to normal temporary teeth [791]. Additionally, their color is often yellow or white but they might represent hypoplastic enamel accompanied by poorly developed or even absent root [792]. A conical shape has been found in 40% of the natal/neonatal teeth and hypoplastic enamel and dentin in 10% of the natal/neonatal teeth [793]. The presence of hypoplastic enamel on natal/neonatal teeth might be explained by immature enamel which is not able to complete its development as soon as the gingival coating disappears and subsequently the underdeveloped enamel starts deteriorating [789]. Specifically, when the enamel becomes unprotected, it generally turns into a yellow-brown color and keeps breaking down as long as it remains exposed [794]. Moreover, the available data from the literature show that the natal/neonatal teeth come in pairs in different percentages varying from study to study, from 38% to 43.3% to 76% [789,792,794]. The shape, size and color of the two natal teeth in

our case report were similar to normal teeth with no hypoplastic enamel and dentin. The plausible reason why the teeth from our case report were whitish is that these teeth were protected by the gingival coating until extraction.

Regarding the gender differences, the available literature shows that more females are affected by natal/neonatal teeth (63.3%) compared to males [789,795,796]. However, no significant differences between males and females are found in the literature regarding natal/neonatal tooth morphology, positive family history or complications [793].

In the literature, numerous congenital syndromes are considered to be associated with natal/neonatal teeth [797–799]. A thorough examination of the available literature shows that the most common congenital syndromes correlated with natal or neonatal teeth are: Ellis-van Creveld, Jadassohn-Lewandowsky, Hallermann-Streiff, Rubinstein-Taybi, steatocystoma multiplex, Pfeiffer, craniofacial dysostosis and adrenogenital syndromes [797–799]. In addition, natal and neonatal teeth are more frequent in children with cleft lip than among the general population [800]. It is important to be mentioned that the patient from our case report was not associated with any anomalies or syndromes.

The most common complication of natal teeth is the ulceration of the tongue's ventral surface, or Riga-Fede disease, which is the result of repetitive trauma of the area [801]. This condition leads to difficulty in feeding or refusal to feed because of the pain. Other complications may include: potential risk of swallowing and aspiration of tooth, due to its great mobility, injuries to the mother's breast and apical abscesses.

Therefore, it is essential to perform a radiographic examination to establish if these natal/neonatal teeth are components of normal dentition or are supernumerary, to determine the amount of root development and to establish differential diagnosis. Bohn's nodules and congenital epulis might be confused with natal teeth. Another advantage of radiography is that it may reveal the relationship between the natal teeth and adjacent teeth. The care plan should be formulated with proper regard for the need to ensure normal dental occlusion.

In addition, factors such as implantation and degree of mobility, breastfeeding interference and the possibility of dislocation followed by swallowing or aspiration of these teeth should be taken into consideration when establishing the treatment plan. Over the years, various management methods of natal teeth have been proposed. For example, in 2010, Padmanabhan et al., recommended that the incisal edges of the natal or neonatal teeth be grinded or smoothed with an abrasive instrument, to prevent the injury of the maternal breast [802]. Moreover, Choi et al., reported rapid healing of a sublingual traumatic ulceration after applying composite resin over the affected teeth [803]. However, this procedure might be limited due to a reduced surface area of enamel available for resin bonding and the expected lack of cooperation from the infant.

Consequently, extraction of these teeth is preferred and should be performed if the teeth are supernumerary or if the teeth are extremely mobile, due to the potential complications mentioned above. However, some authors suggest that natal teeth should be extracted only if they belong to Hebling's category number 1 or 2 and the degree of mobility is more than 2 mm [804]. According to Hebling and Zuanon, if the teeth are components of normal dentition, premature extraction may cause a loss of space and collapse of the developing mandibular arch. Contrary to this, in a study conducted in Hong Kong on 48 children, 56 out of 72 natal teeth were removed with no appreciable space loss occurred following the extractions [805]. Due to high mobility, extraction of these teeth may be done with a forceps or even with the fingers. The fourth category of natal teeth in Hebling's classification, represented by natal teeth covered by gingival mucosa, is less likely to generate complications such as aspiration or swallowing of the teeth. Although, during breastfeeding the thin layer of gingival mucosa may get traumatized, exposing the mobile teeth and therefore may increase the risk for the tooth to be dislodged and inhaled or swallowed by the infant.

Another important risk is represented by possible local hemorrhage. The risk of hemorrhage is directly proportional to the degree of mobility of the natal teeth, so the more mobile the tooth is, the lower the risk of hemorrhage. The American Academy of Pediatrics advises that a single intramuscular dosage of 0.5 to 1 mg of vitamin K should be administered to all newborn babies before extraction, since it is essential for the formation of clots at the extraction site [806]. In the standard Romanian protocol and in our practice every newborn receives a prophylactic dose of vitamin K a few hours after birth. Usually, this vitamin is synthesized by bacteria in the large intestine and since

commensal intestinal flora will not have been formed until the infant is 10 days old, extraction below this age is regularly associated with an increased hemorrhage risk. However, it is the doctor's choice whether to administer prophylactic vitamin K before extraction or not, although it is standard procedure in most of the hospitals to perform a single intramuscular dose of vitamin K immediately after birth [807].

The extraction of the natal teeth should be followed by a gentle curettage of the socket to remove the underlying dental papilla and Hertwig's epithelial root sheath [808]. Failure to curette the socket may cause an ongoing development of the cells of the dental papilla, which may result in eruption of tooth-like structures several months later, referred to by Tsubone et al., as "residual natal tooth" [809]. According to King and Lee (1998), the risk of residual tooth formation is approximately 9.1%. In these cases, if residual tooth formation develops, a second surgical procedure is required [810]. Lately, there is a tendency for much clearer management in the cases of prematurely erupted teeth in newborns [811]. These aspects could bear revelance with regard to the connections between dental, neuropsychiatric and GI processes, having for example OS and other complex factors in the center of these manifestations [811].

Regarding the limitations of our study, we can mention here the lack of intra-oral radiographs, since no written consent was obtained for the radiographic exam.

Legal provisions

The legal implications of these methods can be the subject matter of some debates between lawyers and practitioners specialized in reproductive medicine. In Romania, at the moment, there are no legal norms clearly regulating the status of reproductive medicine, although the number of specialized clinics is increasing. The PGD is not widely spread in Romania. Who can decide when the PGD is recommended and under which conditions? The European member states have various regulations for this matter. Some states totally forbid these procedures, other states partially agree on observing medical directions, and some states are more permissive [812]. The most permissive legislations are to be found in the United Kingdom, Sweden, Denmark, France and Norway. The more restrictive states are those with a Catholic majority, such as Austria, Germany and Switzerland, where a PGD for nonmedical purposes is sanctioned by the Criminal Code. In Germany, since early 1990 there is a normative act, "Embryo Protection Act" regulating the genetic diagnosis. Countries in which the PGD is not regulated and it is permitted are: Belgium, Cyprus, Finland, Greece, Netherlands, and Portugal, Spain. However, there is certainly an increasing demand for such kind of medical services. The solution adopted by couples is that of carrying out the PGD procedures in countries where the legislation allows it. Thus, "medical tourism" emerges, as in other medical fieldss. That is the reason why it is absolutely necessary that in Romania the legislator should present the legal framework under which these medical procedures can be carried out.

Legal provision of health reproduction allowing PGD can prevent widespread, questionable, unregulated practice. The medical directions in cases of X-linked genetic diseases are unanimously accepted. The medical ethics of the subject tackled in this article implies several points of view. Is the selection of embryo sex acceptable in the case of X-linked transmissible genetic diseases? Starting from the premise that the medicine and the medical progress are in the benefit of the individual and of the society he belongs to, the selection of a female embryo that certainly should not be affected by Duchenne muscular dystrophy (DMD) can be accepted. The extension of these directions to the aneuploids' screening can also be accepted. Embryo screening for mutations on tumor protein p53 or breast cancer 1 (BRCA1) and breast cancer 2 (BRCA2) genes should be encouraged, due to the fact that, in this way, the emergence of a neoplasic process with unknown outbreak, later affecting the individual health state, would be prevented. A number of tests can be used to screen for Down syndrome (DS), with varying levels of accuracy and invasiveness. Several blood markers can be measured that can be used as part of combined tests to predict the risk of Down syndrome. Abortion after 12 weeks and called therapeutic abortion may be performed only due to precise medical cause. Down syndrome is not included in the categories of conditions that justify interruption of the pregnancy by therapeutic grounds. Still, most parents decide the interruption of the pregnancy in the case of finding out about the probability of having a child with Down syndrome.

In 2001, Verlinsky et al., reported the first PGD combined with HLA patterns in order to obtain a healthy child and an identical HLA with the sister affected by FA [813]. The "baby design" concept has thus been created. The French law that permitted the PGD under the condition of genetic affectation of a parent extends through Law 2131-4-1/August 2004 Act, the applicability area of the method and to obtain an embryo that later, at birth, will be a donor for hematopoetic stem cells [814].

The restrictive terms of a judicial norm can largely limit the development and the applicability area of the method. The development of this method is going to be carried out mainly in countries with permissive legislation. Legislation will thus play a key role in developing and improving the human life.

The medical act ethics will certainly reject the idea of "baby design", but can anyone decide the destiny of a child affected by one of the following disorders: Fanconi anemia (FA), thalassemia, Wiscott-Aldrich syndrome (WAS), leukemia, Diamond-Blackfan aplastic anemia (DBA), where it was demonstrated that the hematopoetic stem cells transplant with identical HLA compatibility is the only treatment method available [815]? Unfortunately, in Romania, there is legislative void on this matter. The current Romanian judicial norms refer only to the authorization process of some medical units providing medical services of assisted human reproduction. The sex selection of the first child "social sex selection" has not yet appealed to many couples in Romania. A questionnaire-based survey carried out on a group of senior medical students showed that the idea of selecting the sex of the future child was accepted by less than 10% of them.

The only legal norms applicable in Romania for IVF procedures are the national Law 71/2011 and Order no. 860/2013, the European Directive 23/2004/EC of the European Parliament and of the Council4, the Commission Directive 17/2006/EC, and the Commission Directive 2006/86/EC related to donation and transplantation of organs, tissues and cells of human origin.

Overall, there is a list of inclusion criteria stated by the Order of the Minister of Health no. 386/2015, the eligibility of a couple for applying to the program being largely determined by a series of mandatory analyzes the partners have to perform. There are 6 major inclusion criteria, which are briefly listed as follows: the couple should have an indication from a specialist in human assisted reproduction techniques, both partners should possess health insurance, the age of the female patient should be between 24 and 40 years, the BMI should range between 20 and 25 and the ovarian reserve, as measured by the AMH should be minimum 1.1 ng/ml.

In 2016, The Ministry of Health allocated around 2,000,000 RON for this program, which could cover about 330 fertilization procedures, while the estimated number of IVF procedures performed annually in Romania is around 2000. It is worth mentioning that the data is reported voluntarily by the Romanian IVF clinics to an international organism such as ESHRE, and there is no national authority or framework that collects clinical data in order to conduct careful analysis and monitor of the quality of IVF practice [761].

Nevertheless, the participation of IVF clinics in the national IVF program is conditioned by a minimum threshold of 30% successful outcomes. Moreover, this public financial support does not cover the costs of hormonal treatment necessary for ovarian hyperstimulation, nor other medical investigations needed to diagnose infertility or procedures designed to improve their chances of achieving pregnancy, such as ICSI or assisted hatching. Although controversial in some countries, the genetic screening of the embryos is legal to perform in Romania [694], but it is not financially supported by National Program for IVF and ET. Therefore, couples with a history of genetic disorders or recurrent failed implantation have to bear the costs of such investigations themselves.

Through the National Program of IVF and ET, only one IVF procedure is financed per person, while in other countries such as Belgium, France or Germany up to 6 procedures are publicly funded per medically ensured citizen [816]. This raises another ethical concern, since couple who fail in one IVF attempt may not afford to carry out another procedure, so they may justifiably feel that their fundamental right to procreation is infringed.

In economically developed and developing countries across Europe there is currently an upward trend in postponing procreation [817] in spite of the alarm signals drawn by doctors specialized in assisted reproduction, according to whom fertility decreases vertiginously with age. Unfortunately, many women become more and more aware that later is not necessarily better, at least not when it comes to reproduction. Because the ovarian reserve decreases rapidly with age, as can be established by determining the AMH, the chances of conceiving naturally also diminish vertiginously

with each passing year of life [615].

Concurrently, the cultural and social climate has wide implications such as due to religious beliefs. In Romania, 85% of the population is Christian-Orthodox, and the Orthodox Church has been reluctant to accept these assisted reproductive procedures, currently considering the use of oocytes or sperm from donors as adultery , and embryo reduction a form of abortion.

To identify the factors leading to change or to resistance to change, we will examine the correlations between the most influential institutions and people's behavior and perceptions related to procreation. According to the Eurobarometer reports 68.2 and 72, Romanian people place most trust in the Church and in television. These two institutions exert a great deal of social influence on the way Romanian people relate to the issues and realities of the day and future.

The public messaging of the Romanian Orthodox Church has been explicitly for or against medical practice in no subtle terms. It is noteworthy that the Bioethical Commission of the Romanian Orthodox Church considers the practice of tissue and organ transplantation as one of the highest forms of contemporary medical practice, which transforms pain into hope for longer life. The Church blesses medical practice where transplant can transform a health crisis into the opportunity to restore a person back to normal life, but without taking life away from another. Nobody should be killed so that somebody else should live[818], and this includes the unborn - the same document contains one reference to human embryos as unacceptable, since the embryo, although a living being, is incapable of expressing consent.

Therefore, the Romanian Orthodox Church indirectly and tacitly displays a certain degree of tolerance towards new technologies in the field. On the other hand, the Romanian Orthodox Church has taken a firm position against abortion, but, despite this, abortion is legal in Romania. Interestingly, abortions rates from this country have declined in comparison with prior decades. From a religious point of view, abortion is a capital sin, but, on a more general level, it is also a consequence of the direct effects of the precarious economic and social conditions which do not foster family policies enough. History has taught us that restrictive norms and legislation do not yield the expected results.

Considering the relatively tolerant attitude of the Romanian Orthodox Church towards ART and its very influential power, we are tempted to assume that the religious traditionalism specific to this country is not a primordial factor leading to the delay of regulation in the MAR field. On the contrary, the continuous bombardment with ART-related news from the Romanian mass-media devalue these techniques by attributing negative connotations to them, constantly reiterating the bioethical issues related to reproductive tourism, commercialization of human gametes and mercantile gestation. This leads us to believe that public opinion may have selectively and distortedly retained mass-media information related to assisted reproduction, and this contributes to the general population's resistance to change. A connection between perception and behavior is noticeable with regard to ART. Overall, Romanian society is a conformist and imitative society, so it is common for individuals to align their opinions to group and societal norms, and ART is a good example of that. The overwhelming majority of the people who do not have fertility problems become a reference group and, since they do not need to resort to assisted reproduction services to procreate, "ART may not fit into their ideological definition of family". While the infertile population constitutes a dispersed and stigmatized minority, the majority is inoculated with mass-media messages or maintains a passive attitude to these matters.

Public debates launched by the Ministry of Health are practically inexistent, even if the Oviedo Convention urges that a legislative project in human reproduction field be accompanied by such debates. The reality is that, according to the National Transplant Agency, between 2009 and 2011, some 10,105 couples received assisted reproduction procedures with partner donation, and 898 patients received assisted reproduction procedures with the involvement of a donor. The increasing number of couples who resort to ART treatments to conceive underlines the fact that the population affected by infertility is becoming conscious of the fact that ART is a pertinent solution to their health problem. In contrast, Eurobarometer 72 showed the Romanian population perceives national political institutions with the lowest confidence level among other official authorities and demonstrates discontent towards the inability to provide and implement prompt solutions for the current social and economic problems. It is clear that political structures have not mobilized sufficiently to produce a law for the field of assisted reproduction in alignment with existing democratic, ethical and socio cultural values which ensure equal access to reproductive health-care services.

Personal contribution - published papers:

(ESHRE), T.E.I.-M.C. (EIM) for the E.S. of H.R. and E.; Calhaz-Jorge, C.; de Geyter, C.; Kupka, M.S.; de Mouzon, J.; Erb, K.; Mocanu, E.; Motrenko, T.; Scaravelli, G.; Wyns, C.; et al. Assisted reproductive technology in Europe, 2012: results generated from European registers by ESHRE†. *Hum. Reprod.* ***2016****, 31,* 1638–1652. **IF: 6.918**

Study question:

The 16th EIM report presents the data of the treatments involving ART and IUI initiated in Europe during 2012: are there any changes compared to previous years?

Summary answer:

Despite some fluctuations in the number of countries reporting data, the overall number of ART cycles has continued to increase year by year, the pregnancy rates in 2012 remained stable compared with those reported in 2011, and the number of transfers with multiple embryos (3+) and the multiple DRs were lower than ever before.

What is known:

Since 1997, ART data in Europe have been collected and reported in 15 manuscripts, published in Human Reproduction.

Study design, size, duration:

Retrospective data collection of European ART data by the EIM Consortium for the ESHRE. Data for cycles performed between 1 January and 31 December 2012 were collected from National Registers and from individual clinics and organisations on a voluntary basis.

Participants/materials, setting, methods:

1,111 clinics from 34 countries (+1 compared with 2011) reported 640,144 treatment cycles, including 139,978 IVF, 312,600 ICSI, 139,558 FER, 33,605 ED, 421 IVM, 8,433 PGD/PGS, and 5,549 FOR. European data on IUI using husband/partner's semen and donor semen were reported by 1,126 IUI labs in 24 countries. A total of 175,028 IUI-H and 43,497 IUI-D cycles were included in the analysis.

Main results and the role of chance:

In 18 countries where all clinics reported to the corresponding national ART register, a total of 369,081 ART cycles were performed in a population of around 295 million inhabitants, the equivalent of 1,252 cycles per million inhabitants (range 325-2,732 cycles per million inhabitants). For all IVF cycles, the clinical PRs per aspiration and per transfer were stable with 29.4 (29.1% in 2011) and 33.8% (33.2% in 2011), respectively. For ICSI, the corresponding rates also were stable with 27.8 (27.9% in 2011) and 32.3% (31.8% in 2011). In FER cycles, the PR per thawing/warming increased to 23.1% (21.3% in 2011). In ED cycles, the PR per fresh transfer increased to 48.4% (45.8% in 2011) and to 35.9% (33.6% in 2011) per thawed transfer, while it was 45.1% for transfers after FOR. The DR after IUI remained stable, at 8.5% (8.3% in 2011) after IUI-H and 12.0% (12.2% in 2011) after IUI-D. In IVF and ICSI cycles, 1, 2, 3 and 4+ embryos were transferred in 30.2, 55.4, 13.3 and 1.1% of the cycles, respectively.

The rates of singleton, twin and triplet deliveries after IVF and ICSI (added together) were

82.1%, 17.3%, and 0.6%, respectively, resulting in a total multiple DR of 17.9% compared to 19.2% in 2011 and 20.6% in 2010. In FER cycles, the multiple DR was 12.5% (12.2% twins and 0.3% triplets). Twin and triplet DRs associated with IUI cycles were 9.0% / 0.4% and 7.2% / 0.5%, following treatment with husband and donor semen, respectively.

Limitations, reasons for caution:

The reporting method varies among countries, and registers from a number of countries have been unable to provide some of the relevant data such as initiated cycles and deliveries. As long as data are incomplete and generated through different methods of collection, results should be interpreted with caution.

Wider implications of the findings:

The 16th ESHRE report on ART shows a continuing expansion of the number of treatment cycles in Europe, with more than 640,000 cycles reported in 2012 with an increasing contribution to birthrate in many countries. However, the need to improve and standardize the national registries and to establish validation methodologies remains manifest.

Personal contribution - published papers:

De Geyter, C.; Calhaz-Jorge, C.; Kupka, M.S.; Wyns, C.; Mocanu, E.; Motrenko, T.; Scaravelli, G.; Smeenk, J.; Vidakovic, S.; Goossens, V.; et al. ART in Europe, 2014: results generated from European registries by ESHRE†: The European IVF-monitoring Consortium (EIM)‡ for the European Society of Human Reproduction and Embryology (ESHRE). *Hum. Reprod.* ***2018***, 33, 1586–1601. **IF: 6.918**

Study question:

What are the European trends and developments in ART and IUI in 2014 as compared to previous years?

Summary answer:

The 18th ESHRE report on ART shows a continuing expansion of both treatment numbers in Europe and more variability in treatment modalities resulting in a rising contribution to the birth rates in most participating countries.

What is known:

Since 1997, ART data generated by national registries have been collected, analyzed by the EIM Consortium, and reported in 17 manuscripts published in Human Reproduction.

Study design, size, duration:

Continuous collection of European data by the EIM for ESHRE has been the basis for research. The data for treatments performed in 2014 between 1 January and 31 December in 39 European countries were provided by national registries or on a voluntary basis by clinics or professional societies.

Participants/materials, setting, methods:

1,279 institutions from 39 countries reported offering ART services as follows: a total of 776,556 treatment cycles, of which 146,148 IVF, 362,285 ICSI, 192,027 FER, 15,894 PGT, 56,516 ED, 292 IVM, and 3,404 FOR. European data on IUI using husband/partner's semen and donor semen were reported from 1,364 institutions offering IUI in 26 countries and 21 countries, respectively. A

total of 120,789 treatments with IUI-H and 49,163 treatments with IUI-D were included.

Main results and the role of chance:

In 14 countries (17 in 2013), where all institutions contributed to their respective national registers, a total of 291,235 treatment cycles were performed in a population of ~208 million inhabitants, the equivalent of 1,925 cycles per million inhabitants (range: 423-2978 per million inhabitants). After treatment with IVF the clinical PRs per aspiration and per transfer were marginally higher in 2014 than in 2013, at 29.9% and 35.8% versus 29.6% and 34.5%, respectively. After treatment with ICSI the PR per aspiration and per transfer were also higher than those achieved in 2013 (28.4% and 35.0% versus 27.8% and 32.9%, respectively). After FER with own embryos the PR continued to rise, from 27.0% in 2013 to 27.6% in 2014. After ED a similar trend was observed with PR reaching 50.3% per fresh transfer (49.8% in 2013) and 48.7% for FOR (46.4% in 2013). The DR after IUI remained stable at 8.5% after IUI-H (8.6% in 2013) and at 11.6% after IUI-D (11.1% in 2013). In IVF and ICSI together, 1, 2, 3 and ≥4 embryos were transferred in 34.9, 54.5, 9.9 and in 0.7% of all treatments, respectively (corresponding to 31.4%, 56.3, 11.5% and 1% in 2013). This evolution in ET strategy in both IVF and ICSI resulted in a singleton, twin and triplet DR of 82.5%, 17.0% and 0.5%, respectively (compared to 82.0, 17.5 and 0.5%, respectively, in 2013). Treatments with FER in 2014 resulted in a twin and triplet DR of 12.4 and 0.3%, respectively (versus 12.5% and 0.3% in 2013). Twin and triplet DR after IUI were 9.5% and 0.3%, respectively, after IUI-H (in 2013: 9.5% and 0.6%), and 7.7% and 0.3% after IUI-D (in 2013: 7.5% and 0.3%).

Limitation, reasons for caution:

The method of data collection and reporting varies among European countries. The EIM receives aggregated data from various countries with variable levels of completeness. Registries from a number of countries have failed to provide adequate data about the number of initiated cycles and deliveries. As long as incomplete data are provided, the results should be interpreted with caution.

Wider implications of the findings:

The 18th ESHRE report on ART treatments shows a continuously growing trend across Europe. The number of treatments reported, the variability in treatment modalities and the rising contribution to the birth rates in most participating countries point towards the increasing impact of ART on reproduction in Europe. As this is the largest data collection on ART, the report gives comprehensive information about ongoing developments in the field.

Personal contribution - published papers:

The European IVF-monitoring Consortium (EIM)‡ for the European Society of Human Reproduction and Embryology (ESHRE); Wyns, C.; Bergh, C.; Calhaz-Jorge, C.; De Geyter, C.; Kupka, M.S.; Motrenko, T.; Rugescu, I.; Smeenk, J.; Tandler-Schneider, A.; et al. ART in Europe, 2016: results generated from European registries by ESHRE. *Hum. Reprod. Open.* ***2020***, 3, hoaa032

Study question:

What are the reported data on cycles in ART, IUI, and fertility preservation interventions in 2016 as compared to previous years, as well as the main trends over the years?

Summary answer:

The 20th ESHRE report on ART and IUI shows a progressive increase in reported treatment cycle numbers in Europe, with a decrease in the number of transfers with more than one embryo causing a reduction of multiple DRs, as well as higher pregnancy rates and DR after FER compared to fresh IVF and ICSI cycles, while the outcomes for IUI cycles remained stable.

What is known:

Since 1997, ART aggregated data generated by national registries, clinics or professional societies have been collected, analyzed by the EIM, and reported in 19 manuscripts published in Human Reproduction and Human Reproduction Open.

Study design size duration:

Yearly collection of European medically assisted reproduction data by EIM for ESHRE has been the basis for our analysis. The data on treatments performed between 1 January and 31 December 2016 in 40 European countries were provided by either National Registries or registries based on personal initiatives of medical associations and scientific organizations.

Participants/materials setting methods:

In all, 1,347 clinics offering ART services in 40 countries reported a total of 918,159 treatment cycles, of which 156,002 IVF, 407,222 ICSI, 248,407 FER, 27,069 preimplantation genetic testing, 73927 ED, 654 IVM of oocytes, and 4,878 FOR cycles. European data on IUI using husband/partner's semen and donor semen were reported from 1,197 institutions offering IUI in 29 and 24 countries, respectively. A total of 162,948 treatments with IUI-H and 50,467 treatments with IUI-D were included. A total of 13,689 FP interventions from 11 countries including oocyte, ovarian tissue, semen and testicular tissue banking in pre-and postpubertal patients were reported.

Main results and the role of chance:

In 20 countries (18 in 2015) with a total population of approximately 325 million inhabitants, in which all ART clinics reported to the registry, a total of 461,401 treatment cycles were performed, of the equivalent of 1,410 cycles per million inhabitants (range 82-3088 per million inhabitants). In the 40 reporting countries, after IVF the clinical PRs per aspiration and per transfer in 2016 were similar to those observed in 2015 (28.0% and 34.8% vs 28.5% and 34.6%, respectively). After ICSI, the corresponding rates were also similar to those achieved in 2015 (25% and 33.2% vs 26.2% and 33.2%). After FER with own embryos, the PR per thawing is still on the rise, from 29.2% in 2015 to 30.9% in 2016. After ED, the PR per fresh embryo transfer was 49.4% (49.6% in 2015) and per FOR 43.6% (43.4% in 2015). In IVF and ICSI together, the trend towards the transfer of fewer embryos continues with the transfer of 1, 2, 3 and ≥4 embryos in 41.5%, 51.9%, 6.2% and 0.4% of all treatments, respectively (corresponding to 37.7%, 53.9%, 7.9% and 0.5% in 2015). This resulted in a proportion of singleton, twin and triplet DRs of 84.8%, 14.9% and 0.3%, respectively (compared to 83.1%, 16.5% and 0.4%, respectively in 2015). Treatments with FER in 2016 resulted in twin and triplet DR of 11.9% and 0.2%, respectively (vs 12.3% and 0.3% in 2015). After IUI, the DRs remained similar at 8.9% after IUI-H (7.8% in 2015) and at 12.4% after IUI-D (12.0% in 2015). Twin and triplet DRs after IUI-H were 8.8% and 0.3%, respectively (in 2015: 8.9% and 0.5%) and 7.7% and 0.4% after IUI-D (in 2015: 7.3% and 0.6%). The majority of FP interventions included the cryopreservation of ejaculated sperm (n = 7,877 from 11 countries) and of oocytes (n = 4,907 from eight countries).

Limitations reasons for caution:

As the methods of data collection and levels of completeness of reported data vary among European countries, the results should be interpreted with caution. A number of countries failed to provide adequate data about the number of initiated cycles and deliveries.

Wider implications of the findings:

The 20th ESHRE report on ART and IUI shows a continuous increase of reported treatment

numbers and medically assisted reproduction-derived livebirths in Europe. This is the largest data collection framework and opportunity for surveying medically assisted reproduction in Europe, so continuous efforts should be made to stimulate comprehensive data collection and reporting, to ensure transparency of processes and data quality.

Personal contribution - published papers:

Anton, E.; **Doroftei**, **B**.; Lupaşcu, I.A.; Socolov, D.; Ioanid, N. Preimplantation genetic diagnosis. Legal, ethical and medical implications in Romania. *Rev. Rom. Bioet.* ***2009***, *7*, 45-51+113.

Simionescu, G.; **Doroftei**, **B**.; Anton, SC.; Anton, E.; Nicolaiciuc, D.; Bolota, M.; Diaconu, I.; Filipeanu, D. National Program For In Vitro Fertilization And Embryo Transfer In Romania: Ethical, Legal, And Social Challenges. *SEA - Pract. Appl. Sci.* ***2017***, *V*, 161–164.

Doroftei, **B**.; Anton, E.; Edgar. M. ASSISTED REPRODUCTION IN ROMANIA OR RESISTANCE TO CHANGE IN A POST-COMMUNIST COUNTRY? *Rev. Med. Chir. Soc. Med. Nat., Iaşi* ***2017***, *121*, 125–135.

Anton, E.; Ciobica, A.; Mircea-Vicol, R.; Ioanid, N.; Padurariu, M.; **Doroftei**, **B**.; Dumitru, F.; Carmen, A. The triple test and down syndrome: Between feticide and therapeutic abortion. *RCIS* ***2016***, *54*, 182–189.

Simionescu, G.; **Doroftei**, **B**.; Cumpata, S.; Nemtanu, L.; Ivanov, I.; Maftei, R.; Grab, D.; Neculai-Valeanu, S.; Anton, E. EMBRYO SELECTION ON MORPHOKINETIC CRITERIA THROUGH TIME-LAPSE TECHNOLOGY ALONG WITH PREIMPLANTATION GENETIC TESTING (PGT) IN A COUPLE WITH RECURRENT PREGNANCY LOSS. CASE REPORT. *Rev. Med. Chir. Soc. Med. Nat., Iaşi* ***2018***, *122*, 807–812.

II. 6 Can fertility status be explained mathematically?

Superconductivity, fractals, and biological systems

The human body generates extremely small magnetic fields but the measurement of these fields is of great value in medicine. The main device for measuring these fields is the superconducting quantum interference device (SQUID) magnetometer. There are a number of applications of superconducting quantum interference device in medicine, but all of them can be divided into magnetoencephalanography (MEG), magnetocardiography (MCG) and other biomagnetic applications. If two superconductors are separated by a weak link they form a Josephson junction. A superconducting quantum interference device magnetometer consists of one or two of these junctions in a superconducting loop. To keep the inductance low the size of superconducting quantum interference device loop should be a small as possible, although in order to have a small sensor loop, a very sensitive pickup loop is needed. This loop usually couples inductively with the superconducting quantum interference device loop although some high temperature superconductors use a directly coupled pickup loop. Together with the sensor some readout electronics is also needed. There are various readout schemes but the most commonly used one is either a fluxed locked loop or a current locked loop.

Because of the high current carrying capability, superconductors are frequently used to generate high magnetic fields, specifically in the field of MRI, where superconducting magnets have long been used [819]. Advances in the field of cryo free magnets enabled low temperature superconductors to be used without the need of liquid helium, by using low temperature cryo coolers. Using these high intensity magnets a new imaging technology has been developed based on the Hall Effect. An ultrasound beam is used to create vibrations in the tissue sample. This takes place in a strong magnetic field which causes opposite charges in the tissue to diverge and lead to a Hall voltage, which is picked up by electrodes. It can also be accomplished the other way around, using a pulsed current through the electrodes in a strong magnetic field to generate an acoustic wave that is picked up by an ultrasound detector.

Supermagnets are also used in magnetic surgery, where a small magnetic tip is attached to a catheter or guide wire and steered through the body by rapid adjustments to strong magnetic fields (5T). This enables the surgeon to steer around very sensitive structures to the part that needs to be operated instead of taking the straight line approach. It is possible to measure the position of the tip with an accuracy of 1mm and a real time X-ray image in two dimensions is used for control. It is also used to guide magnetized pellets in the brain, for instance, to directly deliver drugs to deep brain tissues [820].

The literature shows that, at the macroscopic scale, the charge transport in physical systems is achieved by one-dimensional cnoidal oscillation modes of the charge current density (Figure 98) [821,822].

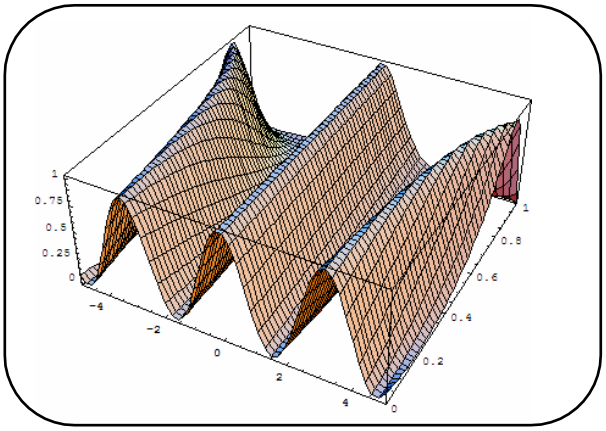

Figure 98. One-dimensional cnoidal oscillation modes as a function of space-timecoordinate and non-linear degree

This process is characterized by a normalized wave length, a normalized phase speed, and a normalized group speed [821]. Let us analyze the consequences of such extention. (1) The parameter *s* measures the charge transfer in biological systems. The one-dimensional cnoidal oscillation modes contain as subsequences: for $s = 0$ the one-dimensional harmonic waves, while for $s \to 0$ the onedimensional waves packet. These two subsequences describe the charge transport in a non-quasi-autonomous regime of the biological systems dynamics. For $s = 1$, the solution becomes the one-dimensional soliton, while for $s \to 1$ the one dimensional solitons packet results. These last two subsequences describe the electric charge transport in a quasi-autonomous regime of the in biological systems dynamics. These two regimes (non-quasi-autonomous and quasi-autonomous) are separated by the 0.7 structure, a value in agreement with the experimental data [823]. (2) Results show, through the normalized group speed, an increase of the charge transport in biological systems by means of quasi-autonomous structures. This can provide a possible explanation for null resistance of the superconductor, such as in arterial blood flow processes, for example [824–826].

Considering that the motions of the complex systems' structural units take place on fractal curves with constant fractal dimension (FD), an extended scale relativity model in its hydrodynamic version is built. In this approach, the harmonic oscillator problem is analyzed. This static system can be associated with a coherent structure (of superconductor or of super-fluid types of behavior), whose structural units are moving on stationary fractal trajectories. In such conjectures, the complex speed field becomes essential: the zero value of the differentiable part specifies the coherence of the structure, while the non-zero value of the fractal part selects, through some "quantization" relations, the "stationary" fractal trajectories (that may correspond to the observables from quantum mechanics). The model yields certain consequences in the morphogenesis of structures at various scale resolutions.

Considering that the movements of complex system entities take place on continuous, but non-differentiable, curves, concepts, like non-differentiable entropy, informational non-differentiable entropy and informational non-differentiable energy, are introduced. First of all, the dynamics equations of the complex system entities (Schrödinger-type or fractal hydrodynamic-type) are obtained. The last one gives a specific fractal potential, which generates uncertainty relations through non-differentiable entropy. Next, the correlation between informational non-differentiable entropy and informational non-differentiable energy implies specific uncertainty relations through a maximization principle of the informational non-differentiable entropy and for a constant value of the informational non-differentiable energy. Finally, for a harmonic oscillator, the constant value of the informational non-differentiable energy is equivalent to a quantification condition.

1. Any complex structure implies test particles, field sources, *etc.*, correlated with various types of forces, together with the non-differentiable medium in which they evolve. The non-

differentiable (fractal) medium is assimilated to a fractal fluid, whose particles are moving on continuous, but non-differentiable, curves. Moreover, the non-differentiable medium that cannot be separated from test particles and field sources is described either by a Schrödinger-type equation or by non-differentiable hydrodynamics with non-differentiable potential, which works simultaneously with standard potentials. The non-differentiable potential is induced by the non-differentiability of the movement curves of fractal fluid entities.

2. The dynamics of a complex system is described by motion equations for a complex speed field and exhibit rheological properties (memory).

3. Separation movements on the interaction scales imply non-differentiable hydrodynamics, which, at the differentiable scale, contains the law of momentum conservation and, at the non-differentiable scale, the law of probability density (states density) conservation.

4. The correlation fractal potential-non-differentiable entropy provides uncertainty relations in the fractal hydrodynamic approach. These relations are explained for the case of a test particle motion in spherically symmetric Coulomb or Newton fields.

5. The correlation informational non-differentiable entropy-informational non-differentiable energy provides specific uncertainty relations through a maximization principle of the informational non-differentiable entropy and for a constant value of the informational non-differentiable energy. For a linear harmonic oscillator, the constant value of the informational non-differentiable energy is equivalent to a quantification condition.

Concepts such as non-differentiable entropy, informational non-differentiable entropy, informational non-differentiable energy, *etc*., can prove to be essential in defining wave-corpuscle duality and, moreover, in the formulation of some fundamental equations in physics, such as the Klein-Gordon equation, the Dirac equation, *etc*.

Assuming that the motions of complex system structural units take place on continuous, but non-differentiable curves of a space-time manifold, the scale relativity model with arbitrary constant fractal dimension (the hydrodynamic and wave function versions) is built. For non-differentiability through stochastic processes of the Markov type, the non-differentiable entropy concept on a space-time manifold in the hydrodynamic version and its correspondence with motion variables (energy, momentum, etc.) are established. Moreover, for the same non-differentiability type, through a scale resolution dependence of a fundamental length and wave function independence with respect to the proper time, a non-differentiable Klein-Gordon-type equation in the wave function version is obtained. For a phase-amplitude functional dependence on the wave function, the non-differentiable spontaneous symmetry breaking mechanism implies pattern generation in the form of Cooper non-differentiable-type pairs, while its non-differentiable topology implies some fractal logic elements (fractal bit, fractal gates, etc.).

1. Assuming that in a Minkowski-type space-time the motions of structural units take place on continuous, but non-differentiable curves, a scale relativity theory with an arbitrary constant fractal dimension is built.

2. Non-differentiable geodesics on a space-time manifold and its diverse variants (the hydrodynamics one and in the wave function) are obtained. Particularly, if the wave function is independent of the motion curve affine parameter and if we consider a scale resolution dependence on a fundamental length, then the non-differentiable geodesics imply a non-differentiable Klein-Gordon-type equation. In this last situation, the standard result (Klein-Gordon equation) is obtained for motions on Peano curves at the Compton scale.

3. The concept of non-differentiable entropy on a space-time manifold (relativistic non-differentiable entropy) is introduced. It is proven that its three-dimensional projection is dependent (through total energy, internal energy and impulse) on the structural unit motion state. In such a context, the Klein-Gordon equation corresponds to a particular case of geodesics that is independent of its proper time, precisely those for which the motion takes place on Peano curves at the Compton scale and constant non-differentiable entropy.

4. Admitting that there exists a functional dependence between the phase and the amplitude of the wave function, in accordance with Consequence (6) of Section 2, the non-differentiable fluid is self-structuring through a spontaneous symmetry breaking-type mechanism. Cooper-type non-differentiable pairs result, which confer superconductibility-type properties to the non-differentiable fluid. Moreover, the motions on such geodesics imply maximum entropy.

5. Since the admissible number of non-differentiable kinks is determined by the non-differentiable topological properties of the symmetry group induced by Equation (11), a non-differentiable topological method can be applied. Then, some elements of a fractal logic, such as fractal bits, fractal gates (fractal IDENTITY, fractal NOT), *etc.*, are obtained.

6. Such formalism can be applied to complex systems in biology, precisely in problems related to fertility: the coupling between ovule and spermatozoon. The efficient interaction between one sperm and one oocyte leading to fertilization relies on specific informational energy exchange events. As a consequence, shortly after fertilization, before the first mitotic cell division, a developmental transition process commences, in order to trigger cell modeling from each gamete to a complex, multipotent zygote [827]. Genetically-encrypted data allow for various pathways to be upregulated, among which autophagy is one of the main players. During this cellular process, paternal mitochondria are selectively destructed in fertilized eggs [828]. The rationale for this event relies on evolutionary conservation strategies to prevent both the transmission of paternal mitochondrial DNA to the offspring and the establishment of heteroplasmy [829]. This is necessary, as, during fertilization, sperms compete with each other to reach and fertilize the oocyte and, in doing so, consume a great amount of energy produced by mitochondria via oxidative phosphorylation, generating reactive oxygen species, which could irreparably damage the integrity of mitochondrial DNA. This may be the main explanation why mitochondrial DNA mutates at a faster rate than nuclear DNA [828]. There are studies sustaining the avoidance of reactive oxygen species-dependent mutation as an evolutionary pressure underlying maternal mitochondrial inheritance and the developmental origin of the female germ line [830]. Most interestingly, it has been postulated that the maintenance of any gene within a bioenergetic organelle may be the result of natural selection with a selective advantage for the individual organelle in its ability to respond to changes in the redox state of its bioenergetic membrane and to regulate the synthesis of proteins in the electron transport chain by means of gene expression [830]. Therefore, in complex systems, complex bioinformatic systems are required to ensure long-term species conservation.

The discovery that cellular membrane systems had fractal properties paved the way for the application of fractal geometry to cell biology. This was due to the uncertainty of observations regarding the extent of cell membranes in the liver, as findings from morphometric studies of liver cell membranes by various laboratories failed to match. Much debate followed, the researchers trying to determine which of these estimates was correct, and whether liver cells contained 6 or 11 m^2 of membranes per cm^3, a significant difference. This cast doubt on the reliability of stereological methods, because they yielded conflicting results when measurements were made under different magnifications of the electron microscope.

Moreover, it was found that the estimates of surface density of liver cell membranes increased with increased resolution [831]. Mandelbrot suggested that these results were attributable to a scaling effect, analogous to the “Coast of Britain” effect [832]. Some results in fractal theory and its implications are given in [821,833–836]. This could explain why measurements of liver cell membranes at higher magnification yielded higher values than at lower magnification [831]. The scaling effect applies mainly to cellular membranes with a folded surface or an indented profile, such as the inner mitochondrial membrane or the rough ER. In fact, the surface density estimate of rough membranes was found to be increased with increasing magnification, while the surface density measure of the smooth outer mitochondrial membrane and of the smooth ER counterpart was only slightly affected by the resolution effect (Figure 99) [831].

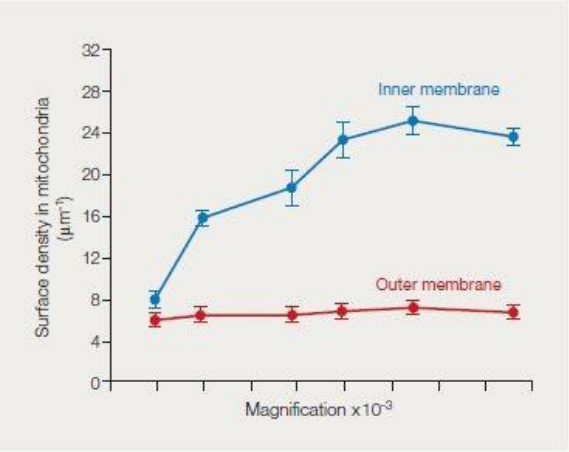

Figure 99. Changes of surface density estimates for outer and inner mitochondrial membranes, with increased magnification (site) [831]

In normal and pathological tissues and cell cultures, fractal analysis proved particularly useful with regard to electron microscopy for the objective investigation of fine cytoplasmic structures and the organization of various types of chromatin, nuclear components, and other subcellular organelles, both. External nuclear membranes (ENM) and nuclear membrane-bound heterochromatin (NMBHC) domains of human breast cancer MCF-7 cells briefly triggered by steroid hormones, such as 17β-estradiol or dexamethasone, were found to undergo ultra-structural changes at the beginning of growth, which were quantified by their fractal dimensionss [837]. Moreover, after a very short treatment (5 min) with 17β-estradiol (1 nM), the ultra-structural irregularity or the DNA unfolding of the nuclear membrane-bound heterochromatin domain was significantly enhanced as shown by an increase in its fractal dimension, whereaswith dexamethasone (1 nM) it was reduced. Neither steroid significantly modified the external nuclear membranes ultrastructure (Figure 100).

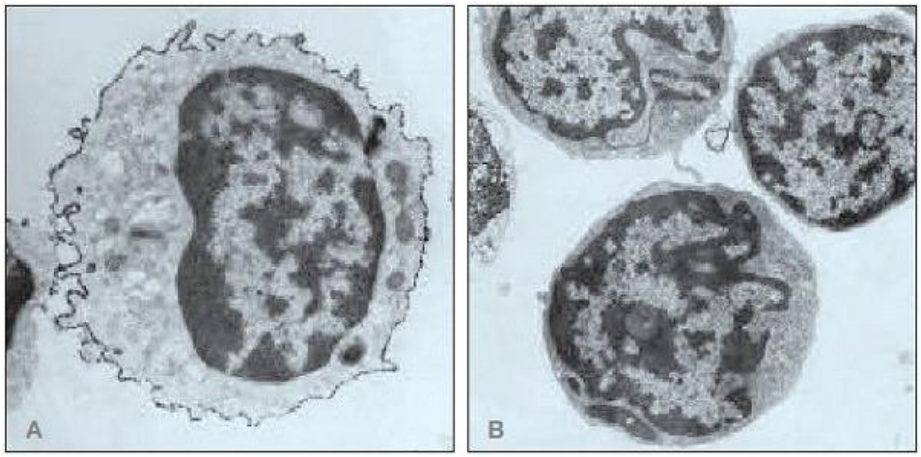

Figure 100. Electron microscopy view of human lymphocytes (site). a) healthy human suppressor T lymphocyte [CD8] haracterized by a wrinkled cell surface. Magnification: 18 400×. b) human lymphoblasts of acute leukemia (T-ALL), characterized by a smooth cell surface and a low fractal dimension [838]

This fractal tool has also been used to document the feasibility of using ultra-structural changes in cell surface and nuclear inter(eu)chromatin to assess the early phases of apoptosis (programmed cell death) induced in human breast cancer SKBR-3 cells by the ionophore calcimycin. The ultra-structural changes that involved a loss in heterochromatin irregularity caused by an increase in its condensation, quantified by a lower fractal dimension were evident well before the detection of conventional cell markers, which could only be measured during the active phases of apoptosis. Similarly, it was shown that the nuclear complexity of human healthy lymphocytes [839] underwent reduction during the apoptotic process. By measuring the fractal dimension of euchromatin and heterochromatin nuclear domains a discrimination of lymphoidcells found in mycosis fungoides from

those in chronic dermatitis was realized.

In histology and cytology, fractal morphometry applied to microscopic examination of cell nuclei and nuclear components has greatly improved the understanding of cell behavior and the diagnosis and prognosis of various disease states [839]. Quantification of nuclear chromatin organization by fractal morphometry is used to evaluate the degree of malignancy in human breast cytology and in aspiration cytology smears of cervical lesions. About 20 recent studies targeting the periphery of cell nuclei have shown fractal properties, making it possible to classify early ovarian cancers and even to distinguish normal from malignant liver cells [840].

Some correlations between biological systems and fractals were presented in a previously published paper, and we summarize them here. Planar and spatial neural networks based on fractal algorithms show morphologic and functional correspondences to biological neural networks. For both of these networks we can find:

1. Biomorphic symmetrical structures like lobes and hemispheres, gyri and sulci and cavities similar to ventricles; the axons of neurons projecting massive parallel, “somatotopic”, some crossing the median line in form of a decussatio.
2. Connections between each neuron with practically all other neurons and only a few functional interneurons.
3. Aperiodic and periodic orbits as bases for deterministic chaotic activities in biological nervous systems [841] as well as in fractal functions, the visualization of functional parameters in fractal nets resemblingto pictures we get by neuroimaging procedures.
4. Activation patterns developing in the course of recurrent projections between peripheral “cortical” and central “thalamic” structures. An according central structure we can find in the Mandelbrot set in which each region has its own periodic sequences coming with a certain frequency relatively close to zero. From these “neurons” of the central structure near zero, the activity will be projected to the periphery again. Like the Thalamus, this central structure of the Mandelbrot set consists of distinct nuclei.
5. Information processing as a task of the entire network [842–844].
6. The possibility to activate the entire net from a circumscribed region (by the recurrent projections of the reversed function in fractal nets, from some hippocampal regions in human brains in epileptic seizures).
7. Wave functions playing a role in network function.
8. The existence (or at least possibility) of associative memory functions. In ontogenetic development of organisms the orientation of growing axonal fibers in fields of concentration gradients of different neurotropic growth factors could reflect the course of trajectories in fractal functions. Thus, neurons and their axons may form spatial neural networks, based on specific fractal algorithms.

Carbon Nanotubes are often employed in contemporary medical research and are being highly researched in the fields of drug delivery and bio sensing methods for disease treatment and health monitoring. Carbon Nanotubes technology has demonstrated the potential to alter drug delivery and bio sensing methods for the better, and thus, carbon nanotubes have recently garnered interest in the field of medicine.

The use of carbon nanotubes in drug delivery and bio sensing technology has the potential to revolutionize medicine. Functionalization of single-walled nanotubes (SWNTs) has been shown to enhance solubility and allow for efficient tumor targeting/drug delivery. It prevents single-walled nanotubes from being cytotoxic and altering the function of immune cells. Cancer, a group of diseases in which cells grow and divide abnormally, is one of the primary diseases being looked at with regards to how it responds to carbon nanotube drug delivery. Current cancer treatment attempts primarily involve chemotherapy, surgery, or radiation therapy. These methods are usually painful and kill normal cells in addition to producing adverse side effects, and their effectiveness is a subject of debate in most cases. Carbon nanotubes as drug delivery vehicles have shown potential in targeting specific cancer cells with a dosage lower than conventional drugs used [845], that is just as effective in killing the cells, however does not harm healthy cells and significantly reduces side effects [846].

Current blood glucose monitoring methods by patients suffering from diabetes are mostly invasive and often painful. For example, one method involves a continuous glucose sensor integrated into a small needle which must be inserted under the skin to monitor glucose levels every couple of days [846]. Another method involves glucose monitoring strips to which blood must be applied.

These methods are not only invasive but they can also yield inaccurate results. It was shown that 70 percent of glucose readings obtained by continuous glucose sensors differed by 10 percent or more and 7 percent differed by over 50 percent [846]. Thus, single-walled nanotubes and multi-walled nanotubes (MWNTs) have a potential use in highly sensitive noninvasive glucose detectors, due to their high electrochemically accessible surface area, high electrical conductivity and useful structural properties [847].

Personal contribution - published papers:

Doroftei, B.; Buzea, C.; Simionescu, G.; Cumpata, S.; Agop, M.; Maftei, R. Fractal analysis and related forms of complexity of embryo development. Is there a new tool for human embryo selection? In Proceedings of the HUMAN REPRODUCTION; OXFORD UNIV PRESS GREAT CLARENDON ST, OXFORD OX2 6DP, ENGLAND, ***2016***; Vol. 31, p. 217.

Study question:

Can fractal analysis of the microscopic image of embryos, using different forms of complexity, predict the embryos with highest implantation potential?

Summary answer:

We reveal a decrease of fractal dimension from 72 h to 110 h morphokinetics for embryos associated to pregnancy and a constant value for those who did not result in pregnancy.

What is known:

Fractal analysis has applications in the detection of coding regions in DNA and measurement of the space-filling properties of tumors, blood vessels and neurons. Fractal concepts have been incorporated into models of biological processes, including epithelial cell growth, blood vessel growth and viral infections. There are various uses for fractal geometry in pathology: molecular biology, tumor development, vascular pathology. Three aspects of texture are considered by fractal geometry: fractal dimension, lacunarity and succolarity. The importance of morphokinetics fractal embryo analyse in IVF process reflected in literature is limited. Previous reported data show accuracy prediction of pregnancy between 67.4% and 74%.

Study design, size, duration:

The reproductive outcome using fractal dimension analysis provided by EmbryoViewer - Fertilitech, Denmark was done with programs ImageJ (IJ) 1.28 and Adobe Photoshop CS4. Fractal dimension was calculated with FracLac for ImageJ using box counting method, and with Fractalyse using grid, mass-radius, correlation and pixel dilation methods. Lacunarity was calculated with FracLac for ImageJ program. Succolarity was calculated using a program we built, on MS VC 2010 Express Edition.

Participants/materials, setting, methods:

168 couples (mean age 36.2 years) were included in the study. OS was performed with gonadotropins: 87% short antagonist protocol and 13% long agonist protocol, and we did ICSI for 72% and IVF for 28%. We obtained a number of 1,092 embryos monitored by time-lapse imaging (EmbryoScope). Patients in whose cases we were able to obtain between 3 and 20 oocytes were included in the study. Transfer was done with single blastocyst to patients who have P4 level at trigger day below 1.5 ng/dl.

Main results and the role of chance:

Fractal dimension was measured by four different methods: mass-radius, box-counting, correlation, and pixel dilation. Fractal dimension decrease from 72 to 110 h evolving time (the difference exceeding the standard error) for embryos led to pregnancy and remain constant (linear) for those who did not result in a pregnancy. For both measured samples of embryos leading to pregnancy or failing to do so, the fractal dimension at 72 h was 1.933 ± 0.002 and 1.932 ± 0.001 respectively, and at 110 h it was 1.928 ± 0.002 and 1.930 ± 0.002, respectively. Fractal analysis of the microscopic image of embryo in a culture dish revealed a decrease of lacunarity from 72 to 110 h evolving time, for both embryos which after implant led to pregnancy or not and the lacunarity slope from 72 to 110 h evolving time, decreased only for embryos which led to pregnancy and was constant for those who did not. For both measured samples, which headed for pregnancy or not, the lacunarity at 72 h was 0.197 ± 0.002 and 0.190 ± 0.002 respectively, and at 110 h was 0.142 ± 0.002 and 0.147 ± 0.002, respectively. For both measured samples, which headed for pregnancy or not, the lacunarity slope at 72 h was 0.0725 ± 0.0004 and 0.0675 ± 0.0005 respectively, and at 110 h was 0.0674 ± 0.0003 and 0.0685 ± 0.0003, respectively.

Limitations, reasons for caution:

More embryo images should be used to improve the accuracy of the prediction model. In this study of embryo morphokinetics, we were only able to use images at 72h and at 110h.

Wider implications of the findings:

Our results show that fractal model could predict pregnancy in 75% of cases. Using a support vector machine related to supervised learning methods in conjunction with learning based intelligent software could improve pregnancy prediction. In a personalised approach, the proposed model predicts pregnancy correctly in 83% of cases, but further research is needed for validation.

Personal contribution - published papers:

Buzea, C.; Paun, M.-A.; Agop, M.; Paun, V.-A.; **Doroftei**, **B**. Fractal Analysis And Related Forms Of Complexity Of Embryo Development. Is There A New Tool For Human Embryo Selection? *Univ. Politeh. Bucharest Sci. Bull. A-Applied Math. Phys.* ***2019*** *81*, 229–240.

Aim of the study

This paper aims at presenting a noninvasive method, which is based on a thorough analysis of the microscopic image of fertilized eggs, using different forms of complexity (fractal dimension, lacunarity and succolarity), that may improve our ability to select embryos with the highest implantation potential.

Materials and methods

A total of 1,092 embryos from 168 couples who underwent IVF cycles were analyzed in this study. ICSI was performed in 72% of the cycles, while IVF in 28%. Different protocols were used for OS, 87% of patients receiving antagonist protocol with gonadotropins, while long agonist protocol was used for 13% of patients.

The mean age of the female patients included in the study was 36.2 years; patients with good ovarian reserve and low ovarian reserved were in approximately equal numbers. Patients from whom less than 3 oocytes or more than 20 were retrieved were excluded from the study. Only day-5 blastocysts were transferred, and single ET was performed. In cases where the progesterone value exceeded 1.5 ng /dl on the day of the trigger administration, all the embryos were frozen (freeze all), and frozen-thawed ET was performed afterwards.

IVF/ICSI/IMSI Protocol

Retrieval of cumulus-oocyte complexes

The OS was monitored by ultrasound and blood analysis. Subsequently, a hCG or agonist trigger was administrated 36 hours prior to the retrieval of cumulus-oocyte complexes. The FF was aspirated by ultrasound-guided transvaginal aspiration and analyzed in the stereomicroscope. After identification, the cumulus-oocyte complexes were transferred to Petri dishes which contained a washing medium. For ICSI and IMSI, which is a variation of ICSI that uses a higher-powered microscope to select sperm, oocytes were firstly denudated 37-40 hours after the trigger administration. Denudation was performed in Petri dishes with a central well, by placing 5-6 cumulus-oocyte complexes and adding an appropriate amount of hyaluronidase. After removal of cumulus cells by repeated pipetting, using a pipette whit top of adequate diameter (135-200 μm), oocytes were evaluated in terms of their maturity. Further on, mature oocytes (MII) were used for ICSI/IMSI.

Sperm preparation for IVF/ICSI/IMSI

The semen sample was processed using density gradient centrifugation. Depending on the semen volume, one or more sterile centrifugation tubes were prepared by loading 1,2 - 2.0 mL of 40%, respectively 80% gradient, in such manner to create a clear interface between the layers. The liquefied sperm sample was carefully pipetted on top of the gradient, centrifugation being performed at 350 g-400 g, for 10-20 min. The resulting deposit after centrifugation was transferred into a tube with washing medium and centrifuged again for 5 minutes at 300 g. The deposit resulting after the second centrifugation was used for IVF/ICSI/IMSI.

Procedures FIV/ICSI/IMSI

For IVF, the insemination volume from the final sample was calculated so that the concentration would be about 200,000 spermatozoa per every insemination dose. Using a pipette, the predetermined volume of semen was added in each Petri containing 5-6 cumulus-oocyte complexes. The fertilization rate was assessed 16-18 hours after insemination.

For ICSI/IMSI, a small amount of the final semen sample was transferred in the Petri dish for injection, while a small a drop was placed in advance in the PVP. Subsequently, the semen sample was transferred in the same Petri dish with the mature oocytes that were to be injected. The oocyte was immobilized using a holding micropipette. One mobile sperm, morphologically normal observed in the microscopic field (x400 for ICSI) was aspirated into the micropipette injection. The oocyte to be injected was rotated so that the first polar body would be positioned at 12 o'clock or at 6 o'clock. After the oocyte was immobilized using the holding micropipette, the injection micropipette was inserted into the oocyte and the sperm could be easily introduced into the cytoplasm. IMSI procedure took place in similar conditions, with the only difference that sperm selection was done at magnifications higher than x1000-x10000, using Nomarski differential contrast, thus enabling a more thorough analysis of the sperm morphology. After injection, all mature oocytes were transferred into the Petri culture, the fertilization progress being evaluated after 16-18 hours.

All fertilized oocytes were transferred to Petri dishes that contained Single Continuous Media CSCM from Irvine Scientific in individual microdrops. The resulting embryos were assessed daily over the next 5/6 days by registering cell number, degree of fragmentation and embryo morphology (form and shape of the blastomere).

The study involved the processing of several images using the program ImageJ (IJ) 1.28. ImageJ is a public domain, Java-based picture handling program created at the National Institutes of Health. ImageJ was designed with an open architecture that gives extensibility through Java plugins and recordable macros. Custom acquisition, analysis and processing modules may be developed using ImageJ's built-in editor and a Java compiler. User-written modules make it conceivable to solve many image processing and analysis issues, from three-dimensional live-cell imaging to radiological picture processing, multiple imaging system data comparisons to automated hematology systems. ImageJ enables users to display, edit, analyze, process, save, and print 8-bit color and gray scale, 16-bit integer, and 32-bit floating point pictures. The program may read many picture file formats (TIFF, PNG, GIF, JPEG, BMP, DICOM, FITS), and also raw formats. ImageJ supports picture stacks, a progression of images that share a single window, and it is multithreaded, so tedious operations may be performed in parallel on multi-CPU hardware equipment. ImageJ may calculate area and pixel value statistics of user-defined selections and intensity-thresholded objects, may measure distances and angles, may determine density histograms and line profile plots. Additionally, the program

supports standard picture processing functions, for example, logical and arithmetical operations between pictures, manipulate contrast, convolution, Fourier analysis, sharpening, smoothing, edge detection, and median filtering. Further on, geometric changes, for example, scaling, rotation, and flips may also be performed. The program supports the processing of many pictures at the same time, the only restriction being related to the accessible memory. The microscopic images of the fertilized eggs and the resulting embryos were thorough analyzed using different forms of complexity (fractal dimension, lacunarity and succolarity).

Results

Fractal dimension was measured by means of 4 different methods: massradius, box-counting, correlation, and pixel dilation using two different softwares: Fractalyse and FracLac for ImageJ. Lacunarity was calculated with FracLac for ImageJ program, while succolarity was calculated by a program built by our team: Succolarity_1F.exe (written in MS VC# 2010 Express Edition). Fractal analysis of the microscopic image of sperm and egg united in a culture dish revealed a decrease of the fractal dimension from 72 to 110 h evolving time (the difference exceeding the standard error) for embryos which after implantation led to pregnancy and a constant (linear) value for those who failed to implant (Figure 101 a,b).

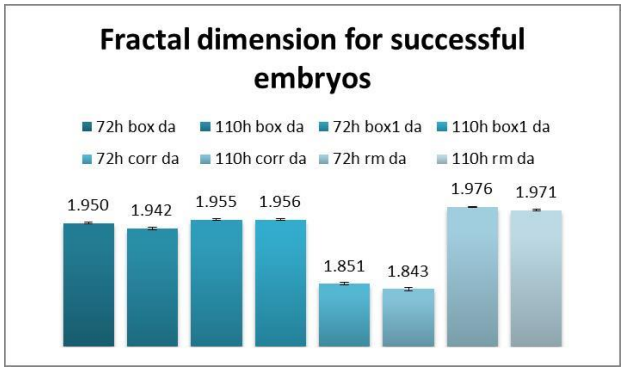

Figure 101a. Fractal dimension for embryos who where successfully implanted

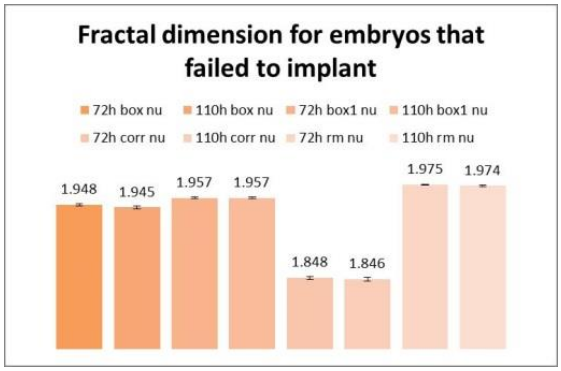

Figure 101b. Fractal dimension calculated for embryos who failed to implant

For both measured samples (those which resulted in pregnancy and those which did not), the fractal dimension at 72 h was 1.933±0.002 and 1.932±0.001 respectively, while at 110 h the value was 1.928±0.002 and 1.930±0.002, respectively.

Fractal analysis of the microscopic image of sperm and egg united in a culture dish revealed the same decrease of lacunarity from 72 to 110 h evolving time, for both (leading to pregnancy and failed implants). Notwithstanding, the lacunarity slope from 72 to 110 h evolving time decreased only for embryos which after implantation led to pregnancy and was almost constant for those who did not (Figure 102a).

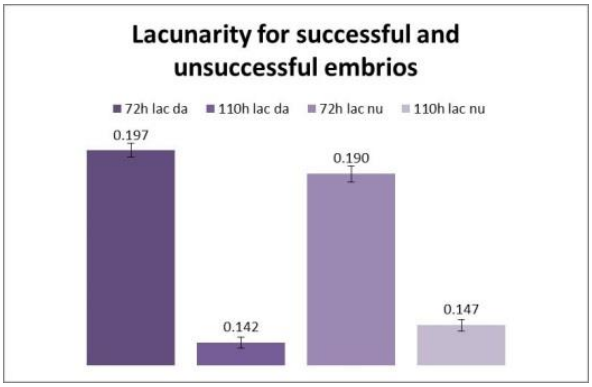

Figure 102a. Lacunarity value plotted for both successful and unsuccessful embryos

For both measured samples, which resulted in pregnancy or not, the lacunarity at 72 h was 0.197±0.002 and 0.190±0.002 respectively, and at 110 h was 0.142±0.002 and 0.147±0.002, respectively – no significant difference. However, for both samples, which resulted in pregnancy or not, the lacunarity slope at 72 h was 0.0725±0.0004 and 0.0675±0.0005 respectively, while at 110 h the values were 0.0674±0.0003, respectively 0.0685±0.0003, (Figure 102b).

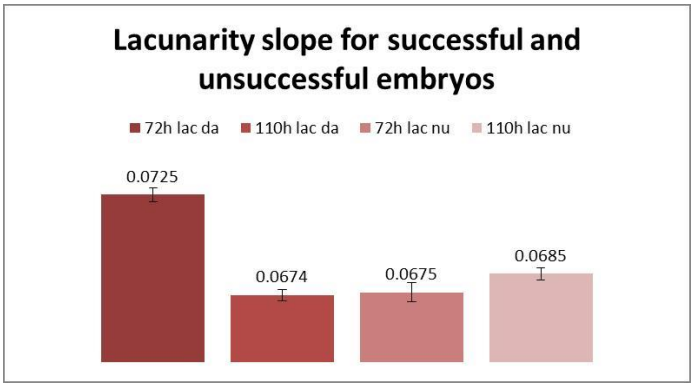

Figure 102b. Lacunarity slope plotted for both successful and unsuccessful embryos

Fractal analysis of the microscopic image of sperm and egg united in a culture dish revealed a higher decrease of succolarity, from 72 to 110 h evolving time, for embryos which after implantation led to pregnancy compared to those who failed (Figure 103).

For both measured samples, the succolarity at 72 h was 0.837±0.001 and 0.836±0.001 respectively, and at 110 h was 0.805±0.002 and 0.815±0.002, respectively. Although the value for succolarity at 72 h was almost the same, the succolarity at 110 h was lower for successful embryos, suggesting there is a much more permeable environment in this case (Figure 103).

The results of our study may be the beginning of a new path in morphokinetic analysis by applying a fractal model in the succession of embryonic development to the blastocyst stage. Validation of this method of selecting the human embryo with the maximum chance of obtaining pregnancy may be achieved by PGT using NGS. This research direction may be applied later to other complementary studies.

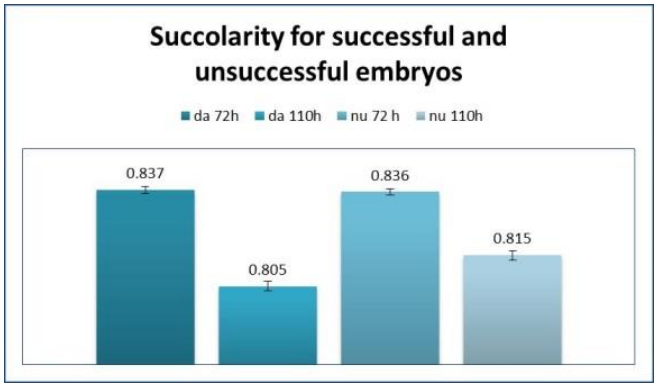

Figure 103. Succolarity value for both successful and unsuccessful embryos

Discussion

Modern time-lapse monitoring system (e.g. EmbryoScope™) has emerged as a method of ensuring continuous monitoring of the embryo development without removing embryos from the incubator, thereby ensuring a stable environment and avoiding changes in temperature and pH. Beside the automated annotation that are generated from the system, a series of morphokinetic parameters specific to different events taking place during the embryo development may be identified, and different research teams have focused on developing a generally applicable morphokinetic algorithm which would predict the implantation potential of embryos [848–850].

Numerous studies have shown that the morphology and morphokinetics of embryos correlate with the embryo implantation rate, which is why several working groups have developed embryonic evaluation and grading criteria, all of which aim to select the embryo with the embryo better implantation rate. Since embryonic evaluation by the classical method involves removing embryos from the incubator (temperature differences, CO_2, O_2 and pH concentrations) and subjecting them to increased intensity light, efforts have been made to produce a time-lapse device that allows embryos to be evaluated in their environment culture without the need to remove them from the incubator and with a much better examination time with images obtained at short intervals (10- 20min).

In 2014, a study published in *Human Reproduction* on the relationship between aneuploidy and morphological and morphokinetic characteristics in patients with PGD/PGS could not find a perfect correlation between the euploid status of the embryo and its morphological and morphokinetic characteristics [691]. However, as a conclusion of the study, morphological and morphokinetic assessment was still considered the best and most cost-effective method of assessing embryos in patients that do not undergo PGT.

According to the ESHRE Consortium (ESHRE PGT Consortium/Embryology Special Interest Group - best practice guidelines for polar body and embryo biopsy for preimplantation genetic testing), the indications for performing PGT-M are: patients at high risk of transmitting genetic abnormality to their children, which includes all monogenic defects (autosomal recessive, autosomal dominant and X-linked disorders) and carriers of balanced translocations, which are at high risk of implantation failure and recurrent abortions [851]. On the other hand, PGT-A has been conducted for infertile patients undergoing IVF with the aim of increasing IVF pregnancy and delivery rates. Cited indications for PGT-A include advanced maternal age, repeated implantation failure, severe male factor and couples with normal karyotypes who have experienced repeated miscarriages.

Fractal analysis of the embryos was used in a study published in 1994 [852], however, the fractal dimension was calculated only on the images obtained on the 5th day of the embryonic development and not in the dynamics. This paper presents a new embryo grading algorithm based on calculating the fractal dimension of the embryos in dynamics, respectively at 72h and 110h.

The definition of a fractal is a self-repeating (self similar) pattern that shows similar properties in different scales. Fractal analysis has found applications in the detection of coding regions in DNA and measurement of the space-filling properties of tumors, blood vessels and neurons. Fractal concepts have also been usefully incorporated into models of biological processes, including epithelial cell growth, blood vessel growth, periodontal disease and viral infections. In other words, one can find various uses of fractal geometry in pathology: molecular biology, tumour, bone and vascular pathology, neuropathology, modeling of biological processes using fractals and other miscellaneous applications [853], or integrative models for fractal description of the particular structure parameters [854,855].

Three aspects of texture are considered by the fractal geometry: Fractal Dimension, Lacunarity and Succolarity. Fractal dimension has been well studied; a great number of approaches have been presented to extract it from images. It can be computed from black and white to gray scale images. There are many approaches also, from the simple Box-dimension to the most complex Hausdorff dimension. The same does not happen with the other two measures. Although Lacunarity has been more and more used in works exploring its characteristics, Succolarity, until now, has not been even computed.

The three fractal characteristics (Fractal Dimension, Lacunarity and Succolarity) explore different aspects of the images in a complementary way. Two images could present the same Fractal Dimension but different Lacunarity or the same Lacunarity but different Succolarity therefore there may be other combination of results. Fractal dimension is a measure that characterizes how much an object occupies the space that contains it. Fractal dimension is a measure that does not change with scale neither with translation nor rotation. Lacunarity measures the size and frequency of gaps in the image. Succolarity measures how much a given „fluid" may flow through an image, considering as obstacles the set of pixels with a defined color (e.g. white) on 2D images analysis.

When the most important desideratum is the birth of a healthy baby, no effort on the part of those involved in assisted human reproduction is too small. Which embryo should be transferred or how many embryos should be transferred are essential questions that many medical teams face in the daily work. Also, which embryo has the greatest chance of becoming a healthy newborn? In order to

answer this question, methods of invasive and non-invasive selection of human embryos have been developed. Among the invasive methods we mentioned previously the morphokinetic timelapse analysis, metabolomics, proteomics and genomics. Promising results are found in the exponential development of molecular genetics techniques and preimplantation genetic screening of embryos. Notwithstanding the improvements in embryo selection made possible by genomic testing, according to some studies, the embryo morphokinetics, especially the inner cell mass (ICM) grade is still one of the basic predictors of pregnancy outcome.

The PGT has the advantage of offering an objective, functional and applicable diagnosis, however, the embryo biopsy, which represents an invasive intervention, may be responsible for inducing iatrogenic damage to a good potential embryo. For this reason, finding a mathematical analysis method for assessing human embryo development may ease the work of an embryologist and contribute to the standardization of embryo selection, implicitly increasing the success rate.

In globozoospermia the main morphological defect is characterized by the absent or severely malformed acrosome. The pathogenesis occurs during spermiogenesis and probably originates in the acrosomic vesicle fusion impairment and cytoskeleton disorders, although precise mechanisms remain to be determined [856]. Total (100% round headed spermatozoa) or partial (less than 100%) globozoospermia have been described [857,858].

The introduction ICSI and then IMSI lead the way for males with severe globozoospermia to have the ability to father their own children. However, rates of fertilization remained poor for this cohort of males and it quickly became evident that round headed sperm did not have the ability to trigger oocyte activation [859–861]. In 1997, the first reports of AOA and improved fertilization could be achieved by applying calcium ionophore in such cases [862]. Here we will report on a successful ongoing pregnancy after IMSI with oocyte activation.

Personal contribution - published papers:

Doroftei, **B**.; Zlei, M.; Simionescu, G.; Maftei, R.; Cumpata, S.; Emerson, G. Report of a successful ongoing pregnancy as a result of IMSI with assisted oocyte activation. *Reprod. Health* ***2015***, *12*, 38. **IF: 3.223**

Case presentation 1

A 32-year-old couple presenting for fertility consultation reported a history of 5 years of unsuccessful attempts to obtain a pregnancy. The investigation of the female partner and the fertility workup included checking the ovarian reserve by antimullerian hormone (3.72 ng/mL), an antral follicle count (18 follicles on both ovaries), an ultrasound examination of the uterus, and in-office diagnostic hysteroscopy, all of which showed no abnormalities. Semen analysis on the male showed a volume of 5.6 mL and a concentration of 23 million/mL spermatozoa of which 44% were motile (and only 5% progressively motile). Sperm morphology was reported as 2% normal with evidence of acrosome abnormalities (strict criteria, Figure 104). The DNA fragmentation index was 10.6% and high DNA stainability was 14.9%, both assessed using the flow-cytometry method.

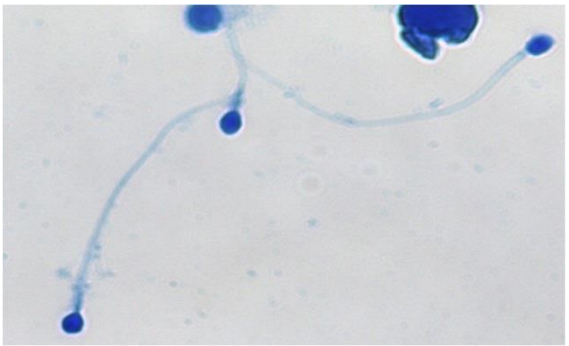

Figure 104. Microscopy image of sperm morphologic assessment. The staining was performed with Sper Blue (Microptic, Spain). Magnification with the oil immersion, 100 x objective (Leica GX, L3200, Leica Application Capture Software

As a result, male factor infertility was diagnosed and the couple was advised to pursue IMSI. Informed consent was obtained. No history was known regarding the fertility of other male family members. The female patient was treated with an antagonist protocol of ganirelix (Orgalutran - MSD) and 150 IU rFSH (Puregon-MSD) daily for 9 days. Oocyte retrieval was undertaken 36 hours post hCG priming 10,000 IU (Pregnyl - MSD). A total of 7 oocytes were collected, of which 5 were mature and suitable for injection. Semen analysis on the day of oocyte retrieval on high magnification using an inverted microscope equipped with Nomarski differential interference contrast optics (Leica AM 6000) showed no normal morphology, only total round heads (globozoospermia). Due to the concern of a total failure to fertilize, the couple was informed that IMSI would be the method of choice to continue to observe the sperm sample, trying to identify any sperm with a partial orsmall acrosome to avoid the use of oocyte activation media. However, none were observed and, post IMSI, the use of oocyte activation media was undertaken.

The couple was fully informed of the limited data available on the use of calcium ionophore with regard to the long-term health of resultant offspring. Written consent was obtained to carry out this procedure. The characteristics of the sperm used for insemination showed total round head nucleus with no acrosome present; howeverall were motile.

Following IMSI, the 5 oocytes were placed into oocyte activation media (GM508, Cult Active, GYNEMED) for 15 minutes at 37 degrees 5% O_2 and 6% CO_2. The oocytes were then washed free of calcium ionophore through 8 drops of culture media. The oocytes were cultured over night in CSCM media (Irvine Scientific, Santa Ana, CA) in the embryoscope time lapse incubator (Fertilitech- Unisence Denmark). Sixteen hours post injection, only one oocyte showed signs of fertilization and developed normally (Figure 105).

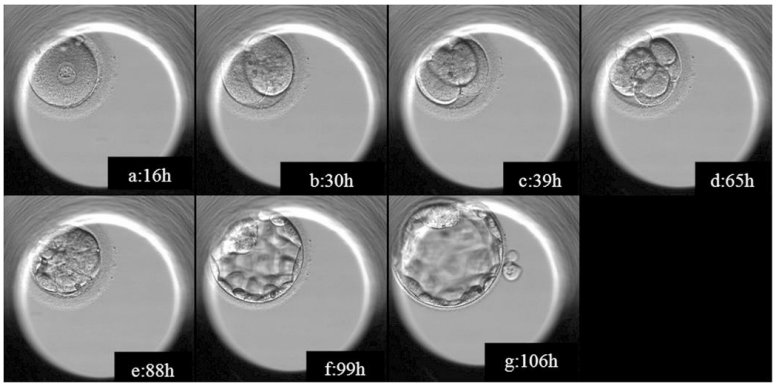

Figure 105. Different stages of embryo development captured with a Time Lapse System. The images were captured (Embrioscope, Fertilitech - Unisence Denmark, Embryo-Viewer Software) at different stages of the embryo's development post injection: a - 2 pro-nucleai, 16 hours, b - 2 cells (30 hours), c - 4 cells (39 hours), d - 8 cells (65 hours), e - start of blastocyst (88 hours), f - expanded blastocyst (99 hour), g - hatching blastocyst (106 hours)

The embryo was cultured to day 5 uninterrupted in the embryoscope (Unisense FertiliTech, Aarhus, Danemarca) and a blastocyst grade 6AA [863] was transferred under ultrasound guidance. BhCG level on day 12 post ET was 468.9 mUI/mL, 2 days later BhCG level was 916.1 mUI/mL. Ultrasound evaluation at 12 weeks and 5 days of gestation (Figure 106) showed Fetal Heart Beat 149 bpm, CRL (crown-rump length 63 mm, nuchal transluency - 1.6 mm and intracranianal translucency 2.1 mm, ductus venosus dopller without notch, nasal bone present and tricuspid doppler in normal range. First trimester biochemical and ultrasound screening revealed low risk for trisomy.

Figure 106. Ultrasound image of the fetus at 12 weeks and 2 days of gestation

It is yet unclear whether patients whose ejaculate contains both 100% globozoospermia or normal and globozoospermic cells (partial globozoospermia) suffer from a variation of the same syndrome [856]. Yon et al., [864] reported the absence of PLCz in both the normal and round-headed sperm of a partial globozoospermic patient, in line with the inability of partial globozoospemic sperm cell types to activate mouse oocytes as reported by Heindryckz et al., [865]. Numerous reports studying familial cases have suggested that globozoospermia is a genetic syndrome [866–870]. However, the specific mode of inheritance remains unclear, despite a recently reported mutation in the SPATA16 gene appearing to be associated with certain types of globozoospermia in men [856].

To our knowledge this is the first reported ongoing pregnancy after IMSI using globozoospermic spermatozoa with AOA in Romania. This report shows the use of high magnification tools such as IMSI in the assessment of sperm morphology can aid in the reduction of complete failure to fertilize in cases of suspected globozoospermia with the introduction of AOA when necessary.

Nanotechnology

Reproductive biology is a constantly developing field that focuses on the structure and function of the reproductive system as well as on the complexity of processes that take place such as gametogenesis, fertilization, implantation and embryo development. In both humans and mammals, the success of fertilization depends on gamete fertility potential, sperm, and oocyte quality being equally important. Assisted reproductive technologies have been used extensively for humans and domestic animals in order to promote reproductive efficiency and preserve valuable genetics.

Due to their small size, nanoparticles may be easily integrated into the physiological processes of the cells and may migrate between different intracellular compartments, making 638 the selective targeting of certain tumoral cells possible (Table 38). Another important characteristic is their high stability, which enables them to be used via long distance, therefore improving drug delivery, for example. According to Navath et al., polyamidoamine (PAMAM) dendrimer-based nanoparticles may be used for the delivery of drugs intravaginal [871]. This application may be very useful in the case of pregnant women with ascending genital infections because by restricting the administration of the drugs to the vaginal area, the passage of the compounds towards the fetal membranes is limited, thus the fetotoxicity is minimized [872]. Nanoparticles have been successfully used for the detection and treatment of various genital infections such as *Chlamydia trachomatis* [873–875]. A nano-carrier may simultaneously carry and deliver a variety of substances (Table 44), the efficiency of targeting being adjustable depending on the physical and chemical proprieties of the carrier [876].

In recent years, the gold standard for several reproductive diseases has been surgical treatment, but the latest studies have shown that nanoparticles may be used for the detection and therapy of both reproductive cancers and non-cancerous diseases such as EMS [877,878], uterine fibroids [879], ectopic pregnancy and trophoblastic diseases [880], offering a less invasive and safer alternative to standard diagnosis and surgical treatment protocol.

Table 44. Application of nanomaterials in reproductive medicine

Applications	Principle
Treatment and imaging of reproductive system-related cancers	Nanobiosensors for measuring cancerbiomarkers Nanoparticles for biomedical imaging Nanoparticle Contrast Agents for ComputedTomography Imaging [881]
Treatment of different gynecologicalaffections	Potentiation of the antitumor effect of chemotherapy by exposure to nanomaterials
Carrier particles	Nanoparticles used for diagnosis, targeting and carriers for drug administration
Nanoparticle-assisted combination Therapies	Simultaneous delivery of different drugs
Gene therapy in reproductivediseases	Therapeutic delivery of nucleic acid polymersusing nanoparticles into a patient's cells as a drug
Sperm-mediated gene transfer	Application in obtaining transgenic animal
Magnetic-Activated Cell Sorting (MACS)	Magnetic nanoparticle-based selection of live sperm with integral (not fragmented) DNA

Improvement of semen quality though nanotechnology

Semen quality measures the ability of semen to accomplish fertilization, thus estimating its fertility potential and implicitly, any decrease in sperm quality leads to reduced fertility. Although the advances in the cryobiology have led to the development of new methods that allow the conservation of gametes at low-temperature, a loss of fertility potential consecutive manipulation and preservation have been observed in both human and animals.

Routine semen assessment is usually done by microscopic evaluation of semen parameters, such as total sperm count, sperm concentration, the percentage of motile sperm and percentage of normal sperm morphology. Some of these may correlate with fertility, though their predictive potential for male fertility appears limited [882].

The introduction of computerized technology in the process of semen evaluation, such as computer-assisted semen analysis (CASA), has increased the accuracy of the analysis by facilitating an objective and rapid count of the sperm cells, as well as by offering essential data regarding the kinetic parameters of the cells.

Due to the fact that standard seminal parameters (concentration, motility and morphology) currently used for routine analysis in most species were insufficient for predicting fertility and detecting sub-fertility situations, a series of additional molecular marker-based tests were designed. Consequently, flow cytometry analysis of semen passed the barrier from research to standard practice and fluorescent markers are now used to assess the acrosomal status, mitochondrial activity, the sperm chromatin integrity or oxidative stress of the sperm cells.

A step forward is being taken by combining flow cytometry analysis and nanotechnology. A series of fluorescent biomarkers have been developed with the purpose of assessing the structural and functional properties of sperm cells such as DNA condensation (sperm chromatin integrity), acrosome integrity, which permits the penetration of the egg during fertilization (acrosome status), mitochondrial membrane integrity which ensures the capacity of the sperm cells to produce the energy essential for sperm motility (mitochondrial membranary potential), as well as cell viability (expressed as live/dead ratio) [883].

Ubiquitin is one example of protein biomarker which was intensively researched and is now used for fertility assessment. This biomarker is located at the surface of abnormal sperm cells and possesses properties similar to lecithin ligands such as peanut agglutinin (PNA) or Pisum sativum agglutinin (PSA), which are commonly used to assess acrosome status in different species [884–886]. The abnormal sperm cells may be targeted by coating nano-particles with ubiquitin-binding antibodies, thus this technique may be useful in the process of nano-purification of semen.

Unlike agglutinin, ubiquitin has the ability to identify both the sperm cells showing abnormal acrosome, as well as those who have abnormalities of the tail and the head [887], including those

with altered sperm DNA. If an ejaculate contains a high proportion of tagged sperm cells, this may indicate a poor quality of the sperm or infertility [888], since ubiquitine-tagged sperm cells are an indicator of sperm quality. Due to this characteristics, a series of ubiquitin-based sperm assay were developed for the diagnosis of male factor infertility in different species such as men [889], boars [887], stallions [890] or bulls.

Additionally, according to Ozanon et al., a negative correlation was observed in humans between sperm ubiquitin and embryo development in the case of assisted fertilization [891]. The results obtained with ubiquitin were a cornerstone for the elaboration of other potential biomarker for male fertility, such as platelet-activating factor receptor (PAFR) or postacrosomal ww domain-binding protein (PAWP) which promotes pronuclear development during fertilization.

The new technology based on biomarkers facilitates the diagnosis of infertility in men and enables the specialist to customize an efficient treatment for each patient. In livestock reproduction, a high correlation has been observed between the routine semen parameters, conception rates after I.A and the parameters evaluated using flow-cytometry analysis based on biomarkers; therefore, this technology may be a predictive tool for fertility potential of young males.

Another possible application of nanotechnology with the purpose of improving sperm quality is nano purification of semen using nanoparticles. Usually, high quality semen is needed for assisted reproduction, so sperm cells with abnormalities are removed from the sample using different techniques such as swim-up, migration, filtration or density gradient centrifugation. These techniques are based on certain specific properties of sperm cells (e.g. motility) or a set of properties (e.g. motility, membrane and chromatin integrity) such is the case of density gradient and aim to select superior quality sperm cells (membrane integrity, normal morphology, chromatin integrity) and even remove virus from the sample by combining the sperm selection techniques [892]. Over the years, different commercial colloids have been developed for gradient centrifugation of both human semen (Percoll, PureSperm, Sage) and mammalian semen from different species (Bovipure, Capripure, Androcoll). Even if this method is quite efficient for selecting highquality spermatozoa, it is time-consuming and requires expensive reagents and equipment, which makes it less suitable if larger amounts of semen must be processed for A.I. Therefore, new approaches are embraced by researches and andrologists, one of them being the magnetic separation method.

Having the antibody and lectins conjugation as example, Clemente Associates (Madison, CT) developed a sperm selection method using magnetite and iron oxides nanoparticles. The particles, coated previously with anti-ubiquitin antibodies or with lectin peanut agglutinin, were projected to target the abnormal sperm cells by binding to the ubiquitin protein located on the surface of these cells. According to the field insemination trails conducted with nano purified semen, there were differences between males and also between heifers and cows which were inseminated but, most importantly, no adverse effect was observed in the study conducted. This encourages further studies and the development of new protocols for nano purification using magnetic separation [893]. The results obtained by Nasri et al., contradict these findings somehat, as iron oxide nanoparticles were found to a potentially negative effect on the Leydig cells at molecular level [894].

Microfluidics

The *in vitro* embryo production is an assisted reproduction biotechnology that consists in the recovery and maturation of female gametes from donors, IVF of the matured gametes using male gametes, and the subsequent *in vitro* culture of the embryos obtained after fertilization [895]. In order to improve the outcomes of *in vitro* embryo production, efforts must be made to improve all IVF stages from female and male gametes sorting to embryo culture.

Applications of microfluidics could be integrated throughout the process of embryo production, starting with the qualitative assessment and sorting of gametes and continuing with embryo culture and vitrification, in order to miniaturize and enable several laborious lab procedures to be carried out using a single compact device, the so called “lab-on-a-chip”.

Sperm sorting using microfluidics

A study conducted by Enciso et al., showed that sperm DNA plays a decisive role in IVP [896].

Sperm with fragmented DNA can fertilize the female gamete [897,898], but it may also adversely affect the quality of the embryo by causing embryonic development interruption, often in the first phase of gestation [576,899] and by subsequentely determining low pregnancy rates after IVF or IA [900–902].

Additionally, a study led by Wdowiak and Bojar has showed that the intracytoplasmatic injection of sperms with a higher degree of DNA fragmentation may negatively influence the morphokinetic parameters of embryos thus the SDF index may be used as a predictive tool for estimating pregnancy rates after ICSI [903].

One of the main objectives of an assisted reproduction program is the selection of high quality cells in order to improve the fertilization rates of IVF, ICSI. Some sperm selection technologies such as swim-up, filtration or gradient centrifugation have proven efficient for sorting sperm cells based on a specific propriety such as motility or a group of characteristics such as normal chromatin, motility and morphology [904], but yet, the outcomes of FIV or ICSI are still lower than expected, one key factor being the subjective approach when it comes to choosing the best sperm cell for fertilization of the egg [905].

The introduction of molecular markers for sperm quality analysis has opened new pathways for research into objective methods of retrieving high quality spermatozoa for fertilization *in vitro*. Some of the microfluidics-based devices use sperm motility as the main mechanism of cell sorting, since non-motile sperm cell and cellular debris lack the ability to traverse streamlines in a laminar flow circuit determined by the hydrostatic pressure [906].

Due to the existing relationship between motility and normal morphology, these devices are able to eliminate abnormal cells from the samples, concomitant with imotile ones. Other passively driven microfluidics devices use gravity as a mechanism for creating several microchannels (Figure 112.B), relying on the capacity of motile sperm to move across the laminar streamlines towards the collection reservoir [907,908]. Both types of devices are equipped with the different chambers for the introduction of sperm sample and media, collection of motile spermatozoa, as well as non-motile cells and cellular debris (Figure 107).

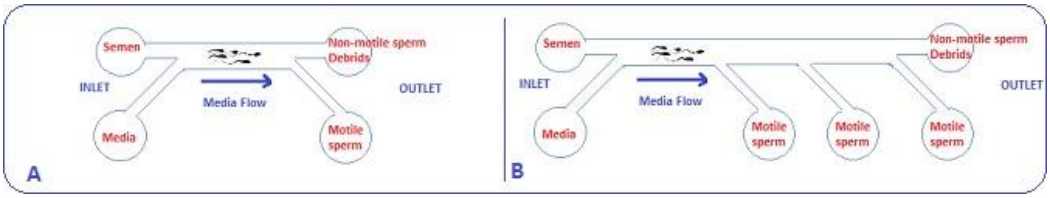

Figure 107. The Passively Driven Integrated Microfluidic System for sperm sorting (A-single reservoir for collection of motile sperm; B- multichannel reservoir for the collection of motile sperm)

A study conducted by Seo [909] showed that the movement of the sperm cells associated with the hydrostatic pressure may facilitate the sorting and alignment of bull, mouse and human spermatozoa through the micro-channel. By integrating a charge-coupled device (CCD) to the microfluidic device, Zhang and collaborators elaborated an automated algorithm capable of sorting sperm populations based on their motility pattern by determining several kinetic parameters such as sperm average velocity, straight line velocity, straightness of swimming path and average acceleration [910]. This algorithm may facilitate a more objective selection of sperm intended for ICSI.

More recently, Chen et al., proposed to use microfluidic resistive pulse technique (RPT) for the development of a device that may enable the quantification of both sperm concentration and motility, thus making this technique an economical alternative to sperm analysis systems such as computer-assisted semen analysis [911]. Furthermore, microfluidics might also prove helpful in improving the sexed semen technology, which enables livestock owners to obtain offspring of a desire sex. Among the methods currently used for obtaining sexed semen are included fluorescence in situ hybridization, polymerase chain reaction [912], density gradient centrifugation and FACS, the latter being the most effective (90% accuracy) [913]. When spermatozoa are sorted using FACS, the sperm DNA must stained a dye called Hoechst 33342, which enables the differentiation between chromosome X and Y. Despite the methods' high efficiency, the main drawback resides in the fact that Hoechst 33342

(Bisbenzimide) has a toxic effect on sperm cells and the sexed sorted semen which is obtained, usually has a much lower fertility compared to semen which is not sex-sorted [914].

Selection of oocytes using microfluidic systems

The quality of oocytes is a factor of great importance for both fertilization and embryo production. The selection of oocytes for IVF is carried out subjectively, based on morpho-structural properties of the cells [915,916].

The challenges in terms of implementing a more sophisticated method for assessing the quality of oocytes consist in developing an objectivity-based technique that would not jeopardize the integrity of cells which may then be used for fertilization. Choi et al., succeded in developing a microfluidic device that can establish the maturity degree of the female gamete by analyzing the index of refraction and optical absorption [917]. Significant differences were observed between mature and immature oocytes regarding the optical absorption spectrum, so this type of device may prove to be key in making oocyte selection less subjective.

Furthermore, in a study conducted in 2009, Szczepanska et al., assessed the micro-spectro-photometric features of bovine and porcine oocytes using a Lab-on-Chip platform in order to establish their potency [918]. Another spectrophotometric methodology utilizing lab-on-a chip device for assessing the quality of bovine oocytes was developed by Walczakand collaborators [919].

Apart from oocyte selection, the denudation of the oocytes represents another essential step during IVM and IVF. This process involves the removal of the cumulus-oocyte complexes by repeated aspiration and flushing with the tip of a narrow Pasteur pipette, thus causing a mechanical stress to the cells [920].

In Vitro fertilization on a chip (IVF-on-a-chip)

Conventionally, during the IVF process, the mature oocytes are coincubated with the washed semen in a culture dish using a fertilization medium, thus facilitating the interaction between spermatozoa and zona-pellucida of the oocyte. Since abnormal sperm function is the principle cause of human infertility, alternative procedures for IVF, such as ICSI or IMSI are used to overcome severe male infertility in patients with a history of repeated conventional IVF failure. Accordingly, the principle of both ICSI and IMSI is the assisted penetration of the oocytes by injecting the sperm into the egg cytoplasm. Unlike ICSI, IMSI is performed with an inverted microscope 400 times more powerful than the one used for ICSI, which allows for the detailed inspection of the internal morphology of sperm cells selected for injection [920].

A series of microfluidics devices destined with weir-type trap design were designed for IVF. Clark et al., worked on one that reduces the polyspermic penetration by limiting the period of time during which the oocytes interact with the spermatozoa [921]. Suhand et al., focus on developing a device that significantly increased the fertilization rates with a low total number and concentration of sperm [922]. In 2013, another group of researchers concentrated their efforts towards a fully automated microfluidic system that may be integrated in the ICSI procedure [923]. Spermatozoa are selected based on their motility and the oocytes are denuded in a separate compartment thorough a chemical and mechanical process. The revolutionary aspect of this device consists in the fact that the processing of both sexual gametes (sperm and oocytes) is fully integrated with the same instrument. Additionally, the system presents individual compartment for the culture and monitoring of a single embryo.

Dynamic embryo culture

Since the achievement of the first successful IVF, researchers and clinicians have made constant efforts to understand aspects of basic biology regarding gametes and embryos in order to improve the success rates in the assisted reproduction programs. Up to now, most of the research has aimed to improve the chemical composition of different media used for fertilization and embryo culture, as well as to optimize and simplify protocols. Unfortunately, the protocols used presently are still extremely laborious and require repeated washing and replacement of culture media, thus

generating changes in temperature, osmolarity, pH and most important, mechanical stress to the embryos [920]. However, the major drawback of the classical protocols for embryo culture is the lack of resemblance to what occurs in vivo. Naturally, after fertilization, the embryos are transported through the fallopian tubes by a continuous flow of fluid that has an extremely complex composition [924].

The success rates of assisted reproduction programs are still below expectations, but new opportunities for advancing ART are being created as revolutionary technologies such as biomimetics and microfluidics are emerging, scientists have started to tap into the potential advantages these new technologies in ART. For instance, a dynamic platform based on microfluidic technology mimics the *in vivo* process of embryo culture, and Hao et al., showed in 2013 that the quality of the embryos cultured using a microfluidic platform was superior as compared to the control group, cultured in standard media [925].

Automatization of vitrification

Cryopreservation is a key technology in biology and scientists are trying to minimize the osmotic stress effects and to improve survivability of the cells that are cryopreserved. The cryopreservation of oocytes and embryos may be achieved either by slow freezing or vitrification, though recent studies point to vitrification as the superior approach leading to a higher cleavage percentage, as well as higher survival and pregnancy rates [926].

Microfluidic systems may facilitate precise control of fluid osmolarity, and this is of great importance in the process of vitrification, where different concentrations of cryoprotectant agents (CPA) are used [920]. The exposure to various concentrations of cryoprotectant agents during the vitrification process increases cryosurvival and development in the bovine oocytes and embryos; however, the application of such a practice is limited since performing numerous precise pipetting steps in a short amount of time it is unlikely to be achieved by manual operation [927]. A microfluidic device for vitrification can provide a continuous, sequential flow using various concentrations of cryoprotectants agents, simultaneously being able to provide real-time images of cells that undergo the process of cryopreservation. Thus, in the future, the entire process of human and mammalian oocyte and embryo vitrification may become automated [927,928].

In 2014, Dai concluded that microfludic systems could perform certain protocols unavailable via conventional methods, reducing both the disadvantages of manual pipetting and the chemical stress to which the cells were subjected.

New mathematical model are being developed to assist understanding of delivery mechanisms from drug release systems. For instance, two drug release systems (based on chitosan and diclofenac sodium salt) were prepared by *in situ* hydrogelation in the presence of salicylaldehyde. The morphology of the systems was analyzed by scanning electron microscopy and polarized light microscopy and the drug release was *in vitro* investigated into a medium mimicking the *in vivo* environment. The drug release mechanism was firstly assessed by fitting the *in vitro* release data on five traditional mathematical models. In the context of pharmacokinetics behavioral analysis, a new mathematical procedure for describing drug release dynamics in polymer-drug complex systems was proposed. Assuming that the dynamics of polymer-drug system's structural units take place on continuous and nondifferentiable curves (multifractal curves), it was showed that in a one-dimensional hydrodynamic formalism of multifractal variables the drug release mechanism is given through synchronous dynamics at a differentiable and non-differentiable scale resolutions.

The *in vitro* release and fitting onto traditional models revealed a prolonged drug delivery mainly controlled by dissolution velocity and diffusion through the matrix. A different drug release rate noticed in the first release stage was attributed to the formation of polymer-drug structural units of different size, controlled by the system viscosity during the hydrogelation step. This indicated the formation of a multifractal system during the hydrogelation which controls the rate of drug release.

A theoretical model in a multi fractal paradigm was developed for understanding the drug release dynamics, considering that these behaviors are described by continuous but nondifferentiable curves. In such a context, the irrotational-type dynamic of the polymer drug structural units implies the functionality of a multifractal type hydrodynamic formalism. For the unidimensional case of this multifractal type hydrodynamic formalism, it was seen that ratio between the differentiable velocity

and the nondifferentiable one for a certain distance depends on a homographic manner on time. The conditions for the simultaneous dynamics involve the synchronization of the drug release mechanisms at the two scale resolutions, expressed through diffusion functions of multifractal type (the diffusion process depends on the scale resolutions).

Personal contribution - published papers:

Doroftei, **B**.; Gatu, I.; Ghizdovat, V. BIOLOGICAL SYSTEMS AND SUPERCONDUCTIVITY. SOME APPLICATIONS OF SUPERCONDUCTIVITY IN MEDICINE (I). *Bul. INSTITUTULUI Politeh. DIN IAŞI ISSN 1223-8139* ***2014****, Tomul LX (LXIV)*.

Doroftei, **B**.; Ghizdovat, V.; Stefanescu, C. BIOLOGICAL SYSTEMS AND SUPERCONDUCTIVITY. IMPLICATIONS OF THE SCALE RELATIVITY THEORY IN BIOLOGICAL SYSTEMS DYNAMICS (II). *Bul. INSTITUTULUI Politeh. DIN IAŞI ISSN 1223-8139* ***2014****, Tomul LX (LXIV)*.

Agop, M.; Gavriluț, A.; Crumpei, G.; **Doroftei**, **B**. Informational Non-Differentiable Entropy and Uncertainty Relations in Complex Systems. *Entropy* ***2014****, 16*. **IF: 2.524**

Agop, M.; Gavriluț, A.; Ştefan, G.; **Doroftei**, **B**. Implications of Non-Differentiable Entropy on a Space-Time Manifold. *Entropy* ***2015****, 17*. **IF: 2.524**

Doroftei, **B**. FRACTALS AND THEIR CORRESPONDENCE WITH BIOLOGICAL SYSTEMS (I). *Bul. INSTITUTULUI Politeh. DIN IAŞI ISSN 1223-8139* ***2014****, Tomul LX (LXIV)*.

Ghizdovat, V.; Doroftei, B. FRACTALS AND THEIR CORRESPONDENCE WITH BIOLOGICAL SYSTEMS. CARBON NANOTUBES AND BIOLOGICAL SYSTEMS (II). *Bul. INSTITUTULUI Politeh. DIN IAŞI ISSN 1223-8139* ***2014****, Tomul LX (LXIV)*.

Doroftei, **B**.; Doina, D.; Iacob, D.; Nicolae, D.; Volovat, S.; Viorel, S.; Agop, M.; Viviana, A. The Harmonic Oscillator Problem in the Scale Relativity Theory. Its Implications in the Morphogenesis of Structures at Various Scale Resolutions. *J. Comput. Theor. Nanosci.* ***2015****, 12*, 5870–5881. **IF: 0.457**

Doroftei, **B**.; Simionescu, G.; Neculai-Valeanu, A.S. APPLICATION OF NANOTECHNOLOGY IN THE IMPROVEMENT OF SEMEN QUALITY – FUTURE TREND IN ASSISTED REPRODUCTION. *Lucr. Stiint. Med. Vet. 1454-7406* ***2015****, 58*, 242–249.

Neculai-Valeanu, A.; Creangă, Ș.; Ruginosu, E.; Ariton, A.; **Doroftei**, **B**. Improving the outcome of in vitro embryo production through microfluidic technology. *Rom Biotechnol Lett*. ***2018,*** *23*, 14178-14186. **IF: 0.765**

Doroftei, **B**.; Mambet, C.; Zlei, M. It's Never over until It's over: How Can Age and Ovarian Reserve Be Mathematically Bound through the Measurement of Serum AMH—A Study of 5069 Romanian Women. *PLoS One* ***2015****, 10*, e0125216. **IF: 3.240**

Iftime, M.M.; Dobreci, D.L.; Irimiciuc, S.A.; Agop, M.; Petrescu, T.; **Doroftei**, **B**. A theoretical mathematical model for assessing diclofenac release from chitosan-based formulations. *Drug Deliv*. ***2020***, 27, 1125–1133. **IF: 6.419**

CONCLUSIONS

Directions for Future Professional Development and Scientific Research – Ongoing Projects and Topics of Further Clinical and Academic Interest

The research I have been conducting in the field of reproductive medicine builds on prior knowledge of medical genetics acquired during the residency, which now proves especially valuable for its relevance and applicability to my area of interest – infertility and human assisted reproduction. I have been able to turn my attention to relatively less studied clinical entities, such as rare diseases that are typically approached by geneticists. This is the basis for my professional goal to establish the first center for rare diseases and molecular genetics in our geographical region, which would work as a multidisciplinary hub for clinicians and researchers, giving them access to state-of-the-art equipment. The center would assist couples dealing with genetic infertility as well as other patients suffering from a wide spectrum of genetic disorders. Unfortunately, at present, such couples and individuals are faced with insurmountable diagnostic challenges and their comprehensive multidisciplinary approach is not yet possible. Most often, they bear the brunt of having to seek expensive, cumbersome, and time-consuming treatment internationally.

Thus, in the future, I plan to pursue new developments in areas such as Preimplantation Genetic Testing (PGT), a technique that promises to become the golden standard for many cases of embryo IVF both via biopsy and cell-free DNA detection. Also, I intend to deepen our current understanding by studying embryo division morphokinetics and fractal cellular division patterns in embryonic cultures, aiming to configure a model suitable for informational energy analysis. This would enable us to create an artificial intelligence algorithm for selecting those embryos with the highest developmental potential.

Another direction for research is to expand on the current knowledge and applicability of CRISPR-Cas9 technology in RUAM. Briefly, CRISPR refers to clustered regularly interspaced short palindromic repeats, or to groups of systematically interspaced short palindromic repeats making up a family of DNA sequences in the genome of all prokaryotic organisms. Cas9, or CRISPR-associated protein 9, is an enzyme that uses CRISPR sequences as a guide to recognize and cut those DNA strands complementary to CRISPR. These Cas9 enzymes together with the CRISPR sequences are the key elements of the technology known as CRISPR-Cas9 by which genes can be edited inside organisms with efficiency and specificity. This can have a wide range of applications, including fundamental biological research, biotechnological product development, and especially in the field of embryology, where genome editing can minimize the risk of anomalous autosomal recessive or dominant inheritance.

With regard to microbiota and the human microbiome, scientists have been able to shed new light on and gain novel perspectives of the countless immunologic, genetic, and histochemical implications of the symbiosis between microorganisms and the human body. Gut microbiota has been intensely studied lately, but my intended approach in this area would be to investigate the microbiota of aspirates from the peritoneal cavity and of follicular fluid in order to establish its role in infertility and human assisted reproduction.

Last but not least, the potential of applied exploratory hysteroscopy in the field of obstetrics may be explored and exploited further. This approach allows for the direct, *in situ* visualization of an embryo that has already been found by other means to contain abnormal genetic material and to therefore present a significant malformation risk. Another benefit of perfecting this method would be a superior detection rate for anomalies incompatible with life by correlating morphological results with paraclinical data from non-invasive prenatal testing (NIPT).

BIBLIOGRAPHIC REFERENCES

1. Greil, A.L.; Slauson-Blevins, K.; McQuillan, J. The experience of infertility: a review of recent literature. *Sociol. Health Illn.* **2010**, *32*, 140–162.
2. Vander Borght, M.; Wyns, C. Fertility and infertility: Definition and epidemiology. *Clin. Biochem.* **2018**, *62*, 2–10.
3. Deshpande, P.S.; Gupta, A.S. Causes and Prevalence of Factors Causing Infertility in a Public Health Facility. *J. Hum. Reprod. Sci.* **2019**, *12*, 287–293.
4. Testing and interpreting measures of ovarian reserve: a committee opinion. *Fertil. Steril.* **2015**, *103*, e9–e17.
5. Olooto, W.; Eniola; Amballi, A.; Adetola; Banjo, T.; Abayomi A review of Female Infertility; important etiological factors and management. *J. Microbiol. Biotechnol. Res.* **2012**, *2*, 379–385.
6. Dean, D.D.; Agarwal, S.; Tripathi, P. Connecting links between genetic factors defining ovarian reserve and recurrent miscarriages. *J. Assist. Reprod. Genet.* **2018**, *35*, 2121–2128.
7. Abrao, M.S.; Muzii, L.; Marana, R. Anatomical causes of female infertility and their management. *Int. J. Gynecol. Obstet.* **2013**, *123*, S18–S24.
8. Wallach, E.E.; Seibel, M.M.; Taymor, M.L. Emotional aspects of infertility. *Fertil. Steril.* **1982**, *37*, 137–145.
9. Nichols, W.C.; Pace-Nichols, M.A. Childless married couples. In *Handbook of family development and intervention.*; Wiley series in couples and family dynamics and treatment.; John Wiley & Sons Inc: Hoboken, NJ, US, 2000; pp. 171–188 ISBN 0-471-29967-7 (Hardcover).
10. Greenfeld, D.A. The course of infertility: Immediate and long-term reactions. *Sess. Psychother. Pract.* **1996**, *2*, 5–16.
11. Cousineau, T.M.; Domar, A.D. Psychological impact of infertility. *Best Pract. Res. Clin. Obstet. Gynaecol.* **2007**, *21*, 293–308.
12. Greil, A.; McQuillan, J.; Slauson-Blevins, K. The Social Construction of Infertility. *Sociol. Compass* **2011**, *5*, 736–746.
13. Schmidt, L. Psychosocial Consequences of Infertility and Treatment BT - Reproductive Endocrinology and Infertility: Integrating Modern Clinical and Laboratory Practice. In; Carrell, D.T., Peterson, C.M., Eds.; Springer New York: New York, NY, 2010; pp. 93–100 ISBN 978-1-4419-1436-1.
14. Verhaak, C.M.; Smeenk, J.M.J.; Evers, A.W.M.; Kremer, J.A.M.; Kraaimaat, F.W.; Braat, D.D.M. Women's emotional adjustment to IVF: a systematic review of 25 years of research. *Hum. Reprod. Update* **2006**, *13*, 27–36.
15. Boivin, J. A review of psychosocial interventions in infertility. *Soc. Sci. Med.* **2003**, *57*, 2325–2341.
16. Donarelli, Z.; Gullo, S.; Lo Coco, G.; Marino, A.; Scaglione, P.; Volpes, A.; Allegra, A. Assessing infertility-related stress: the factor structure of the Fertility Problem Inventory in Italian couples undergoing infertility treatment. *J. Psychosom. Obstet. Gynecol.* **2015**, *36*, 58–65.
17. Omani-Samani, R.; Ghaheri, A.; Navid, B.; Sepidarkish, M.; Maroufizadeh, S. Prevalence of generalized anxiety disorder and its related factors among infertile patients in Iran: a cross-sectional study. *Health Qual. Life Outcomes* **2018**, *16*, 129.
18. Omani-Samani, R.; Maroufizadeh, S.; Almasi-Hashiani, A.; Amini, P. Prevalence of depression and its determinant factors among infertile patients in Iran based on the PHQ-9. *Middle East Fertil. Soc. J.* **2018**, *23*, 460–463.
19. Amiri, M.; Khosravi, A.; Chaman, R.; Sadeghi, Z.; Raei, M.; Jahanitiji, M.; Mehrabian, F. Social Consequences of Infertility on Families in Iran. *Glob. J. Health Sci.* **2015**, *8*, 89–95.
20. Huppelschoten, A.G.; van Dongen, A.J.C.M.; Verhaak, C.M.; Smeenk, J.M.J.; Kremer, J.A.M.; Nelen, W.L.D.M. Differences in quality of life and emotional status between infertile women and their partners. *Hum. Reprod.* **2013**, *28*, 2168–2176.
21. Peterson, B.D.; Sejbaek, C.S.; Pirritano, M.; Schmidt, L. Are severe depressive symptoms associated with infertility-related distress in individuals and their partners? *Hum. Reprod.* **2013**, *29*, 76–82.
22. KLEMETTI, R.; RAITANEN, J.; SIHVO, S.; SAARNI, S.; KOPONEN, P. Infertility, mental disorders and well-being – a nationwide survey. *Acta Obstet. Gynecol. Scand.* **2010**, *89*, 677–682.
23. Gao, J.; Zhang, X.; Su, P.; Liu, J.; Shi, K.; Hao, Z.; Zhou, J.; Liang, C. Relationship between Sexual Dysfunction and Psychological Burden in Men with Infertility: A Large Observational Study in China. *J. Sex. Med.* **2013**, *10*, 1935–1942.
24. Satkunasivam, R.; Ordon, M.; Hu, B.; Mullen, B.; Lo, K.; Grober, E.; Jarvi, K. Hormone abnormalities are not related to the erectile dysfunction and decreased libido found in many men with infertility. *Fertil. Steril.* **2014**, *101*, 1594–1598.
25. Herbert, D.L.; Lucke, J.C.; Dobson, A.J. Depression: an emotional obstacle to seeking medical advice for infertility. *Fertil. Steril.* **2010**, *94*, 1817–1821.

26. Stewart, L.M.; Holman, C.D.J.; Semmens, J.B.; Preen, D.; Mai, Q.; Hart, R. Hospital mental health admissions in women after unsuccessful infertility treatment and in vitro fertilization: an Australian population-based cohort study. *PLoS One* **2015**, *10*, e0120076–e0120076.
27. Yli-Kuha, A.-N.; Gissler, M.; Klemetti, R.; Luoto, R.; Koivisto, E.; Hemminki, E. Psychiatric disorders leading to hospitalization before and after infertility treatments. *Hum. Reprod.* **2010**, *25*, 2018–2023.
28. Eisenberg, M.L.; Li, S.; Cullen, M.R.; Baker, L.C. Increased risk of incident chronic medical conditions in infertile men: analysis of United States claims data. *Fertil. Steril.* **2016**, *105*, 629–636.
29. Baldur-Felskov, B.; Kjaer, S.K.; Albieri, V.; Steding-Jessen, M.; Kjaer, T.; Johansen, C.; Dalton, S.O.; Jensen, A. Psychiatric disorders in women with fertility problems: results from a large Danish register-based cohort study. *Hum. Reprod.* **2012**, *28*, 683–690.
30. Biringer, E.; Kessler, U.; Mykletun, A. PW01-98 - No predictive value of anxiety- and depression symptoms for sub- or infertility. *Eur. Psychiatry* **2010**, *25*, 1529.
31. Biringer, E.; Kessler, U.; Howard, L.M.; Pasupathy, D.; Mykletun, A. Anxiety, depression and probability of live birth in a cohort of women with self-reported infertility in the HUNT 2 Study and Medical Birth Registry of Norway. *J. Psychosom. Res.* **2018**, *113*, 1–7.
32. Rostad, B.; Schmidt, L.; Sundby, J.; Schei, B. Infertility experience and health differentials – a population-based comparative study on infertile and non-infertile women (the HUNT Study). *Acta Obstet. Gynecol. Scand.* **2014**, *93*, 757–764.
33. Sirota, I.; Zarek, S.M.; Segars, J.H. Potential influence of the microbiome on infertility and assisted reproductive technology. *Semin. Reprod. Med.* **2014**, *32*, 35–42.
34. Blenner, J.L. Clomiphene-Induced Mood Swings. *J. Obstet. Gynecol. Neonatal Nurs.* **1991**, *20*, 321–327.
35. Aussedat, M.; Jean-Louis, J.; Brochet*, O.D. and M.-S. Clomiphene for the Treatment of Male Infertility: A Case Report of Mood Change and a Literature Overview. *Curr. Drug Saf.* 2017, *12*, 208–215.
36. Choi, S.-H.; Shapiro, H.; Robinson, G.E.; Irvine, J.; Neuman, J.; Rosen, B.; Murphy, J.; Stewart, D. Psychological side-effects of clomiphene citrate and human menopausal gonadotrophin. *J. Psychosom. Obstet. Gynecol.* **2005**, *26*, 93–100.
37. Gingnell, M.; Engman, J.; Frick, A.; Moby, L.; Wikström, J.; Fredrikson, M.; Sundström-Poromaa, I. Oral contraceptive use changes brain activity and mood in women with previous negative affect on the pill—A double-blinded, placebo-controlled randomized trial of a levonorgestrel-containing combined oral contraceptive. *Psychoneuroendocrinology* **2013**, *38*, 1133–1144.
38. O'Connell, K.; Davis, A.R.; Kerns, J. Oral contraceptives: side effects and depression in adolescent girls. *Contraception* **2007**, *75*, 299–304.
39. Skovlund, C.W.; Mørch, L.S.; Kessing, L.V.; Lidegaard, Ø. Association of Hormonal Contraception With Depression. *JAMA Psychiatry* **2016**, *73*, 1154–1162.
40. Young, E.A.; Kornstein, S.G.; Harvey, A.T.; Wisniewski, S.R.; Barkin, J.; Fava, M.; Trivedi, M.H.; Rush, A.J. Influences of hormone-based contraception on depressive symptoms in premenopausal women with major depression. *Psychoneuroendocrinology* **2007**, *32*, 843–853.
41. Roberts, T.A.; Hansen, S. Association of Hormonal Contraception with depression in the postpartum period. *Contraception* **2017**, *96*, 446–452.
42. Zettermark, S.; Perez Vicente, R.; Merlo, J. Hormonal contraception increases the risk of psychotropic drug use in adolescent girls but not in adults: A pharmacoepidemiological study on 800 000 Swedish women. *PLoS One* **2018**, *13*, e0194773–e0194773.
43. Evans-Hoeker, E.A.; Eisenberg, E.; Diamond, M.P.; Legro, R.S.; Alvero, R.; Coutifaris, C.; Casson, P.R.; Christman, G.M.; Hansen, K.R.; Zhang, H.; et al. Major depression, antidepressant use, and male and female fertility. *Fertil. Steril.* **2018**, *109*, 879–887.
44. Toren, P.; Dor, J.; Mester, R.; Mozes, T.; Blumensohn, R.; Rehavi, M.; Weizman, A. Depression in women treated with a gonadotropinreleasing hormone agonist. *Biol. Psychiatry* **1996**, *39*, 378–382.
45. Yazdani, F.; Elyasi, F.; Peyvandi, S.; Moosazadeh, M.; Galekolaee, K.S.; Kalantari, F.; Rahmani, Z.; Hamzehgardeshi, Z. Counseling-supportive interventions to decrease infertile women's perceived stress: A systematic review. *Electron. physician* **2017**, *9*, 4694–4702.
46. Zahra, O.A.; Soheila, R.; Tahereh, B.; Marzieh, A.; Atefeh, Y. The Effectiveness of Counseling with a Cognitive-Behavioral Approach on Infertile Women's Stress. *Maedica (Buchar).* **2019**, *14*, 363–370.
47. Mosalanejad, L.; Khodabakshi Koolaee, A.; Jamali, S. Effect of cognitive behavioral therapy in mental health and hardiness of infertile women receiving assisted reproductive therapy (ART). *Iran. J. Reprod. Med.* **2012**, *10*, 483–488.
48. Maleki-Saghooni, N.; Amirian, M.; Sadeghi, R.; Latifnejad Roudsari, R. Effectiveness of infertility counseling on pregnancy rate in infertile patients undergoing assisted reproductive technologies: A systematic review and meta-analysis. *Int. J. Reprod. Biomed.* **2017**, *15*, 391–402.

49. Burns, L.H. Psychiatric Aspects of Infertility and Infertility Treatments. *Psychiatr. Clin. North Am.* **2007**, *30*, 689–716.
50. Dumbala, S.; Bhargav, H.; Satyanarayana, V.; Arasappa, R.; Varambally, S.; Desai, G.; Bangalore, G.N. Effect of Yoga on Psychological Distress among Women Receiving Treatment for Infertility. *Int. J. Yoga* **2020**, *13*, 115–119.
51. Oron, G.; Allnutt, E.; Lackman, T.; Sokal-Arnon, T.; Holzer, H.; Takefman, J. A prospective study using Hatha Yoga for stress reduction among women waiting for IVF treatment. *Reprod. Biomed. Online* **2015**, *30*, 542–548.
52. Jasani, S.; Heller, B. Impact of a Structured Yoga Program on Anxiety in Infertility Patients: A Feasibility Study. *J. Fertil. Vitr. - IVF-Worldwide, Reprod. Med. Genet. Stem Cell Biol.* **2016**, *04*.
53. Charlton, H. Neural transplantation in hypogonadal (hpg) mice – physiology and neurobiology. *Reproduction 127*, 3–12.
54. Balmus, I.M.; Ciobica, A.; Trifan, A.; Stanciu, C. The implications of oxidative stress and antioxidant therapies in Inflammatory Bowel Disease: Clinical aspects and animal models. *Saudi J. Gastroenterol.* **2016**, *22*, 3–17.
55. Ciobica, A.; Padurariu, M.; Hritcu, L. The effects of short-term nicotine administration on behavioral and oxidative stress deficiencies induced in a rat model of Parkinson's disease. *Psychiatr. Danub.* **2012**, *24*, 194–205.
56. Wang, S.; Sun, M.; Yu, L.; Wang, Y.; Yao, Y.; Wang, D. Niacin Inhibits Apoptosis and Rescues Premature Ovarian Failure. *Cell. Physiol. Biochem.* **2018**, *50*, 2060–2070.
57. Zhang, J.; Zhao, X.; Jiang, Y.; Zhao, W.; Guo, T.; Cao, Y.; Teng, J.; Hao, X.; Zhao, J.; Yang, Z. Antioxidant status and gut microbiota change in an aging mouse model as influenced by exopolysaccharide produced by Lactobacillus plantarum YW11 isolated from Tibetan kefir. *J. Dairy Sci.* **2017**, *100*, 6025–6041.
58. Zhao, J.; Tian, F.; Yan, S.; Zhai, Q.; Zhang, H.; Chen, W. Lactobacillus plantarum CCFM10 alleviating oxidative stress and restoring the gut microbiota in d-galactose-induced aging mice. *Food Funct.* **2018**, *9*, 917–924.
59. Jose, S.; Bhalla, P.; Suraishkumar, G.K. Oxidative stress decreases the redox ratio and folate content in the gut microbe, Enterococcus durans (MTCC 3031). *Sci. Rep.* **2018**, *8*, 12138.
60. Reese, A.T.; Cho, E.H.; Klitzman, B.; Nichols, S.P.; Wisniewski, N.A.; Villa, M.M.; Durand, H.K.; Jiang, S.; Midani, F.S.; Nimmagadda, S.N.; et al. Antibiotic-induced changes in the microbiota disrupt redox dynamics in the gut. *Elife* **2018**, *7*, e35987..
61. Ge, Y.; Lin, S.; Li, B.; Yang, Y.; Tang, X.; Shi, Y.; Sun, J.; Le, G. Oxidized Pork Induces Oxidative Stress and Inflammation by Altering Gut Microbiota in Mice. *Mol. Nutr. Food Res.* **2020**, *64*, 1901012.
62. de Sousa, A.R.; de Castro Moreira, M.E.; Grancieri, M.; Toledo, R.C.L.; de Oliveira Araújo, F.; Mantovani, H.C.; Queiroz, V.A.V.; Martino, H.S.D. Extruded sorghum (Sorghum bicolor L.) improves gut microbiota, reduces inflammation, and oxidative stress in obese rats fed a high-fat diet. *J. Funct. Foods* **2019**, *58*, 282–291.
63. Ohlsson, B.; Veress, B.; Janciauskiene, S.; Montgomery, A.; Haglund, M.; Wallmark, A. Chronic Intestinal Pseudo-Obstruction due to Buserelin-Induced Formation of Anti-GnRH Antibodies. *Gastroenterology* **2007**, *132*, 45–51.
64. Sharma, R.K.; Agarwal, A. Role of reactive oxygen species in male infertility. *Urology* **1996**, *48*, 835–850.
65. Lipshultz, L.I.; Howards, S.S. Evaluation of the subfertile man. *Infertil. Male. New York Churchill Livingstone* **1983**, 187–192.
66. Aitken, R.J.; Sutton, M.; Warner, P.; Richardson, D.W. Relationship between the movement characteristics of human spermatozoa and their ability to penetrate cervical mucus and zona-free hamster oocytes. *Reproduction 73*, 441–449.
67. Overstreet, J.W.; Yanagimachi, R.; Katz, D.F.; Hayashi, K.; Hanson, F.W. Penetration of Human Spermatozoa into the Human Zona Pellucida and the Zona-Free Hamster Egg: A Study of Fertile Donors and Infertile Patients**Supported in part by a grant from the International Planned Parenthood Federation (to R. Y.). *Fertil. Steril.* **1980**, *33*, 534–542.
68. Aitken, R.J.; Best, F.S.M.; Richardson, D.W.; Djahanbakhch, O.; Lees, M.M. The correlates of fertilizing capacity in normal fertile men*. *Fertil. Steril.* **1982**, *38*, 68–76.
69. Holland, M.K.; Alvarez, J.G.; Storey, B.T. Production of Superoxide and Activity of Superoxide Dismutase in Rabbit Epididymal Spermatozoa. *Biol. Reprod.* **1982**, *27*, 1109–1118.
70. Aitken, R.J.; Best, F.S.M.; Richardson, D.W.; Djahanbakhch, O.; Templeton, A.; Lees, M.M. An analysis of semen quality and sperm function in cases of oligozoospermia**Supported in part by a grant from the Riyadh-Al Kharj Hospital, Riyadh, Saudi Arabia, to Professor D. T. Baird, Department of Obstetrics and Gynaecology, University of Edinburgh. *Fertil. Steril.* **1982**, *38*, 705–711.

71. Aitken, R.J.; Clarkson, J.S. Cellular basis of defective sperm function and its association with the genesis of reactive oxygen species by human spermatozoa. *Reproduction 81*, 459–469.
72. ALVAREZ, J.G.; TOUCHSTONE, J.C.; BLASCO, L.; STOREY, B.T. Spontaneous Lipid Peroxidation and Production of Hydrogen Peroxide and Superoxide in Human Spermatozoa Superoxide Dismutase as Major Enzyme Protectant Against Oxygen Toxicity. *J. Androl.* **1987**, *8*, 338–348.
73. Steiner, A.Z.; Hansen, K.R.; Barnhart, K.T.; Cedars, M.I.; Legro, R.S.; Diamond, M.P.; Krawetz, S.A.; Usadi, R.; Baker, V.L.; Coward, R.M.; et al. The effect of antioxidants on male factor infertility: the Males, Antioxidants, and Infertility (MOXI) randomized clinical trial. *Fertil. Steril.* **2020**, *113*, 552-560.e3.
74. Ruder, E.H.; Hartman, T.J.; Goldman, M.B. Impact of oxidative stress on female fertility. *Curr. Opin. Obstet. Gynecol.* **2009**, *21*.
75. Aitken, R.J.; Clarkson, J.S. Generation of reactive oxygen species by human spermatozoa. *Free radicals Recent Dev. lipid Chem. Exp. Pathol. Med.* **1987**, 333–335.
76. Agarwal, A.; Gupta, S.; Sharma, R.K. Role of oxidative stress in female reproduction. *Reprod. Biol. Endocrinol.* **2005**, *3*, 28.
77. Agarwal, A.; Nallella, K.P.; Allamaneni, S.S.R.; Said, T.M. Role of antioxidants in treatment of male infertility: an overview of the literature. *Reprod. Biomed. Online* **2004**, *8*, 616–627.
78. Szczepańska, M.; Koźlik, J.; Skrzypczak, J.; Mikołajczyk, M. Oxidative stress may be a piece in the endometriosis puzzle. *Fertil. Steril.* **2003**, *79*, 1288–1293.
79. SIRISTATIDIS, C.; VOGIATZI, P.; VAROUNIS, C.; ASKOXYLAKI, M.; CHRELIAS, C.; PAPANTONIOU, N. The Effect of Reactive Oxygen Species on Embryo Quality in IVF. *Vivo* **2016**, *30*, 149–153.
80. Nishihara, T.; Matsumoto, K.; Hosoi, Y.; Morimoto, Y. Evaluation of antioxidant status and oxidative stress markers in follicular fluid for human in vitro fertilization outcome. *Reprod. Med. Biol.* **2018**, *17*, 481–486.
81. Borowiecka, M.; Wojsiat, J.; Polac, I.; Radwan, M.; Radwan, P.; Zbikowska, H.M. Oxidative stress markers in follicular fluid of women undergoing in vitro fertilization and embryo transfer. *Syst. Biol. Reprod. Med.* **2012**, *58*, 301–305.
82. Tulić, L.; Vidaković, S.; Tulić, I.; Ćurčić, M.; Stojnić, J.; Jeremić, K. Oxidative Stress Markers in GnRH Agonist and Antagonist Protocols in IVF. *J. Med. Biochem.* **2017**, *36*, 163–170.
83. Kumar, S.; Mishra, V.; Thaker, R.; Gor, M.; Perumal, S.; Joshi, P.; Sheth, H.; Shaikh, I.; Gautam, A.K.; Verma, Y. Role of environmental factors & oxidative stress with respect to in vitro fertilization outcome. *Indian J. Med. Res.* **2018**, *148*, S125–S133.
84. Singh, A.K.; Chattopadhyay, R.; Chakravarty, B.; Chaudhury, K. Markers of oxidative stress in follicular fluid of women with endometriosis and tubal infertility undergoing IVF. *Reprod. Toxicol.* **2013**, *42*, 116–124.
85. Luddi, A.; Capaldo, A.; Focarelli, R.; Gori, M.; Morgante, G.; Piomboni, P.; De Leo, V. Antioxidants reduce oxidative stress in follicular fluid of aged women undergoing IVF. *Reprod. Biol. Endocrinol.* **2016**, *14*, 57.
86. Fadgyas-Stanculete, M.; Buga, A. (1). nbi.-M.; Popa-Wagner, A.; Dumitrascu, D.L. The relationship between irritable bowel syndrome and psychiatric disorders: from molecular changes to clinical manifestations. *J. Mol. psychiatry* **2014**, *2*, 4.
87. Schmulson, M.J.; Drossman, D.A. What Is New in Rome IV. *J. Neurogastroenterol. Motil.* **2017**, *23*, 151–163.
88. Mayer, E.A. Clinical practice. Irritable bowel syndrome. *N. Engl. J. Med.* **2008**, *358*, 1692–1699.
89. Singh, P.; Agnihotri, A.; Pathak, M.K.; Shirazi, A.; Tiwari, R.P.; Sreenivas, V.; Sagar, R.; Makharia, G.K. Psychiatric, somatic and other functional gastrointestinal disorders in patients with irritable bowel syndrome at a tertiary care center. *J. Neurogastroenterol. Motil.* **2012**, *18*, 324–33.
90. Masand, P.S.; Kaplan, D.S.; Gupta, S.; Bhandary, A.N.; Nasra, G.S.; Kline, M.D.; Margo, K.L. Major depression and irritable bowel syndrome: is there a relationship? *J. Clin. Psychiatry* **1995**, *56*, 363–367.
91. Karling, P.; Danielsson, Å.; Adolfsson, R.; Norrback, K. -f. No difference in symptoms of irritable bowel syndrome between healthy subjects and patients with recurrent depression in remission. *Neurogastroenterol. Motil.* **2007**, *19*, 896–904.
92. Michael, V.; El Hamady, M.; El-Bakry, S.; Awd, M. A study of psychiatric comorbidities in irritable bowel syndrome. *Egypt. J. Psychiatry* **2018**, *39*, 140–149.
93. Fitzgerald, P.; Cassidy Eugene, M.; Clarke, G.; Scully, P.; Barry, S.; Quigley Eamonn, M.M.; Shanahan, F.; Cryan, J.; Dinan Timothy, G. Tryptophan catabolism in females with irritable bowel syndrome: relationship to interferon-gamma, severity of symptoms and psychiatric co-morbidity. *Neurogastroenterol. Motil.* **2008**, *20*, 1291–1297.
94. Majeed, M.; Nagabhushanam, K.; Arumugam, S.; Majeed, S.; Ali, F. Bacillus coagulans MTCC 5856

for the management of major depression with irritable bowel syndrome: a randomised, double-blind, placebo controlled, multi-centre, pilot clinical study. *Food Nutr. Res.* **2018**, *62*, 10.29219/fnr.v62.1218.
95. Romijn, A.R.; Rucklidge, J.J.; Kuijer, R.G.; Frampton, C. A double-blind, randomized, placebo-controlled trial of Lactobacillus helveticus and Bifidobacterium longum for the symptoms of depression. *Aust. N. Z. J. Psychiatry* **2017**, *51*, 810–821.
96. Bardisi, B.; Halawani, A.; Halawani, H.; Alharbi, A.; Turkostany, N.; Alrehaili, T.; Radin, A.; Alkhuzea, N. Efficiency of diet change in irritable bowel syndrome. *J. Fam. Med. Prim. Care* **2018**, *7*, 946–951.
97. Inserra, A.; Rogers, G.B.; Licinio, J.; Wong, M.-L. The Microbiota-Inflammasome Hypothesis of Major Depression. *BioEssays* **2018**, *40*, 1800027.
98. Slyepchenko, A.; Maes, M.; Jacka, F.N.; Köhler, C.A.; Barichello, T.; McIntyre, R.S.; Berk, M.; Grande, I.; Foster, J.A.; Vieta, E.; et al. Gut Microbiota, Bacterial Translocation, and Interactions with Diet: Pathophysiological Links between Major Depressive Disorder and Non-Communicable Medical Comorbidities. *Psychother. Psychosom.* **2017**, *86*, 31–46.
99. Crane, C.; Martin, M.; Johnston, D.; Goodwin, G.M. Does depression influence symptom severity in irritable bowel syndrome? Case study of a patient with irritable bowel syndrome and bipolar disorder. *Psychosom. Med.* **2003**, *65*, 919–923.
100. Mykletun, A.; Jacka, F.; Williams, L.; Pasco, J.; Henry, M.; Nicholson, G.C.; Kotowicz, M.A.; Berk, M. Prevalence of mood and anxiety disorder in self reported irritable bowel syndrome (IBS). An epidemiological population based study of women. *BMC Gastroenterol.* **2010**, *10*, 88.
101. Liu, C.-J.; Hu, L.-Y.; Yeh, C.-M.; Hu, Y.-W.; Chen, P.-M.; Chen, T.-J.; Lu, T. Irritable brain caused by irritable bowel? A nationwide analysis for irritable bowel syndrome and risk of bipolar disorder. *PLoS One* **2015**, *10*, e0118209–e0118209.
102. Tseng, P.-T.; Zeng, B.-S.; Chen, Y.-W.; Wu, M.-K.; Wu, C.-K.; Lin, P.-Y. A meta-analysis and systematic review of the comorbidity between irritable bowel syndrome and bipolar disorder. *Medicine (Baltimore).* **2016**, *95*, e4617–e4617.
103. Lee, Y.-T.; Hu, L.-Y.; Shen, C.-C.; Huang, M.-W.; Tsai, S.-J.; Yang, A.C.; Hu, C.-K.; Perng, C.-L.; Huang, Y.-S.; Hung, J.-H. Risk of Psychiatric Disorders following Irritable Bowel Syndrome: A Nationwide Population-Based Cohort Study. *PLoS One* **2015**, *10*, e0133283–e0133283.
104. Järbrink-Sehgal, E.; Andreasson, A. The gut microbiota and mental health in adults. *Curr. Opin. Neurobiol.* **2020**, *62*, 102–114.
105. Rossato, M.; Foresta, C. Antisperm Antibodies in Inflammatory Bowel Disease. *Arch. Intern. Med.* **2004**, *164*, 2281–2283.
106. Moody, G.A.; Probert, C.; Jayanthi, V.; Mayberry, J.F. The effects of chronic ill health and treatment with sulphasalazine on fertility amongst men and women with inflammatory bowel disease in Leicestershire. *Int. J. Colorectal Dis.* **1997**, *12*, 220–224.
107. Matricon, J.; Meleine, M.; Gelot, A.; Piche, T.; Dapoigny, M.; Muller, E.; Ardid, D. Review article: associations between immune activation, intestinal permeability and the irritable bowel syndrome. *Aliment. Pharmacol. Ther.* **2012**, *36*, 1009–1031.
108. Narendranathan, M.; Sandier, R.S.; Suchindran, C.M.; Savitz, D.A. Male Infertility in Inflammatory Bowel Disease. *J. Clin. Gastroenterol.* **1989**, *11*.
109. Moody, G.A.; Mayberry, J.F. Perceived Sexual Dysfunction amongst Patients with Inflammatory Bowel Disease. *Digestion* **1993**, *54*, 256–260.
110. HEETUN, Z.S.; BYRNES, C.; NEARY, P.; O'MORAIN, C. Review article: reproduction in the patient with inflammatory bowel disease. *Aliment. Pharmacol. Ther.* **2007**, *26*, 513–533.
111. Tavernier, N.; Fumery, M.; Peyrin-Biroulet, L.; Colombel, J.-F.; Gower-Rousseau, C. Systematic review: fertility in non-surgically treated inflammatory bowel disease. *Aliment. Pharmacol. Ther.* **2013**, *38*, 847–853.
112. Lee, S.; Crowe, M.; Seow, C.H.; Kotze, P.G.; Kaplan, G.G.; Metcalfe, A.; Ricciuto, A.; Benchimol, E.I.; Kuenzig, M.E. The impact of surgical therapies for inflammatory bowel disease on female fertility. *Cochrane database Syst. Rev.* **2019**, *7*, CD012711–CD012711.
113. Feagins, L.; Kane, S. Sexual and Reproductive Issues for Men With Inflammatory Bowel Disease. *Am. J. Gastroenterol.* **2009**, *104*, 768–773.
114. Sands, K.; Jansen, R.; Zaslau, S.; Greenwald, D. Review article: the safety of therapeutic drugs in male inflammatory bowel disease patients wishing to conceive. *Aliment. Pharmacol. Ther.* **2015**, *41*, 821–834.
115. Shin, T.; Kobori, Y.; Suzuki, K.; Iwahata, T.; Yagi, H.; Soh, S.; Arai, G.; Okada, H. Inflammatory bowel disease in subfertile men and the effect of mesalazine on fertility. *Syst. Biol. Reprod. Med.* **2014**, *60*, 373–376.
116. Grunnet, E.; Nyfors, A.; Hansen, K.B. Studies on Human Semen in Topical Corticosteroid-Treated and

in Methotrexate-Treated Psoriatics. *Dermatology* **1977**, *154*, 78–84.
117. Shin, T.; Okada, H. Infertility in men with inflammatory bowel disease. *World J. Gastrointest. Pharmacol. Ther.* **2016**, *7*, 361–369.
118. Johnson, P.M. Managing Reduced Fecundity Following IBD-related Surgery. *Gastroenterol. Hepatol. (N. Y).* **2008**, *4*, 267–268.
119. Quigley, E.M.M.; Bytzer, P.; Jones, R.; Mearin, F. Irritable bowel syndrome: The burden and unmet needs in Europe. *Dig. Liver Dis.* **2006**, *38*, 717–723.
120. Zegers-Hochschild, F.; Adamson, G.D.; de Mouzon, J.; Ishihara, O.; Mansour, R.; Nygren, K.; Sullivan, E.; Vanderpoel, S. International Committee for Monitoring Assisted Reproductive Technology (ICMART) and the World Health Organization (WHO) revised glossary of ART terminology, 2009. *Fertil. Steril.* **2009**, *92*, 1520–1524.
121. Conn P. Michael, P..; Crowley, W.F. GONADOTROPIN-RELEASING HORMONE AND ITS ANALOGS. *Annu. Rev. Med.* **1994**, *45*, 391–405.
122. Levine, J.E. New Concepts of the Neuroendocrine Regulation of Gonadotropin Surges in Rats. *Biol. Reprod.* **1997**, *56*, 293–302.
123. González-Martínez, D.; Hu, Y.; Bouloux, P.M. Ontogeny of GnRH and olfactory neuronal systems in man: novel insights from the investigation of inherited forms of Kallmann's syndrome. *Front. Neuroendocrinol.* **2004**, *25*, 108–130.
124. Hammar, O.; Ohlsson, B.; Veress, B.; Alm, R.; Fredrikson, G.N.; Montgomery, A. Depletion of enteric gonadotropin-releasing hormone is found in a few patients suffering from severe gastrointestinal dysmotility. *Scand. J. Gastroenterol.* **2012**, *47*, 1165–1173.
125. Roberts, V.H.J.; Smith, J.; McLea, S.A.; Heizer, A.B.; Richardson, J.L.; Myatt, L. Effect of Increasing Maternal Body Mass Index on Oxidative and Nitrative Stress in The Human Placenta. *Placenta* **2009**, *30*, 169–175.
126. Ehrmann, D.A. Polycystic Ovary Syndrome. *N. Engl. J. Med.* **2005**, *352*, 1223–1236.
127. Stamets, K.; Taylor, D.S.; Kunselman, A.; Demers, L.M.; Pelkman, C.L.; Legro, R.S. A randomized trial of the effects of two types of short-term hypocaloric diets on weight loss in women with polycystic ovary syndrome. *Fertil. Steril.* **2004**, *81*, 630–637.
128. Moran, L.J.; Brinkworth, G.D.; Norman, R.J. Dietary therapy in polycystic ovary syndrome. *Semin. Reprod. Med.* **2008**, *26*, 85–92.
129. El-Tawil, A.M. Zinc deficiency in men with Crohn's disease may contribute to poor sperm function and male infertility. *Andrologia* **2003**, *35*, 337–341.
130. König, J.; Ganda Mall, J.-P.; Rangel, I.; Edebol-Carlman, H.; Brummer, R.-J. The Role of the Gut Microbiota in Brain Function. In; 2014 ISBN 978-1-910190-09-8.
131. Scheperjans, F. The prodromal microbiome. *Mov. Disord.* **2018**, *33*, 5–7.
132. Mertsalmi, T.H.; Aho, V.T.E.; Pereira, P.A.B.; Paulin, L.; Pekkonen, E.; Auvinen, P.; Scheperjans, F. More than constipation – bowel symptoms in Parkinson's disease and their connection to gut microbiota. *Eur. J. Neurol.* **2017**, *24*, 1375–1383.
133. Cassani, E.; Privitera, G.; Pezzoli, G.; Pusani, C.; Madio, C.; Iorio, L.; Barichella, M. Use of probiotics for the treatment of constipation in Parkinson's disease patients. *Minerva Gastroenterol. Dietol.* **2011**, *57*, 117–121.
134. Suzuki, M.; Yoshioka, M.; Hashimoto, M.; Murakami, M.; Noya, M.; Takahashi, D.; Urashima, M. Randomized, double-blind, placebo-controlled trial of vitamin D supplementation in Parkinson disease. *Am. J. Clin. Nutr.* **2013**, *97*, 1004–1013.
135. Smith, M.P.; Fletcher-Turner, A.; Yurek, D.M.; Cass, W.A. Calcitriol Protection against Dopamine Loss Induced by Intracerebroventricular Administration of 6-Hydroxydopamine. *Neurochem. Res.* **2006**, *31*, 533–539.
136. Coimbra, C.G.; Junqueira, V.B.C. High doses of riboflavin and the elimination of dietary red meat promote the recovery of some motor functions in Parkinson's disease patients . *Brazilian J. Med. Biol. Res.* 2003, *36*, 1409–1417.
137. Heintz-Buschart, A.; Pandey, U.; Wicke, T.; Sixel-Döring, F.; Janzen, A.; Sittig-Wiegand, E.; Trenkwalder, C.; Oertel, W.H.; Mollenhauer, B.; Wilmes, P. The nasal and gut microbiome in Parkinson's disease and idiopathic rapid eye movement sleep behavior disorder. *Mov. Disord.* **2018**, *33*, 88–98.
138. Keshavarzian, A.; Green, S.J.; Engen, P.A.; Voigt, R.M.; Naqib, A.; Forsyth, C.B.; Mutlu, E.; Shannon, K.M. Colonic bacterial composition in Parkinson's disease. *Mov. Disord.* **2015**, *30*, 1351–1360.
139. Hill-Burns, E.M.; Debelius, J.W.; Morton, J.T.; Wissemann, W.T.; Lewis, M.R.; Wallen, Z.D.; Peddada, S.D.; Factor, S.A.; Molho, E.; Zabetian, C.P.; et al. Parkinson's disease and Parkinson's disease medications have distinct signatures of the gut microbiome. *Mov. Disord.* **2017**, *32*, 739–749.
140. Bedarf, J.R.; Hildebrand, F.; Coelho, L.P.; Sunagawa, S.; Bahram, M.; Goeser, F.; Bork, P.; Wüllner, U.

Functional implications of microbial and viral gut metagenome changes in early stage L-DOPA-naïve Parkinson's disease patients. *Genome Med.* **2017**, *9*, 39.
141. Unger, M.M.; Spiegel, J.; Dillmann, K.-U.; Grundmann, D.; Philippeit, H.; Bürmann, J.; Faßbender, K.; Schwiertz, A.; Schäfer, K.-H. Short chain fatty acids and gut microbiota differ between patients with Parkinson's disease and age-matched controls. *Parkinsonism Relat. Disord.* **2016**, *32*, 66–72.
142. Barichella, M.; Severgnini, M.; Cilia, R.; Cassani, E.; Bolliri, C.; Caronni, S.; Ferri, V.; Cancello, R.; Ceccarani, C.; Faierman, S.; et al. Unraveling gut microbiota in Parkinson's disease and atypical parkinsonism. *Mov. Disord.* **2019**, *34*, 396–405.
143. Lin, A.; Zheng, W.; He, Y.; Tang, W.; Wei, X.; He, R.; Huang, W.; Su, Y.; Huang, Y.; Zhou, H.; et al. Gut microbiota in patients with Parkinson's disease in southern China. *Parkinsonism Relat. Disord.* **2018**, *53*, 82–88.
144. Scheperjans, F.; Aho, V.; Pereira, P.A.B.; Koskinen, K.; Paulin, L.; Pekkonen, E.; Haapaniemi, E.; Kaakkola, S.; Eerola-Rautio, J.; Pohja, M.; et al. Gut microbiota are related to Parkinson's disease and clinical phenotype. *Mov. Disord.* **2015**, *30*, 350–358.
145. Qian, Y.; Yang, X.; Xu, S.; Wu, C.; Song, Y.; Qin, N.; Chen, S.-D.; Xiao, Q. Alteration of the fecal microbiota in Chinese patients with Parkinson's disease. *Brain. Behav. Immun.* **2018**, *70*, 194–202.
146. Hopfner, F.; Künstner, A.; Müller, S.H.; Künzel, S.; Zeuner, K.E.; Margraf, N.G.; Deuschl, G.; Baines, J.F.; Kuhlenbäumer, G. Gut microbiota in Parkinson disease in a northern German cohort. *Brain Res.* **2017**, *1667*, 41–45.
147. Li, W.; Wu, X.; Hu, X.; Wang, T.; Liang, S.; Duan, Y.; Jin, F.; Qin, B. Structural changes of gut microbiota in Parkinson's disease and its correlation with clinical features. *Sci. China Life Sci.* **2017**, *60*, 1223–1233.
148. Yuzefpolskaya, M.; Bohn, B.; Nasiri, M.; Zuver, A.M.; Onat, D.D.; Royzman, E.A.; Nwokocha, J.; Mabasa, M.; Pinsino, A.; Brunjes, D.; et al. Gut microbiota, endotoxemia, inflammation, and oxidative stress in patients with heart failure, left ventricular assist device, and transplant. *J. Hear. Lung Transplant.* **2020**.
149. Kadariswantiningsih, I.; Thaha, M.; Wibisono, C.; Empitu, M. Thiol-producing microbiota of the intestine modulate oxidative stress and inflammation in Chronic Kidney Disease. *Bali Med. J.* **2019**, *8*, 307.
150. Bhalla, P.; Rengaswamy, R.; Karunagaran, D.; Suraishkumar, G.K.; Sahoo, S. Silver nanoparticle induced oxidative stress augments anticancer gut bacterial metabolites production. *bioRxiv* **2019**, 658609.
151. Chi, L.; Bian, X.; Gao, B.; Tu, P.; Ru, H.; Lu, K. The Effects of an Environmentally Relevant Level of Arsenic on the Gut Microbiome and Its Functional Metagenome. *Toxicol. Sci.* **2017**, *160*, 193–204.
152. Wang, Y.; Bi, Z.; Wang, E.; Sun, B.; Zheng, Y.; Zhong, L.; Yuan, J. Rodent Model of Irritable Bowel Syndrome. *Int. J. Gastroenterol. Disord. Ther.* **2017**, *4*.
153. Yi, L.; Zhang, H.; Sun, H.; Zhou, L.; Chen, Y.; Xuan, L.; Jiang, Y.; Xu, S. Maternal Separation Induced Visceral Hypersensitivity from Childhood to Adulthood. *J. Neurogastroenterol. Motil.* **2017**, *23*, 306–315.
154. Kokkinidis, L.; Anisman, H. Dissociation of the effects of scopolamine and d-amphetamine on a spontaneous alternation task. *Pharmacol. Biochem. Behav.* **1976**, *5*, 293–297.
155. Pellow, S.; Chopin, P.; File, S.E.; Briley, M. Validation of open : closed arm entries in an elevated plus-maze as a measure of anxiety in the rat. *J. Neurosci. Methods* **1985**, *14*, 149–167..
156. Porsolt, R.D.; Bertin, A.; Jalfre, M. Behavioral despair in mice: a primary screening test for antidepressants. *Arch. Int. Pharmacodyn. Ther.* **1977**, *229*, 327–336.
157. Ciobica, A.; Olteanu, Z.; Padurariu, M.; Hritcu, L. The effects of pergolide on memory and oxidative stress in a rat model of Parkinson's disease. *J. Physiol. Biochem.* **2012**, *68*, 59–69.
158. Whitehead, W.E.; Palsson, O.; Jones, K.R. Systematic review of the comorbidity of irritable bowel syndrome with other disorders: What are the causes and implications? *Gastroenterology* **2002**, *122*, 1140–1156.
159. Sanger, G.J.; Yoshida, M.; Yahyah, M.; Kitazumi, K. Increased defecation during stress or after 5-hydroxytryptophan: selective inhibition by the 5-HT4 receptor antagonist, SB-207266. *Br. J. Pharmacol.* **2000**, *130*, 706–712.
160. Vannucchi, M.G.; Evangelista, S. Experimental Models of Irritable Bowel Syndrome and the Role of the Enteric Neurotransmission. *J. Clin. Med.* **2018**, *7*.
161. Saito, K.; Kasai, T.; Nagura, Y.; Ito, H.; Kanazawa, M.; Fukudo, S. Corticotropin-Releasing Hormone Receptor 1 Antagonist Blocks Brain–Gut Activation Induced by Colonic Distention in Rats. *Gastroenterology* **2005**, *129*, 1533–1543.
162. Taché, Y.; Martinez, V.; Million, M.; Rivier, J. Corticotropin-Releasing Factor and the Brain-Gut Motor Response to Stress. *Can. J. Gastroenterol.* **1999**, *13*, 375916.

163. German, A.C.; Cunliffe, N.A.; Morgan, K.L. Faecal consistency and risk factors for diarrhoea and constipation in cats in UK rehoming shelters. *J. Feline Med. Surg.* **2015**, *19*, 57–65.
164. O'Malley, D.; Dinan, T.G.; Cryan, J.F. Neonatal maternal separation in the rat impacts on the stress responsivity of central corticotropin-releasing factor receptors in adulthood. *Psychopharmacology (Berl).* **2011**, *214*, 221–229.
165. Savignac, H.; Dinan, T.; Cryan, J. Resistance to Early-Life Stress in Mice: Effects of Genetic Background and Stress Duration. *Front. Behav. Neurosci.* 2011, *5*, 13.
166. Savignac, H.M.; Finger, B.C.; Pizzo, R.C.; O'Leary, O.F.; Dinan, T.G.; Cryan, J.F. Increased sensitivity to the effects of chronic social defeat stress in an innately anxious mouse strain. *Neuroscience* **2011**, *192*, 524–536.
167. Tramullas, M.; Dinan, T.G.; Cryan, J.F. Chronic psychosocial stress induces visceral hyperalgesia in mice. *Stress* **2012**, *15*, 281–292.
168. Zhang, G.-Y.; Jiang, Y.-P.; Hu, H.-L.; Cao, Z.-J. Establishing rat models of slow transit constipation and chronic stress-induced depression: Correlation of constipation and depression. *Chinese J. Tissue Eng. Res.* **2015**, *19*, 4356–4360.
169. Lieblich, I.; Guttman, R. Analysis of emotional defecation under severe and mild stress — evidence for genotype-situation interaction. *Life Sci.* **1968**, *7*, 301–309.
170. Cryan, J.F.; Markou, A.; Lucki, I. Assessing antidepressant activity in rodents: recent developments and future needs. *Trends Pharmacol. Sci.* **2002**, *23*, 238–245.
171. Cryan, J.F.; Page, M.E.; Lucki, I. Noradrenergic lesions differentially alter the antidepressant-like effects of reboxetine in a modified forced swim test. *Eur. J. Pharmacol.* **2002**, *436*, 197–205.
172. Anyan, J.; Amir, S. Too Depressed to Swim or Too Afraid to Stop? A Reinterpretation of the Forced Swim Test as a Measure of Anxiety-Like Behavior. *Neuropsychopharmacology* **2018**, *43*, 931–933.
173. Carola, V.; D'Olimpio, F.; Brunamonti, E.; Mangia, F.; Renzi, P. Evaluation of the elevated plus-maze and open-field tests for the assessment of anxiety-related behaviour in inbred mice. *Behav. Brain Res.* **2002**, *134*, 49–57.
174. Jiang, Y.-M.; Li, X.-J.; Meng, Z.-Z.; Liu, Y.-Y.; Zhao, H.-B.; Li, N.; Yan, Z.-Y.; Ma, Q.-Y.; Zhang, H.-T.; Chen, J.-X. Effects of Xiaoyaosan on Stress-Induced Anxiety-Like Behavior in Rats: Involvement of CRF1 Receptor. *Evidence-Based Complement. Altern. Med.* **2016**, *2016*, 1238426.
175. Walf, A.A.; Frye, C.A. The use of the elevated plus maze as an assay of anxiety-related behavior in rodents. *Nat. Protoc.* **2007**, *2*, 322–328.
176. Yoon, S.; Kim, B.-H.; Ye, S.-K.; Kim, E. Chronic Non-Social Stress Affects Depressive Behaviors But Not Anxiety in Mice. *Korean J. Physiol. Pharmacol.* **2014**, *18*, 263–268.
177. Kim, J.-W.; Ko, M.J.; Gonzales, E.L.; Kang, R.J.; Kim, D.G.; Kim, Y.; Seung, H.; Oh, H.A.; Eun, P.H.; Shin, C.Y. Social support rescues acute stress-induced cognitive impairments by modulating ERK1/2 phosphorylation in adolescent mice. *Sci. Rep.* **2018**, *8*, 12003.
178. Bian, Y.; Pan, Z.; Hou, Z.; Huang, C.; Li, W.; Zhao, B. Learning, memory, and glial cell changes following recovery from chronic unpredictable stress. *Brain Res. Bull.* **2012**, *88*, 471–476.
179. Riaz, M.S.; Bohlen, M.O.; Gunter, B.W.; Henry, Q.; Stockmeier, C.A.; Paul, I.A. Attenuation of social interaction-associated ultrasonic vocalizations and spatial working memory performance in rats exposed to chronic unpredictable stress. *Physiol. Behav.* **2015**, *152*, 128–134.
180. Lara, V.P.; Caramelli, P.; Teixeira, A.L.; Barbosa, M.T.; Carmona, K.C.; Carvalho, M.G.; Fernandes, A.P.; Gomes, K.B. High cortisol levels are associated with cognitive impairment no-dementia (CIND) and dementia. *Clin. Chim. Acta* **2013**, *423*, 18–22.
181. Sousa, V.C.; Vital, J.; Costenla, A.R.; Batalha, V.L.; Sebastião, A.M.; Ribeiro, J.A.; Lopes, L. V Maternal separation impairs long term-potentiation in CA1-CA3 synapses and hippocampal-dependent memory in old rats. *Neurobiol. Aging* **2014**, *35*, 1680–1685.
182. Novak, M.A.; Hamel, A.F.; Kelly, B.J.; Dettmer, A.M.; Meyer, J.S. Stress, the HPA axis, and nonhuman primate well-being: A review. *Appl. Anim. Behav. Sci.* **2013**, *143*, 135–149.
183. O'Sullivan; Clayton; Breslin; Harman; Bountra; Mclaren; O'Morain Increased mast cells in the irritable bowel syndrome. *Neurogastroenterol. Motil.* **2000**, *12*, 449–457.
184. Mete, R.; Tulubas, F.; Oran, M.; Yılmaz, A.; Avci, B.A.; Yildiz, K.; Turan, C.B.; Gurel, A. The role of oxidants and reactive nitrogen species in irritable bowel syndrome: A potential etiological explanation. *Med. Sci. Monit.* **2013**, *19*, 762–766.
185. Yigit Karakas, E. Evaluating unspecific oxidative stress parameters in the sera of patients with irritable bowel syndrome. *Period. Biol.* **2016**, *118*, 111–116.
186. Zafir, A.; Banu, N. Induction of oxidative stress by restraint stress and corticosterone treatments in rats. *Indian J. Biochem. Biophys.* **2009**, *46 1*, 53–58.
187. Duda, W.; Curzytek, K.; Kubera, M.; Iciek, M.; Kowalczyk-Pachel, D.; Bilska-Wilkosz, A.; Lorenc-Koci, E.; Leśkiewicz, M.; Basta-Kaim, A.; Budziszewska, B.; et al. The Effect of Chronic Mild Stress

and Imipramine on the Markers of Oxidative Stress and Antioxidant System in Rat Liver. *Neurotox. Res.* **2016**, *30*, 173–184.
188. López-López, A.L.; Jaime, H.B.; Escobar Villanueva, M. del C.; Padilla, M.B.; Palacios, G.V.; Aguilar, F.J.A. Chronic unpredictable mild stress generates oxidative stress and systemic inflammation in rats. *Physiol. Behav.* **2016**, *161*, 15–23.
189. Tribble, D.L.; Aw, T.Y.; Jones, D.P. The pathophysiological significance of lipid peroxidation in oxidative cell injury. *Hepatology* **1987**, *7*, 377–386.
190. Campos-Rangel, A.; Torner-Aguilar, L.; Saavedra-Molina, A.; Manzo-Avalos, S. Effect of Maternal Separation on Oxidative and Nitrosative Stress in the Brain of Rat Offspring. *FASEB J.* **2017**, *31*, 779.7-779.7.
191. Diehl, L.A.; Alvares, L.O.; Noschang, C.; Engelke, D.; Andreazza, A.C.; Gonçalves, C.A.S.; Quillfeldt, J.A.; Dalmaz, C. Long-Lasting Effects of Maternal Separation on an Animal Model of Post-Traumatic Stress Disorder: Effects on Memory and Hippocampal Oxidative Stress. *Neurochem. Res.* **2012**, *37*, 700–707.
192. Balmus, I.M.; Lefter, R.; Ciobica, A.; Antioch, I.; Ababei, D.; Dobrin, R. Preliminary Data on Some Behavioral Changes Induced by Short-Term Intraperitoneal Oxytocin Administration in Aged Rats. *Psychiatr. Danub.* **2018**, *30*, 91–98.
193. Stefanescu, C.; Ciobica, A. The relevance of oxidative stress status in first episode and recurrent depression. *J. Affect. Disord.* **2012**, *143*, 34–38.
194. Goyette, P.; Labbé, C.; Trinh, T.T.; Xavier, R.J.; Rioux, J.D. Molecular pathogenesis of inflammatory bowel disease: Genotypes, phenotypes and personalized medicine. *Ann. Med.* **2007**, *39*, 177–199.
195. Foster, J.A.; Rinaman, L.; Cryan, J.F. Stress & the gut-brain axis: Regulation by the microbiome. *Neurobiol. Stress* **2017**, *7*, 124–136.
196. George, E.D.; Bordner, K.A.; Elwafi, H.M.; Simen, A.A. Maternal separation with early weaning: a novel mouse model of early life neglect. *BMC Neurosci.* **2010**, *11*, 123.
197. Cani, P.D. Human gut microbiome: hopes, threats and promises. *Gut* **2018**, *67*, 1716 LP – 1725.
198. Zhu, B.; Wang, X.; Li, L. Human gut microbiome: the second genome of human body. *Protein Cell* **2010**, *1*, 718–725.
199. Bäckhed, F.; Ley, R.E.; Sonnenburg, J.L.; Peterson, D.A.; Gordon, J.I. Host-Bacterial Mutualism in the Human Intestine. *Science (80-.).* **2005**, *307*, 1915 LP – 1920.
200. Sender, R.; Fuchs, S.; Milo, R. Revised Estimates for the Number of Human and Bacteria Cells in the Body. *PLoS Biol.* **2016**, *14*, e1002533–e1002533.
201. Jandhyala, S.M.; Talukdar, R.; Subramanyam, C.; Vuyyuru, H.; Sasikala, M.; Nageshwar Reddy, D. Role of the normal gut microbiota. *World J. Gastroenterol.* **2015**, *21*, 8787–8803.
202. Okumura, R.; Takeda, K. Roles of intestinal epithelial cells in the maintenance of gut homeostasis. *Exp. Mol. Med.* **2017**, *49*, e338–e338.
203. Elphick, D.A.; Mahida, Y.R. Paneth cells: their role in innate immunity and inflammatory disease. *Gut* **2005**, *54*, 1802–1809.
204. Hill, D.A.; Artis, D. Intestinal bacteria and the regulation of immune cell homeostasis. *Annu. Rev. Immunol.* **2010**, *28*, 623–667.
205. Johansson, M.E. V; Phillipson, M.; Petersson, J.; Velcich, A.; Holm, L.; Hansson, G.C. The inner of the two Muc2 mucin-dependent mucus layers in colon is devoid of bacteria. *Proc. Natl. Acad. Sci. U. S. A.* **2008**, *105*, 15064–15069.
206. Randall-Demllo, S.; Chieppa, M.; Eri, R. Intestinal epithelium and autophagy: partners in gut homeostasis. *Front. Immunol.* **2013**, *4*, 301.
207. Bevins, C.L.; Salzman, N.H. Paneth cells, antimicrobial peptides and maintenance of intestinal homeostasis. *Nat. Rev. Microbiol.* **2011**, *9*, 356–368.
208. Nair, M.G.; Guild, K.J.; Du, Y.; Zaph, C.; Yancopoulos, G.D.; Valenzuela, D.M.; Murphy, A.; Stevens, S.; Karow, M.; Artis, D. Goblet cell-derived resistin-like molecule beta augments CD4+ T cell production of IFN-gamma and infection-induced intestinal inflammation. *J. Immunol.* **2008**, *181*, 4709–4715.
209. Williams, A.; Flavell, R.A.; Eisenbarth, S.C. The role of NOD-like Receptors in shaping adaptive immunity. *Curr. Opin. Immunol.* **2010**, *22*, 34–40.
210. Hooper, L. V; Macpherson, A.J. Immune adaptations that maintain homeostasis with the intestinal microbiota. *Nat. Rev. Immunol.* **2010**, *10*, 159–169.
211. Balmus, I.-M.; Ilie-Dumitru, O.; Ciobica, A.; Cojocariu, R.-O.; Stanciu, C.; Trifan, A.; Cimpeanu, M.; Cimpeanu, C.; Gorgan, L. Irritable Bowel Syndrome between Molecular Approach and Clinical Expertise—Searching for Gap Fillers in the Oxidative Stress Way of Thinking. *Medicina (B. Aires).* **2020**, *56*, 38.
212. Varatharaj, A.; Galea, I. The blood-brain barrier in systemic inflammation. *Brain. Behav. Immun.* **2017**,

60, 1–12.
213. Rowland, I.; Gibson, G.; Heinken, A.; Scott, K.; Swann, J.; Thiele, I.; Tuohy, K. Gut microbiota functions: metabolism of nutrients and other food components. *Eur. J. Nutr.* **2018**, *57*, 1–24.
214. Yadav, M.; Verma, M.K.; Chauhan, N.S. A review of metabolic potential of human gut microbiome in human nutrition. *Arch. Microbiol.* **2018**, *200*, 203–217.
215. Turnbaugh, P.J.; Ley, R.E.; Hamady, M.; Fraser-Liggett, C.M.; Knight, R.; Gordon, J.I. The human microbiome project. *Nature* **2007**, *449*, 804–810.
216. Krishnan, S.; Alden, N.; Lee, K. Pathways and functions of gut microbiota metabolism impacting host physiology. *Curr. Opin. Biotechnol.* **2015**, *36*, 137–145.
217. Levy, M.; Blacher, E.; Elinav, E. Microbiome, metabolites and host immunity. *Curr. Opin. Microbiol.* **2017**, *35*, 8–15.
218. Donohoe, D.R.; Garge, N.; Zhang, X.; Sun, W.; O'Connell, T.M.; Bunger, M.K.; Bultman, S.J. The microbiome and butyrate regulate energy metabolism and autophagy in the mammalian colon. *Cell Metab.* **2011**, *13*, 517–526.
219. Chow, J.; Lee, S.M.; Shen, Y.; Khosravi, A.; Mazmanian, S.K. Host-bacterial symbiosis in health and disease. *Adv. Immunol.* **2010**, *107*, 243–274.
220. Nagpal, R.; Mainali, R.; Ahmadi, S.; Wang, S.; Singh, R.; Kavanagh, K.; Kitzman, D.W.; Kushugulova, A.; Marotta, F.; Yadav, H. Gut microbiome and aging: Physiological and mechanistic insights. *Nutr. Heal. aging* **2018**, *4*, 267–285.
221. Bischoff, S.C. Microbiota and aging. *Curr. Opin. Clin. Nutr. Metab. Care* **2016**, *19*.
222. Robertson, R.C.; Manges, A.R.; Finlay, B.B.; Prendergast, A.J. The Human Microbiome and Child Growth - First 1000 Days and Beyond. *Trends Microbiol.* **2019**, *27*, 131–147.
223. Collado, M.C.; Rautava, S.; Aakko, J.; Isolauri, E.; Salminen, S. Human gut colonisation may be initiated in utero by distinct microbial communities in the placenta and amniotic fluid. *Sci. Rep.* **2016**, *6*, 23129.
224. Aagaard, K.; Ma, J.; Antony, K.M.; Ganu, R.; Petrosino, J.; Versalovic, J. The placenta harbors a unique microbiome. *Sci. Transl. Med.* **2014**, *6*, 237ra65-237ra65.
225. Makino, H.; Kushiro, A.; Ishikawa, E.; Kubota, H.; Gawad, A.; Sakai, T.; Oishi, K.; Martin, R.; Ben-Amor, K.; Knol, J.; et al. Mother-to-infant transmission of intestinal bifidobacterial strains has an impact on the early development of vaginally delivered infant's microbiota. *PLoS One* **2013**, *8*, e78331–e78331.
226. Rautava, S.; Collado, M.C.; Salminen, S.; Isolauri, E. Probiotics Modulate Host-Microbe Interaction in the Placenta and Fetal Gut: A Randomized, Double-Blind, Placebo-Controlled Trial. *Neonatology* **2012**, *102*, 178–184.
227. Lauder, A.P.; Roche, A.M.; Sherrill-Mix, S.; Bailey, A.; Laughlin, A.L.; Bittinger, K.; Leite, R.; Elovitz, M.A.; Parry, S.; Bushman, F.D. Comparison of placenta samples with contamination controls does not provide evidence for a distinct placenta microbiota. *Microbiome* **2016**, *4*, 29.
228. de Goffau, M.C.; Lager, S.; Sovio, U.; Gaccioli, F.; Cook, E.; Peacock, S.J.; Parkhill, J.; Charnock-Jones, D.S.; Smith, G.C.S. Human placenta has no microbiome but can contain potential pathogens. *Nature* **2019**, *572*, 329–334.
229. Stout, M.J.; Conlon, B.; Landeau, M.; Lee, I.; Bower, C.; Zhao, Q.; Roehl, K.A.; Nelson, D.M.; Macones, G.A.; Mysorekar, I.U. Identification of intracellular bacteria in the basal plate of the human placenta in term and preterm gestations. *Am. J. Obstet. Gynecol.* **2013**, *208*, 226.e1-226.e2267.
230. Agrawal, V.; Hirsch, E. Intrauterine infection and preterm labor. *Semin. Fetal Neonatal Med.* **2012**, *17*, 12–19.
231. Ananth, C.; Oyelese, Y.; Srinivas, N.; Yeo, L.; Vintzileos, A. Preterm Premature Rupture of Membranes, Intrauterine Infection, and Oligohydramnios. *Obstet. Gynecol.* **2004**, *104*, 71–77,.
232. Steel, J.H.; Malatos, S.; Kennea, N.; Edwards, A.D.; Miles, L.; Duggan, P.; Reynolds, P.R.; Feldman, R.G.; Sullivan, M.H.F. Bacteria and Inflammatory Cells in Fetal Membranes Do Not Always Cause Preterm Labor. *Pediatr. Res.* **2005**, *57*, 404–411.
233. Jones, H.E.; Harris, K.A.; Azizia, M.; Bank, L.; Carpenter, B.; Hartley, J.C.; Klein, N.; Peebles, D. Differing prevalence and diversity of bacterial species in fetal membranes from very preterm and term labor. *PLoS One* **2009**, *4*, e8205–e8205.
234. Ardissone, A.N.; de la Cruz, D.M.; Davis-Richardson, A.G.; Rechcigl, K.T.; Li, N.; Drew, J.C.; Murgas-Torrazza, R.; Sharma, R.; Hudak, M.L.; Triplett, E.W.; et al. Meconium microbiome analysis identifies bacteria correlated with premature birth. *PLoS One* **2014**, *9*, e90784–e90784.
235. Mshvildadze, M.; Neu, J.; Shuster, J.; Theriaque, D.; Li, N.; Mai, V. Intestinal microbial ecology in premature infants assessed with non-culture-based techniques. *J. Pediatr.* **2010**, *156*, 20–25.
236. Hu, J.; Nomura, Y.; Bashir, A.; Fernandez-Hernandez, H.; Itzkowitz, S.; Pei, Z.; Stone, J.; Loudon, H.; Peter, I. Diversified microbiota of meconium is affected by maternal diabetes status. *PLoS One* **2013**, *8*,

e78257–e78257.
237. Jiménez, E.; Marín, M.L.; Martín, R.; Odriozola, J.M.; Olivares, M.; Xaus, J.; Fernández, L.; Rodríguez, J.M. Is meconium from healthy newborns actually sterile? *Res. Microbiol.* **2008**, *159*, 187–193..
238. Hansen, R.; Scott, K.P.; Khan, S.; Martin, J.C.; Berry, S.H.; Stevenson, M.; Okpapi, A.; Munro, M.J.; Hold, G.L. First-Pass Meconium Samples from Healthy Term Vaginally-Delivered Neonates: An Analysis of the Microbiota. *PLoS One* **2015**, *10*, e0133320–e0133320.
239. DiGiulio, D.B.; Romero, R.; Amogan, H.P.; Kusanovic, J.P.; Bik, E.M.; Gotsch, F.; Kim, C.J.; Erez, O.; Edwin, S.; Relman, D.A. Microbial prevalence, diversity and abundance in amniotic fluid during preterm labor: a molecular and culture-based investigation. *PLoS One* **2008**, *3*, e3056–e3056.
240. Shao, Y.; Forster, S.C.; Tsaliki, E.; Vervier, K.; Strang, A.; Simpson, N.; Kumar, N.; Stares, M.D.; Rodger, A.; Brocklehurst, P.; et al. Stunted microbiota and opportunistic pathogen colonization in caesarean-section birth. *Nature* **2019**, *574*, 117–121.
241. Gasparrini, A.J.; Wang, B.; Sun, X.; Kennedy, E.A.; Hernandez-Leyva, A.; Ndao, I.M.; Tarr, P.I.; Warner, B.B.; Dantas, G. Persistent metagenomic signatures of early-life hospitalization and antibiotic treatment in the infant gut microbiota and resistome. *Nat. Microbiol.* **2019**, *4*, 2285–2297.
242. Turnbaugh, P.J.; Quince, C.; Faith, J.J.; McHardy, A.C.; Yatsunenko, T.; Niazi, F.; Affourtit, J.; Egholm, M.; Henrissat, B.; Knight, R.; et al. Organismal, genetic, and transcriptional variation in the deeply sequenced gut microbiomes of identical twins. *Proc. Natl. Acad. Sci. U. S. A.* **2010**, *107*, 7503–7508.
243. Goodrich, J.K.; Davenport, E.R.; Beaumont, M.; Jackson, M.A.; Knight, R.; Ober, C.; Spector, T.D.; Bell, J.T.; Clark, A.G.; Ley, R.E. Genetic Determinants of the Gut Microbiome in UK Twins. *Cell Host Microbe* **2016**, *19*, 731–743.
244. Lee, S.; Sung, J.; Lee, J.; Ko, G. Comparison of the gut microbiotas of healthy adult twins living in South Korea and the United States. *Appl. Environ. Microbiol.* **2011**, *77*, 7433–7437.
245. Schloss, P.D.; Iverson, K.D.; Petrosino, J.F.; Schloss, S.J. The dynamics of a family's gut microbiota reveal variations on a theme. *Microbiome* **2014**, *2*, 25.
246. Kato, K.; Ishida, S.; Tanaka, M.; Mitsuyama, E.; Xiao, J.-Z.; Odamaki, T. Association between functional lactase variants and a high abundance of Bifidobacterium in the gut of healthy Japanese people. *PLoS One* **2018**, *13*, e0206189–e0206189.
247. Liebert, A.; López, S.; Jones, B.L.; Montalva, N.; Gerbault, P.; Lau, W.; Thomas, M.G.; Bradman, N.; Maniatis, N.; Swallow, D.M. World-wide distributions of lactase persistence alleles and the complex effects of recombination and selection. *Hum. Genet.* **2017**, *136*, 1445–1453.
248. Itan, Y.; Jones, B.L.; Ingram, C.J.E.; Swallow, D.M.; Thomas, M.G. A worldwide correlation of lactase persistence phenotype and genotypes. *BMC Evol. Biol.* **2010**, *10*, 36.
249. Mattar, R.; de Campos Mazo, D.F.; Carrilho, F.J. Lactose intolerance: diagnosis, genetic, and clinical factors. *Clin. Exp. Gastroenterol.* **2012**, *5*, 113–121.
250. Odamaki, T.; Bottacini, F.; Mitsuyama, E.; Yoshida, K.; Kato, K.; Xiao, J.; van Sinderen, D. Impact of a bathing tradition on shared gut microbes among Japanese families. *Sci. Rep.* **2019**, *9*, 4380.
251. Odamaki, T.; Bottacini, F.; Kato, K.; Mitsuyama, E.; Yoshida, K.; Horigome, A.; Xiao, J.; van Sinderen, D. Genomic diversity and distribution of Bifidobacterium longum subsp. longum across the human lifespan. *Sci. Rep.* **2018**, *8*, 85.
252. Laursen, M.F.; Zachariassen, G.; Bahl, M.I.; Bergström, A.; Høst, A.; Michaelsen, K.F.; Licht, T.R. Having older siblings is associated with gut microbiota development during early childhood. *BMC Microbiol.* **2015**, *15*, 154..
253. Laursen, M.F.; Laursen, R.P.; Larnkjær, A.; Mølgaard, C.; Michaelsen, K.F.; Frøkiær, H.; Bahl, M.I.; Licht, T.R. Faecalibacterium Gut Colonization Is Accelerated by Presence of Older Siblings. *mSphere* **2017**, *2*, e00448-17.
254. Dill-McFarland, K.A.; Tang, Z.-Z.; Kemis, J.H.; Kerby, R.L.; Chen, G.; Palloni, A.; Sorenson, T.; Rey, F.E.; Herd, P. Close social relationships correlate with human gut microbiota composition. *Sci. Rep.* **2019**, *9*, 703.
255. Voigt, A.Y.; Costea, P.I.; Kultima, J.R.; Li, S.S.; Zeller, G.; Sunagawa, S.; Bork, P. Temporal and technical variability of human gut metagenomes. *Genome Biol.* **2015**, *16*, 73.
256. Roberts, C.L.; Algert, C.S.; Ford, J.B.; Todd, A.L.; Morris, J.M. Pathways to a rising caesarean section rate: a population-based cohort study. *BMJ Open* **2012**, *2*, e001725.
257. Stinson, L.F.; Payne, M.S.; Keelan, J.A. A Critical Review of the Bacterial Baptism Hypothesis and the Impact of Cesarean Delivery on the Infant Microbiome. *Front. Med.* **2018**, *5*, 135.
258. Peters, J.M.; Koo, B.-M.; Patino, R.; Heussler, G.E.; Hearne, C.C.; Qu, J.; Inclan, Y.F.; Hawkins, J.S.; Lu, C.H.S.; Silvis, M.R.; et al. Enabling genetic analysis of diverse bacteria with Mobile-CRISPRi. *Nat. Microbiol.* **2019**, *4*, 244–250.
259. Dethlefsen, L.; Huse, S.; Sogin, M.L.; Relman, D.A. The Pervasive Effects of an Antibiotic on the

Human Gut Microbiota, as Revealed by Deep 16S rRNA Sequencing. *PLOS Biol.* **2008**, *6*, e280.
260. Buttó, L.F.; Haller, D. Dysbiosis in intestinal inflammation: Cause or consequence. *Int. J. Med. Microbiol.* **2016**, *306*, 302–309.
261. Mawdsley, J.E.; Rampton, D.S. Psychological stress in IBD: new insights into pathogenic and therapeutic implications. *Gut* **2005**, *54*, 1481–1491.
262. Ilie, O.-D.; Ciobica, A.; McKenna, J.; Doroftei, B.; Mavroudis, I. Minireview on the Relations between Gut Microflora and Parkinson's Disease: Further Biochemical (Oxidative Stress), Inflammatory, and Neurological Particularities. *Oxid. Med. Cell. Longev.* **2020**, *2020*, 4518023.
263. Lefter, R.; Ciobica, A.; Timofte, D.; Stanciu, C.; Trifan, A. A Descriptive Review on the Prevalence of Gastrointestinal Disturbances and Their Multiple Associations in Autism Spectrum Disorder. *Medicina (Kaunas).* **2019**, *56*, 11.
264. Hritcu, L.; Padurariu, M.; Ciobica, A.; Horhogea, C.; Spataru, C.; Spataru, C.; Burtan, L.; Stefanescu, C. Serum Cortisol Levels Modifications in Patients with Depression and Irritable Bowel Syndrome. *Rev. Chim.* **2019**, *70*, 3383–3386.
265. Gavril, R.; Hritcu, L.; Padurariu, M.; Ciobica, A.; Horhogea, C.; Stefanescu, G.; Spataru, C.; Straulea, C.; Stefanescu, C. Preliminary Study on the Correlations Between Oxytocin Levels and Irritable Bowel Syndrome in Patients with Depression. *Rev. Chim.* **2019**, *70*, 2204–2206.
266. Hritcu, L.; Dumitru, I.; Padurariu, M.; Ciobica, A.; Spataru, C.; Spataru, C.; Stefanescu, G.; Stefanescu, C.; Grecu-Gabos, C. The Modulation of Oxytocin and Cortisol Levels in Major Depression Disorder and Irritable Bowel Syndrome. *Rev. Chim.* **2020**, *71*, 150–154.
267. Verna, E.C.; Lucak, S. Use of probiotics in gastrointestinal disorders: what to recommend? *Therap. Adv. Gastroenterol.* **2010**, *3*, 307–319.
268. Wilkins, T.; Sequoia, J. Probiotics for Gastrointestinal Conditions: A Summary of the Evidence. *Am. Fam. Physician* **2017**, *96*, 170–178.
269. Aktas, B.; Aslim, B. Gut-lung axis and dysbiosis in COVID-19. *Turkish J. Biol. = Turk Biyol. Derg.* **2020**, *44*, 265–272.
270. Guan, W.; Ni, Z.; Hu, Y.; Liang, W.; Ou, C.; He, J.; Liu, L.; Shan, H.; Lei, C.; Hui, D.S.C.; et al. Clinical Characteristics of Coronavirus Disease 2019 in China. *N. Engl. J. Med.* **2020**, *382*, 1708–1720.
271. Huang, C.; Wang, Y.; Li, X.; Ren, L.; Zhao, J.; Hu, Y.; Zhang, L.; Fan, G.; Xu, J.; Gu, X.; et al. Clinical features of patients infected with 2019 novel coronavirus in Wuhan, China. *Lancet* **2020**, *395*, 497–506.
272. Chen, N.; Zhou, M.; Dong, X.; Qu, J.; Gong, F.; Han, Y.; Qiu, Y.; Wang, J.; Liu, Y.; Wei, Y.; et al. Epidemiological and clinical characteristics of 99 cases of 2019 novel coronavirus pneumonia in Wuhan, China: a descriptive study. *Lancet* **2020**, *395*, 507–513.
273. Xu, X.-W.; Wu, X.-X.; Jiang, X.-G.; Xu, K.-J.; Ying, L.-J.; Ma, C.-L.; Li, S.-B.; Wang, H.-Y.; Zhang, S.; Gao, H.-N.; et al. Clinical findings in a group of patients infected with the 2019 novel coronavirus (SARS-Cov-2) outside of Wuhan, China: retrospective case series. *BMJ* **2020**, *368*, m606.
274. Jin, X.; Lian, J.-S.; Hu, J.-H.; Gao, J.; Zheng, L.; Zhang, Y.-M.; Hao, S.-R.; Jia, H.-Y.; Cai, H.; Zhang, X.-L.; et al. Epidemiological, clinical and virological characteristics of 74 cases of coronavirus-infected disease 2019 (COVID-19) with gastrointestinal symptoms. *Gut* **2020**, *69*, 1002 LP – 1009.
275. Zhou, F.; Yu, T.; Du, R.; Fan, G.; Liu, Y.; Liu, Z.; Xiang, J.; Wang, Y.; Song, B.; Gu, X.; et al. Clinical course and risk factors for mortality of adult inpatients with COVID-19 in Wuhan, China: a retrospective cohort study. *Lancet* **2020**, *395*, 1054–1062.
276. Wang, D.; Hu, B.; Hu, C.; Zhu, F.; Liu, X.; Zhang, J.; Wang, B.; Xiang, H.; Cheng, Z.; Xiong, Y.; et al. Clinical Characteristics of 138 Hospitalized Patients With 2019 Novel Coronavirus-Infected Pneumonia in Wuhan, China. *JAMA* **2020**, *323*, 1061–1069.
277. Lin, L.; Jiang, X.; Zhang, Z.; Huang, S.; Zhang, Z.; Fang, Z.; Gu, Z.; Gao, L.; Shi, H.; Mai, L.; et al. Gastrointestinal symptoms of 95 cases with SARS-CoV-2 infection. *Gut* **2020**, *69*, 997 LP – 1001.
278. Zhang, H.; Kang, Z.; Gong, H.; Xu, D.; Wang, J.; Li, Z.; Li, Z.; Cui, X.; Xiao, J.; Zhan, J.; et al. Digestive system is a potential route of COVID-19: an analysis of single-cell coexpression pattern of key proteins in viral entry process. *Gut* **2020**, *69*, 1010 LP – 1018.
279. Ong, J.; Young, B.E.; Ong, S. COVID-19 in gastroenterology: a clinical perspective. *Gut* **2020**, *69*, 1144 LP – 1145.
280. Song, Y.; Liu, P.; Shi, X.L.; Chu, Y.L.; Zhang, J.; Xia, J.; Gao, X.Z.; Qu, T.; Wang, M.Y. SARS-CoV-2 induced diarrhoea as onset symptom in patient with COVID-19. *Gut* **2020**, *69*, 1143 LP – 1144.
281. Liang, W.; Feng, Z.; Rao, S.; Xiao, C.; Xue, X.; Lin, Z.; Zhang, Q.; Qi, W. Diarrhoea may be underestimated: a missing link in 2019 novel coronavirus. *Gut* **2020**, *69*, 1141 LP – 1143.
282. Kibune-Nagasako, C.; García-Montes, C.; Silva-Lorena, S.L.; Aparecida-Mesquita, M. Irritable bowel syndrome subtypes: clinical and psychological features, body mass index and comorbidities . *Rev. Española Enfermedades Dig.* 2016, *108*, 59–64.
283. Martin, C.R.; Osadchiy, V.; Kalani, A.; Mayer, E.A. The Brain-Gut-Microbiome Axis. *Cell. Mol.*

Gastroenterol. Hepatol. **2018**, *6*, 133–148.
284. Chen, T.; Wu, D.; Chen, H.; Yan, W.; Yang, D.; Chen, G.; Ma, K.; Xu, D.; Yu, H.; Wang, H.; et al. Clinical characteristics of 113 deceased patients with coronavirus disease 2019: retrospective study. *BMJ* **2020**, *368*, m1091.
285. Magro, F.; Lopes, J.; Borralho, P.; Lopes, S.; Coelho, R.; Cotter, J.; Castro, F.D. de; Sousa, H.T. de; Salgado, M.; Andrade, P.; et al. Comparison of different histological indexes in the assessment of UC activity and their accuracy regarding endoscopic outcomes and faecal calprotectin levels. *Gut* **2019**, *68*, 594 LP – 603.
286. Effenberger, M.; Grabherr, F.; Mayr, L.; Schwaerzler, J.; Nairz, M.; Seifert, M.; Hilbe, R.; Seiwald, S.; Scholl-Buergi, S.; Fritsche, G.; et al. Faecal calprotectin indicates intestinal inflammation in COVID-19. *Gut* **2020**, gutjnl-2020-321388.
287. Taxonera, C.; Sagastagoitia, I.; Alba, C.; Mañas, N.; Olivares, D.; Rey, E. 2019 novel coronavirus disease (COVID-19) in patients with inflammatory bowel diseases. *Aliment. Pharmacol. Ther.* **2020**, *n/a*.
288. Mazza, S.; Sorce, A.; Peyvandi, F.; Vecchi, M.; Caprioli, F. A fatal case of COVID-19 pneumonia occurring in a patient with severe acute ulcerative colitis. *Gut* **2020**, *69*, 1148 LP – 1149.
289. Wu, Y.; Guo, C.; Tang, L.; Hong, Z.; Zhou, J.; Dong, X.; Yin, H.; Xiao, Q.; Tang, Y.; Qu, X.; et al. Prolonged presence of SARS-CoV-2 viral RNA in faecal samples. *Lancet Gastroenterol. Hepatol.* **2020**, *5*, 434–435.
290. Holshue, M.L.; DeBolt, C.; Lindquist, S.; Lofy, K.H.; Wiesman, J.; Bruce, H.; Spitters, C.; Ericson, K.; Wilkerson, S.; Tural, A.; et al. First Case of 2019 Novel Coronavirus in the United States. *N. Engl. J. Med.* **2020**, *382*, 929–936.
291. Zheng, S.; Fan, J.; Yu, F.; Feng, B.; Lou, B.; Zou, Q.; Xie, G.; Lin, S.; Wang, R.; Yang, X.; et al. Viral load dynamics and disease severity in patients infected with SARS-CoV-2 in Zhejiang province, China, January-March 2020: retrospective cohort study. *BMJ* **2020**, *369*, m1443.
292. Sriwijitalai, W.; Wiwanitkit, V. COVID-19 in forensic medicine unit personnel: Observation from Thailand. *J. Forensic Leg. Med.* **2020**, *72*, 101964.
293. Xiao, F.; Tang, M.; Zheng, X.; Liu, Y.; Li, X.; Shan, H. Evidence for Gastrointestinal Infection of SARS-CoV-2. *Gastroenterology* **2020**, *158*, 1831-1833.e3.
294. Gao, Q.Y.; Chen, Y.X.; Fang, J.Y. 2019 Novel coronavirus infection and gastrointestinal tract. *J. Dig. Dis.* **2020**, *21*, 125–126.
295. Yang, Y.; Shen, C.; Li, J.; Yuan, J.; Yang, M.; Wang, F.; Li, G.; Li, Y.; Xing, L.; Peng, L.; et al. Exuberant elevation of IP-10, MCP-3 and IL-1ra during SARS-CoV-2 infection is associated with disease severity and fatal outcome. *medRxiv* **2020**, 2020.03.02.20029975.
296. Gou, W.; Fu, Y.; Yue, L.; Chen, G.; Cai, X.; Shuai, M.; Xu, F.; Yi, X.; Chen, H.; Zhu, Y.J.; et al. Gut microbiota may underlie the predisposition of healthy individuals to COVID-19. *medRxiv* **2020**, 2020.04.22.20076091.
297. Devaux, C.A.; Rolain, J.-M.; Raoult, D. ACE2 receptor polymorphism: Susceptibility to SARS-CoV-2, hypertension, multi-organ failure, and COVID-19 disease outcome. *J. Microbiol. Immunol. Infect.* **2020**, *53*, 425–435.
298. Hashimoto, T.; Perlot, T.; Rehman, A.; Trichereau, J.; Ishiguro, H.; Paolino, M.; Sigl, V.; Hanada, T.; Hanada, R.; Lipinski, S.; et al. ACE2 links amino acid malnutrition to microbial ecology and intestinal inflammation. *Nature* **2012**, *487*, 477–481.
299. Xu, H.; Zhong, L.; Deng, J.; Peng, J.; Dan, H.; Zeng, X.; Li, T.; Chen, Q. High expression of ACE2 receptor of 2019-nCoV on the epithelial cells of oral mucosa. *Int. J. Oral Sci.* **2020**, *12*, 8.
300. Zheng, M.; Gao, Y.; Wang, G.; Song, G.; Liu, S.; Sun, D.; Xu, Y.; Tian, Z. Functional exhaustion of antiviral lymphocytes in COVID-19 patients. *Cell. Mol. Immunol.* **2020**, *17*, 533–535.
301. Wang, F.; Nie, J.; Wang, H.; Zhao, Q.; Xiong, Y.; Deng, L.; Song, S.; Ma, Z.; Mo, P.; Zhang, Y. Characteristics of Peripheral Lymphocyte Subset Alteration in COVID-19 Pneumonia. *J. Infect. Dis.* **2020**, *221*, 1762–1769.
302. Bellono, N.W.; Bayrer, J.R.; Leitch, D.B.; Castro, J.; Zhang, C.; O'Donnell, T.A.; Brierley, S.M.; Ingraham, H.A.; Julius, D. Enterochromaffin Cells Are Gut Chemosensors that Couple to Sensory Neural Pathways. *Cell* **2017**, *170*, 185-198.e16.
303. Rios, D.; Wood, M.B.; Li, J.; Chassaing, B.; Gewirtz, A.T.; Williams, I.R. Antigen sampling by intestinal M cells is the principal pathway initiating mucosal IgA production to commensal enteric bacteria. *Mucosal Immunol.* **2016**, *9*, 907–916.
304. Yano, J.M.; Yu, K.; Donaldson, G.P.; Shastri, G.G.; Ann, P.; Ma, L.; Nagler, C.R.; Ismagilov, R.F.; Mazmanian, S.K.; Hsiao, E.Y. Indigenous bacteria from the gut microbiota regulate host serotonin biosynthesis. *Cell* **2015**, *161*, 264–276.
305. Zang, R.; Castro, M.F.G.; McCune, B.T.; Zeng, Q.; Rothlauf, P.W.; Sonnek, N.M.; Liu, Z.; Brulois,

K.F.; Wang, X.; Greenberg, H.B.; et al. TMPRSS2 and TMPRSS4 promote SARS-CoV-2 infection of human small intestinal enterocytes. *Sci. Immunol.* **2020**, *5*, eabc3582.
306. Lamers, M.M.; Beumer, J.; van der Vaart, J.; Knoops, K.; Puschhof, J.; Breugem, T.I.; Ravelli, R.B.G.; Paul van Schayck, J.; Mykytyn, A.Z.; Duimel, H.Q.; et al. SARS-CoV-2 productively infects human gut enterocytes. *Science (80-.).* **2020**, eabc1669.
307. Xu, Y.; Li, X.; Zhu, B.; Liang, H.; Fang, C.; Gong, Y.; Guo, Q.; Sun, X.; Zhao, D.; Shen, J.; et al. Characteristics of pediatric SARS-CoV-2 infection and potential evidence for persistent fecal viral shedding. *Nat. Med.* **2020**, *26*, 502–505.
308. Wang, W.; Xu, Y.; Gao, R.; Lu, R.; Han, K.; Wu, G.; Tan, W. Detection of SARS-CoV-2 in Different Types of Clinical Specimens. *JAMA* **2020**, *323*, 1843–1844.
309. Long, Q.-X.; Liu, B.-Z.; Deng, H.-J.; Wu, G.-C.; Deng, K.; Chen, Y.-K.; Liao, P.; Qiu, J.-F.; Lin, Y.; Cai, X.-F.; et al. Antibody responses to SARS-CoV-2 in patients with COVID-19. *Nat. Med.* **2020**.
310. Carrouel, F.; Conte, M.P.; Fisher, J.; Gonçalves, L.S.; Dussart, C.; Llodra, J.C.; Bourgeois, D. COVID-19: A Recommendation to Examine the Effect of Mouthrinses with β-Cyclodextrin Combined with Citrox in Preventing Infection and Progression. *J. Clin. Med.* **2020**, *9*, 1126.
311. Zhou, D.; Dai, S.-M.; Tong, Q. COVID-19: a recommendation to examine the effect of hydroxychloroquine in preventing infection and progression. *J. Antimicrob. Chemother.* **2020**.
312. Bescos, R.; Ashworth, A.; Cutler, C.; Brookes, Z.L.; Belfield, L.; Rodiles, A.; Casas-Agustench, P.; Farnham, G.; Liddle, L.; Burleigh, M.; et al. Effects of Chlorhexidine mouthwash on the oral microbiome. *Sci. Rep.* **2020**, *10*, 5254.
313. Wang, L.; Li, J.; Guo, S.; Xie, N.; Yao, L.; Cao, Y.; Day, S.W.; Howard, S.C.; Graff, J.C.; Gu, T.; et al. Real-time estimation and prediction of mortality caused by COVID-19 with patient information based algorithm. *Sci. Total Environ.* **2020**, *727*, 138394.
314. Kurbalija, V.; Radovanović, M.; Ivanović, M.; Schmidt, D.; von Trzebiatowski, G.L.; Burkhard, H.-D.; Hinrichs, C. Time-series analysis in the medical domain: A study of Tacrolimus administration and influence on kidney graft function. *Comput. Biol. Med.* **2014**, *50*, 19–31.
315. Nsoesie, E.; Beckman, R.; Shashaani, S.; Nagaraj, K.; Marathe, M. A Simulation Optimization Approach to Epidemic Forecasting. *PLoS One* **2013**, *8*, e67164.
316. Orbann, C.; Sattenspiel, L.; Miller, E.; Dimka, J. Defining epidemics in computer simulation models: How do definitions influence conclusions? *Epidemics* **2017**, *19*, 24–32.
317. Thomson, M.C.; Molesworth, A.M.; Djingarey, M.H.; Yameogo, K.R.; Belanger, F.; Cuevas, L.E. Potential of environmental models to predict meningitis epidemics in Africa. *Trop. Med. Int. Heal.* **2006**, *11*, 781–788.
318. Liu, Q.; Li, Z.; Ji, Y.; Martinez, L.; Zia, U.H.; Javaid, A.; Lu, W.; Wang, J. Forecasting the seasonality and trend of pulmonary tuberculosis in Jiangsu Province of China using advanced statistical time-series analyses. *Infect. Drug Resist.* **2019**, *12*, 2311–2322.
319. Ren, H.; Li, J.; Yuan, Z.-A.; Hu, J.-Y.; Yu, Y.; Lu, Y.-H. The development of a combined mathematical model to forecast the incidence of hepatitis E in Shanghai, China. *BMC Infect. Dis.* **2013**, *13*, 421.
320. Zhang, X.; Liu, Y.; Yang, M.; Zhang, T.; Young, A.; Li, X. Comparative Study of Four Time Series Methods in Forecasting Typhoid Fever Incidence in China. *PLoS One* **2013**, *8*, e63116.
321. Wang, Y.; Shen, Z.; Jiang, Y. Comparison of ARIMA and GM(1,1) models for prediction of hepatitis B in China. *PLoS One* **2018**, *13*, e0201987.
322. Zhang, L.; Wang, L.; Zheng, Y.; Wang, K.; Zhang, X.; Zheng, Y. Time Prediction Models for Echinococcosis Based on Gray System Theory and Epidemic Dynamics. *Int. J. Environ. Res. Public Health* **2017**, *14*, 262.
323. Tunnicliffe Wilson, G. Time Series Analysis: Forecasting and Control,5th Edition, by George E. P. Box, Gwilym M. Jenkins, Gregory C. Reinsel and Greta M. Ljung, 2015. Published by John Wiley and Sons Inc., Hoboken, New Jersey, pp. 712. ISBN: 978-1-118-67502-1. *J. Time Ser. Anal.* **2016**, *37*, n/a-n/a.
324. Fanoodi, B.; Malmir, B.; Jahantigh, F.F. Reducing demand uncertainty in the platelet supply chain through artificial neural networks and ARIMA models. *Comput. Biol. Med.* **2019**, *113*, 103415.
325. Benvenuto, D.; Giovanetti, M.; Vassallo, L.; Angeletti, S.; Ciccozzi, M. Application of the ARIMA model on the COVID-2019 epidemic dataset. *Data Br.* **2020**, *29*, 105340.
326. Li, X.; Zhang, C.; Zhang, B.; Liu, K. A comparative time series analysis and modeling of aerosols in the contiguous United States and China. *Sci. Total Environ.* **2019**, *690*, 799–811.
327. Elevli, S.; Uzgören, N.; Bingöl, D.; Elevli, B. Drinking water quality control: control charts for turbidity and pH. *J. Water, Sanit. Hyg. Dev.* **2016**, *6*, 511–518.
328. He, Z.; Tao, H. Epidemiology and ARIMA model of positive-rate of influenza viruses among children in Wuhan, China: A nine-year retrospective study. *Int. J. Infect. Dis.* **2018**, *74*, 61–70.
329. Chakraborty, T.; Ghosh, I. Real-time forecasts and risk assessment of novel coronavirus (COVID-19) cases: A data-driven analysis. *Chaos, Solitons & Fractals* **2020**, *135*, 109850.

330. Ahmar, A.S.; del Val, E.B. SutteARIMA: Short-term forecasting method, a case: Covid-19 and stock market in Spain. *Sci. Total Environ.* **2020**, *729*, 138883.
331. Chintalapudi, N.; Battineni, G.; Amenta, F. COVID-19 virus outbreak forecasting of registered and recovered cases after sixty day lockdown in Italy: A data driven model approach. *J. Microbiol. Immunol. Infect.* **2020**, *53*, 396–403.
332. Kırbaş, İ.; Sözen, A.; Tuncer, A.D.; Kazancıoğlu, F. Comparative analysis and forecasting of COVID-19 cases in various European countries with ARIMA, NARNN and LSTM approaches. *Chaos Solitons & Fractals* **2020**, 110015.
333. Ceylan, Z. Estimation of COVID-19 prevalence in Italy, Spain, and France. *Sci. Total Environ.* **2020**, *729*, 138817.
334. Singh, R.K.; Rani, M.; Bhagavathula, A.S.; Sah, R.; Rodriguez-Morales, A.J.; Kalita, H.; Nanda, C.; Sharma, S.; Sharma, Y.D.; Rabaan, A.A.; et al. Prediction of the COVID-19 Pandemic for the Top 15 Affected Countries: Advanced Autoregressive Integrated Moving Average (ARIMA) Model. *JMIR Public Heal. Surveill* **2020**, *6*, e19115.
335. Modeling and Forecasting for the number of cases of the COVID-19 pandemic with the Curve Estimation Models, the Box-Jenkins and Exponential Smoothing Methods. *EURASIAN J. Med. Oncol.* **2020**, *4*, 160–165.
336. Demongeot, J.; Flet-Berliac, Y.; Seligmann, H. Temperature Decreases Spread Parameters of the New Covid-19 Case Dynamics. *Biology (Basel).* **2020**, *9*, 10.
337. Papastefanopoulos, V.; Linardatos, P.; Kotsiantis, S. COVID-19: A Comparison of Time Series Methods to Forecast Percentage of Active Cases per Population. *Appl. Sci.* **2020**, *10*, 3880.
338. López, L.; Rodó, X. The end of social confinement and COVID-19 re-emergence risk. *Nat. Hum. Behav.* **2020**.
339. Williamson, E.J.; Walker, A.J.; Bhaskaran, K.; Bacon, S.; Bates, C.; Morton, C.E.; Curtis, H.J.; Mehrkar, A.; Evans, D.; Inglesby, P.; et al. Factors associated with COVID-19-related death using OpenSAFELY. *Nature* **2020**, *584*, 430–436.
340. Miller, I.F.; Becker, A.D.; Grenfell, B.T.; Metcalf, C.J.E. Disease and healthcare burden of COVID-19 in the United States. *Nat. Med.* **2020**.
341. Brockwell, P.J.; Davis, R.A. ARMA Models BT - Introduction to Time Series and Forecasting. In; Brockwell, P.J., Davis, R.A., Eds.; Springer International Publishing: Cham, 2016; pp. 73–96 ISBN 978-3-319-29854-2.
342. Al-Douri, Y.; Hamodi, H.; Lundberg, J. *Time Series Forecasting Using a Two-level Multi-Objective Genetic Algorithm: A Case Study of Maintenance Cost Data for Tunnel Fans*; 2018;
343. Chen, P.; Niu, A.; Liu, D.; Jiang, W.; Ma, B. Time Series Forecasting of Temperatures using SARIMA: An Example from Nanjing. *IOP Conf. Ser. Mater. Sci. Eng.* **2018**, *394*, 52024.
344. Contoyiannis, Y.; Stavrinides, S.; Hanias, M.; Kampitakis, M.; Papadopoulos, P.; Picos, R.; POTIRAKIS, S. A Universal Physics-Based Model Describing COVID-19 Dynamics in Europe. *Int. J. Environ. Res. Public Health* **2020**, *17*.
345. Demertzis, K.; Tsiotas, D.; Magafas, L. Modeling and Forecasting the COVID-19 Temporal Spread in Greece: An Exploratory Approach based on Complex Network Defined Splines. *Int. J. Environ. Res. Public Health* **2020**, *17*, 4693.
346. Tsiotas, D.; Magafas, L. *The effect of anti-COVID-19 policies on the evolution of the disease: A complex network analysis of the successful case of Greece (arXiv:2004.06536)*; 2020;
347. Chatterjee, K.; Chauhan, V.S. Epidemics, quarantine and mental health. *Med. journal, Armed Forces India* **2020**, *76*, 125–127.
348. Sharon, G.; Sampson, T.R.; Geschwind, D.H.; Mazmanian, S.K. The Central Nervous System and the Gut Microbiome. *Cell* **2016**, *167*, 915–932.
349. Xu, S.; Li, Y. Beware of the second wave of COVID-19. *Lancet* **2020**, *395*, 1321–1322.
350. Toyoshima, Y.; Nemoto, K.; Matsumoto, S.; Nakamura, Y.; Kiyotani, K. SARS-CoV-2 genomic variations associated with mortality rate of COVID-19. *J. Hum. Genet.* **2020**.
351. Gherghel, I.; Bulai, M. Is Romania ready to face the novel coronavirus (COVID-19) outbreak? The role of incoming travelers and that of Romanian diaspora. *Travel Med. Infect. Dis.* **2020**, *34*, 101628.
352. Pierantozzi, M.; Pietroiusti, A.; Sancesario, G.; Lunardi, G.; Fedele, E.; Giacomini, P.; Frasca, S.; Galante, A.; Marciani, M.G.; Stanzione, P. Reduced L-dopa absorption and increased clinical fluctuations in Helicobacter pylori-infected Parkinson's disease patients. *Neurol. Sci.* **2001**, *22*, 89–91.
353. Senkovich, O.A.; Yin, J.; Ekshyyan, V.; Conant, C.; Traylor, J.; Adegboyega, P.; McGee, D.J.; Rhoads, R.E.; Slepenkov, S.; Testerman, T.L. Helicobacter pylori AlpA and AlpB bind host laminin and influence gastric inflammation in gerbils. *Infect. Immun.* **2011**, *79*, 3106–3116.
354. Tan, A.H.; Mahadeva, S.; Marras, C.; Thalha, A.M.; Kiew, C.K.; Yeat, C.M.; Ng, S.W.; Ang, S.P.; Chow, S.K.; Loke, M.F.; et al. Helicobacter pylori infection is associated with worse severity of

Parkinson's disease. *Parkinsonism Relat. Disord.* **2015**, *21*, 221–225.
355. Rees, K.; Stowe, R.; Patel, S.; Ives, N.; Breen, K.; Clarke, C.E.; Ben-Shlomo, Y. Helicobacter pylori eradication for Parkinson's disease. *Cochrane Database Syst. Rev.* **2011**.
356. Barker, R.A.; Cahn, A.P. Parkinson's Disease: An Autoimmune Process. *Int. J. Neurosci.* **1988**, *43*, 1–7.
357. Arai, H.; Furuya, T.; Mizuno, Y.; Mochizuki, H. Inflammation and infection in Parkinsons disease. *Histol. Histopathol.* **2006**.
358. Gabrielli, M.; Bonazzi, P.; Scarpellini, E.; Bendia, E.; Lauritano, E.C.; Fasano, A.; Ceravolo, M.G.; Capecci, M.; Rita Bentivoglio, A.; Provinciali, L.; et al. Prevalence of Small Intestinal Bacterial Overgrowth in Parkinson's Disease. *Mov. Disord.* **2011**, *26*, 889–892.
359. Tan, A.H.; Mahadeva, S.; Thalha, A.M.; Gibson, P.R.; Kiew, C.K.; Yeat, C.M.; Ng, S.W.; Ang, S.P.; Chow, S.K.; Tan, C.T.; et al. Small intestinal bacterial overgrowth in Parkinson's disease. *Parkinsonism Relat. Disord.* **2014**, *20*, 535–540.
360. Fasano, A.; Bove, F.; Gabrielli, M.; Petracca, M.; Zocco, M.A.; Ragazzoni, E.; Barbaro, F.; Piano, C.; Fortuna, S.; Tortora, A.; et al. The role of small intestinal bacterial overgrowth in Parkinson's disease. *Mov. Disord.* **2013**, *28*, 1241–1249.
361. Bu, X.-L.; Wang, X.; Xiang, Y.; Shen, L.-L.; Wang, Q.-H.; Liu, Y.-H.; Jiao, S.-S.; Wang, Y.-R.; Cao, H.-Y.; Yi, X.; et al. The association between infectious burden and Parkinson's disease: A case-control study. *Parkinsonism Relat. Disord.* **2015**, *21*, 877–881.
362. Matheoud, D.; Cannon, T.; Voisin, A.; Penttinen, A.-M.; Ramet, L.; Fahmy, A.M.; Ducrot, C.; Laplante, A.; Bourque, M.-J.; Zhu, L.; et al. Intestinal infection triggers Parkinson's disease-like symptoms in Pink1−/− mice. *Nature* **2019**, *571*, 565–569.
363. Yildiz, S.; Mazel-Sanchez, B.; Kandasamy, M.; Manicassamy, B.; Schmolke, M. Influenza A virus infection impacts systemic microbiota dynamics and causes quantitative enteric dysbiosis. *Microbiome* **2018**, *6*, 9.
364. Nerius, M.; Doblhammer, G.; Tamgüney, G. GI infections are associated with an increased risk of Parkinson's disease. *Gut* **2020**, *69*, 1154 LP – 1156.
365. Dutta, S.K.; Verma, S.; Jain, V.; Surapaneni, B.K.; Vinayek, R.; Phillips, L.; Nair, P.P. Parkinson's Disease: The Emerging Role of Gut Dysbiosis, Antibiotics, Probiotics, and Fecal Microbiota Transplantation. *J. Neurogastroenterol. Motil.* **2019**, *25*, 363–376.
366. Chiang, H.-L.; Lin, C.-H. Altered Gut Microbiome and Intestinal Pathology in Parkinson's Disease. *J. Mov. Disord.* **2019**, *12*, 67–83.
367. Ness, R.B.; Goodman, M.T.; Shen, C.; Brunham, R.C. Serologic Evidence of Past Infection with Chlamydia trachomatis in Relation to Ovarian Cancer. *J. Infect. Dis.* **2003**, *187*, 1147–1152.
368. Baud, D.; Goy, G.; Jaton, K.; Osterheld, M.-C.; Blumer, S.; Borel, N.; Vial, Y.; Hohlfeld, P.; Pospischil, A.; Greub, G. Role of Chlamydia trachomatis in miscarriage. *Emerg. Infect. Dis.* **2011**, *17*, 1630–1635.
369. Shanmughapriya, S.; SenthilKumar, G.; Vinodhini, K.; Das, B.C.; Vasanthi, N.; Natarajaseenivasan, K. Viral and bacterial aetiologies of epithelial ovarian cancer. *Eur. J. Clin. Microbiol. Infect. Dis.* **2012**, *31*, 2311–2317.
370. Leli, C.; Mencacci, A.; Bombaci, J.; D'Alò, F.; Farinelli, S.; Vitali, M.; Montagna, P.; Bietolini, C.; Meucci, M.; Perito, S.; et al. Prevalence and antimicrobial susceptibility of Ureaplasma urealyticum and Mycoplasma hominis in a population of Italian and immigrant outpatients. *Infez. Med.* **2012**, *20*, 82–87.
371. Zhang, N.; Wang, R.; Li, X.; Liu, X.; Tang, Z.; Liu, Y. Are Ureaplasma spp. a Cause of Nongonococcal Urethritis? A Systematic Review and Meta-Analysis. *PLoS One* **2014**, *9*, e113771.
372. Tibaldi, C.; Cappello, N.; Latino, M.A.; Masuelli, G.; Marini, S.; Benedetto, C. Vaginal and endocervical microorganisms in symptomatic and asymptomatic non-pregnant females: risk factors and rates of occurrence. *Clin. Microbiol. Infect.* **2009**, *15*, 670–679.
373. Lanzafame, M.; Delama, A.; Emanuela, L.; Faggian, F.; Padovani, G.; Concia, E.; Vento, S. Prevalence and clinical significance of Ureaplasma urealyticum and Mycoplasma hominis in the lower genital tract of HIV-1-infected women. *Infez. Med.* **2007**, *14*, 213–215.
374. Stellrecht, K.A.; Woron, A.M.; Mishrik, N.G.; Venezia, R.A. Comparison of multiplex PCR assay with culture for detection of genital mycoplasmas. *J. Clin. Microbiol.* **2004**, *42*, 1528–1533.
375. Mihai, M.; Valentin, N.; Bogdan, D.; Carmen, C.M.; Coralia, B.; Demetra, S. Antibiotic susceptibility profiles of Mycoplasma hominis and ureaplasma urealyticum isolated during a population-based study concerning women infertility in northeast romania. *Braz. J. Microbiol.* **2011**, *42*, 256–260.
376. Imudia, A.N.; Detti, L.; Puscheck, E.E.; Yelian, F.D.; Diamond, M.P. The prevalence of ureaplasma urealyticum, mycoplasma hominis, chlamydia trachomatis and neisseria gonorrhoeae infections, and the rubella status of patients undergoing an initial infertility evaluation. *J. Assist. Reprod. Genet.* **2008**, *25*, 43–46.
377. Oliveira, N.; Adelaide, F.; Timenetsky, J. Sensitivity of rabbit fibrochondrocytes to mycoplasmas. *Brazilian J. Microbiol.* **2002**, *33*.

378. Taylor-Robinson, D.; Bébéar, C. Antibiotic susceptibilities of mycoplasmas and treatment of mycoplasmal infections. *J. Antimicrob. Chemother.* **1997**, *40*, 622–630.
379. Xie, X.; Zhang, J. Trends in the rates of resistance of Ureaplasma urealyticum to antibiotics and identification of the mutation site in the quinolone resistance-determining region in Chinese patients. *FEMS Microbiol. Lett.* **2006**, *259*, 181–186.
380. Bébéar, C.M.; Renaudin, H.; Charron, A.; Clerc, M.; Pereyre, S.; Bébéar, C. DNA gyrase and topoisomerase IV mutations in clinical isolates of Ureaplasma spp. and Mycoplasma hominis resistant to fluoroquinolones. *Antimicrob. Agents Chemother.* **2003**, *47*, 3323–3325.
381. Bebear, C.M.; Renaudin, H.; Charron, A.; Gruson, D.; Lefrancois, M.; Bebear, C. In vitro activity of trovafloxacin compared to those of five antimicrobials against mycoplasmas including Mycoplasma hominis and Ureaplasma urealyticum fluoroquinolone-resistant isolates that have been genetically characterized. *Antimicrob. Agents Chemother.* **2000**, *44*, 2557 LP – 2560.
382. Duffy, L.; Glass, J.; Hall, G.; Avery, R.; Rackley, R.; Peterson, S.; Waites, K. Fluoroquinolone Resistance in Ureaplasma parvum in the United States. *J. Clin. Microbiol.* **2006**, *44*, 1590 LP – 1591.
383. Pfaller, M.A.; Diekema, D.J.; Gibbs, D.L.; Newell, V.A.; Ellis, D.; Tullio, V.; Rodloff, A.; Fu, W.; Ling, T.A. Results from the ARTEMIS DISK Global Antifungal Surveillance Study, 1997 to 2007: a 10.5-year analysis of susceptibilities of Candida Species to fluconazole and voriconazole as determined by CLSI standardized disk diffusion. *J. Clin. Microbiol.* **2010**, *48*, 1366 LP – 1377.
384. Pfaller, M.A.; Espinel-Ingroff, A.; Boyken, L.; Hollis, R.J.; Kroeger, J.; Messer, S.A.; Tendolkar, S.; Diekema, D.J. Comparison of the broth microdilution (BMD) method of the European Committee on Antimicrobial Susceptibility Testing with the 24-hour CLSI BMD method for testing susceptibility of Candida species to fluconazole, posaconazole, and voriconazole by use of epidemiological cutoff values. *J. Clin. Microbiol.* **2011**, *49*, 845 LP – 850.
385. Lyon, G.M.; Karatela, S.; Sunay, S.; Adiri, Y. Antifungal susceptibility testing of Candida isolates from the Candida surveillance study. *J. Clin. Microbiol.* **2010**, *48*, 1270 LP – 1275.
386. Ostrosky-Zeichner, L.; Rex, J.H.; Pappas, P.G.; Hamill, R.J.; Larsen, R.A.; Horowitz, H.W.; Powderly, W.G.; Hyslop, N.; Kauffman, C.A.; Cleary, J.; et al. Antifungal susceptibility survey of 2,000 bloodstream Candida isolates in the United States. *Antimicrob. Agents Chemother.* **2003**, *47*, 3149–3154.
387. Quindós, G.; Sánchez-Vargas, L.O.; Villar-Vidal, M.; Eraso, E.; Alkorta, M.; Hernández-Almaraz, J.L. Activities of fluconazole and voriconazole against bloodstream isolates of Candida glabrata and Candida krusei: a 14-year study in a Spanish tertiary medical centre. *Int. J. Antimicrob. Agents* **2008**, *31*, 266–271.
388. Vermes, A.; Guchelaar, H.-J.; Dankert, J. Flucytosine: a review of its pharmacology, clinical indications, pharmacokinetics, toxicity and drug interactions. *J. Antimicrob. Chemother.* **2000**, *46*, 171–179.
389. Szejtli, J. Past, Present, and Future of Cyclodextrin Research. *Pure Appl. Chem. - PURE APPL CHEM* **2004**, *76*, 1825–1845.
390. Spulber, M.; Miron, L.; Mares, M.; Nastasa, V.; Pinteala, M.; Fifere, A.; Harabagiu, V.; Simionescu, B.C. Water soluble 5 FC complexes, preliminary pharmacological studies. *J. Incl. Phenom. Macrocycl. Chem.* **2009**, *65*, 431.
391. Miron, L.; Mares, M.; Nastasa, V.; Spulber, M.; Fifere, A.; Pinteala, M.; Harabagiu, V.; Simionescu, B.C. Water soluble sulconazole-β-cyclodextrin complex: physico-chemical characterization and preliminary pharmacological studies. *J. Incl. Phenom. Macrocycl. Chem.* **2009**, *63*, 159–162.
392. Mares, M.; Ştefanache, A.; Popovici, I.; Valica, V.; Buiuc, D. [Evaluation of the antifungal effect of a new propiconazole derivative against 64 yeast strains isolated from vaginal mycosis]. *Rev. medico-chirurgicală a Soc. Medici şi Nat. din Iaşi* **2007**, *111*, 768–772.
393. Goetz, A.K.; Dix, D.J. Mode of Action for Reproductive and Hepatic Toxicity Inferred from a Genomic Study of Triazole Antifungals. *Toxicol. Sci.* **2009**, *110*, 449–462.
394. Chen, P.-J.; Moore, T.; Nesnow, S. Cytotoxic effects of propiconazole and its metabolites in mouse and human hepatoma cells and primary mouse hepatocytes. *Toxicol. Vitr.* **2008**, *22*, 1476–1483.
395. Organization, W.H.; Safety, I.P. on C. The WHO recommended classification of pesticides by hazard and guidelines to classification 2009 2010.
396. *Pfizer Inc. Vfend (Voriconazole) Powder for oral suspension. Material safety data sheet; version 1.2; 2007.*;
397. Bensadoun, R.-J.; Patton, L.L.; Lalla, R. V; Epstein, J.B. Oropharyngeal candidiasis in head and neck cancer patients treated with radiation: update 2011. *Support. Care Cancer* **2011**, *19*, 737–744.
398. Bremenkamp, R.M.; Caris, A.R.; Jorge, A.O.C.; Back-Brito, G.N.; Mota, A.J.; Balducci, I.; Brighenti, F.L.; Koga-Ito, C.Y. Prevalence and antifungal resistance profile of Candida spp. oral isolates from patients with type 1 and 2 diabetes mellitus. *Arch. Oral Biol.* **2011**, *56*, 549–555.

399. Sobel, J.D. Genital candidiasis. *Medicine (Baltimore).* **2010**, *38*, 286–290.
400. A., P.M.; J., D.D.; L., G.D.; A., N. V; F., M.J.; M., G.I.; W., F.; L., C.A.; E., R.-N. Results from the ARTEMIS DISK Global Antifungal Surveillance Study, 1997 to 2005: an 8.5-Year Analysis of Susceptibilities of Candida Species and Other Yeast Species to Fluconazole and Voriconazole Determined by CLSI Standardized Disk Diffusion Testing. *J. Clin. Microbiol.* **2007**, *45*, 1735–1745.
401. Schmalreck, A.F.; Willinger, B.; Haase, G.; Blum, G.; Lass-Flörl, C.; Fegeler, W.; Becker, K.; Group, for the A.S.T. (AFST) S. Species and susceptibility distribution of 1062 clinical yeast isolates to azoles, echinocandins, flucytosine and amphotericin B from a multi-centre study. *Mycoses* **2012**, *55*, e124–e137.
402. Manuel, C.-E.; Alicia, G.-L.; Emilia, M.; Araceli, M.; J., B.M.; L., R.-T.J. Activity Profile In Vitro of Micafungin against Spanish Clinical Isolates of Common and Emerging Species of Yeasts and Molds. *Antimicrob. Agents Chemother.* **2009**, *53*, 2192–2195.
403. Yang, Y.-L.; Chen, H.-T.; Lin, C.-C.; Chu, W.-L.; Lo, H.-J. Species distribution and drug susceptibilities of Candida isolates in TSARY 2010. *Diagn. Microbiol. Infect. Dis.* **2013**, *76*, 182–186.
404. Rodloff, A.C.; Koch, D.; Schaumann, R. Epidemiology and antifungal resistance in invasive candidiasis. *Eur. J. Med. Res.* **2011**, *16*, 187.
405. Espinel-Ingroff, A.; Cuenca-Estrella, M.; Cantón, E. EUCAST and CLSI: Working Together Towards a Harmonized Method for Antifungal Susceptibility Testing. *Curr. Fungal Infect. Rep.* **2013**, *7*, 59–67.
406. Cisterna, R.; Tellería, O.; Hernaez, S.; Ezpeleta, G. Impact of the New Clinical Breaking Points Proposed by the Clinical and Laboratory Standards Institute (CLSI) in the Antifungal Susceptibility Profile of Clinical Strains Isolated from Invasive Bloodstream Candida Spp. Infections in Spain. *Clin. Med. Insights Ther.* **2012**, *4*, CMT.S8293.
407. Clinical and Laboratory Standards Institute (CLSI) (2008) Reference method for broth dilution antifungal susceptibility testing of yeasts; Approved Standard—Third Edition. CLSI document M27-A3.
408. Lockhart, S.R.; Iqbal, N.; Cleveland, A.A.; Farley, M.M.; Harrison, L.H.; Bolden, C.B.; Baughman, W.; Stein, B.; Hollick, R.; Park, B.J.; et al. Species identification and antifungal susceptibility testing of Candida bloodstream isolates from population-based surveillance studies in two U.S. cities from 2008 to 2011. *J. Clin. Microbiol.* **2012**, *50*, 3435 LP – 3442.
409. Clinical and Laboratory Standards Institute (CLSI) (2004) Method for antifungal disk diffusion susceptibility testing of yeasts; Approved Guideline. CLSI document M44-A.
410. Rodriguez-Tudela, J.L.; Arendrup, M.C.; Barchiesi, F.; Bille, J.; Chryssanthou, E.; Cuenca-Estrella, M.; Dannaoui, E.; Denning, D.W.; Donnelly, J.P.; Dromer, F.; et al. EUCAST Definitive Document EDef 7.1: method for the determination of broth dilution MICs of antifungal agents for fermentative yeasts: Subcommittee on Antifungal Susceptibility Testing (AFST) of the ESCMID European Committee for Antimicrobial Susceptibili. *Clin. Microbiol. Infect.* **2008**, *14*, 398–405.
411. Pemán, J.; Cantón, E.; Linares-Sicilia, M.J.; Roselló, E.M.; Borrell, N.; Ruiz-Pérez-de-Pipaon, M.T.; Guinea, J.; García, J.; Porras, A.; García-Tapia, A.M.; et al. Epidemiology and Antifungal Susceptibility of Bloodstream Fungal Isolates in Pediatric Patients: a Spanish Multicenter Prospective Survey. *J. Clin. Microbiol.* **2011**, *49*, 4158 LP – 4163.
412. Mareş, M.; Năstasă, V.; Moraru Ramona, F.; Doroftei, B.; Ştefanache, A. Comparative In Vitro Activities of Fluconazole, Voriconazole, and MXP-4509 Against Romanian Blood Yeast Isolates. *Mycopathologia* **2011**, *172*, 487–492.
413. Taylor-Robinson, D. Mollicutes in vaginal microbiology: Mycoplasma hominis, Ureaplasma urealyticum, Ureaplasma parvum and Mycoplasma genitalium. *Res. Microbiol.* **2017**, *168*, 875–881.
414. Baka, S.; Kouskouni, E.; Antonopoulou, S.; Sioutis, D.; Papakonstantinou, M.; Hassiakos, D.; Logothetis, E.; Liapis, A. Prevalence of Ureaplasma urealyticum and Mycoplasma hominis in women with chronic urinary symptoms. *Urology* **2009**, *74*, 62–66.
415. Egawa, T.; Morioka, I.; Morisawa, T.; Yokoyama, N.; Nakao, H.; Ohashi, M.; Matsuo, M. Ureaplasma urealyticum and Mycoplasma hominis presence in umbilical cord is associated with pathogenesis of funisitis. *Kobe J. Med. Sci.* **2007**, *53*, 241–249.
416. Goldenberg, R.L.; Andrews, W.W.; Goepfert, A.R.; Faye-Petersen, O.; Cliver, S.P.; Carlo, W.A.; Hauth, J.C. The Alabama Preterm Birth Study: umbilical cord blood Ureaplasma urealyticum and Mycoplasma hominis cultures in very preterm newborn infants. *Am. J. Obstet. Gynecol.* **2008**, *198*, 43.e1-43.e435.
417. Zeng, X.-Y.; Xin, N.; Tong, X.-N.; Wang, J.-Y.; Liu, Z.-W. Prevalence and antibiotic susceptibility of Ureaplasma urealyticum and Mycoplasma hominis in Xi'an, China. *Eur. J. Clin. Microbiol. Infect. Dis.* **2016**, *35*, 1941–1947.
418. Zheng, W.; Zhang, W.; Cui, D.; Nie, Z.; Ding, B.; Cheng, J.; Mei, C. Examination of Ureaplasma urealyticum and Mycoplasma hominis in 4082 Chinese patients . *Brazilian J. Med. Biol. Res.* 2021, *54*.
419. Wang, Q.-Y.; Li, R.-H.; Zheng, L.-Q.; Shang, X.-H. Prevalence and antimicrobial susceptibility of

Ureaplasma urealyticum and Mycoplasma hominis in female outpatients, 2009–2013. *J. Microbiol. Immunol. Infect.* **2014**, *49*.
420. Huang, C.; Long, X.; Jing, S.; Fan, L.; Xu, K.; Wang, S.; Zhu, W. Ureaplasma urealyticum and Mycoplasma hominis infections and semen quality in 19,098 infertile men in China. *World J. Urol.* **2016**, *34*, 1039–1044.
421. Zhu, C.; Liu, J.; Ling, Y.; Dong, C.; Wu, T.; Yu, X.; Hou, Y.; Dong, L.; Cheng, X. Prevalence and antimicrobial susceptibility of Ureaplasma urealyticum and Mycoplasma hominis in Chinese women with genital infectious diseases. *Indian J. Dermatol. Venereol. Leprol.* **2012**, *78*, 406–407.
422. Lee, J.S.; Kim, K.T.; Lee, H.S.; Yang, K.M.; Seo, J.T.; Choe, J.H. Concordance of Ureaplasma urealyticum and Mycoplasma hominis in infertile couples: impact on semen parameters. *Urology* **2013**, *81*, 1219–1224.
423. Salmeri, M.; Valenti, D.; Vignera, S.; Bellanca, S.; Morello, A.; Toscano, M.; Mastrojeni, S.; Calogero, A. Prevalence of Ureaplasma urealyticum and Mycoplasma hominis infection in unselected infertile men. *J. Chemother.* **2012**, *24*, 81–86.
424. Moridi, K.; Hemmaty, M.; Azimian, A.; Fallah, M.H.; Khaneghahi Abyaneh, H.; Ghazvini, K. Epidemiology of genital infections caused by Mycoplasma hominis, M. genitalium and Ureaplasma urealyticum in Iran; a systematic review and meta-analysis study (2000–2019). *BMC Public Health* **2020**, *20*, 1020.
425. Daniele, M.; Ruiz, F.; Pascual, L.; Barberis, L. Ureaplasma urealyticum and Mycoplasma hominis Sensitivity to Bacteriocins Produced by Two Lactobacilli Strains. *Curr. Microbiol.* **2011**, *63*, 360.
426. Michou, I.V.; Constantoulakis, P.; Makarounis, K.; Georgoulias, G.; Kapetanios, V.; Tsilivakos, V. Molecular investigation of menstrual tissue for the presence of Chlamydia trachomatis, Ureaplasma urealyticum and Mycoplasma hominis collected by women with a history of infertility. *J. Obstet. Gynaecol. Res.* **2014**, *40*, 237–242.
427. Witkin, S.S.; Kligman, I.; Grifo, J.A.; Rosenwaks, Z. Ureaplasma urealyticum andMycoplasma hominis detected by the polymerase chain reaction in the cervices of women undergoingin vitro fertilization: Prevalence and consequences. *J. Assist. Reprod. Genet.* **1995**, *12*, 610–614.
428. Aydin, Y.; Atis, A.; Ocer, F.; Isenkul, R. Association of cervical infection of Chlamydia trachomatis, Ureaplasma urealyticum and Mycoplasma hominis with peritoneum colonisation in pregnancy. *J. Obstet. Gynaecol. (Lahore).* **2010**, *30*, 809–812.
429. Garzon, S.; Laganà, A.S.; Casarin, J.; Raffaelli, R.; Cromi, A.; Sturla, D.; Franchi, M.; Ghezzi, F. An update on treatment options for interstitial cystitis. *Prz. menopauzalny = Menopause Rev.* **2020**, *19*, 35–43.
430. Patnaik, S.S.; Laganà, A.S.; Vitale, S.G.; Butticè, S.; Noventa, M.; Gizzo, S.; Valenti, G.; Rapisarda, A.M.C.; La Rosa, V.L.; Magno, C.; et al. Etiology, pathophysiology and biomarkers of interstitial cystitis/painful bladder syndrome. *Arch. Gynecol. Obstet.* **2017**, *295*, 1341–1359.
431. Bébéar, C. *Mycoplasmes et chlamydiae*; Elsevier Masson, 2002; ISBN 2842993373.
432. Waites, K.B.; Schelonka, R.L.; Xiao, L.; Grigsby, P.L.; Novy, M.J. Congenital and opportunistic infections: Ureaplasma species and Mycoplasma hominis. *Semin. Fetal Neonatal Med.* **2009**, *14*, 190–199.
433. Donders, G.G.; Van Bulck, B.; Caudron, J.; Londers, L.; Vereecken, A.; Spitz, B. Relationship of bacterial vaginosis and mycoplasmas to the risk of spontaneous abortion. *Am. J. Obstet. Gynecol.* **2000**, *183*, 431–437.
434. Fowlkes, D.M.; Macleod, J.; O'leary, W.M. T-Mycoplasmas and Human Infertility: Correlation of Infection with Alterations in Seminal Parameters**Supported by grants from The Population Council and from Hoffmann-LaRoche, Inc. *Fertil. Steril.* **1975**, *26*, 1212–1218.
435. Gerber, S.; Vial, Y.; Hohlfeld, P.; Witkin, S.S. Detection of Ureaplasma urealyticum in Second-Trimester Amniotic Fluid by Polymerase Chain Reaction Correlates with Subsequent Preterm Labor and Delivery. *J. Infect. Dis.* **2003**, *187*, 518–521.
436. GUILLET-ROSSO, F.; FARI, A.; TAYLOR, S.; FORMAN, R.; BELAISCH-ALLART, J.; TESTART, J.; FRYDMAN, R. Systematic semen culture and its influence on IVF management. *BJOG An Int. J. Obstet. Gynaecol.* **1987**, *94*, 543–547.
437. Montagut, J.M.; Leprêtre, S.; Degoy, J.; Rousseau, M. Ureaplasma in semen and IVF. *Hum. Reprod.* **1991**, *6*, 727–729.
438. Reichart, M.; Kahane, I.; Bartoov, B. In Vivo and In Vitro Impairment of Human and Ram Sperm Nuclear Chromatin Integrity by Sexually Transmitted Ureaplasma urealyticum Infection1. *Biol. Reprod.* **2000**, *63*, 1041–1048.
439. Williams, C.M.; Okada, D.M.; Marshall, J.R.; Chow, A.W. Clinical and microbiologic risk evaluation for post-cesarean section endometritis by multivariate discriminant analysis: role of intraoperative mycoplasma, aerobes, and anaerobes. *Am. J. Obstet. Gynecol.* **1987**, *156*, 967–974.

440. Gruson, D.; Pereyre, S.; Renaudin, H.; Charron, A.; Bébéar, C.; Bébéar, C.M. In vitro development of resistance to six and four fluoroquinolones in Mycoplasma pneumoniae and Mycoplasma hominis, respectively. *Antimicrob. Agents Chemother.* **2005**, *49*, 1190 LP – 1193.
441. Dannaoui, E.; Lortholary, O.; Raoux, D.; Bougnoux, M.E.; Galeazzi, G.; Lawrence, C.; Moissenet, D.; Poilane, I.; Hoinard, D.; Dromer, F.; et al. Comparative in vitro activities of caspofungin and micafungin, determined using the method of the European Committee on Antimicrobial Susceptibility Testing, against yeast isolates obtained in France in 2005-2006. *Antimicrob. Agents Chemother.* **2008**, *52*, 778–781.
442. EUCAST technical note on fluconazole. *Clin. Microbiol. Infect. Off. Publ. Eur. Soc. Clin. Microbiol. Infect. Dis.* **2008**, *14*, 193–195.
443. EUCAST Technical Note on voriconazole. *Clin. Microbiol. Infect. Off. Publ. Eur. Soc. Clin. Microbiol. Infect. Dis.* **2008**, *14*, 985–987.
444. Espinel-Ingroff, A.; Pfaller, M.; Cantón, E.; Pemán, J. Emerging Resistance to Azoles and Echinocandins: Clinical Relevance and Laboratory Detection. *Curr. Fungal Infect. Rep.* **2010**, *4*, 186–195.
445. Kuhn, D.; Ghannoum, M. Candida biofilms: Antifungal resistance and emerging therapeutic options. *Curr. Opin. Investig. Drugs* **2004**, *5*, 186–197.
446. Pfaller, M.A.; Diekema, D.J.; Gibbs, D.L.; Newell, V.A.; Barton, R.; Bijie, H.; Bille, J.; Chang, S.-C.; da Luz Martins, M.; Duse, A.; et al. Geographic variation in the frequency of isolation and fluconazole and voriconazole susceptibilities of Candida glabrata: an assessment from the ARTEMIS DISK Global Antifungal Surveillance Program. *Diagn. Microbiol. Infect. Dis.* **2010**, *67*, 162–171.
447. Sellami, A.; Sellami, H.; Néji, S.; Makni, F.; Abbes, S.; Cheikhrouhou, F.; Chelly, H.; Bouaziz, M.; Hammami, B.; Ben Jemaa, M.; et al. Antifungal Susceptibility of Bloodstream Candida Isolates in Sfax Hospital: Tunisia. *Mycopathologia* **2011**, *171*, 417–422.
448. Romeo, O.; Criseo, G. Candida africana and its closest relatives. *Mycoses* **2011**, *54*, 475–486.
449. Anna, K.; Kantarawee, K.; Marizeth, G.; Bart, T.; Michael, A.; Aristea, V.; Markus, K.; Mihai, M.; J., T.-A.S.; Teun, B. Identification of Medically Relevant Species of Arthroconidial Yeasts by Use of Matrix-Assisted Laser Desorption Ionization–Time of Flight Mass Spectrometry. *J. Clin. Microbiol.* **2013**, *51*, 2491–2500.
450. E., C.-B.; A., K.; A., A.-I.; B., T.; M., G.; M., K.; M., C.-E.; A., G.-L.; T., B. Reclassification of the Candida haemulonii Complex as Candida haemulonii (C. haemulonii Group I), C. duobushaemulonii sp. nov. (C. haemulonii Group II), and C. haemulonii var. vulnera var. nov.: Three Multiresistant Human Pathogenic Yeasts . *J. Clin. Microbiol.* **2012**, *50*, 3641–3651.
451. White, T.; Bruns, T.; Lee, S.; Taylor, J.; Innis, M.; Gelfand, D.; Sninsky, J. Amplification and Direct Sequencing of Fungal Ribosomal RNA Genes for Phylogenetics. In *Pcr Protocols: a Guide to Methods and Applications,*; 1990; Vol. 31, pp. 315–322.
452. Vilgalys, R.; Hester, M. Rapid genetic identification and mapping of enzymatically amplified ribosomal DNA from several Cryptococcus species. *J. Bacteriol.* **1990**, *172*, 4238–4246.
453. Arendrup, M.C.; Cuenca-Estrella, M.; Lass-Flörl, C.; Hope, W. EUCAST technical note on the EUCAST definitive document EDef 7.2: method for the determination of broth dilution minimum inhibitory concentrations of antifungal agents for yeasts EDef 7.2 (EUCAST-AFST)*. *Clin. Microbiol. Infect.* **2012**, *18*, E246–E247.
454. European Committee on Antimicrobial Susceptibility Testing (EUCAST) (2013) Antifungal agents. Breakpoint tables for interpretation of MICs. Version 6.1, valid from 2013-03-11. Available online: https://eucast.org/fileadmin/src/media/PDFs/EUCAST_files/AFST/Antifungal_breakpoints_v_6.1.pdf.
455. E., D.; O., L.; D., R.; E., B.M.; G., G.; C., L.; D., M.; I., P.; D., H.; F., D. Comparative In Vitro Activities of Caspofungin and Micafungin, Determined Using the Method of the European Committee on Antimicrobial Susceptibility Testing, against Yeast Isolates Obtained in France in 2005-2006. *Antimicrob. Agents Chemother.* **2008**, *52*, 778–781.
456. Kurtzman, C.P.; Fell, J.W.; Boekhout, T. *The Yeasts: A Taxonomic Study*; The Yeasts: A Taxonomic Study; Elsevier, 2011; ISBN 9780123847072.
457. Ahmad, S.; Khan, Z.U.; Johny, M.; Ashour, N.M.; Al-Tourah, W.H.; Joseph, L.; Chandy, R. Isolation of *Lodderomyces elongisporus* from the Catheter Tip of a Fungemia Patient in the Middle East. *Case Rep. Med.* **2013**, *2013*, 560406.
458. Martinez, M.; López-Ribot, J.L.; Kirkpatrick, W.R.; Coco, B.J.; Bachmann, S.P.; Patterson, T.F. Replacement of Candida albicans with C. dubliniensis in human immunodeficiency virus-infected patients with oropharyngeal candidiasis treated with fluconazole. *J. Clin. Microbiol.* **2002**, *40*, 3135 LP – 3139.
459. Moran, G.P.; Sullivan, D.J.; Henman, M.C.; McCreary, C.E.; Harrington, B.J.; Shanley, D.B.; Coleman, D.C. Antifungal drug susceptibilities of oral Candida dubliniensis isolates from human

immunodeficiency virus (HIV)-infected and non-HIV-infected subjects and generation of stable fluconazole-resistant derivatives in vitro. *Antimicrob. Agents Chemother.* **1997**, *41*, 617–623.
460. Arendrup, M.C.; Boekhout, T.; Akova, M.; Meis, J.F.; Cornely, O.A.; Lortholary, O. ESCMID and ECMM joint clinical guidelines for the diagnosis and management of rare invasive yeast infections. *Clin. Microbiol. Infect.* **2014**, *20*, 76–98.
461. Vazquez, J.A. Trichosporon Infection. *Curr. Fungal Infect. Rep.* **2010**, *4*, 52–58.
462. J., D.D.; B., P.; A., M.S.; J., H.R.; A, P.M. Activities of Available and Investigational Antifungal Agents against Rhodotorula Species. *J. Clin. Microbiol.* **2005**, *43*, 476–478.
463. Sobel, J. The emergence of non-albicans Candida species as causes of invasive candidiasis and candidemia. *Curr. Infect. Dis. Rep.* **2006**, *8*, 427–433.
464. Lass-Flörl, C. The changing face of epidemiology of invasive fungal disease in Europe. *Mycoses* **2009**, *52*, 197–205.
465. Falagas, M.E.; Roussos, N.; Vardakas, K.Z. Relative frequency of albicans and the various non-albicans Candida spp among candidemia isolates from inpatients in various parts of the world: a systematic review. *Int. J. Infect. Dis.* **2010**, *14*, e954–e966.
466. Toubas, D. Epidémiologie des candidoses invasives. *Rev. Francoph. des Lab.* **2013**, *2013*, 27–36.
467. Arendrup, M.C.; Bruun, B.; Christensen, J.J.; Fuursted, K.; Johansen, H.K.; Kjældgaard, P.; Knudsen, J.D.; Kristensen, L.; Møller, J.; Nielsen, L.; et al. National Surveillance of Fungemia in Denmark (2004 to 2009). *J. Clin. Microbiol.* **2011**, *49*, 325 LP – 334.
468. Sifuentes-Osornio, J.; Corzo-León, D.E.; Ponce-de-León, L.A. Epidemiology of Invasive Fungal Infections in Latin America. *Curr. Fungal Infect. Rep.* **2012**, *6*, 23–34.
469. Colombo, A.L.; Guimarães, T.; Silva, L.R.B.F.; Monfardini, L.P. de A.; Cunha, A.K.B.; Rady, P.; Alves, T.; Rosas, R.C. Prospective Observational Study of Candidemia in São Paulo, Brazil: Incidence Rate, Epidemiology, and Predictors of Mortality. *Infect Control Hosp Epidemiol.* **2007**, *28*, 570–576.
470. Montagna, M.T.; Caggiano, G.; Lovero, G.; De Giglio, O.; Coretti, C.; Cuna, T.; Iatta, R.; Giglio, M.; Dalfino, L.; Bruno, F.; et al. Epidemiology of invasive fungal infections in the intensive care unit: results of a multicenter Italian survey (AURORA Project). *Infection* **2013**, *41*, 645–653.
471. Taj-Aldeen, S.J.; Kolecka, A.; Boesten, R.; Alolaqi, A.; Almaslamani, M.; Chandra, P.; Meis, J.F.; Boekhout, T. Epidemiology of candidemia in Qatar, the Middle East: performance of MALDI-TOF MS for the identification of Candida species, species distribution, outcome, and susceptibility pattern. *Infection* **2014**, *42*, 393–404.
472. Tortorano, A.M.; Kibbler, C.; Peman, J.; Bernhardt, H.; Klingspor, L.; Grillot, R. Candidaemia in Europe: epidemiology and resistance. *Int. J. Antimicrob. Agents* **2006**, *27*, 359–366.
473. Charlier, C.; Hart, E.; Lefort, A.; Ribaud, P.; Dromer, F.; Denning, D.W.; Lortholary, O. Fluconazole for the management of invasive candidiasis: where do we stand after 15 years? *J. Antimicrob. Chemother.* **2006**, *57*, 384–410.
474. Alexander, B.D.; Johnson, M.D.; Pfeiffer, C.D.; Jiménez-Ortigosa, C.; Catania, J.; Booker, R.; Castanheira, M.; Messer, S.A.; Perlin, D.S.; Pfaller, M.A. Increasing Echinocandin Resistance in Candida glabrata: Clinical Failure Correlates With Presence of FKS Mutations and Elevated Minimum Inhibitory Concentrations. *Clin. Infect. Dis.* **2013**, *56*, 1724–1732.
475. Guillermo, G.-E.; K., K.S.; Steven, P.; D., E.T.; S., P.D. A Naturally Occurring Proline-to-Alanine Amino Acid Change in Fks1p in Candida parapsilosis, Candida orthopsilosis, and Candida metapsilosis Accounts for Reduced Echinocandin Susceptibility. *Antimicrob. Agents Chemother.* **2008**, *52*, 2305–2312.
476. Bassetti, M.; Taramasso, L.; Nicco, E.; Molinari, M.P.; Mussap, M.; Viscoli, C. Epidemiology, Species Distribution, Antifungal Susceptibility and Outcome of Nosocomial Candidemia in a Tertiary Care Hospital in Italy. *PLoS One* **2011**, *6*, e24198.
477. Chitasombat, M.N.; Kofteridis, D.P.; Jiang, Y.; Tarrand, J.; Lewis, R.E.; Kontoyiannis, D.P. Rare opportunistic (non-Candida, non-Cryptococcus) yeast bloodstream infections in patients with cancer. *J. Infect.* **2012**, *64*, 68–75.
478. Lunardi, L.W.; Aquino, V.R.; Zimerman, R.A.; Goldani, L.Z. Epidemiology and Outcome of Rhodotorula Fungemia in a Tertiary Care Hospital. *Clin. Infect. Dis.* **2006**, *43*, e60–e63.
479. Mashburn, J. Etiology, Diagnosis, and Management of Vaginitis. *J. Midwifery Womens. Health* **2006**, *51*, 423–430.
480. Sobel, J.D. Vulvovaginal candidosis. *Lancet* **2007**, *369*, 1961–1971.
481. F, K.; AR, K.; V, K.; M, H.; AA, K.; M, R. In vitro antifungal susceptibility of oral candida species from Iranian HIV infected patients TT - حساسیت گونه های کاندیدای دهانی جدا شده از افراد آلوده به HIV نسبت به داروهای ضد قارچی تحت شرایط برون تنی در ایران. *Tehran-Univ-Med-J* **2012**, *70*, 96–103.
482. Thompson III, G.R.; Patel, P.K.; Kirkpatrick, W.R.; Westbrook, S.D.; Berg, D.; Erlandsen, J.; Redding, S.W.; Patterson, T.F. Oropharyngeal candidiasis in the era of antiretroviral therapy. *Oral Surgery, Oral*

Med. Oral Pathol. Oral Radiol. Endod. **2010**, *109*, 488–495.
483. Ahmad, A.; Khan, A.U. Prevalence of Candida species and potential risk factors for vulvovaginal candidiasis in Aligarh, India. *Eur. J. Obstet. Gynecol. Reprod. Biol.* **2009**, *144*, 68–71.
484. Al Mubarak, S.; Robert, A.A.; Baskaradoss, J.K.; Al-Zoman, K.; Al Sohail, A.; Alsuwyed, A.; Ciancio, S. The prevalence of oral Candida infections in periodontitis patients with type 2 diabetes mellitus. *J. Infect. Public Health* **2013**, *6*, 296–301.
485. Katiraee, F.; Khosravi, A.R.; Khalaj, V.; Hajiabdolbaghi, M.; Khaksar, A.; Rasoolinejad, M.; Yekaninejad, M.S. Oropharyngeal candidiasis and oral yeast colonization in Iranian Human Immunodeficiency Virus positive patients. *J. Mycol. Med.* **2010**, *20*, 8–14.
486. Mañas, A.; Cerezo, L.; de la Torre, A.; García, M.; Alburquerque, H.; Ludeña, B.; Ruiz, A.; Pérez, A.; Escribano, A.; Manso, A.; et al. Epidemiology and prevalence of oropharyngeal candidiasis in Spanish patients with head and neck tumors undergoing radiotherapy treatment alone or in combination with chemotherapy. *Clin. Transl. Oncol.* **2012**, *14*, 740–746.
487. Corsello, S.; Spinillo, A.; Osnengo, G.; Penna, C.; Guaschino, S.; Beltrame, A.; Blasi, N.; Festa, A. An epidemiological survey of vulvovaginal candidiasis in Italy. *Eur. J. Obstet. Gynecol. Reprod. Biol.* **2003**, *110*, 66–72.
488. Bohbot, J.-M.; Sednaoui, P.; Verriere, F.; Achhammer, I. Diversité étiologique des vaginites. *Gynécologie Obs. Fertil.* **2012**, *40*, 578–581.
489. Grigoriou, O.; Baka, S.; Makrakis, E.; Hassiakos, D.; Kapparos, G.; Kouskouni, E. Prevalence of clinical vaginal candidiasis in a university hospital and possible risk factors. *Eur. J. Obstet. Gynecol. Reprod. Biol.* **2006**, *126*, 121–125.
490. Sojakova, M.; Liptajova, D.; Borovsky, M.; Subik, J. Fluconazole and itraconazole susceptibility of vaginal yeast isolates from Slovakia. *Mycopathologia* **2004**, *157*, 163–169.
491. Bulacio, L.; Paz, M.; Ramadán, S.; Ramos, L.; Pairoba, C.; Sortino, M.; Escovich, L.; López, C. Oral infections caused by yeasts in patients with head and neck cancer undergoing radiotherapy. Identification of the yeasts and evaluation of their antifungal susceptibility. *J. Mycol. Med.* **2012**, *22*, 348–353.
492. Kamikawa, Y.; Nagayama, T.; Fujisaki, J.; Hirabayashi, D.; Kawasaki, K.; Hamada, T.; Mori, Y.; Kamikawa, Y.; Mukai, H.; Sato, T.; et al. Clinical study on anti-fungal drug activity against clinically isolated strains of oral Candida species. *Oral Sci. Int.* **2013**, *10*, 87–94.
493. Mulu, A.; Kassu, A.; Anagaw, B.; Moges, B.; Gelaw, A.; Alemayehu, M.; Belyhun, Y.; Biadglegne, F.; Hurissa, Z.; Moges, F.; et al. Frequent detection of 'azole' resistant Candida species among late presenting AIDS patients in northwest Ethiopia. *BMC Infect. Dis.* **2013**, *13*, 82.
494. Migliorati, C.A.; Birman, E.G.; Cury, A.E. Oropharyngeal candidiasis in HIV-infected patients under treatment with protease inhibitors. *Oral Surgery, Oral Med. Oral Pathol. Oral Radiol. Endod.* **2004**, *98*, 301–310.
495. Pasqualotto, A.C. Candida and the paediatric lung. *Paediatr. Respir. Rev.* **2009**, *10*, 186–191.
496. Beck, J.M.; Young, V.B.; Huffnagle, G.B. The microbiome of the lung. *Transl. Res.* **2012**, *160*, 258–266.
497. Pfaller, M.A.; Castanheira, M.; Lockhart, S.R.; Jones, R.N. Candida glabrata: Multidrug Resistance and Increased Virulence in a Major Opportunistic Fungal Pathogen. *Curr. Fungal Infect. Rep.* **2012**, *6*, 154–164.
498. Marangoci, N.; Mares, M.; Silion, M.; Fifere, A.; Varganici, C.; Nicolescu, A.; Deleanu, C.; Coroaba, A.; Pinteala, M.; Simionescu, B.C. Inclusion complex of a new propiconazole derivative with β-cyclodextrin: NMR, ESI–MS and preliminary pharmacological studies. *Results Pharma Sci.* **2011**, *1*, 27–37.
499. Romeo, O.; Criseo, G. First molecular method for discriminating between Candida africana, Candida albicans, and Candida dubliniensis by using hwp1 gene. *Diagn. Microbiol. Infect. Dis.* **2008**, *62*, 230–233.
500. *Motulsky Harvey. Intuitive Biostatistics: A Nonmathematical Guide to Statistical Thinking. Oxford University Press, USA; 2nd Revised & enlarged edition (January 20, 2010)*;
501. Subcommittee on Antifungal Susceptibility Testing (AFST) of the ESCMID European Committee for Antimicrobial Susceptibility Testing (EUCAST). (2012) EUCAST DEFINITIVE DOCUMENT EDef 7.2 Revision. Method for the determination of broth dilution minimum Inhibi.
502. European Committee for Antimicrobial Susceptibility Testing. (2013) Antifungal Agents. Breakpoint tables for interpretation of MICs. Version 6.1.
503. Lunenfeld, B.; Bilger, W.; Longobardi, S.; Alam, V.; D'Hooghe, T.; Sunkara, S.K. The Development of Gonadotropins for Clinical Use in the Treatment of Infertility . *Front. Endocrinol.* 2019, *10*, 429.
504. Leo, V. De; Musacchio, M.C.; Sabatino, A. Di; Tosti, C.; Petraglia, G.M. and F. Present and Future of Recombinant Gonadotropins in Reproductive Medicine. *Curr. Pharm. Biotechnol.* 2012, *13*, 379–391.

505. Bungum, L.; Tagevi, J.; Jokubkiene, L.; Bungum, M.; Giwercman, A.; Macklon, N.; Andersen, C.Y.; Klausen, T.W.; Tørring, N.; Kumar, A.; et al. The Impact of the Biological Variability or Assay Performance on AMH Measurements: A Prospective Cohort Study With AMH Tested on Three Analytical Assay-Platforms. *Front. Endocrinol. (Lausanne).* **2018**, *9*, 603.
506. Arce, J.-C.; La Marca, A.; Mirner Klein, B.; Nyboe Andersen, A.; Fleming, R. Antimüllerian hormone in gonadotropin releasing-hormone antagonist cycles: prediction of ovarian response and cumulative treatment outcome in good-prognosis patients. *Fertil. Steril.* **2013**, *99*, 1644-1653.e1.
507. Arce, J.-C.; Nyboe Andersen, A.; Fernández-Sánchez, M.; Visnova, H.; Bosch, E.; García-Velasco, J.A.; Barri, P.; de Sutter, P.; Klein, B.M.; Fauser, B.C.J.M. Ovarian response to recombinant human follicle-stimulating hormone: a randomized, antimüllerian hormone-stratified, dose-response trial in women undergoing in vitro fertilization/intracytoplasmic sperm injection. *Fertil. Steril.* **2014**, *102*, 1633-1640.e5.
508. Croxtall, J.D.; McKeage, K. Corifollitropin Alfa. *BioDrugs* **2011**, *25*, 243–254.
509. Arce, J.-C.; Klein, B.; Erichsen, L. Using amh for determining a stratified gonadotropin dosing regimen for IVF/ICSI and optimizing outcomes. In *Anti-Müllerian Hormone: Biology, Role in Ovarian Function and Clinical Significance*; 2016; pp. 83–102.
510. Fleming, R.; Broekmans, F.; Calhaz-Jorge, C.; Dracea, L.; Alexander, H.; Nyboe Andersen, A.; Blockeel, C.; Jenkins, J.; Lunenfeld, B.; Platteau, P.; et al. Can anti-Müllerian hormone concentrations be used to determine gonadotrophin dose and treatment protocol for ovarian stimulation? *Reprod. Biomed. Online* **2013**, *26*, 431–439.
511. La Marca, A.; Sunkara, S.K. Individualization of controlled ovarian stimulation in IVF using ovarian reserve markers: from theory to practice. *Hum. Reprod. Update* **2014**, *20*, 124–140.
512. Nelson, S.M. Biomarkers of ovarian response: current and future applications. *Fertil. Steril.* **2013**, *99*, 963–969.
513. Toner, J.P.; Seifer, D.B. Why we may abandon basal follicle-stimulating hormone testing: a sea change in determining ovarian reserve using antimüllerian hormone. *Fertil. Steril.* **2013**, *99*, 1825–1830.
514. Havelock, J.C.; Claman, P.; Martin, F.S.; Gothberg, M.; Andersen, E.; Mannaerts, B. A prospective follow-up on neonatal health following controlled ovarian stimulation with follitropin delta or follitropin alfa. *Fertil. Steril.* **2018**, *110*, e198.
515. Leijdekkers, J.A.; van Tilborg, T.C.; Torrance, H.L.; Oudshoorn, S.C.; Brinkhuis, E.A.; Koks, C.A.M.; Lambalk, C.B.; de Bruin, J.P.; Fleischer, K.; Mochtar, M.H.; et al. Do female age and body weight modify the effect of individualized FSH dosing in IVF/ICSI treatment? A secondary analysis of the OPTIMIST trial. *Acta Obstet. Gynecol. Scand.* **2019**, *98*, 1332–1340.
516. Anckaert, E.; Denk, B.; He, Y.; Torrance, H.L.; Broekmans, F.; Hund, M. Evaluation of the Elecsys ® anti-Müllerian hormone assay for the prediction of hyper-response to controlled ovarian stimulation with a gonadotrophin-releasing hormone antagonist protocol. *Eur. J. Obstet. Gynecol. Reprod. Biol.* **2019**, *236*, 133–138.
517. Iliodromiti, S.; Salje, B.; Dewailly, D.; Fairburn, C.; Fanchin, R.; Fleming, R.; Li, H.W.R.; Lukaszuk, K.; Ng, E.H.Y.; Pigny, P.; et al. Non-equivalence of anti-Müllerian hormone automated assays-clinical implications for use as a companion diagnostic for individualised gonadotrophin dosing. *Hum. Reprod.* **2017**, *32*, 1710–1715.
518. Nyboe Andersen, A.; Nelson, S.M.; Fauser, B.C.J.M.; García-Velasco, J.A.; Klein, B.M.; Arce, J.-C.; Tournaye, H.; De Sutter, P.; Decleer, W.; Petracco, A.; et al. Individualized versus conventional ovarian stimulation for in vitro fertilization: a multicenter, randomized, controlled, assessor-blinded, phase 3 noninferiority trial. *Fertil. Steril.* **2017**, *107*, 387-396.e4.
519. Bosch, E.; Havelock, J.; Martin, F.S.; Rasmussen, B.B.; Klein, B.M.; Mannaerts, B.; Arce, J.-C. Follitropin delta in repeated ovarian stimulation for IVF: a controlled, assessor-blind Phase 3 safety trial. *Reprod. Biomed. Online* **2019**, *38*, 195–205.
520. Koechling, W.; Plaksin, D.; Croston, G.E.; Jeppesen, J. V; Macklon, K.T.; Andersen, C.Y. Comparative pharmacology of a new recombinant FSH expressed by a human cell line. *Endocr. Connect.* **2017**, *6*, 297–305.
521. Arce, J.-C.; Larsson, P.; García-Velasco, J.A. Establishing the follitropin delta dose that provides a comparable ovarian response to 150 IU/day follitropin alfa. *Reprod. Biomed. Online* **2020**, *41*, 616–622.
522. Nastri, C.O.; Ferriani, R.A.; Rocha, I.A.; Martins, W.P. Ovarian hyperstimulation syndrome: pathophysiology and prevention. *J. Assist. Reprod. Genet.* **2010**, *27*, 121–128.
523. Youssef, M.A.F.M.; van Wely, M.; Hassan, M.A.; Al-Inany, H.G.; Mochtar, M.; Khattab, S.; van der Veen, F. Can dopamine agonists reduce the incidence and severity of OHSS in IVF/ICSI treatment cycles? A systematic review and meta-analysis. *Hum. Reprod. Update* **2010**, *16*, 459–466.
524. Ovarian hyperstimulation syndrome. *Fertil. Steril.* **2008**, *90*, S188–S193.
525. Neulen, J.; Yan, Z.; Raczek, S.; Weindel, K.; Keck, C.; Weich, H.A.; Marmé, D.; Breckwoldt, M.

Human chorionic gonadotropin-dependent expression of vascular endothelial growth factor/vascular permeability factor in human granulosa cells: importance in ovarian hyperstimulation syndrome. *J. Clin. Endocrinol. Metab.* **1995**, *80*, 1967–1971.
526. Pellicer, A.; Albert, C.; Mercader, A.; Bonilla-Musoles, F.; Remohí, J.; Simón, C. The pathogenesis of ovarian hyperstimulation syndrome: in vivo studies investigating the role of interleukin-1beta, interleukin-6, and vascular endothelial growth factor. *Fertil. Steril.* **1999**, *71*, 482–489.
527. Kovács, P.; Mátyás, S.; Kaali, S.G. Effect of coasting on cycle outcome during in vitro fertilization/intracytoplasmic sperm injection cycles in hyper-responders. *Fertil. Steril.* **2006**, *85*, 913–917.
528. Shmorgun, D.; Claman, P.; Gysler, M.; Hemmings, R.; Cheung, A.P.; Goodrow, G.J.; Hughes, E.G.; Min, J.K.; Roberts, J.; Senikas, V.; et al. The Diagnosis and Management of Ovarian Hyperstimulation Syndrome. *J. Obstet. Gynaecol. Canada* **2011**, *33*, 1156–1162.
529. Soares, S.R. Etiology of OHSS and use of dopamine agonists. *Fertil. Steril.* **2012**, *97*, 517–522.
530. Vandoorne, K.; Addadi, Y.; Neeman, M. Visualizing vascular permeability and lymphatic drainage using labeled serum albumin. *Angiogenesis* **2010**, *13*, 75–85.
531. Abramov, Y.; Naparstek, Y.; Elchalal, U.; Lewin, A.; Schechter, E.; Schenker, J.G. Plasma immunoglobulins in patients with severe ovarian hyperstimulation syndrome. *Fertil. Steril.* **1999**, *71*, 102–105.
532. RCOG *The management of ovarian hyperstimulation syndrome. Green-top guideline, number 5.*; 2016;
533. Sansone, P.; Aurilio, C.; Pace, M.C.; Esposito, R.; Passavanti, M.B.; Pota, V.; Pace, L.; Pezzullo, M.G.; Bulletti, C.; Palagiano, A. Intensive care treatment of ovarian hyperstimulation syndrome (OHSS). *Ann. N. Y. Acad. Sci.* **2011**, *1221*, 109–118.
534. Kumar, R.; Kumar, S.; Lata, S. Albumin infusion may deleteriously promote extracellular fluid overload without improving circulating hypovolemia in patients of advanced cirrhosis with diabetes mellitus and sepsis. *Med. Hypotheses* **2013**, *80*, 452–455.
535. Orvieto, R.; Achiron, A.; Margalit, R.; Ben-Rafael, Z. The role of intravenous immunoglobulin in the prevention of severe ovarian hyperstimulation syndrome. *J. Assist. Reprod. Genet.* **1998**, *15*, 46–49.
536. Qublan, H.S.; Al-Taani, M.I.; Megdadi, M.F.; Metri, R.M.; Al-Ahmad, N. Multiple transvaginal ascitic fluid aspirations improves the clinical and reproductive outcome in patients undergoing in vitro fertilisation treatment complicated by severe early ovarian hyperstimulation syndrome. *J. Obstet. Gynaecol. (Lahore).* **2012**, *32*, 379–382.
537. Braunstein, G.D.; Rasor, J.; Adler, D.; Danzer, H.; Wade, M.E. Serum human chorionic gonadotropin levels throughout normal pregnancy. *Am. J. Obstet. Gynecol.* **1976**, *126*, 678–681.
538. Ben-Chetrit, A.; Eldar-Geva, T.; Gal, M.; Huerta, M.; Mimon, T.; Algur, N.; Diamant, Y.Z.; Margalioth, E.J. The questionable use of albumin for the prevention of ovarian hyperstimulation syndrome in an IVF programme: a randomized placebo-controlled trial. *Hum. Reprod.* **2001**, *16*, 1880–1884.
539. Kissler, S.; Neidhardt, B.; Siebzehnrübl, E.; Schmitt, H.; Tschaikowsky, K.; Wildt, L. The detrimental role of colloidal volume substitutes in severe ovarian hyperstimulation syndrome: a case report. *Eur. J. Obstet. Gynecol. Reprod. Biol.* **2001**, *99*, 131–134.
540. Papanikolaou, E.G.; Pozzobon, C.; Kolibianakis, E.M.; Camus, M.; Tournaye, H.; Fatemi, H.M.; Van Steirteghem, A.; Devroey, P. Incidence and prediction of ovarian hyperstimulation syndrome in women undergoing gonadotropin-releasing hormone antagonist in vitro fertilization cycles. *Fertil. Steril.* **2006**, *85*, 112–120.
541. Ocal, P.; Sahmay, S.; Cetin, M.; Irez, T.; Guralp, O.; Cepni, I. Serum anti-Müllerian hormone and antral follicle count as predictive markers of OHSS in ART cycles. *J. Assist. Reprod. Genet.* **2011**, *28*, 1197–1203.
542. Lee, T.-H.; Liu, C.-H.; Huang, C.-C.; Wu, Y.-L.; Shih, Y.-T.; Ho, H.-N.; Yang, Y.-S.; Lee, M.-S. Serum anti-müllerian hormone and estradiol levels as predictors of ovarian hyperstimulation syndrome in assisted reproduction technology cycles. *Hum. Reprod.* **2008**, *23*, 160–167.
543. Steward, R.G.; Lan, L.; Shah, A.A.; Yeh, J.S.; Price, T.M.; Goldfarb, J.M.; Muasher, S.J. Oocyte number as a predictor for ovarian hyperstimulation syndrome and live birth: an analysis of 256,381 in vitro fertilization cycles. *Fertil. Steril.* **2014**, *101*, 967–973.
544. Engmann, L.; DiLuigi, A.; Schmidt, D.; Nulsen, J.; Maier, D.; Benadiva, C. The use of gonadotropin-releasing hormone (GnRH) agonist to induce oocyte maturation after cotreatment with GnRH antagonist in high-risk patients undergoing in vitro fertilization prevents the risk of ovarian hyperstimulation syndrome: a prospective rando. *Fertil. Steril.* **2008**, *89*, 84–91.
545. Radesic, B.; Tremellen, K. Oocyte maturation employing a GnRH agonist in combination with low-dose hCG luteal rescue minimizes the severity of ovarian hyperstimulation syndrome while maintaining excellent pregnancy rates. *Hum. Reprod.* **2011**, *26*, 3437–3442.
546. Seyhan, A.; Ata, B.; Polat, M.; Son, W.-Y.; Yarali, H.; Dahan, M.H. Severe early ovarian

hyperstimulation syndrome following GnRH agonist trigger with the addition of 1500 IU hCG. *Hum. Reprod.* **2013**, *28*, 2522–2528.
547. Humaidan, P.; Ejdrup Bredkjær, H.; Westergaard, L.G.; Yding Andersen, C. 1,500 IU human chorionic gonadotropin administered at oocyte retrieval rescues the luteal phase when gonadotropin-releasing hormone agonist is used for ovulation induction: a prospective, randomized, controlled study. *Fertil. Steril.* **2010**, *93*, 847–854.
548. Fawcett, D.W. The mammalian spermatozoon. *Dev. Biol.* **1975**, *44*, 394–436.
549. Moreno, R.D.; Alvarado, C.P. The mammalian acrosome as a secretory lysosome: New and old evidence. *Mol. Reprod. Dev.* **2006**, *73*, 1430–1434.
550. Zhao, L.; Burkin, H.R.; Shi, X.; Li, L.; Reim, K.; Miller, D.J. Complexin I is required for mammalian sperm acrosomal exocytosis. *Dev. Biol.* **2007**, *309*, 236–244.
551. Steven Ward, W.; Coffey, D.S. DNA Packaging and Organization in Mammalian Spermatozoa: Comparison with Somatic Cell. *Biol. Reprod.* **1991**, *44*, 569–574.
552. Steger, K.; Pauls, K.; Klonisch, T.; Franke, F.E.; Bergmann, M. Expression of protamine-1 and -2 mRNA during human spermiogenesis. *Mol. Hum. Reprod.* **2000**, *6*, 219–225.
553. EVENSON, D.P.; LARSON, K.L.; JOST, L.K. Sperm Chromatin Structure Assay: Its Clinical Use for Detecting Sperm DNA Fragmentation in Male Infertility and Comparisons With Other Techniques. *J. Androl.* **2002**, *23*, 25–43.
554. Oliva, R. Protamines and male infertility. *Hum. Reprod. Update* **2006**, *12*, 417–435.
555. Zini, A.; Bielecki, R.; Phang, D.; Zenzes, M.T. Correlations between two markers of sperm DNA integrity, DNA denaturation and DNA fragmentation, in fertile and infertile men. *Fertil. Steril.* **2001**, *75*, 674–677.
556. Surmon, L.; Fleming, S.D.; Aitken, R.; De Iuliis, G.; Zieschang, J.-A.; Clark, A.M. Cryopreservation-induced human sperm DNA damage is predominantly mediated by oxidative stress rather than apoptosis. *Hum. Reprod.* **2009**, *24*, 2061–2070.
557. Mukhopadhyay, C.S.; Gupta, A.K.; Yadav, B.R.; Chauhan, I.S.; Gupta, A.; Mohanty, T.K.; Raina, V.S. Effect of cryopreservation on sperm chromatin integrity and fertilizing potential in bovine semen. *Livest. Sci.* **2011**, *136*, 114–121.
558. Tandara, M.; Bajić, A.; Tandara, L.; Sunj, M.; Jurisic, Z.; Jukić, M. Correlation between proportions of sperm with DNA fragmentation assessed by Halosperm test and values of standard quality parameters of semen and possible impact on embryo quality. *Zdr. Vestn 2013; 82 298–307* **2013**, *82*, 298–307.
559. Cho, C.; Jung-Ha, H.; Willis, W.D.; Goulding, E.H.; Stein, P.; Xu, Z.; Schultz, R.M.; Hecht, N.B.; Eddy, E.M. Protamine 2 Deficiency Leads to Sperm DNA Damage and Embryo Death in Mice1. *Biol. Reprod.* **2003**, *69*, 211–217.
560. Januskauskas, A.; Johannisson, A.; Rodriguez-Martinez, H. Subtle membrane changes in cryopreserved bull semen in relation with sperm viability, chromatin structure, and field fertility. *Theriogenology* **2003**, *60*, 743–758.
561. Khalifa, T.A.A.; Rekkas, C.A.; Lymberopoulos, A.G.; Sioga, A.; Dimitriadis, I.; Papanikolaou, T. Factors affecting chromatin stability of bovine spermatozoa. *Anim. Reprod. Sci.* **2008**, *104*, 143–163.
562. Dobrinski, I.; Hughes, H.P.A.; Barth, A.D. Flow cytometric and microscopic evaluation and effect on fertility of abnormal chromatin condensation in bovine sperm nuclei. *Reproduction 101*, 531–538.
563. Madrid-Bury, N.; Pérez-Gutiérrez, J.F.; Pérez-Garnelo, S.; Moreira, P.; Sanjuanbenito, B.P.; Gutiérrez-Adán, A.; Martínez, J. de la F. Relationship between non-return rate and chromatin condensation of deep frozen bull spermatozoa. *Theriogenology* **2005**, *64*, 232–241.
564. Petrunkina, A.M.; Harrison, R.A.P. Cytometric solutions in veterinary andrology: Developments, advantages, and limitations. *Cytom. Part A* **2011**, *79A*, 338–348.
565. Rodriguez-Martinez, H.; Barth, A.D. In vitro evaluation of sperm quality related to in vivo function and fertility. *Soc. Reprod. Fertil. Suppl.* **2007**, *64*, 39–54.
566. Aravindan, G.R.; Bjordahl, J.; Jost, L.K.; Evenson, D.P. Susceptibility of Human Sperm toin SituDNA Denaturation Is Strongly Correlated with DNA Strand Breaks Identified by Single-Cell Electrophoresis. *Exp. Cell Res.* **1997**, *236*, 231–237.
567. ERENPREISS, J.; HLEVICKA, S.; ZALKALNS, J.; ERENPREISA, J. Effect of Leukocytospermia on Sperm DNA Integrity: A Negative Effect in Abnormal Semen Samples. *J. Androl.* **2002**, *23*, 717–723.
568. Mello, M.; Beletti, M.E. Methods for abnormal spermatozoa chromatin condensation identification in buffaloes (Bubalus bubalis). *Bubalus bubalis* **2002**, *1*, 57–65.
569. Beletti, M.E.; Mello, M.L.S. Comparison between the toluidine blue stain and the Feulgen reaction for evaluation of rabbit sperm chromatin condensation and their relationship with sperm morphology. *Theriogenology* **2004**, *62*, 398–402.
570. Erenpreisa, J.; Erenpreiss, J.; Freivalds, T.; Slaidina, M.; Krampe, R.; Butikova, J.; Ivanov, A.; Pjanova, D. Toluidine blue test for sperm DNA integrity and elaboration of image cytometry algorithm. *Cytom.*

Part A **2003**, *52A*, 19–27.
571. Beletti, M.; da F. Costa, L.; Guardieiro, M. Morphometric features and chromatin condensation abnormalities evaluated by Toluidine Blue staining in bull spermatozoa. *Braz J Morphol Sci* **2005**, *22*.
572. Sardoy, M.; Carretero, M.; Neild, D. Evaluation of stallion sperm DNA alterations during cryopreservation using Toluidine Blue. *Anim. Reprod. Sci.* **2008**, *107*, 349–350.
573. Erenpreiss, J.; Jepson, K.; Giwercman, A.; Tsarev, I.; Erenpreisa, J.; Spano, M. Toluidine blue cytometry test for sperm DNA conformation: comparison with the flow cytometric sperm chromatin structure and TUNEL assays. *Hum. Reprod.* **2004**, *19*, 2277–2282.
574. Tamuli, M.K.; Watson, P.F. Use of a simple staining technique to distinguish acrosomal changes in the live sperm sub-population. *Anim. Reprod. Sci.* **1994**, *35*, 247–254.
575. A, Awarwal, TM, S. Sperm chromatin assessment. In *Textbook of ART*; DK Gardner, A Weissman, CM Howles, Z.S., Ed.; Taylor & Francis Group, London: UK, 2005; pp. 93–106.
576. Evenson, D.P.; Jost, L.K.; Marshall, D.; Zinaman, M.J.; Clegg, E.; Purvis, K.; de Angelis, P.; Claussen, O.P. Utility of the sperm chromatin structure assay as a diagnostic and prognostic tool in the human fertility clinic. *Hum. Reprod.* **1999**, *14*, 1039–1049.
577. Gatewood, J.M.; Cook, G.R.; Balhorn, R.; Bradbury, E.M.; Schmid, C.W. Sequence-specific packaging of DNA in human sperm chromatin. *Science (80-.).* **1987**, *236*, 962 LP – 964.
578. Bench, G.S.; Friz, A.M.; Corzett, M.H.; Morse, D.H.; Balhorn, R. DNA and total protamine masses in individual sperm from fertile mammalian subjects. *Cytometry* **1996**, *23*, 263–271.
579. IRVINE, D.S.; TWIGG, J.P.; GORDON, E.L.; FULTON, N.; MILNE, P.A.; AITKEN, R.J. DNA Integrity in Human Spermatozoa: Relationships With Semen Quality. *J. Androl.* **2000**, *21*, 33–44.
580. Corzett, M.; Mazrimas, J.; Balhorn, R. Protamine 1: Protamine 2 stoichiometry in the sperm of eutherian mammals*. *Mol. Reprod. Dev.* **2002**, *61*, 519–527.
581. Kim, H.-S.; Kang, M.J.; Kim, S.A.; Oh, S.K.; Kim, H.; Ku, S.-Y.; Kim, S.H.; Moon, S.Y.; Choi, Y.M. The utility of sperm DNA damage assay using toluidine blue and aniline blue staining in routine semen analysis. *Clin. Exp. Reprod. Med.* **2013**, *40*, 23–28.
582. Bochenek, M.; Smorąg, Z.; Pilch, J. Sperm chromatin structure assay of bulls qualified for artificial insemination. *Theriogenology* **2001**, *56*, 557–567.
583. Larson, K.L.; DeJonge, C.J.; Barnes, A.M.; Jost, L.K.; Evenson, D.P. Sperm chromatin structure assay parameters as predictors of failed pregnancy following assisted reproductive techniques. *Hum. Reprod.* **2000**, *15*, 1717–1722.
584. Devi, K.R.; Kuruvila, S.; Musa, M.M. Pathological prognostic factors in breast carcinoma. *Saudi Med. J.* **2000**, *21*, 372–375.
585. Fitzgibbons, P.L.; Page, D.L.; Weaver, D.; Thor, A.D.; Allred, D.C.; Clark, G.M.; Ruby, S.G.; O'Malley, F.; Simpson, J.F.; Connolly, J.L.; et al. Prognostic Factors in Breast Cancer: College of American Pathologists Consensus Statement 1999. *Arch. Pathol. Lab. Med.* **2000**, *124*, 966–978.
586. Hamilton, A.; Piccart, M. The contribution of molecular markers to the prediction of response in the treatment of breast cancer: a review of the literature on HER-2, p53 and BCL-2. *Ann. Oncol.* **2000**, *11*, 647–663.
587. Vitucci, C.; Tirelli, C.; Graziano, F.; Santoro, E. Results of conservative surgery for limited-sized infiltrating breast cancer: Analysis of 962 tested patients: 24 years of experience. *J. Surg. Oncol.* **2000**, *74*, 108–115.
588. Goldhirsch, A.; Wood, W.C.; Gelber, R.D.; Coates, A.S.; Thürlimann, B.; Senn, H.-J. Progress and promise: highlights of the international expert consensus on the primary therapy of early breast cancer 2007. *Ann. Oncol.* **2007**, *18*, 1133–1144.
589. Cibula, D.; Slama, J.; Fischerova, D. Update on abdominal radical trachelectomy. *Gynecol. Oncol.* **2008**, *111*, S111–S115.
590. Morice, P.; Denschlag, D.; Rodolakis, A.; Reed, N.; Schneider, A.; Kesic, V.; Colombo, N. Recommendations of the Fertility Task Force of the European Society of Gynecologic Oncology About the Conservative Management of Ovarian Malignant Tumors. *Int. J. Gynecol. Cancer* **2011**, *21*, 951 LP – 963.
591. Wilkinson, E.J.; Teixeira, M.R. Epithelial tumours, squamous tumours. *World Heal. Organ. Classif. Tumours Pathol. Genet. Tumours Breast Female Genit. Organs* **2003**, *270*, 316–320.
592. Morice, P.; Camatte, S.; El Hassan, J.; Pautier, P.; Duvillard, P.; Castaigne, D. Clinical outcomes and fertility after conservative treatment of ovarian borderline tumors. *Fertil. Steril.* **2001**, *75*, 92–96.
593. Charafe-Jauffret, E.; Ginestier, C.; Iovino, F.; Wicinski, J.; Cervera, N.; Finetti, P.; Hur, M.-H.; Diebel, M.E.; Monville, F.; Dutcher, J.; et al. Breast Cancer Cell Lines Contain Functional Cancer Stem Cells with Metastatic Capacity and a Distinct Molecular Signature. *Cancer Res.* **2009**, *69*, 1302 LP – 1313.
594. Leitner, S.P.; Swern, A.S.; Weinberger, D.; Duncan, L.J.; Hutter, R.V.P. Predictors of recurrence for patients with small (one centimeter or less) localized breast cancer (T 1 a,b NO MO). *Cancer* **1995**, *76*,

2266–2274.
595. Baselga, J.; Zambetti, M.; Llombart-Cussac, A.; Manikhas, G.; Kubista, E.; Steger, G.G.; Makhson, A.; Tjulandin, S.; Ludwig, H.; Verrill, M.; et al. Phase II Genomics Study of Ixabepilone as Neoadjuvant Treatment for Breast Cancer. *J. Clin. Oncol.* **2008**, *27*, 526–534.
596. Colleoni, M.; Rotmensz, N.; Peruzzotti, G.; Maisonneuve, P.; Viale, G.; Renne, G.; Casadio, C.; Veronesi, P.; Intra, M.; Torrisi, R.; et al. Minimal and small size invasive breast cancer with no axillary lymph node involvement: the need for tailored adjuvant therapies. *Ann. Oncol.* **2004**, *15*, 1633–1639.
597. Spooner, D.; Morrison, J.M.; Oates, G.; Ellis, D.; Lee, M.J.; Aukland, A.; Grieve, R.; Blunt, R.; Bishop, H.; Jevons, C.; et al. 16. The role of radiotherapy in early breast cancer (stage I). A West Midlands Breast Group prospective randomized collaborative study (BR 3002). *The Breast* **1995**, *4*, 231–232.
598. Fisher, B.; Redmond, C.; Poisson, R.; Margolese, R.; Wolmark, N.; Wickerham, L.; Fisher, E.; Deutsch, M.; Caplan, R.; Pilch, Y.; et al. Eight-Year Results of a Randomized Clinical Trial Comparing Total Mastectomy and Lumpectomy with or without Irradiation in the Treatment of Breast Cancer. *N. Engl. J. Med.* **1989**, *320*, 822–828.
599. McCloud, P. Slide presentation during the 11th International Conference on Primary Therapy of Early Breast Cancer.; St Gallen, Switzerlend, 2009.
600. Rosen, P.P.; Groshen, S.; Saigo, P.E.; Kinne, D.W.; Hellman, S. Pathological prognostic factors in stage I (T1N0M0) and stage II (T1N1M0) breast carcinoma: a study of 644 patients with median follow-up of 18 years. *J. Clin. Oncol.* **1989**, *7*, 1239–1251.
601. Hughes, KS, Schnaper D, B.D. Comparison of lumpectomy plus tamoxifen with and without radiotherapy (RT) in women 70 years of age or older who have clinical stage I estrogen receptor positive (ER+) breast carcinoma. *Proc. Am. Soc. Clin. Oncol* **2001**, *20*.
602. Gonzalez-Angulo, A.M.; Hortobágyi, G.N.; Esteva, F.J. Adjuvant Therapy with Trastuzumab for HER-2/neu-Positive Breast Cancer. *Oncologist* **2006**, *11*, 857–867.
603. Dowsett, M.; Dunbier, A.K. Emerging Biomarkers and New Understanding of Traditional Markers in Personalized Therapy for Breast Cancer. *Clin. Cancer Res.* **2008**, *14*, 8019 LP – 8026.
604. GROUP, E.B.C.T.C. Systemic treatment of early breast cancer by hormonal, cytotoxic, or immune therapy: 133 randomised trials involving 31 000 recurrences and 24 000 deaths among 75 000 women. *Lancet* **1992**, *339*, 1–15.
605. Sun, X.; Sandhu, R.; Figueroa, J.D.; Gierach, G.L.; Sherman, M.E.; Troester, M.A. Benign Breast Tissue Composition in Breast Cancer Patients: Association with Risk Factors, Clinical Variables, and Gene Expression. *Cancer Epidemiol Biomarkers Prev.* **2014**, *23*, 2810 LP – 2818.
606. Hayes, D.F. Prognostic and predictive factors revisited. *The Breast* **2005**, *14*, 493–499.
607. Gershenson, D.M. Clinical management potential tumours of low malignancy. *Best Pract. Res. Clin. Obstet. Gynaecol.* **2002**, *16*, 513–527.
608. Harris, R.; Whittemore, A.S.; Itnyre, J.; Group, the C.O.C. Characteristics Relating to Ovarian Cancer Risk: Collaborative Analysis of 12 US Case-Control Studies: III. Epithelial Tumors of Low Malignant Potential in White Women. *Am. J. Epidemiol.* **1992**, *136*, 1204–1211.
609. Riman, T.; Dickman, P.W.; Nilsson, S.; Correia, N.; Nordlinder, H.; Magnusson, C.M.; Persson, I.R. Risk factors for epithelial borderline ovarian tumors: results of a Swedish case-control study. *Gynecol. Oncol.* **2001**, *83*, 575–585.
610. Winter, W.E. 3rd; Kucera, P.R.; Rodgers, W.; McBroom, J.W.; Olsen, C.; Maxwell, G.L. Surgical staging in patients with ovarian tumors of low malignant potential. *Obstet. Gynecol.* **2002**, *100*, 671–676.
611. Zanetta, G.; Rota, S.; Chiari, S.; Bonazzi, C.; Bratina, G.; Mangioni, C. Behavior of Borderline Tumors With Particular Interest to Persistence, Recurrence, and Progression to Invasive Carcinoma: A Prospective Study. *J. Clin. Oncol.* **2001**, *19*, 2658–2664.
612. Seracchioli, R.; Venturoli, S.; Colombo, F.M.; Govoni, F.; Missiroli, S.; Bagnoli, A. Fertility and tumor recurrence rate after conservative laparoscopic management of young women with early-stage borderline ovarian tumors. *Fertil. Steril.* **2001**, *76*, 999–1004.
613. Chang, H.J.; Han, S.H.; Lee, J.R.; Jee, B.C.; Lee, B.I.; Suh, C.S.; Kim, S.H. Impact of laparoscopic cystectomy on ovarian reserve: serial changes of serum anti-Müllerian hormone levels. *Fertil. Steril.* **2010**, *94*, 343–349.
614. Iwase, A.; Hirokawa, W.; Goto, M.; Takikawa, S.; Nagatomo, Y.; Nakahara, T.; Manabe, S.; Kikkawa, F. Serum anti-Müllerian hormone level is a useful marker for evaluating the impact of laparoscopic cystectomy on ovarian reserve. *Fertil. Steril.* **2010**, *94*, 2846–2849.
615. Doroftei, B.; Mambet, C.; Zlei, M. It's Never over until It's over: How Can Age and Ovarian Reserve Be Mathematically Bound through the Measurement of Serum AMH—A Study of 5069 Romanian Women. *PLoS One* **2015**, *10*, e0125216.
616. Somigliana, E.; Ragni, G.; Benedetti, F.; Borroni, R.; Vegetti, W.; Crosignani, P.G. Does laparoscopic

excision of endometriotic ovarian cysts significantly affect ovarian reserve? Insights from IVF cycles. *Hum. Reprod.* **2003**, *18*, 2450–2453.
617. Ho, H.-Y.; Lee, R.K.-K.; Hwu, Y.-M.; Lin, M.-H.; Su, J.-T.; Tsai, Y.-C. Poor response of ovaries with endometrioma previously treated with cystectomy to controlled ovarian hyperstimulation. *J. Assist. Reprod. Genet.* **2002**, *19*, 507–511.
618. Nicolaiciuc D, Simionescu G, Doroftei B, Anton SC, Bolota M, Ioanid N, A.E. Abdominal radical trachelectomy as a method of preserving fertility in patients with cervical cancer. *Med. Rev. Chir.* **2018**, *122*, 96–101.
619. Kardakis, S. Fertility-Preserving Surgery in Patients with Early Stage Cervical Carcinoma. *ISRN Oncol.* **2012**, *2012*, 817065.
620. Mitildzans, A.; Bazarova, J.; Brikune, J.; Gelderina, E.; Isajevs, S.; Lakutins, J.; Mumdzjans, A.; Rezeberga, D.; Romanovskis, Z.; Vitina, S. First Successful Full Term Pregnancy Outcome in Latvia Following a Radical Trachelectomy for the Patient with a Combined Pathology of a Cervical Cancer and Severe Subfertility. *Acta Chir. Latv.* **2016**, *16*.
621. Outwater, E.K.; Siegelman, E.S.; Hunt, J.L. Ovarian Teratomas: Tumor Types and Imaging Characteristics. *RadioGraphics* **2001**, *21*, 475–490.
622. Stany, M.P.; Hamilton, C.A. Benign Disorders of the Ovary. *Obstet. Gynecol. Clin. North Am.* **2008**, *35*, 271–284.
623. Stein, I.F.; Cohen, M.R. Surgical treatment of bilateral polycystic ovaries—Amenorrhea and sterility. *Am. J. Obstet. Gynecol.* **1939**, *38*, 465–480.
624. Zárate, A.; Hernández-Ayup, S.; Rios-Montiel, A. Treatment of Anovulation in the Stein-Leventhal Syndrome. Analysis of 90 Cases. *Fertil. Steril.* **1971**, *22*, 188–193.
625. Zárate-Treviño A, Hernández-Valencia M, Morán M, Manuel L, S.R. Conveniencia clínica de redefinir al síndrome de poliquistosis ovárica (Stein-Leventhal). *Ginecol Obs. Mex* **2014**, *84*, 246–251.
626. Vieriu-Moţoc, R.; Anton, E.; Ioanid, N. [Laparoscopic approach of the ovarian cyst tumors]. *Rev. Med. Chir. Soc. Med. Nat. Iasi* **2011**, *115*, 401–404.
627. Sandler, M.A.; Karo, J.J. The Spectrum of Ultrasonic Findings in Endometriosis. *Radiology* **1978**, *127*, 229–231.
628. Guerriero, S.; Condous, G.; van den Bosch, T.; Valentin, L.; Leone, F.P.G.; Van Schoubroeck, D.; Exacoustos, C.; Installé, A.J.F.; Martins, W.P.; Abrao, M.S.; et al. Systematic approach to sonographic evaluation of the pelvis in women with suspected endometriosis, including terms, definitions and measurements: a consensus opinion from the International Deep Endometriosis Analysis (IDEA) group. *Ultrasound Obstet. Gynecol.* **2016**, *48*, 318–332.
629. Bazot, M.; Daraï, E. Sonography and MR imaging for the assessment of deep pelvic endometriosis. *J. Minim. Invasive Gynecol.* **2005**, *12*, 178–185.
630. Hudelist, G.; English, J.; Thomas, A.E.; Tinelli, A.; Singer, C.F.; Keckstein, J. Diagnostic accuracy of transvaginal ultrasound for non-invasive diagnosis of bowel endometriosis: systematic review and meta-analysis. *Ultrasound Obstet. Gynecol.* **2011**, *37*, 257–263.
631. Guerriero, S.; Ajossa, S.; Orozco, R.; Perniciano, M.; Jurado, M.; Melis, G.B.; Alcazar, J.L. Accuracy of transvaginal ultrasound for diagnosis of deep endometriosis in the rectosigmoid: systematic review and meta-analysis. *Ultrasound Obstet. Gynecol.* **2016**, *47*, 281–289.
632. Timmerman, D.; Valentin, L.; Bourne, T.H.; Collins, W.P.; Verrelst, H.; Vergote, I. Terms, definitions and measurements to describe the sonographic features of adnexal tumors: a consensus opinion from the International Ovarian Tumor Analysis (IOTA) group. *Ultrasound Obstet. Gynecol.* **2000**, *16*, 500–505.
633. Guerriero, S.; Van Calster, B.; Somigliana, E.; Ajossa, S.; Froyman, W.; De Cock, B.; Coosemans, A.; Fischerová, D.; Van Holsbeke, C.; Alcazar, J.L.; et al. Age-related differences in the sonographic characteristics of endometriomas. *Hum. Reprod.* **2016**, *31*, 1723–1731.
634. Chapron, C.; Pietin-Vialle, C.; Borghese, B.; Davy, C.; Foulot, H.; Chopin, N. Associated ovarian endometrioma is a marker for greater severity of deeply infiltrating endometriosis. *Fertil. Steril.* **2009**, *92*, 453–457.
635. Van den Bosch, T.; Dueholm, M.; Leone, F.P.G.; Valentin, L.; Rasmussen, C.K.; Votino, A.; Van Schoubroeck, D.; Landolfo, C.; Installé, A.J.F.; Guerriero, S.; et al. Terms, definitions and measurements to describe sonographic features of myometrium and uterine masses: a consensus opinion from the Morphological Uterus Sonographic Assessment (MUSA) group. *Ultrasound Obstet. Gynecol.* **2015**, *46*, 284–298.
636. Chapron, C.; Chopin, N.; Borghese, B.; Foulot, H.; Dousset, B.; Vacher-Lavenu, M.C.; Vieira, M.; Hasan, W.; Bricou, A. Deeply infiltrating endometriosis: pathogenetic implications of the anatomical distribution. *Hum. Reprod.* **2006**, *21*, 1839–1845.
637. Guerriero, S.; Ajossa, S.; Minguez, J.A.; Jurado, M.; Mais, V.; Melis, G.B.; Alcazar, J.L. Accuracy of transvaginal ultrasound for diagnosis of deep endometriosis in uterosacral ligaments, rectovaginal

septum, vagina and bladder: systematic review and meta-analysis. *Ultrasound Obstet. Gynecol.* **2015**, *46*, 534–545.
638. Bergqvist, A. Different types of extragenital endometriosis: A review. *Gynecol. Endocrinol.* **1993**, *7*, 207–221.
639. Koger, K.E.; Shatney, C.H.; Hodge, K.; McClenathan, J.H. Surgical scar endometrioma. *Surg. Gynecol. Obstet.* **1993**, *177*, 243–246.
640. Ramdani, A.; Rais, K.; Rockson, O.; Serji, B.; Harroudi, T. Parietal Mass: Two Case Reports of Rare Cesarean Scar Endometriosis. *Cureus* **2020**, *12*.
641. Rezvani, M.; Shaaban, A.; Kennedy, A. The Role of Multimodality Imaging After Cesarean Delivery. *Ultrasound Q.* **2015**, *31*, 5–18.
642. Mkhinini; Kaabia; and Khairi Parietal Endometriosis a Caesarian Section Complication.; 2015.
643. Burney, R.O.; Giudice, L.C. Pathogenesis and pathophysiology of endometriosis. *Fertil. Steril.* **2012**, *98*, 511–519.
644. Rivlin, M.E.; Das, S.K.; Patel, R.B.; Meeks, G.R. Leuprolide acetate in the management of cesarean scar endometriosis. *Obstet. Gynecol.* **1995**, *85*, 838–839.
645. Batioglu, S.; Celikkanat, H.; Ugur, M.; Mollamahmutoglu, L.; Yesilyurt, H.; Kundakci, M. The use of GnRH agonists in the treatment of endometriomas with or without drainage. *J. Pak. Med. Assoc.* **1996**, *46*, 30–32.
646. Takeuchi, H.; Kobori, H.; Kikuchi, I.; Sato, Y.; Mitsuhashi, N. A Prospective Randomized Study Comparing Endocrinological and Clinical Effects of Two Types of GnRH Agonists in Cases of Uterine Leiomyomas or Endometriosis. *J. Obstet. Gynaecol. Res.* **2000**, *26*, 325–331.
647. Rana, N.; Thomas, S.; Rotman, C.; Dmowski, W.P. Decrease in the size of ovarian endometriomas during ovarian suppression in stage IV endometriosis. Role of preoperative medical treatment. *J. Reprod. Med.* **1996**, *41*, 384–392.
648. Agarwal, S.K.; Foster, W.G. Reduction in Endometrioma Size with Three Months of Aromatase Inhibition and Progestin Add-Back. *Biomed Res. Int.* **2015**, *2015*, 878517.
649. Seal, S.L.; Kamilya, G.; Mukherji, J.; De, A.; Ghosh, D.; Majhi, A.K. Aromatase inhibitors in recurrent ovarian endometriomas: report of five cases with literature review. *Fertil. Steril.* **2011**, *95*, 291.e15-291.e18.
650. Ashfaq, S.; Can, A.S. Danazol. In; Treasure Island (FL), 2020.
651. Murji, A.; Biberoğlu, K.; Leng, J.; Mueller, M.D.; Römer, T.; Vignali, M.; Yarmolinskaya, M. Use of dienogest in endometriosis: a narrative literature review and expert commentary. *Curr. Med. Res. Opin.* **2020**, *36*, 895–907.
652. Kavoussi, S.K.; Odenwald, K.C.; As-Sanie, S.; Lebovic, D.I. Incidence of ovarian endometrioma among women with peritoneal endometriosis with and without a history of hormonal contraceptive use. *Eur. J. Obstet. Gynecol. Reprod. Biol.* **2017**, *215*, 220–223.
653. Practice Bulletin No. 114: Management of Endometriosis. *Obstet. Gynecol.* **2010**, *116*.
654. Leyland, N.; Casper, R.; Laberge, P.; Singh, S.S.; Allen, L.; Arendas, K.; Leyland, N.; Allaire, C.; Awadalla, A.; Best, C.; et al. Endometriosis: Diagnosis and Management. *J. Obstet. Gynaecol. Canada* **2010**, *32*, S1–S3.
655. Vercellini, P.; De Matteis, S.; Somigliana, E.; Buggio, L.; Frattaruolo, M.; Fedele, L. Long-term adjuvant therapy for the prevention of postoperative endometrioma recurrence: A systematic review and meta-analysis. *Acta Obstet. Gynecol. Scand.* **2012**, *92*.
656. Takamura, M.; Koga, K.; Osuga, Y.; Takemura, Y.; Hamasaki, K.; Hirota, Y.; Yoshino, O.; Taketani, Y. Post-operative oral contraceptive use reduces the risk of ovarian endometrioma recurrence after laparoscopic excision. *Hum. Reprod.* **2009**, *24*, 3042–3048.
657. Seracchioli, R.; Mabrouk, M.; Frascà, C.; Manuzzi, L.; Montanari, G.; Keramyda, A.; Venturoli, S. Long-term cyclic and continuous oral contraceptive therapy and endometrioma recurrence: a randomized controlled trial. *Fertil. Steril.* **2010**, *93*, 52–56.
658. Vercellini, P.; Somigliana, E.; Viganò, P.; De Matteis, S.; Barbara, G.; Fedele, L. Post-operative endometriosis recurrence: a plea for prevention based on pathogenetic, epidemiological and clinical evidence. *Reprod. Biomed. Online* **2010**, *21*, 259–265.
659. Muneyyirci-Delale, O.; Anopa, J.; Charles, C.; Mathur, D.; Parris, R.; Cutler, J.B.; Salame, G.; Abulafia, O. Medical management of recurrent endometrioma with long-term norethindrone acetate. *Int. J. Womens. Health* **2012**, *4*, 149–154.
660. Bozkurt, M.; Çil, A.S.; Bozkurt, D.K. Intramuscular abdominal wall endometriosis treated by ultrasound-guided ethanol injection. *Clin. Med. Res.* **2014**, *12*, 160–165.
661. Bektaş, H.; Bilsel, Y.; Sarı, Y.S.; Ersöz, F.; Koç, O.; Deniz, M.; Boran, B.; Huq, G.E. Abdominal Wall Endometrioma; A 10-Year Experience and Brief Review of the Literature. *J. Surg. Res.* **2010**, *164*, e77–e81.

662. Rehmer, J.M.; Flyckt, R.L.; Goodman, L.R.; Falcone, T. Management of Endometriomas. *Obstet. Gynecol. Surv.* **2019**, *74*, 232–240.
663. Hsu, A.L.; Khachikyan, I.; Stratton, P. Invasive and noninvasive methods for the diagnosis of endometriosis. *Clin. Obstet. Gynecol.* **2010**, *53*, 413–419.
664. Scardapane, A.; Lorusso, F.; Scioscia, M.; Ferrante, A.; Stabile Ianora, A.A.; Angelelli, G. Standard high-resolution pelvic MRI vs. low-resolution pelvic MRI in the evaluation of deep infiltrating endometriosis. *Eur. Radiol.* **2014**, *24*, 2590–2596.
665. Bermot, C.; Labauge, P.; Limot, O.; Louboutin, A.; Fauconnier, A.; Huchon, C. Performance of MRI for the detection of anterior pelvic endometriotic lesions. *J. Gynecol. Obstet. Hum. Reprod.* **2018**, *47*, 499–503.
666. Burkett, B.J.; Cope, A.; Bartlett, D.J.; Burnett, T.L.; Jones, T.; Venkatesh, S.K.; VanBuren, W.M. MRI impacts endometriosis management in the setting of image-based multidisciplinary conference: a retrospective analysis. *Abdom. Radiol.* **2020**, *45*, 1829–1839.
667. Yap, S.Z.L.; Leathersich, S.; Lu, J.; Fender, L.; Lo, G. Pelvic MRI staging of endometriosis at 3 T without patient preparation or anti-peristaltic: Diagnostic performance outcomes. *Eur. J. Radiol.* **2018**, *105*, 72–80.
668. Bazot, M.; Jarboui, L.; Ballester, M.; Touboul, C.; Thomassin-Naggara, I.; Daraï, E. The value of MRI in assessing parametrial involvement in endometriosis. *Hum. Reprod.* **2012**, *27*, 2352–2358.
669. Valentini, A.L.; Gui, B.; Miccò, M.; Mingote, M.C.; Ninivaggi, V.; Guido, M.; Zannoni, G.F.; Marrucci, E.; Bonomo, L. How to improve MRI accuracy in detecting deep infiltrating colorectal endometriosis: MRI findings vs. laparoscopy and histopathology. *Radiol. Med.* **2014**, *119*, 291–297.
670. Sengul, I.; Sengul, D.; Kahyaoglu, S.; Kahyaoglu, I. Incisional endometriosis: a report of 3 cases. *Can. J. Surg.* **2009**, *52*, 444–445.
671. Bujold, E. The optimal uterine closure technique during cesarean. *N. Am. J. Med. Sci.* **2012**, *4*, 362–363.
672. March, C.M. Management of Asherman's syndrome. *Reprod. Biomed. Online* **2011**, *23*, 63–76.
673. Fayez, J.A.; Mutie, G.; Schneider, P.J. The diagnostic value of hysterosalpingography and hysteroscopy in infertility investigation. *Am. J. Obstet. Gynecol.* **1987**, *156*, 558–560.
674. Raziel, A.; Arieli, S.; Bukovsky, I.; Caspi, E.; Golan, A. Investigation of the uterine cavity in recurrent aborters. *Fertil. Steril.* **1994**, *62*, 1080–1082.
675. Soares, S.R.; dos Reis, M.M.B.B.; Camargos, A.F. Diagnostic accuracy of sonohysterography, transvaginal sonography, and hysterosalpingography in patients with uterine cavity diseases. *Fertil. Steril.* **2000**, *73*, 406–411.
676. Seshadri, S.; El-Toukhy, T.; Douiri, A.; Jayaprakasan, K.; Khalaf, Y. Diagnostic accuracy of saline infusion sonography in the evaluation of uterine cavity abnormalities prior to assisted reproductive techniques: a systematic review and meta-analyses. *Hum. Reprod. Update* **2014**, *21*, 262–274.
677. Acholonu, U.C.; Silberzweig, J.; Stein, D.E.; Keltz, M. Hysterosalpingography versus sonohysterography for intrauterine abnormalities. *JSLS J. Soc. Laparoendosc. Surg.* **2011**, *15*, 471–474.
678. Sylvestre, C.; Child, T.J.; Tulandi, T.; Tan, S.L. A prospective study to evaluate the efficacy of two- and three-dimensional sonohysterography in women with intrauterine lesions. *Fertil. Steril.* **2003**, *79*, 1222–1225.
679. Confino, E.; Friberg, J.; Giglia, R. V; Gleicher, N. Sonographic imaging of intrauterine adhesions. *Obstet. Gynecol.* **1985**, *66*, 596–598.
680. Schlaff, W.D.; Hurst, B.S. Preoperative sonographic measurement of endometrial pattern predicts outcome of surgical repair in patients with severe Asherman's syndrome*. *Fertil. Steril.* **1995**, *63*, 410–413.
681. Salle, B.; Gaucherand, P.; de Saint Hilaire, P.; Rudigoz, R.C. Transvaginal sonohysterographic evaluation of intrauterine adhesions. *J. Clin. Ultrasound* **1999**, *27*, 131–134.
682. Lo, S.; Ramsay, P.; Pierson, R.; Manconi, F.; Munro, M.; Fraser, I. Endometrial thickness measured by ultrasound scan in women with uterine outlet obstruction due to intrauterine or upper cervical adhesions. *Hum. Reprod.* **2008**, *23*, 306–309.
683. Kresowik, J.D.; Syrop, C.H.; Van Voorhis, B.J.; Ryan, G.L. Ultrasound is the optimal choice for guidance in difficult hysteroscopy. *Ultrasound Obstet. Gynecol.* **2012**, *39*, 715–718.
684. Pal, A.; Babinszki, A.; Vajda, G.; Kovacs, L. Diagnosis of Asherman's syndrome with three-dimensional ultrasound. *Ultrasound Obstet. Gynecol.* **2000**, *15*, 341–343.
685. Makris, N.; Kalmantis, K.; Skartados, N.; Papadimitriou, A.; Mantzaris, G.; Antsaklis, A. Three-dimensional hysterosonography versus hysteroscopy for the detection of intracavitary uterine abnormalities. *Int. J. Gynecol. Obstet.* **2007**, *97*, 6–9.
686. Abou-Salem, N.; El-Mazny, A.; Sherbiny, W. Value of 3-Dimensional Sonohysterography for Detection of Intrauterine Lesions in Women with Abnormal Uterine Bleeding. *J. Minim. Invasive Gynecol.* **2010**, *17*, 200–204.

687. Kim, M.J.; Lee, Y.; Lee, C.; Chun, S.; Kim, A.; Kim, H.Y.; Lee, J.Y. Accuracy of three dimensional ultrasound and treatment outcomes of intrauterine adhesion in infertile women. *Taiwan. J. Obstet. Gynecol.* **2015**, *54*, 737–741.
688. Yu, D.; Wong, Y.-M.; Cheong, Y.; Xia, E.; Li, T.-C. Asherman syndrome--one century later. *Fertil. Steril.* **2008**, *89*, 759–779.
689. Dreisler, E.; Kjer, J.J. Asherman's syndrome: current perspectives on diagnosis and management. *Int. J. Womens. Health* **2019**, *11*, 191–198.
690. Tesarik, J.; Mendoza-Tesarik, R.; Mendoza, N. Virtual ultrasonographic hysteroscopy followed by conventional operative hysteroscopy, enabling pregnancy. *Am. J. Obstet. Gynecol.* **2017**, *216*, 188.e1.
691. Harton, G.L.; Magli, M.C.; Lundin, K.; Montag, M.; Lemmen, J.; Harper, J.C. ESHRE PGD Consortium/Embryology Special Interest Group—best practice guidelines for polar body and embryo biopsy for preimplantation genetic diagnosis/screening (PGD/PGS)†. *Hum. Reprod.* **2010**, *26*, 41–46.
692. Kuliev, A.; Verlinsky, O.; Rechitsky, S. Safety, Accuracy and Reproductive Outcome of Preimplantation Genetic Diagnosis. *J. Fertil. Vitr. - IVF-Worldwide, Reprod. Med. Genet. Stem Cell Biol.* **2013**, *01*.
693. Stern, H.J. Preimplantation Genetic Diagnosis: Prenatal Testing for Embryos Finally Achieving Its Potential. *J. Clin. Med.* **2014**, *3*, 280–309.
694. Anton, E.; Doroftei, B.; Lupaşcu, I.A.; Socolov, D.; Ioanid, N. Preimplantation genetic diagnosis. Legal, ethical and medical implications in Romania. *Rev. Rom. Bioet.* **2009**, *7*, 45-51+113.
695. Grünewald, S.; Matthijs, G.; Jaeken, J. Congenital Disorders of Glycosylation: A Review. *Pediatr. Res.* **2002**, *52*, 618–624.
696. Freeze, H.H.; Eklund, E. Chapter 17 - Introduction to Human Glycosylation Disorders. In; Cummings, R.D., Pierce, J.M.B.T.-H. of G., Eds.; Academic Press: San Diego, 2010; pp. 431–464 ISBN 978-0-12-373600-0.
697. Jaeken, J.; Vanderschueren-Lodeweyckx, M.; Casaer, P.; Snoeck, L.; Corbeel, L.; Eggermont, E.; Eeckels, R. Familial psychomotor retardation with markedly fluctuating serum prolactin, FSH and GH levels, partial TBG-deficiency, increased serum arylsulphatase A and increased CSF protein: a new syndrome?: 90. *Pediatr. Res.* **1980**, *14*, 179.
698. Ganetzky, R.; Reynoso, F.J.; He, M. Chapter 15 - Congenital disorders of glycosylation. In; Garg, U., Smith, L.D.B.T.-B. in I.E. of M., Eds.; Elsevier: San Diego, 2017; pp. 343–360 ISBN 978-0-12-802896-4.
699. Jaeken, J. Glycosylation and its Disorders: General Overview. In *Reference Module in Biomedical Sciences*; 2016 ISBN 9780128012383.
700. Scott, K.; Gadomski, T.; Kozicz, T.; Morava, E. Congenital disorders of glycosylation: new defects and still counting. *J. Inherit. Metab. Dis.* **2014**, *37*, 609–617.
701. Phosphomannomutase deficiency is a cause of carbohydrate-deficient glycoprotein syndrome type I. *FEBS Lett.* **1995**, *377*, 318–320.
702. Goreta, S.S.; Dabelic, S.; Dumic, J. Insights into complexity of congenital disorders of glycosylation. *Biochem. medica* **2012**, *22*, 156–170.
703. Ohtsubo, K.; Marth, J.D. Glycosylation in Cellular Mechanisms of Health and Disease. *Cell* **2006**, *126*, 855–867.
704. Vega, A.I.; Pérez-Cerdá, C.; Abia, D.; Gámez, A.; Briones, P.; Artuch, R.; Desviat, L.R.; Ugarte, M.; Pérez, B. Expression analysis revealing destabilizing mutations in phosphomannomutase 2 deficiency (PMM2-CDG). *J. Inherit. Metab. Dis.* **2011**, *34*, 929–939.
705. Haeuptle, M.A.; Hennet, T. Congenital disorders of glycosylation: an update on defects affecting the biosynthesis of dolichol-linked oligosaccharides. *Hum. Mutat.* **2009**, *30*, 1628–1641.
706. Jaeken, J. Congenital disorders of glycosylation. *Ann. N. Y. Acad. Sci.* **2010**, *1214*, 190–198.
707. Erlandson, A.; Bjursell, C.; Stibler, H.; Kristiansson, B.; Wahlström, J.; Martinsson, T. Scandinavian CDG-Ia patients: genotype/phenotype correlation and geographic origin of founder mutations. *Hum. Genet.* **2001**, *108*, 359–367.
708. Imtiaz, F.; Worthington, V.; Champion, M.; Beesley, C.; Charlwood, J.; Clayton, P.; Keir, G.; Mian, N.; Winchester, B. Genotypes and phenotypes of patients in the UK with carbohydrate-deficient glycoprotein syndrome type 1. *J. Inherit. Metab. Dis.* **2000**, *23*, 162–174.
709. Le Bizec, C.; Vuillaumier-Barrot, S.; Barnier, A.; Dupré, T.; Durand, G.; Seta, N. A new insight into PMM2 mutations in the French population. *Hum. Mutat.* **2005**, *25*, 504–505.
710. Enns, G.M.; Steiner, R.D.; Buist, N.; Cowan, C.; Leppig, K.A.; McCracken, M.F.; Westphal, V.; Freeze, H.H.; O'Brien, J.F.; Jaeken, J.; et al. Clinical and molecular features of congenital disorder of glycosylation in patients with type 1 sialotransferrin pattern and diverse ethnic origins. *J. Pediatr.* **2002**, *141*, 695–700.
711. Ohno, K.; Yuasa, I.; Akaboshi, S.; Itoh, M.; Yoshida, K.; Ehara, H.; Ochiai, Y.; Takeshita, K. The

carbohydrate deficient glycoprotein syndrome in three Japanese children. *Brain Dev.* **1992**, *14*, 30–35..
712. Briones, P.; Vilaseca, M.A.; Schollen, E.; Ferrer, I.; Maties, M.; Busquets, C.; Artuch, R.; Gort, L.; Marco, M.; van Schaftingen, E.; et al. Biochemical and molecular studies in 26 Spanish patients with congenital disorder of glycosylation type Ia. *J. Inherit. Metab. Dis.* **2003**, *25*, 635–646.
713. de Lonlay, P.; Seta, N.; Barrot, S.; Chabrol, B.; Drouin, V.; Gabriel, B.M.; Journel, H.; Kretz, M.; Laurent, J.; Le Merrer, M.; et al. A broad spectrum of clinical presentations in congenital disorders of glycosylation I: a series of 26 cases. *J. Med. Genet.* **2001**, *38*, 14–19.
714. Pérez-Dueñas, B.; García-Cazorla, A.; Pineda, M.; Poo, P.; Campistol, J.; Cusí, V.; Schollen, E.; Matthijs, G.; Grunewald, S.; Briones, P.; et al. Long-term evolution of eight Spanish patients with CDG type Ia: Typical and atypical manifestations. *Eur. J. Paediatr. Neurol.* **2009**, *13*, 444–451.
715. Monin, M.-L.; Mignot, C.; De Lonlay, P.; Héron, B.; Masurel, A.; Mathieu-Dramard, M.; Lenaerts, C.; Thauvin, C.; Gérard, M.; Roze, E.; et al. 29 French adult patients with PMM2-congenital disorder of glycosylation: outcome of the classical pediatric phenotype and depiction of a late-onset phenotype. *Orphanet J. Rare Dis.* **2014**, *9*, 207.
716. Vals, M.-A.; Pajusalu, S.; Kals, M.; Mägi, R.; Õunap, K. The Prevalence of PMM2-CDG in Estonia Based on Population Carrier Frequencies and Diagnosed Patients. *JIMD Rep.* **2018**, *39*, 13–17.
717. Krasnewich, D.; O'Brien, K.; Sparks, S. Clinical features in adults with congenital disorders of glycosylation type Ia (CDG-Ia). *Am. J. Med. Genet. Part C Semin. Med. Genet.* **2007**, *145C*, 302–306.
718. Stefanits, H.; Konstantopoulou, V.; Kuess, M.; Milenkovic, I.; Matula, C. Initial diagnosis of the congenital disorder of glycosylation PMM2-CDG (CDG1a) in a 4-year-old girl after neurosurgical intervention for cerebral hemorrhage. *J. Neurosurg. Pediatr. PED* **2014**, *14*, 546–549.
719. Miossec-Chauvet, E.; Mikaeloff, Y.; Heron, D.; Merzoug, V.; Cormier-Daire, V.; Lonlay, P.; Matthijs, G.; Hulle, C.; Ponsot, G.; Seta, N. Neurological Presentation in Pediatric Patients with Congenital Disorders of Glycosylation Type Ia. *Neuropediatrics* **2003**, *34*, 1–6.
720. McKenzie, F.A.; Fietz, M.; Fletcher, J.; Smith, R.L.L.; Wright, I.M.R.; Jaeken, J. A previously undescribed form of congenital disorder of glycosylation with variable presentation in siblings: Early fetal loss with hydrops fetalis, and infant death with hypoproteinemia. *Am. J. Med. Genet. Part A* **2007**, *143A*, 2029–2034.
721. Wolthuis, D.F.G.J.; Janssen, M.C.; Cassiman, D.; Lefeber, D.J.; Morava-Kozicz, E. Defining the phenotype and diagnostic considerations in adults with congenital disorders of N-linked glycosylation. *Expert Rev. Mol. Diagn.* **2014**, *14*, 217–224.
722. Stibler, H.; Blennow, G.; Kristiansson, B.; Lindehammer, H.; Hagberg, B. Carbohydrate-deficient glycoprotein syndrome: clinical expression in adults with a new metabolic disease. *J. Neurol. Neurosurg. Psychiatry* **1994**, *57*, 552–556.
723. Kjaergaard, S.; Schwartz, M.; Skovby, F. Congenital disorder of glycosylation type Ia (CDG-Ia): phenotypic spectrum of the R141H/F119L genotype. *Arch. Dis. Child.* **2001**, *85*, 236–239.
724. Coman, D.; McGill, J.; MacDonald, R.; Morris, D.; Klingberg, S.; Jaeken, J.; Appleton, D. Congenital disorder of glycosylation type 1a: Three siblings with a mild neurological phenotype. *J. Clin. Neurosci.* **2007**, *14*, 668–672.
725. Parveen, Z.; Tongson-Ignacio, J.E.; Fraser, C.R.; Killeen, J.L.; Thompson, K.S. Placental Mesenchymal Dysplasia. *Arch. Pathol. Lab. Med.* **2007**, *131*, 131–137.
726. Moscoso, G.; Jauniaux, E.; Hustin, J. Placental Vascular Anomaly with Diffuse Mesenchymal Stei Villuos Hyperplasia: A New Clinico-Pathological Entity? *Pathol. - Res. Pract.* **1991**, *187*, 324–328.
727. Arizawa, M.; Nakayama, M. Suspected involvement of the X chromosome in placental mesenchymal dysplasia. *Congenit. Anom. (Kyoto).* **2002**, *42*, 309–317.
728. Lage, J.M. Placentomegaly with massive hydrops of placental stem villi, diploid DNA content, and fetal omphaloceles: Possible association with Beckwith-Wiedemann syndrome. *Hum. Pathol.* **1991**, *22*, 591–597.
729. Paradinas, F.J.; Sebire, N.J.; Fisher, R.A.; Rees, H.C.; Foskett, M.; Seckl, M.J.; Newlands, E.S. Pseudo-partial moles: placental stem vessel hydrops and the association with Beckwith–Wiedemann syndrome and complete moles. *Histopathology* **2001**, *39*, 447–454.
730. Jauniaux, E.; Nicolaides, K.H.; Hustin, J. Perinatal features associated with placental mesenchymal dysplasia. *Placenta* **1997**, *18*, 701–706.
731. Werner, M.; Reh, A.; Grifo, J.; Perle, M.A. Characteristics of chromosomal abnormalities diagnosed after spontaneous abortions in an infertile population. *J. Assist. Reprod. Genet.* **2012**, *29*, 817–820.
732. Hardy, K.; Hardy, P.J. 1(st) trimester miscarriage: four decades of study. *Transl. Pediatr.* **2015**, *4*, 189–200.
733. Choi, B.H.; Kim, U.H.; Lee, K.S.; Ko, C.W. Various endocrine disorders in children with t(13;14)(q10;q10) Robertsonian translocation. *Ann Pediatr Endocrinol Metab* **2013**, *18*, 111–115.
734. Kar, B.; Sivamani, S.; Kundavi, S.; Varma, T.R. The Importance of Cytogenetics and Associated

Molecular Techniques in the Management of Patients Carrying Robertsonian Translocation and Their Pregnancy Outcome by Intracytoplasmic Sperm Injection. *J. Obstet. Gynaecol. India* **2018**, *68*, 93–97.
735. Colaco, S.; Modi, D. Genetics of the human Y chromosome and its association with male infertility. *Reprod. Biol. Endocrinol.* **2018**, *16*, 14.
736. Mierla, D.; Jardan, D.; Stoian, V. Chromosomal abnormality in men with impaired spermatogenesis. *Int. J. Fertil. Steril.* **2014**, *8*, 35–42.
737. Singh, R.; Kaleem, A.M.; Narayana, S.S.; Mahdi, A.A. A case of oligoasthenoteratozoospermia with AZFc deletion and persistent oxidative stress. *Indian J. Hum. Genet.* **2012**, *18*, 359–362.
738. Rozen, S.G.; Marszalek, J.D.; Irenze, K.; Skaletsky, H.; Brown, L.G.; Oates, R.D.; Silber, S.J.; Ardlie, K.; Page, D.C. AZFc deletions and spermatogenic failure: a population-based survey of 20,000 Y chromosomes. *Am. J. Hum. Genet.* **2012**, *91*, 890–896.
739. Girardi, S.K.; Mielnik, A.; Schlegel, P.N. Submicroscopic deletions in the Y chromosome of infertile men. *Hum. Reprod.* **1997**, *12*, 1635–1641.
740. Kremer, J.A.; Tuerlings, J.H.; Meuleman, E.J.; Schoute, F.; Mariman, E.; Smeets, D.F.; Hoefsloot, L.H.; Braat, D.D.; Merkus, H.M. Microdeletions of the Y chromosome and intracytoplasmic sperm injection: from gene to clinic. *Hum. Reprod.* **1997**, *12*, 687–691.
741. Liu, X.; Qiao, J.; Li, R.; Yan, L.; Chen, L. Y chromosome AZFc microdeletion may not affect the outcomes of ICSI for infertile males with fresh ejaculated sperm. *J. Assist. Reprod. Genet.* **2013**, *30*, 813–819.
742. Souza Setti, A.; Borges Junior, E. Response: Gender incidence of intracytoplasmic morphologically selected sperm injection-derived embryos: A prospective randomized study. *Reprod. Biomed. Online* **2012**, *25*, 334.
743. Franco Jr., J.G.; Pedroso, D.C.C.; Mauri, A.L.; Petersen, C.G.; Baruffi, R.; Oliveira, J.B.A. The effect of intracytoplasmic morphologically selected sperm injection (IMSI) procedure on human sex ratio. *Fertil. Steril.* **2013**, *100*, S461–S462.
744. Bortot, B.; Cosentini, D.; Faletra, F.; Biffi, S.; De Martino, E.; Carrozzi, M.; Severini, G.M. PMM2-CDG: Phenotype and genotype in four affected family members. *Gene* **2013**, *531*, 506–509.
745. Grünewald, S. The clinical spectrum of phosphomannomutase 2 deficiency (CDG-Ia). *Biochim. Biophys. Acta - Mol. Basis Dis.* **2009**, *1792*, 827–834.
746. Grünewald, S.; Schollen, E.; Van Schaftingen, E.; Jaeken, J.; Matthijs, G. High residual activity of PMM2 in patients' fibroblasts: possible pitfall in the diagnosis of CDG-Ia (phosphomannomutase deficiency). *Am. J. Hum. Genet.* **2001**, *68*, 347–354.
747. Citro, V.; Cimmaruta, C.; Monticelli, M.; Riccio, G.; Hay Mele, B.; Cubellis, M.V.; Andreotti, G. The Analysis of Variants in the General Population Reveals That PMM2 Is Extremely Tolerant to Missense Mutations and That Diagnosis of PMM2-CDG Can Benefit from the Identification of Modifiers. *Int. J. Mol. Sci.* **2018**, *19*, 2218.
748. Thirumal Kumar, D.; Jain, N.; Udhaya Kumar, S.; George Priya Doss, C.; Zayed, H. Identification of potential inhibitors against pathogenic missense mutations of PMM2 using a structure-based virtual screening approach. *J. Biomol. Struct. Dyn.* **2019**, 1–17.
749. Casado, M.; O'Callaghan, M.M.; Montero, R.; Pérez-Cerda, C.; Pérez, B.; Briones, P.; Quintana, E.; Muchart, J.; Aracil, A.; Pineda, M.; et al. Mild Clinical and Biochemical Phenotype in Two Patients with PMM2-CDG (Congenital Disorder of Glycosylation Ia). *The Cerebellum* **2012**, *11*, 557–563.
750. Jaeken, J.; Lefeber, D.; Matthijs, G. Clinical utility gene card for: Phosphomannomutase 2 deficiency. *Eur. J. Hum. Genet.* **2014**, *22*.
751. de Koning, T.J.; Toet, M.; Dorland, L.; de Vries, L.S.; van den Berg, I.E.T.; Duran, M.; Poll-The, B.T. Recurrent nonimmune hydrops fetalis associated with carbohydrate-deficient glycoprotein syndrome. *J. Inherit. Metab. Dis.* **1998**, *21*, 681–682.
752. Schwarz, M.; Thiel, C.; Lübbehusen, J.; Dorland, B.; de Koning, T.; von Figura, K.; Lehle, L.; Körner, C. Deficiency of GDP-Man:GlcNAc2-PP-dolichol mannosyltransferase causes congenital disorder of glycosylation type Ik. *Am. J. Hum. Genet.* **2004**, *74*, 472–481.
753. Vesela, K.; Honzik, T.; Hansikova, H.; Haeuptle, M.A.; Semberova, J.; Stranak, Z.; Hennet, T.; Zeman, J. A new case of ALG8 deficiency (CDG Ih). *J. Inherit. Metab. Dis.* **2009**, *32*, 259–264.
754. Aronica, E.; van Kempen, A.A.M.W.; van der Heide, M.; Poll-The, B.T.; van Slooten, H.J.; Troost, D.; Rozemuller-Kwakkel, J.M. Congenital disorder of glycosylation type Ia: a clinicopathological report of a newborn infant with cerebellar pathology. *Acta Neuropathol.* **2005**, *109*, 433–442.
755. Noelle, V.; Knuepfer, M.; Pulzer, F.; Schuster, V.; Siekmeyer, W.; Matthijs, G.; Vogtmann, C. Unusual presentation of congenital disorder of glycosylation type 1a: congenital persistent thrombocytopenia, hypertrophic cardiomyopathy and hydrops-like aspect due to marked peripheral oedema. *Eur. J. Pediatr.* **2005**, *164*, 223–226.
756. van de Kamp, J.M.; Lefeber, D.J.; Ruijter, G.J.G.; Steggerda, S.J.; den Hollander, N.S.; Willems, S.M.;

Matthijs, G.; Poorthuis, B.J.H.M.; Wevers, R.A. Congenital disorder of glycosylation type Ia presenting with hydrops fetalis. *J. Med. Genet.* **2007**, *44*, 277–280.
757. Wurm, D.; Löffler, G.; Lindinger, A.; Gortner, L. Congenital disorders of glycosylation type Ia as a cause of mirror syndrome. *J. Perinatol.* **2007**, *27*, 802–804.
758. Truin, G.; Guillard, M.; Lefeber, D.J.; Sykut-Cegielska, J.; Adamowicz, M.; Hoppenreijs, E.; Sengers, R.C.A.; Wevers, R.A.; Morava, E. Pericardial and abdominal fluid accumulation in Congenital Disorder of Glycosylation type Ia. *Mol. Genet. Metab.* **2008**, *94*, 481–484.
759. Schollen, E.; Kjaergaard, S.; Martinsson, T.; Vuillaumier-Barrot, S.; Dunoe, M.; Keldermans, L.; Seta, N.; Matthijs, G. Increased recurrence risk in congenital disorders of glycosylation type Ia (CDG-Ia) due to a transmission ratio distortion. *J. Med. Genet.* **2004**, *41*, 877 LP – 880.
760. McAllister, M.; Moldovan, R.; Paneque, M.; Skirton, H. The need to develop an evidence base for genetic counselling in Europe. *Eur. J. Hum. Genet.* **2016**, *24*, 504–505.
761. Nahman, M. Romanian IVF: A brief history through the 'lens' of labour, migration and global egg donation markets. *Reprod. Biomed. Soc. Online* **2016**, *2*.
762. Chen, C.-P.; Chern, S.-R.; Wang, T.-Y.; Huang, Z.-D.; Huang, M.-C.; Chuang, C.-Y. Case Report: Pregnancy with concomitant chorangioma and placental vascular malformation with mesenchymal hyperplasia. *Hum. Reprod.* **1997**, *12*, 2553–2556.
763. Pham, T.; Steele, J.; Stayboldt, C.; Chan, L.; Benirschke, K. Placental Mesenchymal Dysplasia Is Associated With High Rates of Intrauterine Growth Restriction and Fetal Demise: A Report of 11 New Cases and a Review of the Literature. *Am. J. Clin. Pathol.* **2006**, *126*, 67–78.
764. Kaiser-Rogers, K.A.; McFadden, D.E.; Livasy, C.A.; Dansereau, J.; Jiang, R.; Knops, J.F.; Lefebvre, L.; Rao, K.W.; Robinson, W.P. Androgenetic/biparental mosaicism causes placental mesenchymal dysplasia. *J. Med. Genet.* **2006**, *43*, 187–192.
765. Ohira, S.; Ookubo, N.; Tanaka, K.; Takatsu, A.; Kobara, H.; Kikuchi, N.; Ohya, A.; Kanai, M.; Shiozawa, T. Placental Mesenchymal Dysplasia: Chronological Observation of Placental Images during Gestation and Review of the Literature. *Gynecol. Obstet. Invest.* **2013**, *75*, 217–223.
766. Faye-Petersen, O.M.; Kapur, R.P. Placental Mesenchymal Dysplasia. *Surg. Pathol. Clin.* **2013**, *6*, 127–151.
767. Cohen, M.C.; Roper, E.C.; Sebire, N.J.; Stanek, J.; Anumba, D.O.C. Placental mesenchymal dysplasia associated with fetal aneuploidy. *Prenat. Diagn.* **2005**, *25*, 187–192.
768. Mittal, D.; Anand, R.; Sisodia, N.; Singh, S.; Biswas, R. Placental mesenchymal dysplasia: What every radiologist needs to know. *Indian J. Radiol. Imaging* **2017**, *27*, 62–64.
769. ZHU, J.; King, D. Natal and neonatal teeth. *J. Dent. Child.* **1995**, *62*, 123–128.
770. Basile, N.; Nogales, M. del C.; Bronet, F.; Florensa, M.; Riqueiros, M.; Rodrigo, L.; García-Velasco, J.; Meseguer, M. Increasing the probability of selecting chromosomally normal embryos by time-lapse morphokinetics analysis. *Fertil. Steril.* **2014**, *101*, 699-704.e1.
771. Zidi-Jrah, I.; Hajlaoui, A.; Mougou-Zerelli, S.; Kammoun, M.; Meniaoui, I.; Sallem, A.; Brahem, S.; Fekih, M.; Bibi, M.; Saad, A.; et al. Relationship between sperm aneuploidy, sperm DNA integrity, chromatin packaging, traditional semen parameters, and recurrent pregnancy loss. *Fertil. Steril.* **2016**, *105*, 58–64.
772. Moraru, E.; Diaconu, R.; Anton, E.; Bozomitu, L.; Carmen, A.; Alin, C.; Timofte, D.; Oprisa, C.; Azoicăi, A. Understanding the relevance of pain, depression and anxiety-like manifestations in the management of cystic fibrosis. *Arch. Biol. Sci.* **2015**, *67*, 71.
773. RPL, T.E.G.G. on; Bender Atik, R.; Christiansen, O.B.; Elson, J.; Kolte, A.M.; Lewis, S.; Middeldorp, S.; Nelen, W.; Peramo, B.; Quenby, S.; et al. ESHRE guideline: recurrent pregnancy loss. *Hum. Reprod. Open* **2018**, *2018*.
774. Ikuma, S.; Sato, T.; Sugiura-Ogasawara, M.; Nagayoshi, M.; Tanaka, A.; Takeda, S. Preimplantation Genetic Diagnosis and Natural Conception: A Comparison of Live Birth Rates in Patients with Recurrent Pregnancy Loss Associated with Translocation. *PLoS One* **2015**, *10*, e0129958.
775. Wong, C.; Chen, A.A.; Behr, B.; Shen, S. Time-lapse microscopy and image analysis in basic and clinical embryo development research. *Reprod. Biomed. Online* **2013**, *26*, 120–129.
776. Simionescu, G.; Maftei, R.; Anton, E.; Valeanu, S.; Doroftei, B. TIME-LAPSE MICROSCOPY ROLE IN IMPROVING THE OUTCOME OF IVF/ICSI CYCLES BY MONITORING AND SELECTION OF EARLY EMBRYO. *Manag. Intercult.* **2016**, 345–349.
777. Rubio, I.; Galán, A.; Larreategui, Z.; Ayerdi, F.; Bellver, J.; Herrero, J.; Meseguer, M. Clinical validation of embryo culture and selection by morphokinetic analysis: a randomized, controlled trial of the EmbryoScope. *Fertil. Steril.* **2014**, *102*, 1287-1294.e5.
778. Chawla, M.; Fakih, M.; Shunnar, A.; Bayram, A.; Hellani, A.; Perumal, V.; Divakaran, J.; Budak, E. Morphokinetic analysis of cleavage stage embryos and its relationship to aneuploidy in a retrospective time-lapse imaging study. *J. Assist. Reprod. Genet.* **2015**, *32*, 69–75.

779. Del Carmen Nogales, M.; Bronet, F.; Basile, N.; Martínez, E.M.; Liñán, A.; Rodrigo, L.; Meseguer, M. Type of chromosome abnormality affects embryo morphology dynamics. *Fertil. Steril.* **2017**, *107*, 229-235.e2.
780. Yang, Z.; Zhang, J.; Salem, S.A.; Liu, X.; Kuang, Y.; Salem, R.D.; Liu, J. Selection of competent blastocysts for transfer by combining time-lapse monitoring and array CGH testing for patients undergoing preimplantation genetic screening: a prospective study with sibling oocytes. *BMC Med. Genomics* **2014**, *7*, 38.
781. Patel, D.; Shah, P.; Kotdawala, A.; Herrero, J.; Rubio, I.; Banker, M. Morphokinetic behavior of euploid and aneuploid embryos analyzed by time-lapse in embryoscope. *J. Hum. Reprod. Sci.* **2016**, *9*, 112–118.
782. Pribenszky, C.; Nilselid, A.-M.; Montag, M. Time-lapse culture with morphokinetic embryo selection improves pregnancy and live birth chances and reduces early pregnancy loss: a meta-analysis. *Reprod. Biomed. Online* **2017**, *35*, 511–520.
783. Griffin, D.K.; Ogur, C. Chromosomal analysis in IVF: just how useful is it? *Reproduction 156*, F29–F50.
784. Maheswari, N.; Kumar, B.; Kumaran, S. "'Early baby teeth'": Folklore and facts. *J. Pharm. Bioallied Sci.* **2012**, *4*, 329–333.
785. Anderson, R.A. Natal and neonatal teeth: Histologic investigation of two black females. *ASDC J Dent Child* **1982**, *49*, 300–303.
786. Hals, E. Natal and neonatal teeth: Histologic investigations in two brothers. *Oral Surgery, Oral Med. Oral Pathol.* **1957**, *10*, 509–521.
787. BOYD, J.D.; MILES, A.E.W. An erupted tooth in a cyclops foetus. *Br. Dent. J.* **1951**, *91*, 173–181.
788. Portela, M.B.; Damasceno, L.; Primo, L.G. Unusual case of multiple natal teeth. *J. Clin. Pediatr. Dent.* **2008**, *29*, 37–3.
789. Kates, G.A.; Needleman, H.L.; Holmes, L.B. Natal and neonatal teeth: a clinical study. *J. Am. Dent. Assoc.* **1984**, *109*, 441–443.
790. Štamfelj, I.; Jan, J.; Cvetko, E.; Gašperšič, D. Size, ultrastructure, and microhardness of natal teeth with agenesis of permanent successors. *Ann. Anat. - Anat. Anzeiger* **2010**, *192*, 220–226.
791. Basavanthappa, N.N.; Kagathur, U.; Basavanthappa, R.N.; Suryaprakash, S.T. Natal and Neonatal Teeth: A Retrospective Study of 15 Cases. *Eur J Dent* **2011**, *05*, 168–172.
792. Leung, A.K.C.; Robson, W.L.M. Natal teeth: a review. *J. Natl. Med. Assoc.* **2006**, *98*, 226.
793. Wang, C.-H.; Lin, Y.-T.; Lin, Y.-T.J. A survey of natal and neonatal teeth in newborn infants. *J. Formos. Med. Assoc.* **2017**, *116*, 193–196.
794. Bjuggren, G. Premature eruption in the primary dentition--a clinical and radiological study. *Sven. Tandlak. Tidskr.* **1973**, *66*, 343–355.
795. Chow, M.H. Natal and Neonatal Teeth. *J. Am. Dent. Assoc.* **1980**, *100*, 215–216.
796. Tomizawa, M.; Yamada, Y.; Tonouchi, K.; Watanabe, H.; Noda, T. [Treatment of Riga-Fede's disease by resin-coverage of the incisal edges and seven cases of natal and neonatal teeth]. *Shoni Shikagaku Zasshi.* **1989**, *27*, 182–190.
797. Weiss, H. Chondroectodermal dysplasia: Report of a case and review of the literature. *J. Pediatr.* **1955**, *46*, 268–275.
798. Dyment, H.; Anderson, R.; Humphrey, J.; Chase, I. Residual neonatal teeth: a case report. *J Can Dent Assoc* **2005**, *71*, 394–397.
799. Hennekam, R.C.M.; Van Doorne, J.M. Oral aspects of Rubinstein-Taybi syndrome. *Am. J. Med. Genet.* **1990**, *37*, 42–47.
800. Ziai, M.N.; Bock, D.J.; Da Silveira, A.; Daw, J.L. Natal Teeth: A Potential Impediment to Nasoalveolar Molding in Infants With Cleft Lip and Palate. *J. Craniofac. Surg.* **2005**, *16*.
801. Khandelwal, V.; Nayak, U.A.; Nayak, P.A.; Bafna, Y. Management of an infant having natal teeth. *BMJ Case Rep.* **2013**, *2013*, bcr2013010049.
802. Padmanabhan, M.Y.; Pandey, R.K.; Aparna, R.; Radhakrishnan, V. Neonatal sublingual traumatic ulceration – case report & review of the literature. *Dent. Traumatol.* **2010**, *26*, 490–495.
803. Choi, S.C.; Park, J.H.; Choi, Y.C.; Kim, G.-T. Sublingual traumatic ulceration (a Riga-Fede disease): report of two cases. *Dent. Traumatol.* **2009**, *25*, e48–e50.
804. Singh, S.; Subba Reddy, V. V; Dhananjaya, G.; Patil, R. Reactive fibrous hyperplasia associated with a natal tooth. *J. Indian Soc. Pedod. Prev. Dent.* **2004**, *22*, 183–186.
805. TO, E.W.H. A study of natal teeth in Hong Kong Chinese. *Int. J. Paediatr. Dent.* **1991**, *1*, 73–76.
806. Bhutta, Z.A.; Darmstadt, G.L.; Hasan, B.S.; Haws, R.A. Community-Based Interventions for Improving Perinatal and Neonatal Health Outcomes in Developing Countries: A Review of the Evidence. *Pediatrics* **2005**, *115*, 519 LP – 617.
807. Ng, E.; Loewy, A.D. Guidelines for vitamin K prophylaxis in newborns. *Paediatr. Child Health* **2018**, *23*, 394–397.

808. Ooshima, T.; Mihara, J.; Saito, T.; Sobue, S. Eruption of tooth-like structure following the exfoliation of natal tooth: report of case. *ASDC J. Dent. Child.* **1986**, *53*, 275–278.
809. Tsubone, H.; Onishi, T.; Hayashibara, T.; Sobue, S.; Ooshima, T. Clinico-pathological aspects of a residual natal tooth: a case report. *J. Oral Pathol. Med.* **2002**, *31*, 239–241.
810. King, N.M.; Lee, A.M.P. Prematurely erupted teeth in newborn infants. *J. Pediatr.* **1989**, *114*, 807–809.
811. Ciobica, A.; Padurariu, M.; Curpan, A.; Antioch, I.; Chirita, R.; Stefanescu, C.; Luca, A.-C.; Tomida, M. Minireview on the Connections between the Neuropsychiatric and Dental Disorders: Current Perspectives and the Possible Relevance of Oxidative Stress and Other Factors. *Oxid. Med. Cell. Longev.* **2020**, *2020*, 6702314.
812. Soini, S. Preimplantation genetic diagnosis (PGD) in Europe: Diversity of legislation a challenge to the community and its citizens. *Med. Law* **2007**, *26*, 309–323.
813. Verlinsky, Y.; Rechitsky, S.; Schoolcraft, W.; Strom, C.; Kuliev, A. Preimplantation Diagnosis for Fanconi Anemia Combined With HLA Matching. *JAMA* **2001**, *285*, 3130–3133.
814. KULIEV, A.; RECHITSKY, S.; TUR-KASPA, I.; VERLINSKY, Y. Preimplantation Genetics: Improving Access to Stem Cell Therapy. *Ann. N. Y. Acad. Sci.* **2005**, *1054*, 223–227.
815. Steffann, J.; Frydman, N.; Burlet, P.; Gigarel, N.; Feyereisen, E.; Kerbrat, V.; Tachdjian, G.; Munnich, A.; Frydman, R. Le diagnostic préimplantatoire couplé au typage HLA : l'expérience parisienne. *Gynécologie Obs. Fertil.* **2005**, *33*, 824–827.
816. Berg Brigham, K.; Cadier, B.; Chevreul, K. The diversity of regulation and public financing of IVF in Europe and its impact on utilization. *Hum. Reprod.* **2013**, *28*, 666–675.
817. Mills, M.; Rindfuss, R.R.; McDonald, P.; te Velde, E.; Force, on behalf of the E.R. and S.T. Why do people postpone parenthood? Reasons and social policy incentives. *Hum. Reprod. Update* **2011**, *17*, 848–860.
818. Ziebe, S.; Devroey, P.; Group, on behalf of the S. of the A.R.T. 2007 W. Assisted reproductive technologies are an integrated part of national strategies addressing demographic and reproductive challenges. *Hum. Reprod. Update* **2008**, *14*, 583–592.
819. Burgoyne, J.W.; Daniels, P.D.; Timms, K.W.; Vale, S.H. Advances in superconducting magnets for commercial and industrial applications. *IEEE Trans. Appl. Supercond.* **2000**, *10*, 703–709.
820. McNeil, R.G.; Ritter, R.C.; Wang, B.; Lawson, M.A.; Gillies, G.T.; Wika, K.G.; Quate, E.G.; Howard, M.A.; Grady, M.S. Characteristics of an improved magnetic-implant guidance system. *IEEE Trans. Biomed. Eng.* **1995**, *42*, 802–808.
821. Agop, M.; Ioannou, P.D.; Nica, P. Superconductivity by means of the subquantum medium coherence. *J. Math. Phys.* **2005**, *46*, 62110.
822. Agop, M.; Ioannou, P.D.; Buzea, C.G.; Nica, P. Hydrodynamic formulation of scale relativity theory and unified superconductivity by means of a fractal string. *Phys. C Supercond.* **2003**, *390*, 37–55.
823. Chiatti, O.; Nicholls, J.T.; Proskuryakov, Y.Y.; Lumpkin, N.; Farrer, I.; Ritchie, D.A. Quantum Thermal Conductance of Electrons in a One-Dimensional Wire. *Phys. Rev. Lett.* **2006**, *97*, 56601.
824. Burns, G. High-Temperature Superconductivity: An Introduction.; 1991.
825. Poole CP, Farach HA, C.R. *Superconductivity*; Academic Press, San DiegoNew York-Boston-London-Sydney-Tokyo-Toronto, 1995;
826. Chiroiu, V.; Stiuca, P.; Munteanu, L.; Donescu, S. Introduction in nanomechanics. *Publ. House Acad. Române, Bucureşti* **2005**.
827. Sato, M.; Sato, K. Dynamic Regulation of Autophagy and Endocytosis for Cell Remodeling During Early Development. *Traffic* **2013**, *14*, 479–486.
828. Zhou, Q.; Li, H.; Xue, D. Elimination of paternal mitochondria through the lysosomal degradation pathway in C. elegans. *Cell Res.* **2011**, *21*, 1662–1669.
829. Al Rawi, S.; Louvet-Vallée, S.; Djeddi, A.; Sachse, M.; Culetto, E.; Hajjar, C.; Boyd, L.; Legouis, R.; Galy, V. Postfertilization Autophagy of Sperm Organelles Prevents Paternal Mitochondrial DNA Transmission. *Science (80-.).* **2011**, *334*, 1144 LP – 1147.
830. de Paula, W.B.M.; Lucas, C.H.; Agip, A.-N.A.; Vizcay-Barrena, G.; Allen, J.F. Energy, ageing, fidelity and sex: oocyte mitochondrial DNA as a protected genetic template. *Philos. Trans. R. Soc. B Biol. Sci.* **2013**, *368*, 20120263.
831. Paumgartner, D.; Losa, G.; Weibel, E.R. Resolution effect on the stereological estimation of surface and volume and its interpretation in terms of fractal dimensions. *J. Microsc.* **1981**, *121*, 51–63.
832. B, M. *Les Objetes Fractals: Forme, Hazard et Dimension*; Paris: Flammarion, 1972;
833. Gottlieb, I. *L'hypothèse d'un modèle de la structure de la matière*; Revista Ma.; Tucuman, Argentina, 1964;
834. Gottlieb, I. Some Hypotheses on Space-Time and Gravitation. In *Studies in Gravitation Theory*; Gottlieb, I, Ionescu-Pallas, I., Ed.; CIP Press, 1988; pp. 227–234.
835. Gottlieb, I. *Overlaped Universes*; Ed. Tehnica, 1995;

836. Gottlieb, I.; Agop, M. El Naschie's ε(∞) theory and an alternative to gauged spacetime scale relativity theory. *Chaos, Solitons & Fractals* **2007**, *34*, 1025–1029.
837. CROSS, S.S. FRACTALS IN PATHOLOGY. *J. Pathol.* **1997**, *182*, 1–8.
838. Losa, G.A.; Baumann, G.; Nonnenmacher, T.F. Fractal dimension of pericellular membranes in human lymphocytes and lymphoblastic leukemia cells. *Pathol. - Res. Pract.* **1992**, *188*, 680–686.
839. Castelli, C.; Losa, G.A. Ultrastructural complexity of nuclear components during early apoptotic phases in breast cancer cells. *Anal. Cell. Pathol.* **2001**, *23*, 1–9.
840. Nielsen, B.; Albregtsen, F.; Danielsen, H.E. Fractal Analysis of Monolayer Cell Nuclei from Two Different Prognostic Classes of Early Ovarian Cancer BT - Fractals in Biology and Medicine.; Losa, G.A., Merlini, D., Nonnenmacher, T.F., Weibel, E.R., Eds.; Birkhäuser Basel: Basel, 2005; pp. 175–186.
841. Freeman, W.J. Simulation of chaotic EEG patterns with a dynamic model of the olfactory system. *Biol. Cybern.* **1987**, *56*, 139–150.
842. A, L.M. *Les Geometries Fractales*; Paris, Hermes, 1990;
843. Gouyet, J.-F. *Physique et structures fractales. Préface de Benoît Mandelbrot*; 1992; ISBN 2-225-82777-X.
844. Feder J, A.A. *Fractals in Physics*; Amsterdam, North Holland, 1990;
845. Srinivasan, C. Carbon nanotubes in cancer therapy. *Curr. Sci.* **2008**, *94*, 300–301.
846. Metzger, M.; Leibowitz, G.; Wainstein, J.; Glaser, B.; Raz, I. Reproducibility of Glucose Measurements Using the Glucose Sensor. *Diabetes Care* **2002**, *25*, 1185 LP – 1191.
847. Clendenin, J.; Kim, J.; Tung, S. An Aligned Carbon Nanotube Biosensor for DNA Detection. In Proceedings of the 2007 2nd IEEE International Conference on Nano/Micro Engineered and Molecular Systems; 2007; pp. 1028–1033.
848. Petersen, B.M.; Boel, M.; Montag, M.; Gardner, D.K. Development of a generally applicable morphokinetic algorithm capable of predicting the implantation potential of embryos transferred on Day 3. *Hum. Reprod.* **2016**, *31*, 2231–2244.
849. Liu, Y.; Chapple, V.; Feenan, K.; Roberts, P.; Matson, P. Time-lapse deselection model for human day 3 in vitro fertilization embryos: the combination of qualitative and quantitative measures of embryo growth. *Fertil. Steril.* **2016**, *105*, 656-662.e1.
850. Barrie, A.; Homburg, R.; McDowell, G.; Brown, J.; Kingsland, C.; Troup, S. Examining the efficacy of six published time-lapse imaging embryo selection algorithms to predict implantation to demonstrate the need for the development of specific, in-house morphokinetic selection algorithms. *Fertil. Steril.* **2017**, *107*, 613–621.
851. Filho, E.; Noble, J.; Poli, M.; Griffiths, T.; Emerson, G.; Wells, D. A method for semi-automatic grading of human blastocyst microscope images. *Hum. Reprod.* **2012**, *27*, 2641–2648.
852. Cross, S.S. The application of fractal geometric analysis to microscopic images. *Micron* **1994**, *25*, 101–113.
853. Nazem, T.G.; Sekhon, L.; Lee, J.A.; Overbey, J.; Pan, S.; Duke, M.; Briton-Jones, C.; Copperman, A.B. In an era of euploid single embryo transfers: does oocyte age matter? *Fertil. Steril.* **2017**, *108*, e98.
854. Paun, V.-P. Creep model for polymeric materials. **2003**, *40*, 25–26.
855. Paun, V.-P. Relaxation model for polymeric materials in the hereditary theory of elasticity. *Mater. Plast.* **2003**, *40*, 81–82.
856. Dam, A.H.D.M.; Koscinski, I.; Kremer, J.A.M.; Moutou, C.; Jaeger, A.-S.; Oudakker, A.R.; Tournaye, H.; Charlet, N.; Lagier-Tourenne, C.; van Bokhoven, H.; et al. Homozygous mutation in SPATA16 is associated with male infertility in human globozoospermia. *Am. J. Hum. Genet.* **2007**, *81*, 813–820.
857. Holstein, A.F.; Schirren, C.G.; Mauß, J. Rundköpfige Spermatozoen: eine Ursache der Infertilität des Mannes. *Dtsch Med Wochenschr* **1973**, *98*, 61–62.
858. Dam, A.H.; Ramos, L.; Dijkman, H.B.; Woestenenk, R.; Robben, H.; van den Hoven, L.; Kremer, J.A. Morphology of Partial Globozoospermia. *J. Androl.* **2011**, *32*, 199–206.
859. Saunders, C.M.; Larman, M.G.; Parrington, J.; Cox, L.J.; Royse, J.; Blayney, L.M.; Swann, K.; Lai, F.A. PLCζ: a sperm-specific trigger of Ca2+ oscillations in eggs and embryo development. *Development* **2002**, *129*, 3533–3544.
860. Grasa, P.; Coward, K.; Young, C.; Parrington, J. The pattern of localization of the putative oocyte activation factor, phospholipase Cζ, in uncapacitated, capacitated, and ionophore-treated human spermatozoa. *Hum. Reprod.* **2008**, *23*, 2513–2522.
861. Ikawa, M.; Inoue, N.; Benham, A.M.; Okabe, M. Fertilization: a sperm's journey to and interaction with the oocyte. *J. Clin. Invest.* **2010**, *120*, 984–994.
862. Rybouchkin, A. V; Van der Straeten, F.; Quatacker, J.; De Sutter, P.; Dhont, M. Fertilization and pregnancy after assisted oocyte activation and intracytoplasmic sperm injection in a case of round-headed sperm associated with deficient oocyte activation capacity. *Fertil. Steril.* **1997**, *68*, 1144–1147.

863. Embryology, A.S. in R.M. and E.S.I.G. of The Istanbul consensus workshop on embryo assessment: proceedings of an expert meeting†. *Hum. Reprod.* **2011**, *26*, 1270–1283.
864. Yoon, S.-Y.; Jellerette, T.; Salicioni, A.M.; Lee, H.C.; Yoo, M.; Coward, K.; Parrington, J.; Grow, D.; Cibelli, J.B.; Visconti, P.E.; et al. Human sperm devoid of PLC, zeta 1 fail to induce Ca2+ release and are unable to initiate the first step of embryo development. *J. Clin. Invest.* **2008**, *118*, 3671–3681.
865. Heindryckx, B.; Gheselle, S.; Gerris, J.; Dhont, M.; De Sutter, P. Efficiency of assisted oocyte activation as a solution for failed intracytoplasmic sperm injection. *Reprod. Biomed. Online* **2008**, *17*, 662–668.
866. Kullander, S.; Rausing, A. On round-headed human spermatozoa. *Int. J. Fertil.* **1975**, *20*, 33–40.
867. FLÖRKE-GERLOFF, S.; TÖPFER-PETERSEN, E.; MÜLLER-ESTERL, W.; MANSOURI, A.; SCHATZ, R.; SCHIRREN, C.; SCHILL, W.; ENGEL, W. Biochemical and Genetic Investigation of Round-headed Spermatozoa in Infertile Men including two Brothers and their Father. *Andrologia* **1984**, *16*, 187–202.
868. Dale, B.; Iaccarino, M.; Fortunato, A.; Gragnaniello, G.; Kyozuka, K.; Tosti, E. A morphological and functional study of fusibility in round-headed spermatozoa in the human. *Fertil. Steril.* **1994**, *61*, 336–340.
869. Kilani, Z.; Ismail, R.; Ghunaim, S.; Mohamed, H.; Hughes, D.; Brewis, I.; Barratt, C.L.R. Evaluation and treatment of familial globozoospermia in five brothers. *Fertil. Steril.* **2004**, *82*, 1436–1439.
870. Heindryckx, B.; Van der Elst, J.; De Sutter, P.; Dhont, M. Treatment option for sperm- or oocyte-related fertilization failure: assisted oocyte activation following diagnostic heterologous ICSI. *Hum. Reprod.* **2005**, *20*, 2237–2241.
871. Navath, R.S.; Menjoge, A.R.; Dai, H.; Romero, R.; Kannan, S.; Kannan, R.M. Injectable PAMAM dendrimer-PEG hydrogels for the treatment of genital infections: formulation and in vitro and in vivo evaluation. *Mol. Pharm.* **2011**, *8*, 1209–1223.
872. Ensign, L.M.; Cone, R.; Hanes, J. Nanoparticle-based drug delivery to the vagina: A review. *J. Control. Release* **2014**, *190*, 500–514.
873. Tang, J.; Xu, Z.; Zhou, L.; Qin, H.; Wang, Y.; Wang, H. Rapid and simultaneous detection of Ureaplasma parvum and Chlamydia trachomatis antibodies based on visual protein microarray using gold nanoparticles and silver enhancement. *Diagn. Microbiol. Infect. Dis.* **2010**, *67*, 122–128.
874. Toti, U.S.; Guru, B.R.; Hali, M.; McPharlin, C.M.; Wykes, S.M.; Panyam, J.; Whittum-Hudson, J.A. Targeted delivery of antibiotics to intracellular chlamydial infections using PLGA nanoparticles. *Biomaterials* **2011**, *32*, 6606–6613.
875. Taha, M.A.; Singh, S.R.; Dennis, V.A. Biodegradable PLGA85/15 nanoparticles as a delivery vehicle forChlamydia trachomatisrecombinant MOMP-187 peptide. *Nanotechnology* **2012**, *23*, 325101.
876. Menjoge, A.R.; Navath, R.S.; Asad, A.; Kannan, S.; Kim, C.J.; Romero, R.; Kannan, R.M. Transport and biodistribution of dendrimers across human fetal membranes: Implications for intravaginal administration of dendrimer-drug conjugates. *Biomaterials* **2010**, *31*, 5007–5021.
877. Weissleder, R.; Elizondo, G.; Wittenberg, J.; Lee, A.S.; Josephson, L.; Brady, T.J. Ultrasmall superparamagnetic iron oxide: an intravenous contrast agent for assessing lymph nodes with MR imaging. *Radiology* **1990**, *175*, 494–498.
878. Zhao, Z.; Han, Y.; Lin, C.; Hu, D.; Wang, F.; Chen, X.; Chen, Z.; Zheng, N. Multifunctional Core–Shell Upconverting Nanoparticles for Imaging and Photodynamic Therapy of Liver Cancer Cells. *Chem. – An Asian J.* **2012**, *7*, 830–837.
879. Ali, H.; Kilic, G.; Vincent, K.; Motamedi, M.; Rytting, E. Nanomedicine for uterine leiomyoma therapy. *Ther. Deliv.* **2013**, *4*, 161–175.
880. Kaitu'u-Lino, T.J.; Pattison, S.; Ye, L.; Tuohey, L.; Sluka, P.; MacDiarmid, J.; Brahmbhatt, H.; Johns, T.; Horne, A.W.; Brown, J.; et al. Targeted Nanoparticle Delivery of Doxorubicin Into Placental Tissues to Treat Ectopic Pregnancies. *Endocrinology* **2013**, *154*, 911–919.
881. Cormode, D.P.; Naha, P.C.; Fayad, Z.A. Nanoparticle contrast agents for computed tomography: a focus on micelles. *Contrast Media Mol. Imaging* **2014**, *9*, 37–52.
882. Sutovsky, P.; Lovercamp, K. Molecular markers of sperm quality. *Soc. Reprod. Fertil. Suppl.* **2010**, *67*, 247–256.
883. Payan-Carreira, R. Molecular Markers in Sperm Analysis. In; Borges, P., Ed.; IntechOpen: Rijeka, 2013; p. Ch. 6.
884. Mortimer, D.; Curtis, E.F.; Camenzind, A.R. Combined use of fluorescent peanut agglutinin lectin and Hoechst 33258 to monitor the acrosomal status and vitality of human spermatozoa. *Hum. Reprod.* **1990**, *5*, 99–103.
885. CHENG, F.-P.; FAZELI, A.; VOORHOUT, W.I.M.F.; MARKS, A.; BEVERS, M.M.; COLENBRANDER, B.E.N. Use of Peanut Agglutinin to Assess the Acrosomal Status and the Zona Pellucida-Induced Acrosome Reaction in Stallion Spermatozoa. *J. Androl.* **1996**, *17*, 674–682.
886. Esteves, S.; Sharma, R.; Thomas, A.; Agarwal, A. Evaluation of acrosomal status and sperm viability in

fresh and cryopreserved specimens by the use of fluorescent peanut agglutinin lectin in conjunction with hypo-osmotic swelling test. *Int. Braz J Urol* **2007**, *33*, 364–74; discussion 375.
887. Kuster, C.E.; Hess, R.A.; Althouse, G.C. Immunofluorescence Reveals Ubiquitination of Retained Distal Cytoplasmic Droplets on Ejaculated Porcine Spermatozoa. *J. Androl.* **2004**, *25*, 340–347.
888. Sutovsky, P.; Moreno, R.D.; Ramalho-Santos, J.; Dominko, T.; Simerly, C.; Schatten, G. Ubiquitinated Sperm Mitochondria, Selective Proteolysis, and the Regulation of Mitochondrial Inheritance in Mammalian Embryos1. *Biol. Reprod.* **2000**, *63*, 582–590.
889. Sutovsky, P.; Terada, Y.; Schatten, G. Ubiquitin-based sperm assay for the diagnosis of male factor infertility. *Hum. Reprod.* **2001**, *16*, 250–258.
890. Sutovsky, P.; Turner, R.M.; Hameed, S.; Sutovsky, M. Differential Ubiquitination of Stallion Sperm Proteins: Possible Implications for Infertility and Reproductive Seasonality1. *Biol. Reprod.* **2003**, *68*, 688–698.
891. Ozanon, C.; Chouteau, J.; Sutovsky, P. Clinical adaptation of the sperm ubuquitin tag immunoassay (SUTI): relationship of sperm ubiquitylation with sperm quality in gradient-purified semen samples from 93 men from a general infertility clinic population. *Hum. Reprod.* **2005**, *20*, 2271–2278.
892. Galuppo, A.G.; Junior, N.B.; Arruda, N.S.; Corbellini, A.O.; Chiappetta, C.M.; Pavão, D.L.; D'Angelo, M.; Canal, C.W.; Rodrigues, J.L. Evaluation of the effectiveness of semen processing techniques to remove bovine viral diarrhea virus from experimentally contaminated semen samples. *J. Virol. Methods* **2013**, *187*, 443–448.
893. Sutovsky, P.; Kennedy, C.E. Biomarker-Based Nanotechnology for the Improvement of Reproductive Performance in Beef and Dairy Cattle. *Ind. Biotechnol.* **2013**, *9*, 24–30.
894. Nasri, S.; Rezai-Zarchi, S.; Kerishchi Khiabani, P.; Sadeghi, S. The Effect of Iron Oxide Nanoparticles on Sperm Numbers and Mobility in Male Mice. *Zahedan J. Res. Med. Sci.* **2015**, *17*.
895. Sirard, M.-A.; Coenen, K. In Vitro Maturation and Embryo Production in Cattle BT - Nuclear Transfer Protocols: Cell Reprogramming and Transgenesis. In; Verma, P.J., Trounson, A.O., Eds.; Humana Press: Totowa, NJ, 2006; pp. 35–42 ISBN 978-1-59745-154-3.
896. Enciso, M.; Muriel, L.; Fernández, J.L.; Goyanes, V.; Segrelles, E.; Marcos, M.; Montejo, J.M.; Ardoy, M.; Pacheco, A.; Gosálvez, J. Infertile Men With Varicocele Show a High Relative Proportion of Sperm Cells With Intense Nuclear Damage Level, Evidenced by the Sperm Chromatin Dispersion Test. *J. Androl.* **2006**, *27*, 106–111.
897. Carrell, D.T.; Emery, B.R.; Hammoud, S. The aetiology of sperm protamine abnormalities and their potential impact on the sperm epigenome. *Int. J. Androl.* **2008**, *31*, 537–545.
898. Bansal, A.K.; Bilaspuri, G.S. Impacts of oxidative stress and antioxidants on semen functions. *Vet. Med. Int.* **2010**, *2010*, 686137.
899. Maciuc, V.; Creangă, S.; Chelmu, S.S. The reproductive capacity and specific applied biotechnologies in rendering cows reproduction efficient. *Rom. Biotechnol. Lett.* **2014**, *19*, 9155–9161.
900. Virro, M.R.; Larson-Cook, K.L.; Evenson, D.P. Sperm chromatin structure assay (SCSA) parameters are related to fertilization, blastocyst development, and ongoing pregnancy in in vitro fertilization and intracytoplasmic sperm injection cycles. *Fertil. Steril.* **2004**, *81*, 1289–1295.
901. Waterhouse, K.; Haugan, T.; Kommisrud, E.; Tverdal, A.; Flatberg, G.; Farstad, W.; Evenson, D.; De Angelis, P. Sperm DNA damage is related to field fertility of semen from young Norwegian Red bulls. *Reprod. Fertil. Dev.* **2006**, *18*, 781–788.
902. Sakkas, D.; Alvarez, J.G. Sperm DNA fragmentation: mechanisms of origin, impact on reproductive outcome, and analysis. *Fertil. Steril.* **2010**, *93*, 1027–1036.
903. Wdowiak, A.; Bojar, I. Relationship between pregnancy, embryo development, and sperm deoxyribonucleic acid fragmentation dynamics. *Saudi J. Biol. Sci.* **2016**, *23*, 598–606.
904. Neculai-Valeanu, A.S.; Drugociu, D.; Rosca, P. Effect of Single layer centrifugation using Bovipure on frozen-thawed bovine sperm during a 6 hours survival test. *Rom. Biotechnol. Lett.* **2015**, *20*, 10327–10333.
905. Said, T.M.; Land, J.A. Effects of advanced selection methods on sperm quality and ART outcome: a systematic review. *Hum. Reprod. Update* **2011**, *17*, 719–733.
906. Cho, B.S.; Schuster, T.G.; Zhu, X.; Chang, D.; Smith, G.D.; Takayama, S. Passively Driven Integrated Microfluidic System for Separation of Motile Sperm. *Anal. Chem.* **2003**, *75*, 1671–1675.
907. Xie, L.; Ma, R.; Han, C.; Su, K.; Zhang, Q.; Qiu, T.; Wang, L.; Huang, G.; Qiao, J.; Wang, J.; et al. Integration of Sperm Motility and Chemotaxis Screening with a Microchannel-Based Device. *Clin. Chem.* **2010**, *56*, 1270–1278.
908. Ko, Y.-J.; Maeng, J.-H.; Lee, B.-C.; Lee, S.; Hwang, S.; Ahn, Y. Separation of Progressive Motile Sperm from Mouse Semen Using On-chip Chemotaxis. *Anal. Sci.* **2012**, *28*, 27–32.
909. D, S. A development of the motile sperm sorting microfluidic devices, University of Missouri-Columbia, 2007.

910. Zhang, X.; Khimji, I.; Gurkan, U.A.; Safaee, H.; Catalano, P.N.; Keles, H.O.; Kayaalp, E.; Demirci, U. Lensless imaging for simultaneous microfluidic sperm monitoring and sorting. *Lab Chip* **2011**, *11*, 2535–2540.
911. Chen, W.; Huang, N.-T.; Li, X.; Yu, Z.; Kurabayashi, K.; Fu, J. Emerging Microfluidic Tools for Functional Cellular Immunophenotyping: A New Potential Paradigm for Immune Status Characterization. *Front. Oncol.* 2013, *3*, 98.
912. Cenariu, M.; Groza, I.; Páll, E.; Bogdan, L.; Morar, I.; Maria, C.; Pop, R. Sexing of bovine embryos using polymerase chain reaction (PCR) and fluorescent in situ hybridization (FISH). *Rom. Biotechnol. Lett.* **2011**, *16*, 6055–6061.
913. Rath, D.; Barcikowski, S.; de Graaf, S.; Garrels, W.; Grossfeld, R.; Klein, S.; Knabe, W.; Knorr, C.; Kues, W.; Meyer, H.; et al. Sex selection of sperm in farm animals: status report and developmental prospects. *REPRODUCTION 145*, R15–R30.
914. Wheeler, M.B.; Rutledge, J.J.; Fischer-Brown, A.; VanEtten, T.; Malusky, S.; Beebe, D.J. Application of sexed semen technology to in vitro embryo production in cattle. *Theriogenology* **2006**, *65*, 219–227.
915. Rienzi, L.; Vajta, G.; Ubaldi, F. Predictive value of oocyte morphology in human IVF: a systematic review of the literature. *Hum. Reprod. Update* **2011**, *17*, 34–45.
916. Bukowska, D.; Kempisty, B.; Piotrowska, H.; Walczak, R.; Śniadek, P.; Dziuban, J.; Brüssow, K.-P.; Jaskowski, J.M.; Nowicki, M. The invasive and new non-invasive methods of mammalian oocyte and embryo quality assessment: A review. *Vet. Med. (Praha).* **2012**, *57*, 169–176.
917. Choi, W.; Kim, J.-S.; Lee, D.-H.; Lee, K.-K.; Koo, D.-B.; Park, J.-K. Dielectrophoretic oocyte selection chip for in vitro fertilization. *Biomed. Microdevices* **2008**, *10*, 337–345.
918. Szczepanska, P.; Walczak, R.; Dziuban, J.; Jackowska, M.; Kempisty, B.; Jaskowski, J.; Bargiel, S. Lab-on-chip quality classification of porcine/bovine oocytes. *Procedia Chem.* **2009**, *1*, 341–344.
919. Walczak, R.; Szczepańska, P.; Dziuban, J.; Kempisty, B.; Jackowska, M.; Antosik, P.; Jaśkowski, J.; Chelmońska-Soyta, A. Lab-on-a-chip for developmental competence assessment of bovine oocytes. In Proceedings of the Proceedings of the 17th International Conference Mixed Design of Integrated Circuits and Systems - MIXDES 2010; 2010; pp. 633–636.
920. Lai, D. Microfluidic Reduction of Osmotic Stress in Oocyte and Zygote Vitrification. **2014**.
921. Clark, S.G.; Haubert, K.; Beebe, D.J.; Ferguson, C.E.; Wheeler, M.B. Reduction of polyspermic penetration using biomimetic microfluidic technology during in vitro fertilization. *Lab Chip* **2005**, *5*, 1229–1232.
922. Suh, R.S.; Zhu, X.; Phadke, N.; Ohl, D.A.; Takayama, S.; Smith, G.D. IVF within microfluidic channels requires lower total numbers and lower concentrations of sperm. *Hum. Reprod.* **2006**, *21*, 477–483.
923. Giglio, A.; Cheong, S.H.; Neri, Q. V; Rosenwaks, Z.; Palermo, G.D. ICSI-on-a-chip. *Fertil. Steril.* **2013**, *100*, S479.
924. Croxatto, H.B. Physiology of gamete and embryo transport through the Fallopian tube*. *Reprod. Biomed. Online* **2002**, *4*, 160–169.
925. Hao, Z.; Kieslinger, D.C.; Vergouw, C.G.; Kostelijk, H.; Lambalk, C.; Gac, S. Microfluidic protocol for in vitro culture of human embryos.; 2013.
926. Smith, R.L.; Demers, C.J.; Collins, S.D. Microfluidic device for the combinatorial application and maintenance of dynamically imposed diffusional gradients. *Microfluid. Nanofluidics* **2010**, *9*, 613–622.
927. Pyne, D.G.; Liu, J.; Abdelgawad, M.; Sun, Y. Digital microfluidic processing of mammalian embryos for vitrification. *PLoS One* **2014**, *9*, e108128–e108128.
928. Meng, L.; Huezo, X.; Stone, B.A.; Baek, K.; Ringler, G.; Marrs, R.P. Development of a microfluidic device for automated vitrification human embryo. *Fertil. Steril.* **2011**, *96*, S207.